In vitro systems to predict hepatotoxicity: models based on hepatocarcinoma cell lines

Catherine Anne Mowbray

Thesis submitted in partial fulfilment of the requirements
of the regulations for the degree of Doctor of Philosophy

Newcastle University

Faculty of Medical Sciences

Institute of Cell and Molecular Biosciences

Epithelial Research Group

August 2011

Abstract

The liver has a major role in the metabolism of both endogenous and exogenous compounds. In drug development, reliable and reproducible results regarding the toxicity of a new compound must be obtained. The gold standard is freshly isolated primary human hepatocytes; however, these are costly, difficult to obtain regularly and cannot be cultured extensively. Secondary hepatocyte cell lines are cheaper with a much longer lifespan in culture but do not accurately reflect the expression profile of a hepatocyte. The aim of this work was to promote differentiation of hepatic carcinoma cell lines towards the *in vivo* hepatic profile and potentially create a well defined and easily accessible model for early stage drug testing.

Initial profiling of HepG2 and Huh7 for differentiation markers, transporters and enzymes was carried out by qPCR. Differentiation was attempted by use of growth factors and dimethyl sulfoxide (DMSO) for periods of up to thirty days. Analysis of differentiation markers by qPCR indicated that 1% DMSO treatment for at least 15 days promoted maturation most effectively. Cells treated with 1% DMSO were analysed for mRNA expression of selected transporters and enzymes, followed by treatment with typical inducers, Western blotting and functional assays to assess the presence and function of certain proteins.

Although initial results showed potential, further analyses of the 1% DMSO treated cells were less promising. Analysis of transporter and enzyme mRNA expression revealed that many levels did not change favourably towards those observed in liver, or significantly changed from control but remained vastly removed from liver. Results from protein and induction experiments also indicated no benefit of 15-day DMSO treatment in either cell line. In conclusion, 1% DMSO treatment does not promote differentiation towards a more representative hepatic profile in either cell line; alternative methods are needed to develop a more heptocyte-like model using these cells.

For my Mam, who always encouraged me to be the best I could be.

For Hookbones, who is always there for me.

Acknowledgements

I would like to thank my supervisors Prof. Barry Hirst, Dr. Alison Howard and Dr. Janine Morsman for their help, advice and support throughout this project. I would also like to thank Mrs Maxine Geggie for her invaluable help and advice with tissue culture. Members of the Epithelial Research Group and ICaMB both past and present are thanked for their help and advice ranging from experimental setup and the teaching of new techniques to providing the stimulating discussion and questions essential in the development and progress of any research project.

I am also appreciative of the support from my family, friends and work colleagues throughout my research career both past and present. Prof. Patrick Chinnery and colleagues are thanked for giving me the experience I needed to progress from a new graduate to potential PhD student, and for encouraging me to take that step. My current work colleagues, in particular Dr. Marie Smith, are thanked for their advice and understanding as I completed this thesis. Finally, I would like to thank my mam for her continued support throughout my education and Steven for the unconditional support and encouragement throughout my PhD.

This studentship was funded by a BBSRC-CASE award in partnership with Sanofi Aventis.

Table of Contents

Chapter 1 – Introduction

1.1 General introduction.....1

1.2 Liver physiology.....2

1.2.1 Overview of liver structure and function.....2

1.2.2 Liver development and regeneration.....3

1.2.3 Signalling in liver regeneration.....4

1.2.4 Progenitor cells in the liver.....6

1.3 Key enzymes and transporters in hepatocytes.....7

1.3.1 Uptake transporters.....7

1.3.2 Phase I drug metabolising enzymes.....8

1.3.3 Phase II drug metabolising enzymes.....10

1.3.4 Phase III drug transporters.....12

1.4 Model systems for hepatic transport and metabolism.....14

1.4.1 Enzyme only systems.....14

1.4.1.1 Liver fractions.....14

1.4.1.2 Liver microsomes.....15

1.4.1.3 Supersomes™.....15

1.4.2 Liver slices.....15

1.4.3 Hepatocytes.....16

1.4.3.1 Primary hepatocytes.....16

1.4.3.2 Cryopreserved human hepatocytes.....17

1.4.3.3 Immortalised hepatocytes.....18

1.5 Hepatic tumour-derived cell lines.....19

1.5.1 HepG2 cells.....19

1.5.2 Huh7 cells.....20

1.5.3 Additional cell lines.....21

1.6 Stem cell derived hepatocytes.....22

1.6.1 Human embryonic stem cell derived hepatocyte-like cells.....22

1.6.2 Adult stem cell derived hepatocyte-like cells.....23

1.6.3 Umbilical cord blood derived hepatocyte like cells.....24

1.7 Differentiation of existing models.....24

1.7.1 Dimethyl sulfoxide treatment.....24

1.7.2 Transdifferentiation.....25

1.7.3 Oxygen rich environments.....25

1.8 Summary.....26

1.9 Aims.....27

Chapter 2 – Materials and Methods

2.1 Cell culture.....37

2.1.1 Routine culture of HepG2 and Huh7 cells.....37

2.1.2 Subculture of HepG2 and Huh7 cells.....37

2.1.3 Cell cryopreservation.....38

2.2 Differentiation treatments.....38

2.2.1 Initial growth factor treatments.....38

2.2.2 Dimethyl sulfoxide (DMSO) treatments.....39

2.2.3 Extended growth factor treatments.....39

2.2.4 HepatoZYME medium.....39

2.3 Induction treatments.....40

2.4 RNA extraction and reverse transcription.....40

2.5 End point PCR, cloning and qPCR.....41

2.6 Functional studies.....43

2.6.1 Hoechst 33342 experiments.....43

2.6.2 Calcein-AM experiments....44

2.7 Western blotting....45

2.8 Extraction of cells from umbilical cord blood....46

2.9 Statistical analysis....47

Chapter 3 – Characterisation of HepG2 and Huh7 cells: PCR assay development

3.1 Introduction....50

3.2 Methods....56

3.3 Results....56

3.3.1 Primer design....56

3.3.2 End point PCR....56

3.3.3 Sequence and BLAST results....57

3.3.4 qPCR assay validation....57

3.3.5 Summary of gene expression....59

3.4 Discussion....60

Chapter 4 – Differentiation of secondary hepatic cell lines to show a more *in vivo* hepatic profile

4.1 Introduction....110

4.2 Methods....112

4.3 Results....113

4.3.1 Selection of differentiation markers....113

4.3.2 Preliminary growth factor treatments....116

4.3.3 1% DMSO treatment on HepG2 and Huh7 cells....117

4.3.4 2% DMSO treatment on HepG2 and Huh7 cells....119

4.3.5 HepG2 cells plus treatment 1....121

4.3.6 HepG2 cells plus treatment 2....122

4.3.7 HepG2 cells plus treatment 3....122

4.3.8 Huh7 cells plus treatment 1.....123

4.3.9 Huh7 cells plus treatment 2.....123

4.3.10 Huh7 cells plus treatment 3.....124

4.3.11 Comparison of treatments in HepG2 and Huh7 cells.....125

4.4 Discussion.....126

Chapter 5 – Transporter and enzyme levels in DMSO-treated HepG2 and Huh7 cells

5.1 Introduction.....160

5.1.1 Influx transporters.....161

5.1.2 Efflux transporters.....162

5.1.3 Phase I metabolising enzymes.....162

5.1.4 Phase II metabolising enzymes.....163

5.2 Methods.....164

5.3 Results.....165

5.3.1 Influx transporters.....165

5.3.2 Efflux transporters.....167

5.3.3 Phase I metabolising enzymes.....168

5.3.4 Phase II metabolising enzymes.....170

5.3.5 GOI mRNA levels in HepG2 cells.....171

5.3.6 GOI mRNA levels in Huh7 cells.....173

5.4 Discussion.....175

Chapter 6 – Induction via CAR, PXR and AhR nuclear receptor pathways

6.1 Introduction.....200

6.2 Methods.....203

6.3 Results.....203

6.3.1 Rifampicin treatments.....203

6.3.2 Phenobarbital treatments.....204

6.3.3 BNF treatments.....205

6.4 Discussion.....206

Chapter 7 – Functional studies using Hoechst 33342 and calcein-AM

7.1 Introduction.....217

7.2 Methods.....218

7.3 Results.....219

7.3.1 Hoechst 33342 – confluent HepG2 cells.....219

7.3.2 Hoechst 33342 – DMSO-treated HepG2 cells.....220

7.3.3 Hoechst 33342 – confluent Huh7 cells.....221

7.3.4 Hoechst 33342 – prolonged untreated Huh7 cells.....222

7.3.5 Hoechst 33342 – DMSO-treated Huh7 cells.....223

7.3.6 Calcein-AM – preliminary experiments.....223

7.3.7 Calcein-AM – confluent HepG2 cells.....224

7.3.8 Calcein-AM – confluent Huh7 cells.....225

7.3.9 Calcein-AM – DMSO treated HepG2 cells.....226

7.3.10 Calcein-AM – prolonged untreated Huh7 cells.....228

7.3.11 Calcein-AM – DMSO treated Huh7 cells.....229

7.4 Discussion.....230

7.4.1 Hoechst 33342 experiments.....231

7.4.2 Calcein-AM experiments.....232

Chapter 8 – Detection of proteins by Western blotting

8.1 Introduction.....256

8.2 Methods.....260

8.3 Results.....261

8.3.1 Assessment of antibodies.....261

8.3.2 Effect of DMSO on BCRP levels.....263

8.3.3 Effect of BNF on BCRP levels.....264

8.3.4 Transferrin and ADPGK protein levels.....265

8.4 Discussion.....266

Chapter 9 – Concluding discussion.....283

Appendix A.....300

Appendix B.....302

References.....304

List of Tables

Table 1.1 – Influx tranporters.....31

Table 1.2 – CYP450 families.....32

Table 1.3 – Phase I metabolising enzymes.....33

Table 1.4 – Phase II metabolising enzymes (UGT enzymes).....34

Table 1.5 – Phase II metabolising enzymes (SULT, GST and NAT enzymes).....35

Table 1.6 – Efflux transporters.....36

Table 3.1 – Coefficient of Variation (CV) for qPCR assays.....107

Table 3.2 – Summary of gene expression in confluent HepG2 and Huh7 cells.....109

Table 4.1 – Preliminary growth factor treatments.....115

Table 4.4 – Extended treatments.....120

Table 4.3 – Markers of differentiation in HepG2 and Huh7 cells relative to control at 15 days.....136

Table 5.1 – Substrates of influx transporters.....178

Table 5.2 – Substrates of efflux transporters.....179

Table 5.3 – Substrates of phase I metabolising enzymes.....180

Table 5.4 – Substrates of phase II metabolising enzymes.....181

Table 5.5 – Transporter and enzyme mRNA levels in HepG2 relative to control.....198

Table 5.6 – Transporter and enzyme mRNA levels in Huh7 cells relative to control.....199

Table 6.1 – Protein targets of CAR, PXR and AhR.....210

Table 7.1 – Statistical analysis of data from figure 7.1.....236

Table 7.2 – Statistical analysis of data from figure 7.2.....238

Table 7.3 – Statistical analysis of data from figure 7.3.....240

Table 7.4 – Statistical analysis of data from figure 7.4.....242

Table 7.5 – Statistical analysis of data from figure 7.5.....244

Table 7.6 – Statistical analysis of data from figure 7.7.....247

Table 7.7 – Statistical analysis of data from figure 7.8.....249

Table 7.8 – Statistical analysis of data from figure 7.9.....251

Table 7.9 – Statistical analysis of data from figure 7.10.....253

Table 7.10 – Statistical analysis of data from figure 7.11.....255

Table 8.1 – Primary antibodies used for the detection of protein in Western blots.....272

Table 8.2 – Secondary antibodies used for the detection of protein in Western blots.....273

List of Figures

Figure 1.1 – Structure of a liver lobule.....29

Figure 1.2 – Hepatic drug transporters.....30

Figure 2.1 – Experimental protocol for HepG2 cells.....48

Figure 2.2 – Experimental protocol for Huh7 cells.....49

Figure 3.1 – Albumin PCR assay development.....67 & 68

Figure 3.2 – Transferrin PCR assay development.....69 & 70

Figure 3.3 – AFP PCR assay development.....71 & 72

Figure 3.4 – A1AT PCR assay development.....73 & 74

Figure 3.5 – HNF4a PCR assay development.....75 & 76

Figure 3.6 – MRP1 PCR assay development.....77 & 78

Figure 3.7 – MRP2 PCR assay development.....79 & 80

Figure 3.8 – MDR1 PCR assay development.....81 & 82

Figure 3.9 – BCRP PCR assay development.....83 & 84

Figure 3.10 – OCT3 PCR assay development.....85 & 86

Figure 3.11 – OATPB PCR assay development.....87 & 88

Figure 3.12 – OATPC PCR assay development.....89 & 90

Figure 3.13 – OATP8 PCR assay development.....91 & 92

Figure 3.14 – CYP1A2 PCR assay development.....93 & 94

Figure 3.15 – CYP2E1 PCR assay development.....95 & 96

Figure 3.16 – CYP3A4 PCR assay development.....97 & 98

Figure 3.17 – GSTA PCR assay development.....99 & 100

Figure 3.18 – GSTA4 PCR assay development.....101 & 102

Figure 3.19 – UGT1A1 PCR assay development.....103 & 104

Figure 3.20 – FMO3 PCR assay development.....105 & 106

Figure 3.21 – Sample dilution series for high, medium and low expression assays.....108

Figure 4.1 – Analysis of markers of differentiation in HepG2 cells.....132 & 133

Figure 4.2 – Analysis of markers of differentiation in Huh7 cells.....134 & 135

Figure 4.3 – Preliminary growth factor treatments on HepG2 cells.....137

Figure 4.4 – Preliminary growth factor treatments on Huh7 cells.....138

Figure 4.5 – HepG2 cells treated with 1% DMSO and analysed for differentiation markers...139

Figure 4.6 – Prolonged untreated culture and 1% DMSO treatment of Huh7 cells analysed for differentiation markers.....140 & 141

Figure 4.7 – HepG2 cells treated with DMSO and analysed for differentiation markers.....142 & 143

Figure 4.8 – Untreated and DMSO treated Huh7 cells analysed for differentiation markers.....144 & 145

Figure 4.9 – HepG2 cells with treatment 1 and 1% DMSO analysed for differentiation markers.....146 & 147

Figure 4.10 – HepG2 cells with treatment 2 and 1% DMSO analysed for differentiation markers.....148 & 149

Figure 4.11 – HepG2 cells with treatment 3 and 1% DMSO analysed for differentiation markers.....150 & 151

Figure 4.12 – Untreated and DMSO treated Huh7 cells with treatment 1 analysed for differentiation markers.....152 & 153

Figure 4.13 – Untreated and DMSO treated Huh7 cells with treatment 2 analysed for differentiation markers.....154 & 155

Figure 4.14 – Untreated and DMSO treated HepG2 cells with treatment 3 analysed for differentiation markers.....156 & 157

Figure 4.15 – Albumin, transferrin and AFP mRNA levels in 1% DMSO, 2% DMSO and treatments 1, 2 and 3 applied to HepG2 cells for 15 days.....158

Figure 4.16 – Albumin, transferrin and AFP mRNA levels in untreated, 1% DMSO, 2% DMSO and treatments 1, 2 and 3 applied to Huh7 cells for 15 days.....159

Figure 5.1 – DMSO treated HepG2 cells – OATPB, OATPC, OATP8 and OCT3 mRNA levels.....182 & 183

Figure 5.2 – Untreated and DMSO treated Huh7 cells – OATPB, OATPC, OATP8 and OCT3 mRNA levels.....184 & 185

Figure 5.3 – DMSO treated HepG2 cells – MRP1, MRP2, MDR1 and BCRP mRNA levels.....186 & 187

Figure 5.4 – Untreated and DMSO treated Huh7 cells – MRP1, MRP2, MDR1 and BCRP levels.....188 & 189

Figure 5.5 – DMSO treated HepG2 cells – CYP1A2, 2E1, 3A4 and FMO3 mRNA levels..190 & 191

Figure 5.6 – Untreated and DMSO treated Huh7 cells – CYP1A2, 2E1, 3A4 and FMO3 mRNA levels.....192 & 193

Figure 5.7 – DMSO treated HepG2 cells – GSTA, GSTA4 and UGT1A1 mRNA levels.....194 & 195

Figure 5.8 – Untreated and DMSO treated Huh7 cells – GSTA, GSTA4 and UGT1A1 mRNA levels.....196 & 197

Figure 6.1 – Rifampicin induction of MDR1 mRNA levels in confluent and 15 day 1% DMSO treated HepG2 cells.....211

Figure 6.2 – Rifampicin induction of MDR1 mRNA levels in confluent and 15 day 1% DMSO treated Huh7 cells.....212

Figure 6.3 – Phenobarbital induction of MRP2 mRNA levels in confluent and 15 day 1% DMSO treated HepG2 cells.....213

Figure 6.4 – Phenobarbital induction of MRP2 mRNA levels in confluent and 15 day 1% DMSO treated Huh7 cells.....214

Figure 6.5 – Beta-naphthoflavone (BNF) induction of BCRP mRNA in confluent and 15 day 1% DMSO treated HepG2 cells.....215

Figure 6.6 – Beta-naphthoflavone (BNF) induction of BCRP mRNA in confluent and 15 day 1% DMSO treated Huh7 cells.....216

Figure 7.1 – Hoechst 33342 accumulation in confluent HepG2 cells in the presence of P-gp and BCRP inhibitors.....235

Figure 7.2 – Hoechst 33342 accumulation in 15 day DMSO treated HepG2 cells in the presence of P-gp and BCRP inhibitors.....237

Figure 7.3 – Hoechst 33342 accumulation in confluent Huh7 cells in the presence of P-gp and BCRP inhibitors.....239

Figure 7.4 – Hoechst 33342 accumulation in 15 day untreated Huh7 cells in the presence of P-gp inhibitors.....241

Figure 7.5 – Hoechst 33342 accumulation in 15 day DMSO treated Huh7 cells in the presence of P-gp and BCRP inhibitors.....243

Figure 7.6 – Calcein uptake into confluent HepG2 and Huh7 cells.....245

Figure 7.7 – Confluent HepG2 cells analysed for calcein-AM uptake and calcein efflux.....246

Figure 7.8 – Confluent Huh7 cells analysed for calcein-AM uptake and calcein efflux.....248

Figure 7.9 – HepG2 cells treated for 15 days with 1% DMSO and analysed for calcein-AM uptake and calcein efflux.....250

Figure 7.10 – Huh7 cells grown untreated for 15 days and analysed for calcein-AM uptake and calcein efflux.....252

Figure 7.11 – Huh7 cells treated for 15 days with 1% DMSO and analysed for calcein-AM uptake and calcein efflux.....254

Figure 8.1 – Titration of sample for Western blot analysis using anti-BCRP.....274

Figure 8.2 – Titration of sample for Western blot analysis using anti-transferrin, anti-ADPGK and anti-GAPDH.....275 & 276

Figure 8.3 – Titration of sample for Western blot analysis using anti-actin and anti-GAPDH..277

Figure 8.4 – DMSO treated HepG2 and Huh7 cells analysed using anti-BCRP, anti-actin and anti-GAPDH.....278

Figure 8.5 – HepG2 and Huh7 cells treated with BNF and analysed using anti-BCRP, anti-actin and anti-GAPDH.....279

Figure 8.6 – HepG2 and Huh7 cells treated with DMSO plus BNF and analysed using anti-BCRP, anti-actin and anti-GAPDH.....280

Figure 8.7 – HepG2 and Huh7 cells treated with DMSO and analysed using anti-TF, anti-actin and anti-GAPDH.....281

Figure 8.8 – HepG2 and Huh7 cells treated with DMSO and analysed using anti-ADPGK, anti-actin and anti-GAPDH.....282

Abbreviations

A1AT	Alpha-1-antiproteinasse, antitrypsin
ABC	ATP-binding cassette
ADPGK	ADP-dependent glucokinase
AFP	Alpha-fetoprotein
AhR	Aryl hydrocarbon receptor
ARNT	AhR nuclear translocator
BAL	Bioartificial liver
BCRP	Breast cancer resistance protein
BMP	Bone morphogenic protein
BMSC	Bone marrow stem cell
BNF	Beta-naphthoflavone
BSEP	Bile salt export pump
BSP	Bromosulphophathanlin
CAR	Constitutive androstane receptor
C/EBPβ	CCAAT enhancer binding protein β
CFTR	Cystic fibrosis transmembrane conductance regulator
CHH	Cryopreserved human hepatocytes
CP	Crossing point
CSA	Cyclosporin A
CV	Coefficient of Variation
CYP	Cytochrome P-450
DDIs	Drug-drug interactions
DMEs	Drug metabolising enzymes

DMSO	Dimethyl sulfoxide
DNA	Deoxyribonucleic acid
dsDNA	Double stranded DNA
DTT	Dithiothreitol
EGF	Epidermal growth factor
EGFR	Epidermal growth factor receptor
ELAD	Extracorporeal liver device
EpCAM	Epithelial cell adhesion molecule
EST	Estrogen sulfotransferase
FGF	Fibroblast growth factor
FMO	Flavin containing mono-oxygenase
G6P	Glucose-6-phosphatase
GAPDH	Glyceraldehyde-3-phosphate dehydrogenase
gDNA	Genomic DNA
GOI	Gene of interest
GST	Glutathione-S-transferase
hATP5b	ATP synthase, H^+ transporting, mitochondrial F1 complex, beta polypeptide
HB EGF	Heparin binding EGF
hESCs	Human embryonic stem cells
HGF	Hepatocyte growth factor
HNF4a	Hepatocyte nuclear factor 4, alpha
HPC	Hepatic progenitor cell
HSC	Hepatic stellate cell
IGF1	Insulin-like growth factor 1

IL-6	Interleukin-6
ITS	Insulin-selenium-transferrin
MDR1	Multidrug resistance protein 1
miRNA	Micro RNA
MMLV	Moloney murin leukaemia virus
mRNA	Messenger RNA
MRP	Multidrug resistance associated protein
MTX	Methotrexate
NAT	N-acetyltransferase
NTCP	Na^+-taurochlorate co-transporting polypeptide
OAT	Organic anion transporter
OATP	Organic ion transporting polypeptide
OCT	Organic cation transporter
OSM	Oncostatin M
PB	Phenobarbital
PCR	Polymerase chain reaction
P-gp	P-glycoprotein
PXR	Pregnane X receptor
qPCR	Quantitative PCR
RNA	Ribonucleic acid
ROS	Reactive oxygen species
RT	Reverse transcription
SC	Stem cell
SDS	Sodium dodecyl sulphate

SLC	Solute carrier family
SNP	Single nucleotide polymorphism
SULT	Sulphotransferases
SUR	Sulfonylurea receptors
TCDD	2,3,7,8-tetrachlorodibenzo-p-dioxin (dioxin)
TEA	Tetraethylammonium
TGF	Transforming growth factor
Tm	Melting temperature
TNF	Tumour necrosis factor
TOP1	Topoisomerase 1
Tr1-3	Treatments 1-3
TTFs	Tail-tip fibroblasts
UCB	Umbilical cord blood
UCB-SC	Umbilical cord blood-derived stem cells
UGT	UDP glucuronosyltransferase
VEGF	Vascular endothelial growth factor

Chapter 1 – Introduction

1.1 – General introduction

Drugs and other xenobiotics undergo metabolism and/or elimination as part of the body's mechanism to avoid toxicity. A large number of systems and pathways combine to flush these xenobiotics from the body and the liver plays a central role in this process, utilising a variety of uptake and excretion systems as well as conducting phase I and phase II metabolism. It is often during uptake and metabolism of compounds that toxicity can occur. This is a major hurdle during development of new drugs; a compound producing an unacceptable toxic effect in the body cannot be used.

A high percentage of drug withdrawals from the market are due to toxicity issues. Lasser *et al.* (Lasser *et al.*, 2002) found that during the previous 40 years, 2.9% of drugs released on to the market were withdrawn as a result of causing severe adverse effects. With the pre-approval cost of drug development estimated to range from $800 million to $2 billion (Orloff *et al.*, 2009; DiMasi *et al.*, 2003), it is vital that toxicity and drug-drug interactions (DDIs) are identified as early as possible during testing. Any potential model must have certain features in order to be useful to the drug development industry. These include being readily available, easy to use, giving reproducible results and allowing high throughput testing. It would also be beneficial for any potential model to be human-based as differences in species metabolism of compounds does occur, which has been reviewed in several publications (Bode *et al.*, 2010; Strom *et al.*, 2010; Singh, 2006; Lin and Yamazaki, 2003; Lin, 1995). A system which will accurately predict toxicity during the early stages of testing is therefore a key area for development and would be an extremely valuable tool in industry.

Hepatocytes play a key role in the metabolism of xenobiotics so a system to predict toxicity and DDIs would ideally be focused on these cells. Specific enzymes and transporters which play important roles in uptake, transformation and efflux of xenobiotics should be present in an effective model in order to be of relevance to hepatocytes *in vivo*. These are classified as phase I and phase II drug metabolizing enzymes (DMEs) and phase III transporters and although there is a basal and/or inducible level of these proteins in most tissues, they are most abundant in metabolizing tissues such as intestine and liver. This introduction to the thesis will provide a background on the groups of transporters and enzymes and then outline the currently available hepatocyte models along with their advantages and disadvantages.

1.2 – Liver physiology

1.2.1 – Overview of liver structure and function

The liver is a key organ involved in a variety of physiological processes including synthesis, storage, distribution and metabolism of molecules such as amino acids, urea, proteins and carbohydrates. It is also a key method in the detoxification of xenobiotics introduced into the body and waste products of the body itself such as haemoglobin and insulin. The liver itself is divided into hexagonal lobules which have a hepatic artery, portal vein and bile duct at each corner; blood flow into the liver originates from both the hepatic artery, which supplies oxygenated blood from the heart, and the portal vein which carries venous blood from the intestines, spleen and pancreas. Blood exits the liver via the central vein. During transit through the liver, xenobiotics, hormones and other substances can be taken up into the hepatocytes and subjected to metabolic processes resulting in exit of the metabolites back into the blood or into the bile ducts. Various cell types in the liver allow this process to occur efficiently – parenchymal cells (hepatocytes) account for up to 65% of the liver cell population and up to 80% of the liver volume (Tanaka *et al.*, 2011; Zheng *et al.*, 2009; Gebhardt, 1992), with the remaining 20% of non-parenchymal cells consisting of lymphocytes, Kupffer cells, stellate cells, epithelial cells and oval cells. Figure 1.1 shows the structure and placement of these cell types within the liver.

As well as being the main drug-metabolising component of the liver, hepatocytes also perform functions such as glycogen storage and bile acid synthesis which are essential for normal homeostasis. Hepatocytes are highly polarised cells which form tight junctions and can be bi-nuclear. They contain many important drug-metabolising enzymes such as members of the cytochrome P450 family and transporters such as those belonging to the ATP-binding cassette (ABC) superfamily. Under-expression of metabolic enzymes can result in an accumulation of toxic substances, whereas over-expression of efflux transporters can lead to drugs being removed from the body before they can act – this can be the case where resistance to chemotherapy treatments is observed. Pro-drugs which require cleavage before they attain their active form can also be affected by altered expression levels of both enzymes and transporters.

Lining the vascular channels (sinusoids) are hepatic sinusoidal epithelial cells. These constitute approximately 50% of the non-parenchymal hepatic cell population and provide a barrier between the blood and hepatic cells which allows diffusion of substances through a fenestrated monolayer, the average pore size being 120 nm (Zheng *et al.*, 2009; Oda *et al.*, 2003). These cells play a role in the metabolism of substances such as glycoproteins,

lipoproteins, immune complexes and transferrin and the secretion of substances such as hepatocyte growth factor (HGF) and cytokines (Mohammed and Khokha, 2005; Kmiec, 2001). Biliary epithelial cells (cholangiocytes) line the bile ducts in the liver. These cells are thought to transport water, ions and solutes while also being involved in secretion of molecules involved in cell-cell signalling such as growth factors and cytokines (Tietz and Larusso, 2006; Mohammed and Khokha, 2005). The Canals of Herring separate the hepatocytes along the bile canaliculus and the cholangiocytes of the bile duct – this is thought to be where hepatic progenitor cells originate (Zheng *et al.*, 2009).

Between the hepatocytes and the hepatic sinusoidal epithelial cells is the space of Disse where hepatic stellate cells can be found. In a healthy liver, these cells are quiescent and constitute approximately 5-8% of liver cells and are responsible for controlling the contractility of the sinusoids as well as being a major storage site for retinol (vitamin A) homeostasis (Senoo *et al.*, 2010; Winau *et al.*, 2007; Mohammed and Khokha, 2005; Kmiec, 2001). In a damaged liver, for example during liver fibrosis or cirrhosis, the stellate cells emerge from their quiescent state after activation by hepatocytes, release their vitamin A stores and instead generate extracellular matrix components and secrete substances such as HGF and fibroblast growth factor (FGF) (Senoo *et al.*, 2010; Henderson and Forbes, 2008; Mohammed and Khokha, 2005). Kupffer cells can also be found in the liver within the sinusoids (Winau *et al.*, 2007). These cells are macrophages and so play an important role in clearing waste products such as old or damaged red blood cells. If the liver becomes damaged or unhealthy, these cells are activated and proceed to release agents such as cytokines which in turn promote a response in hepatocytes and aid in the process of liver regeneration (Malato *et al.*, 2008).

1.2.2 – Liver development and regeneration

Foetal liver development occurs when endoderm cells in the foregut are exposed to a number of signals prompting hepatic development. In mice this process occurs at embryonic day 8.5, while studies in several animal models have shown that this occurs after exposure to FGF from the heart and bone morphogenic protein (BMP) from the septum transversum mesenchyme (Shin *et al.*, 2007; Zhang *et al.*, 2004; Deutsch *et al.*, 2001; Rossi *et al.*, 2001; Jung *et al.*, 1999). Foetal liver development in the mouse is continued between 9 and 9.5 days when expression of liver specific genes such as alpha-fetoprotein (AFP) and albumin occurs, while in the rat this expression occurs one day later. At this stage cells are referred to as hepatoblasts and proliferate in response to a variety of growth factors such as HGF, FGF, epidermal growth factor (EGF), transforming growth factor (TGF)-β and the cytokine interleukin-6 (IL-6). Many of these factors originate from the surrounding endothelial cells which are essential for normal

liver development at this stage (Tanaka *et al.*, 2011; Kung *et al.*, 2010; Oertel and Shafritz, 2008). After hepatoblasts are formed two developmental routes are possible; hepatocytes and cholangiocytes. Exposure to oncostatin M, which is a member of the IL-6 family, has proved to be effective for the induction of the hepatoblast to hepatocyte transition and is thought to help co-ordinate liver development (Kinoshita *et al.*, 1999).

Less is known about human foetal liver development as appropriate samples are more difficult to procure and so a definition of human foetal liver as determined by expression of markers remains an area of discussion (Kung *et al.*, 2010). Although groups have claimed to use other sources of stem cells to create hepatocytes, it is unknown whether these truly represent the path or indeed the endpoint of a genuine foetal liver stem cell. Success in isolating liver progenitor cells has been achieved by selection of cells expressing the epithelial cell adhesion molecule (EpCAM) which could be directed into either cholangiocytes or hepatocytes in culture and could also be transplanted into immunodeficient mice, resulting in the presence of functioning mature human liver tissue (Schmelzer *et al.*, 2007).

The liver has a remarkable capacity to regenerate. Studies in rodents have demonstrated that removal of two thirds of the liver, leaving one third undamaged, allows for regeneration of the total liver mass in five to seven days in the rat and eight to fifteen days in humans (Michalopoulos, 2007). Using the rat model has allowed for reliable and reproducible study of the liver regeneration process. Normal regeneration does not involve stem cells; instead, the remaining hepatocytes undergo one mitotic cycle with a smaller proportion of cells undergoing a second cycle of mitosis followed by some apoptosis which is thought to reduce any over-proliferation back to the original liver mass (Sakamoto *et al.*, 1999; Stocker *et al.*, 1973; Stocker and Heine, 1971). This hepatic proliferation in the rat peaks at 24 hours after partial hepatectomy, whereas proliferation of other cell types occurs later than that of hepatocytes; endothelial cell proliferation occurs from two to five days after partial hepatectomy while that of stellate cells is not yet fully understood (Michalopoulos, 2007). Although normal liver mass has been attained at the end of this period, the architecture is not identical to that of the original liver; the individual liver lobules are much larger and fewer in number and the normal single cell thickness of the hepatocytes is lost in some places (Michalopoulos and DeFrances, 1997). Liver re-organisation then takes place over several weeks, eventually becoming identical to the original liver structure (Wagenaar *et al.*, 1993).

1.2.3 – Signalling in liver regeneration

Clearly the understanding of this process of tightly controlled hepatocyte proliferation would be extremely useful if it could be applied *in vitro*, where isolated primary hepatocytes have a

limited lifespan. Investigations into the processes governing proliferation have been undertaken, in particular using the model of partial hepatectomy in rats as outlined earlier. HGF plays a key role in promoting hepatocyte proliferation – plasma levels of HGF are known to increase up to 20-fold after partial hepatectomy (Lindroos *et al.*, 1991) and the HGF receptor, cMET, is activated within 30-60 minutes of the procedure (Monga *et al.*, 2002). Experiments looking into the effects of siRNA to block cMET expression resulted in stalling of the cell cycle until the siRNA effect was active, indicating a key role for HGF signalling in liver regeneration (Michalopoulos, 2010; Paranjpe *et al.*, 2007). The production of HGF affecting hepatic proliferation by non-parenchymal cells has been observed, predominantly by stellate cells but also by sinusoidal epithelial cells (LeCouter *et al.*, 2003; Schirmacher *et al.*, 1993). Although HGF production is not the first signal observed to occur in hepatic regeneration, it is thought to be key in initiating this cascade of events and is generally considered to be one of the most important, irreplaceable steps in the process (Michalopoulos, 2007).

Although HGF is a key factor it is only one of a multitude of signalling mechanisms involved in heptic regeneration. Ligands of the epidermal growth factor receptor (EGFR) such as EGF itself, TGF-α, heparin binding EGF (HB EGF) and amphiregulin have had their importance proven in terms of liver regeneration. The EGFR is phosphorylated within an hour of partial hepatectomy; however, the ability of the liver to regenerate in the absence of this receptor by suppression or targeted elimination has not been investigated (Michalopoulos, 2007). EGF is consistently available via the portal vein of the liver and changes in expression levels have not been directly studied during regeneration, although catecholamines such as epinephrine are known to stimulate EGF production and are raised after partial hepatectomy (Michalopoulos, 2007; Bucher *et al.*, 1977). It has been shown that TGFα is raised from two hours after partial hepatectomy and remains highly expressed for over 48 hours (Mead and Fausto, 1989). TGFα is produced by the hepatocyte itself, indicating that an autocrine loop may be involved. It has also been shown that although overexpression of TGFα promotes liver enlargement in mice, a knockout of the gene does not affect regeneration (Webber *et al.*, 1994). Other cell types affected by TGFα include the sinusoidal epithelial cells and the biliary epithelium (Michalopoulos, 2007). HB EGF increases within 90 minutes of partial hepatectomy, originating from both endothelial and Kupffer cells (Kiso *et al.*, 1995). HB EGF knockout mouse models have a reduced capacity for regeneration, whereas overproduction leads to enhanced regeneration (Mitchell *et al.*, 2005; Kiso *et al.*, 1995). Reduced expression of the final EGFR ligand studied, amphiregulin, has also been shown to result in less efficient regeneration of the liver in mouse models (Berasain *et al.*, 2005).

Other compounds such as tumour necrosis factor (TNF), IL-6, epinephrine, norepinephrine and bile acids are thought to be important in properly functioning homeostasis and regeneration without having a leading role in regeneration itself. TNF itself does not result in mitosis if applied to primary hepatocytes in culture; however, it does enhance the response to HGF and TGFα (Pierce *et al.*, 2000; Webber *et al.*, 1998). Plasma levels of TNF do increase after partial hepatectomy with the source thought to be Kupffer cells (Michalopoulos, 2007). IL-6 itself does not initiate hepatic mitosis nor does it enhance the effects of mitotic activators such as HGF, however, it is known to affect biliary cell proliferation (Liu *et al.*, 1998). Epinephrine and norepinephrine both increase in plasma concentration after partial hepatectomy and enhance the proliferative effects of both HGF and EGF (Cruise *et al.*, 1985), while depletion of bile acids in the blood after partial hepatectomy results in decreased regeneration (Huang *et al.*, 2006).

1.2.4 – Progenitor cells in the liver

True stem cells are ones which have the capacity to proliferate indefinitely and can differentiate into a number of defined lineages. Although stem cells are clearly involved during initial foetal liver development, this is not the case in adult liver. Regeneration, as discussed previously, involves proliferation of the remaining hepatocytes. However, if the liver is too damaged to regenerate using the normal methods observed after partial hepatectomy, another cell type can contribute to the process of rebuilding. These cells reside in the Canals of Herring (see figure 1.1) and are known as hepatic progenitor cells (HPCs) or oval cells. HPCs are not true stem cells in that they do not have the capacity to generate any cell lineage but they are capable of differentiating into both hepatocytes and cholangiocytes.

In order for HPCs to become activated there must be injury to the liver above that which can be healed by the normal process of regeneration, such as continuous damage of the mature epithelial cells, inhibited replication of the hepatocytes or where there has been severe loss over that seen in partial hepatectomy, where roughly one third of the liver remains. Activation of HPCs has been shown to require loss of at least 50% of the hepatocyte mass along with severely inhibited replication capacity; significant activation of HPCs has also been observed in the majority of advanced chronic liver diseases (Bird *et al.*, 2008; Katoonizadeh *et al.*, 2006; Libbrecht and Roskams, 2002). In these scenarios the HPCs begin to expand into either intermediate hepatocytes, which mature into true hepatocytes, or into immature cholangiocytes, after which differentiation into mature cholangiocytes takes place (Gaudio *et al.*, 2009). HPC proliferation occurs within one week of extensive liver damage, with differentiation into mature hepatocytes occurring two weeks post-injury (Gaudio *et al.*, 2009).

As with hepatic regeneration, HPC activation requires specific signalling. Hepatic stellate cells (HSCs) are known to interact with HPCs as they release growth factors pertinent to HPC activation such as TGFα, HGF and acidic fibroblast growth factor (Kuwahara *et al.*, 2008; Sanchez-Munoz *et al.*, 2007; Santoni-Rugiu *et al.*, 2005). The pattern of activation is not as clearly understood as that for hepatic regeneration; although it is known that HSC activation occurs alongside that of HPCs, it is unknown which occurs first, or indeed whether a common factor activates both followed by HSCs affecting HPCs (Svegliati-Baroni *et al.*, 2008). Compounds known to affect proliferation of HPCs include steroid hormones, growth factors (insulin-like growth factor (IGF1) and vascular endothelial growth factor (VEGF)), bile acids and neurotransmitters, although at the present time more is known about compounds affecting differentiation towards the cholangiocyte rather than the hepatocyte lineage (Tanaka *et al.*, 2011; Gaudio *et al.*, 2009; Glaser *et al.*, 2009; Oertel and Shafritz, 2008; Alvaro *et al.*, 2002a; Alvaro *et al.*, 2002b).

1.3 – Key enzymes and transporters in hepatocytes

1.3.1 – Uptake transporters

In order for drug metabolism and elimination to occur within a hepatocyte, the compounds must first be taken into the cell. Although it is possible for this to occur via diffusion across the lipid membrane, the majority of compounds enter the cell via transporters. An overview of some influx transporters and their expression and function in the body can be found in table 1.1. Major uptake transporters in hepatocytes include the organic anion transporters (OATs), the organic cation transporters (OCTs/OCTNs) and the organic anion transporting polypeptides (OATPs). Clearly, for xenobiotics to be able to enter efficiently, physiological levels of functional influx transporters would be required in any hepatic model.

Members of the solute carrier family (SLC) in the basolateral membrane of the hepatocyte play a major role in transporting organic anions and cations both into the hepatocyte from the blood and from the hepatocyte to the blood. Different classes of transporter provide sodium dependent and independent uptake of compounds into the cell. Sodium dependent uptake is carried out via the Na^+-taurocholate co-transporting polypeptide (NTCP), which is expressed solely in the liver and transports conjugated bile salts from the blood into the hepatocyte (Schroeder *et al.*, 1998; Boyer *et al.*, 1994).

Sodium independent transport of organic anions is conducted by organic anion transporting polypeptides (OATPs) and organic anion transporters (OATs), while transport of organic cations is carried out by organic cation transporters (OCTs). The OATP transporter family has five

members expressed in the liver, with OATPB, OATPC and OATP8 being the predominant isoforms expressed in liver (Konig *et al.*, 2000a; Konig *et al.*, 2000b; Tamai *et al.*, 2000). Protein levels of OATP8 and C are known to be reduced in hepatocellular carcinoma (Oswald *et al.*, 2001). Substrate specificity of the OATP family members is known to overlap and cover a broad spectrum of compounds such as bile acids and thyroxine (OATPC and 8), bilirubin and rifampicin (OATPC), benzylpenicillin (OATPB), monoglucuronosyl bilirubin and digoxin (OATP8) (Hagenbuch and Meier, 2004; Cui *et al.*, 2001; Kullak-Ublick *et al.*, 2001; Tamai *et al.*, 2000).

Five family members belonging to OAT have been described, with three, OAT2, OAT4 and OAT5, expressed in the liver (Anzai *et al.*, 2006; Sun *et al.*, 2001; Sekine *et al.*, 1998). The OAT transporters are located at the basolateral membrane of the hepatocyte and have overlapping substrate specificities, transporting organic anions between the hepatocyte and the blood. OAT2 transports compounds such as indomethacin; both OAT2 and OAT4 transport tetracycline and prostaglandin, while OAT4 alone transports methotrexate and ketoprofen (Koepsell and Endou, 2004; Enomoto *et al.*, 2002; Takeda *et al.*, 2002a; Sekine *et al.*, 2000). OAT5 is known to transport NSAIDS and penicillin (Koepsell and Endou, 2004).

Organic cations are transported by the OCT family which has three family members. Of these, OCT1 and OCT3 are expressed in the liver while OCT2 is expressed primarily in the kidney (Koepsell *et al.*, 2003; Zhang *et al.*, 1997). Human OCT1 is located on the sinusoidal membrane of the hepatocyte and is predominantly expressed in the liver. Substrates include N-methylquinine, N-methylquinidine, tetraethylammonium (TEA), desipramine and prostaglandins E_2 and $F_{2\alpha}$ (Molderings *et al.*, 2003; Kimura *et al.*, 2002; Takeda *et al.*, 2002b; Zhang *et al.*, 1999). OCT3 is also located at the sinusoidal membrane of the hepatocyte and is expressed in skeletal muscle, placenta, kidney and heart as well as in the liver (Koepsell *et al.*, 2003). OCT3 does have some substrate overlap with OCT1; for example, both transport TEA, while OCT3 alone transports substance such as dopamine, noradrenaline and histamine (Kekuda *et al.*, 1998; Wu *et al.*, 1998).

1.3.2 – Phase I drug metabolising enzymes

After uptake of substances into the hepatocyte drug metabolism can take place in two stages, the first of which is phase I drug metabolism. Phase I metabolising enzymes are largely located in the endoplasmic reticulum, while phase II enzymes are often cytosolic, a notable exception being the UDP glucuronosyltransferase (UGT) family which is located in the endoplasmic reticulum alongside many phase I enzymes. Metabolism alters the initial compound to produce either a new functional group or modifies an existing functional group to make it more accessible to phase II enzymes. This first stage of metabolism generally contributes to making

the compound more polar by oxidation, reduction, hydrolysis or hydration; however, this alone may not be sufficient to enable excretion from the cell. If this is the case, the compound passes on to phase II metabolism. Typical phase I drug metabolising enzymes include the cytochrome P450 (CYP) superfamily of enzymes and the flavin containing mono-oxygenases (FMOs).

Human genome sequencing of the CYP superfamily has revealed a total of 107 genes, with 48 of these being pseudogenes. This leaves a total of 59 active CYP genes divided into 18 families, although not all of these contribute to hepatic metabolism of xenobiotics. An overview of the CYP superfamily can be seen in table 1.2, with more information on expression and substrates of selected enzymes in table 1.3. Briefly, CYP families 5 to 51 are known to have mainly endogenous substrates and remain highly conserved during evolution (Bozina *et al.*, 2009). CYP families 1 to 3 are less well conserved through evolution and also have a much broader substrate range; these are more involved in the metabolism of xenobiotics, while CYP4 enzymes metabolise fatty acids along with some xenobiotics (Bozina *et al.*, 2009). Enzymes important in metabolism of xenobiotics are CYP2C9, -2C19, -2D6 and -3A4, while chemical biotransformation and activation of pre-carcinogens are carried out mainly by CYP1A2, -1B1, -2A6, -2E1, and -3A4 (Bozina *et al.*, 2009; Lewis *et al.*, 1998). One CYP enzyme in particular, CYP3A4, can comprise up to 60% of all hepatic CYP content and is responsible for full or partial metabolism of up to 50% of all therapeutic drugs, while CYP2C8/9/18, CYP1A2 and CYP2E1 comprise 20%, 15% and 10% of expression respectively (Guengerich, 1999; Shimada *et al.*, 1994). All CYP enzymes, CYP3A4 in particular, are known to show a large degree of inter-individual variation in activity which can be caused by both variations in expression levels and polymorphisms (Bozina *et al.*, 2009).

While the FMO enzymes may not be as well-known as the CYP superfamily for their involvement in drug metabolism, they do play an important role. There are five genes and six pseudogenes currently identified in this family; the five functional genes share 55-60% amino acid homology (Zhou and Shephard, 2006). Of the five genes (FMO1-5), FMO1 is predominantly expressed in foetal liver with FMO3 as the main isoform expressed in adult liver (Hines, 2006; Zhou and Shephard, 2006). FMO3 is known to have expression levels in adult liver similar to those of the most abundant CYP enzymes and metabolises xenobiotics such as cimetidine, ranitidine and tamoxifen, agricultural compounds such as organophosphates and carbamates as well as dietary compounds such as trimethylamine (Bain *et al.*, 2005; Chung *et al.*, 2000; Hodgson *et al.*, 2000; Ziegler-Skylakakis *et al.*, 1998; Hodgson *et al.*, 1995; Al-Waiz *et al.*, 1987). The metabolism of trimethylamine is particularly pertinent as mutations in FMO3

can result in the failure of oxidation of the compound, causing the disease trimethylaminurea, more commonly known as “fish-odour” syndrome (Zhou and Shephard, 2006).

1.3.3 – Phase II drug metabolising enzymes

Phase II drug metabolism is based around the premise of a polar group being present on a molecule inside the cell. This can either be present on the compound initially or it can have been introduced via phase I metabolism. Generally phase II metabolism creates a more polar compound by conjugation with a hydrophilic molecule, enabling excretion from the cell either via biliary or renal routes. This mechanism is also helpful in reducing toxicity in the cell, as products are generally less toxic than the initial compounds or the products of phase I metabolism. Typical examples of phase II drug metabolising enzymes are UDP-glucuronosyltransferases (UGTs), sulphotransferases (SULTs) and glutathione-S-transferases (GSTs). The conjugation reactions carried out by these enzymes, such as glucuronidation and sulphonation, result in a compound which is much more easily excreted from the cell and thus eliminated from the body. These phase II DMEs are important to a hepatocyte model, especially if it is being used for toxicity or elimination investigations. An overview of some of the enzymes involved in phase II metabolism is given in tables 1.4 and 1.5.

The UGT superfamily of enzymes catalyses the conjugation of alpha-D-glucuronic acid to a wide range of both xenobiotics and endogenous compounds, allowing subsequent excretion from the cell (Tukey and Strassburg, 2000). There are two UGT families, UGT1 and UGT2, with a total of 19 isoforms between them; of these, 10 are expressed in adult human liver (Bock, 2010; Tukey and Strassburg, 2000). Although liver levels of UGT2B4 and -2B10 are particularly high, these are mainly involved in maintenance of homeostasis by metabolism of eicosaniods and bile acids (Bock, 2010). The UGT1A1 enzyme is known to be responsible for metabolism of a wide range of xenobiotics, including paracetamol, irinotecan and its toxic metabolite SN38, as well as being the only mechanism for metabolism of the heme metabolite bilirubin (Tukey and Strassburg, 2000). This is particularly important as bilirubin accumulation is toxic; lack of functional UGT1A1 results in Crigler-Najjar syndrome which is fatal if untreated, although treatment of the disease is difficult and a limited lifespan of 30 years is expected, with brain damage caused by persistent jaundice (Bock, 2010). UGT2B7 is also an important drug-metabolising enzyme with a wide range of substrates including morphine, as well as endogenous substrates like retinoids, eicosanoids and bile acids (Burchell *et al.*, 2005; Court, 2005; Little *et al.*, 2004; Samokyszyn *et al.*, 2000; Wietholtz *et al.*, 1996). Other UGT enzymes such as UGT1A4, -1A6, -2B4, 2B10 and -2B15 also have a role in drug metabolism, although the

range of substrates in these proteins is thought to be smaller (Bock, 2010; Tukey and Strassburg, 2000).

The SULT family of enzymes includes four gene families, SULT1, -2, -4 and -6. As a family, sulfotranseferases are responsible for the sulphate conjugation of a wide range of xenobiotics, neurotransmitters and hormones and are thought to be the major detoxification method used in the foetal liver, where SULT expression is high and UGT expression low (Strassburg *et al.*, 2002). SULT1A1 is expressed in the liver and catalyses the conjugation of sulphate to many phenolic compounds, with substrates such as phenol, p-nitrophenol, estradiol, minoxidil and tamoxifen (Jancova *et al.*, 2010; Adjei *et al.*, 2008; Hines, 2008). SULT1A2 is an example of an enzyme which can increase toxicity through metabolism rather than decreasing it; the conjugation of sulphates to some aromatic hydroxylamines results in compounds which are considerably more reactive and mutagenic than the original compound (Meinl *et al.*, 2002). SULT1B1 is expressed in the liver and GI tract and has a fairly narrow substrate specificity, conjugating substrates such as thyroid hormones and small phenols (Jancova *et al.*, 2010). SULT1E1 is expressed in the liver and jejunum and was also known as estrogen sulfotransferase (EST) due to its high affinity for estrogen sulfation; this enzyme is also known to have some metabolic activity for compounds such as 1-naphtol and genistein (Gamage *et al.*, 2006; Falany *et al.*, 1995). Of the SULT family members, SULT2A1 is the most highly expressed in the liver as well as being expressed in the adrenal glands and duodenum (Jancova *et al.*, 2010). This enzyme increases in expression from foetal to adult liver unlike SULT1E1 which is more highly expressed in foetal liver tissue (Hines, 2008). SULT2A1 was also known by an alternative name, dehydroepiandrosterone-sulfotransferase (DHEA ST) as it is known to conjugate hydroxysteroids such as DHEA as well as bile acids and androgens (Comer *et al.*, 1993).

Glutathione conjugation is catalysed by the GST family of transporters which are of high importance in protecting the cells from reactive oxygen species (ROS) produced through normal cellular processes such as phase I drug metabolism by CYP enzymes (Jancova *et al.*, 2010; Sheehan *et al.*, 2001). Two GST superfamiles have been identified, one of soluble enzymes and the other of membrane bound proteins designated MAPEGs (Jancova *et al.*, 2010). GSTs are divided into five groups, GSTA, GSTM, GSTP, GSTK and GSTT – these families have up to 30% sequence homology between classes and over 60% within a class (Jancova *et al.*, 2010). GSTs are expressed in the brain, pancreas, liver, kidney, testis, heart, lung, intestine, skeletal muscle and spleen (Hayes and Strange, 2000) and are known to metabolise a wide range of compounds such as quinones, peroxides, ozonides, esters and sulfoxides (Jancova *et al.*, 2010). Over-expression of GST enzymes can result in resistance to certain drugs; for

example, many anticancer and antiasthmatic treatments are metabolised by a member of the GST family (Hayes and Pulford, 1995). GSTA1, -A2, -A3 and -A4 are expressed in a variety of tissues including liver, whereas in liver GSTA5 is undetectable (Lo and Ali-Osman, 2007; Desmots *et al.*, 2001). GSTA1 is expressed in liver and kidney and catalyses the conjugation of many anti-cancer drugs such as chloroambucil, doxorubicin, melphalan and busulfan (Lo and Ali-Osman, 2007; Kusama *et al.*, 2006; Tew, 1994; Ciaccio *et al.*, 1991). GSTA2 is expressed in liver, kidney, lung, prostate and pancreas and metabolises substrates such as chloroambucil, chloroquine, ceramide and busulfan (Lo and Ali-Osman, 2007; Hayes *et al.*, 2005). GSTA3 plays a role in the production of the steroid hormones testosterone and progesterone as well as contributing to the conjugation of glutathione to both endogenous and exogenous compounds (Lo and Ali-Osman, 2007; Hayes *et al.*, 2005). GSTA3 is expressed in the lung, liver, kidney, pancreas and prostate (Lo and Ali-Osman, 2007; Hayes *et al.*, 2005). GSTA4 is expressed at low levels in a wide range of tissues including the liver and expression has been shown to increase with liver injury such as cirrhosis (Desmots *et al.*, 2001).

The N-acetyltransferase (NAT) family of enzymes includes two isoforms, NAT1 and NAT2, which catalyze the activation and detoxification of amines (Hein *et al.*, 2000). NAT1 expression has been determined to be ubiquitous whereas NAT2 expression is localised to the liver, colon and intestine (Jancova *et al.*, 2010). Despite having 85% sequence homology, NAT1 and 2 have different substrate specificities with NAT2 in particular being an important metabolic route for some drugs including sulphonamides and isoniazid (Kawamura *et al.*, 2005).

1.3.4 – Phase III drug transporters

After compounds have been taken up into the cell from the blood they are effluxed into either bile or blood for excretion from the system. This can be done immediately after uptake or after phase I or II metabolism by enzymes. Major transporters involved in this process are mainly from the ATP-binding cassette superfamily (ABC superfamily), which hydrolyse ATP in order to facilitate transport. These include P-glycoprotein (alternatively known as ABCB1 and multidrug resistance protein 1 (MDR1)), the ABCC family (multidrug resistance-associated proteins (MRP proteins)) and ABCG2 (also known as breast cancer resistance protein (BCRP)). P-gp and MRP proteins have an extremely broad range of substrates including amino acids, sugars, lipids, xenobiotics and many drugs (Dean *et al.*, 2001). As a result, a lot of these transporters have overlapping substrate specificities. It is also common for one or more of these proteins to be over-expressed in drug-resistant carcinoma cells, which can result in drugs being effluxed too quickly from the cell to have the desired effect. These transporters are vital to a hepatocyte model but must be present in the correct quantities – an over-expressed transporter could just

as easily give erroneous results as an under-expressed one. An overview of expression and substrate specificity of some transporters in this group is shown in table 1.6.

P-gp is one of the most well-known drug efflux transporters in the cell as a result of its role in conferring multidrug resistance in multiple cell types (Gerlach *et al.*, 1986a; Gerlach *et al.*, 1986b). It is located on the canalicular membrane and transports a wide range of substances such as steroid hormones, digoxin, verapamil and cyclosporine A from the cell into the bile (Leslie *et al.*, 2005). Over-expression of this transporter is particularly prevalent in chemotherapy-resistant cancer cells, making any potential inhibitor of this transporter particularly interesting in terms of medical use. However, potential drug-drug interactions must also be considered under normal physiological conditions as with such a broad range of substrates accumulation could easily result due to lack of available transporters. The only family member of P-gp, MDR3, is known to be a phospholipid transporter rather than a broad substrate one and is not thought to have a significant role in drug transport or to confer multidrug resistance (Smit *et al.*, 1993). The bile salt export pump (BSEP) is predominantly expressed in liver and does have a role in drug transport. It is known to aid in the disposition of drugs such as vinblastine, but its major role is to efflux bile salts from the hepatocyte (Childs *et al.*, 1998).

BCRP (ABCG2) is a fairly new addition to the ABC superfamily which was discovered in 1998, and is located on the canalicular membrane of the hepatocyte (Doyle *et al.*, 1998). This transporter is known to confer multi-drug resistance but to a lesser extent then either P-gp or the MRPs 1 and 2. Although substrates of these four proteins do overlap, BCRP has a narrower range and includes substances such as anthracyclines, mitoxantrone and topoisomerase I inhibitors (Allen and Schinkel, 2002; Allen *et al.*, 2002).

The human ABCC family includes nine MRPs, the cystic fibrosis transmembrane conductance regulator (CFTR) plus two sulfonylurea receptors (SUR1 and SUR2A/B). MRP1 is not expressed at detectable levels in a healthy human liver but is present at the basolateral membrane in the kidney, lung, muscle, testis and placenta. However, this expression pattern can change dramatically in a liver carcinoma where increased MRP1 protein levels can confer multidrug resistance to a cell. MRP1 was the second protein discovered to confer multidrug resistance when over-expressed after P-gp (Cole *et al.*, 1992). Typical substrates of MRP1 include leukotrines, verapamil, vincristine, folate and oxidised glutathione (Loe *et al.*, 2000; Keppler *et al.*, 1998; Jedlitschky *et al.*, 1997; Jedlitschky *et al.*, 1996; Loe *et al.*, 1996; Leier *et al.*, 1994).

MRP2 is expressed in several tissues including liver, kidney, small intestine, colon and placenta (Keppler, 2011). Expression of this protein is localised to the apical (canalicular) membrane and

the substrate spectrum is quite similar to that of MRP1, although differing kinetic properties have been observed (Cui *et al.*, 1999). MRP2 is responsible for the secretion of a wide range of conjugated xenobiotics and endogenous substances such as leukotrines, conjugated bilirubin and estradiol (Cui *et al.*, 1999; Kamisako *et al.*, 1999).

MRP3, 4 and 6 are also known to be expressed at the basolateral membrane of the hepatocyte. All three transporters are also expressed in the kidney, while MRP3 also shows expression in the cholangiocytes, gallbladder, pancreas, GI tract and spleen (Keppler, 2011). MRP4 is expressed in the prostate, blood-brain barrier and the epithelial cells of the pancreatic duct (Keppler, 2011). Less is known about MRP6 expression and action, although leukotrines are known to be substrates (Ilias *et al.*, 2002). MRP3 substrates include leukotrines, conjugated bilirubin and estradiol, while MRP4 has a longer list of known substrates, including cGMP, cAMP, leukotrines, prostaglandins, thromboxane, cholate, folate and ADP (Rius *et al.*, 2008; Rius *et al.*, 2005; Jedlitschky *et al.*, 2004; Lee *et al.*, 2004b; Rius *et al.*, 2003; Chen *et al.*, 2001; Zeng *et al.*, 2000).

1.4 – Model systems for hepatic transport and metabolism

1.4.1 – Enzyme only systems

These allow enzyme-specific actions on a compound to be seen which can make it easier to identify metabolites and the metabolic pathway for a particular substance. There are several different enzyme preparations which are used for this purpose: S9 liver fractions, liver microsomes and recombinant CYPs e.g. Supersomes™.

1.4.1.1 – Liver fractions

S9 human liver fractions consist of both microsomal and cytosolic fractions from cells. Most phase I enzymes are found in the microsome, while phase II enzymes are often found in the cytosol. This S9 fraction therefore contains most of the enzymes which would combine to form the metabolic profile of a compound. However, a lot of the co-factors they require to function properly will not be there as they are found outside of the cell environment. This can affect any results obtained via this system. Another drawback of there being no whole cells in this model is that there is no guarantee that a compound would ever come into contact with any of the enzymes represented here. It is entirely possible that a new compound could fail to enter the cell, or be effluxed so quickly that very little metabolism occurs, and these interactions would not be seen in this model.

1.4.1.2 – Liver microsomes

Microsomes are obtained by differential centrifugation (Raucy and Lasker, 1991) and only contain enzymes located in the endoplasmic reticulum (CYPs, UGTs and FMOs). Clearly this does not represent the full metabolic complement found in a whole cell, and so all the possible metabolites of a compound cannot be reliably detected using this model. However there are advantages to using this model as human liver microsomes are widely available from commercial sources at relatively low cost. There is also the option of choosing the origin of the microsomes; for example they can be a mixed sample from several donors to eliminate inter-individual variation or specifically chosen to have a certain profile, allowing examination of ethnicity, age or sex-specific responses to a compound. However, this system cannot be used to definitively determine the outcome of a compounds metabolism as cytosolic enzymes are not included in the fraction.

1.4.1.3 – Supersomes™

Supersomes are derived from yeast or insect cells which have been engineered to express a single human drug metabolising enzyme (DME), allowing cellular fractions containing a specific DME for testing a drug's metabolic pathway to be obtained (Asseffa *et al.*, 1989). As the endogenous yeast/insect DMEs are very different from human ones it is effectively a system to see how a single human DMEs interacts with a compound. This has a benefit over microsomes as any co-factors that the DME needs to function correctly can also be engineered into the cell, allowing the true interaction between enzyme and compound to be observed. As with microsomes, only enzymes found in the endoplasmic reticulum can be studied with this system, and of course any contribution to metabolism by other DMEs is excluded from these studies. The major use of Supersomes™ is therefore to support findings from other systems with regard to the role of a single DME.

1.4.2 – Liver slices

Liver slices were first used in the early 20th century but were not used for metabolic studies until the 1970s when advances in technology meant that slices of a consistent thickness with little damage from harvesting were able to be produced (as reviewed in Vermeir (Vermeir *et al.*, 2005)). A major advantage is that the cell architecture, cell-cell contacts and metabolic co-operation between cell types are preserved as they appear *in vivo*. These are particularly useful when looking at the route of metabolism of a compound as additional information can be gained over what would be observed in, for example, a hepatocyte-only system. As is also the case for most isolated whole cell systems, enzyme levels in liver slices quickly decrease following isolation and preparation. It has been observed that the activity of some CYPs drop

by ≥64% after just 24 hours and are undetectable after 96 hours (VandenBranden *et al.*, 1998). Olinga *et al.* (Olinga *et al.*, 2008) successfully demonstrated expression and induction of phase I and II metabolising enzymes plus phase III transporters after both 5 and 24 hours incubation with typical inducers in liver slices, including that of several CYP enzymes. Some studies have looked at methods of maintaining slices in culture to minimise loss of activity; for example, Martin *et al.* (Martin *et al.*, 2002) showed that incubation in a rotating culture system with a 70% oxygen concentration improved both structure and expression in comparison to slices incubated with 20% oxygen. However, studies with liver slices are still restricted by their sustainability in culture, with estimates that they remain viable for three to four days in optimal conditions (Van de Bovenkamp *et al.*, 2007). Difficulties in obtaining fresh liver slices are comparable to those concerning isolation of primary hepatocytes, resulting in the model being low throughput and not readily available.

1.4.3 – Hepatocytes

As the majority of drugs and xenobiotic compounds are metabolised in the liver, specifically in hepatocytes, an ideal model would be a hepatocyte itself. Although there are many such models in existence none are perfect. The following section looks at the range of hepatocyte systems available and their various advantages and disadvantages.

1.4.3.1 – Primary hepatocytes

Primary hepatocytes are isolated from liver tissue, cultured and used for metabolic studies. These are currently considered to be the most appropriate model for investigating drug metabolism as they initially retain a large proportion of the DMEs and transporters that are involved. The cell structure is maintained so transport into and out of the hepatocytes can also be taken into account and any co-factors required for proper enzyme function should be present. The use of primary hepatocytes for drug metabolism, induction and interaction studies is well known and has been reviewed in several publications (Hewitt *et al.*, 2007; Soars *et al.*, 2007a; Soars *et al.*, 2007b; Vermeir *et al.*, 2005; Gomez-Lechon *et al.*, 2004; Gomez-Lechon *et al.*, 2003a; Gomez-Lechon *et al.*, 2003b).

Although primary hepatocytes are considered to be the closest *in vitro* model to the *in vivo* liver, they do have many features which restrict their use. Supply is a major issue; tissue from human liver cannot be easily sourced on a regular basis and there are legal and ethical issues tied to their use (Skett *et al.*, 1995). Inter-individual variability is also a factor; this can be overcome to an extent by pooling donor hepatocytes, and can prove useful if variations such as age or sex are factors which need to be considered (Parkinson *et al.*, 2004).

The metabolic profile of primary hepatocytes can change within 7 days of culture due to de-differentiation. This is especially true for some of the CYP enzymes and limits the usefulness of primary hepatocytes after this period, as CYP activity accounts for a large proportion of drug metabolism within the cell (Gomez-Lechon *et al.*, 2004; Parkinson *et al.*, 2004; Gomez-Lechon *et al.*, 2003a; Gomez-Lechon *et al.*, 2003b). Attempts at altering culture conditions in order to preserve the metabolic profile have met with varying amounts of success. A common addition to culturing conditions is to overlay an extracellular matrix of matrigel or collagen I and create a sandwich culture; this has been reported to preserve the metabolic profile of a hepatocyte more effectively than standard culture and to potentially restore de-differentiated cells to a more mature phenotype (Gkretsi *et al.*, 2007; Olsavsky *et al.*, 2007; Page *et al.*, 2007; Sidhu *et al.*, 2004). This was measured by features such as increased albumin production, enhanced connexin-32 expression (a gap junction marker), increased CYP levels and improved responses to typical inducers such as phenobarbital (Gkretsi *et al.*, 2007; Olsavsky *et al.*, 2007; Page *et al.*, 2007; Sidhu *et al.*, 2004). Improved results from co-culture with epithelial, stellate and Kupffer cells, which mimic the role played by non-parenchymal cells in the *in vivo* liver, have also been reported and showed improvements in the longevity and functional expression of hepatocytes (as reviewed in Dash *et al.* (Dash *et al.*, 2009)). For example, primary hepatocytes cultured alongside hepatic stellate cells have been shown to retain CYP and albumin expression after two months of culture (Riccalton-Banks *et al.*, 2003). This could be as a result of growth factors such as hepatocyte growth factor (HGF) secreted by stellate cells having a positive impact on the hepatocytes.

1.4.3.2 – Cryopreserved human hepatocytes

Ideally primary hepatocytes would be used routinely in drug development, but as discussed above, de-differentiation in culture and unpredictable availability means this is not possible using fresh hepatocytes. Attempts to increase the usefulness of these cells have looked at cryopreservation as a means of improving availability and consistency. Initially, yields upon resuscitation were very low but the advent of better cryopreservation techniques (Lloyd *et al.*, 2003) has led to several recent studies on the potential uses of cryopreserved human hepatocytes (CHHs) in drug metabolism and induction assays. Roymans *et al.* (Roymans *et al.*, 2005) examined levels of CYP activity and found that the induction response was of the same magnitude as is seen in fresh primary hepatocytes, although for some enzymes basal activity was lower. However, cryopreservation does not yet yield the readily available source of healthy hepatocytes that is desired and results in changes in both cell structure and function, as reviewed by Stephenne *et al.* (Stephenne *et al.*, 2010). Li *et al.* (Li, 2007) reviewed cryopreserved hepatocytes as a model in comparison to primary hepatocytes and observed

that although levels of important enzymes and transporters are similar initially, limitations of the model include having to culture in suspension for the majority of cryopreserved lots. This not only limits the type of experiment which can be performed, but expression deteriorates very quickly and cells last hours rather than days. This review also reports that when using cells which can be successfully plated, the useful lifespan is approximately three days, with reductions in CYP1A2 and 3A4 expression of approximately 50% every 24 hours. Although cryopreserved hepatocytes are certainly more readily available than freshly isolated ones, the associated limitations of the model mean that fresh primary hepatocytes remain more true to the *in vivo* hepatic state. CHHs may not provide the definitive metabolic data that can be obtained with primary hepatocytes but are still useful for applications such as ranking test compounds in order of toxicity where a comparative rather than an absolute measure is required.

1.4.3.3 – Immortalised hepatocytes

Another technique to try and overcome de-differentiation of human hepatocytes is to artificially immortalise the cells. This can be done by transfection with SV40 large T-antigen, which inactivates tumour suppressor genes such as p53 and results in a senescent state where replication is no longer limited to a few population doublings (Pfeifer *et al.*, 1993). Immortalised human hepatocytes are useful in that they proliferate indefinitely and the sample variation seen with fresh hepatocytes is eliminated. These two features could allow immortalised hepatocytes to be used in industry as a high-throughput screening model for drug development. However, these cell lines do not always express the full metabolic profile of the *in vivo* liver so thorough investigation of expression is needed at several points to ensure that expression is maintained during cell expansion. Two notable lines of immortalised hepatocytes are Fa2N-4 and HC-04, which are looked at in more detail in the following paragraphs.

The Fa2N-4 cell line was generated by transfection of human hepatocytes with SV40 large T-antigen (Mills *et al.*, 2004). Expression and induction of proteins in these cells has been investigated with varied results. As stated previously, CYP1A2 and -3A4 account for a large proportion of drug metabolism in the body. The mRNA of both of these enzymes was found to be inducible to a similar extent as in primary human hepatocytes (Mills *et al.*, 2004). This paper also showed that CYP2C9 and MDR1 were induced by prototypical inducing agents (e.g. rifampicin, phenobarbital) with a similar level of response to primary hepatocytes. These initial characterisations were built upon by Ripp *et al.* (Ripp *et al.*, 2006) who examined the effects of known inducers and non-inducers of CYPs in primary hepatocytes and Fa2N-4 cells. The results suggested that Fa2N-4 cells have a very similar response to that of primary hepatocytes when

looking at CYP3A4 induction. Hariparsad *et al.* (Hariparsad *et al.*, 2008) looked at basal mRNA levels of genes involved in drug metabolism and at CYP3A4 induction in Fa2N-4 in comparison to CHHs. It was observed that the basal level of constitutive androstane receptor (CAR) was a lot lower in Fa2N-4 cells than in CHHs; this is significant as CAR is one of the pathways of induction of CYP3A4. The other route of CYP3A4 activation, the pregnane X receptor (PXR), was seen at a similar level in Fa2N-4 cells and CHHs. The study found that CAR-only activators (e.g. artemisinin) failed to provoke a response in Fa2N-4, while other activators which act via both CAR and PXR (e.g. phenobarbital) evoked a lower response in Fa2N-4 than in CHHs. Rifampicin induced CYP3A4 mRNA to a similar level in both Fa2N-4 and CHHs and is a PXR-only activator. These results, suggesting reduced or absent CAR function, cast some doubt over whether Fa2N-4 can be used as a predictor of DDIs and drug metabolism.

The HC-04 cell line is slightly different from Fa2N-4 in that it spontaneously immortalised rather than being treated to achieve that state. Lim *et al.* (Lim *et al.*, 2007) found that CYP1A2, -3A4 and -3A5 but not -1A1, -2C9 or -2E1 transcripts were expressed in HC-04 cells and it was observed that CYP3A4, -1A2, -2C9 and -2E1 could all be induced at the protein level. Functional assays for these enzymes also demonstrated CYP-dependent metabolism and toxicity in this cell line. These are promising results for this cell line, but the absence of some of the CYPs and transporters such as OATPC may limit its usefulness (Lim *et al.*, 2007). More investigations into the level of functionality achievable in HC-04 cells needs to be undertaken before any significant conclusions can be drawn.

1.5 – Hepatic tumour-derived cell lines

Cell lines can be derived from hepatocarcinomas, specifically from primary tumours of the liver parenchymal cells which occur after cirrhosis or chronic hepatitis. The levels of DMEs and drug transporters found in cell lines of this type tend to be low compared to those seen in *in vivo* liver and in primary hepatocytes. This is especially true of the CYP enzymes, which can often show little or no expression in a tumour-derived cell line.

1.5.1 – HepG2 cells

The most commonly-used hepatoma cell line is HepG2 which was derived in 1979 (Aden *et al.*, 1979) and has since been extensively characterised in terms of both phase 1 and phase 2 enzymes. Numerous studies have shown that the basal levels of several of the major CYPs are severely reduced in HepG2 (Westerink and Schoonen, 2007a; Elizondo and Medina-Diaz, 2003) but other enzymes and transporters are present at levels which resemble an *in vivo* hepatocytes more closely although they remain at a reduced level in many cases (Sivertsson *et*

al., 2010; Olsavsky *et al.*, 2007; Westerink and Schoonen, 2007b; Westerink and Schoonen, 2007a; Hewitt and Hewitt, 2004; Elizondo and Medina-Diaz, 2003). Other changes in comparison to primary hepatocytes are also evident; for example, the detection of alpha-fetoprotein is reported in HepG2 and other cell line systems but not in primary or *in vivo* hepatocytes, as AFP is known to be a marker of a more foetal liver phenotype and is not expressed in the mature adult liver, while albumin and transferrin (markers of maturation) are usually lower in cell lines than primary hepatocytes (Page *et al.*, 2007; Sainz and Chisari, 2006; Snykers *et al.*, 2006; Sidhu *et al.*, 2004; Raul Cassia, 1997).

The low expression levels of some proteins in this cell line prevent it from being used as a definitive model for drug metabolism and DDIs, resulting in several studies looking to enhance the function of HepG2 cells. An example of this is a study by Bokhari *et al.* (Bokhari *et al.*, 2007a) which looked at the effect of growing the cells in a 3D culture system rather than a 2D one. Under 3D conditions HepG2 cells formed spherical aggregates which maintained an improved liver function as determined by albumin production and also showed improved cell viability compared to 2D cell growth. This study also looked at the cytotoxic effect of methotrexate (MTX) on cells grown in both 2D and 3D configurations and found that the 3D-cultured cells reacted to a similar concentration of MTX as *in vivo* cells, whereas 2D-cultured cells reacted to a much lower level of the compound, indicating that a 3D culture system may be more suitable for HepG2 culture in terms of producing a realistic response to utilise in drug testing. Another study by Dannenberg *et al.* (Dannenberg and Edenberg, 2006) investigated the effect of DNA methylation on expression in HepG2 cells by inhibition of the methylation process using the compound 5-aza-dC. Assessment of the treated cells by microarray revealed increases in levels of important metabolising genes such as CYP3A4, -3A5 and -3A7 along with CCAAT element-binding proteins including C/EBPβ, which has been implicated in transdifferentiation studies as being involved in liver development (Al-Adsani *et al.*, 2010; Wallace *et al.*, 2009; Shen *et al.*, 2000).

1.5.2 – Huh7 cells

Another cell line with potential for use as a realistic *in vivo* hepatocyte model is Huh7, derived in 1982 by Nakabayashi *et al.* (Nakabayashi *et al.*, 1982). This has been characterised to a much lesser extent than HepG2 and therefore needs to be investigated in more depth to determine whether it can be useful as a model. Some studies have looked at the expression profile in these cells and have found that they are similar to the HepG2 cell line at confluence (Sivertsson *et al.*, 2010; Bokhari *et al.*, 2007a; Bokhari *et al.*, 2007b; Olsavsky *et al.*, 2007). As with HepG2 cells, studies have been undertaken using Huh7 cells to attempt to create a cell

line with an expression profile more resembling that *in vivo*. An example of this is in work published by Sivertsson *et al.* (Sivertsson *et al.*, 2010), which reports that levels of many hepatic differentiation markers, enzymes and transporters are very similar at the mRNA level in confluent HepG2 and Huh7 cells, but prolonged growth in standard media for up to four weeks results in an increase in the level of some major enzymes. A major observation here is the increase in CYP3A4 mRNA which is accompanied by an increase in function within the cell, resulting in expression more comparable to primary hepatocytes. Other published data has stated that Huh7 cells have no detectable CYP3A4 mRNA at confluence, highlighting possible differences in the expression profiles of Huh7 and other cells from different sources (Olsavsky *et al.*, 2007). These could be due to passage number, media differences, culturing and experimental techniques among other things. Data showing that Huh7 cells become more differentiated towards the *in vivo* hepatic profile when incubated with 1% dimethyl sulfoxide (DMSO) for 20 days, with increased expression of albumin, CYP1A2, -2E1 and -3A4 and UGT1A1 at mRNA level accompanied by functional increases in CYP metabolism (Choi *et al.*, 2009; Sainz and Chisari, 2006). Although more work will need to be done in order to validate these cells as a suitable *in vitro* model, prolonged growth in standard media or media supplemented with 1% DMSO appear to produce promising results.

1.5.3 – Additional cell lines

The last hepatoma-derived cell line I will be looking at is HepaRG which was developed by Gripon *et al.* in 2002 (Gripon *et al.*, 2002). Although this is only a recently developed cell line, there have been several papers published on its metabolic profile and functionality which indicate that HepaRG may be a good *in vitro* liver model. A striking difference in this cell line compared to many others is the requirement for a differentiation period consisting of at least two weeks culture in media containing 2% DMSO after high-density seeding. Aninat *et al.* (Aninat *et al.*, 2006) looked at expression and function of various CYPs in these cells and reported that expression was comparable to those seen in primary human hepatocytes with evidence of appropriate functionality of these proteins. Two studies by Kanebratt *et al.* (Kanebratt and Andersson, 2008a; Kanebratt and Andersson, 2008b) evaluated levels of CYPs and other enzymes and transporters involved in liver metabolism. This found that mRNA levels for CYPs, transporter proteins and transcription factors were stable in HepaRG cells over six weeks when cultured in media containing 2% DMSO. Although expression tended to be lower than in primary hepatocytes (with a few exceptions e.g. levels of CYP3A4 mRNA were higher), it was consistently higher than in HepG2 cells. The whole genome expression profile of HepaRG has been analysed and compared to both primary hepatocytes and the HepG2 cell line; results revealed that HepaRG exhibited an expression profile which more closely matched

primary hepatocytes than HepG2 cells did and were more suited to identifying the biological consequences of exposure to toxic substances than were HepG2 cells (Hart *et al.*, 2010; Jennen *et al.*, 2010). Overall results indicate that HepaRG may be a good candidate for the development of a representative hepatocyte cell line.

1.6 – Stem cell-derived hepatocytes

A recent development in the search for an *in vitro* liver model is the use of stem cells (SC); once isolated stem cells can be differentiated into hepatocyte-like cells. Stem cells are capable of self-renewal, going through multiple cycles of cell division and remaining undifferentiated, and are able to differentiate into a variety of specialised cell types. This technology is relatively new and at the moment a lot of the work in this area is centred around the process of differentiation into hepatocyte-like cells rather than metabolic studies.

As stem cells can be grown indefinitely without de-differentiation, one of the major requirements of an *in vitro* model could be fulfilled – the ability to create a sustainable source of cells for experimentation. Once differentiation has taken place this will most likely not be the case, but before the stem cells are directed towards becoming hepatocyte-like cells they are a sustainable source. Specific protocols vary for different sources of stem cells and between laboratories, but there are a few basic steps which are followed in all cases. The stem cells are isolated from the relevant source and kept in sustaining media until the time comes for differentiation to be induced. This is typically done by the addition of various supplements which direct the cells to differentiate into the appropriate cell type. The three main sources of stem cells used for this type of work are human embryonic stem cells (hESCs), adult stem cells, and stem cells derived from umbilical cord blood (UCB). Several reviews on this technology and the state of development at the moment have been recently published (Wobus and Loser, 2011; Greenhough *et al.*, 2010; Medine *et al.*, 2010; Phillips and Crook, 2010); a brief outline of current developments using embryonic, adult and umbilical cord blood derived-stem cells is given below.

1.6.1 – Human embryonic stem cell-derived hepatocyte-like cells

Stem cells are isolated from the inner mass of a blastocyst and cultured along with feeder cells for one to two weeks. At this point the cells growing outwards from the initial cell masses are removed and further cultured or differentiated into various cell types. Ameen *et al.* (Ameen *et al.*, 2008) reviews various techniques employed in culture and differentiation of hESCs in more detail.

In order for hESC derived hepatocyte-like cells to be useful as a model they must be validated in terms of phase I and II DMEs and the phase III transporters along with their induction potential and functionality. This technology is quite new (spontaneous differentiation was first shown in the year 2000 (Schuldiner *et al.*, 2000)) and so only a few studies have been carried out in this area. As techniques of expansion and differentiation improve, so will the level of validation of DMEs and transporters in these cells.

Hay *et al.* (Hay *et al.*, 2007) have looked at basic functional characterisation of hESC derived hepatocyte-like cells and found some promising results. Typical hepatocellular morphology was observed, along with hepatic markers such as alpha-feto protein and albumin. Functional CYPs and the storage of glycogen in cells were also seen. Similar findings to these have also been reported by Ameen *et al.* (Ameen *et al.*, 2008) and by Ek *et al.* (Ek *et al.*, 2007). The latter study also looked at expression and function of specific CYPs in more detail. In the three cell lines tested, protein levels and functionality of CYPs were lower than in primary hepatocytes. However, in one of the lines the mRNA levels of CYPs, various transporters and transcription factors were consistently higher than those found in HepG2 cells. This shows promise for future uses of these hepatocyte-like cells in drug metabolism and drug-drug interaction (DDI) studies once improvements in differentiation quality and quantity of hESCs has been achieved. However, the issues of availability, ethical considerations and regulations remain and could hinder widespread use of this technology.

1.6.2 – Adult stem cell-derived hepatocyte-like cells

The main source for adult stem cells for differentiation into hepatocyte-like cells is bone marrow. This has been found to be the source of hepatic progenitor cells and so is the best option to date as hepatic stem cells have been difficult to isolate (Vessey and de la Hall, 2001). The isolated adult stem cells are cultured and differentiated in a similar way to hESCs (see Lee *et al.* (Lee *et al.*, 2004a) for more detail). As with hESC-derived hepatocyte-like cells, these show hepatic cell morphology and testing of DMEs and transporters has produced some promising results. Both Lee *et al.* (Lee *et al.*, 2004a) and Schwartz *et al.* (Schwartz *et al.*, 2002) showed that the cells expressed albumin, showed glycogen storage and some CYP functional activity. These preliminary results led to the same conclusions as for hESC-derived hepatocyte-like cells. Bone marrow stem cells (BMSCs) have also been used by Snykers *et al.* (Snykers *et al.*, 2006), where differentiation using specific growth factor combinations at different time points during culture resulted in increases in albumin secretion, glycogen storage, urea production and levels of CYP enzymes along with a decrease in AFP, all of which are indicative

of a more mature hepatocyte-like cell. As there are fewer ethical issues when using adult SCs rather than hESCs this source of cells may be the preferred option for future development.

1.6.3 – Umbilical cord blood-derived hepatocyte-like cells

Stem cells can also be extracted from umbilical cord blood. This is a less controversial source than hESCs and has the advantage over adult SCs in that the cells are in a less differentiated state at the time of harvest. The procedures used for generation of embryonic-like cells from the cord blood and subsequent differentiation into hepatocyte-like cells are still being refined. In 2005 McGuckin *et al.* (McGuckin *et al.*, 2005) reported the first reproducible generation of embryonic-like SCs from UCB. Within this study there were also some results concerning differentiation of the UCB SCs towards hepatocyte-like cells. However, as this procedure is extremely new and still requires refining, very little data from testing of expression levels and functionality of various proteins in these cells has been published. If these UCB-derived hepatocyte-like cells do show promise in terms of being a useful model the implications could be far-reaching as the availability of UCB is much greater than that of both hESCs and adult SCs; with 100 million births worldwide every year UCB could be a huge potential source of stem cells.

1.7 – Differentiation of existing models

The differentiation of an existing model to show a more *in vivo* hepatic profile could be another route through which an acceptable model may be created. Two of the more promising experimental processes are briefly described below.

1.7.1 – Dimethyl sulfoxide treatment

Dimethyl sulfoxide (DMSO) is a compound which has been used in several different circumstances to try to aid in differentiation of a hepatic cell line. DMSO applied at a concentration of 1% v/v to Huh7 cells resulted in higher expression of hepatic markers and higher mRNA and protein expression of some metabolising enzymes such as CYP1A2 (Choi *et al.*, 2009; Sainz and Chisari, 2006) indicating a higher level of differentiation and promising in terms of creating a realistic hepatic model. A higher concentration of DMSO (2% v/v) is routinely applied to the cell line HepaRG to differentiate the cells to a state more closely resembling that of a mature hepatocyte. These differentiated cells have been shown to be closer in mRNA, protein and functional assessments to primary hepatocytes than either the parental cell line or other secondary hepatocytes and may be a promising avenue to explore for the development of a toxicity prediction model (Antherieu *et al.*, 2010; Kanebratt and Andersson, 2008a; Le Vee *et al.*, 2006).

1.7.2 – Transdifferentiation

Transdifferentiation is the reprogramming of one cell type to another. Several publications describing attempts to transdifferentiate pancreatic to hepatic cells have shown some promising results. Human foetal pancreatic cells have been reported to have transdifferentiated into cells with more hepatic expression markers, although these have not been fully tested as a hepatic model (Sumitran-Holgersson *et al.*, 2009). Another route which has been explored is to attempt to differentiate an established cell line, in particular the pancreatic exocrine line AR42J-B13, into cells more resembling a hepatocyte. This has also met with some success with the potential signalling mechanisms for differentiation being identified, but again have not been fully tested as a hepatocyte model (Al-Adsani *et al.*, 2010; Shen and Tosh, 2010; Wallace *et al.*, 2009; Shen *et al.*, 2000).

Mouse tail-tip fibroblasts (TTFs) have also been subjected to attempted transdifferentiation into hepatocyte-like cells. Huang *et al.* (Huang *et al.*, 2011) attempted to do this and named the induced hepatocyte-like cells produced iHep cells. This was done by lentiviral infection with the transcription factors Gata4, Hnf1 and Foxa3, along with inactivation of $p19^{Arf}$ in order to bypass the proliferative limitations of the cells in culture. After 15 days cells showed expression of liver markers such as albumin, alpha fetoprotein and transferring at RNA level and metabolism of compounds using the Cyp1a2, Cyp2a and Cyp3a enzymes at roughly one third of the metabolic capacity of primary hepatocytes. This is a good indication that the cells are progressing towards hepatic functionality. These iHep cells have also been used to restore liver function to $Fah^{-/-}$ mice, indicating that with the correct signalling induction can be continued to create a fully representative hepatocyte model using this method (Huang et al., 2011).

1.7.3 – Oxygen rich environments

As discussed previously, although primary hepatocytes are the gold standard model for investigations into drug metabolism and toxicity, they cannot be maintained indefinitely in culture due to de-differentiation. Attempts at increasing the longevity of this model have included culture in different formats, for example co-culture with non-parenchymal cells, 3D culture and sandwich culture (Bhatia *et al.*, 1999; Bhatia *et al.*, 1997; Dunn *et al.*, 1992; Dunn *et al.*, 1989; Morin and Normand, 1986; Landry *et al.*, 1985). Another attempted strategy to prolong the useful life of primary heptocytes has been to culture in a high oxygen environment as the oxygen levels available to cells in standard culture conditions are far lower than those found *in vivo* (Nahmias *et al.*, 2007; Nahmias *et al.*, 2006). However, although metabolic rates were shown to decrease under restricted oxygen conditions, increased oxygen availability

alone did not improve on the model (Tilles *et al.*, 2001; Yanagi and Ohshima, 2001; Rotem *et al.*, 1994; Suleiman and Stevens, 1987). Kidambi *et al.* (Kidambi *et al.*, 2009) described a combination of these techniques which appear to increase the longevity of the primary hepatocytes as a useful model in culture. This work combined co-culture of primary hepatocytes with endothelial cells on collagen coated plates cultured in a high oxygen environment in serum-free media. Results revealed that levels of mRNA expression, albumin and urea production and metabolic function were improved over those from cells cultured with serum or in suspension and were more comparable to those in primary hepatocytes for prolonged periods of time; for example, albumin production peaked and stabilised after 11 days of culture. Another notable finding was that hepatocytes cultured in this fashion were able to be used before hepatocytes cultured in suspension with metabolic stability obtained earlier. Culturing techniques such as these are promising for extending the life of a primary hepatic model, although they still rely on the cells being available for isolation and culture initially.

1.8 – Summary

Studying drug metabolism and DDIs effectively requires a reproducible model which has functional expression of hepatic proteins at a relevant physiological level. Although there are many systems which have some of these desired features, as yet none have them all. Liver microsomes and Supersomes™ allow the study of a particular enzyme in great detail but fail to take into account physiological factors, such as where the enzyme is located in the cell and the transporters it encounters *in vivo*. Liver slices maintain cell structure, cell-cell contacts and reflect protein location *in vivo* but protein levels, especially those of CYPs, decrease dramatically. As a result liver slices have a limited time frame of use, affecting the potential for use in induction assays which in turn limits their usefulness in DME and DDI testing.

Primary hepatocytes are deemed to be the “gold standard” model for use in DME and DDI assays. They are the model which most consistently represents the *in vivo* liver when freshly isolated. However, these cells tend to lose expression of some proteins after a short time in culture which affects reproducibility of results. Additionally, supply is unpredictable as a good quality source of fresh human liver tissue cannot be obtained regularly. To try and combat the downfalls of primary hepatocytes, attempts at cryopreservation and immortalisation have been tried and are partially successful. Although the metabolic profile of these cells is never quite as good a match to *in vivo* liver as primary hepatocytes are, the relative responses to inducers can often be useful in DME and DDI assays. The longevity of these cells also allows for reproducibility between assays and a more permanent source of cells than primary

hepatocytes. A more complete set of proteins with expression levels matching *in vivo* liver would be preferred in order to reliably use these models.

Cell lines derived from hepatic tumours have been in use for a number of decades now, the most established being the HepG2 cell line. Although this does have the benefit of indefinite growth and so provides a constant source of cells, the metabolic profile is lacking when compared to primary hepatocytes. Cell lines of this type are still being developed, with the recent HepaRG line looking like it has the potential to be of use in drug metabolism and DDI assays.

A future possibility is the use of stem-cell derived hepatocyte-like cells. Although adult stem cells have been differentiated into hepatocyte-like cells they are a few steps further into the differentiation process to begin with than are hESCs. As yet there is no evidence to indicate whether this will alter the phenotype or genotype of the hepatocyte-like cells produced. Adult stem cells may be more readily available than hESCs and would also carry fewer ethical issues, making them more acceptable for use in the drug industry if they were ever to be validated as a model. Potentially an even greater source for stem cells could be UCB; umbilical-cord blood-derived embryonic-like stem cells have been produced and further differentiated into hepatocyte-like cells. Extensive validation of any hepatocyte-like cell would be needed before use as a high-throughput model for industry could be considered.

In conclusion, the ideal model for a high-throughput system of analysis for potential drug toxicity and DDIs would contain a full metabolic profile of phase I and II DMEs and phase III transporters. It would also need to have appropriate expression levels and functional properties of the *in vivo* liver, to give reproducible results and be in ready supply. This model does not currently exist; the closest available at this time are freshly isolated primary hepatocytes. However, current work with cell lines and stem cells does point towards this goal drawing closer with future studies.

1.9 – Aims

The main aim of the series of experiments described in this thesis was to test the hypothesis that the cell lines HepG2 and Huh7 can be successfully differentiated into a more mature hepatic state. If the hypothesis is positive, this would potentially allow easy access to a well defined and easily accessible model for early stage drug testing and could potentially help to define culture conditions with which to generate a hepatocyte-like cell from other sources such as adult and embryonic stem cells. The hypothesis was investigated by attempting differentiation of the cells utilising a variety of treatment strategies, including growth factor

treatments applied to stem cells from different sources and the DMSO treatments which have already been reported to be producing good results in secondary hepatocyte cell lines. Treated cells have been analysed for a wide range of genes of interest including hepatic differentiation markers, influx and efflux transporters and both phase I and II drug metabolising enzymes by qPCR. Following this, more specific analysis was carried out using protein and functional tests to analyse the extent of treatments on the function of the cells.

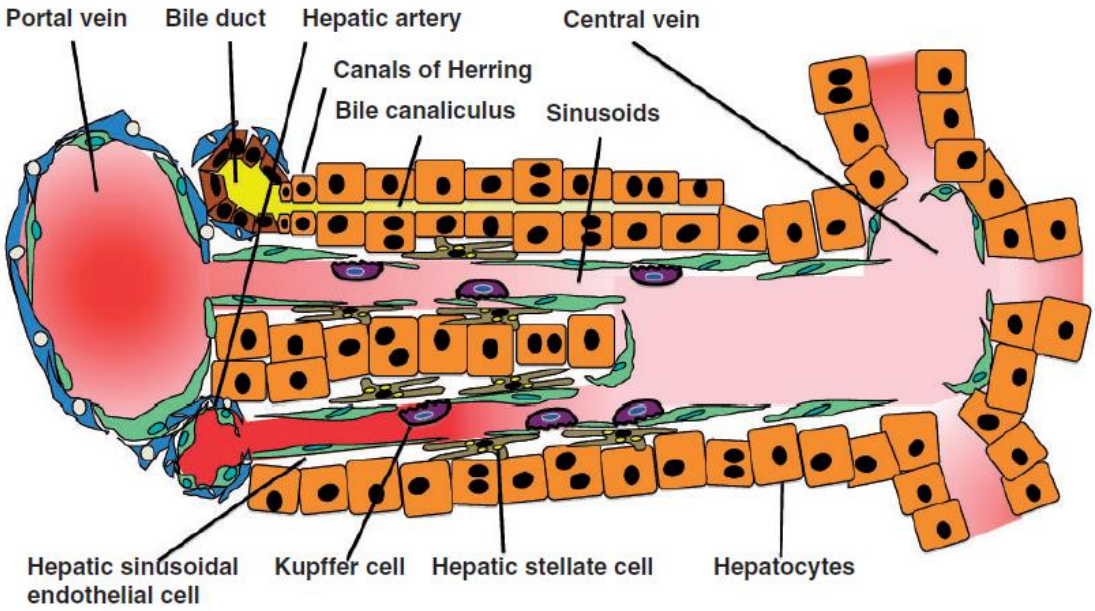

Figure 1.1 – Structure of a liver lobule. Diagram reproduced with permission from Tanaka *et al.* (Tanaka *et al.*, 2011).

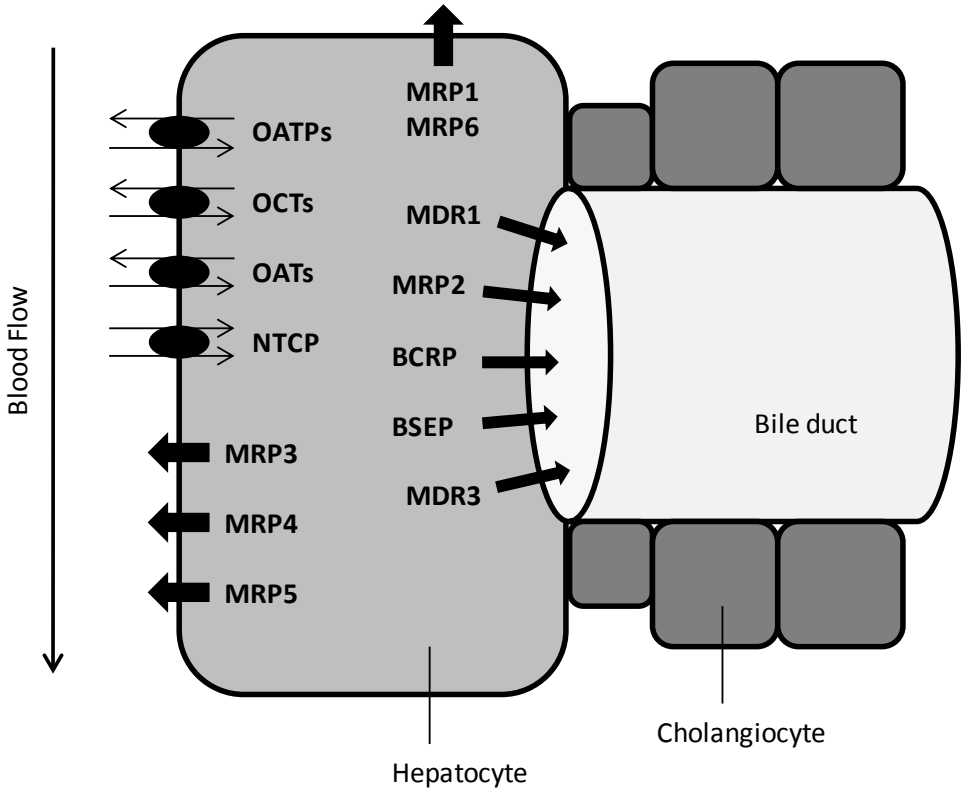

Figure 1.2 – Drug transporters and their location in the hepatocyte

Protein Name	Alternate names	Tissue expression	Substrates
OATP1A2	OATPA, OATP, SLCO1A2, SLC21A3	Brain, liver, kidney, ciliary body	Bile salts, organic cations and anions
OATP1B1	OATPC, OATP2, SLCO1B1, SLC21A6	Liver	Bile salts, organic anions
OATP1B3	OATP8, SLCO1B3, SLC21A8	Liver, cancer cell lines	Bile salts, organic anions, digoxin
OATP1C1	OATPF, SLCO1C1, SLC21A14	Brain, testis, intestine, kidney	Bromosulphophathanlin (BSP)
OATP2A1	PGT, SLCO2A1, SLC21A2	Ubiquitous	Prostaglandin
OATP2B1	OATPB, SLCO2B1, SLC21A9	Liver, placenta, intestine, ciliary body	BSP
OCT1	SLC22A1	Liver (sinusoidal)	Organic cations
OCT2	SLC22A2	Kidney, brain	Organic cations
OCT3	SLC22A3	Liver, muscle, placenta, kidney, heart, lung, brain	Organic cations
OAT1	SLC22A6	Kidney, placenta, brain	Organic anions
OAT2	SLC22A7	Liver, kidney	Organic anions
OAT3	SLC22A8	Kidney, brain, muscle, developing bone	Organic anions
OAT7	SLC22A9, OAT4	Liver	Estrone sulfate
NTCP	SLC10A1	Liver (basolateral), pancreas	Bile acids

Table 1.1 – Influx transporters. Information from the following sources (Schroeder *et al.*, 1998; Boyer *et al.*, 1994; Hagenbuch and Meier, 2004; Cui *et al.*, 2001; Kullak-Ublick *et al.*, 2001; Tamai *et al.*, 2000; Koepsell and Endou, 2004; Enomoto *et al.*, 2002; Takeda *et al.*, 2002; Sekine *et al.*, 2000; Molderings *et al.*, 2003; Kimura *et al.*, 2002; Takeda *et al.* 2002b; Zhang *et al.*, 1999; Kekuda *et al.*, 1998; Wu *et al.*, 1998).

Family	Subfamilies	Genes	Function
CYP1	3 subfamilies, 3 genes, 1 pseudogene	CYP1A1, -1A2, -1B1	Drug and steroid metabolism, in particular estrogen
CYP2	13 subfamilies, 15 genes, 16 pseudogenes	CYP2A6, -2A7, -2A13, -2B6, -2C8, -2C9, -2C18, -2C19, -2D6, -2E1, -2F1, -2J2, -2R1, -2S1, -2U1, -2W1	Drug and steroid metabolism
CYP3	1 subfamily, 4 genes,2 pseudogenes	CYP3A4, -3A5, -3A6, -3A43	Drug and steroid metabolism, including testosterone
CYP4	6 subfamilies, 12 genes, 10 pseudogenes	CYP4A11, -4A22, -4B1, -4F2, -4F3, -4F8, -4F11, -4F12, -4F22, -4V2, -4X1, -4Z1	Fatty acid metabolism
CYP5	1 subfamily, 1 gene	CYP5A1	Thromboxine A_2 synthesis
CYP7	2 subfamilies, 2 genes	CYP7A1, CYP7B1	Bile acid biosynthesis
CYP8	2 subfamilies, 2 genes	CYP8A1, CYP8B1	Bile acid and prostacyclin synthesis
CYP11	2 subfamilies, 3 genes	CYP11A1, -11B1, -11B2	Steroid biosynthesis
CYP17	1 subfamily, 1 gene	CYP17A1	Steroid biosynthesis
CYP19	1 subfamily, 1 gene	CYP19A1	Steroid biosynthesis
CYP20	1 subfamily, 1 gene	CYP20A1	Unknown function
CYP21	2 subfamilies, 1 gene, 1 psseudogene	CYP21A2	Steroid biosynthesis
CYP24	1 subfamily, 1 gene	CYP24A1	Vitamin D degradation
CYP26	3 subfamilies, 3 genes	CYP26A1, -26B1, -26C1	Retinoic acid hydroxylase
CYP27	3 subfamilies, 3 genes	CYP27A1, -27B1, -27C1	Bile acid biosynthesis, vitamin D activation
CYP39	1 subfamily, 1 gene	CYP39A1	Cholesterol hydroxylase
CYP46	1 subfamily, 1 gene	CYP46A1	Cholesterol hydroxlyase
CYP51	1 subfamily, 1 gene, 3 pseudogenes	CYP51A1	Cholesterol biosynthesis

Table 1.2 – CYP450 families. Information from the following sources (Bozina *et al.*, 2009; Lewis *et al.*, 1998; Guengerich, 1999; Shimada *et al.*, 1994).

Protein name	Alternate names	Tissue expression	Substrates
CYP1A1	CYP1, CP11, P1-450	Extrahepatic	Pre-carcinogens, PAHs
CYP1A2	CP12, P3-450	Liver	Aromatic amines
CYP1B1	CP1B, P4501B1	Extrahepatic	Oestradiol
CYP2A6	CPA6, P450C2A	Liver	Nicotine
CYP2A7	CYPA7, P450-IIA4	Liver	Steroids, fatty acids, some xenobiotics
CYP2B6	CPB6, P450-IIB6	Liver, lower levels in other tissues	Xenobiotics, in particular anti-cancer drugs
CYP2C9	CPC9, P450-IIC9	Liver	Many xenobiotics
CYP2C19	CPCJ, P450-IIC19	Liver	Many xenobiotics
CYP2D6	CPD6	Liver	Many xenobiotics
CYP2E1	CPE1, P450C2E	Liver	Many xenobiotics, solvents, pre-carcinogens
CYP3A4	CP34, P450C3N P450PCN1	Liver, intestine	Many xenobiotics, pre-carcinogens, dietary components
CYP3A5	CP35, P450PCN3	Liver, intestine	Many xenobiotics, pre-carcinogens, dietary components
CYP3A7	CP37, P450-HFLA	Mainly foetal liver	Many xenobiotics, pre-carcinogens, dietary components
CYP7A1	CP7A, CYP7	Liver	Bile acid synthesis
CYP7B1	CP7B	Extrahepatic	Cholesterol to bile acid conversion
FMO1	None	Foetal liver and kidney, adult kidney	Anti-histamine promethazine, insecticide alicarb
FMO2	FMO1B1	Unknown – high prevalence of polymorphism causing non-function	Unknown
FMO3	FMOII, TMAU	Adult liver, kidney and lung	Xenobiotics such as cimetidine, agricultural chemicals such as organophosphates, dietary trimethylamine
FMO4	FMO2	Very low levels in foetal and adult tissues	Variety of xenobiotics and pesticides
FMO5	None	Adult liver (low levels)	Unknown – possibly not a DME

Table 1.3 – Phase I metabolising enzymes. Information from the following sources (Bozina *et al.*, 2009; Lewis *et al.*, 1998; Guengerich, 1999; Shimada *et al.*, 1994; Zhou and Shepard, 2006; Hines, 2006; Bain *et al.*, 2005; Chung *et al.*, 2000; Hodgson *et al.*, 2000; Ziegler-Skylakakis *et al.*, 1998; Hodgson *et al.*, 1995, Al-Waiz *et al.*, 1987).

Protein name	Alternate names	Tissue expression	Substrates
UGT1A1	UGT1, UDPGT 1-1	Liver, kidney	Bilirubin, estradiol, thyroxin, paracetamol
UGT1A3	UGT1C, UDPGT 1-3	Liver, kidney	Estrogens, bile acids
UGT1A4	UGT1D, UDPGT 1-4	Liver, kidney	Estrogens, eicosaniods, nicotine
UGT1A6	UGT1F, UDPGT 1-6	Liver, kidney	Serotonin, paracetamol
UGT1A7	UGT1G, UDPGT 1-7	GI tract	Phenols, irinotecan, uridine
UGT1A8	UGT1H, UDPGT 1-8	GI tract	Phenols, flavones, opioids
UGT1A9	UGT1I, UDPGT 1-9	Liver, kidney	Estrogens, eicosanoids
UGT1A10	UGT1J, UGT 1.10	GI tract	Mycophenolic acid, coumarins
UGT2A1	None	Nasal tissue	Unknown
UGT2B4	UGT2B11, UDPGT2B4	Liver	Bile acids, arachidonic acid, codeine
UGT2B7	UGT2B9, UDPGT2B7	Liver, kidney	Bile acids, estradiol, progesterone, glucocorticoids
UGT2B10	UDPGT2B10	Liver, kidney	Eicosanoids, nicotine
UGT2B15	UGT2B8, UDPGT2B15	Liver, pancreas, prostate, kidney	Testosterone, paracetamol
UGT2B17	UDPGT2B17	Liver	Testosterone

Table 1.4 – Phase II metabolising enzymes (UGT enzymes). Information from the following sources (Bock, 2010; Tukey and Strassburg, 2000; Burchell *et al.*, 2005; Court, 2005; Little *et al.*, 2004; Samokyszyn *et al.*, 2000; Wietholtz *et al.*, 1996; Jancova *et al.*, 2010).

Protein name	Alternate names	Tissue expression	Substrates
SULT1A1	ST1A1	Liver, pancreas, prostate, kidney, lung	Phenolic compounds
SULT1A2	ST1A2	Liver, pancreas, prostate, kidney, lung	Aromatic amines
SULT1B1	ST1B1	Liver, GI tract	Thyroid hormones, small phenols
SULT1E1	ST1E1	Liver, jejunum	Estrogen, genistein, 1-naphtol
SULT2A1	ST2A1	Liver, adrenal glands, duodenum	Hydroxysteroids
SULT4A1	SULTX3	Brain	Unknown
SULT6B1	None	Testis, kidney	Unknown
GSTA1	GSTA1-1, GST2, GTH1	Liver, kidney	Anti-cancer drugs e.g. chloroambucil, doxorubicin, busulfan
GSTA2	GSTA2-2, GST2, GTH2	Liver, kidney, lung, prostate, pancreas	Chloroambucil, chloroquinine, ceramide, busulfan
GSTA3	GSTA3-3, GTA3	Lung, liver, kidney, pancreas, prostate	Steroid hormone production, endogenous and exogenous conjugation
GSTA4	GSTA4-4, GTA4	Wide range of tissues including liver	4-hydroxyalkenals such as 4-hydroxynonenal (4-HNE)
GSTA5	None	Unknown	Unknown
GSTM1-5	GSTM1-1 to 5-5, GST4	Wide range including liver, heart, kidney and testis	Endogenous and exogenous conjugation
GSTP1	GSTP, GST3	Wide range including kidney, lung, liver, heart and pancreas	Endogenous and exogenous conjugation
GSTT1/2	None	Wide range including kidney, lung, liver, heart and pancreas	Endogenous and exogenous conjugation
NAT2	AAC2, PNAT	Liver, GI tract	Sulphonamides, isoniazid

Table 1.5 – Phase II metabolising enzymes (SULT, GST and NAT enzymes). Information from the following sources (Jancova *et al.*, 2010; Strassburg *et al.*, 2002; Adjei *et al.*, 2008; Hines, 2008; Meinl *et al.*, 2002; Gamage *et al.*, 2006; Falany *et al.*, 1995; Comer *et al.*, 1993; Hayes and Strange, 2000; Hayes and Pulford, 1995; Lo and Ali-Osman, 2007; Desmots *et al.*, 2001; Kusama *et al.*, 2006; Tew, 1994; Ciaccio *et al.*, 1991; Hayes *et al.*, 2005; Hein *et al.*, 2000; Kawamura *et al.*, 2005).

Protein name	Alternate names	Tissue expression	Substrates
MRP1	ABCC1	Kidney, lung, muscle, testis, placenta, multi-drug resistant carcinoma	Conjugated drugs, verapamil, vincristine, folate
MRP2	ABCC2	Liver, kidney, GI tract, placenta	Conjugated bilirubin, estradiol, leukotrines
MRP3	ABCC3	Kidney, cholangiocytes, pancreas, GI tract, spleen	Conjugated bilirubin, leukotrines, estradiol
MRP4	ABCC4	Kidney, prostate, brain, pancreas	Conjugated nucleosides, cGMP, cAMP, ADP, folate
MRP5	ABCC5	Wide range including liver, kidney, lung and muscle	Thiopurine anticancer drugs, some anti-HIV drugs
MRP6	ABCC6	Kidney, lower liver levels	Drugs such as doxorubicin, cisplatin, probenacid
BCRP	ABCG2	Blood-brain barrier, placenta, kidney, intestine, liver	Hydrophobic drugs, mitoxantrone, anthracycline
BSEP	ABCB11	Liver	Bile salts, vinblastine
P-gp	MDR1, ABCB1	Blood-brain barrier, kidney, intestine, liver	Hydrophobic drugs – digoxin, verapamil, cyclosporin A, steroid hormones
MDR3	ABCB4	Liver, colon	Phosphatidylcholine, phospholipids

Table 1.6 – Efflux transporters. Information from the following sources (Rius *et al.*, 2008; Rius *et al.*, 2005; Jedlitschky *et al.*, 2004; Lee *et al.*, 2004b; Rius *et al.*, 2003; Chen *et al.*, 2001; Zeng *et al.*, 2000; Keppler, 2011; Ilias *et al.*, 2002; Cui *et al.*, 1999; Kamisako *et al.*, 1999; Allen and Schinkel, 2002; Allen *et al.*, 2002; Loe *et al.*, 2000; Keppler *et al.*, 1998; Jedlitschky *et al.*, 1997; Jedlitschky *et al.*, 1996; Loe *et al.*, 1996; Leier *et al.*, 1994; Childs *et al.*, 1998; Leslie *et al.*, 2005).

Chapter 2 – Materials and Methods

Detailed in this section is the methodology used in obtaining the experimental results shown in the following chapters. All reagents and cell culture media were purchased from Sigma (Dorset, UK) unless otherwise stated. Buffer recipes can be found in Appendix 1.

2.1 – Cell culture

2.1.1 – Routine culture of HepG2 and Huh7 cells

All manipulations were carried out in the sterile environment of a class II laminar flow cabinet (S@feflow 1.2, BIOAIR, Italy) using aseptic techniques to avoid contamination. Sterility was maintained by UV irradiation and spraying with 70% ethanol and TriGene (Starlab, UK). All glassware was autoclaved at 121^{o}C for 20 minutes before use and nitrile gloves were worn at all times. Sterile plastics were purchased from Corning Costar. All medium was stored at 4^{0}C and warmed to 37^{0}C prior to use.

HepG2 cells (passages 71-90) were originally obtained from American Type Culture Collection (ATCC HB-8065). HepG2 cells were maintained in high glucose DMEM supplemented with 10% foetal calf serum (v/v), penicillin/streptomycin (100U/ml and 100µg/ml respectively), 1% glutamine (v/v) and 1% non-essential amino acids (v/v). This cell line was grown in 75cm^2 flasks at 37^{o}C in 5% CO_2 in air until confluent (approximately 7 days, determined by light microscopy), at which time they were sub-cultured and re-seeded at a density of 2.5 x10^6 cells per flask. Growth medium was replaced every three to four days.

Huh7 cells (passages 5-18) were kindly donated by Paul Sharp (Kings College, London, UK). These were maintained in high glucose DMEM supplemented with 10% foetal calf serum (v/v), penicillin/streptomycin (100U/ml and 100µg/ml respectively) and 1% glutamine (v/v). This cell line was grown in 162cm^2 flasks at 37^{o}C in 5% CO_2 in air until 90% confluent (approximately 7 days, determined by light microscopy), at which time they were sub-cultured and re-seeded at a density of 1.8 to 2.5 x10^6 cells per flask. Growth medium was replaced every three to four days.

2.1.2 – Subculture of HepG2 and Huh7 cells

When ready to be subcultured, cells were washed twice with PBS and incubated at 37^{o}C in trypsin-EDTA (10ml/162cm^2, 5ml/75cm^2) for approximately 5 minutes. Once detached they were transferred into a sterile universal tube and the flask was washed with medium to retrieve any remaining cells. Addition of serum-containing medium deactivated the trypsin.

Cells were then centrifuged at 400 xg for 3 minutes, after which the supernatant was discarded and the cell pellet resuspended in 10mls of fresh medium using a wide-bore needle and syringe. The number of cells was quantified using a Coulter Particle Counter Z1 (Beckman Coulter, UK) and seeded accordingly into sterile culture flasks at the previously stated densities. For experimental purposes HepG2 cells were seeded onto 6, 12 and 24 well plates at densities of 5 $x10^5$ (6 well) or 1 $x10^5$ (12 and 24 well) cells per well. Huh7 cells were seeded onto 6 well and 24 well plates at densities of 4 $x10^5$ and 8 $x10^4$ cells per well respectively. Medium was changed every two to three days at which point all cells were visually assessed for effects of treatment on viability and morphology using a light microscope.

2.1.3 – Cell cryopreservation

Periodically cells from both lines were frozen in liquid nitrogen in order to maintain a low passage stock. Cells ready to be subcultured were dissociated from the flask with trypsin and a count obtained as previously described, after which the cells in suspension were re-pelleted by centrifugation. The pellet was resuspended in freezing medium consisting of 80% growth medium, 10% serum and 10% DMSO) so that 1ml of medium contained 3 to $5x10^6$ cells. 1ml aliquots of cell suspension in 2ml cryopreservation vials were slowly frozen at a rate of 1^oC/min until a temperature of -196^oC was reached, at which point the vials were transferred into a liquid nitrogen storage facility.

In order to grow cells from frozen stocks, a vial was removed from the liquid nitrogen store and immediately thawed in a water bath at 37^oC whilst being vigorously shaken to minimise bursting of the cells. Once thawed, cells were added to a new sterile culture flask along with prewarmed growth medium. The following day the medium was changed to remove any traces of the freezing medium. Culturing was then commenced as previously described, allowing at least one passage before cells were used for experimental purposes.

2.2 – Differentiation treatments

2.2.1 – Initial growth factor treatments

HepG2 and Huh7 cells were seeded onto 6 well plates at the previously stated densities and allowed to grow for two days. HepG2 cells were also seeded onto 3 cm diameter plastic plates at the same density to allow imaging on the stage of a confocal microscope. On the third day cells were at approximately 90% confluence (acceptable range was approximately 85% to 95%, cells not meeting this criteria or showing signs of infection were discarded) and the applicable growth factor cocktail was added to the standard growth medium, passed through a sterile 0.22 µm syringe-driven filter (Millipore, Ireland) and added to the growing cells (for growth

factor treatments see table 4.2). Every two days medium was changed and images were taken of HepG2 cells using a Zeiss LSM 510 inverted confocal microscope (Zeiss, Germany) at 20x zoom and excitation wavelength of 633 nm using an HeNe2 laser. On day five of treatment (day eight total growth) total RNA was extracted from the cells as described in chapter 2.4. However, as no clear changes were observed in morphology with this treatment and it was not feasible to conduct this in prolonged treatments due to the time the cells were out of the sterile environment, no images from this method are included.

2.2.2 – Dimethyl sulfoxide (DMSO) treatments

HepG2 and Huh7 cells were seeded onto 6 well plates at the previously described densities and allowed to grow for two days. On the third day the cells were at approximately 90% confluence and treatment began with the addition of either 1% or 2% DMSO (v/v) to the standard growth medium. Medium was changed every two to three days and total RNA was extracted at specific time points. Untreated Huh7 cells were grown and extracted at the same time points. The timing of treatments and RNA or protein extraction for both HepG2 and Huh7 cell lines can be seen in figures 2.1 and 2.2 respectively.

2.2.3 – Extended growth factor treatments

HepG2 and Huh7 cells were seeded onto 6 well plates at the previously described densities and allowed to grow for two days. On the third day the cells were at approximately 90% confluence and treatment commenced with the addition of growth factor treatment 1, 2 or 3 (see table 4.3). The cocktail was added to standard growth medium and passed through a sterile 0.22 µm syringe-driven filter before being added to the cells. Medium was changed every two to three days and total RNA was extracted at specific time points (figures 2.1 and 2.2).

2.2.4 – HepatoZYME medium

HepatoZYME is a specialised medium designed for long term maintenance of primary hepatocytes which can be purchased from Invitrogen (UK). It is designed to be used in a serum-free state and contains carefully balanced growth factor mixtures. This medium was tested on both HepG2 and Huh7 cells as an alternative to standard growth medium or supplemented medium using combinations of growth factors to attempt to produce a more heptocyte-like cell using a widely available commercial product. Normal growth conditions for both HepG2 and Huh7 cells require the addition of 10% foetal calf serum; however, adding 10% serum to this medium would reduce its specificity so various methods of growing both cell lines with a lower serum content were attempted. Both cell lines were grown on 6 well plates

to confluence in standard growth medium which was subsequently replaced by HepatoZYME containing no serum or with 2% serum. In both media, cells began to dissociate from the flask surface very quickly and after four to five days very few whole cells were present. Next, in an attempt to habituate the cells to low serum concentrations, both cell lines were cultured in standard growth medium with gradual reductions in serum content from 10% to 2% over a period of two weeks. Both cell lines grew more slowly at low serum concentration but still appeared healthy. After five to seven days of growth at 2% serum, cells were subcultured and seeded into 6 well plates with the continuation of growth medium at 2% serum. When cells were confluent this was replaced with HepatoZYME medium with or without 2% serum. Unfortunately cells did not survive in serum-supplemented or standard HepatoZYME medium for more than ten days, and after approximately five days there were so few viable cells present that only small quantities of RNA could be extracted and what was obtained was of too poor quality to be of use. In view of these results it was concluded that the HepatoZYME medium with a low serum concentration was not suitable for prolonged growth of these cell lines and no further experiments were conducted using this medium.

2.3 – Induction treatments

Rifampicin, phenobarbital and β-naphthoflavone (BNF) were added to HepG2 and Huh7 cells in 6 well plates at confluency and after 15 days of 1% DMSO treatment. Each experiment included a control and three different concentrations of the inducing agent. Phenobarbital was dissolved in water to a stock concentration of 30mM; control cells were incubated in standard growth medium with the maximal volume of water added to treated cells; treated cells contained either 0.5, 1.5 or 3 mM phenobarbital in standard growth media with the maximum vehicle volume (water) in each concentration (i.e. the vehicle volume in each of the lower concentrations and the control was equal to that present in the 3 mM treatment). Rifampicin and BNF were both dissolved in DMSO to stock concentrations of 30 mM and 10 mM respectively. Control cells were incubated with growth medium plus the maximum volume of DMSO added to treated cells. When used as a vehicle DMSO concentration was always <1%. Cells were treated with 10 µM, 50 µM or 100 µM rifampicin, and with 1 µM, 10 µM or 100 µM BNF. All treatments were applied for 24 hours, after which total RNA was extracted.

2.4 – RNA extraction and reverse transcription

Total RNA was isolated from HepG2 and Huh7 cells using the SV Total RNA Isolation System according to the manufacturer's instructions (Promega). RNA was quantified and purity assessed using a spectrophotometer with a quartz cuvette at absorbances 260 nm, 230 nm

and 280 nm. RNA concentration was determined by the measurement of absorbtion at 260 nm, while the ratios 260/280 and 260/230 were recorded to detect contamination by phenols, proteins and other organic compounds – ideally in pure RNA preparations both of these ratios would give a value of 2. Where values under 1.8 were observed for either ratio the sample was not used. Total RNA (1 µg and 0.5 µg for HepG2 cells and Huh7 cells respectively) was reverse transcribed into cDNA. A lower concentration of RNA was reverse transcribed for Huh7 samples due to the lower RNA yield from the cells, allowing the sample to be used for more experiments; this concentration still allowed subsequent PCR experiments to be carried out reliably. Reverse transcription was carried out using random priming and Moloney murine leukaemia virus (MMLV) reverse transcriptase (RT) (Promega), in a reaction volume of 20 µl. This RT also has an endogenous RNase H^+ function which ensures degradation of the RNA template after it has been subjected to reverse transcription; RNase inhibitor (RNAsin, Promega) was included to ensure that RNA degradation did not occur in the mixture before reverse transcription has taken place. This enzyme inhibits common eukaryotic RNases and does not affect MMLV reverse transcriptase or RNase H^+ function. Negative control reactions from which either MMLV-RT enzyme or RNA were omitted were included to check for genomic DNA contamination in the samples and other contaminants in the RT components. Briefly, RNA was mixed with 1 µl of 0.5 mg/ml random hexamers and heated for 5 minutes at 65^{o}C in order to remove any secondary structure, then cooled on ice for a further 2 minutes to ensure that the secondary structure did not reform. The rest of the reaction mixture was then added (0.5 µl MMLV-RT (200 U/µl), 4 µl 5xRT buffer, 5 µl 2mM dNTPs and 0.25 µl RNase inhibitor (40 U/µl, Promega)) and samples incubated at 42^{o}C for 2 hours, followed by 10 minutes at 70^{o}C. Reverse transcription products and negative controls were subject to end point PCR to ensure that the reverse transcription had worked and that no contamination was present.

2.5 – End point PCR, cloning and qPCR

Details of primer sequences, annealing temperatures, exon locations, product length sequencing results and qPCR parameters such as melting temperatures, assay efficiency and error used in this work are included in chapter 3. All primers were designed using the LUX primer design program by Invitrogen (www.invitrogen.com) with the criteria of a product size of around 100 base pairs, primer length of approximately 20 base pairs, a melting temperature of between 55 and 60^{o}C and ideally would cross an exon:exon boundary. The inclusion of an exon:exon boundary is particularly useful as the intron which would be included in the genomic DNA sequence would create a longer product during PCR. This can both help with identifying potential genomic DNA amplification during end-point PCR and can prevent

genomic amplification during the much shorter amplification stage in qPCR. As part of the design program predicted product sequences were tested for specificity using the BLAST program (http://blast.ncbi.nlm.nih.gov/Blast.cgi). Primers were ordered from either VHBio (Gateshead, UK) or IDT (Belgium). Primers were initially purchased with standard desalting purification; if these proved to be unsuitable for either end-point or qPCR due to mispriming, lack of product or poor qPCR efficiency, HPLC purified primers were ordered. If primers were still found to be unsuitable they were redesigned.

End point PCRs were carried out for all primer pairs. Reaction volumes were 20 µl, comprised of 0.25 µl GoTaq DNA polymerase (5 U/µl, Promega), 2 µl 2mM dNTPs, 0.5 µM of each primer (1 µl of a 10 µM stock) and 4 µl 5x Green GoTaq Flexibuffer. Amplification protocol was as follows: 95^{o}C for 2minutes, 35 cycles of 95^{o}C (30 seconds), χ^{o}C (30 seconds, χ = annealing temperature) and 72^{o}C (30 seconds), then an end stage of 72^{o}C for 10 minutes (carried out on a Px2 Thermo Cycler, Thermo Scientific, USA). Cycle number was increased to 40 if insufficient amplification was seen. PCR products were separated by gel electrophoresis using 1.5% agarose gels and visualised with SafeView (5 µl per 100 ml of agarose, NBS Biologicals Ltd, UK) under UV light (Alphaimager, Flowgen). Products were excised, cloned using pGem T-easy vector system 2 with JM109 competent cells according to manufacturers instructions (Promega), and sequenced to verify that the correct product had been amplified. Sequencing was outsourced to Cogenics (Essex, UK).

Quantitative PCR (qPCR) was carried out on a Roche LightCycler 480 using LightCycler 480 SYBR-green Master Mix (Roche, UK). The suitability of six reference genes to be used in data normalisation was determined using GeNorm software ((Vandesompele *et al.*, 2002), website medgen.ugent.be/genorm/, PrimerDesign, Southampton, UK) using cDNA samples harvested at confluence over several passages of each cell line. Of the six, the two most stable reference genes were chosen for each cell line; these were GAPDH and hATP5b for HepG2 cells and GAPDH and TOP1 for Huh7 cells. Pre-designed primer mixes for these genes were purchased from Primer Design (Southampton, UK) and used in PCR with LightCycler 480 SYBR-green Master Mix. For amplification of genes of interest the protocol was as follows: 95^{o}C for 10 minutes, 45 cycles of 95^{o}C (10 seconds), χ^{o}C (20 seconds, χ = annealing temperature) and 72^{o}C (10 seconds), followed by melt curve analysis (cooling to 65^{o}C followed by heating to 97^{o}C during which a continuous fluorescent reading is recorded) and a cooling step. For reference genes the protocol was as follows: 95^{o}C for 10 minutes, 35 cycles of 95^{o}C (15 seconds), 60^{o}C (30 seconds) and 72^{o}C (10 seconds), followed by melt curve analysis and a cooling step. All data was normalised to a geometric mean derived from the two appropriate reference genes. Coefficient of variation (CV) calculations were carried out for each assay to ensure

reproducibility using the first and second clone dilutions from standard curves which were repeated up to ten times. An average value for each clone dilution from each repetition was calculated, from which an overall mean and standard deviation was generated for each clone dilution. These values were used to generate a CV for each assay (standard deviation/mean) with a smaller value being representative of a more stable, consistent assay.

2.6 – Functional studies

2.6.1 – Hoechst 33342 experiments

Hoechst 33342 dye is effluxed from cells mainly by MDR1 and BCRP. The functionality of these transporters in cells can be investigated using inhibitors such as cyclosporin A (CSA, vehicle 100% methanol), verapamil (vehicle 100% ethanol) (both MDR1) and Ko143 (vehicle DMSO) (BCRP). Both confluent and 15 day 1% DMSO-treated HepG2 and Huh7 cells plus prolonged untreated Huh7 cells were subject to Hoechst 33342 accumulation experiments. Huh7 cells were grown on 24 well plates for confluent, prolonged untreated and DMSO Hoechst experiments. HepG2 cells were grown on 24 well plates for confluent experiments and on 12 well plates for 15 day 1% DMSO experiments, as a larger volume of medium was needed to sustain the cells than the 24 well plates could hold. Cells were treated with DMSO as previously stated.

For experiments, cells were washed with warm Krebs buffer and incubated for 30 minutes in Krebs with or without inhibitors (10 µM CSA, 100 µM verapamil or 10 µM Ko143) on a heating plate at 37^{o}C. Krebs containing Hoechst dye at concentrations ranging from 0.1 µM to 30 µM (vehicle water) was applied with or without inhibitors (matching those applied in the previous 30 minutes) for 60 minutes. Cells were then washed twice with ice cold Krebs buffer and lysed in lysis buffer (appendix A) for at least 30 minutes at 37^{o}C, harvested and collected. Fluorescence was measured in one of two ways; either in UV grade cuvettes (Fisher) and analysed in a Perkin-Elmer LS-5 luminescence spectrometer (Perkin Elmer, Massachusetts, USA) at excitation wavelength 360 nm and emission wavelength 480 nm or in black plastic 96 well plates (Sterilin, purchased through Fisher Scientific, UK) and analysed on a fluorescent plate reader (FLUOstar Omega, BMG Labtech, Germany) using excitation filter 355 ± 10 nm and emission filter 480 ± 20 nm. For analysis, background fluorescence measured in cuvettes or wells containing lysis buffer only was subtracted from sample readings. Protein concentration of each sample was determined using Bradford reagent and measured in 96 well clear plastic plates on a spectrometer at 595 nm (FLUOstar Omega, BMG Labtech, Germany). For each well, fluorescent data was normalised to protein concentration.

2.6.2 – Calcein-AM experiments

Confluent and 1% DMSO treated HepG2 and Huh7 cells were grown as described for Hoechst 33342 experiments. Calcein-AM is not fluorescent but is cleaved by cellular esterases into calcein, which does fluoresce. The uncleaved form, calcein-AM, is lipid soluble and is effluxed by MDR1 and MRP1. Calcein is not lipid soluble and is effluxed from the cell by MRP1 and MRP2. Verapamil at 100 µM was used to inhibit MDR1 and MRP1 function and MK571 (Sigma) at 20 µM was used to inhibit MRP1 and MRP2 efflux. All solutions were made in Krebs buffer and heated to 37^{o}C before use. All experiments were carried out on a heated surface. Cells were washed in warm Krebs and incubated for 30 minutes with 2 µM calcein-AM (vehicle DMSO) with or without MDR1 inhibitors (verapamil and CSA), washed with Krebs and incubated in 500 µl Krebs solution with or without inhibitors (verapamil, CSA and MK571). After 20 minutes either all Krebs solution was collected and kept for analysis in cuvettes or 200 µl was collected for analysis in 96 well plates with the remaining solution being removed and discarded. Warm Krebs buffer (with or without inhibitors) was added again and the process repeated. Solutions were collected at four time points (0-20, 20-40, 40-60 and 60-80 minutes) in order to minimise the influx of calcein back into the cells and to enable the rate of efflux to be calculated if necessary. After the final collection water was added, the samples were protected from light and left overnight to lyse at 4^{o}C. Lysed cells were harvested into 1.7 ml microcentrifuge tubes, centrifuged at 9660 xg for 10 minutes and the supernatant analysed for calcein fluorescence and protein content.

Fluorescent samples were analysed using optical grade cuvettes on a fluorimeter at excitation wavelength 492 nm and emission wavelength 518 nm, or on black plastic plates in a fluorescent plate reader with excitation filter 480 ± 20 nm and emission filter 520 ± 10 nm. Background fluorescence was subtracted from readings for all samples before analysis and corrected readings were normalised to protein concentration for each well. Before experiments were commenced, the effects of overnight storage on calcein fluorescence were assessed and it was determined to be stable while protected from light at 4^{o}C for at least 72 hours. Total calcein content was determined by adding efflux and lysate fluorescence values.

Calcein influx was assessed by loading the cells for 20 minutes with concentrations of calcein (vehicle water) from 0.2 µM to 2 µM in warm Krebs, representing 10% to 100% of calcein-AM cleavage. Cells were then washed twice with cold Krebs, lysed in water overnight and treated as previously described. Analysis of all samples and loading solutions was carried out on a fluorescent plate reader using black plastic 96 well plates. Protein levels were assessed using

Bradford reagent and read on a spectrometer. Background fluorescence was subtracted and data normalised to protein levels.

2.7 – Western blotting

Protein was extracted from HepG2 and Huh7 cells at confluence and at 10, 15 and 20 days of 1% DMSO treatment. Cells treated at confluence and for 15 days with 1% DMSO were treated with BNF at the same concentrations as previously described (section 2.3) and protein harvested. Cells were washed twice with ice-cold 1x PBS and incubated at 4^{o}C for 45 minutes with lysis buffer (recipe in appendix A). After being scraped and collected into 1.7 ml eppendorf tubes, samples were passed through a 25G needle three times, centrifuged at 9660 xg for 15 minutes and the supernatant collected, aliquoted and stored at -80^{o}C. Sample protein values were obtained by Bradford assay using a spectrometer at 595 nm. Protein concentration by acetone precipitation was carried out when necessary; this was done by adding acetone to the protein sample in a ratio of 1:4 (e.g. 25 µl acetone for every 100 µl of sample). This was incubated at room temperature for 20 minutes followed by centrifugation at 9660 xg for 15 minutes. Supernatant was discarded and samples air-dried for 5 minutes before being re-suspended in an appropriate volume of sample loading buffer (Invitrogen).

All reagents used in the process of Western blotting were from Invitrogen unless otherwise stated. Samples were thawed on ice; initially, maximum sample loading volume (13 µl) was used which was later refined to 20 µg of sample per well. Pre-cast NuPAGE Novex 4-12% Bis-Tris Gels (1.0 mm, 12 well) were used as per the manufacturer's instructions (NuPAGE technical guide, www.invitrogen.com). Denaturing conditions using SDS and reducing agents were applied and gels were run for 50-55 minutes at 200V. Transfer of the protein from gel to nitrocellulose membrane (0.45 µm pore, Invitrogen) was in a semi-dry transfer tank (OWL HEP-1, Thermo Scientific, USA), for 24 minutes at 20V, again as per manufacturer's instructions. Membranes were air dried for 30 minutes, re-wet in 1x PBS and incubated in Odyssey blocking buffer (Licor, Cambridge, UK) diluted 1:1 with 1x PBS at room temperature for 1 hour prior to addition of antibodies.

Antibodies used were as follows; transferrin (1:1000), GAPDH (1:1000 and 1:5000), ADPGK (1:500) (all Genetex, Texas, USA), UGT1A1 (1:30 D-16, Santa Cruz, California, USA), albumin (1:100 AbCam, Cambridge, UK), BCRP (1:50 BXP-21, Santa Cruz, California, USA), MDR1 (1:100 C219, Santa Cruz, California, USA) and actin (I-19, 1:2000 Santa Cruz, California, USA). Secondary IRDye antibodies were purchased from Licor as follows; donkey anti-rabbit IgG (680LT, red), goat anti-mouse IgG (680LT, red) and donkey anti-goat IgG (800CW, green). All

were used at 1:5000 dilution. All antibodies were diluted in blocking buffer with 0.1% Tween-20; secondary antibodies also had 0.1% SDS added. Membranes were scanned using an Odyssey Licor v1.2 and bands were quantified using ImageJ software (version 1.44p, http://imagej.nih.gov/ij). After use membranes were stored in 1x PBS at 4^{o}C until being air dried. Membranes were protected from light at all times after the secondary antibody had been added.

2.8 – Extraction of cells from umbilical cord blood

Umbilical cord blood was obtained from patients undergoing Caesarean section and kindly donated to us by Jola Weaver (Queen Elizabeth Hospital, Gateshead, UK and Newcastle University, UK) with full consent and ethical approval. The process of cell extraction is detailed below.

UCB was decanted into 50 ml Falcon tubes and diluted 1:1 with 1x PBS (maximum total volume of 35ml). Into a separate 50 ml tube, 15 ml of Biocoll Separating Solution (density 1.077 g/ml, Biochrom AG, Germany) was added and all of the UCB:PBS from one Falcon (35 mls) was decanted by pipetting so that the Biocoll solution remained as a separate layer in the bottom of the tube. This was centrifuged at 800 xg for 20 minutes with no brake applied at the end of the spin as this disturbs the layers formed. Following centrifugation, four layers should be apparent – from the top, serum; a small layer of cells; biocoll and finally red blood cells. The cell layer must be transferred to a new tube. Serum can be transferred with the cells but no Biocoll. At this point, cells were amalgamated into as few tubes as possible and centrifuged again at 800 xg for 10 minutes, this time with the brake on full. The supernatant was discarded and the pellet resuspended in 5ml of PBS; all cells were collected into one Falcon if not already in one tube, which was filled with PBS and centrifuged again at 800 xg for 10 minutes. Once again, the supernatant was discarded and the cells resuspended in PBS and counted. Cells can be seeded at this point; a typical seeding density is 15 x10^{6} cells in 5ml of media. However, the suspension contains all cells except red blood cells at this point, so platelets, white blood cells and so on are still present. If seeded these should detach within two weeks; if further separation is required before seeding, magnetic beads must be used.

Unfortunately UCB was only provided once. Cells were extracted and grown in 25cm^{2} flasks with either HepatoZYME plus 2% serum (10% serum for the first 3 days to help cells attach) or DMEM HEPES plus 10% serum. Cells were split at confluence using trypsin which proved to be too strong an agent and the cells did not thrive afterwards. This resulted in few cells surviving and no RNA could be extracted for analysis.

2.9 – Statistical analysis

Data is shown as mean ± SEM. Statistical analysis by one-way ANOVA with Dunnett's or Bonferroni's post test and using Student's T-test were also carried out with Prism. All graphs and statistics were produced using GraphPad Prism v5.00 (www.graphpad.com).

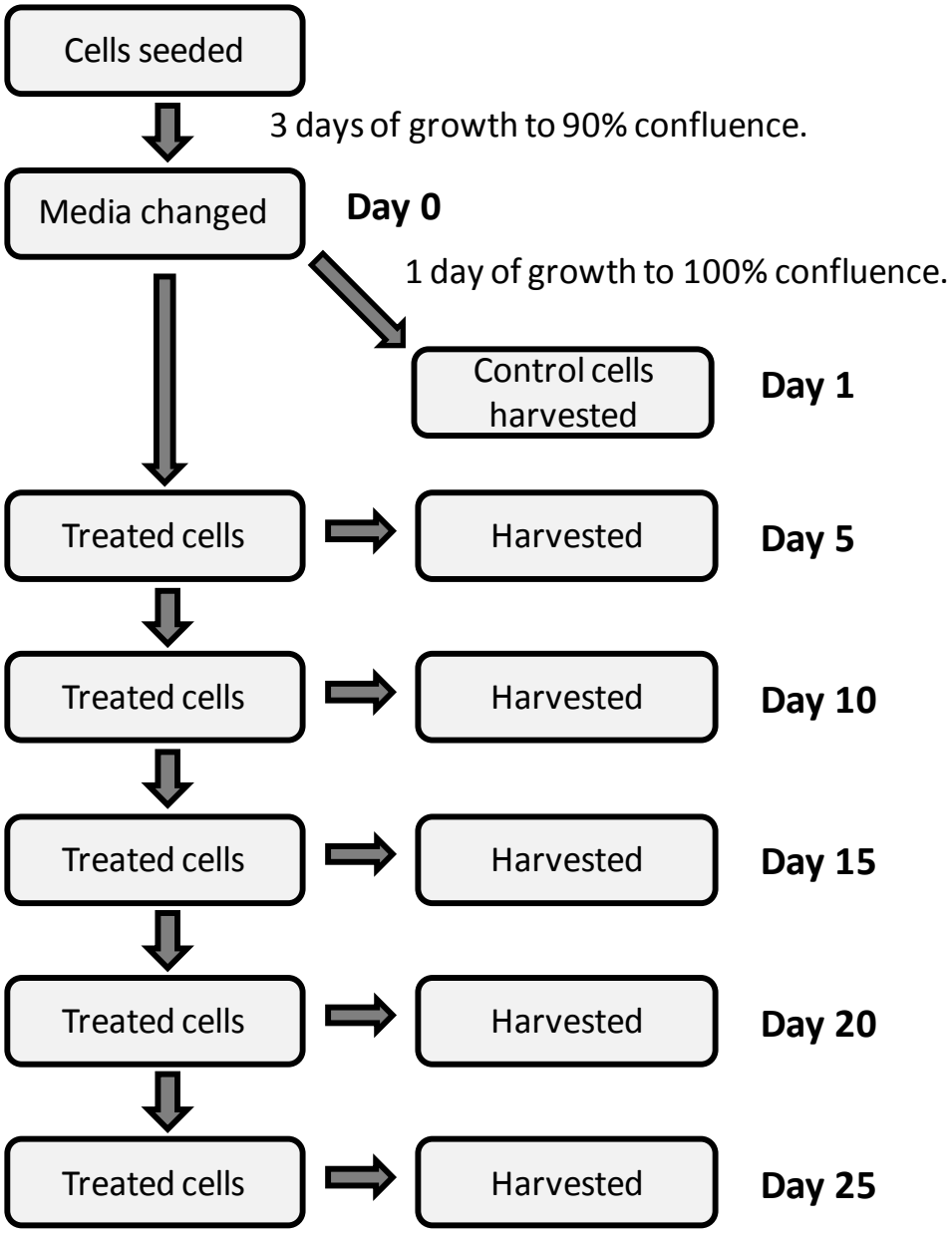

Figure 2.1 – **Experimental protocol for HepG2 cells.** Cells were seeded and grown in standard growth medium on six well plastic plates. On day 0 media was changed to either fresh standard growth medium (control cells) or growth medium plus the applicable treatment. Following this, media was replaced every two to three days. Cells were harvested at the indicated points for either protein or total RNA dependent on the experiment. Matched controls of untreated cells were not sustainable for the duration of the experiment, with widespread cell death due to overgrowth observed after 5 to 7 days.

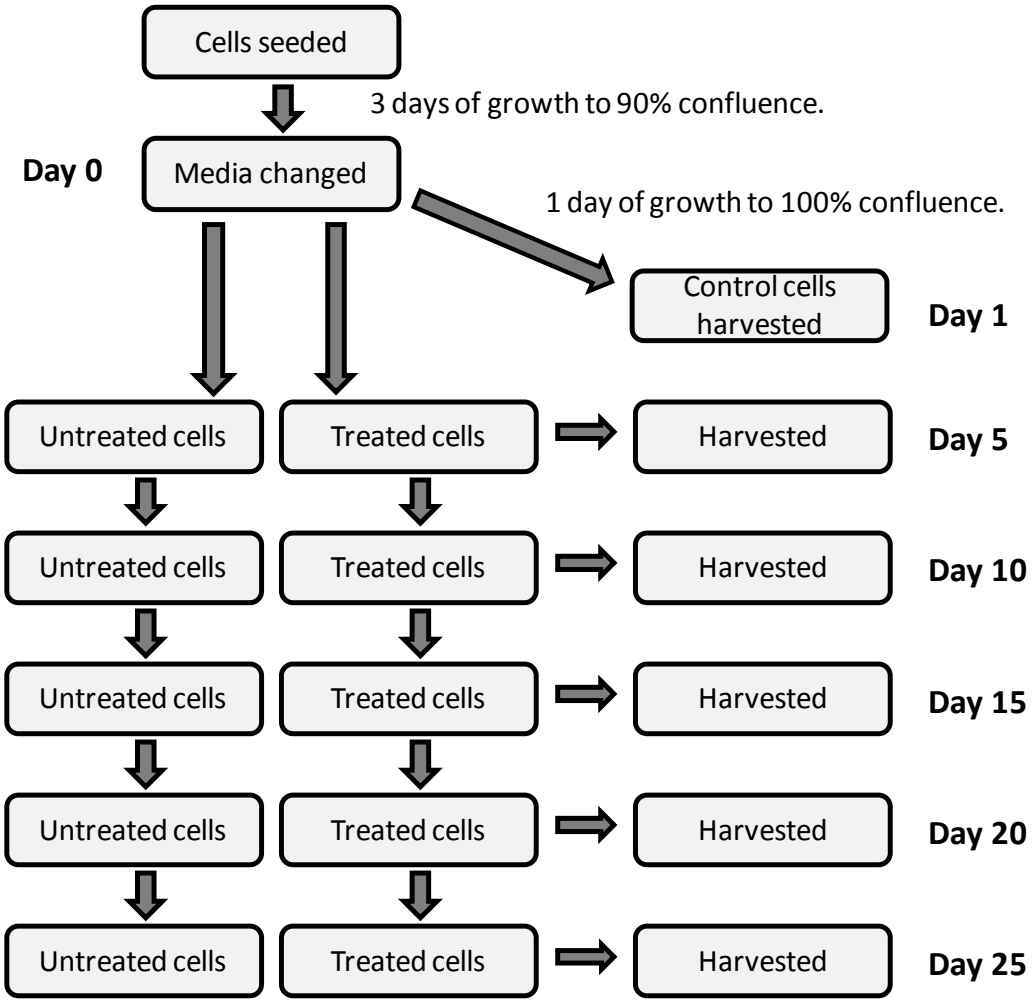

Figure 2.2 – **Experimental protocol for Huh7 cells.** Cells were seeded and grown in standard growth medium on six well plastic plates. On day 0 media was changed to either fresh standard growth medium (control and untreated cells) or growth medium plus the applicable treatment. Following this, media was changed every two to three days. Cells were harvested at the indicated points for either protein or total RNA dependent on the experiment. In addition to the control at confluence, matched controls of untreated cells grown in standard growth media were harvested at each time point of the experiment.

Chapter 3 – Characterisation of HepG2 and Huh7 cells: PCR assay development

Chapter aim: To develop quantitative PCR assays for a variety of differentiation markers, transporters and drug metabolising enzymes in order to characterise the hepatic carcinoma cell lines HepG2 and Huh7 relative to liver.

3.1 – Introduction

Hepatic carcinoma cell lines are known to have markedly different mRNA and protein expression profiles to those found in healthy *in vivo* hepatocytes. As well as being initially altered due to their carcinogenic nature, the repeated passaging necessary to maintain these cells *in vitro* is known to contribute to genetic drift, further changing the expression profile of transporters and enzymes.

The two human hepatocarcinoma cell lines being characterised in this chapter are HepG2 and Huh7. HepG2 cells are sometimes used in the pharmaceutical industry in the very early stage assessment of drug toxicity; however, these cells are known to be hugely different from *in vivo* hepatocytes in the expression and activity of a number of major enzymes and transporters (Sivertsson *et al.*, 2010; Ek *et al.*, 2007; Hilgendorf *et al.*, 2007; Olsavsky *et al.*, 2007; Westerink and Schoonen, 2007a; Westerink and Schoonen, 2007b; Elizondo and Medina-Diaz, 2003). A key example of this is the drug metabolising enzyme CYP3A4, which is reported to have expression levels 100-fold lower than both liver and primary hepatocytes in HepG2 cells at best; some variants of the cell line have no detectable CYP3A4 at mRNA or protein level (Sivertsson *et al.*, 2010; Olsavsky *et al.*, 2007). HepG2 cells have been extensively characterised by a large number of groups; however, due to the variability between the same cell lines when grown in different laboratories the HepG2 cells used here have been assessed for basal mRNA expression levels of several differentiation markers, enzymes and transporters.

Huh7 cells were isolated in 1982 and were found to excrete hepatocyte-specific plasma proteins such as albumin, transferrin and alpha 1-antitrypsin (Nakabayashi *et al.*, 1982). Recent studies have since reported a similar mRNA expression profile for hepatic markers, transporters and enzymes in these cells as in HepG2s (Sivertsson *et al.*, 2010; Olsavsky *et al.*, 2007). The mRNA expression profile of key transporters and enzymes in Huh7 cells used in these experiments has been examined due to both the lack of reported expression profiles and to characterise them under the conditions employed.

In order to characterise the cell lines in question the mRNA levels of several hepatocyte differentiation markers, transporters and enzymes were analysed. These genes of interest (GOI) were chosen to provide an overview of the maturation status of HepG2 and Huh7 cells at confluence in comparison to a human whole liver cDNA sample comprised of a pool of three human liver samples (37 year old Caucasian male, 64 year old Caucasian male, 70 year old Caucasian female; purchased from Primer Design, UK). Five markers of differentiation were selected for initial observations of differentiation status; these were albumin, transferrin, alpha-fetoprotein (AFP), serpin peptidase inhibitor, clade A, member 1 (SERPINA1 or alpha-1 antiproteinase, antitrypsin (A1AT)) and hepatocyte nuclear factor 4, alpha (HNF4a). These will be discussed in more detail later in this chapter and in chapter 4.

Both influx and efflux transporters along with phase I and II metabolising enzymes are vital for hepatic function; a selection of key genes were selected for characterisation by assessment of mRNA levels. Four influx transporters were selected; three from the solute carrier organic anion transporter family (OATPB, C and 8) and solute carrier family 22 (extraneuronal monoamine transporter) member 3 (OCT3) which transports organic cations into the cell. Members of the ATP-binding cassette (ABC) superfamily comprise the majority of efflux transporters in the hepatocyte and four were chosen for this study. These were multidrug resistance protein 1, also known as P-glycoprotein (MDR1, P-gp or ABCB1), multidrug resistance associated proteins 1 and 2 (MRP1 and 2, or ABCC1 and 2) and breast cancer resistance protein (BCRP or ABCG2).

Finally, several drug metabolising enzymes were chosen for analysis. These included three cytochrome P450 (CYP) enzymes, CYP1A2, 2E1 and 3A4 which are well known phase I metabolising enzymes and are critical for hepatic function. Phase II conjugating enzymes were also included for assessment – members of the glutathione S-transferase alpha (GSTA) family were assessed in two reactions, one specifically targeting GSTA4 and one which detected GSTA1, 2 and 5. UDP glucuronosyltransferase 1 family polypeptide A1 (UGT1A1) and flavin containing monooxygenase 3 (FMO3) were the other two enzymes assayed.

Quantitative PCR (qPCR) was chosen as the method to analyse basal mRNA levels of this range of differentiation markers, enzymes and transporters for several reasons. It is a high throughput analytical method, allowing large numbers of samples generated in subsequent experiments to be quickly assessed. Accuracy of quantification in each PCR assay can be verified by inclusion of a standard curve (Larionov *et al.*, 2005).

Within qPCR there are several choices to be made in the design of an assay. These include probe type, detection method, quantification method and data analysis. There are several

types of qPCR probes to choose from, some of which incorporate a fluorescent signal either as a primer or a probe. The simplest and one of the most commonly used detection systems available is the use of an intercalating dye which binds to double stranded DNA (dsDNA) whilst utilising standard primers; the SYBR green system is an example of this. When the SYBR green dye binds to dsDNA its fluorescence significantly increases, resulting in the fluorescent intensity increasing proportionally to the amount of dsDNA present. An advantage of this method is that multiple fluorophore molecules bind along the whole product rather than just a single primer or probe-bound fluorophore, allowing more sensitive detection of low expression products. SYBR green detection also allows for melting temperature (Tm) analysis which is important for verification of a single assay-specific product. A disadvantage of this method is that products of non-specific amplification are more likely to be detected and therefore carefully designed primer pairs and good quality reagents are essential.

Primer-based detection systems such as LUX fluorogenic primers (Invitrogen (www.invitrogen.com: D-Lux assays) incorporate a fluorophore bound to the 3' end of one primer in a hairpin structure. This hairpin effectively quenches the fluorescent signal so no separate quenching molecule is required; the fluorescent signal is slightly increased upon deformation of the secondary structure and increases significantly upon extension during PCR. An advantage of this system is that multiplexes composed of two or more assays can be conducted simultaneously by utilising fluorophores which emit fluorescence at different wavelengths; this method of detection also allows for Tm analysis. Disadvantages are that the assays are not as sensitive as SYBR green when detecting low level expression and the labelled primers are more expensive.

Finally, probe based detection methods such as the TaqMan® system utilise two primers alongside a probe with both fluorophore and quencher attached. The probe is designed to bind to the template between the two primers and as the Taq enzyme travels along the DNA during extension, the fluorescent reporter is cleaved from the probe and dequenched, resulting in an increase in fluorescence. As this detection method requires both primer pairs and a probe, assay design is more complex and usually more costly than the previous two methods. Advantages are also imposed by the necessary specificity of designing three binding elements rather than only two as this ensures more accuracy in product detection. As with the primer-bound assays, multiplexing here is possible if different fluorophores are employed.

Other choices in qPCR involve quantification method and analysis of the data. Two types of quantification, absolute and relative, are commonly used. Absolute quantification requires a standard with a known copy number and a robust assay which shows identical amplification

efficiencies between runs in order to extrapolate an exact copy number value for an unknown sample. Relative quantification assigns values to samples to enable comparison between them; this can be done either using the crossing point (CP) value (the cycle number at which fluorescence is deemed to be first significantly increased from background) or by using a standard curve to extrapolate relative abundance in arbitrary units rather than exact copy number. Absolute quantification is much more difficult to utilise and is more often employed in applications such as determining viral titre. For most instances relative quantification allows sufficient data to be collected to provide an answer to the question and is often the method of choice in gene expression studies. Data analysis for relative quantification depends upon which data output has been generated. If CP values are solely being used, the method of choice is PCR efficiency assessment, commonly referred to as $\Delta\Delta C_t$ quantification (Fleige *et al.*, 2006). Standard curve quantification of data has been shown to be a viable and arguably more simple alternative to this calculation, and despite its more common use in absolute quantification, there is no reason it cannot be employed in relative quantification assays (Larionov *et al.*, 2005).

With careful consideration of the positives and negatives discussed previously for all stages of qPCR assay design, several conclusions were reached regarding techniques best suited to this study. Firstly, SYBR green detection was utilised for all assays. This allows for detection of low expression genes of interest and is the most cost-effective option when designing and running multiple assays for a potentially large number of samples. This detection method also allows for generation of Tm data to ensure that a single product is being generated. Relative quantification of data was employed with a standard curve of positive controls generated by cloning of PCR products; derivation of absolute copy number is unnecessary here. A standard curve was used over $\Delta\Delta C_t$ calculations to extract data as it is simple, minimising the opportunity for mistakes to occur, and the generation of the standard curve allows efficiency of the PCR reaction to be accurately assessed as well as being an automatic inclusion of a positive control for use in Tm analysis.

When designing primers for use in qPCR it is recommended to aim to generate products which are around 100 base pairs in length to ensure that the whole product is amplified in every cycle thus improving PCR efficiency. This is also important as in assays utilising SYBR green the fluorescence reading is taken at the end of the extension step in each cycle; this is how the amount of DNA is quantified and an accurate assay will not be produced if whole length PCR products are not guaranteed. It is also beneficial to design the primers so that an exon-exon boundary is encompassed where possible. As these assays are aiming to quantify mRNA levels, genomic DNA (gDNA) amplification must be avoided. Although a DNase step was included in

the sample generation process to eradicate gDNA, the PCR environment is intentionally ideal for amplification so any small amount of gDNA remaining could interfere with the true results. Inclusion of an exon-exon boundary within a primer minimises the chance of it binding to gDNA as the binding site itself will be interrupted by an intron. Where the exon-exon boundaries occur within the product but between primers, amplification from gDNA rather than cDNA will be clear due to the much larger product, which can be seen in end point PCR as a larger band on the gel, and in qPCRs utilising SYBR green as a second product with a different melting temperature to that of the correct product. Conditions of the PCR can also be altered to ensure that genomic amplification does not occur, such as keeping the extension time relatively short. For example, a Taq polymerase which amplifies at a rate of 25 base pairs per second coupled with an extension time of 10 seconds allows for an amplicon 250 base pairs in length to be produced, which would eliminate effective gDNA amplification if the target sequence spanned an intron greater than this in size.

In order to ensure that the correct PCR product was being amplified, products from all primer pairs were cloned and sequenced as described in chapter 2. Briefly, sequence fragments were amplified from HepG2, Huh7 and whole liver cDNA by end point PCR, separated on an agarose gel and the products excised. Products were eluted from the gel and pooled to ensure enough template was recovered to allow cloning. Clones were produced and purified and the insert was sequenced from at least two clone preparations. Sequencing results are shown in the figures of this chapter (figures 3.1 – 3.20), along with end point PCR and qPCR assessment of GOI mRNA levels in HepG2 and Huh7 cells and human whole liver cDNA for comparison. Once clones had been produced and verified they were used in qPCR to create the standard curves for assay verification. This served two purposes; the range of standards was much wider than could be produced using cDNA generated from experimental samples and so could be altered to encompass crossing points (CPs) of the samples in order to produce a relevant standard curve, and the melting point analysis at the end of the PCR allows verification of the correct product being amplified. Each standard curve was run several times, at which point the suitability of the assay was evaluated by looking at the calculated efficiency and error of the amplification. These are generated by the inbuilt Lightcycler 480 software (version 1.4.2) by comparing dilution factors assigned to samples identified as standards and assessing them with regard to the recorded CP value. These data are used to assess whether a doubling of the product occurs with each cycle – the software gives a standard curve showing an exact doubling a value of 2, with numbers above or below this representing more or less template being generated with each cycle. Error values are calculated both from replicates within the standard curve and from variation of points on the curve from the overall efficiency calculated.

If efficiency is consistently around 2 with a small error margin, the amount of DNA in the PCR is doubling in every cycle which is what would be expected in a truly exponential reaction. Values outside the range 1.7-2.3 can be potentially improved upon by altering variables such as annealing temperature and primer concentration.

Melting point analysis functions by slowly heating the final PCR products up to 95^{o}C whilst constantly taking a fluorescence reading in each well – this cannot be utilised with all qPCR systems and is an advantage of using SYBR green as a fluorescent probe. This heat causes the secondary structures within the DNA to deform and the double stranded DNA to become single stranded. In qPCR assays using SYBR green the fluorescence of the probe is maximal when bound to double stranded DNA. The failing of secondary structure results in a decrease in fluorescence which occurs at a specific temperature and is diagnostic for the product of a PCR amplification generated using a specific set of primers. For this reason, a positive control in the form of a diluted sample of the cloned PCR product was included in every qPCR assay so verification of the PCR product from each sample could be performed. This is especially crucial if non-specific amplification such as primer-dimer formation occurs. The inclusion of a positive control also helps to assess whether each assay is performing as expected in terms of efficiency; a control which is suddenly significantly different from previous runs points to an error in that particular plate and if this occurred was repeated.

To analyse qPCR data for the GOI, reference gene levels must be quantified in every sample. A reference gene is one that has constant, stable expression in the cell regardless of treatment or growth stage. Historically only one reference gene was used, often GAPDH, 18S ribosomal RNA or β-actin. However, this method has been proven to be less accurate than the use of multiple reference genes which have been tested and selected for each applicable cell line (Gutierrez *et al.*, 2008). Assessment of reference gene suitability for HepG2 and Huh7 cells was carried out using the geNorm software ((Vandesompele *et al.*, 2002), website medgen.ugent.be/genorm/), which allows determination of the required number and the most stable high and low expression reference genes from a panel of at least six primer pairs.

This chapter outlines the process of assay design for each GOI used in qPCR experiments in subsequent chapters. Included are the details of primer sequences, exon positions, sequences of the inserts in clones created for validation, and both end point and qPCR assessment of mRNA levels in whole liver cDNA and confluent HepG2 and Huh7 cells.

3.2 – Methods

Collection and processing of RNA samples from six-well plates for both cell lines was executed as described in materials and methods (chapter 2.4). End point PCR assays were developed and products analysed by gel electrophoresis and characterised by cloning and sequencing; from these qPCR assays were developed and evaluated using SYBR green fluorescence on a Roche LightCycler 480. Pre-designed reference gene primers and human whole liver cDNA were purchased from Primer Design. LightCycler 480 SYBR Green 1 Master mix (Roche) was used in all assays.

3.3 – Results

3.3.1 – Primer design

All primer sets incorporate an exon-exon boundary either in the forward or reverse primer or within the product between primers with three exceptions. OATP8, CYP3A4 and UGT1A1 assays all have both forward and reverse primers located on the same exons. The OATP8 assay was already in use and validated within the laboratory; in the latter two cases this was unavoidable. The CYP3A family includes CYP3A4, A5, A7 and A43; these are very closely related with amino acid homologies within a subfamily typically over 55% (Nelson *et al.*, 1996) and so it was difficult to design primers which only detect one family member. As a result several primer pairs were tested before finding ones which uniquely bound to CYP3A4 and the less desirable single exon binding and 200bp+ product length were overlooked in favour of the specific product. The UGT1A family has nine members that each have a unique first exon followed by four common exons. This made it necessary to design primers to anneal to the first exon only. GSTA primers were initially designed to anneal only to GSTA1; however, after cloning and sequencing it was found that products from GSTA1, 2 and 5 were generated and it was decided that the cumulative information from these three genes would be useful to this analysis.

3.3.2 – End point PCR

End point PCR assays were executed as described in chapter 2.5 using cDNA from confluent HepG2 and Huh7 cells along with a purchased whole human liver cDNA sample. In all assays the end point PCR showed only one band with occasional instances of faint primer-dimers being observed where there was low gene expression in template cDNA. An example of this was the CYP3A4 assay, where more primer-dimer was observed with HepG2 and Huh7 template cDNA due to the lesser amount of target cDNA present. Product band sizes ranged

from 54 to 226 base pairs, with specific band sizes identified for each assay in figures 3.1 to 3.20. The bands were excised and pooled before being cloned and sequenced. As the qPCR cycling protocols differ from those used in end point PCR, primer-dimers are not certain to form if they are seen in end point PCR and so this was not considered a reason to re-design assays unless very strong non-specific bands were produced.

3.3.3 – Sequence and BLAST results

Two clones for each assay were sequenced externally (Cogenics, Essex, UK) and the results are displayed in figures 3.1 to 3.20. Each clone was analysed using the Basic Local Alignment Search Tool (BLAST) (http://blast.ncbi.nlm.nih.gov/Blast.cgi) which searches for areas of similarity between the input sequence and NCBI reference sequences. The alignment output from this service is shown as part E in all of the figures in this chapter and reveals any mismatches between the input and reference sequences. Occasional mismatches can be seen in a few of the alignments, probably due to PCR or sequencing errors or polymorphisms, however none of these are registered in the NCBI SNP database as being known SNPs (Single Nucleotide Polymorphisms). As these mismatches do not occur in more than one or two positions per product they do not significantly affect overall specificity of the cloned sequence. BLAST outputs also show which reference sequences a particular clone matches. In order to be a valid assay, PCR products must only match to the desired sequence or sequences. In the case of the assays assessed here, all PCR products only matched with the appropriate reference sequences – in most cases this is just one sequence. In the case of the GSTA primers (figure 3.17) the product matched to all three expected genes (GSTA1, 2 and 5).

In cases where the pooled end point PCR samples used to generate the clone had a much stronger product band in liver than in the cell lines, it is likely that the clones analysed have an insert from only the liver cDNA. By including melting point analysis, it was possible to confirm that even though the sequence may represent only one source of cDNA, the products generated during PCR for other templates were correct.

3.3.4 – qPCR assay validation

For all assays a standard curve generated using serial dilutions of the cloned PCR products was run on multiple occasions. Very little optimisation was required whilst developing these assays as the LightCycler 480 SYBR Green I mastermix was developed to allow for ease of use with most templates and primers. Occasionally a slight alteration in annealing temperature was necessary to eliminate non-specific amplification. Once an assay produced consistent results over several runs as determined by coefficient of variation (CV) calculations (table 3.1, method

of calculation as described in chapter 2.5) to show variation between runs was less than 10% and replicates of samples within runs were within 10% of each other, the assay was deemed suitable to use. From that point onwards one representative standard curve was selected for calculating sample concentrations in every subsequent run of that assay. Two clone dilutions corresponding to points on the standard curve were included on every plate as positive control samples. Data from the relevant standard curve are displayed in part F of each figure. These show efficiency and error values along with the range of values seen in melting temperature analysis. The melting temperatures are typically within 0.5^{o}C of each other across the plate. The diagram of melting temperatures generated from the qPCR assay is shown in part G of each figure. Most assays typically show one peak indicating amplification of a single product, for example as shown in figure 3.1 for albumin. Some assays show an additional smaller peak at a lower melting temperature than the main peak; this usually indicates the presence of primer-dimer in the reaction product; an example of this can be seen in figure 3.16 for CYP3A4. The presence of primer-dimers is not a problem if it is occurring in negative reactions as seen for CYP3A4, where it is clear that any sample which has the lower Tm peak does not also have a major peak known to be the correct product. Occasionally other unidentified peaks were also seen, such as those in figures 3.10 and 3.19 (OCT3 and UGT1A1). If this occurred, the relevant samples were identified from the data output, excluded from analysis and repeated at a later date. Usually samples which were repeated for this reason produced a similar result during the second analysis and further inspection regarding levels of reference genes revealed lower mRNA levels throughout the expression profile, which resulted in some non-specific amplification in low expression GOI assays. The few samples in which this occurred were excluded from analysis.

For each cell line a high and low expression reference gene was chosen; GAPDH (glyceraldehyde-3-phosphate dehydrogenase, NM_001082253) and hATP5b (ATP synthase, H^{+} transporting, mitochondrial F1 complex, beta polypeptide, NM_001686) in HepG2, and GAPDH and TOP1 (topoisomerase (DNA) I, NM_003286) in Huh7. GAPDH and hATP5b reference genes were used to normalise whole liver cDNA. When all data had been collected for a specific sample, that from the two reference genes were used to determine a geometric mean; the data from the gene in question were divided by this geometric mean in order to take into account the amount of cDNA originally in the sample. This process was applied to all data presented in this and the following chapters. Graph H on all figures in this chapter shows the results from qPCR assays comparing these normalised values for a whole liver cDNA sample and samples from each cell line extracted from confluent cells. Confluence was reached after four days of growth as defined in figures 2.1 and 2.2 for HepG2 and Huh7 cells, respectively.

In all assays reverse transcription (RT) controls containing no reverse transcriptase enzyme were included in the qPCR as well as being tested by end-point PCR to ensure that no gDNA was present in the initial RNA samples. This was especially important in the three assays that have both primers on the same exon, where it is possible for gDNA to be amplified and unidentified by melting point analysis. RT negative controls and negative controls containing water plus qPCR mastermix were always a minimum of five cycles away from sample results; failing this the plate or individual samples were repeated at another time. Melting temperature analysis was always performed for every sample and compared to the positive control; any samples which did not match the positive control were excluded to be repeated at another time as this indicates non-specific amplification. As stated previously, this rarely occurred and was usually observed in samples which had low overall mRNA expression combined with an assay for a low expression GOI, in which case repetition produced a similar result and the sample was excluded from analysis.

3.3.5 – Summary of gene expression

Table 3.2 shows basal expression of all GOI in confluent HepG2 and Huh7 cells expressed relative to liver (liver = 1). These data have been calculated from qPCR results (graph H) shown in figures 3.1 to 3.20 in this chapter. The cell lines are represented by data compiled from two experiments at passages 73 and 75 for HepG2 cells and 6 and 11 for Huh7 cells. All data have been normalised to two reference genes as described. It is clear that the majority of genes assessed have lower mRNA levels in both HepG2 and Huh7 than in liver. Albumin and transferrin mRNAs were lower in both cell lines than liver and transferrin levels appeared comparable in HepG2 and Huh7 cells; albumin mRNA was slightly higher in HepG2 cells than in Huh7 cells but still 19-fold lower than in liver. Alpha fetoprotein mRNA levels were much higher in HepG2 cells (93-fold) than in liver and 19-fold greater in Huh7 cells in comparison to liver. Alpha-1-antitrypsin mRNA was only 6-fold reduced in HepG2 cells but almost 30-fold lower in Huh7 than in liver, while HNF4a mRNA levels were largely similar to liver, with approximately 2-fold greater and 2-fold lower levels seen in HepG2 and Huh7 cells, respectively.

Of the influx transporters assessed, MRP1 mRNA showed the largest variation from liver. Approximately 2100-fold greater expression was seen in HepG2 cells compared to liver while in Huh7 cells expression was 89-fold greater, which while not as dramatic is still highly over-expressed in comparison to liver. MRP2 mRNA levels were largely similar to liver in HepG2 cells (1.6-fold greater), while Huh7 cells were 12-fold lower. HepG2 cells also showed relatively similar levels of MDR1 and BCRP mRNAs, being 2.7-fold greater and 2.8-fold lower,

respectively. Huh7 cells were more removed from liver for these two transporters, having 5.6- and 21-fold lower MDR1 and BCRP mRNA levels, respectively.

mRNA levels of four influx transporters OCT3 and OATPB, C and 8 were also measured. HepG2 cells showed relatively similar levels of OCT3 and OATPB mRNA with 1.4-fold and 4.8-fold decreases compared with liver, respectively. However, OATPC and 8 mRNA levels were much lower in comparison to liver; 51000-fold and 19000-fold lower, respectively. In Huh7 cells the genes closest to liver in expression levels were OATPB and 8, which were 11- and 82-fold lower, respectively. OCT3 mRNA levels were 24-fold decreased and OATPC mRNA 363-fold decreased in Huh7 cells in comparison to liver.

Of the phase I and II drug metabolising and conjugating enzymes assessed, only GSTA and GSTA4 mRNAs in HepG2 cells show levels approaching those in liver (6.2-fold and 1.6-fold lower, respectively). In Huh7 cells both transcripts were much lower than in HepG2 – GSTA mRNA was 357-fold lower while GSTA4 mRNA showed a 13-fold decrease from liver. All three of the cytochrome P450 enzymes (CYP1A2, 2E1 and 3A4) showed much lower mRNA levels than liver in each cell line. For example, the closest in expression to liver levels was CYP1A2 mRNA in Huh7, which was decreased by 44000-fold. A similar situation was seen with UGT1A1 and FMO3 mRNAs with extremely large decreases from liver seen in both HepG2 and Huh7 cells.

3.4 – Discussion

The information included in the figures of this chapter is as required in the MIQE guidelines (Bustin *et al.*, 2009), which outline the minimum information required for publication of qPCR experiments. Primers were designed as per the specifications outlined in the introduction to this chapter where possible, which was the case in the majority of assays. End-point PCRs were optimised and products were cloned and sequenced. All products were proved to be specific to the desired genes bar a few sequencing errors, which did not introduce any similarity to other genes when subjected to BLAST analysis. Parameters for standard curve variables for all assays were within acceptable limits and assays all amplified only a single product, with some rare instances of primer-dimer seen in negative controls. CV values for each assay showed variation below 10% when all values were taken into account (table 3.1 part A) and little difference was observed in the CV recorded for clone dilutions 1 and 2. Changes in CV over time are displayed in table 3.1 part B for both clone dilutions and no significant differences were seen between runs 1-5 and 6-10 in either dilution. Sample dilution series for high, medium and low expression GOI (figure 3.21, albumin, BCRP and CYP2E1 assays respectively)

revealed that dilutions of RT products of 1:30 for high expression genes and 1:3 for medium and low expression genes were acceptable as exponential increases were seen at these points. In conclusion, these qPCR assays are validated sufficiently to allow use in further analysis of experimental samples.

This preliminary work allowed an approximate comparison of mRNA levels of genes of interest between the two cell lines used and a human liver sample. Although the comparison with human liver rather than hepatic cells alone does have its limitations, it remains a useful indicator of cellular maturity. Hepatocytes make up approximately 65% of the cells in the liver and occupy 80% of the cellular volume (Gebhardt, 1992). However, the bi-nuclear nature of a proportion of hepatocytes means that in terms of DNA abundance, the hepatocyte contributes approximately 69% of the DNA found in a sample of whole liver (Carlile *et al.*, 1997). This suggests that whilst a sample of whole liver is not ideal, it will provide an indication of hepatic expression within the liver. The fact that this liver sample is comprised of three donors which include a wide age range and both genders also contributes to its suitability as an indicator of hepatic expression in the population. Of course, ideally comparisons would be drawn with an isolated hepatocyte population from a large number of donors but in reality these would be difficult and costly to obtain. In a study such as this where an overview of hepatic maturity is required a definitive hepatocyte-only sample is not essential. If this preliminary data was to indicate much improved hepatic expression in these carcinoma cell lines, a truly hepatic sample would be vital to continuing the investigation.

The five markers of differentiation analysed in this chapter, albumin, transferrin, AFP, A1AT and HNF4a have given a picture of the differentiation status of these cells which will be discussed further in later chapters. Comparison of this data with other papers describing relative mRNA levels of these genes draws a similar picture, but with some notable differences in magnitude of change from liver to cell line. Albumin mRNA is reported to be lower in HepG2 cells than in liver by anything from 1000- to 10-fold (Sivertsson *et al.*, 2010; Ek *et al.*, 2007) and 4-fold higher than liver by Olsavsky *et al.* (Olsavsky *et al.*, 2007). Huh7 cells have been reported as having albumin mRNA levels from 100- to 2-fold lower than liver (Sivertsson *et al.*, 2010; Olsavsky *et al.*, 2007). This range of changes does fit with those observed here, with levels 19-fold and 27-fold lower than liver in HepG2 and Huh7 cells, respectively. Transferrin has been verified as a useful marker of hepatic differentiation in several publications (Page *et al.*, 2007; Hengstler *et al.*, 2005; Sidhu *et al.*, 2004; Raul Cassia, 1997) but has not yet been analysed relative to liver. Results found here indicate that both HepG2 and Huh7 cells express transferrin mRNA at levels approximately 10-fold lower than liver. AFP is a well known indicator of reversion to a more foetal rather than adult liver state (Page *et al.*, 2007; Snykers

et al., 2007) and has been shown to be around 100,000-fold higher in both HepG2 and Huh7 cells than in liver (Olsavsky *et al.*, 2007). The results obtained here agree that AFP is increased in both cell lines but not to such extremes as this; data indicate that HepG2 and Huh7 are 92-fold and 18-fold higher than in liver respectively, showing Huh7 cells to be closer to liver expression. A1AT mRNA is described as being between 100- and 10-fold lower than liver in both HepG2 and Huh7 cells (Olsavsky *et al.*, 2007), which is approximately the same as seen here. Huh7 cells had a 29-fold decrease in expression relative to liver, while HepG2 cells are closer to liver with only a 6-fold decrease. The final differentiation marker, HNF4a, has been reported to have equal expression in liver and Huh7 cells (Sivertsson *et al.*, 2010; Olsavsky *et al.*, 2007) and in HepG2 cells to be between that of liver and a 10-fold reduction (Sivertsson *et al.*, 2010; Ek *et al.*, 2007; Olsavsky *et al.*, 2007). Data here show approximately 2-fold greater levels in HepG2 cells than in liver and 2-fold lower levels in Huh7 cells; neither of these is better than the other with regard to similarity to liver expression. Taking into consideration all five differentiation markers measured here, neither cell line appears to be more hepatocyte-like than the other.

Four influx transporters, MRP1, MRP2, MDR1 and BCRP were assessed for expression in HepG2 and Huh7 cells and compared to liver. MRP1 has been reported to be up to 10-fold higher in HepG2 cells than in liver and only slightly increased from liver in Huh7 cells (Hilgendorf *et al.*, 2007; Olsavsky *et al.*, 2007). However, the data obtained here shows a much larger increase in both cell lines, with expression over 2000-fold higher in HepG2 cells and around 89-fold higher in Huh7 cells. Although Huh7 expression is closer to that of liver, it is still an extremely large increase and if it is mirrored by an increase in functionality would be expected to drastically alter the efflux function of the cell. MRP2 is reported to have expression either comparable to or 10-fold lower than liver in both cell lines (Sivertsson *et al.*, 2010; Ek *et al.*, 2007; Olsavsky *et al.*, 2007). Data here agree with the literature, showing a very slight increase in HepG2 MRP2 mRNA expression and a 12-fold decrease in Huh7 cells compared to liver. MDR1 mRNA is reported to be expressed either at levels seen in liver or up to 10-fold lower in both HepG2 and Huh7 cells (Sivertsson *et al.*, 2010; Ek *et al.*, 2007; Hilgendorf *et al.*, 2007; Olsavsky *et al.*, 2007). Data obtained here show an increase of 2.6-fold in HepG2 cells, while Huh7 cells express MDR1 mRNA at levels approximately 5-fold lower than liver; again, both are close to previously reported levels. BCRP mRNA levels are reported to be slightly lower than liver in HepG2 cells (Hilgendorf *et al.*, 2007); data comparing Huh7 cells to liver have not been published. Data obtained here indicate that HepG2 cells are the closest of the two to liver in terms of BCRP mRNA expression, with HepG2 having 2-fold lower and Huh7 21-fold lower transcript levels in comparison to liver. Overall, Huh7 cells are probably the most suitable

system for efflux analysis in an hepatocyte-like system as neither of the major drug-resistance conferring proteins, MDR1 and MRP1, are over-expressed; however, Huh7 remains a less than ideal model for hepatic efflux transporters.

Expression levels of four influx transporters were analysed – OCT3 and OATPB, C and 8. OCT3 is reported to have approximately equal mRNA expression in liver and HepG2 cells (Hilgendorf *et al.*, 2007; Olsavsky *et al.*, 2007) while Huh7 cells have been shown to express OCT3 at levels approximately 4-fold lower than those seen in liver (Olsavsky *et al.*, 2007). Data obtained here agree with predictions for HepG2 cells which show a small reduction of 1.4-fold from liver but Huh7 cells expressed OCT3 mRNA approximately 124-fold lower than levels seen in liver, a much lower figure than expected. OATPB mRNA is reported to be expressed in Huh7 cells at 3-fold lower levels than in liver (Olsavsky *et al.*, 2007), which is slightly higher than results obtained here that show 11-fold lower OATPB mRNA expression. HepG2 cells are variable in their expression of OATPB mRNA, with one paper reporting similar expression to liver (Hilgendorf *et al.*, 2007) and another stating that no transcript at all could be detected (Olsavsky *et al.*, 2007); data here suggests a 4.8-fold lower expression than in liver. OATPC and 8 transcripts are both reported to be much lower in HepG2 cells than in liver (Hilgendorf *et al.*, 2007) and in two publications OATPC is said to be undetected at mRNA level (Sivertsson *et al.*, 2010; Ek *et al.*, 2007). Huh7 cells are also reported to have no detectable OATPC transcripts (Sivertsson *et al.*, 2010), while no data are available at this time for comparison of OATP8 expression in liver. mRNA was detected for both OATPC and 8 in both cell lines here, although in HepG2 cells this was at a very reduced level; expression of mRNA stood at 51000- and 19000-fold lower than liver for OATPC and OATP8, respectively. Huh7 cells also showed reduced expression of these transcripts, although they were markedly higher than levels observed in HepG2 cells. OATPC mRNA expression was approximately 363-fold lower than that in liver, while OATP8 mRNA expression was 82-fold lower than seen in liver. Overall, neither cell line appears improved over the other in expression of influx transporters, with HepG2 closer to liver in expression of OCT3 and OATPB and Huh7 closer to liver expression of OATPC and -8, albeit at substantially reduced levels.

Cytochrome P450 enzymes are responsible for a large proportion of drug metabolism within the cell. Three CYP enzymes have been quantified here – CYP1A2, 2E1 and 3A4, all of which have low expression in HepG2 and Huh7 cells. Both HepG2 and Huh7 cells are reported to have either no or very low (over 1000-fold lower than liver) CYP1A2 expression (Sivertsson *et al.*, 2010; Ek *et al.*, 2007; Olsavsky *et al.*, 2007). Data here show CYP1A2 mRNA as being $1.4x10^{6}$-fold lower than liver in HepG2 cells and $4.4x10^{4}$-fold lower in Huh7 cells, so although Huh7 cells do show the higher expression level of the two cell lines, levels are still extremely reduced

relative to liver – both of these figures agree with previously published data. CYP2E1 mRNA expression in HepG2 cells is reported to be either undetectable or over 1000-fold reduced from liver (Sivertsson *et al.*, 2010; Ek *et al.*, 2007; Olsavsky *et al.*, 2007). In Huh7 cells estimates range from 400-fold to over 1000-fold decrease relative to liver expression (Sivertsson *et al.*, 2010; Olsavsky *et al.*, 2007). Data obtained here suggest that transcript levels for both cell lines are extremely low, with HepG2 and Huh7 cells having a $2.6x10^6$-fold and a $1.9x10^6$-fold decrease respectively. Published data available for CYP3A4 record HepG2 cells as having anywhere between 100-fold and over 1000-fold decrease from liver (Sivertsson *et al.*, 2010; Ek *et al.*, 2007; Olsavsky *et al.*, 2007) and Huh7 cells as having either undetectable mRNA levels or expression 1000-fold lower than seen in liver (Sivertsson *et al.*, 2010; Olsavsky *et al.*, 2007). From results obtained here, CYP3A4 mRNA levels appear very low in both cells lines, with HepG2 showing expression $1.2x10^5$-fold lower than liver and Huh7 cells with expression $3.1x10^5$-fold lower than those seen in liver, values which agree with data in the literature. Neither cell line could be considered closer to hepatocyte-like expression of these three CYP enzymes as levels are so severely reduced from those *in vivo* that any differences are not likely to be physiologically relevant and would not be useful in measuring drug metabolism in any potential drug development model.

As well as the phase I CYP enzymes several phase II metabolising enzymes were assessed for mRNA levels relative to liver. The GSTA mRNA assay which assesses levels of GSTA1, 2 and 5 expression shows HepG2 cells as having mRNA levels 6-fold lower than that of liver, while Huh7 cells have much lower expression with a 350-fold decrease relative to liver. Data specific to GSTA1 mRNA levels in these cell lines have been published and show that HepG2 cells have around 3-fold lower expression than liver with that in Huh7 cells approximately 50-fold lower than liver levels (Olsavsky *et al.*, 2007) – here mRNA levels in HepG2 cells were very close to published data but in Huh7 cells much lower levels of expression were found than stated in the literature. Published data for GSTA4 mRNA levels are not available; data here show that HepG2 expression is very similar to that in liver, with only a 1.6-fold decrease observed. Huh7 cells showed a 13-fold decrease relative to liver levels and so is further away from the ideal than HepG2; however, bearing in mind the extremes which have been observed in previous assays this still seems comparatively close to liver levels. Published data for the UGT1A family of enzymes show mRNA expression in HepG2 cells as over 1000-fold lower than in liver and in Huh7 cells as between 100- and 1000-fold decreased relative to liver (Sivertsson *et al.*, 2010; Ek *et al.*, 2007). The data obtained here specifically relate to UGT1A1 mRNA rather than the whole family and show a 2800-fold decrease in expression in HepG2 and a 1000-fold decrease in Huh7 cells, both of which agree with previously published data. Finally, for FMO3 there are

no published data for analysis; data here show extreme decreases from liver mRNA levels in both HepG2 and Huh7 cells, which have a $4.6x10^{9}$-fold decrease and a $3.9x10^{5}$-fold decrease in expression respectively. HepG2 cells appear to be more useful in assessment of GSTA functions, whereas Huh7 cells have more hepatocyte-like expression of UGT1A1 and FMO3 although both are expressed at levels far lower than those seen *in vivo.*

The variation observed between reported levels of mRNA in the literature and levels observed here are quite marked for some GOI; for example, albumin mRNA levels in HepG2 cells are reported as being anywhere from 1000-fold lower to 4-fold higher than liver. These differences between cells which are identically named are important in a project such as this where differentiation to a more hepatic profile is the aim, as basal levels of genes and thus the starting point is potentially very variable. These differences could be due to variations in culture conditions, plating density and passage number to name a few. For example, HepG2 cells used here were cultured in high glucose DMEM with 10% FCS, 1% glutamine, 1% NEAA and penicillin/streptomycin. Sivertsson *et al.* (Sivertsson *et al.*, 2010) cultured HepG2 cells in DMEM with 10% heat inactivated FCS, NEAA, penicillin/streptomycin and 1mM sodium pyruvate, while Olsavsky *et al.* (Olsavsky *et al.*, 2007) used DMEM with 10% FCS, 0.1mM NEAA, penicillin/streptomycin, 10mM HEPES and 1mM sodium pyruvate. These are but two examples from the literature; many other papers for both HepG2 and Huh7 cells describe culture conditions with very slight differences from each other which could potentially affect basal expression of some or all genes and result in the variable results published in the literature. Details of other variables are not so easily extracted from the literature such as source and batch of foetal calf serum used, frequency of mycoplasma testing (carried out periodically on cells used here), number of passages the cells were grown for after removal from liquid nitrogen stocks before commencement of experiments and intervals between feeding and passaging the cells. Genetic drift of cells can also become a factor if the passage number of cells used is high, particularly in carcinoma-derived cell lines, which can result in an expression profile differing from that in the original ATCC cells. All of these could affect cellular phenotype and lead to the variations in expression described here. Evidence that HepG2 cells do have the potential to form distinct subtypes is seen in the existence of the clonal cell line HepG2/C3A (ATCC number CRL-10741) which shows some differences to the original HepG2 cells such as the ability to grow in glucose deficient medium, strong contact inhibition of growth and high levels of albumin and AFP secretion.

Table 3.2 also shows which of the two cell lines express the mRNA for each gene at a level most resembling that of liver. Neither cell line is closer to liver mRNA levels in transferrin or HNF4a, with transferrin being approximately 10-fold lower in both cell lines and HNF4a being

2-fold higher in HepG2 and 2-fold lower in Huh7. Comparison of the two cell lines with regard to the remaining GOIs reveals that neither is more suitable as a hepatocyte model than the other. HepG2 cells have eleven genes which are closer in expression to those in liver, whereas Huh7 cells are closer in the remaining seven GOIs. It could be argued that, for example, Huh7 cells are more suitable than HepG2 if OATP transporters are specifically of interest, or that HepG2 cells could be useful for efflux transporter analysis if an effective MRP1 inhibitor was employed. However, as both cell lines have severe limitations in enzyme mRNA levels with at least some transporters expressed at low levels it would be difficult to prove that any effects seen were not contributed to by the absence of a fully functioning hepatic profile. The conclusion can therefore be drawn that it would be highly beneficial to attempt to increase the similarity of one or both of these cell lines to the *in vivo* hepatocyte by means of differentiation to a more mature hepatic phenotype.

A

		Albumin (NM_000477)
Primers	Forward	CTTATTCCAGGGGTGTGTTTCG
	Reverse	CGATGAGCAACCTCACTCTTGTG
Exon Location	Forward	1
	Reverse	1, 2
Product length (bp)		55
Annealing temperature (°C)		59

B

Reference sequence (5' – 3'). Exon-exon boundary is located at position 152-153.
120 – **CTTATTCCAGGGGTGTGTTTCG**TCGAGATGCA**CACAAGAGTGAGGTTGCTCATCG** – 174

C

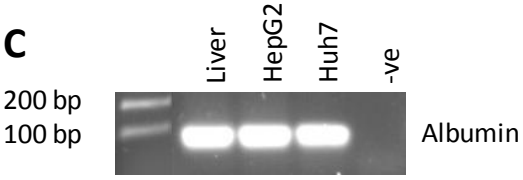

D Clone sequence – insert is in the forward orientation

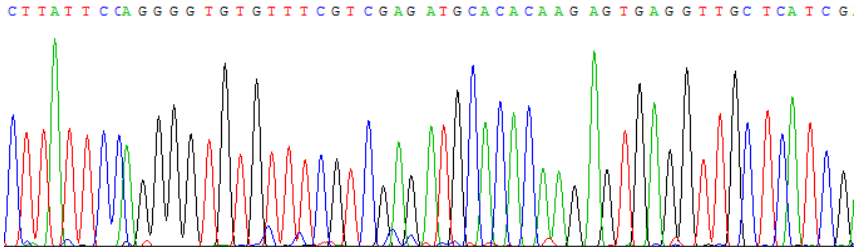

E BLAST results for cloned sequence against reference sequence.

```
Clone      CTTATTCCAGGGGTGTGTTTCGTCGAGATGCACACAAGAGTGAGGTTGCTCATCG
           ||||||||||||||||||||||||||||||||||||||||||||||||||||||||
Reference  CTTATTCCAGGGGTGTGTTTCGTCGAGATGCACACAAGAGTGAGGTTGCTCATCG
```

F

Albumin qPCR assay		
Standard Curve	Efficiency	2.003
	Error	0.0565
Melting temperature range (°C)		80.2 – 80.6

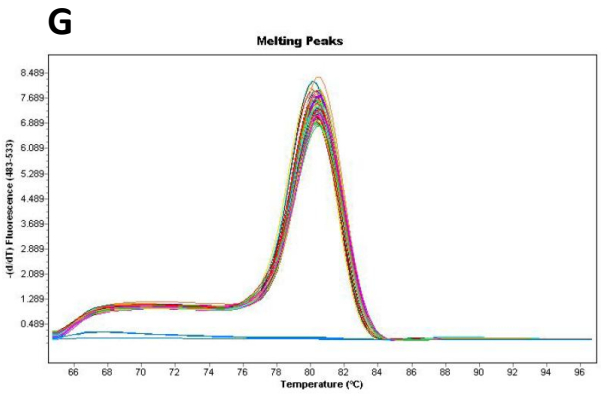

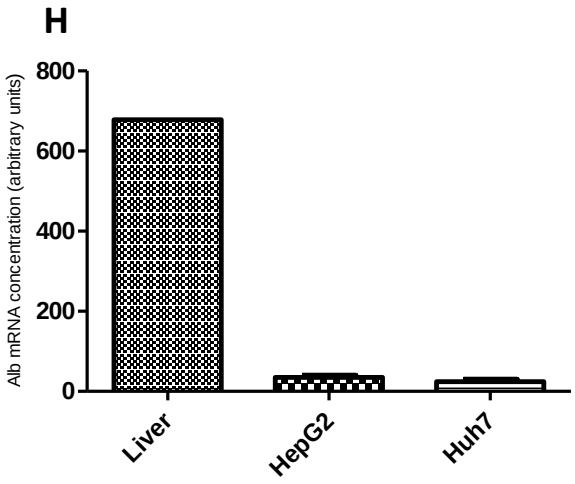

Figure 3.1 – Albumin PCR assay development. Primer sequences, exon location, product length and annealing temperature for both end point and quantitative PCR are shown in the table A. The reference sequence with primers highlighted is displayed in B. End point PCR products visualised on an agarose gel under UV light are shown in C. These products were excised, cloned and sequenced as described in chapter 2; the chromatogram of the cloned sequence can be seen in D, with results from a BLAST analysis shown in E. Data from qPCR assays is displayed in parts F, G and H. Table F includes standard curve details and product melting temperatures, with figure G being an example of a typical melt point plot obtained through this assay. Finally, graph H shows data from the albumin qPCR assay normalised to two reference genes.

A

		Transferrin (NM_001063)
Primers	Forward	GTCAACTGTGTCCAGGGTGTGG
	Reverse	TCAGACACTTGAAGGCTCCCG
Exon Location	Forward	5
	Reverse	5, 6
Product length (bp)		75
Annealing temperature (°C)		58

B

Reference sequence (5'-3'). Exon-exon boundary is located at position 943-944.
877 – **GTCAACTGTGTCCAGGGTGTGG**CTGCTCCACCCTTAACCAATACTTCGGCTACT**CGGGAGCCT TCAAGTGTCTGA** – 951

C

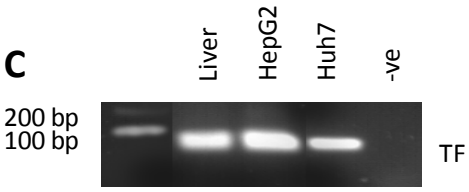

D Clone sequence – insert is in the reverse orientation

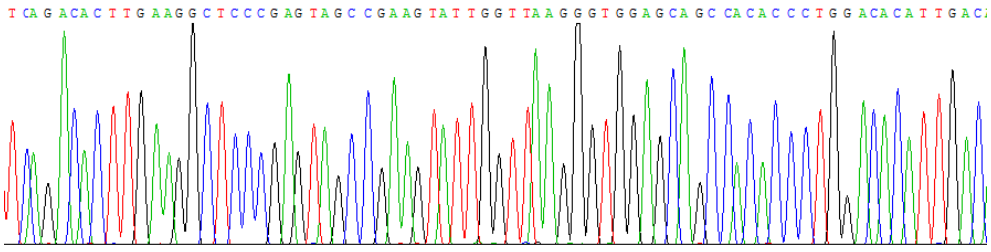

E BLAST results for cloned sequence against reference sequence.

```
Clone      TCAGACACTTGAAGGCTCCCGAGTAGCCGAAGTATTGGTTAAGGGTGGAGCAGCCACACC CTGGACACA-TTGAC
           |||||||||||||||||||||||||||||||||||||||||||||||||||||||||||| ||||||||| |||||
Reference  TCAGACACTTGAAGGCTCCCGAGTAGCCGAAGTATTGGTTAAGGGTGGAGCAGCCACACC CTGGACACAGTTGAC
```

F

Transferrin qPCR assay		
Standard Curve	Efficiency	2.045
	Error	0.0317
Melting temperature range (°C)		83.1 – 83.5

G

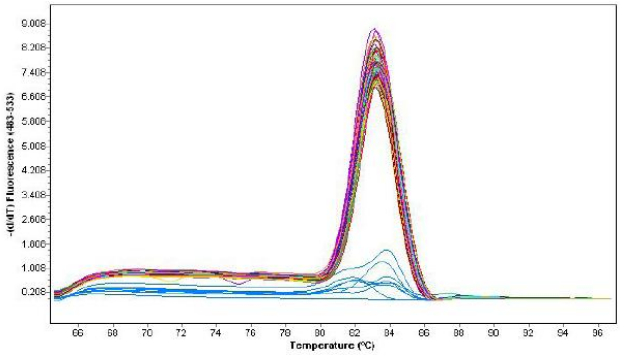

H

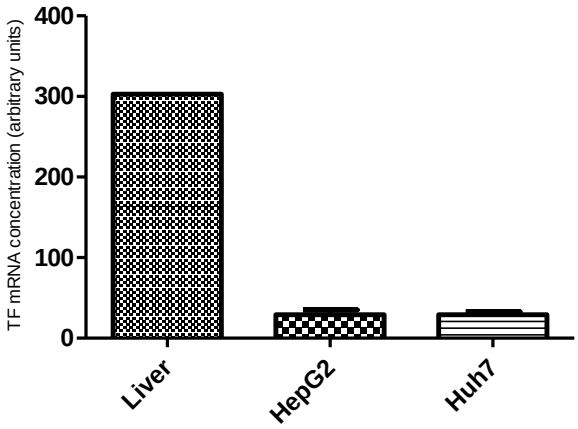

Figure 3.2 – Transferrin PCR assay development. Primer sequences, exon location, product length and annealing temperature for both end point and quantitative PCR are shown in the table A. The reference sequence with primers highlighted is displayed in B. End point PCR products visualised on an agarose gel under UV light are shown in C. These products were excised, cloned and sequenced as described in chapter 2; the chromatogram of the cloned sequence can be seen in D, with results from a BLAST analysis shown in E. Data from qPCR assays is displayed in parts F, G and H. Table F includes standard curve details and product melting temperatures, with figure G being an example of a typical melt point plot obtained through this assay. Finally, graph H shows data from the transferrin qPCR assay normalised to two reference genes.

A

		Alpha-fetoprotein (NM_001134)
Primers	Forward	GGAGCGGCTGACATTATTATCG
	Reverse	GGCCAACACCAGGGTTTACTG
Exon Location	Forward	11, 12
	Reverse	12
Product length (bp)		72
Annealing temperature (°C)		58

B

Reference sequence (5'-3'). Exon-exon boundary is located at position 1475-1476.
1471 – **GGAGCGGCTGACATTATTATCG**GACACTTATGTATCAGACATGAAATGACTC**CAGTAAA CCCTGGTGTTGGCC** – 1542

C

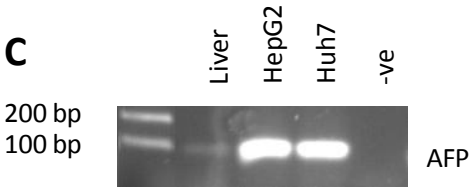

D

Clone sequence – insert is in the reverse orientation

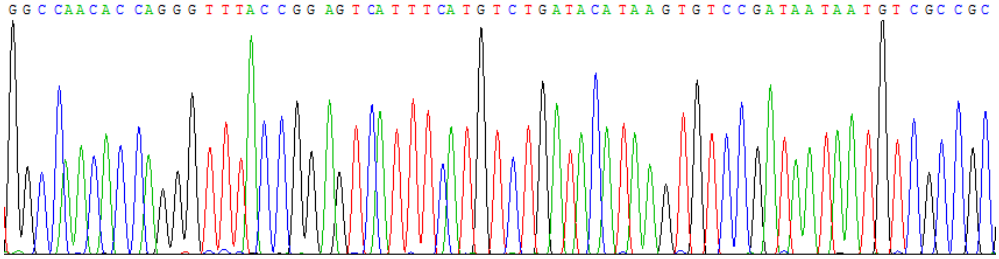

E

BLAST results for cloned sequence against reference sequence.

```
Clone      GGCCAACACCAGGGTTTACCGGAGTCATTTCATGTCTGATACATAAGTGTCCGATAATAATGTC-GCCGC
           |||||||||||||||||||| ||||||||||||||||||||||||||||||||||||||||| |||||
Reference  GGCCAACACCAGGGTTTACTGGAGTCATTTCATGTCTGATACATAAGTGTCCGATAATAATGTCAGCCGC
```

F

AFP qPCR assay		
Standard Curve	Efficiency	2.098
	Error	0.0180
Melting temperature range (°C)		79.6 – 79.9

G

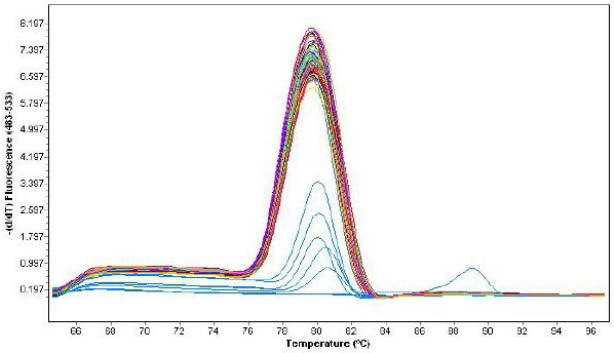

H

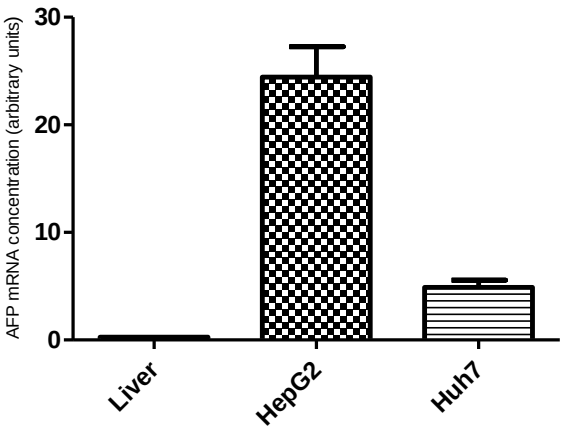

Figure 3.3 – AFP PCR assay development. Primer sequences, exon location, product length and annealing temperature for both end point and quantitative PCR are shown in the table A. The reference sequence with primers highlighted is displayed in B. End point PCR products visualised on an agarose gel under UV light are shown in C. These products were excised, cloned and sequenced as described in chapter 2; the chromatogram of the cloned sequence can be seen in D, with results from a BLAST analysis shown in E. Data from qPCR assays is displayed in parts F, G and H. Table F includes standard curve details and product melting temperatures, with figure G being an example of a typical melt point plot obtained through this assay. Finally, graph H shows data from the AFP qPCR assay normalised to two reference genes.

A

		A1AT (NM_000295)
Primers	Forward	GGTCTGCCAGCTTACATTTACCC
	Reverse	CCCATTGCTGAAGACCTTAGTG
Exon Location	Forward	4, 5
	Reverse	5
Product length (bp)		103
Annealing temperature (°C)		55

B

Reference sequence (5'-3'). Exon-exon boundary is located at position 1178-1179.
1176 – **GGTCTGCCAGCTTACATTTACCC**AAACTGTCCATTACTGGAACCTATGATCTGAAGAG
CGTCCTGGGTCAACTGGGCAT**CACTAAGGTCTTCAGCAATGGG** – 1278

C

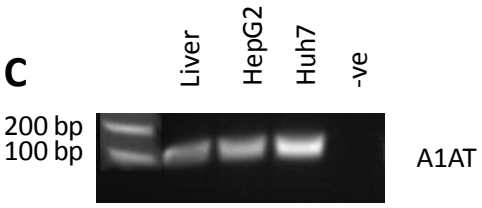

D

Clone sequence – insert is in the reverse orientation

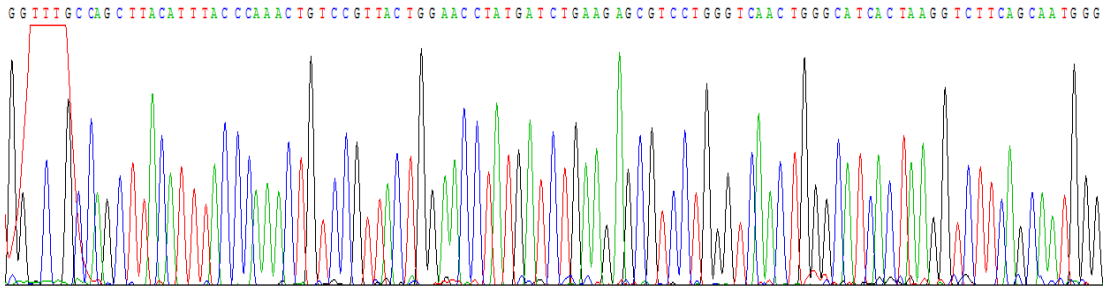

E

BLAST results for cloned sequence against reference sequence.

```
Clone       GGTTTGCCAGCTTACATTTACCCAAACTGTCCGTTACTGGAACCTATGATCTGAAGAGCG
            |||  ||||||||||||||||||||||||||||  ||||||||||||||||||||||||
Reference   GGTCTGCCAGCTTACATTTACCCAAACTGTCCATTACTGGAACCTATGATCTGAAGAGCG

Clone       TCCTGGGTCAACTGGGCATCACTAAGGTCTTCAGCAATGGG
            |||||||||||||||||||||||||||||||||||||||
Reference   TCCTGGGTCAACTGGGCATCACTAAGGTCTTCAGCAATGGG
```

F

A1AT qPCR assay		
Standard Curve	Efficiency	2.306
	Error	0.0475
Melting temperature range (°C)		81.6 – 82.1

G

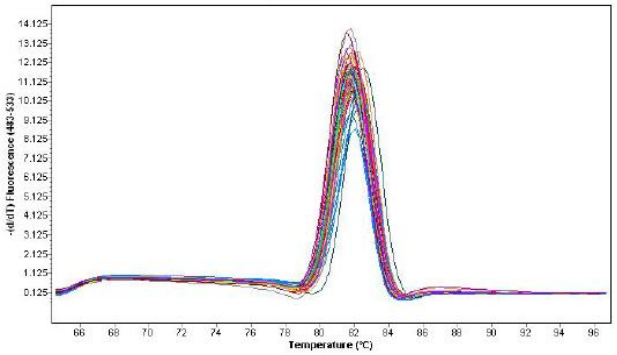

H

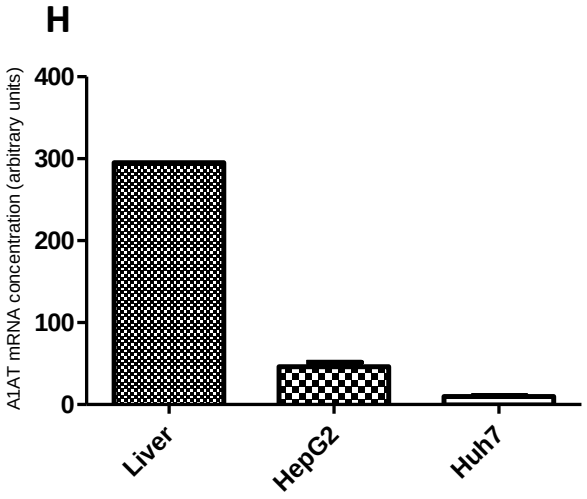

Figure 3.4 – A1AT PCR assay development. Primer sequences, exon location, product length and annealing temperature for both end point and quantitative PCR are shown in the table A. The reference sequence with primers highlighted is displayed in B. End point PCR products visualised on an agarose gel under UV light are shown in C. These products were excised, cloned and sequenced as described in chapter 2; the chromatogram of the cloned sequence can be seen in D, with results from a BLAST analysis shown in E. Data from qPCR assays is displayed in parts F, G and H. Table F includes standard curve details and product melting temperatures, with figure G being an example of a typical melt point plot obtained through this assay. Finally, graph H shows data from the A1AT qPCR assay normalised to two reference genes.

A

		HNF4a (NM_000457)
Primers	Forward	CCTGTCCCGACAGATCACCTC
	Reverse	TGGACTCACACACATCTGCG
Exon Location	Forward	5, 6
	Reverse	6
Product length (bp)		92
Annealing temperature (°C)		59

B

Reference sequence (5'-3'). Exon-exon boundary is located at position 581-582.
569 – **CCTGTCCCGACAGATCACCTC**CCCCGTCTCCGGGATCAACGGCGACATTCGGGCGAAGAA
GATTGCCAGCAT**CGCAGATGTGTGTGAGTCCA** – 660

C

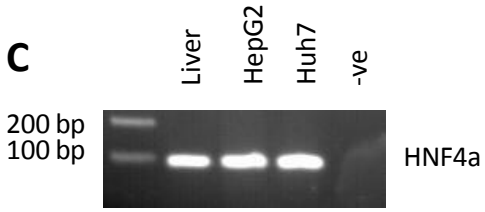

D

Clone sequence – insert is in the forward orientation

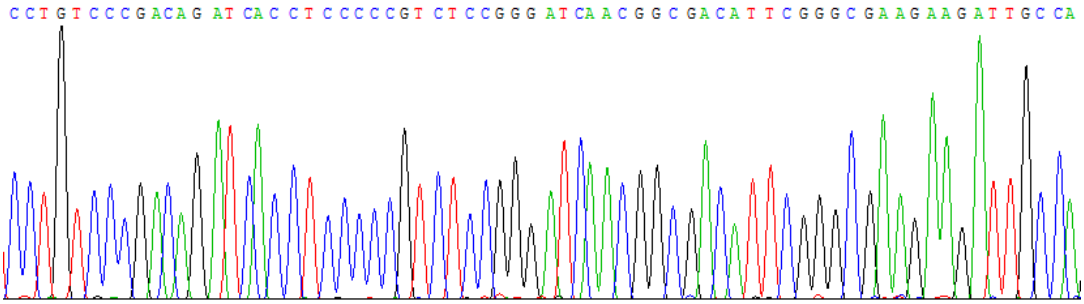

E

BLAST results for cloned sequence against reference sequence.

```
Clone      CCTGTCCCGACAGATCACCTCCCCCGTCTCCGGGATCAACGGCGACATTCGGGCGAAGAA
           ||||||||||||||||||||||||||||||||||||||||||||||||||||||||||||
Reference  CCTGTCCCGACAGATCACCTCCCCCGTCTCCGGGATCAACGGCGACATTCGGGCGAAGAA

Clone      GATTGCCAGCATCGCAGATGTGTGTGAGTCCA
           ||||||||||||||||||||||||||||||||
Reference  GATTGCCAGCATCGCAGATGTGTGTGAGTCCA
```

F

HNF4a qPCR assay		
Standard Curve	Efficiency	2.112
	Error	0.0424
Melting temperature range (°C)		85.4 – 86.0

G

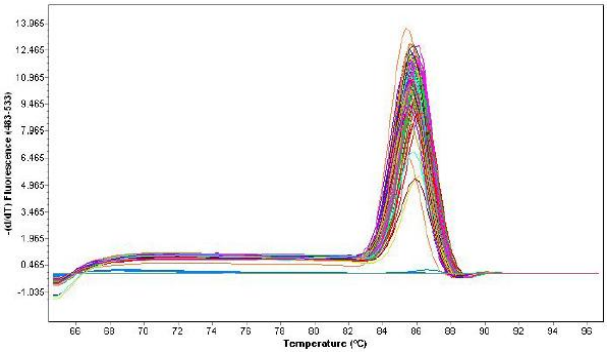

H

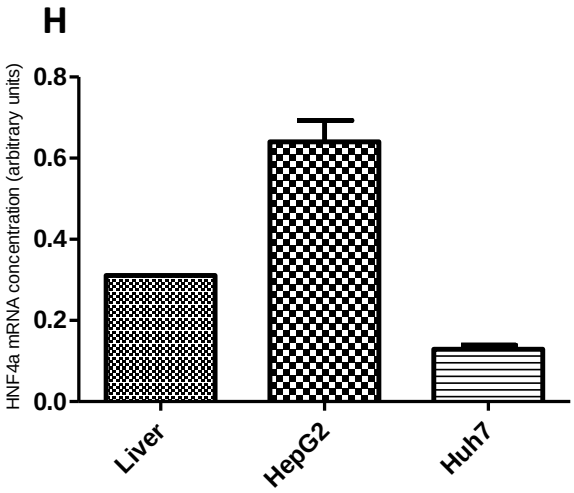

Figure 3.5 – HNF4a PCR assay development. Primer sequences, exon location, product length and annealing temperature for both end point and quantitative PCR are shown in the table A. The reference sequence with primers highlighted is displayed in B. End point PCR products visualised on an agarose gel under UV light are shown in C. These products were excised, cloned and sequenced as described in chapter 2; the chromatogram of the cloned sequence can be seen in D, with results from a BLAST analysis shown in E. Data from qPCR assays is displayed in parts F, G and H. Table F includes standard curve details and product melting temperatures, with figure G being an example of a typical melt point plot obtained through this assay. Finally, graph H shows data from the HNF4a qPCR assay normalised to two reference genes.

A

		MRP1 (NM_004996)
Primers	Forward	TGGCATCACCTTCTCCATCC
	Reverse	GAGAGCAGGGACGACTTTCCG
Exon Location	Forward	15, 16
	Reverse	16
Product length (bp)		81
Annealing temperature (°C)		58

B

Reference sequence (5'-3'). Exon-exon boundary is located at position 2163-2164.
2161 – **TGGCATCACCTTCTCCATCC**CCGAAGGTGCTTTGGTGGCCGTGGTGGGCCAGGTGGGC
TG**CGGAAAGTCGTCCCTGCTCTC** – 2241

C

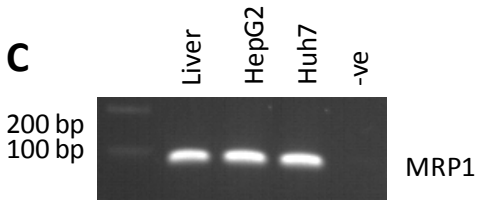

D

Clone sequence – insert is in the forward orientation

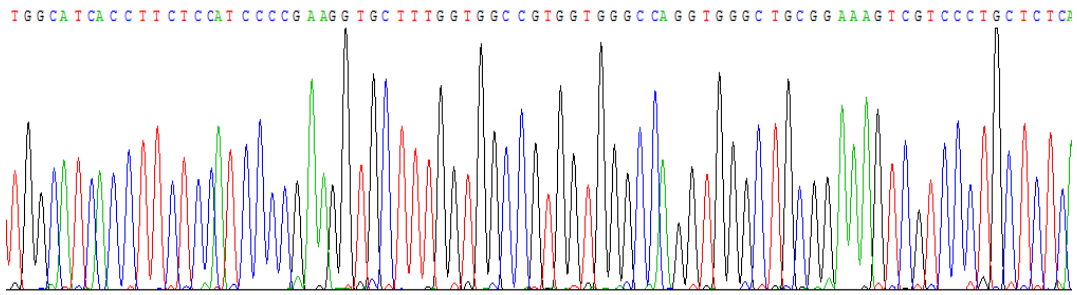

E

BLAST results for cloned sequence against reference sequence.

```
Clone      TGGCATCACCTTCTCCATCCCCGAAGGTGCTTTGGTGGCCGTGGTGGGCCAGGTGGGCTG
           ||||||||||||||||||||||||||||||||||||||||||||||||||||||||||||
Reference  TGGCATCACCTTCTCCATCCCCGAAGGTGCTTTGGTGGCCGTGGTGGGCCAGGTGGGCTG

Clone      CGGAAAGTCGTCCCTGCTCTC
           |||||||||||||||||||||
Reference  CGGAAAGTCGTCCCTGCTCTC
```

F

MRP1 qPCR assay		
Standard Curve	Efficiency	1.924
	Error	0.0414
Melting temperature range (°C)		86.7 – 87.1

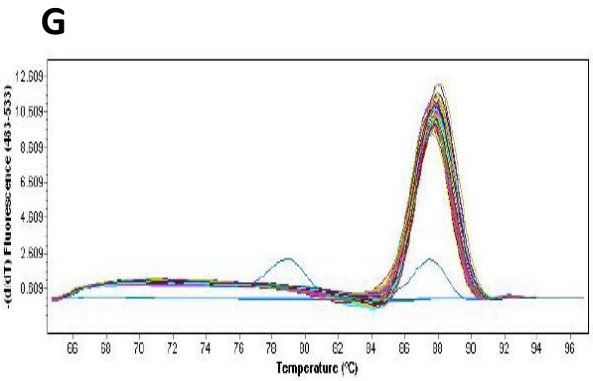

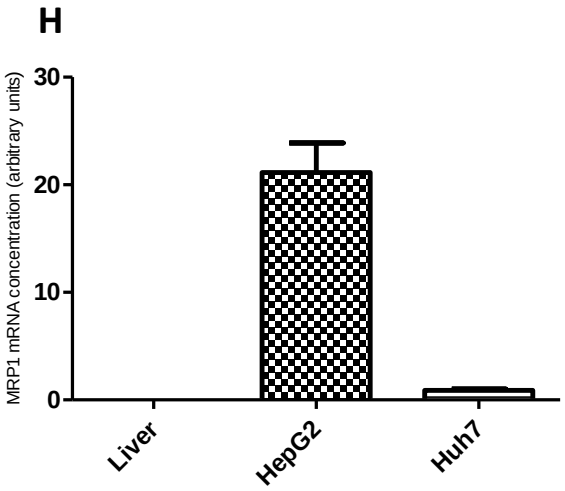

Figure 3.6 – MRP1 PCR assay development. Primer sequences, exon location, product length and annealing temperature for both end point and quantitative PCR are shown in the table A. The reference sequence with primers highlighted is displayed in B. End point PCR products visualised on an agarose gel under UV light are shown in C. These products were excised, cloned and sequenced as described in chapter 2; the chromatogram of the cloned sequence can be seen in D, with results from a BLAST analysis shown in E. Data from qPCR assays is displayed in parts F, G and H. Table F includes standard curve details and product melting temperatures, with figure G being an example of a typical melt point plot obtained through this assay. Finally, graph H shows data from the MRP1 qPCR assay normalised to two reference genes.

A

		MRP2 (NM_000392)
Primers	Forward	CACCATCATGGACAGTGACAAGG
	Reverse	GAGAGCAGGGACGACTTTCCG
Exon Location	Forward	31, 32
	Reverse	32
Product length (bp)		60
Annealing temperature (°C)		58

B Reference sequence (5'-3'). Exon-exon boundary is located at position 4647-4648.
4627 – **CACCATCATGGACAGTGACAAGG**TAATGGTCCTAGACAA**CGGGAAGATTATAGAGT GCGG** – 4686

C

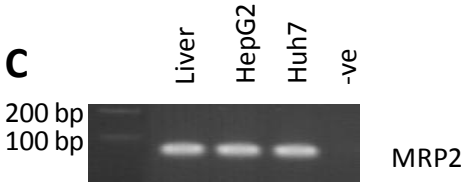

D Clone sequence – insert is in the forward orientation

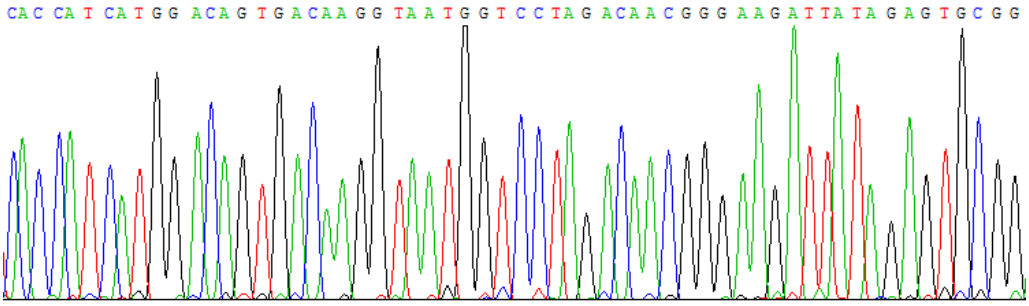

E BLAST results for cloned sequence against reference sequence.

```
Clone       CACCATCATGGACAGTGACAAGGTAATGGTCCTAGACAACGGGAAGATTATAGAGTGCGG
            ||||||||||||||||||||||||||||||||||||||||||||||||||||||||||||
Reference   CACCATCATGGACAGTGACAAGGTAATGGTCCTAGACAACGGGAAGATTATAGAGTGCGG
```

F

MRP2 qPCR assay		
Standard Curve	Efficiency	2.105
	Error	0.0319
Melting temperature range (°C)		78.9 – 79.3

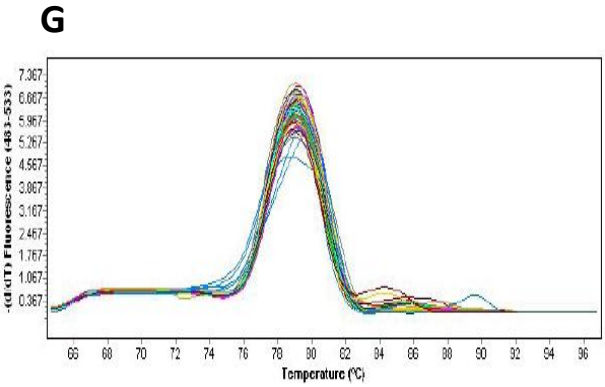

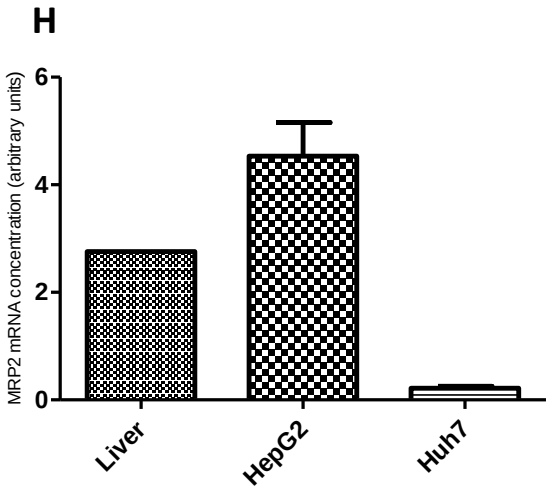

Figure 3.7 – MRP2 PCR assay development. Primer sequences, exon location, product length and annealing temperature for both end point and quantitative PCR are shown in the table A. The reference sequence with primers highlighted is displayed in B. End point PCR products visualised on an agarose gel under UV light are shown in C. These products were excised, cloned and sequenced as described in chapter 2; the chromatogram of the cloned sequence can be seen in D, with results from a BLAST analysis shown in E. Data from qPCR assays is displayed in parts F, G and H. Table F includes standard curve details and product melting temperatures, with figure G being an example of a typical melt point plot obtained through this assay. Finally, graph H shows data from the MRP2 qPCR assay normalised to two reference genes.

A

		MDR1 (NM_000927)
Primers	Forward	TTCACTTCAGTTACCCATCTCG
	Reverse	GTCTGCCCACTCTGCACCTTC
Exon Location	Forward	12
	Reverse	13
Product length (bp)		77
Annealing temperature (°C)		58

B Reference sequence (5'-3'). Exon-exon boundary is located at position 1642-1643.
1607 – **TTCACTTCAGTTACCCATCTCG**AAAAGAAGTTAAGATCTTGAAGGGTCTGAACCT**G AAGGTGCAGAGTGGGCAGAC** – 1683

C

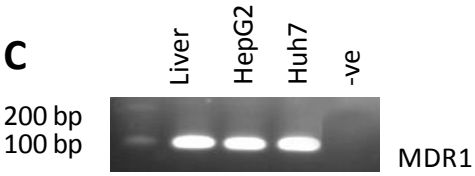

D Clone sequence – insert is in the forward orientation

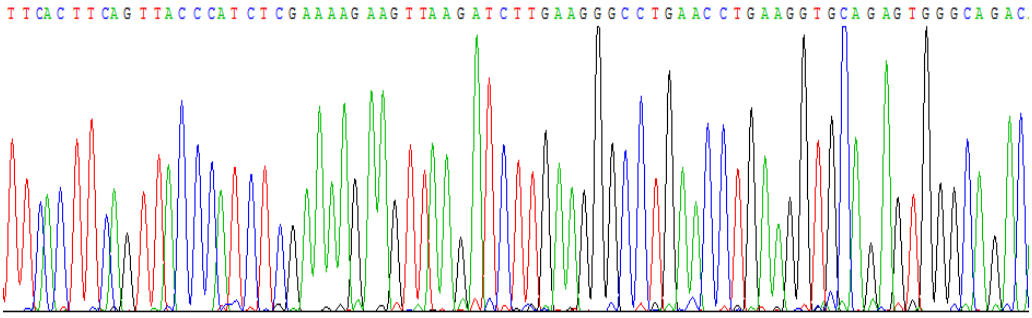

E BLAST results for cloned sequence against reference sequence.

```
Clone       TTCACTTCAGTTACCCATCTCGAAAAGAAGTTAAGATCTTGAAGGGTCTGAACCTGAAGG
            ||||||||||||||||||||||||||||||||||||||||||||||||||||||||||||
Reference   TTCACTTCAGTTACCCATCTCGAAAAGAAGTTAAGATCTTGAAGGGTCTGAACCTGAAGG

Clone       TGCAGAGTGGGCAGAC
            ||||||||||||||||
Reference   TGCAGAGTGGGCAGAC
```

F

MDR1 qPCR assay		
Standard Curve	Efficiency	2.040
	Error	0.0416
Melting temperature range (°C)		79.5 – 80.0

G

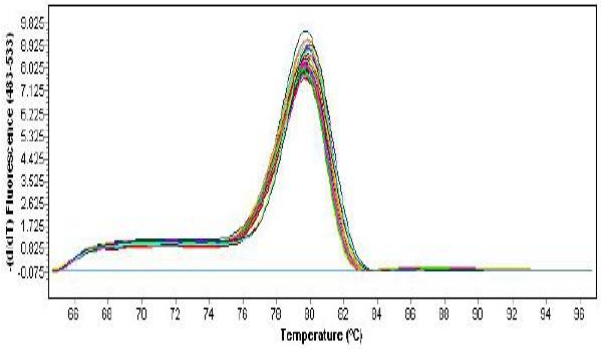

H

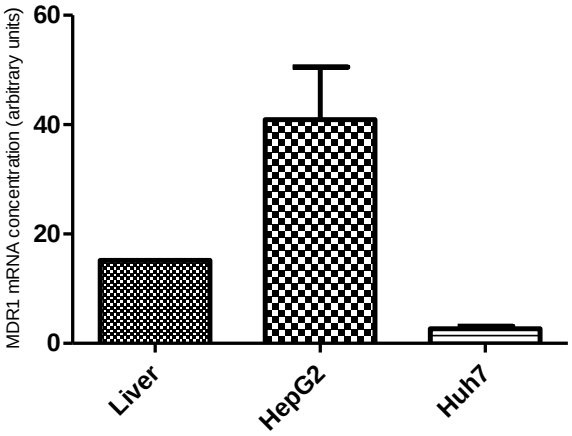

Figure 3.8 – MDR1 PCR assay development. Primer sequences, exon location, product length and annealing temperature for both end point and quantitative PCR are shown in the table A. The reference sequence with primers highlighted is displayed in B. End point PCR products visualised on an agarose gel under UV light are shown in C. These products were excised, cloned and sequenced as described in chapter 2; the chromatogram of the cloned sequence can be seen in D, with results from a BLAST analysis shown in E. Data from qPCR assays is displayed in parts F, G and H. Table F includes standard curve details and product melting temperatures, with figure G being an example of a typical melt point plot obtained through this assay. Finally, graph H shows data from the MDR1 qPCR assay normalised to two reference genes.

A

		BCRP (NM_004827)
Primers	Forward	CAGGTGGAGGCAAATCTTCG
	Reverse	TTGGATCTTTCCTTGCAGCTAA
Exon Location	Forward	3, 4
	Reverse	4
Product length (bp)		54
Annealing temperature (°C)		58

B

Reference sequence (5'-3'). Exon-exon boundary is located at position 756-757
738 – **CAGGTGGAGGCAAATCTTCG**TTATTAGATGTC**TTAGCTGCAAGGAAAGATCCAA** – 791

C

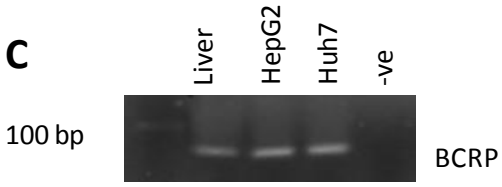

D

Clone sequence – insert is in the reverse orientation

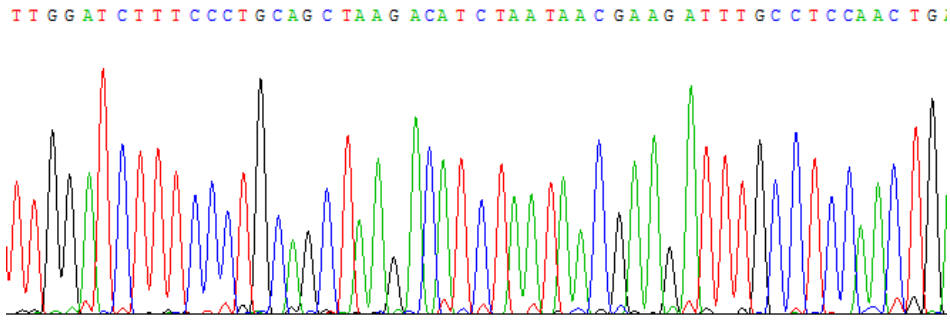

E

BLAST results for cloned sequence against reference sequence.

```
Clone      TTGGATCTTTCCCTGCAGCTAAGACATCTAATAACGAAGATTTGCCTCCAACTG
           |||||||||||| ||||||||||||||||||||||||||||||||||||| |||
Reference  TTGGATCTTTCCTTGCAGCTAAGACATCTAATAACGAAGATTTGCCTCCACCTG
```

F

BCRP qPCR assay		
Standard Curve	Efficiency	2.040
	Error	0.0416
Melting temperature range (°C)		79.5 – 80.0

G

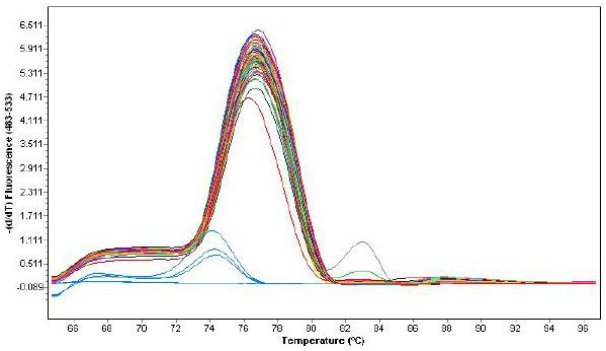

H

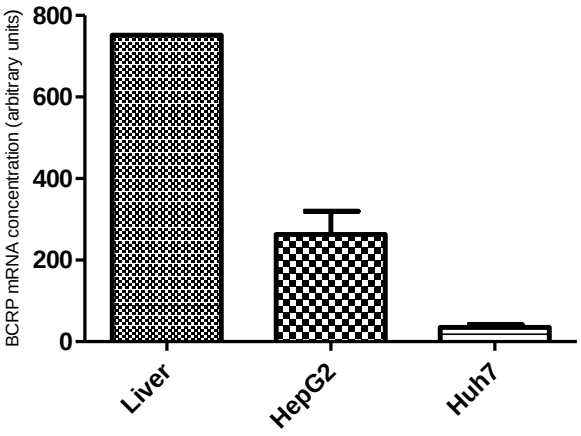

Figure 3.9 – BCRP PCR assay development. Primer sequences, exon location, product length and annealing temperature for both end point and quantitative PCR are shown in the table A. The reference sequence with primers highlighted is displayed in B. End point PCR products visualised on an agarose gel under UV light are shown in C. These products were excised, cloned and sequenced as described in chapter 2; the chromatogram of the cloned sequence can be seen in D, with results from a BLAST analysis shown in E. Data from qPCR assays is displayed in parts F, G and H. Table F includes standard curve details and product melting temperatures, with figure G being an example of a typical melt point plot obtained through this assay. Finally, graph H shows data from the BCRP qPCR assay normalised to two reference genes.

A

		OCT3 (NM_021977)
Primers	Forward	CCAAGCCATCCTGAACCTCG
	Reverse	TGCCATACCTGTCTGCTGCAT
Exon Location	Forward	2
	Reverse	2, 3
Product length (bp)		71
Annealing temperature (°C)		58

B

Reference sequence (5'-3'). Exon-exon boundary is located at position 560-561.
498 – **CCAAGCCATCCTGAACCTCG**GCTTCCTGACTGGAGCATTCACCTTAGGCT**ATGCAGCAG ACAGGTATGGCA** – 568

C

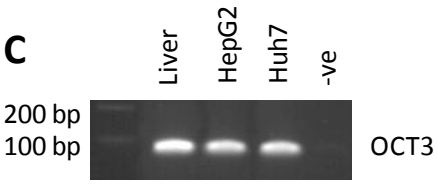

D

Clone sequence – insert is in the reverse orientation

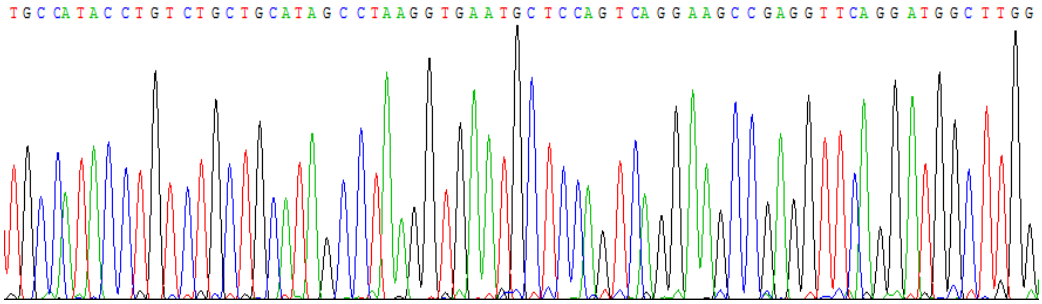

E

BLAST results for cloned sequence against reference sequence.

```
Clone       TGCCATACCTGTCTGCTGCATAGCCTAAGGTGAATGCTCCAGTCAGGAAGCCGAGGTTCA
            ||||||||||||||||||||||||||||||||||||||||||||||||||||||||||||
Reference   TGCCATACCTGTCTGCTGCATAGCCTAAGGTGAATGCTCCAGTCAGGAAGCCGAGGTTCA

Clone       GGATGGCTTGG
            ||||||||||||
Reference   GGATGGCTTGG
```

F

OCT3 qPCR assay		
Standard Curve	Efficiency	2.040
	Error	0.0416
Melting temperature range (°C)		79.5 – 80.0

G

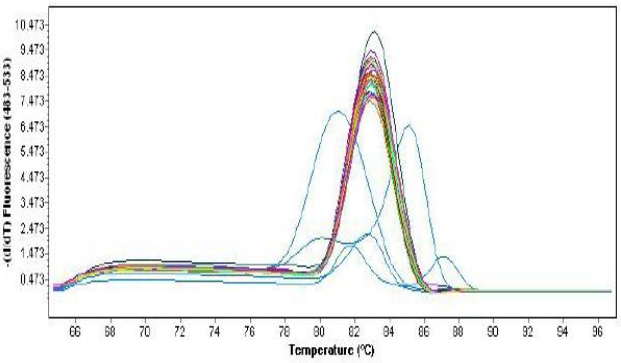

H

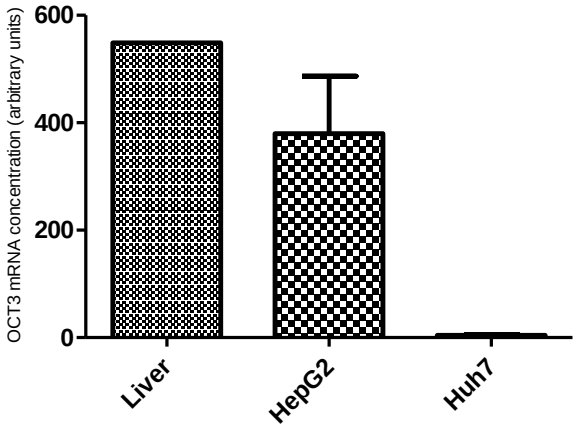

Figure 3.10 – OCT3 PCR assay development. Primer sequences, exon location, product length and annealing temperature for both end point and quantitative PCR are shown in the table A. The reference sequence with primers highlighted is displayed in B. End point PCR products visualised on an agarose gel under UV light are shown in C. These products were excised, cloned and sequenced as described in chapter 2; the chromatogram of the cloned sequence can be seen in D, with results from a BLAST analysis shown in E. Data from qPCR assays is displayed in parts F, G and H. Table F includes standard curve details and product melting temperatures, with figure G being an example of a typical melt point plot obtained through this assay. Finally, graph H shows data from the OCT3 qPCR assay normalised to two reference genes.

A

		OATPB (NM_007256)
Primers	Forward	CCTGCCGCTCTTCTTTATCG
	Reverse	CATGCAGCTTGGAGACAGCTC
Exon Location	Forward	10
	Reverse	11
Product length (bp)		100
Annealing temperature (°C)		59

B

Reference sequence (5'-3'). Exon-exon boundary is located at position 1820-1821.
1758 – **CTGCCGCTCTTCTTTATCG**GCTGCTCCAGCCACCAGATTGCGGGCATCACACACC
AGACCAGTGCCCACCCTGGGCTG**GAGCTGTCTCC AAGCTGCATG** – 1857

C

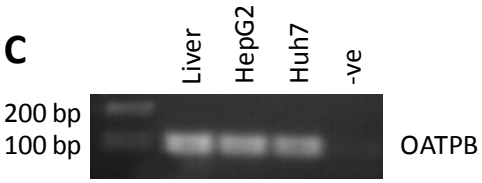

D

Clone sequence – insert is in the forward orientation

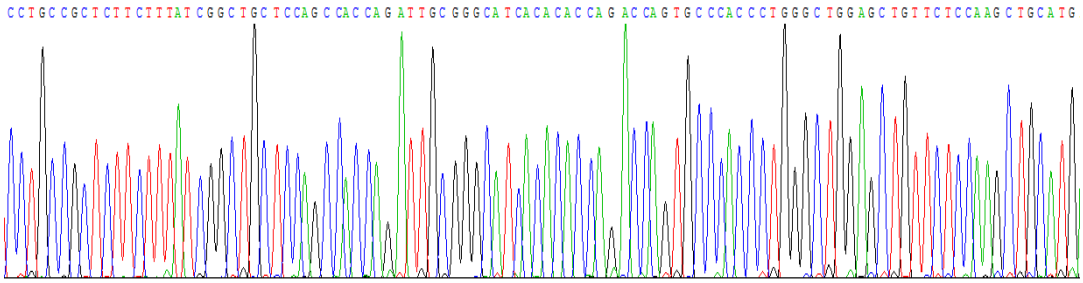

E

BLAST results for cloned sequence against reference sequence.

```
Clone      CCTGCCGCTCTTCTTTATCGGCTGCTCCAGCCACCAGATTGCGGGCATCACACACCAGAC
           ||||||||||||||||||||||||||||||||||||||||||||||||||||||||||||
Reference  CCTGCCGCTCTTCTTTATCGGCTGCTCCAGCCACCAGATTGCGGGCATCACACACCAGAC

Clone      CAGTGCCCACCCTGGGCTGGAGCTGTTCTCCAAGCTGCATG
           |||||||||||||||||||||||||| ||||||||||||||
Reference  CAGTGCCCACCCTGGGCTGGAGCTGT-CTCCAAGCTGCATG
```

F

OATPB qPCR assay		
Standard Curve	Efficiency	1.952
	Error	0.0856
Melting temperature range (°C)		87.9 – 88.4

G

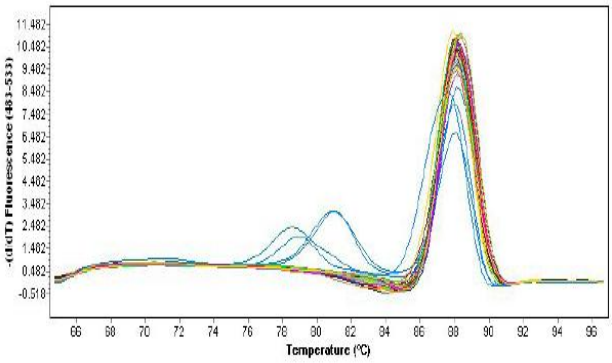

H

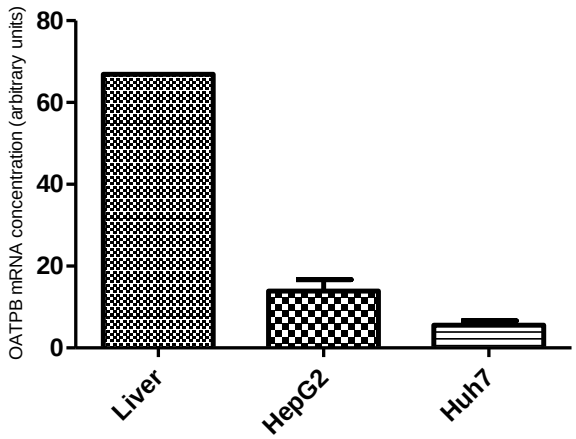

Figure 3.11 – OATPB PCR assay development. Primer sequences, exon location, product length and annealing temperature for both end point and quantitative PCR are shown in the table A. The reference sequence with primers highlighted is displayed in B. End point PCR products visualised on an agarose gel under UV light are shown in C. These products were excised, cloned and sequenced as described in chapter 2; the chromatogram of the cloned sequence can be seen in D, with results from a BLAST analysis shown in E. Data from qPCR assays is displayed in parts F, G and H. Table F includes standard curve details and product melting temperatures, with figure G being an example of a typical melt point plot obtained through this assay. Finally, graph H shows data from the OATPB qPCR assay normalised to two reference genes.

A

		OATPC (NM_006446)
Primers	Forward	TGTGTTCATGGGTAATATGCTTCG
	Reverse	AGATCCCAGGGTAAAGCCAATG
Exon Location	Forward	6
	Reverse	7
Product length (bp)		166
Annealing temperature (°C)		59

B

Reference sequence (5'-3'). Exon-exon boundary is located in position 732-733.
623 – **TGTGTTCATGGGTAATATGCTTCG**TGGAATAGGGGAGACTCCCATAGTACCATTGGG
GCTTTCTTACATTGATGATTTCGCTAAAGAAGGACATTCTTCTTTGTATTTAGGTATATTGAAT
GCAATAGCAATGATTGGTCCAAT**CATTGGCTTTACCCTGGGATCT** – 788

C

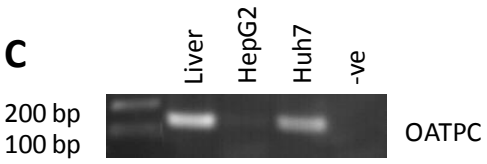

D

Clone sequence – insert is in the reverse orientation

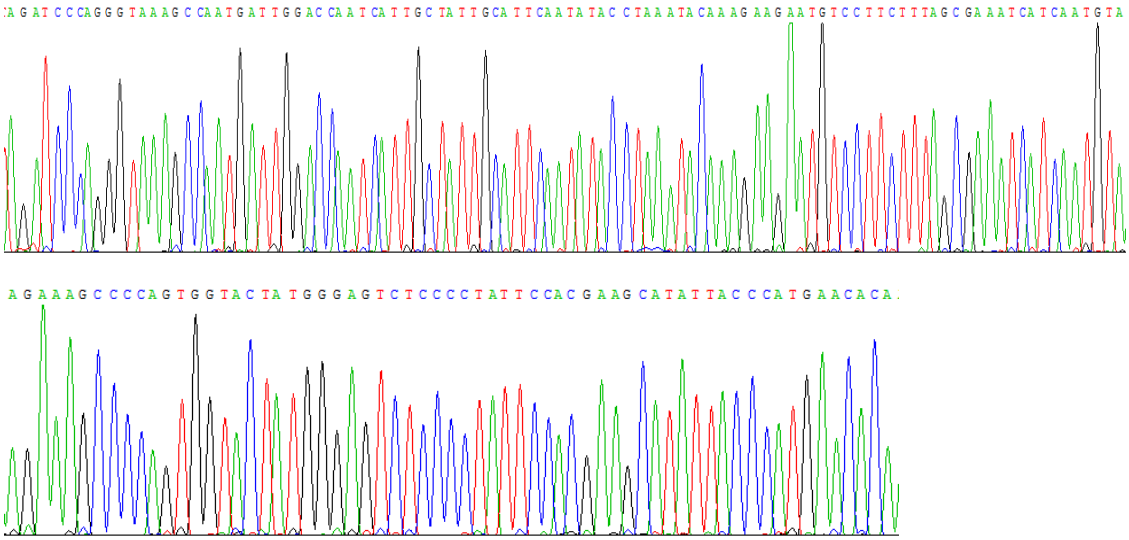

E

BLAST results for cloned sequence against reference sequence.

```
Clone      AGATCCCAGGGTAAAGCCAATGATTGGACCAATCATTGCTATTGCATTCAATATACCTAA
           ||||||||||||||||||||||||||||||||||||||||||||||||||||||||||||
Reference  AGATCCCAGGGTAAAGCCAATGATTGGACCAATCATTGCTATTGCATTCAATATACCTAA

Clone      ATACAAAGAAGAATGTCCTTCTTTAGCGAAATCATCAATGTAAGAAAGCCCCAGTGGTAC
           ||||||||||||||||||||||||||||||||||||||||||||||||||||| ||||||
Reference  ATACAAAGAAGAATGTCCTTCTTTAGCGAAATCATCAATGTAAGAAAGCCCCAATGGTAC

Clone      TATGGGAGTCTCCCCTATTCCACGAAGCATATTACCCATGAACACA
           |||||||||||||||||||||||||||||||||||||||||||||
Reference  TATGGGAGTCTCCCCTATTCCACGAAGCATATTACCCATGAACACA
```

F

OATPC qPCR assay		
Standard Curve	Efficiency	1.978
	Error	0.0200
Melting temperature range (°C)		79.5 – 79.9

G

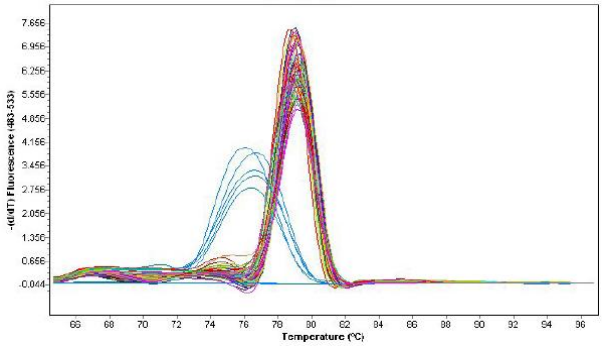

H

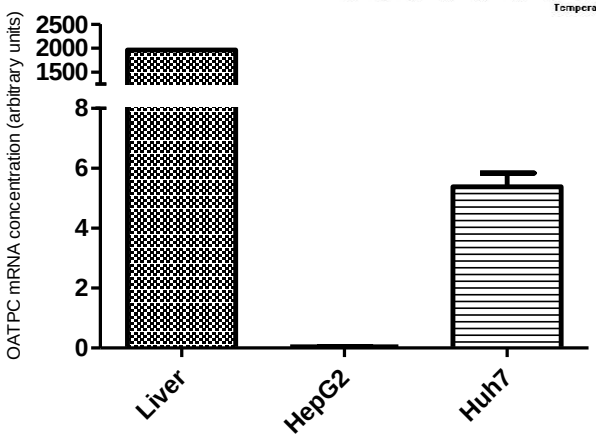

Figure 3.12 – OATPC PCR assay development. Primer sequences, exon location, product length and annealing temperature for both end point and quantitative PCR are shown in the table A. The reference sequence with primers highlighted is displayed in B. End point PCR products visualised on an agarose gel under UV light are shown in C. These products were excised, cloned and sequenced as described in chapter 2; the chromatogram of the cloned sequence can be seen in D, with results from a BLAST analysis shown in E. Data from qPCR assays is displayed in parts F, G and H. Table F includes standard curve details and product melting temperatures, with figure G being an example of a typical melt point plot obtained through this assay. Finally, graph H shows data from the OATPC qPCR assay normalised to two reference genes.

A

		OATP8 (NM_019844)
Primers	Forward	TACTCAGCACACTTGGGTGAATG
	Reverse	CCTCCTGTTGCAGAGAACAAAGA
Exon Location	Forward	12
	Reverse	12
Product length (bp)		107
Annealing temperature (°C)		59

B

Reference sequence (5'-3').
1675 – **TACTCAGCACACTTGGGTGAATG**CCCAAGAGATAATACTTGTACAAGGAAATTTTTCAT
CTATGTTGCAATTCAAGTCATAAAC**TCT TTGTTCTCTGCAACAGGAGG** – 1781

C

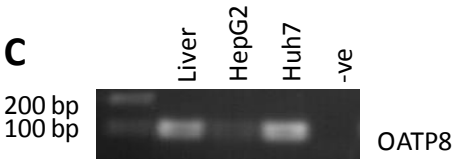

D

Clone sequence – insert is in the forward orientation

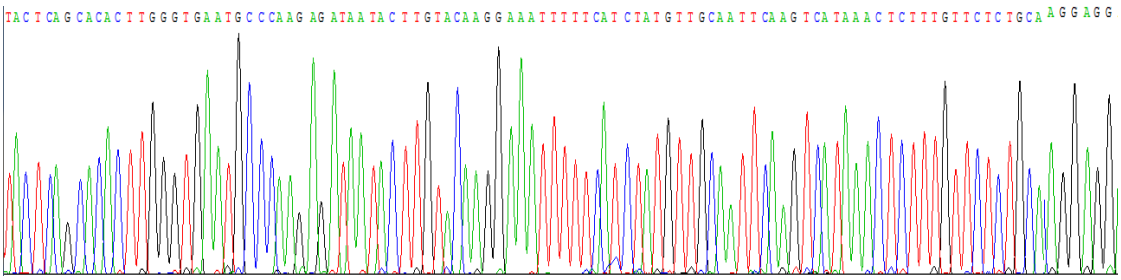

E

BLAST results for cloned sequence against reference sequence.

```
Clone      TACTCAGCACACTTGGGTGAATGCCCAAGAGATAATACTTGTACAAGGAAATTTTTCATC
           ||||||||||||||||||||||||||||||||||||||||||||||||||||||||||||
Reference  TACTCAGCACACTTGGGTGAATGCCCAAGAGATAATACTTGTACAAGGAAATTTTTCATC

Clone      TATGTTGCAATTCAAGTCATAAACTCTTTGTTCTCTGCAACAGGAGG
           |||||||||||||||||||||||||||||||||||||||||||||
Reference  TATGTTGCAATTCAAGTCATAAACTCTTTGTTCTCTGCAACAGGAGG
```

F

OATP8 qPCR assay		
Standard Curve	Efficiency	2.104
	Error	0.0111
Melting temperature range (°C)		78.0 – 78.4

G

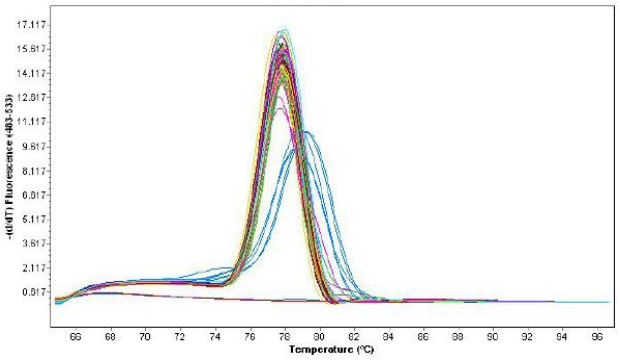

H

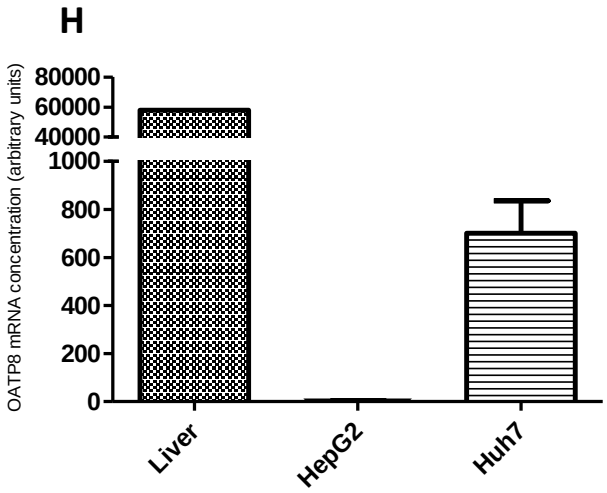

Figure 3.13 – OATP8 PCR assay development. Primer sequences, exon location, product length and annealing temperature for both end point and quantitative PCR are shown in the table A. The reference sequence with primers highlighted is displayed in B. End point PCR products visualised on an agarose gel under UV light are shown in C. These products were excised, cloned and sequenced as described in chapter 2; the chromatogram of the cloned sequence can be seen in D, with results from a BLAST analysis shown in E. Data from qPCR assays is displayed in parts F, G and H. Table F includes standard curve details and product melting temperatures, with figure G being an example of a typical melt point plot obtained through this assay. Finally, graph H shows data from the OATP8 qPCR assay normalised to two reference genes.

A

		CYP1A2 (NM_000761)
Primers	Forward	GACTTTGACAAGAACAGTGTCCG
	Reverse	TTCTCCTGTGGGATGAGGTTGC
Exon Location	Forward	2, 3
	Reverse	3
Product length (bp)		98
Annealing temperature (°C)		59

B

Reference sequence (5'-3'). Exon-exon boundary is located at position 895-896.
884 – **GACTTTGACAAGAACAGTGTCCG**GGACATCACGGGTGCCCTGTTCAAGCACAGCAA
GAAGGGGCCTAGAGCCAGCG**GCAACCTCATCCCACAGGAGAA** – 981

C

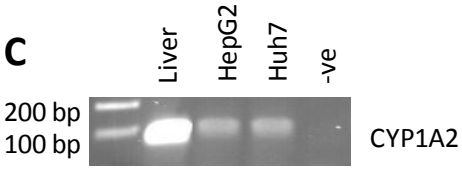

D

Clone sequence – insert is in the forward orientation

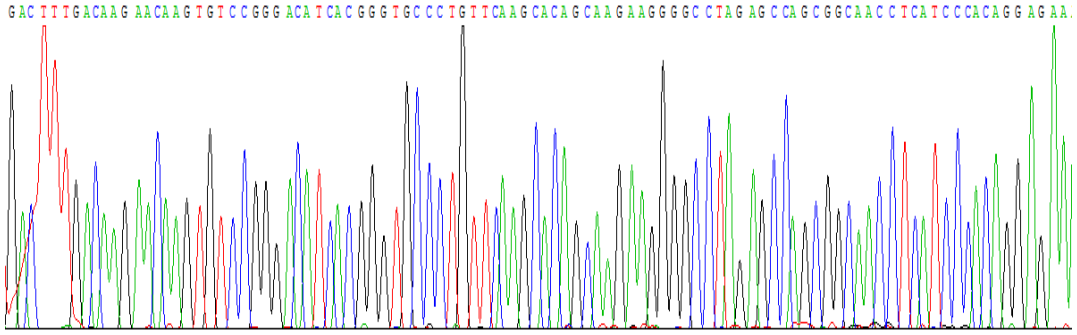

E

BLAST results for cloned sequence against reference sequence.

```
Clone       GACTTTGACAAGAACAAGTGTCCGGGACATCACGGGTGCCCTGTTCAAGCACAGCAAGAA
            ||||||||||||||| ||||||||||||||||||||||||||||||||||||||||||
Reference   GACTTTGACAAGAAC-AGTGTCCGGGACATCACGGGTGCCCTGTTCAAGCACAGCAAGAA

Clone       GGGGCCTAGAGCCAGCGGCAACCTCATCCCACAGGAGAA
            |||||||||||||||||||||||||||||||||||||||
Reference   GGGGCCTAGAGCCAGCGGCAACCTCATCCCACAGGAGAA
```

F

CYP1A2 qPCR assay		
Standard Curve	Efficiency	2.104
	Error	0.0111
Melting temperature range (°C)		78.0 – 78.4

G

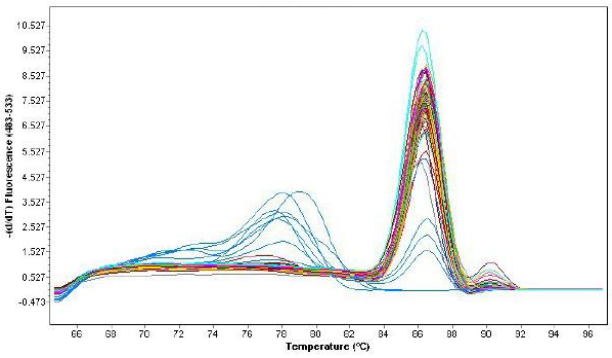

H

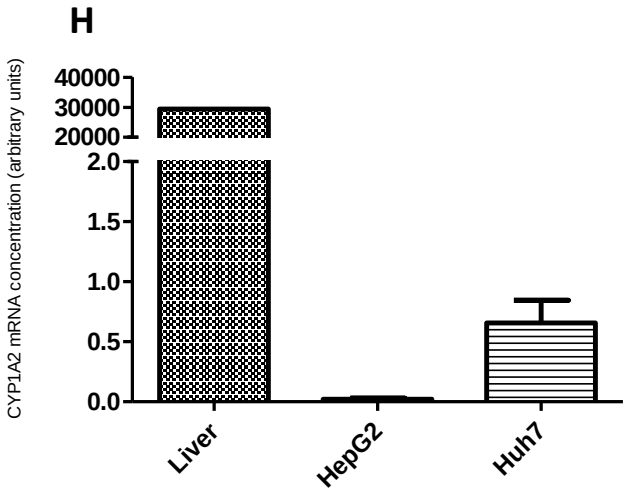

Figure 3.14 – CYP1A2 PCR assay development. Primer sequences, exon location, product length and annealing temperature for both end point and quantitative PCR are shown in the table A. The reference sequence with primers highlighted is displayed in B. End point PCR products visualised on an agarose gel under UV light are shown in C. These products were excised, cloned and sequenced as described in chapter 2; the chromatogram of the cloned sequence can be seen in D, with results from a BLAST analysis shown in E. Data from qPCR assays is displayed in parts F, G and H. Table F includes standard curve details and product melting temperatures, with figure G being an example of a typical melt point plot obtained through this assay. Finally, graph H shows data from the CYP1A2 qPCR assay normalised to two reference genes.

A

		CYP2E1 (NM_000773)
Primers	Forward	ATAGCCGACATCCTCTTCCG
	Reverse	GTAAAGCTGGAGCCAGGGAGTG
Exon Location	Forward	4
	Reverse	4, 5
Product length (bp)		117
Annealing temperature (°C)		59

B

Reference sequence (5'-3'). Exon-exon boundary is located at position 681-682.
571 – **ATAGCCGACATCCTCTTCCG**CAAGCATTTTGACTACAATGATGAGAAGTTTCTAAGGCT
GATGTATTTGTTTAATGAGAACTTCCACCTAC TCAG**CACTCCCTGGCTCCAGCTTTAC** – 687

C

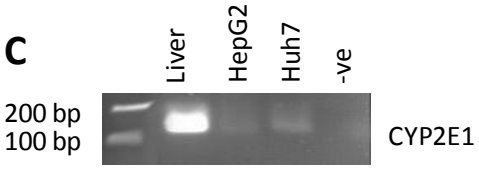

D

Clone sequence – insert is in the reverse orientation

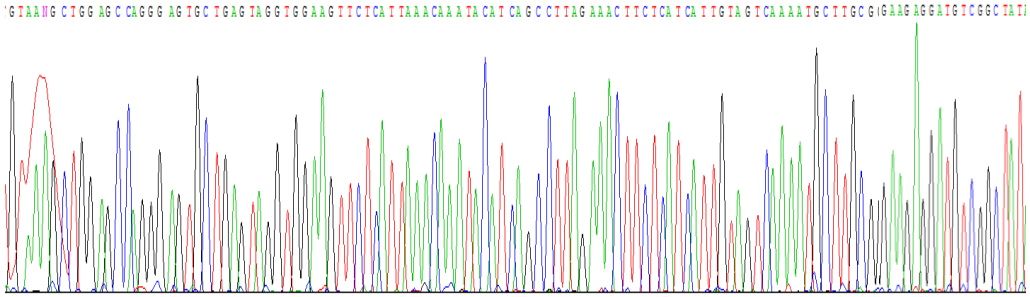

E

BLAST results for cloned sequence against reference sequence.

```
Clone      GTAANGCTGGAGCCAGGGAGTGCTGAGTAGGTGGAAGTTCTCATTAAACAAATACATCAG
           ||||  ||||||||||||||||||||||||||||||||||||||||||||||||||||||
Reference  GTAAAGCTGGAGCCAGGGAGTGCTGAGTAGGTGGAAGTTCTCATTAAACAAATACATCAG

Clone      CCTTAGAAACTTCTCATCATTGTAGTCAAAATGCTTGCGGAAGAGGATGTCGGCTAT
           ||||||||||||||||||||||||||||||||||||||||||||||||||||||||||
Reference  CCTTAGAAACTTCTCATCATTGTAGTCAAAATGCTTGCGGAAGAGGATGTCGGCTAT
```

F

CYP2E1 qPCR assay		
Standard Curve	Efficiency	2.009
	Error	0.0455
Melting temperature range (°C)		80.4 – 80.8

G

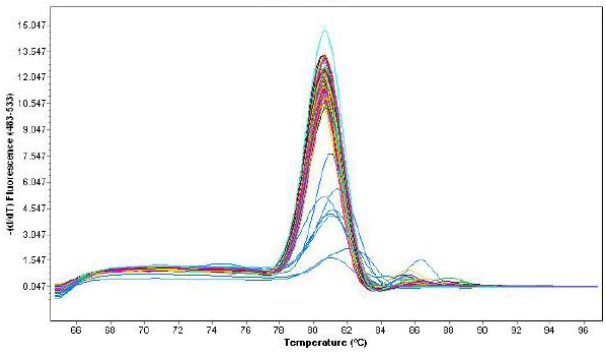

H

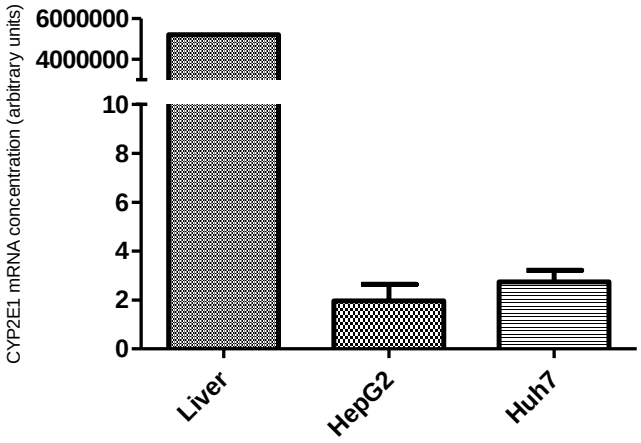

Figure 3.15 – CYP2E1 PCR assay development. Primer sequences, exon location, product length and annealing temperature for both end point and quantitative PCR are shown in the table A. The reference sequence with primers highlighted is displayed in B. End point PCR products visualised on an agarose gel under UV light are shown in C. These products were excised, cloned and sequenced as described in chapter 2; the chromatogram of the cloned sequence can be seen in D, with results from a BLAST analysis shown in E. Data from qPCR assays is displayed in parts F, G and H. Table F includes standard curve details and product melting temperatures, with figure G being an example of a typical melt point plot obtained through this assay. Finally, graph H shows data from the CYP2E1 qPCR assay normalised to two reference genes.

A

		CYP3A4 (NM_017460)
Primers	Forward	TGTGCCTGAGAACACCAGAG
	Reverse	GTGGTGGAAATAGTCCCGTG
Exon Location	Forward	13
	Reverse	13
Product length (bp)		226
Annealing temperature (°C)		58

B

Sequence 5'-3'.

1655 – **TGTGCCTGAGAACACCAGAG**ACCTCAAATTACTTTGTGAATAGAACTCTGAAATGAAGAT
GGGCTTCATCCAATGGACTGCATAAATAACCGGGGATTCTGTACATGCATTGAGCTCTCTCATTGTCT
GTGTAGAGTGTTATACTTGGGAATATAAAGGAGGTGACCAAATCAGTGTGAGGAGGTAGATTTGG
CTCCTCTGCTTCT**CACGGGACTATTTCCACCAC** – 1880

C

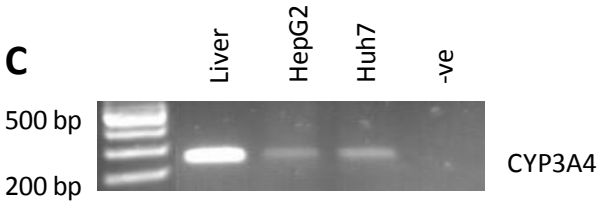

D

Clone sequence – insert is in the forward orientation

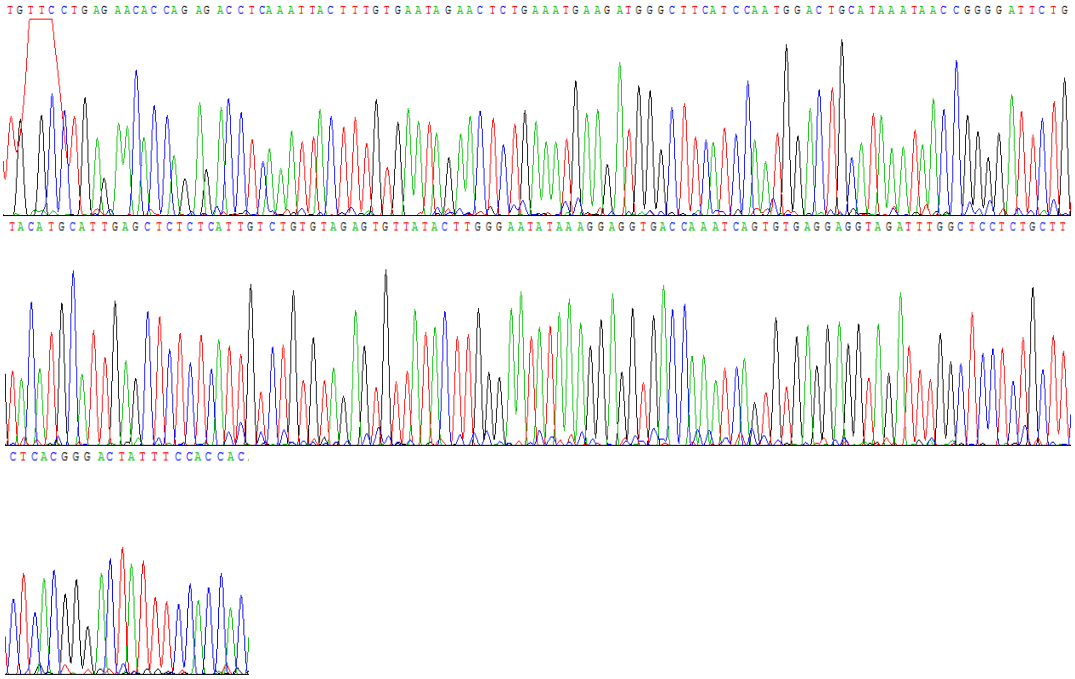

E BLAST results for cloned sequence against reference sequence.

```
Clone      TGTTCCTGAGAACACCAGAGACCTCAAATTACTTTGTGAATAGAACTCTGAAATGAAGAT
           ||| ||||||||||||||||||||||||||||||||||||||||||||||||||||||||
Reference  TGTGCCTGAGAACACCAGAGACCTCAAATTACTTTGTGAATAGAACTCTGAAATGAAGAT
Clone      GGGCTTCATCCAATGGACTGCATAAATAACCGGGGATTCTGTACATGCATTGAGCTCTCT
           ||||||||||||||||||||||||||||||||||||||||||||||||||||||||||||
Reference  GGGCTTCATCCAATGGACTGCATAAATAACCGGGGATTCTGTACATGCATTGAGCTCTCT
Clone      CATTGTCTGTGTAGAGTGTTATACTTGGGAATATAAAGGAGGTGACCAAATCAGTGTGAG
           ||||||||||||||||||||||||||||||||||||||||||||||||||||||||||||
Reference  CATTGTCTGTGTAGAGTGTTATACTTGGGAATATAAAGGAGGTGACCAAATCAGTGTGAG
Clone      GAGGTAGATTTGGCTCCTCTGCTTCTCACGGGACTATTTCCACCAC
           ||||||||||||||||||||||||||||||||||||||||||||||
Reference  GAGGTAGATTTGGCTCCTCTGCTTCTCACGGGACTATTTCCACCAC
```

F

CYP3A4 qPCR assay		
Standard Curve	Efficiency	2.069
	Error	0.264
Melting temperature range (°C)		81.6 – 81.9

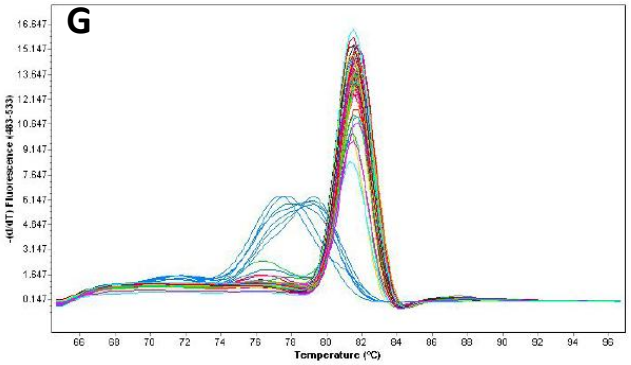

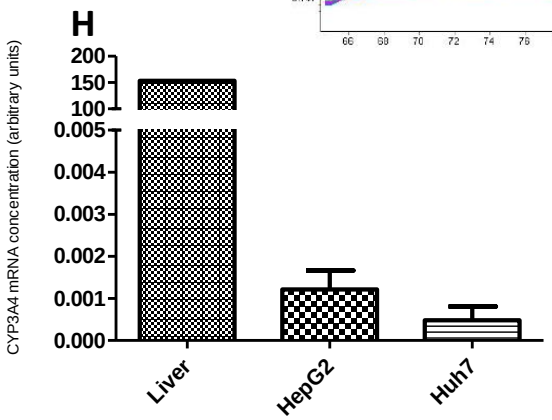

Figure 3.16 – CYP3A4 PCR assay development. Primer sequences, exon location, product length and annealing temperature for both end point and quantitative PCR are shown in the table A. The reference sequence with primers highlighted is displayed in B. End point PCR products visualised on an agarose gel under UV light are shown in C. These products were excised, cloned and sequenced as described in chapter 2; the chromatogram of the cloned sequence can be seen in D, with results from a BLAST analysis shown in E. Data from qPCR assays is displayed in parts F, G and H. Table F includes standard curve details and product melting temperatures, with figure G being an example of a typical melt point plot obtained through this assay. Finally, graph H shows data from the CYP3A4 qPCR assay normalised to two reference genes.

A

		GSTA Primers anneal to GSTA1, 2 and 5 (NM_145740, NM_000846, NM_153699)
Primers	Forward	AATCGCTACTTCCCTGCCTTTG
	Reverse	ACCAGATGAATGTCAGCCCG
Exon Location	Forward	5
	Reverse	6
Product length (bp)		95
Annealing temperature (°C)		59

B

Reference sequence (5'-3'). Exon-exon boundary is located at position 526-527.
500 – **AATCGCTACTTCCCTGCCTTTG**AAAAAGTCTTAAAGAGCCATGGACAAGACTACCTTGTT
GGCAACAAGCTGAGC**CGGGCTGACATTCA TCTGGT** – 594

C

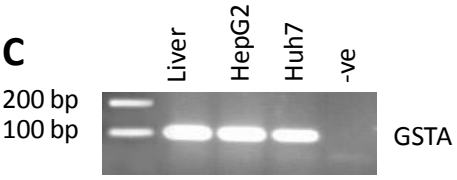

D

Clone sequence – insert is in the forward orientation

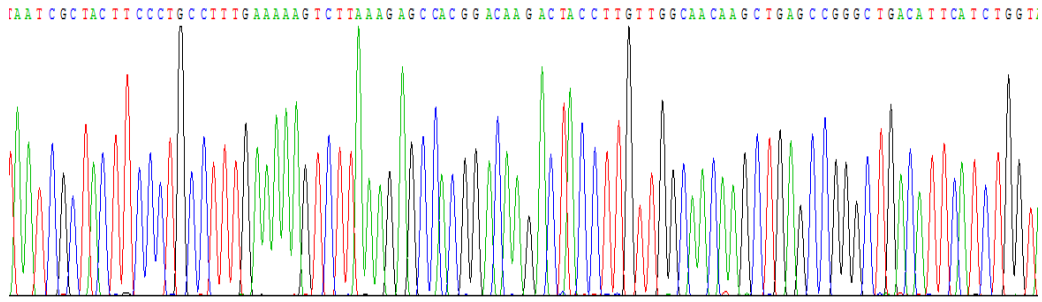

E

BLAST results for cloned sequence against reference sequence.

```
Clone       AATCGCTACTTCCCTGCCTTTGAAAAAGTCTTAAAGAGCCACGGACAAGACTACCTTGTT
            ||||||||||||||||||||||||||||||||||||||| ||||||||||||||||||
Reference   AATCGCTACTTCCCTGCCTTTGAAAAAGTCTTAAAGAGCCATGGACAAGACTACCTTGTT

Clone       GGCAACAAGCTGAGCCGGGCTGACATTCATCTGGT
            ||||||||||||||||||||||||||||||||||
Reference   GGCAACAAGCTGAGCCGGGCTGACATTCATCTGGT
```

F

GSTA qPCR assay		
Standard Curve	Efficiency	2.242
	Error	0.0217
Melting temperature range (°C)		81.7 – 82.1

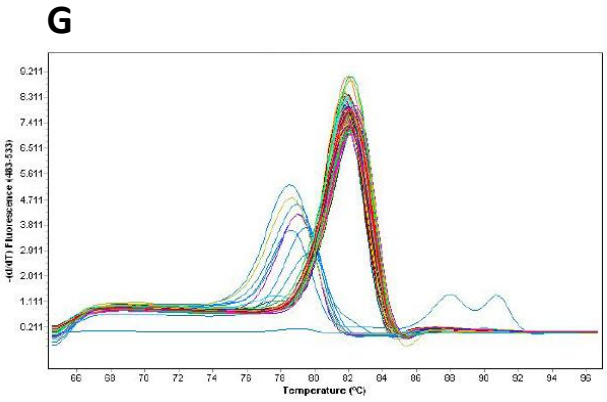

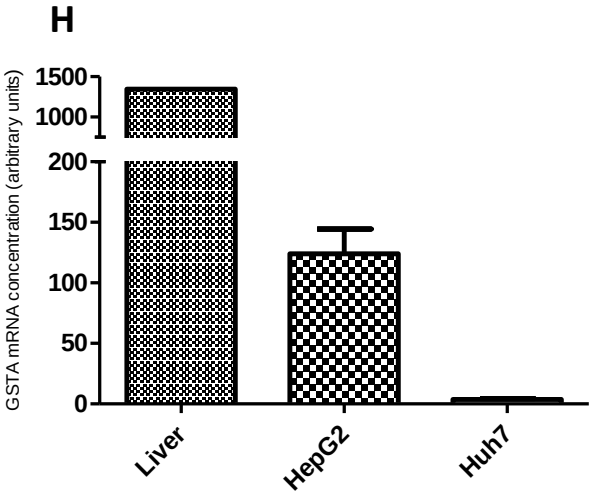

Figure 3.17 – GSTA PCR assay development. Primer sequences, exon location, product length and annealing temperature for both end point and quantitative PCR are shown in the table A. The reference sequence with primers highlighted is displayed in B. End point PCR products visualised on an agarose gel under UV light are shown in C. These products were excised, cloned and sequenced as described in chapter 2; the chromatogram of the cloned sequence can be seen in D, with results from a BLAST analysis shown in E. Data from qPCR assays is displayed in parts F, G and H. Table F includes standard curve details and product melting temperatures, with figure G being an example of a typical melt point plot obtained through this assay. Finally, graph H shows data from the GSTA qPCR assay normalised to two reference genes.

A

		GSTA4 (NM_001512)
Primers	Forward	ATGGTAACCACCTGCTGTTCC
	Reverse	GTCTGTACCAACTTCATCCCG
Exon Location	Forward	3, 4
	Reverse	4
Product length (bp)		67
Annealing temperature (°C)		58

B

Reference sequence (5'-3'). Exon-exon boundary is located at position 289-290.
287 – **ATGGTAACCACCTGCTGTTCC**AACAAGTGCCCATGGTTGAAATTGA**CGGGATGAAGTT GGTACAGAC** – 353

C

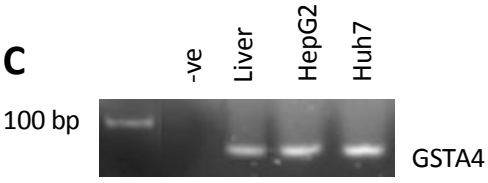

D

Clone sequence – insert is in the forward orientation

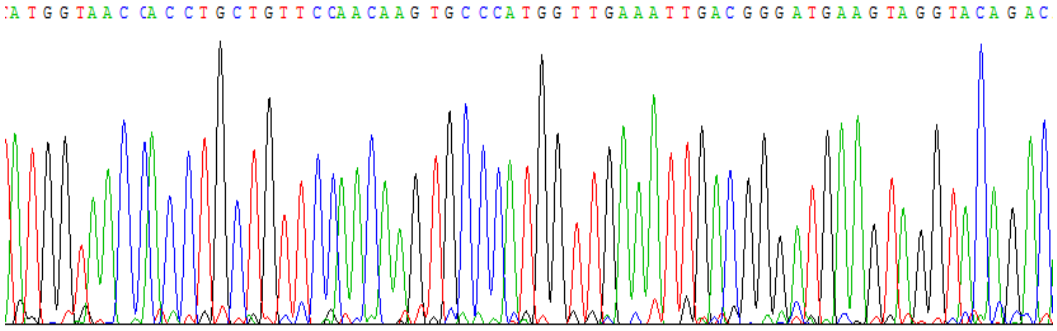

E

BLAST results for cloned sequence against reference sequence.

```
Clone      ATGGTAACCACCTGCTGTTCCAACAAGTGCCCATGGTTGAAATTGACGGGATGAAGTAGG TACAGAC
           |||||||||||||||||||||||||||||||||||||||||||||||||||||||||| || |||||||
Reference  ATGGTAACCACCTGCTGTTCCAACAAGTGCCCATGGTTGAAATTGACGGGATGAAGTTGG TACAGAC
```

F

GSTA4 qPCR assay		
Standard Curve	Efficiency	2.362
	Error	0.0317
Melting temperature range (°C)		80.2 – 80.5

G

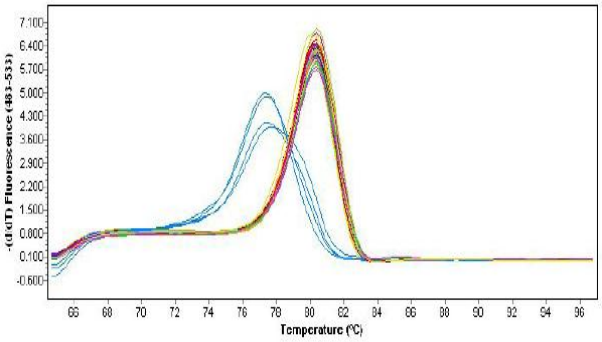

H

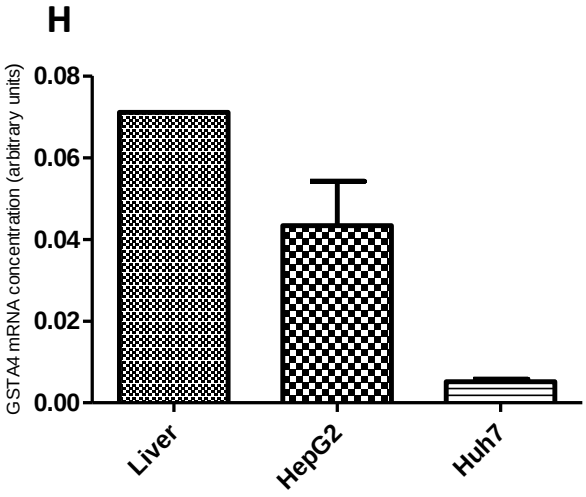

Figure 3.18 – GSTA4 PCR assay development. Primer sequences, exon location, product length and annealing temperature for both end point and quantitative PCR are shown in the table A. The reference sequence with primers highlighted is displayed in B. End point PCR products visualised on an agarose gel under UV light are shown in C. These products were excised, cloned and sequenced as described in chapter 2; the chromatogram of the cloned sequence can be seen in D, with results from a BLAST analysis shown in E. Data from qPCR assays is displayed in parts F, G and H. Table F includes standard curve details and product melting temperatures, with figure G being an example of a typical melt point plot obtained through this assay. Finally, graph H shows data from the GSTA4 qPCR assay normalised to two reference genes.

A

		UGT1A1 (NM_000463)
Primers	Forward	AAATAGTTGTCCTAGCACCTGACG
	Reverse	GGAATGGCACAGGGTACGTCTT
Exon Location	Forward	1
	Reverse	1
Product length (bp)		84
Annealing temperature (°C)		56

B Reference sequence (5'-3').
182 – **AAATAGTTGTCCTAGCACCTGACG**CCTCGTTGTACATCAGAGACGGAGCATTTTACACCT TG**AAGACGTACCCTGTGCCATTCC** – 265

C

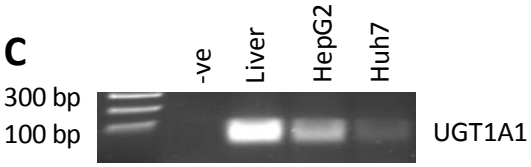

D Clone sequence – insert is in the forward orientation

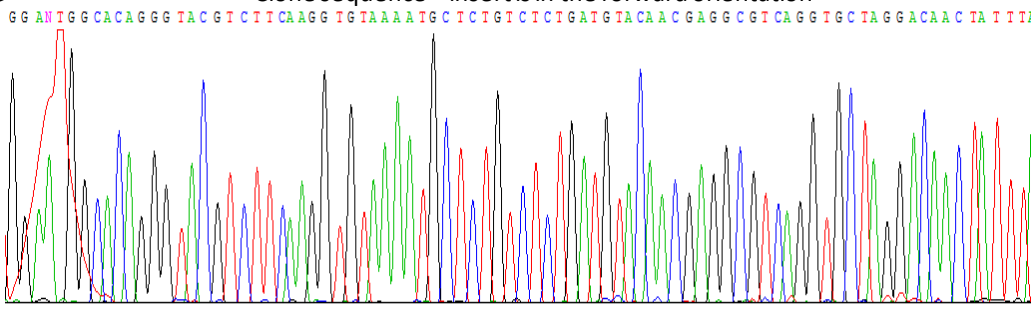

E BLAST results for cloned sequence against reference sequence.

```
Clone       TGGCACAGGGTACGTCTTCAAGGTGTAAAATGCTCTGTCTCTGATGTACAACGAGGCGTC
            ||||||||||||||||||||||||||||||||| |||||||||||||||||||||||||
Reference   TGGCACAGGGTACGTCTTCAAGGTGTAAAATGCTCCGTCTCTGATGTACAACGAGGCGTC

Clone       AGGTGCTAGGACAACTATTT
            ||||||||||||||||||||
Reference   AGGTGCTAGGACAACTATTT
```

F

UGT1A1 qPCR assay		
Standard Curve	Efficiency	2.030
	Error	0.0116
Melting temperature range (°C)		81.7 – 82.0

G

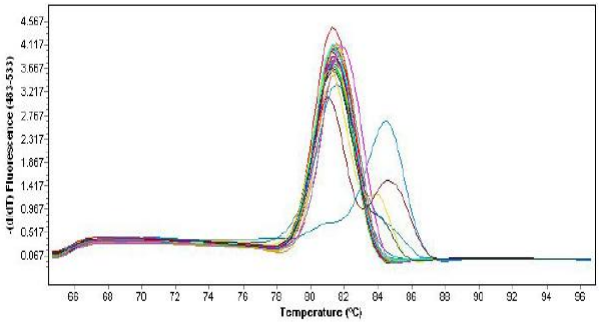

H

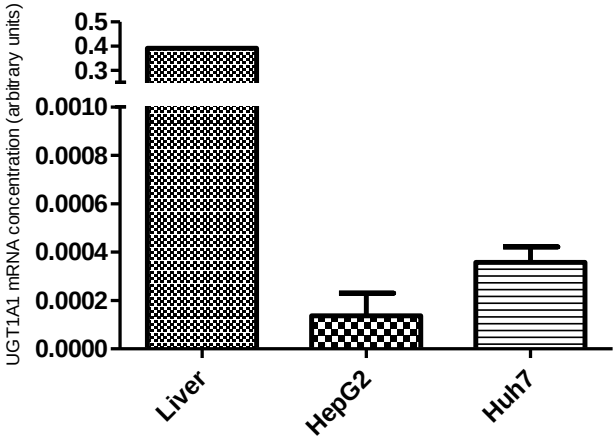

Figure 3.19 – UGT1A1 PCR assay development. Primer sequences, exon location, product length and annealing temperature for both end point and quantitative PCR are shown in the table A. The reference sequence with primers highlighted is displayed in B. End point PCR products visualised on an agarose gel under UV light are shown in C. These products were excised, cloned and sequenced as described in chapter 2; the chromatogram of the cloned sequence can be seen in D, with results from a BLAST analysis shown in E. Data from qPCR assays is displayed in parts F, G and H. Table F includes standard curve details and product melting temperatures, with figure G being an example of a typical melt point plot obtained through this assay. Finally, graph H shows data from the UGT1A1 qPCR assay normalised to two reference genes.

A

		FMO3 (NM_006894)
Primers	Forward	TATTCAATGGAAAGCGTGTCCTG
	Reverse	ATGACCTGTTCTGCTGTGCG
Exon Location	Forward	5
	Reverse	5, 6
Product length (bp)		91
Annealing temperature (°C)		58

B

Reference sequence (5'-3'). Exon-exon boundary is located at position 721-722.
636 – **TATTCAATGGAAAGCGTGTCCTG**GTGGTTGGCCTGGGGAATTCGGGCTGTGATATTGCC
ACAGAACTCAGC**CGCACAGCAGAAC AGGTCAT** – 726

C

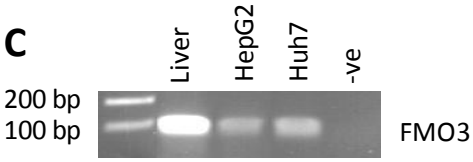

D

Clone sequence – insert is in the reverse orientation

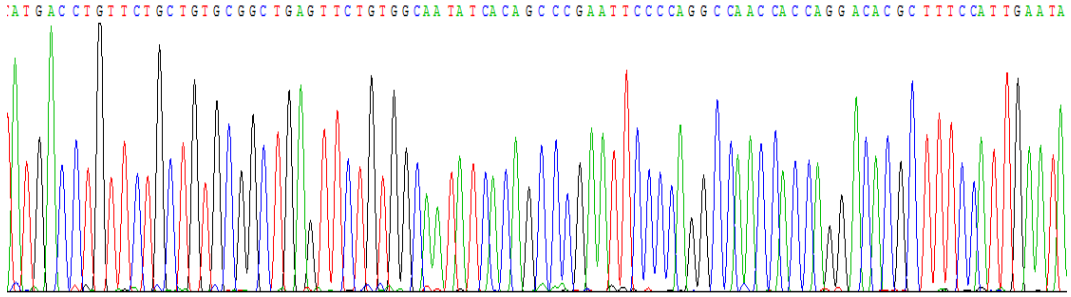

E

BLAST results for cloned sequence against reference sequence.

```
Clone       ATGACCTGTTCTGCTGTGCGGCTGAGTTCTGTGGCAATATCACAGCCCGAATTCCCCAGG
            ||||||||||||||||||||||||||||||||||||||||||||||||||||||||||||
Reference   ATGACCTGTTCTGCTGTGCGGCTGAGTTCTGTGGCAATATCACAGCCCGAATTCCCCAGG

Clone       CCAACCACCAGGACACGCTTTCCATTGAATA
            |||||||||||||||||||||||||||||||
Reference   CCAACCACCAGGACACGCTTTCCATTGAATA
```

F

FMO3 qPCR assay		
Standard Curve	Efficiency	1.836
	Error	0.0203
Melting temperature range (°C)		84.2 – 84.7

G

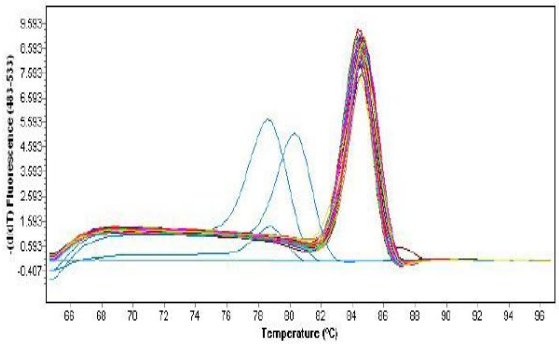

H

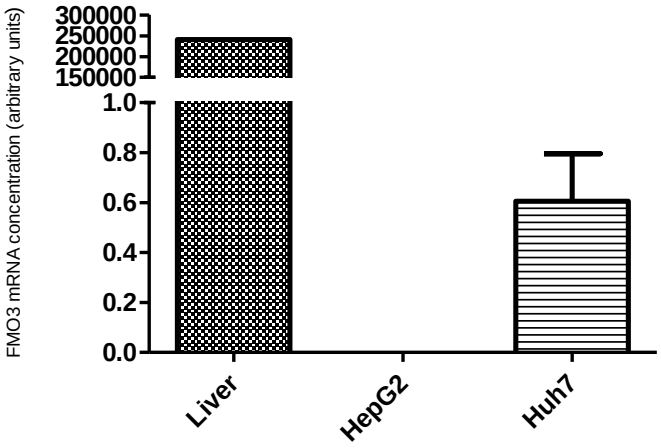

Figure 3.20 – FMO3 PCR assay development. Primer sequences, exon location, product length and annealing temperature for both end point and quantitative PCR are shown in the table A. The reference sequence with primers highlighted is displayed in B. End point PCR products visualised on an agarose gel under UV light are shown in C. These products were excised, cloned and sequenced as described in chapter 2; the chromatogram of the cloned sequence can be seen in D, with results from a BLAST analysis shown in E. Data from qPCR assays is displayed in parts F, G and H. Table F includes standard curve details and product melting temperatures, with figure G being an example of a typical melt point plot obtained through this assay. Finally, graph H shows data from the FMO3 qPCR assay normalised to two reference genes.

A

Assay	Number of runs	Clone 1 CV	Clone 2 CV
Albumin	10	0.041	0.037
Transferrin	10	0.042	0.057
AFP	10	0.050	0.051
HNF4a	5	0.052	0.057
A1AT	5	0.047	0.046
OATPB	5	0.085	0.051
OATPC	5	0.060	0.067
OATP8	5	0.038	0.042
OCT3	5	0.020	0.032
MRP1	5	0.061	0.095
MRP2	7	0.021	0.051
MDR1	10	0.068	0.068
BCRP	8	0.034	0.026
CYP1A2	10	0.057	0.081
CYP2E1	6	0.047	0.079
CYP3A4	10	0.029	0.037
FMO3	5	0.041	0.071
UGT1A1	10	0.059	0.043
GSTA	5	0.075	0.065
GSTA4	10	0.094	0.068

B

Assay	Clone 1 CV 1-5	Clone 1 CV 6-10	Clone 2 CV 1-5	Clone 2 CV 6-10
Albumin	0.034	0.051	0.025	0.050
Transferrin	0.020	0.048	0.030	0.078
AFP	0.053	0.029	0.026	0.055
MDR1	0.034	0.092	0.082	0.044
CYP1A2	0.048	0.056	0.069	0.081
CYP3A4	0.015	0.035	0.034	0.041
UGT1A1	0.071	0.052	0.037	0.052
GSTA4	0.120	0.036	0.098	0.025

Table 3.1 – Coefficient of Variation (CV) for qPCR assays. Table A shows CV values for all assays detailed in figures 3.1-3.20 calculated using data from two dilutions of the cloned PCR product over the number of runs specified. Table B shows data from those assays which had ten data points available (ten runs) with the first and second five data points analysed separately to highlight any changes over time for both clone dilutions.

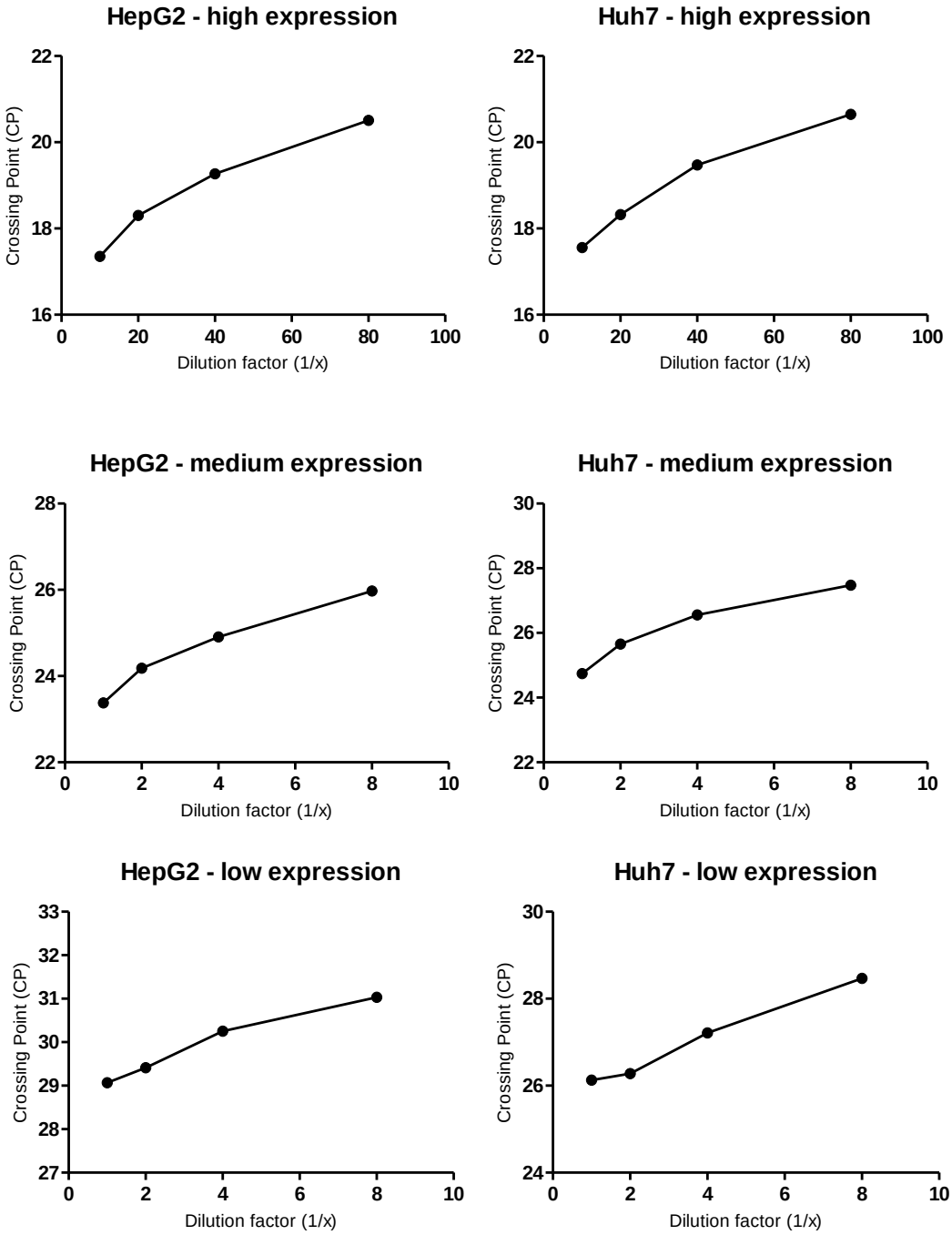

Figure 3.21 – Sample dilution series for high, medium and low expression assays. Samples were serially diluted and used in three assays representative of high (albumin), medium (BCRP) and low (CYP2E1) expression GOIs.

Gene	Expression relative to liver		
	Liver	HepG2	Huh7
Albumin	1.0	0.05	0.04
Transferrin	1.0	0.10	0.10
AFP	1.0	93	19
A1AT	1.0	0.16	0.03
HNF4a	1.0	2.1	0.42
MRP1	1.0	2110	89
MRP2	1.0	1.6	0.08
MDR1	1.0	2.7	0.18
BCRP	1.0	0.35	0.05
OCT3	1.0	0.69	8.0×10^{-3}
OATPB	1.0	0.21	0.08
OATPC	1.0	1.9×10^{-5}	2.8×10^{-3}
OATP8	1.0	5.1×10^{-5}	0.01
CYP1A2	1.0	7.1×10^{-7}	2.2×10^{-5}
CYP2E1	1.0	3.8×10^{-7}	5.3×10^{-7}
CYP3A4	1.0	7.9×10^{-6}	3.2×10^{-6}
GSTA	1.0	0.16	2.8×10^{-3}
GSTA4	1.0	0.61	0.07
UGT1A1	1.0	3.5×10^{-4}	9.1×10^{-4}
FMO3	1.0	2.2×10^{-10}	2.5×10^{-6}

Table 3.2 – Summary of gene expression in confluent HepG2 and Huh7 cells. This table summarises the results of the qPCR data displayed as part of figures 3.1 to 3.21. Confluent HepG2 and Huh7 cells were harvested for RNA and cDNA obtained as described in chapter 2. Whole liver cDNA was purchased and used as an indicator of *in vivo* hepatic levels. Results shown for HepG2 cells are from two experiments with a minimum of eight total replicates (N = 2, n = 8) and for Huh7 cells are from two experiments with a minimum of ten total replicates (N = 2, n = 10). All data has been normalised to two housekeeping genes and is displayed as relative change to liver. Numbers highlighted in grey denote mRNA levels closest to those observed in liver.

Chapter 4 – Differentiation of secondary hepatic cell lines to show a more *in vivo* hepatic profile

Chapter aim: To analyse the suitability of the previously identified differentiation markers and subsequently investigate whether various treatment regimes can be used to differentiate HepG2 and Huh7 cells into a more mature, hepatocyte-like cell.

4.1 – Introduction

As shown in the previous chapter, HepG2 and Huh7 cells are far from being ideal hepatocyte models showing both higher and lower mRNA levels of major enzymes and transporters compared to liver. In order to try and improve these cell lines several treatments were applied to attempt to differentiate them and induce a profile more resembling the *in vivo* hepatocyte. These treatments have been adapted from methods published in the literature and will be explained in more detail in this chapter.

A major area of development in recent years is the process of differentiating hepatocyte-like cells from stem cells. These attempts at creating a functional hepatocyte have been applied to cells from various sources such as human embryonic stem cells (hESCs) (Agarwal *et al.*, 2008; Hay *et al.*, 2008; Hay *et al.*, 2007; Jun Cai, 2007), umbilical cord blood derived stem cells (UCB-SCs) (Sensken *et al.*, 2007; Teramoto *et al.*, 2005) and adult sources such as adipose tissue and bone marrow stem cells (BMSCs) (Philippe A. Lysy, 2008; Snykers *et al.*, 2006). Interesting results have also been obtained using the rat pancreatic cell line AR42J treated with dexamethasone to create transdifferentiated hepatocytes (Eberhard *et al.*, 2010; Shen and Tosh, 2010; Burke *et al.*, 2006) and with human fetal pancreatic cells treated with fibroblast growth factor 2 and dexamethasone to generate hepatocyte-like cell (Sumitran-Holgersson *et al.*, 2009). Results from these attempts at differentiation have been studied in order to develop potential differentiation protocols applicable to HepG2 and Huh7 cells. Other more direct attempts at creating a more desirable hepatic profile in cell lines have met with some success, such as treatment of cell lines with dimethyl sulfoxide (DMSO) (Choi *et al.*, 2009; Sainz and Chisari, 2006) and inhibition of DNA methylation and histone deacetylation (Dannenberg and Edenberg, 2006); ideas from these studies have also been implemented in treatment development here.

A number of different protocols have been published by many separate groups regarding stem cell differentiation from human embryos, umbilical cord blood and adult cell sources. A common feature of these attempts at creating hepatocyte-like cells is a multi-step protocol

where treatments are applied at specific time points for a pre-determined period of time. These treatments typically last at least ten days and extend up to thirty days with two or three changes of growth-factor cocktails being applied. It would be expected that secondary hepatocyte cell lines such as HepG2 and Huh7 will already be pre-programmed towards hepatic development, compared with freshly isolated stem cells. Therefore, where a multiple-step protocol was described only the final maturation cocktail was applied to the cell lines.

An alternative protocol to application of growth factor cocktails is to use DMSO to induce hepatic differentiation. DMSO is used in primary hepatocyte culture to maintain the hepatic profile (Le Vee *et al.*, 2009), and with the hepatocarcinoma cell line HepaRG to create a more differentiated cell which more closely resembles the hepatocyte (Aninat *et al.*, 2006; Le Vee *et al.*, 2006; Gripon *et al.*, 2002). Both of these applications utilise DMSO at 2% v/v in the growth medium. Sumida *et al.* (Sumida *et al.*, 2011) have shown that DMSO at a concentration of up to 2% is not cytotoxic to either rat or human primary hepatocytes and that concentrations over 0.75% were required to significantly alter expression of the majority of probe sets assayed. Some genes which were shown to be up-regulated by DMSO included the cytochrome-P450 enymes (CYP) CYP3A4 and CYP2B6, whereas genes including multidrug-resistance associated proteins (MRPs) -2 to -5 and UDP glucuronosyltransferase (UGT) -1A6 were seen to be down-regulated with higher DMDO concentrations. Primary human hepatocytes have also been treated with concentrations of DMSO up to 2.5% and assessed for mRNA levels of several different enzymes and transporters by Nishimura *et al.* (Nishimura *et al.*, 2003). Results indicated that some genes were upregulated as a result of incubation with higher DMSO concentrations; these included CYP3A4, CYP2E1 and CYP1B1.

A study by Sainz *et al.* in 2006 (Sainz and Chisari, 2006) demonstrated that 1% DMSO applied to Huh7 cells resulted in a more differentiated cell line. This was supported by a further publication from the same group in 2009 (Choi *et al.*, 2009) which examined more thoroughly the expression of drug metabolising enzymes and found that in these DMSO-treated cells, both mRNA levels and functional activity were enhanced towards those seen in an *in vivo* hepatocyte. Use of DMSO at 1-2% has been described for HepG2 cells, however the effects on differentiation were not assessed (Chodon *et al.*, 2007; Galbraith *et al.*, 1986). Although this treatment does seem to have potential for use in Huh7 cells, results have been reported by one group only. As described earlier in chapter 3, there are high levels of variation between the same cell lines under different culture conditions so it is unknown whether this treatment would be effective on all Huh7 cells or indeed on all hepatic carcinoma cell lines. The precise mechanism through which DMSO functions is currently unknown (Aninat *et al.*, 2006; Sainz and Chisari, 2006) but several studies have been conducted which show some effects of the

compound on a cell. DMSO has been shown to be a scavenger of reactive oxygen species (ROS) (Villa *et al.*, 1991) and an anti-apoptotic agent (Gilot *et al.*, 2002), both in primary rat hepatocytes. It has also been shown to alter intracellular signalling in Chinese hamster ovary (CHO) cells (Fiore and Degrassi, 1999) and to affect cell membrane integrity in a variety of cells (Melkonyan *et al.*, 1996) and alternative splicing in HeLa cell nuclear extracts (Bolduc *et al.*, 2001). A combination of these factors or other unknown effect(s) of DMSO may be responsible for any differentiation seen in cell lines or maintenance of primary hepatocyte profiles *in vitro*.

In order to assess the extent of differentiation, the mRNA levels of five known markers of hepatic maturation were studied – albumin, transferrin, AFP, A1AT and HNF4a. Albumin and transferrin are both expected to be increased in the mature hepatocyte in comparison to the immature one, whereas AFP should decrease as maturation increases (Page *et al.*, 2007; Sainz and Chisari, 2006; Snykers *et al.*, 2006; Sidhu *et al.*, 2004; Raul Cassia, 1997). A1AT and HNF4a mRNA levels are also expected to increase with differentiation to a more mature hepatocyte (Sainz and Chisari, 2006). Although these alone do not define a hepatocyte, they can be used to indicate potential maturation of the cell towards a more hepatocyte-like profile. By quantifying mRNA changes in treated cells over time, the effectiveness of the treatments can be assessed for the specific differentiation markers and cell lines used here. Subsequently, marker expression can be used to predict potential maturation of a cell.

In the previous chapter, basal levels of these differentiation markers were assessed in comparison to liver. These indicated that neither cell line could be considered more hepatocyte-like than the other, with relatively equal levels of albumin and transferrin mRNA at approximately 20-fold and 10-fold lower expression than liver respectively, AFP mRNA levels closer to liver in Huh7 cells at 19-fold higher expression in comparison to 93-fold higher expression in HepG2 cells, A1AT mRNA levels closer in HepG2 cells at approximately 6-fold lower than liver and HNF4a mRNA levels 2-fold higher than liver in HepG2 cells and 2-fold lower than liver in Huh7 cells. The aims of this chapter were to identify the most suitable markers for preliminary assessment of differentiation and subsequently use this information to analyse the effects of a variety of potential differentiation protocols utilising combinations of growth factors and DMSO on both HepG2 and Huh7 cells, giving an indication as to whether a more hepatic phenotype was produced.

4.2 – Methods

All cells were seeded, grown and treated as described in chapter 2. Briefly, cells were seeded in six-well plastic plates. Treatments were initiated at 90% confluence as described by Sainz *et*

al. (Sainz and Chisari, 2006) and continued for the number of days specified for each experiment with a medium change every two to three days. Preliminary and extended growth factor treatments are detailed in tables 4.1 and 4.2 respectively. Total RNA was extracted at specific time points, reverse transcribed into cDNA and utilised in qPCR assessment of gene expression. Figures 2.1 and 2.2 detail experimental layout for each cell line. qPCR assays were conducted as described in chapters 2 and 3. Whole liver data are shown relative to control HepG2 and Huh7 cells (untreated confluent); these were calculated relative to all control cells for each particular cell line and the mean displayed on each figure in this chapter.

4.3 – Results

4.3.1 – Selection of differentiation markers

Five markers of hepatic maturation were assessed for their usefulness in indicating differentiation in treated cells. Criteria that were required to be met were that the assay was accurate and reliable in both treated and untreated cells and that as a result of treatment with DMSO, which produces a more hepatic phenotype in Huh7 cells (Sainz and Chisari, 2006), expression of the marker mRNA moved towards that in adult liver. A single experiment in which three identical samples were treated with 1% DMSO was used for each cell line in order to make these preliminary observations. HepG2 cells were treated for 20 days with RNA extracted every five days; Huh7 cells were treated for 25 days and RNA was extracted every five days. Both experiments included a control of 100% confluent cells consisting of a pool of six samples harvested after a total of four days of growth from seeding – see figures 2.1 and 2.2 for experimental layout. A1AT, albumin and transferrin mRNAs are predicted to increase if cells become more differentiated towards the *in vivo* hepatocyte, whereas AFP mRNA level is predicted to decrease. HNF4a mRNA expression is reported to increase with differentiation in the literature but data from chapter 3 showed that HepG2 cells already have HNF4a expression exceeding that in liver by 2.1-fold.

Results from treated HepG2 cells analysed by qPCR for these five markers of differentiation are shown in figure 4.1 where data from a sample of human liver cDNA are included for comparison. A1AT mRNA was significantly increased at 15 and 20 days of 1% DMSO treatment, with the level at 15 days approximately two thirds of liver expression and approximately 4-fold higher than control (figure 4.1 A). This indicated that cells were becoming differentiated by 15 days of treatment and that this was sustained through to 20 days. HNF4a mRNA in HepG2 control cells showed double the expression of HNF4a mRNA found in liver (figure 4.1 B). Significant increases over control were seen at 5 and 15 days, but these were not sustained at 10 and 20 days which remained much closer to control level. Both albumin and transferrin

mRNA levels (figure 4.1 C and E) in treated HepG2 cells increased significantly after 15 days and were sustained through to 20 days. AFP mRNA (figure 4.1 D) showed an initial significant increase at both 5 and 10 days of treatment but decreased to control level by 15 and 20 days; liver AFP mRNA level was notably lower than in control and treated cells.

Results from Huh7 cells treated with 1% DMSO for 25 days and analysed by qPCR for levels of maturation markers are shown in figure 4.2. A1AT mRNA level in control cells was roughly 30-fold lower than in liver and did not increase throughout the experiment. HNF4a results are much the same as were seen in HepG2 cells, with significant increases at 5 and 20 days which are not evident at other time points. Albumin mRNA level increases steadily throughout the 1% DMSO treatment, with significant increases from control level at 10, 20 and 25 days. AFP mRNA level would be expected to decrease as maturation increases, and in these treated Huh7 cells an initial increase was seen at 10 days followed by significant decreases compared to control at 15 and 20 days. The level increased slightly at 25 days but was still lower than control. The decreases in AFP mRNA observed at 15 to 20 days were to levels approaching those seen in liver. Transferrin mRNA showed significant increases from control at 15 and 20 days as would be expected in a more hepatocyte-like cell but still remained at a level approximately 75% lower than that in liver (figure 4.2 E).

These results are summarised in table 4.3 which shows fold change from control at 15 days of treatment for both cell lines along with expression in liver shown normalised to that in confluent HepG2 and Huh7 cells (data recalculated from table 3.1). In HepG2 cells, A1AT and albumin mRNA levels approached those seen in liver. HNF4a and transferrin data showed that mRNA levels of these genes increased above liver levels obtained in chapter 3. However, transferrin level in liver relative to the HepG2 control from this particular experiment remained higher than that in treated cells at all time points. This discrepancy is probably due to relatively low sample numbers in these initial experiments and transferrin levels are analysed with a larger sample number in figure 4.5. AFP mRNA levels in both cell lines were higher than liver and in HepG2 cells remained noticeably higher than in Huh7 cells – AFP should decrease with maturation. Huh7 cells had lower expression of A1AT at confluence than HepG2 cells as indicated by comparison of values for liver relative to confluent cells; liver expression relative to confluent Huh7 cells was 29.8-fold increased, whereas liver relative to HepG2 cells was 6.4-fold increased. Huh7 cells also failed to show significantly increased A1AT expression as a result of DMSO treatment, although levels were approximately 3-fold higher than control. HNF4a mRNA levels were very similar in 15 day treated Huh7 cells and liver, but these levels were not stable throughout the treatment. Albumin mRNA level in Huh7 cells increased

	Dexamethasone	10 ng/ml FGF4	20 ng/ml HGF	10 ng/ml OSM	1% ITS	0.2 mM Sodium pyruvate
Treatment 1	X (5^{-8}M)	-	X	-	X	X
Treatment 2	X (10^{-6}M)	-	-	X	X	X
Treatment 3	X (10^{-7}M)	-	X	X	-	-
Treatment 4	X (5^{-8}M)	X	X	-	X	X
Treatment 5	X (10^{-7}M)	X	X	X	-	-
Treatment 6	X (10^{-7}M)	-	X	X	X	X
Treatment 7	X (10^{-7}M)	X	X	X	X	X

Table 4.1 – Preliminary growth factor treatments adapted from published protocols (Agarwal *et al.*, 2008; Hay *et al.*, 2008; Hossein Baharvand, 2008; Philippe A. Lysy, 2008; Hay *et al.*, 2007; Jun Cai, 2007; Snykers *et al.*, 2006; Kurash *et al.*, 2004) and applied to HepG2 and Huh7 cells. Hepatocyte growth factor (HGF), oncostatin M (OSM) and insulin-transferrin-selenium (ITS) were purchased from Invitrogen, UK. Dexamethasone, fibroblast growth factor 4 (FGF4) and sodium pyruvate were purchased from Sigma, UK.

relative to control after 15 days of treatment but did not approach liver expression, while transferrin levels increased and by 15 days of treatment were closer to levels observed in liver. AFP mRNA expression decreased with treatment as would be expected in a more mature cell and became close to liver expression. This analysis of differentiation markers by a single experiment for each cell line gave an indication as to which of the markers would be most informative in terms of helping to indicate maturation of hepatic cells. For subsequent treatments, mRNA levels of albumin, transferrin and AFP were assessed to indicate whether further hepatic maturation occurred. HNFa was not selected as levels in both cell lines were already close to those in liver and any significant differences to control were not sustained in adjacent time points. A1AT was also omitted due to a lack of significant response observed in Huh7 cells when both albumin and transferrin did increase with treatment – in HepG2 cells, A1AT, albumin and transferrin all increased simultaneously, indicating a possible discrepancy in the response of A1AT in Huh7 cells.

Summary

- HepG2 – significant increases in albumin, transferrin and A1AT after 15 days of treatment. HNF4a and AFP did not decrease closer to liver levels.
- Huh7 – significant increases in albumin and transferrin, significant decreases in AFP with prolonged DMSO treatment. No sustained effect on HNF4a and A1AT.
- Overall, albumin, transferrin and AFP markers were determined to be the most informative of differentiation status after 1% DMSO treatment of at least 15 days.

4.3.2 – Preliminary growth factor treatments

Initially, seven treatments were adapted from published protocols describing generation of hepatocyte-like cells from sources such as hESCs, BMSCs and the rat pancreatic cell line AR42J (Agarwal *et al.*, 2008; Hay *et al.*, 2008; Hossein Baharvand, 2008; Philippe A. Lysy, 2008; Jun Cai, 2007; Snykers *et al.*, 2006; Kurash *et al.*, 2004). These are described in table 4.1 and were applied to both HepG2 and Huh7 cell lines. Cells were allowed to grow for three days after seeding to 90% confluence at which point treatments one to seven were applied for four additional days with media changed after two days. Control cells remained in standard growth medium without additional supplements for the whole seven days, with medium changes applied alongside treated cells. During this time frame control cells were able to maintain confluence and remain attached to the plate surface. RNA was extracted from all samples on the final day. These samples were analysed by qPCR for albumin, transferrin and AFP mRNA levels, the results of which are shown in figures 4.3 and 4.4 for HepG2 and Huh7 cells

respectively. If hepatic maturation had occurred an increase in both albumin and transferrin levels and a decrease in AFP levels compared to control would be expected. A human liver sample was included as an indication of *in vivo* levels.

In HepG2 cells no large increases in albumin or transferrin mRNA levels were seen; only treatments 4 and 5 resulted in significantly increased albumin and transferrin mRNAs respectively. These are not large changes when compared to levels in the liver. AFP mRNA level in control HepG2 cells was much higher than in liver; however, none of the treated cells showed a significant reduction in AFP. Treatments 6 and 7 produced an AFP mRNA level approximately half that of control but these decreases were not statistically significant. The effect of treatments 1 to 7 on Huh7 cells are shown in figure 4.4. Although albumin mRNA level in control cells was much lower than in liver, no increase was seen in any of the treated cells. In fact, treatments 3, 5, 6 and 7 resulted in significantly reduced expression compared to control. Transferrin mRNA level in Huh7 control cells was approximately 1.5 times that in HepG2 control cells and only one tenth of liver expression, but again no increases were observed in the treated cells; levels were generally lower than in control cells, although none of the changes were statistically significant. The AFP mRNA level in Huh7 control cells was approximately 10-fold lower than in HepG2 control cells but still three times higher than that in liver. Although none of the treatments resulted in levels which were significantly lower than control, neither did they increase AFP mRNA above control level. It is notable that the two treatments which produced the lowest AFP levels, 3 and 6, also resulted in significantly decreased albumin mRNA levels and lowered transferrin levels, indicating that perhaps the decrease in AFP is due to an overall decrease in global mRNA expression and not an indicator of increased hepatic maturation.

Summary

- Growth factor treatments did not result in a markedly more differentiated cell in either HepG2 or Huh7 cells; the short treatment time of four days was not sufficient.

4.3.3 – 1% DMSO treatment on HepG2 and Huh7 cells

Figure 4.5 shows results from HepG2 cells treated with 1% DMSO and analysed for the differentiation markers albumin, transferrin and AFP. Unlike the data used for differentiation marker assessment in figure 4.1, these data are compiled from three experiments with treatment extended to 25 days to allow for the possibility of maturation only after an extended period of treatment. Although matched controls could be generated for Huh7 cells (prolonged untreated growth), HepG2 cells did not survive for the duration of the experiment

in standard media, becoming over-confluent to such an extent that widespread cell death occurred. 1% DMSO is therefore required for prolonged growth of HepG2 cells, arresting the cell cycle and preventing over-growth. Albumin mRNA level increased significantly after 15 days of treatment and remained at a similar, but not significantly increased, level after 20 days before returning to control level at 25 days. Transferrin mRNA levels showed a similar pattern, with increases at both 15 and 20 days of treatment (significant at 20 days). At 25 days the expression of transferrin mRNA was reduced to control level. HepG2 cells treated with 1% DMSO showed no sustained or significant change in AFP mRNA level at any point.

Results from Huh7 cells treated with 1% DMSO and analysed for albumin, transferrin and AFP levels are shown in figure 4.6. As is the case with the previous figure, this displays data for three 1% DMSO experiments rather than just one as in figure 4.2. This figure displays data from both confluent control cells (as in HepG2 experiments) along with untreated cells matched to each time point, which were grown for the specified number of days in standard growth medium. The experimental layout used in this treatment can be seen in figure 2.2. Albumin mRNA levels showed a steady increase throughout the experiment in both treated and untreated cells, with the 1% DMSO treatment resulting in a significant increase from 10 days onwards and untreated cells showing significant increases from 15 days onwards. No difference between treated and untreated cells was seen at any time point when assessed by Student's t-test. Transferrin mRNA levels were significantly increased after 15 and 20 days of 1% DMSO treatment but remained at control level in untreated cells. Significant differences between untreated and DMSO-treated cells were seen at 10 to 25 days inclusive; in all cases 1% DMSO treated cells had increased expression over untreated cells. The difference in levels of transferrin mRNA between treated and untreated cells indicate an effect of DMSO rather than of prolonged or arrested growth. AFP mRNA levels decreased steadily throughout both experiments and were significantly different from control at all time points in both untreated and DMSO-treated Huh7 cells. DMSO treated cells had significantly lower AFP mRNA than untreated cells at 25 days; at all other time points there was no difference between treated and untreated cells.

Summary

- HepG2 – significant increases in albumin and transferrin after 15 days of treatment, no significant changes in AFP level. 1% DMSO is required for prolonged treatment.
- Huh7 – 1% DMSO treatment produced significant increases in albumin and transferrin plus significant decreases in AFP. Prolonged untreated growth also resulted in significant albumin and AFP changes but no effect on transferrin was observed.

- Huh7 1% DMSO treatment appears to be more effective at differentiation than prolonged untreated growth, indicating DMSO is inducing maturation as well as slowing growth.

4.3.4 – 2% DMSO treatment on HepG2 and Huh7 cells

In figure 4.7 data are shown from the 1% DMSO HepG2 experiments previously displayed in figure 4.5 alongside results from cells treated with 2% DMSO; this allows direct comparison of the two treatments. The 2% DMSO treatment produced a significant increase in albumin mRNA over control level at both 10 and 15 days, while with 1% DMSO the level only became significantly higher at 15 days. A significant difference between the two treatments was seen at 10 days, with 2% DMSO treated cells showing a higher level of albumin mRNA than cells treated with the lower concentration of DMSO. The trend in 2% DMSO treated cells followed that observed in earlier experiments where the increase was not sustained throughout the later time points.

Transferrin mRNA level in 2% DMSO treated cells increased steadily from initiation of the experiment until 15 days when a significant increase from control was observed. Again, the effect of 1% DMSO lagged slightly behind with increases at 15 and 20 days. Significantly higher levels in 2% treated cells over 1% treated cells were seen at 5 and 10 days. A decrease in transferrin mRNA to a level comparable to that in control was apparent from 20 days in 2%, and at 25 days in 1% DMSO treated cells respectively. AFP mRNA level increased initially with 2% DMSO treatment and returned to control level from 10 days onwards. In general, AFP mRNA levels were higher in 2% DMSO treated cells than in 1% DMSO treated cells at matched time points, with significant increases at 5, 10 and 20 days. AFP mRNA level was significantly lower in 2% than in 1% DMSO treated cells at 25 days.

Figure 4.8 displays data from Huh7 cells treated with 2% DMSO for up to 25 days and analysed for albumin, transferrin and AFP mRNA levels. This is displayed alongside data from figure 4.6 showing mRNA levels of these genes in untreated and 1% DMSO treated cells. Albumin mRNA levels were increased by 2% DMSO and reached significance compared to control at 15 days of treatment, although the standard error was large. No significant differences between untreated, 1% and 2% DMSO treated cells were seen at any time point. Transferrin mRNA levels in 2% DMSO treated cells increased earlier than with either 1% DMSO or extended

	DMSO (1%)	Dexamethasone (10^{-7}M)	HGF (20 ng/ml)	OSM (10 ng/ml)
Control and untreated cells	-	-	-	-
DMSO (1%)	X	-	-	-
DMSO (2%)	X (2%)	-	-	-
Treatment 1	X	X	X	-
Treatment 2	X	X	-	X
Treatment 3	X	X	X	X

Table 4.3 – Extended treatments applied to HepG2 and Huh7 cells for up to 25 days. Treatments 1-3 were adapted from preliminary growth factor experiments.

growth, with significant increases compared to control at 5, 10, 15 and 25 days. Cells treated with 2% DMSO had significantly raised transferrin mRNA compared to untreated cells at 5 and 10 days, the mRNA level was significantly increased over 1% DMSO treated cells at day 10 only. 2% DMSO treated cells had a similar level of transferrin to untreated cells after 20 days when 1% DMSO treatment resulted in transferrin mRNA levels significantly higher than both of the other treatments. AFP mRNA level in 2% DMSO treated Huh7 cells did not significantly decrease in comparison to control at any time. This was in contrast to both untreated and 1% treated cells, which both showed significant decreases from control at all time points. The level of AFP mRNA in 2% DMSO treated cells was significantly higher than in both untreated and 1% treated cells at 5, 10 and 20 days of treatment and higher than 1% DMSO treated cells at 25 days of treatment.

Summary

- HepG2 – albumin and transferrin levels increased earlier with 2% DMSO treatment than with 1% DMSO. AFP levels in 2% DMSO cells were higher than in 1% at 5, 10 and 20 days, indicating no advantage over 1% treatment.

- Huh7 – significant increases over control were seen in albumin after 15 days and transferrin at all times points except 20 days. AFP did not decrease significantly.

- 2% DMSO treatment also resulted in a less healthy cell population than 1% DMSO with cell detatchment and lower RNA yields. Results from differentiation marker analysis combined with this observation reveal no advantage in 2% over 1% DMSO treatment.

4.3.5 – HepG2 cells plus treatment 1

Treatments 1, 2 and 3 are detailed in Table 4.2. Figure 4.9 shows data for HepG2 cells with treatment 1 (Tr1). Tr1 consisted of 1% DMSO, 10^{-7}M dexamethasone and 20 ng/ml hepatocyte growth factor (HGF) in standard growth medium. These data are displayed alongside previously presented data for 1% DMSO treated cells. A significant increase in albumin mRNA level was seen at 10 days both in comparison to control and to 1% DMSO treated cells. However, this increase was not sustained at later time points. Transferrin mRNA levels in Tr1 cells were increased from control throughout the experiment, with significant changes from control at 10 and 15 days and significant increases from 1% DMSO treated cells at 10 and 25 days. AFP mRNA levels remained largely unchanged from control with the only significant difference observed being a slight increase in 1% DMSO treated cells transferrin level over that in Tr1 cells at 25 days.

Summary

- Although significant increases in transferrin were apparent earlier than in 1% treatment, no advantage was observed in albumin and AFP expression with Tr1.

4.3.6 – HepG2 cells plus treatment 2

Treatment 2 (Tr2) consisted of 1% DMSO, 10^{-7}M dexamethasone and 10 ng/ml oncostatin M (OSM) in standard growth medium; data for HepG2 cells plus Tr2 are shown in figure 4.10. Again, data for 1% DMSO treated cells are displayed alongside these results for comparison. No change from control level of albumin mRNA was seen at any time point for Tr2 cells, while significant increases from control were observed in transferrin mRNA levels at 15, 20 and 25 days of treatment. This increase in transferrin level was maintained at 25 days unlike with the 1% DMSO treatment, where mRNA level was significantly lower than in Tr2 treated cells. In contrast to the 1% DMSO treated cells where no decrease in AFP mRNA was detected, Tr2 cells showed a significant and time-dependent decrease compared to control from 10 days onwards. Tr2 treated cells were also significantly lower in AFP mRNA than 1% DMSO treated cells from 15 days onwards.

Summary

- AFP was significantly decreased in comparison to both control and 1% DMSO from 10 days onwards; however, no increase in albumin and lower increases in transferrin indicate that a more mature cell type was not produced with Tr2.

4.3.7 – HepG2 cells plus treatment 3

Treatment 3 (Tr3) consisted of 1% DMSO, 10^{-7}M dexamethasone, 20 ng/ml HGF and 10 ng/ml OSM in standard growth medium; data for HepG2 cells plus Tr3 alongside data from 1% DMSO treated cells are shown in figure 4.11. Albumin mRNA levels increased slightly at 10 and 15 days with Tr3 but do not reach significance. Transferrin mRNA was consistently above control levels and reached significance at 10 and 15 days. Tr3 treated cells also showed significantly higher transferrin mRNA levels than 1% DMSO treated cells at all time points except 20 days. AFP mRNA levels in Tr3 cells were lower than control from day 15 onwards but only reached significance at 25 days. Tr3 AFP mRNA levels were significantly lower than those in 1% DMSO treated cells at 15 and 25 days.

Summary

- Transferrin was increased over both control and 1% DMSO at 10 and 15 days; however, no significant albumin increases occurred, with AFP significantly decreasing only after 25 days. No clear advantage of Tr3 over 1% DMSO was apparent.

4.3.8 – Huh7 cells plus treatment 1

Treatments 1 to 3 are as described in Table 4.2, and are identical to those applied to HepG2 cells. Treatment 1 (Tr1) consisted of 1% DMSO, 10^{-7}M dexamethasone and 20 ng/ml HGF; data for Huh7 cells plus Tr1 are shown in figure 4.12. Displayed alongside results for this treatment are those previously described for prolonged untreated culture and 1% DMSO alone. Albumin mRNA levels were significantly increased compared to control in Tr1 cells at 15 and 25 days but were at control level at day 20. At 15 days albumin mRNA level was significantly increased over both untreated and 1% DMSO treated cells by Tr1; however, at 20 days the level was significantly lower than that seen in 1% DMSO treated cells. Transferrin mRNA levels in Tr1 cells appeared to increase in comparison to control throughout the experiment (similar to results with 1% DMSO), but did not reach significance at any time point. Significant differences were seen between untreated and Tr1 cells at 5, 10 and 25 days, while 1% DMSO treated cells had higher levels of transferrin mRNA than both untreated and Tr1 treated cells at 20 days. Although AFP mRNA levels steadily decreased from 5 days onwards in Tr1 cells they did not decrease significantly in comparison to control levels and remained substantially higher than in untreated and 1% DMSO treated cells. The AFP level in Tr1 cells was significantly increased over that in untreated cells at 5, 10 and 15 days, and in 1% DMSO treated cells at 10 and 15 days.

Summary

- Albumin and transferrin levels were generally similar to both untreated and 1% DMSO but AFP did not significantly decrease from control as was observed with untreated and 1% DMSO cells. No advantage of Tr1 over 1% DMSO was observed.

4.3.9 – Huh7 cells plus treatment 2

Treatment 2 (Tr2) consisted of 1% DMSO, 10^{-7}M dexamethasone and 10 ng/ml OSM in standard growth medium; data for Huh7 cells plus Tr2 along with data from untreated and 1% DMSO treated cells are shown in figure 4.13. Albumin mRNA levels remained around control level except at 15 days, at which point a statistically significant but unsustained increase was observed. At this time point, Tr2-treated cells showed a significantly higher level of albumin

mRNA than both untreated and 1% DMSO treated cells. At 25 days the reverse was observed as Tr2 cells had a significantly lower level of albumin mRNA than the two other data sets. Transferrin mRNA in Tr2 cells was significantly raised at 5 and 15 days compared to control. At 20 days 1% DMSO treated cells showed significantly increased transferrin mRNA level over both untreated and Tr2 cells. AFP mRNA levels in Tr2 cells generally decreased from control level and all (except the 15 day time point increase) reached significance. AFP mRNA level at day 15 appeared to be an anomalous result as data from 10 and 20 days did not support this value, which was almost as high as the original control level and was significantly higher than that in both untreated and 1% DMSO treated cells.

Summary

- Significant increases in both albumin and AFP occurred with Tr2 at 15 days but were not sustained – AFP was not significantly lower than that in untreated or 1% DMSO cells. No benefit of Tr2 over 1% DMSO was observed.

4.3.10 – Huh7 cells plus treatment 3

Treatment 3 (Tr3) consisted of 1% DMSO, 10^{-7}M dexamethasone, 20 ng/ml HGF and 10 ng/ml OSM in standard growth medium; data for Huh7 cells plus Tr3 alongside data from untreated and 1% DMSO treated cells are shown in figure 4.14. Tr3 cells showed albumin mRNA levels largely unchanged from control with no significant increases or decreases. At 10 and 20 days of treatment, cells were significantly lower in albumin mRNA than 1% DMSO treated cells and significantly lower than untreated cells at 20 and 25 days. Transferrin mRNA levels in Tr3 cells also remained close to control level with no significant increase or decrease. After 20 days of treatment, 1% DMSO treated cells had higher transferrin mRNA level than both untreated and Tr3 cells and Tr3 cells were significantly lower in transferrin than both 1% DMSO and untreated cells. After 25 days of treatment Tr3 cells had a significantly lower level of transferrin mRNA than 1% DMSO treated cells. AFP mRNA levels steadily decreased from control in Tr3 cells and were significantly reduced at 15 and 25 days. Tr3 cells also showed significantly lower AFP level at 25 days than both untreated and 1% DMSO treated cells.

Summary

- Neither albumin nor transferrin levels were significantly increased over control; AFP levels did decrease but only reached significance after 15 and 25 days of treatment. Tr3 did not show a significant advantage over 1% DMSO.

4.3.11 – Comparison of treatments in HepG2 and Huh7 cells

Figure 4.15 shows results from each treatment at 15 days plus control levels and liver data. Control and treated data were taken from figures 4.5, 4.7, 4.9, 4.10 and 4.11. Liver data have been included from previous figures in this chapter (labelled 'liver') and recalculated from table 3.1 (labelled 'liver 3.1') to be displayed as relative to confluent HepG2 levels. The time point of 15 days was chosen for this analysis as the majority of treatments that showed an effect exhibited a change in differentiation marker mRNA levels at this stage of treatment. Results for one-way ANOVA with Dunnett's post test to enable comparison to control are included as displayed on the original figures. Results for one-way ANOVA with Bonferroni's post test are also displayed; these were calculated for 15 day treated cells only, excluding values for control and liver samples.

When compared to control, the only treatments which resulted in significantly higher albumin mRNA levels were 1% and 2% DMSO. No differences were seen between 1- or 2% DMSO and treatments 1-3. With regard to transferrin mRNA, the only treatment which did not produce a significant change from control at 15 days was 1% DMSO. However, the mean value for this treatment was extremely close to that calculated for 2% DMSO treated cells and was higher than that seen in Tr2 cells, both of which were significant. A comparison between the effects of 1- and 2% DMSO and treatments 1-3 showed a significant difference between Tr2 and Tr3, with Tr3 having the greater effect of the two. AFP mRNA level was significantly decreased from control by both Tr2 and Tr3 but remained higher than that in liver. Tr2 also produced a significantly lower AFP mRNA level than both 1% and 2% DMSO treatments.

In Huh7 cells, albumin mRNA levels were significantly increased in comparison to control by all treatments except Tr3, with no significant differences between the differently treated cells (fig 4.16). Transferrin mRNA levels were increased over control in 1%- and 2%- DMSO and in Tr2-treated cells after 15 days of treatment. Again, no significant differences in effect were seen between 1 and 2% DMSO and treatments 1-3. AFP mRNA levels were significantly decreased in 1-and 2% DMSO- and in Tr3-treated cells. Significant increases in AFP mRNA level were seen in cells with Tr2 when compared to untreated cells and those exposed to 1% DMSO. Tr3 treated cells had significantly lower AFP mRNA levels than Tr1 and Tr2 cells.

Summary

- HepG2 – overall, 1% DMSO is the preferable differentiation treatment with increases in both albumin and transferrin. Tr1, 2 and 3 did not increase albumin, while 2% DMSO caused some cell death.

- Huh7 – only prolonged untreated growth, 1% DMSO and Tr3 produced significant AFP decreases; of these, only 1% DMSO also showed significant increases in albumin and transferrin. Therefore, 1% DMSO is the preferable treatment for Huh7 cells.

- Relative liver levels were stable from the cells analysed at confluence in chapter 3 to the confluent cells used in experiments here, indicating that basal levels of the differentiation markers were stable with passaging of both cell lines.

4.4 – Discussion

In order to assess the hepatic maturation status of HepG2 and Huh7 cells, measurement of informative markers was required. Five potential markers of differentiation, albumin, transferrin, AFP, A1AT and HNF4a were assessed in both cell lines treated with 1% DMSO. All five of these markers had previously been reported in the literature as being indicative of a more mature hepatic cell when an appropriate increase or decrease in expression was seen (Page *et al.*, 2007; Sainz and Chisari, 2006; Snykers *et al.*, 2006; Sidhu *et al.*, 2004; Raul Cassia, 1997). Results are shown in figures 4.1 and 4.2 for HepG2 and Huh7 cells respectively. Changes observed in these experiments indicated that of the five markers selected, three were more suitable for assessment of maturation status in these cell lines; these were albumin, transferrin and AFP as the responses observed matched those reported in the literature as being those expected in a more mature hepatic cell.

Preliminary experiments with seven different growth factor mixtures applied to HepG2 and Huh7 cells (figures 4.3 and 4.4) showed no clear effect on differentiation. This may be because treatments were only applied for four days whereas the literature demonstrates that extended exposure to specific cocktails of growth factors are ideally required for differentiation, e.g. at least 10 days (Agarwal *et al.*, 2008; Hay *et al.*, 2008; Hossein Baharvand, 2008; Philippe A. Lysy, 2008; Jun Cai, 2007; Snykers *et al.*, 2006). Extended treatment durations with these mixes were attempted but continued proliferation led to cells overgrowing and dying soon after the 4 day time point. As very little informative data were gained from this restricted growth time, the literature was re-assessed to see which treatments may be most beneficial. As a result of this analysis, treatments 1, 2 and 3 were adapted and selected for further investigation. All further treatments included dexamethasone as it is essential for liver maturation (Kinoshita and Miyajima, 2002; Zaret, 2002) and is included in the majority of protocols attempting to differentiate hepatocytes. HGF was used in the final stage of a stepped protocol by Snykers *et al.* (Snykers *et al.*, 2006) using rat BMSCs, which resulted in raised albumin levels, alongside a transient increase then decrease of AFP as the cells matured. OSM has been used in the

differentiation of pancreatic cells into hepatocytes (Kurash *et al.*, 2004) and with hESCs (Hay *et al.*, 2008) with promising results. HGF and OSM have been used together on hESCs by Baharvand *et al.* (Hossein Baharvand, 2008), which reported promising results in terms of hepatic marker expression. Sodium pyruvate and ITS (insulin-selenium-transferrin) were omitted from prolonged treatments as they are intended for use in serum-free medium as partial replacement of the hormones and other additives usually contributed by serum supplementation (Sigma datasheet I2521, appendix B); as all treatments contained 10% serum this was unnecessary.

In order to prolong the duration of growth factor treatments on both cell lines, a mechanism of slowing or halting growth was required, particularly for HepG2 cells. Several compounds have been described that slow growth of HepG2 and Huh7 cells including vitamin K2 (Yamamoto *et al.*, 2009) and vitamin K2 analogues such as menatetrenone (Ozaki *et al.*, 2007) and panaxydol (Guo *et al.*, 2009). 1% DMSO treatment has been reported to halt growth after approximately 6 days of treatment and to induce differentiation in Huh7 cells (Choi *et al.*, 2009; Sainz and Chisari, 2006). This treatment seemed to be the most promising and had already been seen to effectively enable prolonged incubation and induce differentiation in both cell lines here. As extended treatment periods were required with growth factor cocktails, 1% DMSO was added in order to prolong treatments one, two and three (table 4.3). A 2% DMSO treatment is used in the cell line HepaRG to induce differentiation to a more mature hepatic profile (Aninat *et al.*, 2006; Le Vee *et al.*, 2006; Gripon *et al.*, 2002); both concentrations were applied experimentally here.

Thus, following the initial experiments, further treatments of 1% and 2% DMSO were applied to both cell lines. HepG2 cells showed significant increases in albumin and transferrin mRNA levels after 15 and 20 days respectively with 1% DMSO treatment, while 2% DMSO produced significant increases in expression of both genes earlier than observed following 1% DMSO. Taken alone, these results indicate that 2% DMSO enhances maturation after shorter incubation times than 1% DMSO. AFP mRNA levels were generally lower in 1%- than in 2% DMSO treated HepG2 cells but did not reach significance in comparison to control. Observations of the cells made during treatment revealed that HepG2 cells appeared unhealthier when subject to 2% DMSO than untreated or 1% DMSO treated cells with noticeable cell death and unattached cells. Comparison of results combined with these observations led to the conclusion that the higher concentration of DMSO treatment provided no discernable advantage.

As it was possible to culture Huh7 cells for the duration of the experiment without addition of DMSO, effects of DMSO inclusion over those observed with prolonged untreated growth were able to be assessed. Both untreated Huh7 cells and those with 1% DMSO showed a steady increase in albumin mRNA levels with statistical significance first achieved at 15 and 10 days of treatment respectively. While 2% DMSO treated cells also showed a significant increase in albumin after 15 days of treatment, no further significant changes were observed. Despite the mean level in 2% DMSO treated cells (figure 4.8) not being vastly different from that seen in untreated or 1%-treated cells, a large standard error resulting from widespread data points prevents it from reaching significance at time points other than 15 days. These increased error margins are likely due to the adverse effects of 2% DMSO on the cells, which as in HepG2 cells, caused some cell death and detachment of cells from the growth surface. Transferrin mRNA levels in untreated Huh7 cells did not increase significantly above control; this was not the case in either DMSO experiment, with significant increases recorded at 15 and 20 days in 1% DMSO treated cells and at all time points except 20 days with 2% DMSO. This indicates that DMSO is having an effect above that seen solely by prolonging growth in standard medium. Untreated and 1% DMSO treated Huh7 cells had similar AFP mRNA levels throughout the experiment with significant decreases in comparison to control at all time points. However, 2% DMSO treatment did not follow this pattern and no significant change from control was observed. Overall, results for these three experiments indicate that 1% DMSO is the treatment most likely to produce a more mature hepatic cell, with transferrin levels above those seen in untreated cells and AFP levels below those in 2% DMSO treated cells.

Increases in albumin mRNA with 1% DMSO treatment in DMSO-treated Huh7 cells were observed by Choi *et al.* (Choi *et al.*, 2009) and Sainz *et al.* (Sainz and Chisari, 2006) where a maximal increase in albumin mRNA was observed after 14 days of treatment and were shown to be comparable to levels in primary human hepatocytes after 20 days of growth. While neither cell line here showed comparable albumin levels to those in liver, maximal expression was observed at 15 to 20 days which agrees with the published data. Increased albumin levels were also observed after 4 weeks of prolonged untreated growth of both HepG2 and Huh7 cells in comparison to control but did not quite reach levels in liver (Sivertsson *et al.*, 2010). This publication also indicated that Huh7 cells reached the maximal level of albumin expression observed after 2 weeks of culture, while data between 0 and 4 weeks of growth for HepG2 cells was not shown. Albumin mRNA increases have also been observed in HepaRG cells, where DMSO is included in routine culture over a prolonged period of time in order to produce a more mature cell and levels 70% of those observed in freshly isolated human hepatocytes were recorded after 30 days of culture with DMSO (Aninat *et al.*, 2006). AFP

mRNA levels in HepaRG cells lower than those observed in freshly isolated hepatocytes were also recorded, whereas the confluent HepG2 cells analysed for AFP in this publication showed an 89-fold increase in comparison to those in fresh hepatocytes (Aninat *et al.*, 2006). These comparisons to published data indicate that the observed time period required for significant changes to take place is as would be expected, and the response in terms of an increase in albumin and a decrease in AFP mRNA levels, while perhaps not as close to liver levels as observed in some publications, remains substantial enough to indicate that some degree of maturation may be taking place.

Both HepG2 and Huh7 cells were subsequently treated with 1% DMSO plus growth factors for prolonged periods of time; these three treatments are described in table 4.3. In HepG2 cells, albumin mRNA level in cells exposed to Treatment one was significantly higher than control after 10 days but this was not sustained; following Treatments two and three no significant increase or decreases from control were observed. Although all three treatments significantly increased transferrin levels, the absence of increases in albumin mRNA by Tr2 and 3 cast doubt upon whether they have truly induced a more hepatic profile in HepG2 cells. The only treatment which resulted in significantly decreased AFP mRNA level was Tr2 but this did not produce a corresponding increase in albumin levels. Tr1, 3 and 1% DMSO all showed little effect on AFP level – Tr3 did result in a significant decrease from control after 25 days of treatment but this did not correspond with increases in either albumin or transferrin mRNA. Overall, 1% DMSO treated HepG2 cells showed the most promising result in terms of differentiation towards a more mature hepatic phenotype. The changes became apparent at around 15 days of treatment, when albumin mRNA levels were significantly raised over control with increases in transferrin mRNA following soon after. However, AFP mRNA levels did not decrease from control, indicating that treated cells had not yet achieved a fully mature hepatic profile.

Treatments one and two on Huh7 cells produced significant increases in albumin mRNA level from control by day 15 which were not sustained at further time points; treatment three resulted in no increase in albumin or transferrin mRNA at any time point. Treatment one also showed no significant effect on transferrin, whilst treatment two only increased expression at 15 days of treatment. However, Tr2 also showed a solitary increase in AFP mRNA at 15 days which questions whether these albumin and transferrin increases are truly indicative of a more mature hepatic profile, or if a global RNA increase in mRNAs of all types has resulted in these observations; however, levels of housekeeping genes GAPDH and TOP1 remained stable. Tr1 resulted in no significant AFP mRNA decrease at any time point, whereas Tr3 had significantly lower levels of AFP than control at 15 and 25 days of treatment. Overall, none of the three

growth factor treatments produced results surpassing those of 1% DMSO alone. This could indicate that the growth factors selected for treatment were not applicable for the maturation level already seen in these cell lines. Although growth factor combinations were purposely selected from the literature as those which were used in the latter stages of differentiation protocols, it could be that for carcinoma cell lines different factors are required to induce maturation. Alternatively, the growth factors may not have had the desired effect on the cell due to low receptor levels or the factors themselves being masked by the serum included in all media recipes used here. Expression of cMET (HGF receptor), FGF receptors and OSMR (OSM receptor) was checked via end-point PCR and were determined to be expressed at least at the mRNA level in both cell lines.

Figures 4.15 and 4.16 show overall results for HepG2 and Huh7 cells respectively after 15 days of treatment with 1% and 2% DMSO and treatments 1-3. The 15 day time point was chosen as in most treatments any effect that occurred was manifest by this time. Values for 'liver' levels of these three genes were taken from previous figures in this chapter, and 'liver 3.1' values are from table 3.1 calculated relative to confluent control cells for each cell line and are displayed on the appropriate graph. Results for albumin, transferrin and AFP mRNA levels in treated HepG2 cells indicate that there is not much difference in the effect of 1% and 2% DMSO. Of the three growth factor treatments, Tr2 and 3 look promising in terms of AFP decrease and transferrin increase, but neither show a significant increase in albumin mRNA levels. This indicates that an ingredient in these treatment media is suppressing the response which increases albumin expression in DMSO-only treated cells. As a result of this, 1% DMSO treated HepG2 cells will be analysed further to determine the extent of maturation which has taken place.

Data from Huh7 cells after 15 days of treatment are shown in figure 4.16. Here, 1% DMSO does stand out clearly as the preferred method of differentiation – this is the only treatment which resulted in a significant increase in both albumin and transferrin mRNA and a decrease in AFP mRNA levels. It is also worth noting that for both HepG2 and Huh7 cells the expression levels in liver of all three genes are approximately the same in samples from these experiments and in those from earlier experiments displayed in table 3.1. The cells used in these two sets of experiments were at a different passage number and had undergone one cycle of freeze-thaw between the experiments. This indicates that the basal levels of the three markers in these cells are stable throughout a range of passages and following storage in liquid nitrogen. It was also observed that confluent HepG2 cells are closer to liver in respect of albumin and transferrin mRNA concentrations than confluent Huh7 cells are. The two cell lines appear to

have comparable AFP mRNA levels in confluent cells; with the addition of 1% DMSO for 15 days Huh7 cells display an AFP mRNA level more comparable to liver than HepG2 cells.

In conclusion, both cell lines show the most promising results with application of 1% DMSO for a minimum of 15 days. However, this is based only on mRNA expression of three differentiation markers. In order to assess the maturation status of the treated cells further, hepatic features such as levels of transporters and enzymes which contribute to the function of a fully differentiated hepatocyte need to be analysed. Results from this assessment are shown in the following chapter.

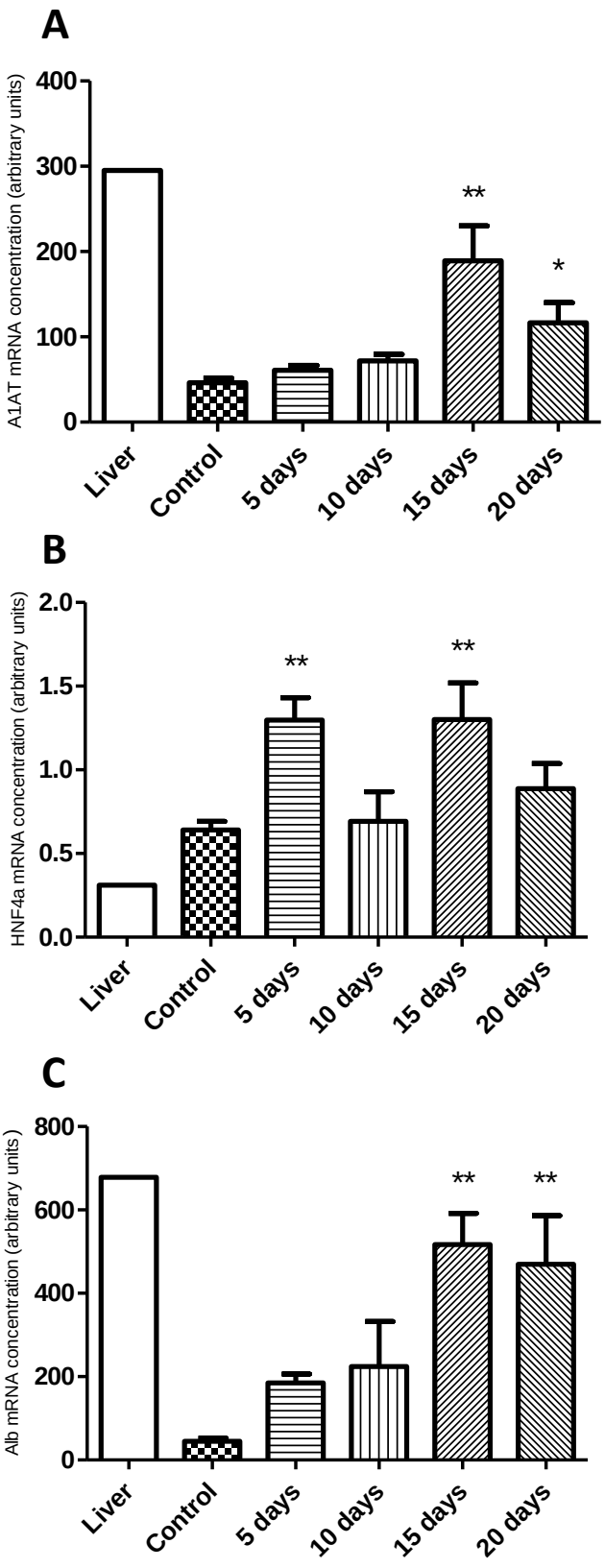
A
A1AT mRNA concentration (arbitrary units)
400
300
200
100
0
**
*
Liver
Control
5 days
10 days
15 days
20 days
B
HNF4a mRNA concentration (arbitrary units)
2.0
1.5
1.0
0.5
0.0
**
**
Liver
Control
5 days
10 days
15 days
20 days
C
Alb mRNA concentration (arbitrary units)
800
600
400
200
0
**
**
Liver
Control
5 days
10 days
15 days
20 days

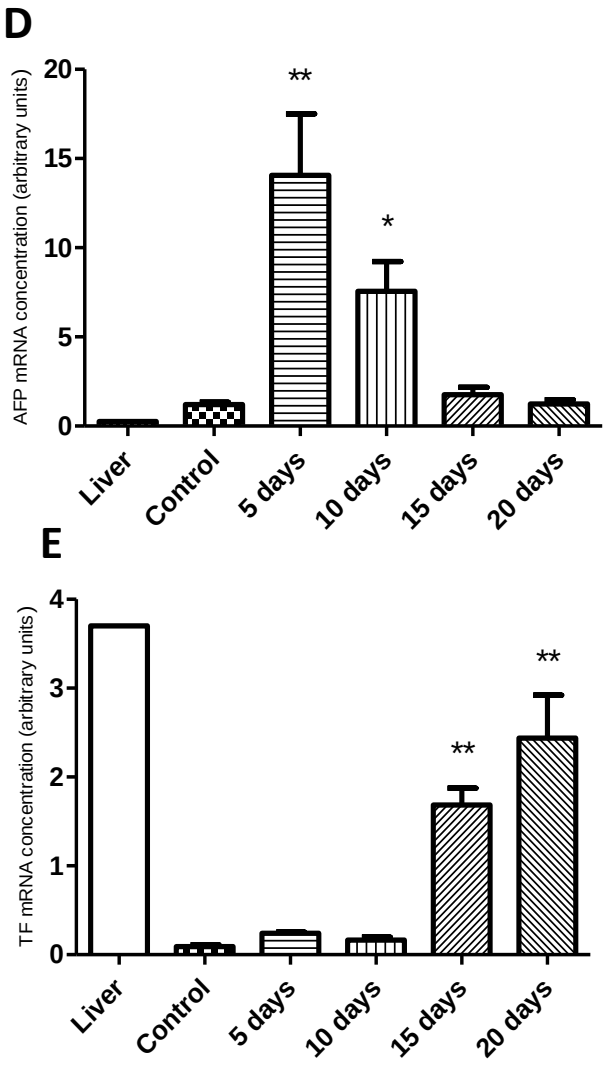

Figure 4.1 – Analysis of markers of differentiation in HepG2 cells. Results for five markers of hepatic maturation are shown in graphs A to E – A1AT, HNF4a, albumin, AFP and transferrin respectively. Cells were seeded and grown for three days to 90% confluence and treated with 1% DMSO for up to twenty days. RNA was harvested every five days, reverse transcribed and analysed for the appropriate gene using qPCR. Cells grown to confluence were used as a control. Whole liver cDNA is included as an indicator of *in vivo* hepatic mRNA levels. Results shown are from one experiment with three replicates (N = 1, n = 3), confluent cells have six replicates (n = 6). Data is displayed as mean ± SEM and analysed statistically using one-way ANOVA with Dunnett's post test. * = $p<0.05$, ** = $p<0.01$.

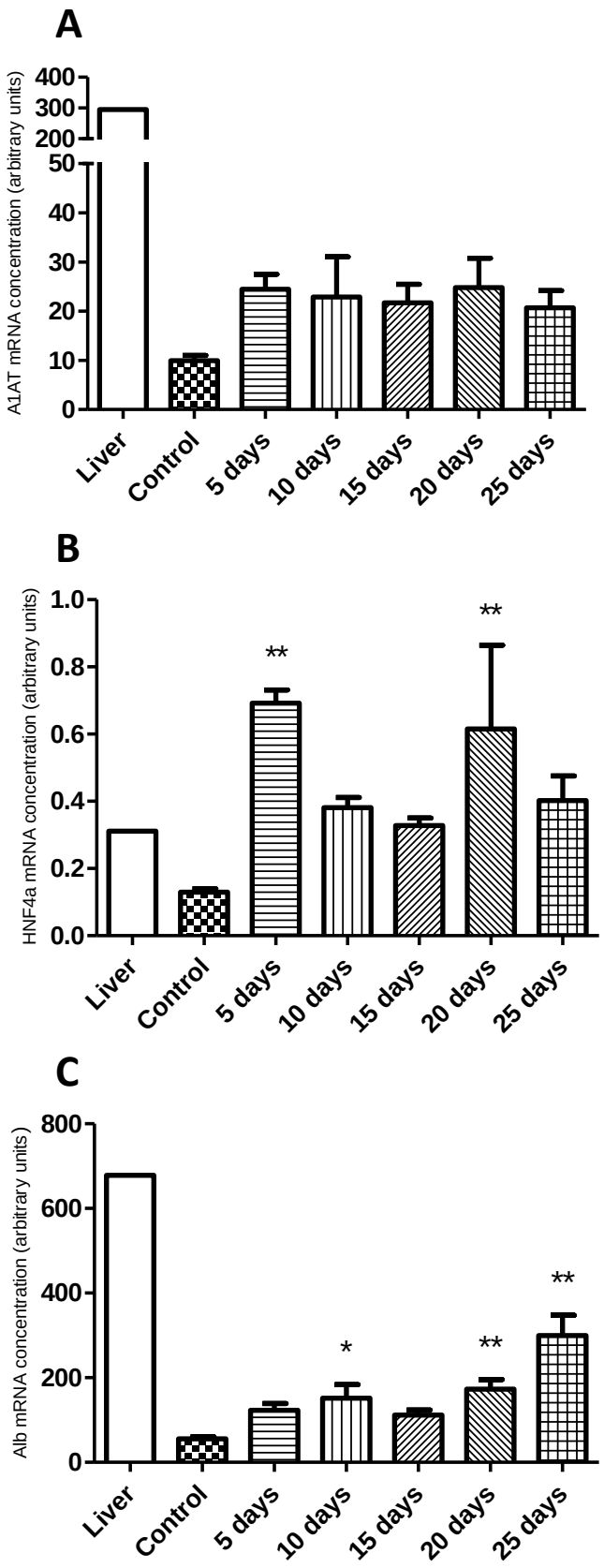
A
A1AT mRNA concentration (arbitrary units)
400
300
200
50
40
30
20
10
0
Liver
Control
5 days
10 days
15 days
20 days
25 days
B
HNF4a mRNA concentration (arbitrary units)
1.0
0.8
0.6
0.4
0.2
0.0
**
**
Liver
Control
5 days
10 days
15 days
20 days
25 days
C
Alb mRNA concentration (arbitrary units)
800
600
400
200
0
*
**
**
Liver
Control
5 days
10 days
15 days
20 days
25 days

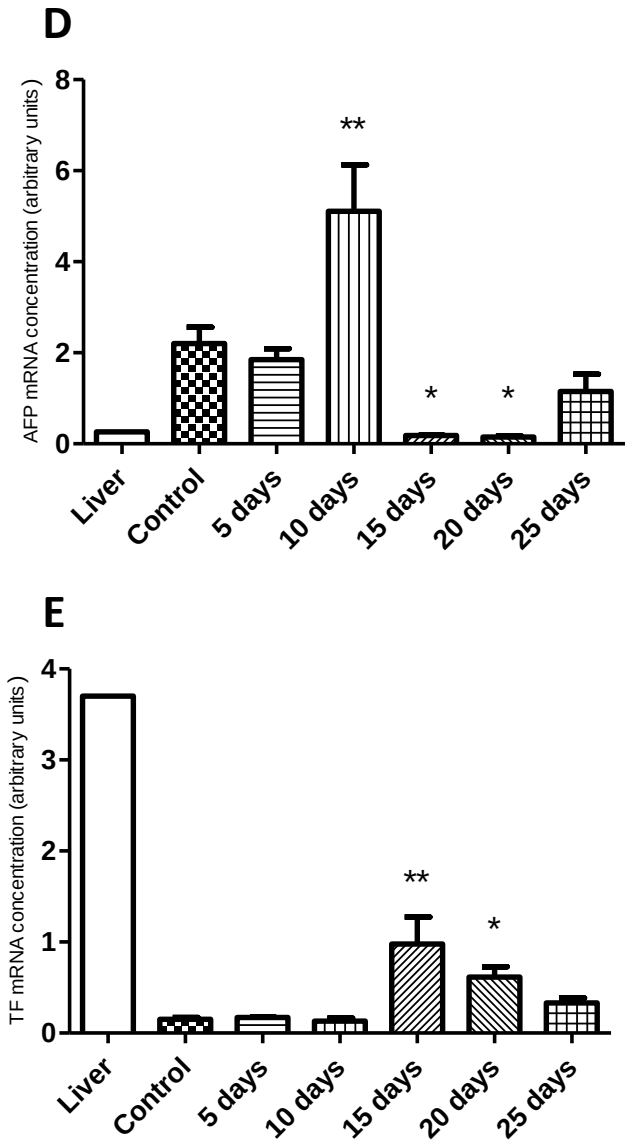

Figure 4.2 – Analysis of markers of differentiation in Huh7 cells. Results for five markers of hepatic maturation are shown in graphs A to E – A1AT, HNF4a, albumin, AFP and transferrin respectively. Cells were seeded and grown for three days to 90% confluence and treated with 1% DMSO for up to twenty five days. RNA was harvested, reverse transcribed and analysed for the appropriate gene using qPCR. Cells grown to confluence were used as a control. Whole liver cDNA was included as an indicator of *in vivo* hepatic mRNA levels. Results shown are from one experiment with three replicates (N = 1, n = 3), confluent cells have six replicates (n = 6). Data is displayed as mean ± SEM and analysed statistically using one-way ANOVA with Dunnett's post test. * = $p < 0.05$, ** = $p < 0.01$.

	HepG2 levels at 15 days relative to control *	Liver levels relative to HepG2 cells at confluence **	Huh7 levels at 15 days relative to control *	Liver levels relative to Huh7 cells at confluence **
A1AT	4.0	6.4	2.2	29.8
HNF4a	2.0	0.49	2.5	2.4
Albumin	11.4	19.4	2.0	27.6
AFP	1.5	0.01	0.08	0.05
Transferrin	18.4	10.4	6.4	10.4

* Experimental control cells are confluent, control values are set at 1.

** Data recalculated from table 3.1

Table 4.3 – Markers of differentiation in HepG2 and Huh7 cells relative to control at 15 days. Data from figures 4.1 and 4.2 has been amalgamated into this table and altered to be displayed relative to control in order to better demonstrate the effects of treatment. Data for liver levels compared to confluent cells has been recalculated from table 3.1 and is included for comparison in order to provide a larger sample number for more accurate data.

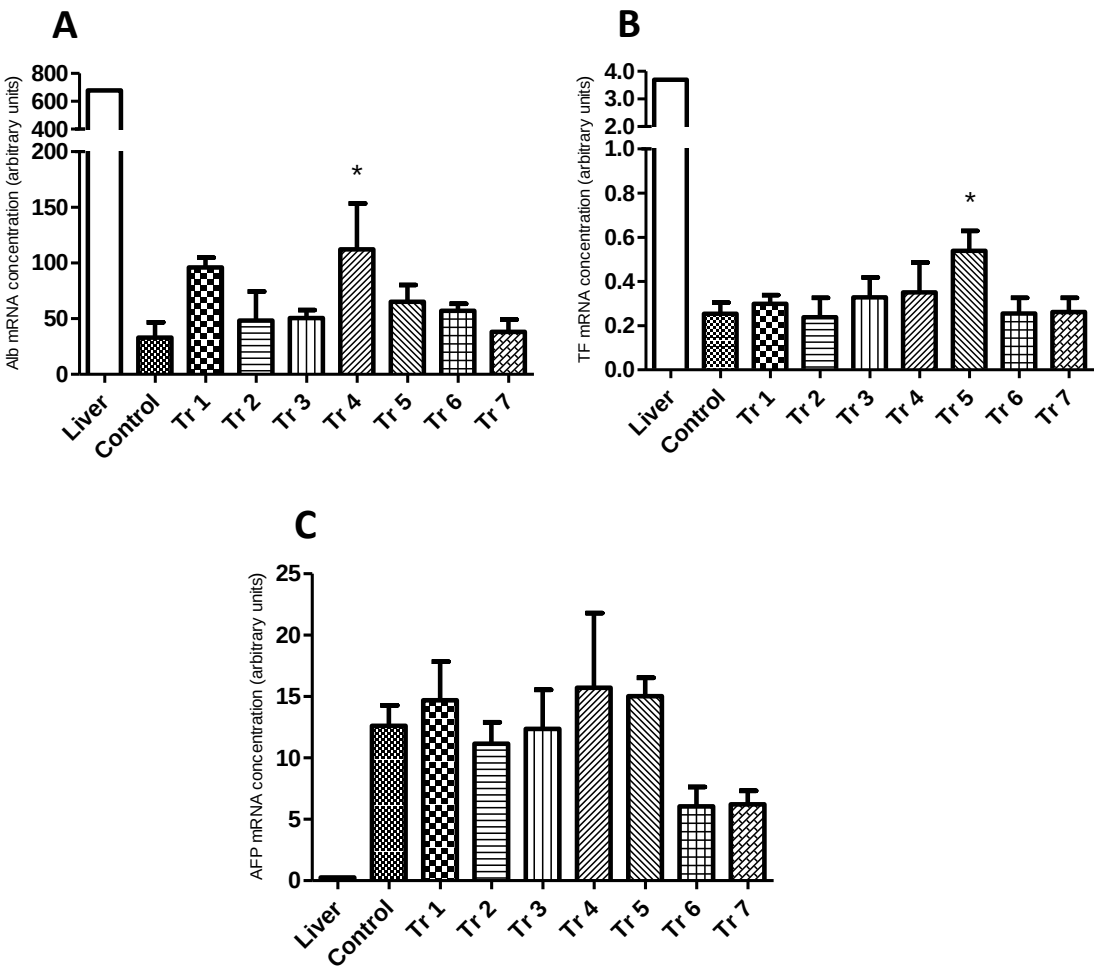

Figure 4.3 – Preliminary growth factor treatments on HepG2 cells. Graphs A, B and C show mRNA levels of albumin, transferrin and AFP respectively in HepG2 cells treated for four days with seven different growth factor treatments as detailed in Table 4.2. Briefly, cells were grown for three days to 90% confluence, at which point the appropriate treatment was applied for four days and RNA harvested after a total of seven days growth. Control cells remained in media without growth factors for the entire seven days. Whole liver cDNA is included as an indicator of *in vivo* hepatic levels. Results are from two experiments, each with two replicates (N = 2, n = 4). Data is displayed as mean ±SEM and analysed using one-way ANOVA with Dunnett's post test. * = $p<0.05$.

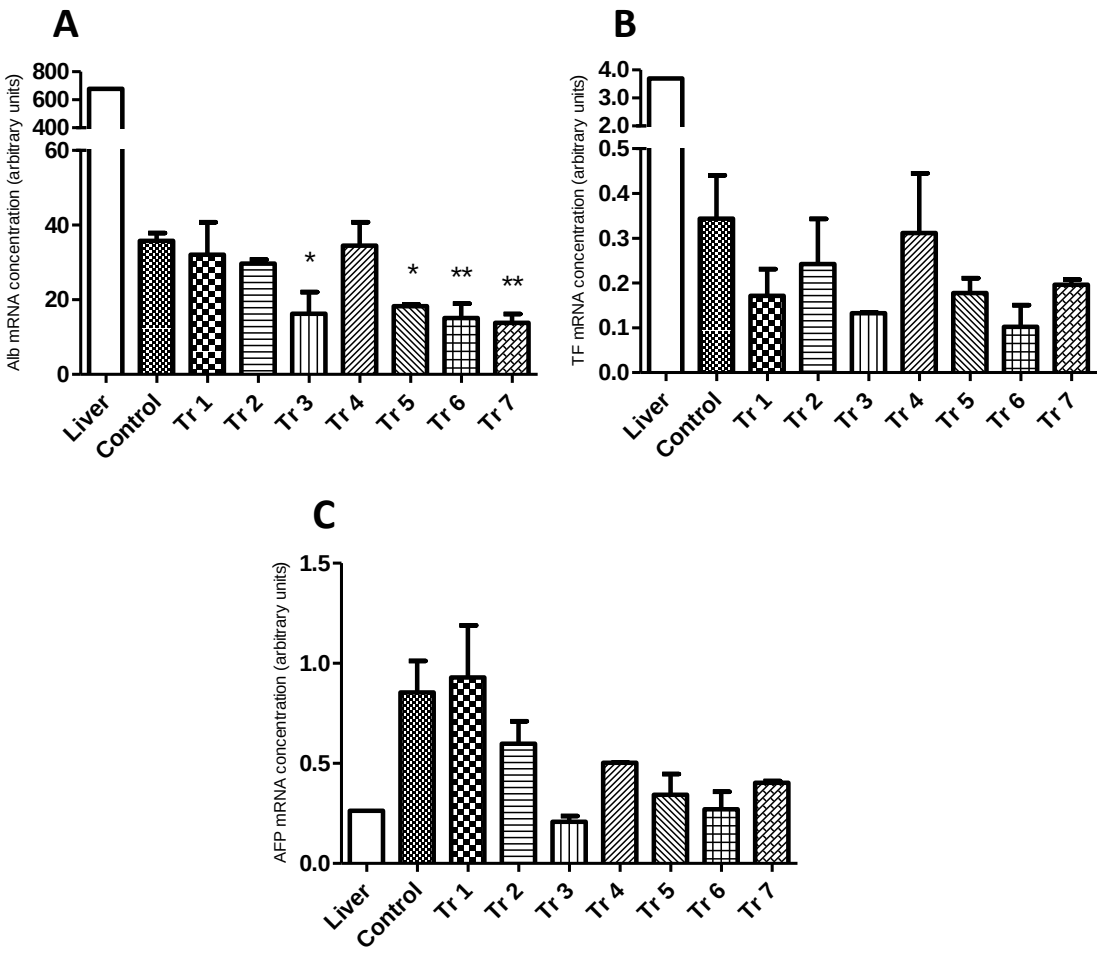

Figure 4.4 – Preliminary growth factor treatments on Huh7 cells. Graphs A, B and C show mRNA levels of albumin, transferrin and AFP respectively in Huh7 cells treated for four days with seven different growth factor treatments as detailed in Table 4.2. Briefly, cells were grown for three days to 90% confluence, at which point the appropriate treatment was applied for four days and RNA harvested after a total of seven days growth. Control cells remained in media without growth factors for the entire seven days. Whole liver cDNA is included as an indicator of *in vivo* hepatic levels. Results are from one experiment with two replicates (N = 1, n = 2). Data is displayed as mean ±SEM and analysed using one-way ANOVA with Dunnett's post test. * = $p<0.05$, ** = $p<0.01$.

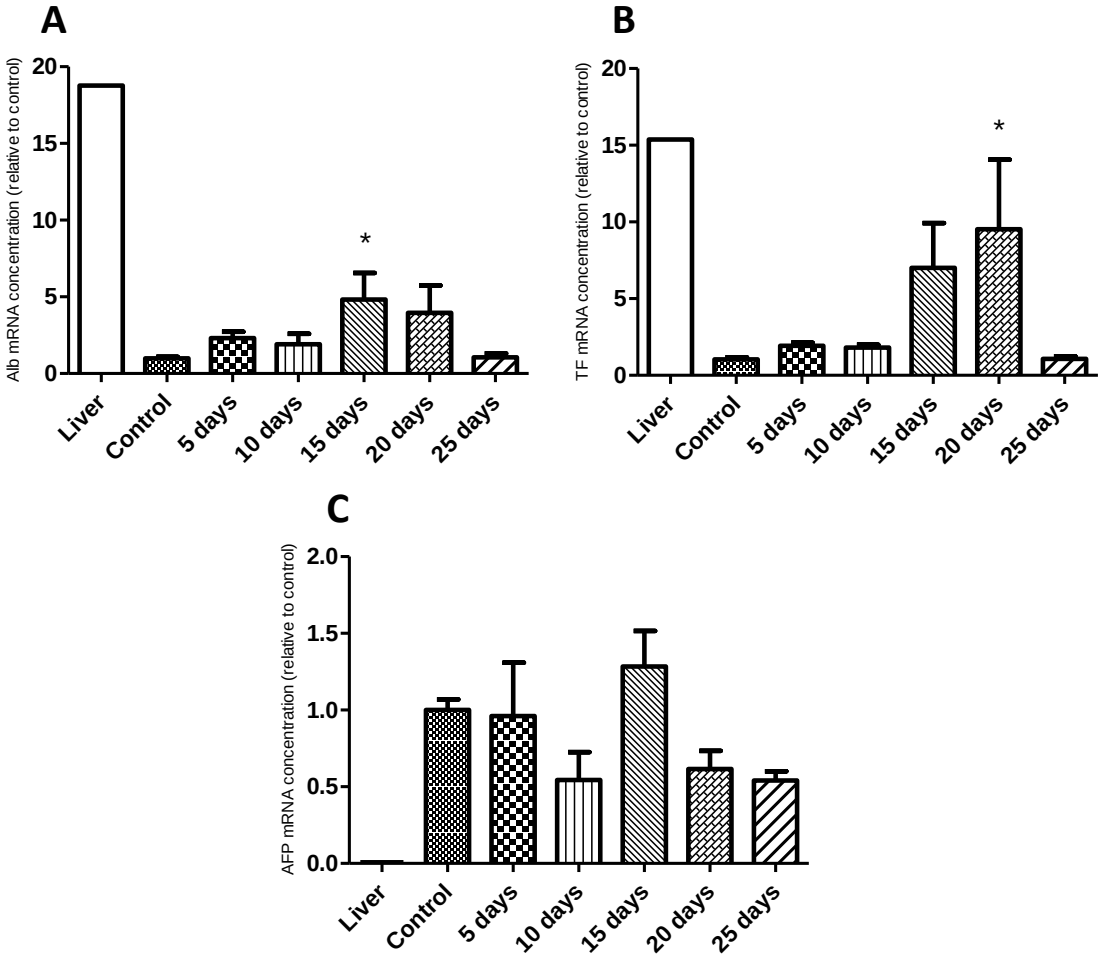

Figure 4.5 – HepG2 cells treated with 1% DMSO and analysed for differentiation markers. Results for albumin, transferrin and AFP are shown in graphs A, B and C respectively. Cells were seeded and grown for three days until 90% confluent then treated with 1% DMSO for up to 25 days. RNA was harvested, reverse transcribed and analysed for the appropriate genes using qPCR. Cells grown to confluence were used as a control. Whole liver cDNA is included as an indication of *in vivo* hepatic mRNA levels. Results shown are from three experiments with a minimum of nine total replicates (N = 3, n = 9), confluent cells having twelve replicates (N = 3, n = 12). Data is displayed as mean ± SEM and analysed statistically using one-way ANOVA with Dunnett's post test. * = $p < 0.05$.

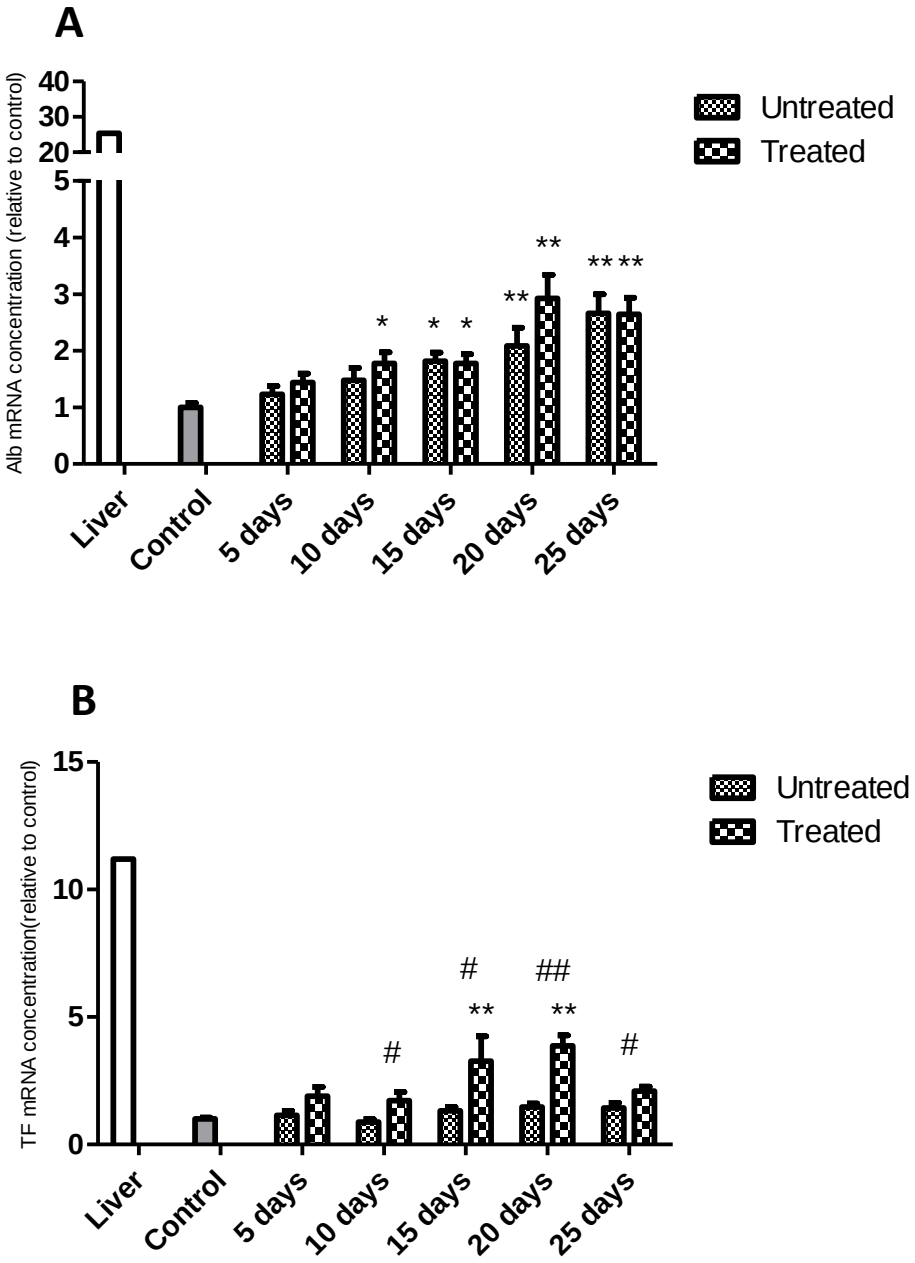
A
Alb mRNA concentration (relative to control)
40
30
20
5
4
3
2
1
0
Untreated
Treated
*
* *
**
**
** **
Liver
Control
5 days
10 days
15 days
20 days
25 days
B
TF mRNA concentration(relative to control)
15
10
5
0
Untreated
Treated
#
#
##
**
**
Liver
Control
5 days
10 days
15 days
20 days
25 days

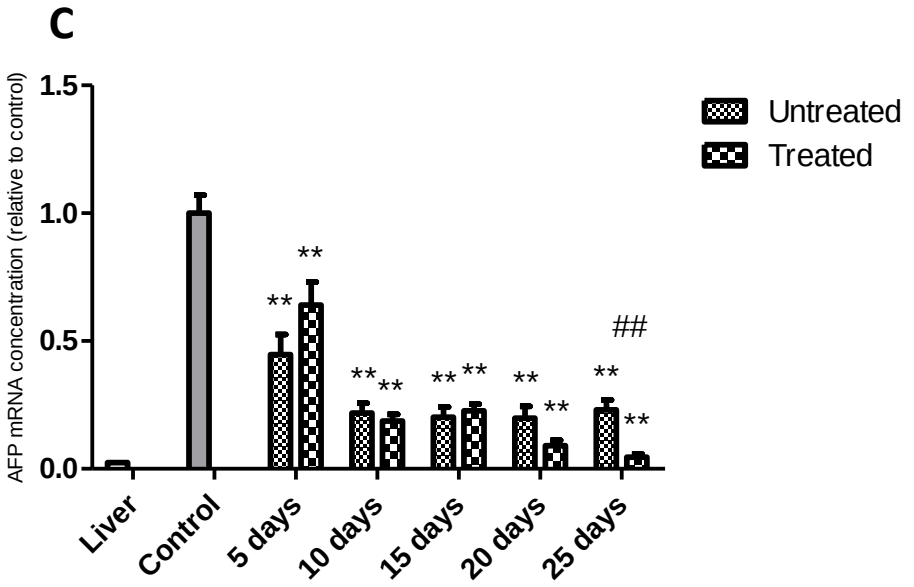

Figure 4.6 – Prolonged untreated culture and 1% DMSO treatment of Huh7 cells analysed for differentiation markers. Results for albumin, transferrin and AFP are shown in graphs A, B and C respectively. Cells were seeded and grown for three days until 90% confluent then treated with 1% DMSO for up to 25 days; untreated cells were allowed to continue growing without DMSO treatment and extracted at the same time points. RNA was harvested, reverse transcribed and analysed for the appropriate genes using qPCR. Cells grown to confluence were used as a control. Whole liver cDNA is included as an indication of *in vivo* hepatic mRNA levels. Results shown for both untreated and 1% DMSO treated cells are from three experiments with a minimum of nine total replicates (N = 3, n = 9). Control data was pooled and experiments normalised to this pool of data; total control replicates number a minimum of 30 from six experiments (N = 6, n = 30). Data is displayed as mean ± SEM and analysed statistically against control using one-way ANOVA with Dunnett's post test (* = $p < 0.05$, ** = $p < 0.01$). Analysis of untreated against treated data was by Student's t-test (# = $p < 0.05$, ## = $p < 0.01$).

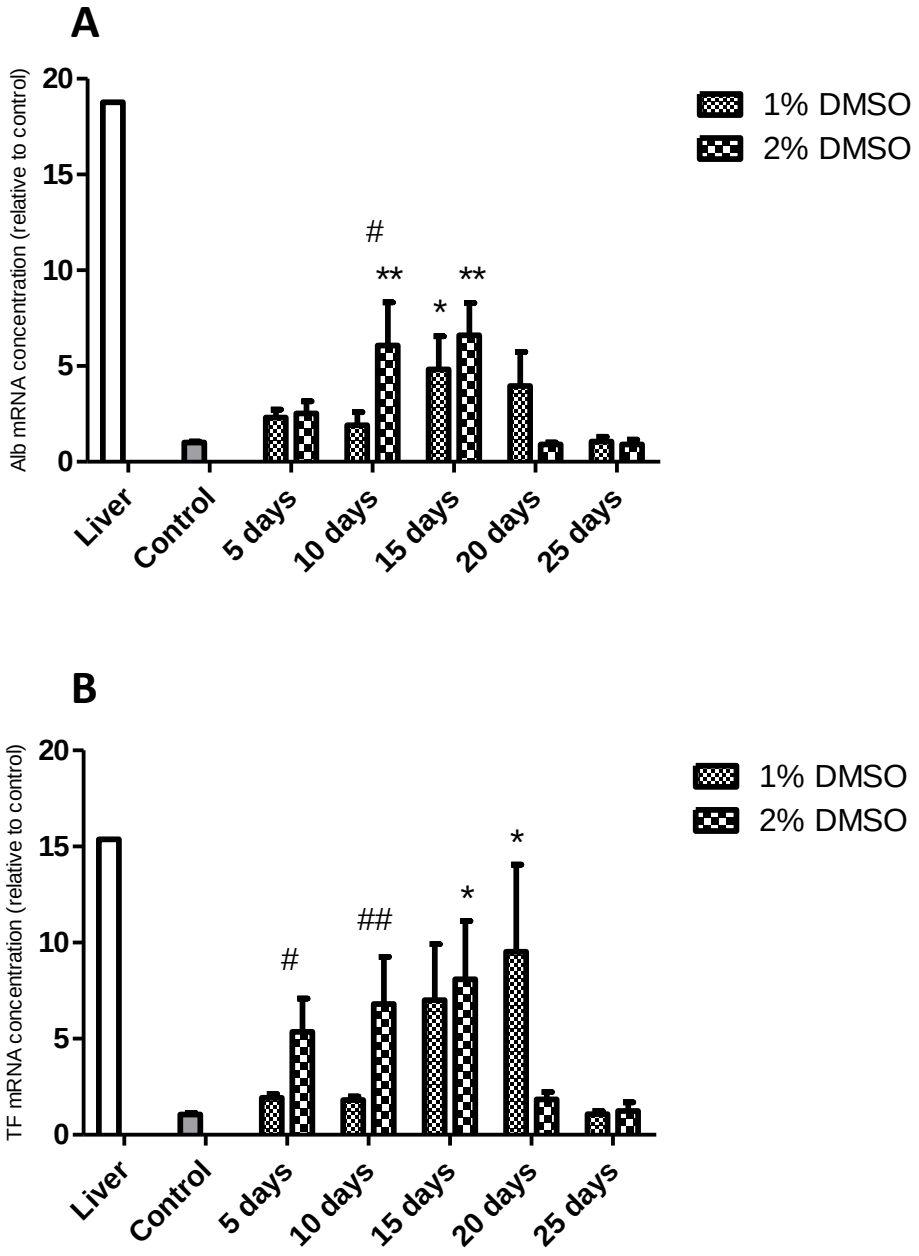
A
Alb mRNA concentration (relative to control)
20
15
10
5
0
#
**
*
**
1% DMSO
2% DMSO
Liver
Control
5 days
10 days
15 days
20 days
25 days
B
TF mRNA concentration (relative to control)
20
15
10
5
0
#
##
*
*
1% DMSO
2% DMSO
Liver
Control
5 days
10 days
15 days
20 days
25 days

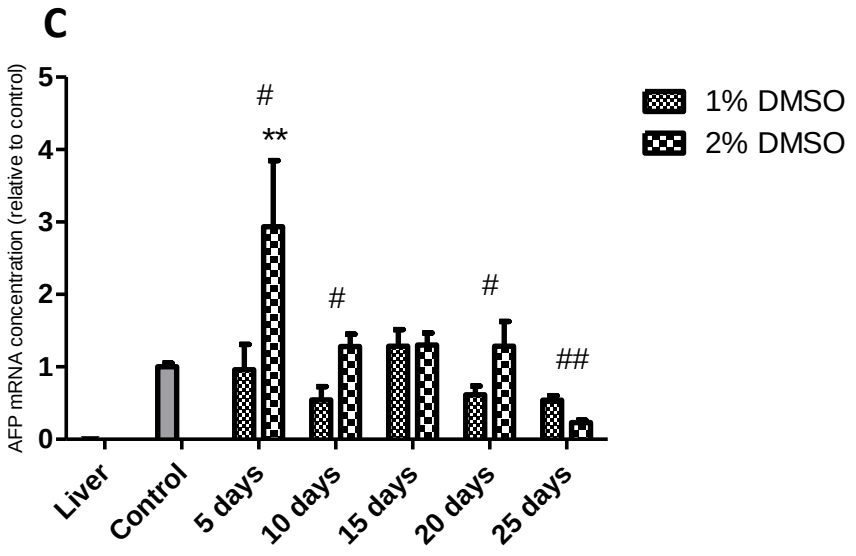

Figure 4.7 – HepG2 cells treated with DMSO and analysed for differentiation markers. Results for albumin, transferrin and AFP are shown in graphs A, B and C respectively. Cells were seeded and grown for three days until 90% confluent then treated with 1 or 2% DMSO for up to 25 days. RNA was harvested, reverse transcribed and analysed for the appropriate genes using qPCR. Cells grown to confluence were used as a control. Data from 1% DMSO is included for comparison. Whole liver cDNA is included as an indication of *in vivo* hepatic mRNA levels. Results shown for 2% DMSO treated cells are from two experiments with a minimum of five total replicates (N = 2, n = 5). Control data from 2% DMSO experiments was pooled with that from 1% DMSO data and experiments normalised to this pool of data; total control replicates number a minimum of 21 from five experiments (N = 5, n = 21). Data is displayed as mean ± SEM and analysed statistically against control using one-way ANOVA with Dunnett's post test (* = $p < 0.05$, ** = $p < 0.01$). Analysis of 1% DMSO against 2% DMSO data was by Student's t-test (# = $p < 0.05$, ## = $p < 0.01$).

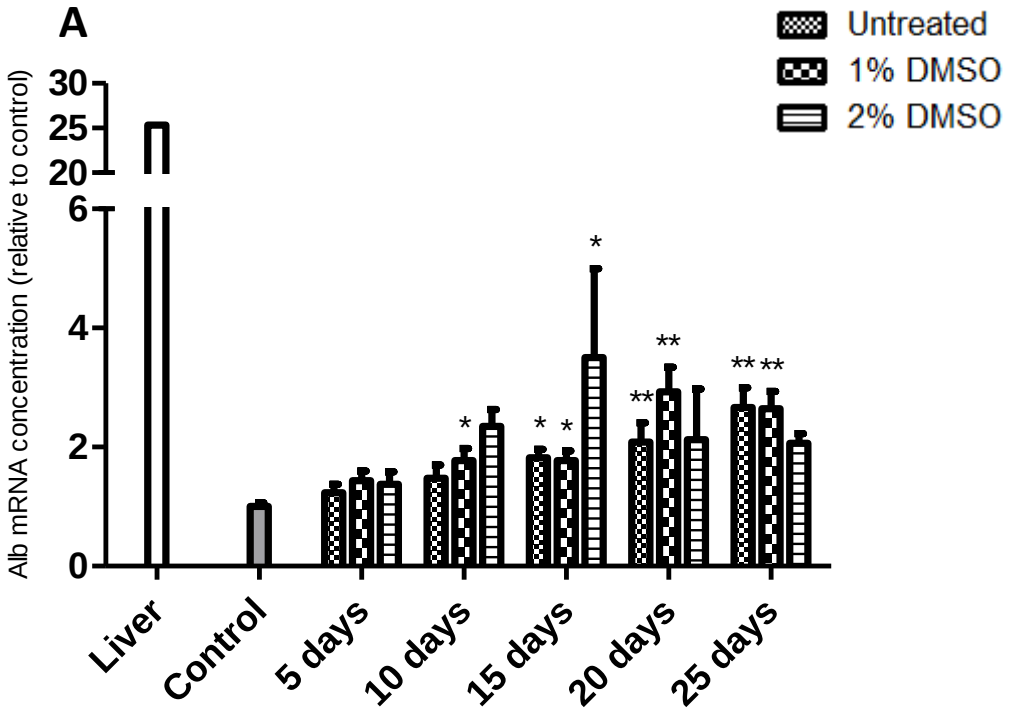
A
Untreated
1% DMSO
2% DMSO
Alb mRNA concentration (relative to control)
30
25
20
6
4
2
0
Liver
Control
5 days
10 days
15 days
20 days
25 days

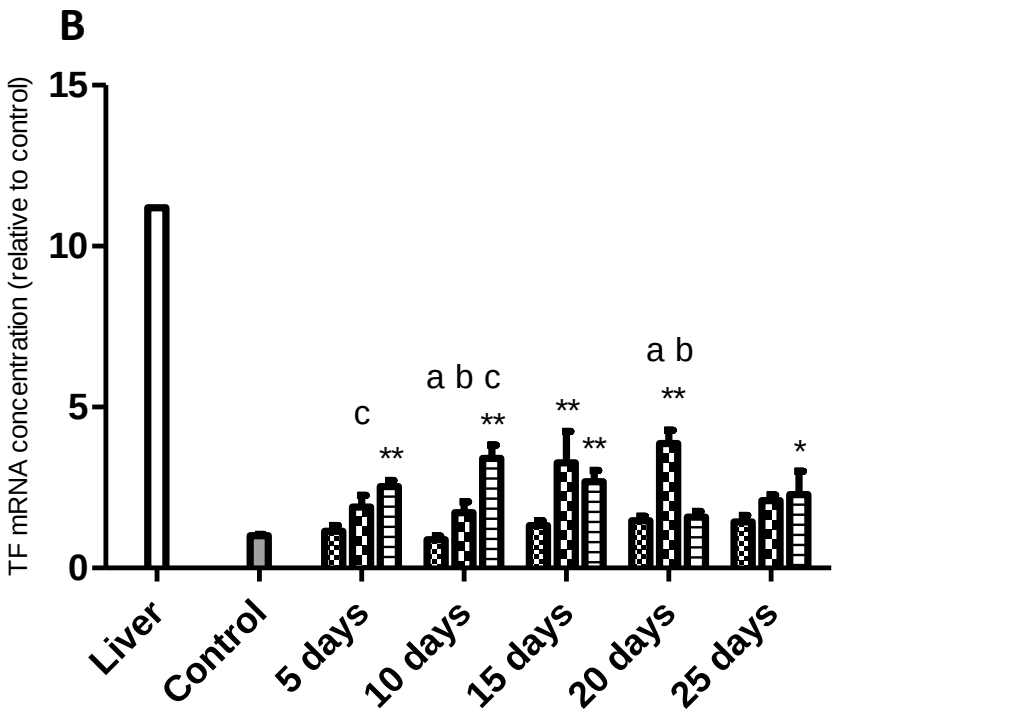
B
TF mRNA concentration (relative to control)
15
10
5
0
Liver
Control
5 days
10 days
15 days
20 days
25 days

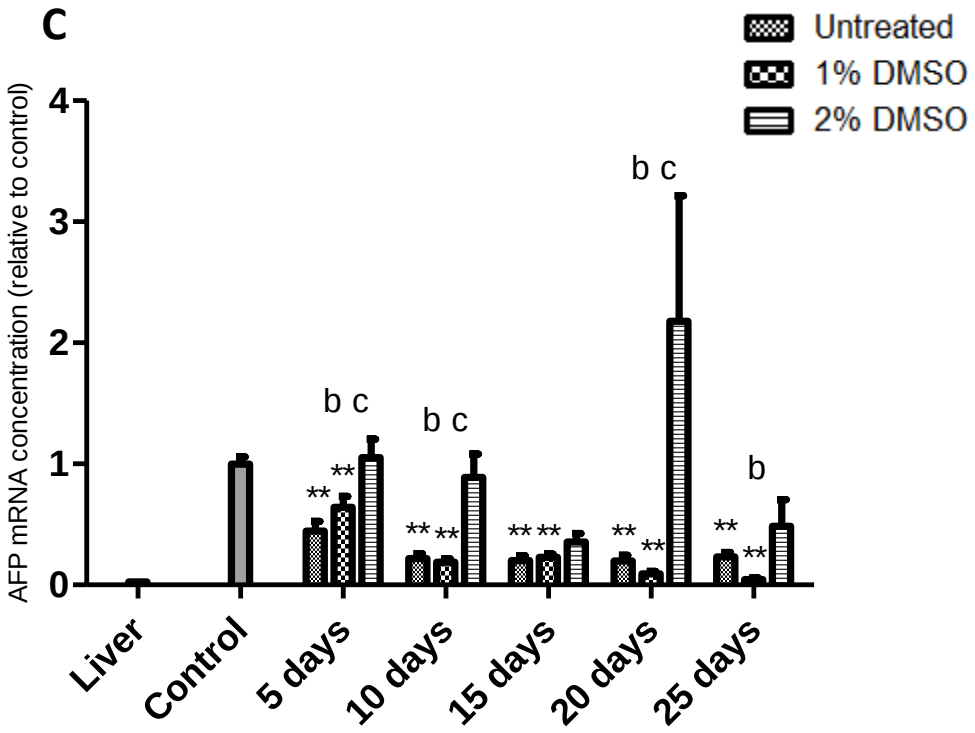

Figure 4.8 – Untreated and DMSO treated Huh7 cells analysed for differentiation markers. Results for albumin, transferrin and AFP are shown in graphs A, B and C respectively. Cells were seeded and grown for three days until 90% confluent then treated with 1 or 2% DMSO for up to 25 days; untreated cells were allowed to continue growing without DMSO treatment and extracted at the same time points. RNA was harvested, reverse transcribed and analysed for the appropriate genes using qPCR. Cells grown to confluence were used as a control. Data from 1% DMSO treatment is included for comparison. Whole liver cDNA is included as an indication of *in vivo* hepatic mRNA levels. Results shown for 2% DMSO treated cells are from three experiments with a minimum of nine total replicates (N = 3, n = 9). Control data from all three experiments was pooled and experiments normalised to this pool of data; total control replicates number a minimum of 42 from nine experiments (N = 9, n = 42) Data is displayed as mean ± SEM and analysed statistically against control using one-way ANOVA with Dunnett's post test (* = $p < 0.05$, ** = $p < 0.01$). Each time point is analysed individually testing all data columns against each other by one way ANOVA with Bonferroni's post test (a = untreated vs. 1% DMSO is $p < 0.05$, b = 1% DMSO vs. 2% DMSO is $p < 0.05$, c = untreated vs. 2% DMSO is $p < 0.05$).

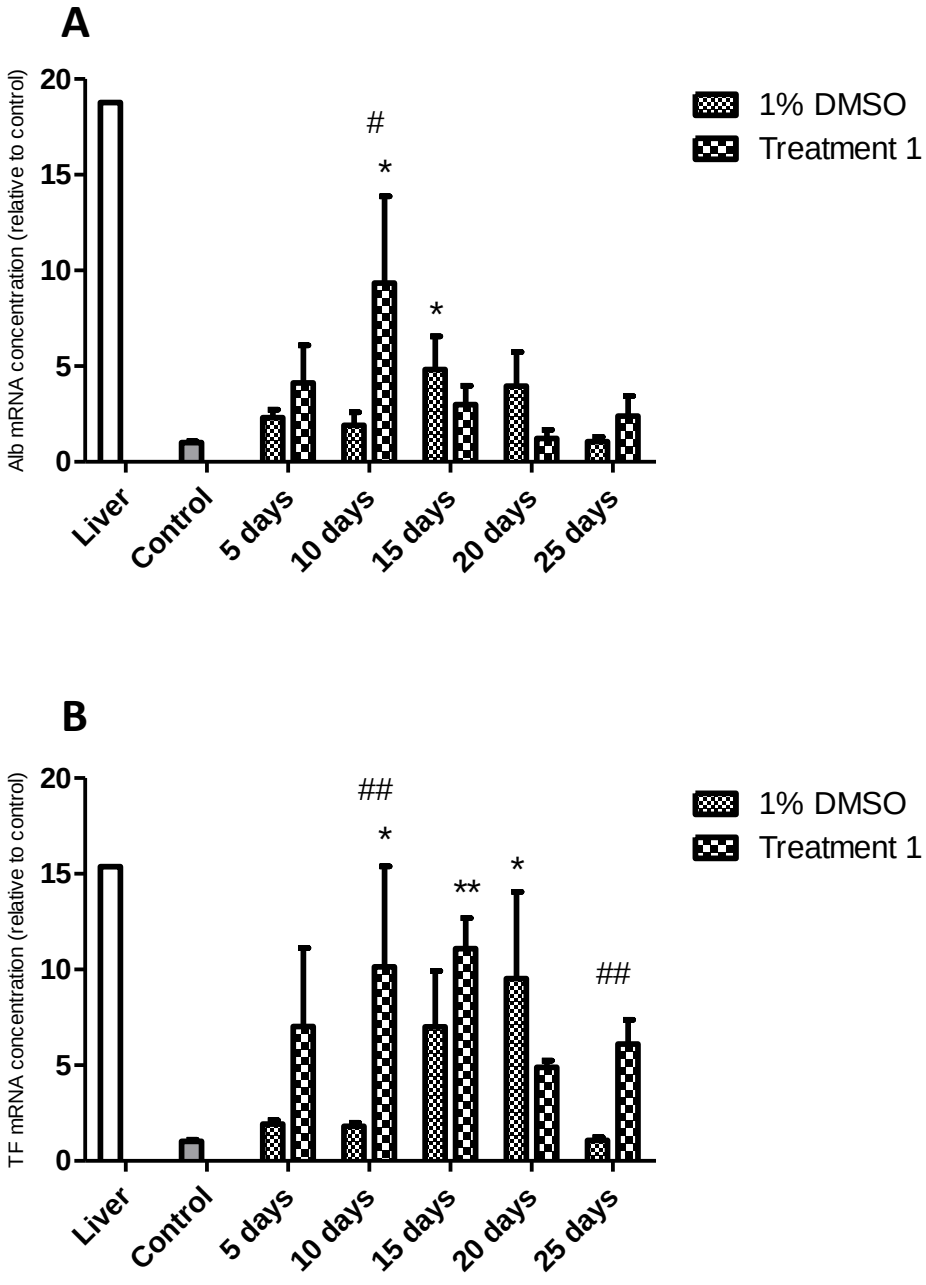
A
Alb mRNA concentration (relative to control)
20
15
10
5
0
#
*
*
Liver
Control
5 days
10 days
15 days
20 days
25 days
1% DMSO
Treatment 1
B
TF mRNA concentration (relative to control)
20
15
10
5
0
##
*
**
*
##
Liver
Control
5 days
10 days
15 days
20 days
25 days
1% DMSO
Treatment 1

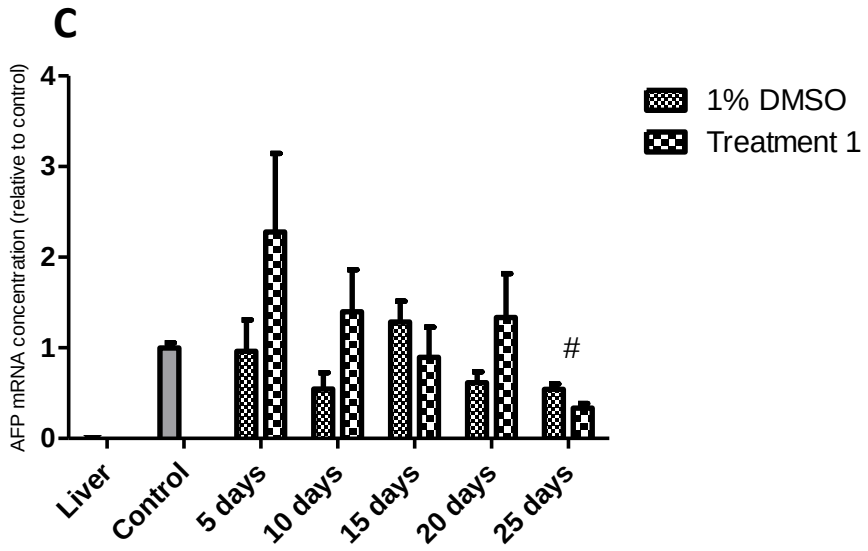

Figure 4.9 – HepG2 cells with treatment 1 and 1% DMSO analysed for differentiation markers. Results for albumin, transferrin and AFP are shown in graphs A, B and C respectively. Cells were grown to 90% confluence and treated with 1% DMSO, 10^{-7}M dexamethasone and 20 ng/ml hepatic growth factor (HGF). RNA was isolated, reverse transcribed and analysed for the appropriate genes by qPCR. Cells grown to confluence were used as a control. Results shown for Tr1 cells are from two experiments with a minimum of four total replicates (N = 2, n = 4). Control data from both experiments was pooled and experiments normalised to this pool of data; total control replicates number a minimum of 18 from five experiments (N = 5, n = 18). Data from 1% DMSO is included for comparison. Whole liver cDNA is included as an indicator of *in vivo* hepatic mRNA levels. Data is displayed as mean ± SEM and analysed statistically against control using one-way ANOVA with Dunnett's post test (* = $p < 0.05$, ** = $p < 0.01$). Analysis of 1% DMSO against treatment 1 data is by Student's t-test (# = $p < 0.05$, ## = $p < 0.01$).

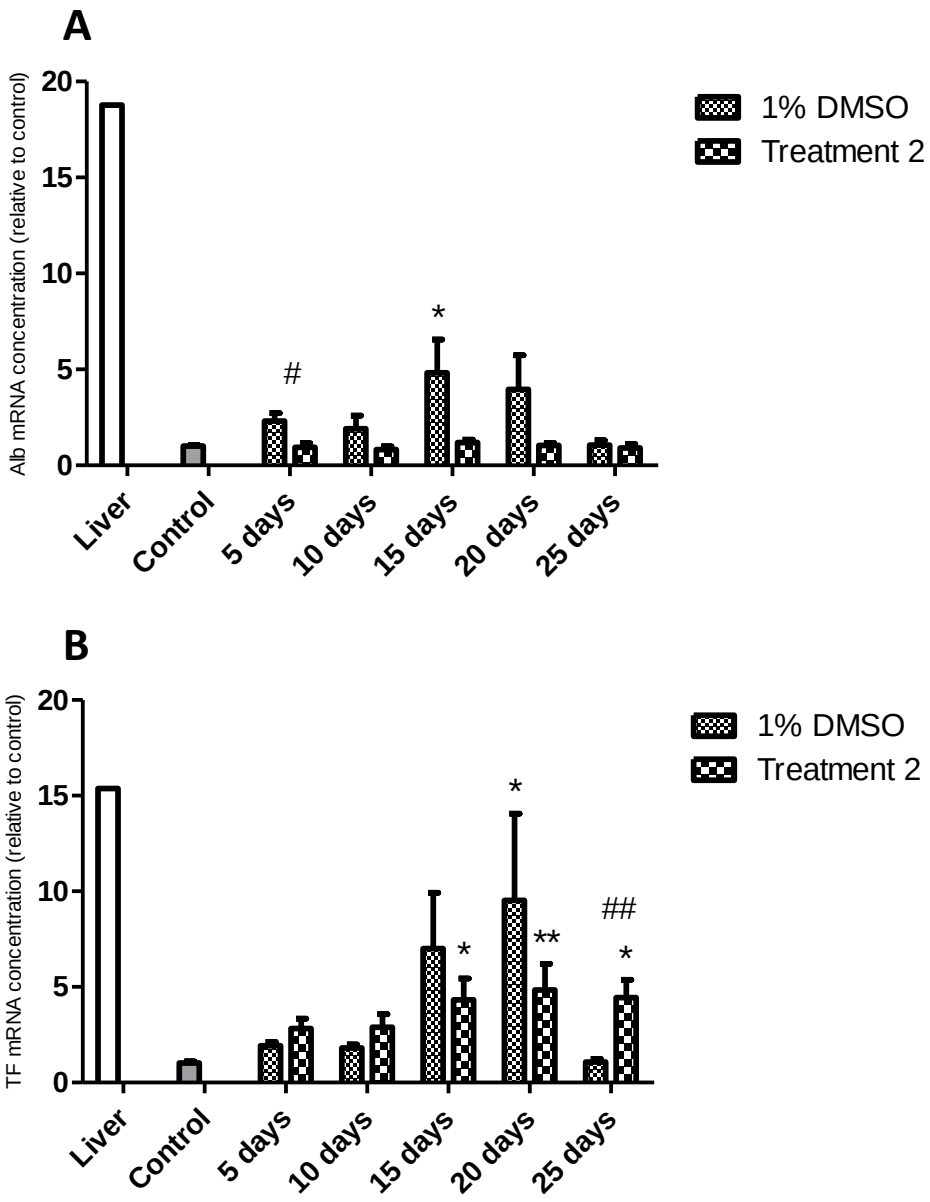
A
Alb mRNA concentration (relative to control)
20
15
10
5
0
#
*
Liver
Control
5 days
10 days
15 days
20 days
25 days
1% DMSO
Treatment 2
B
TF mRNA concentration (relative to control)
20
15
10
5
0
*
*
**
##
*
Liver
Control
5 days
10 days
15 days
20 days
25 days
1% DMSO
Treatment 2

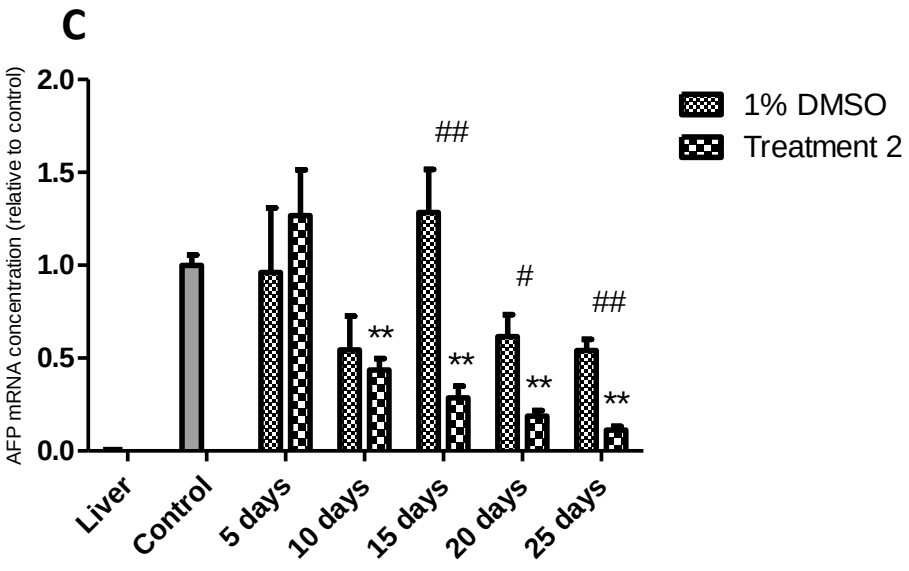

Figure 4.10 – HepG2 cells with treatment 2 and 1% DMSO analysed for differentiation markers. Results for albumin, transferrin and AFP are shown in graphs A, B and C respectively. Cells were grown to 90% confluence and treated with 1% DMSO, 10^{-7}M dexamethasone and 10 ng/ml oncostatin M (OSM). RNA was isolated, reverse transcribed and analysed for the appropriate genes by qPCR. Cells grown to confluence were used as a control. Results shown for Tr2 cells are from two experiments with a minimum of six total replicates (N = 2, n = 6). Control data from both experiments was pooled and experiments normalised to this pool of data; total control replicates number a minimum of 21 from five experiments (N = 5, n = 21). Data from 1% DMSO is included for comparison. Whole liver cDNA is included as an indicator of *in vivo* hepatic mRNA levels. Data is displayed as mean ± SEM and analysed statistically against control using one-way ANOVA with Dunnett's post test (* = $p < 0.05$, ** = $p < 0.01$). Analysis of 1% DMSO against treatment 2 data is by Student's t-test (# = $p < 0.05$, ## = $p < 0.01$).

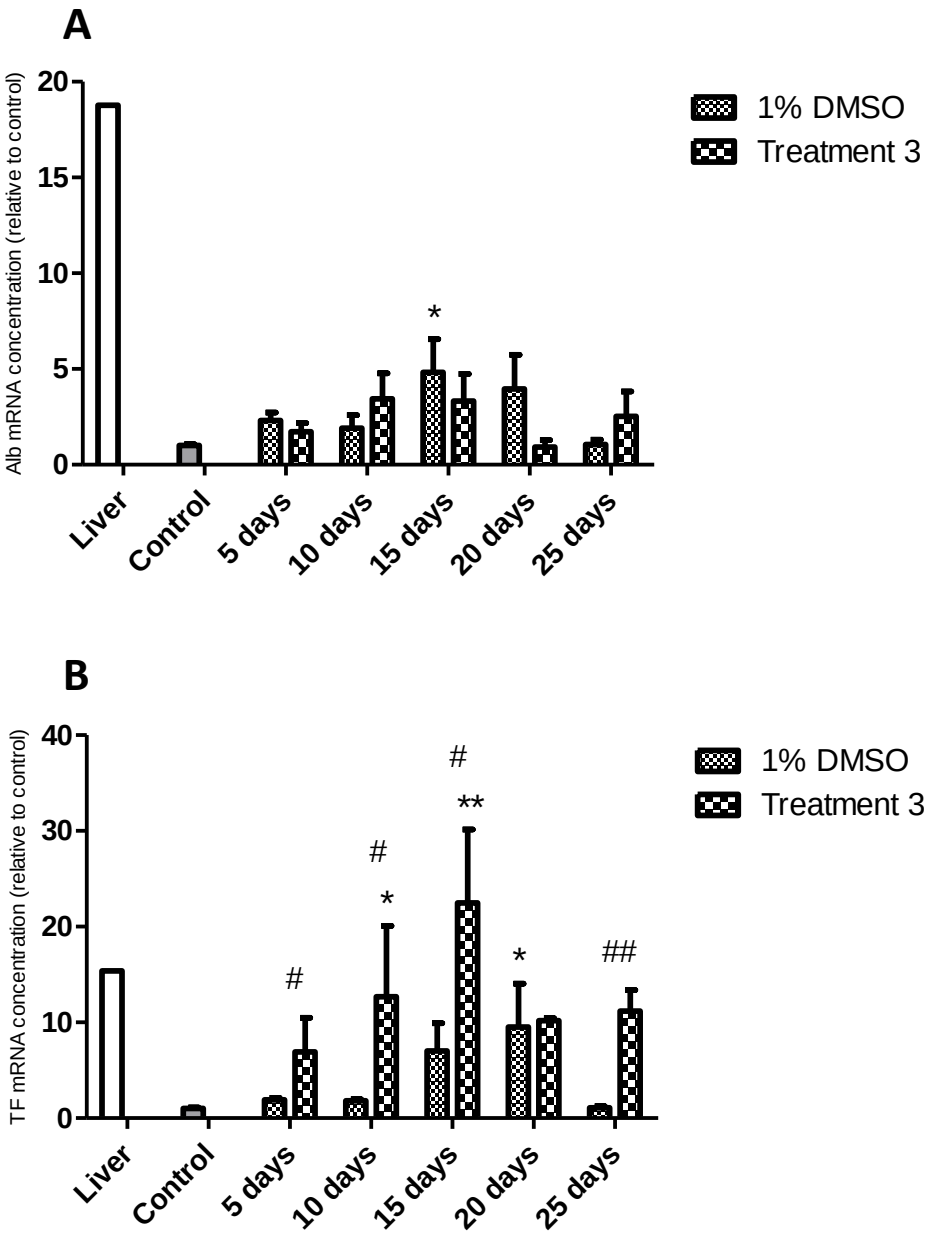
A
Alb mRNA concentration (relative to control)
20
15
10
5
0
*
1% DMSO
Treatment 3
Liver
Control
5 days
10 days
15 days
20 days
25 days
B
TF mRNA concentration (relative to control)
40
30
20
10
0
#
#
*
#
**
*
##
1% DMSO
Treatment 3
Liver
Control
5 days
10 days
15 days
20 days
25 days

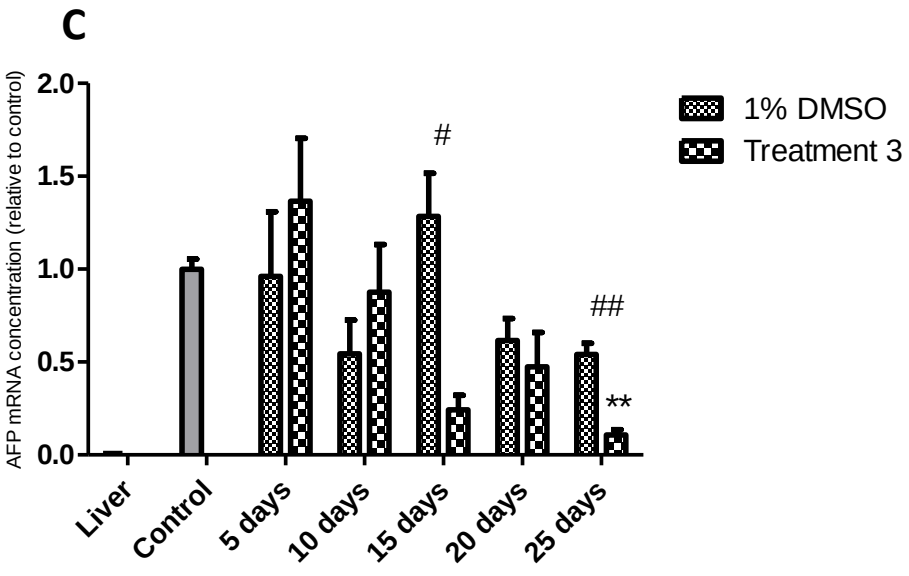

Figure 4.11 – HepG2 cells with treatment 3 and 1% DMSO analysed for differentiation markers. Results for albumin, transferrin and AFP are shown in graphs A, B and C respectively. Cells were grown to 90% confluence and treated with 1% DMSO, 10^{-7}M dexamethasone, 20 ng/ml hepatic growth factor (HGF) and 10 ng/ml oncostatin M (OSM). RNA was harvested, reverse transcribed and analysed for the appropriate genes by qPCR. Cells grown to confluence were used as a control. Results shown for Tr3 cells are from two experiments with a minimum of four total replicates (N = 2, n = 4). Control data from both experiments was pooled and experiments normalised to this pool of data; total control replicates number a minimum of 18 from five experiments (N = 5, n = 18). Data from 1% DMSO is included for comparison. Whole liver cDNA is included as an indicator of *in vivo* hepatic mRNA levels. Data is displayed as mean ± SEM and analysed statistically against control using one-way ANOVA with Dunnett's post test (* = $p < 0.05$, ** = $p < 0.01$). Analysis of 1% DMSO against treatment 3 data is by Student's t-test (# = $p < 0.05$, ## = $p < 0.01$).

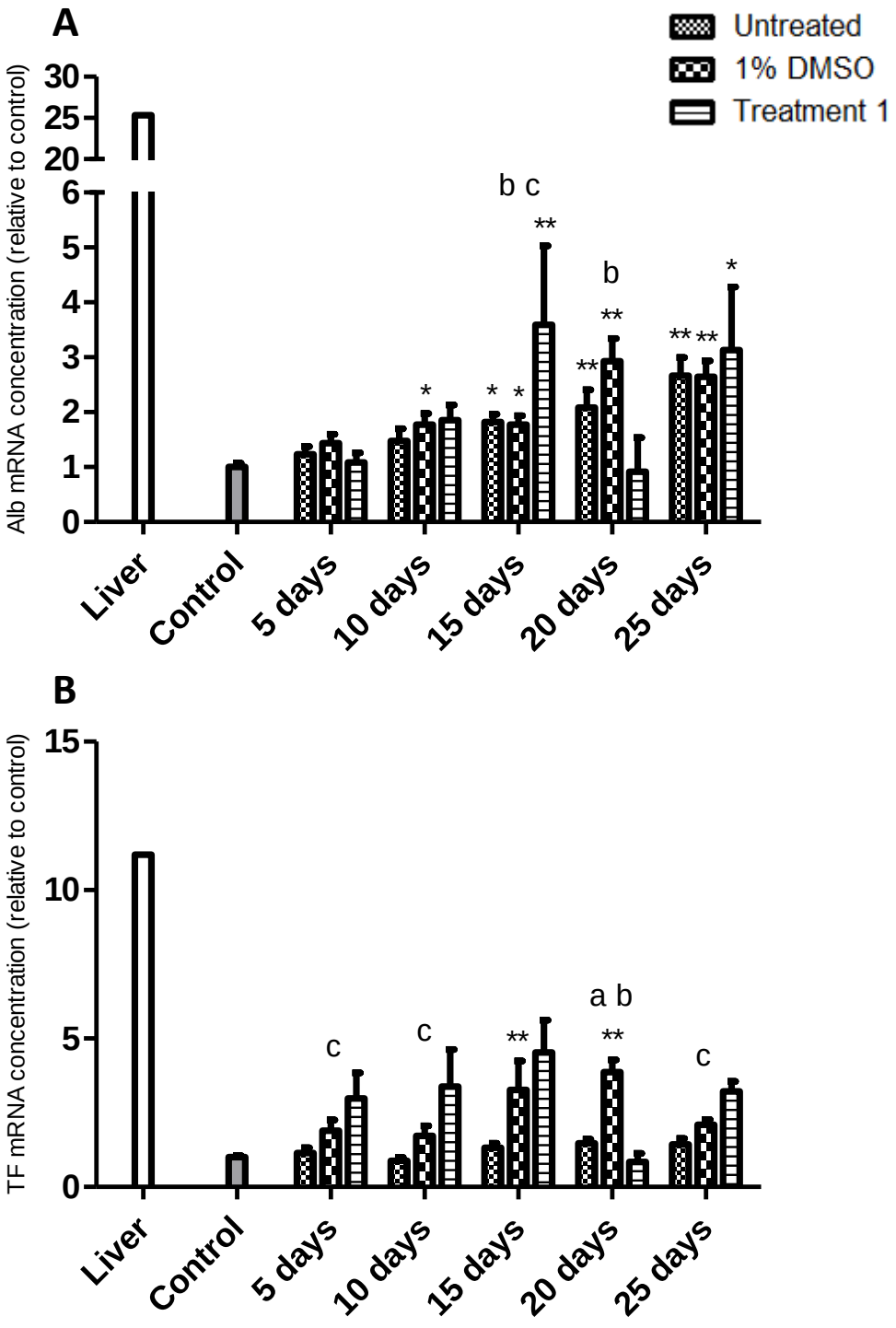
A
Untreated
1% DMSO
Treatment 1
Alb mRNA concentration (relative to control)
30
25
20
6
5
4
3
2
1
0
b c
**
b
**
*
* *
*
** **
**
*
Liver
Control
5 days
10 days
15 days
20 days
25 days
B
TF mRNA concentration (relative to control)
15
10
5
0
c
c
**
a b
**
c
Liver
Control
5 days
10 days
15 days
20 days
25 days

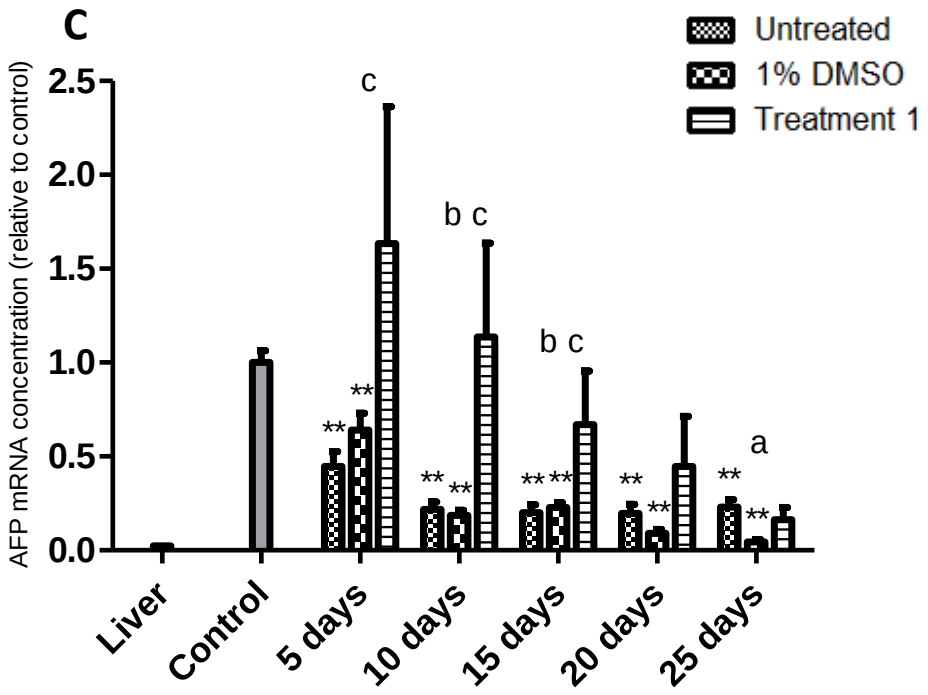

Figure 4.12 – Untreated and DMSO treated Huh7 cells with treatment 1 analysed for differentiation markers. Results for albumin, transferrin and AFP are shown in graphs A, B and C respectively. Cells were grown to 90% confluence and treated with 1% DMSO, 10^{-7}M dexamethasone and 20 ng/ml hepatic growth factor (HGF) for up to 25 days; untreated cells were allowed to continue growing without treatment and extracted at the same time points. mRNA was harvested, reverse transcribed and analysed for the appropriate genes using qPCR. Cells grown to confluence were used as a control. Data from untreated cells and 1% DMSO treatment is included for comparison. Whole liver cDNA is included as an indication of *in vivo* hepatic mRNA levels. Results for treated cells are from two experiments with a minimum of three total replicates (N = 2, n = 3). Control data from all three experiments was pooled and experiments normalised to this pool of data; total control replicates number a minimum of 36 from eight experiments (N = 8, n = 36). Data is displayed as mean ± SEM and analysed statistically against the appropriate control using one-way ANOVA with Dunnett's post test (* = $p < 0.05$, ** = $p < 0.01$). Each time point was also analysed individually testing all data columns against each other by one way ANOVA with Bonferroni's post test (a = untreated vs. 1% DMSO is $p < 0.05$, b = 1% DMSO vs. treatment 1 is $p < 0.05$, c = untreated vs. treatment 1 is $p < 0.05$).

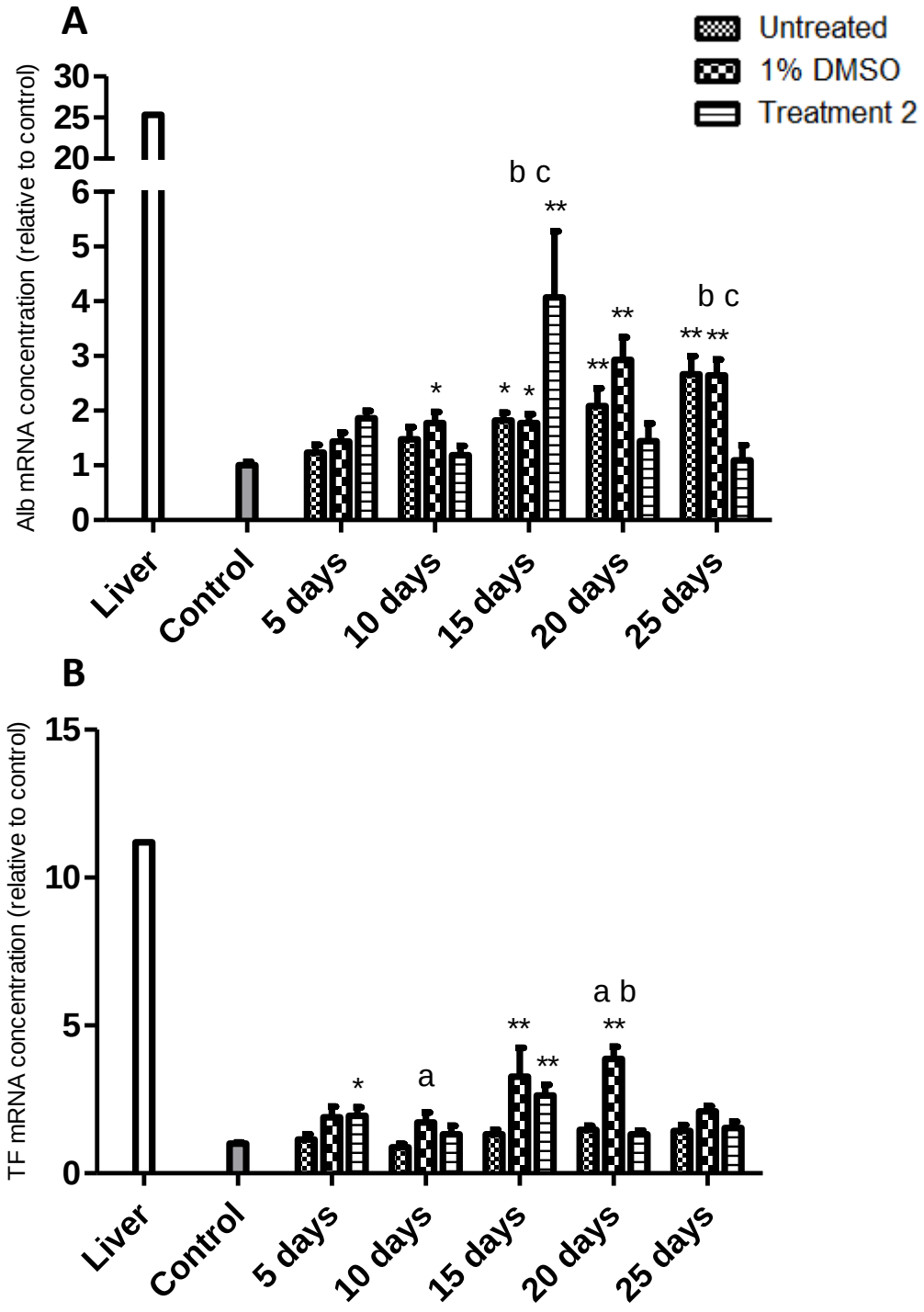
A
Untreated
1% DMSO
Treatment 2
Alb mRNA concentration (relative to control)
30
25
20
6
5
4
3
2
1
0
b c
**
b c
**
**
**
**
**
*
* *
Liver
Control
5 days
10 days
15 days
20 days
25 days
B
TF mRNA concentration (relative to control)
15
10
5
0
a b
**
**
*
a
Liver
Control
5 days
10 days
15 days
20 days
25 days

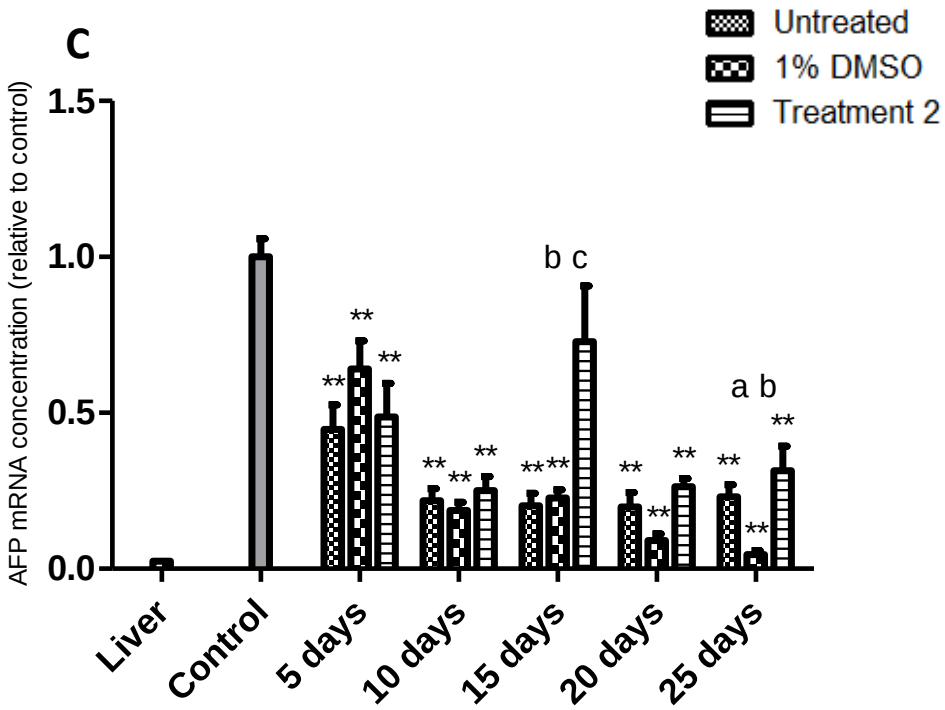

Figure 4.13 – Untreated and DMSO treated Huh7 cells with treatment 2 analysed for differentiation markers. Results for albumin, transferrin and AFP are shown in graphs A, B and C respectively. Cells were grown to 90% confluence and treated with 1% DMSO, 10^{-7}M dexamethasone and 10 ng/ml oncostatin M (OSM) for up to 25 days; untreated cells were allowed to continue growing without treatment and extracted at the same time points. RNA was harvested, reverse transcribed and analysed for the appropriate genes using qPCR. Cells grown to confluence were used as a control. Data from untreated cells and 1% DMSO treatment is included for comparison. Whole liver cDNA is included as an indication of *in vivo* hepatic mRNA levels. Results for treated cells are from two experiments with a minimum of six total replicates (N = 2, n = 6). Control data from all three experiments was pooled and experiments normalised to this pool of data; total control replicates number a minimum of 42 from eight experiments (N = 8, n = 42). Data is displayed as mean ± SEM and analysed statistically against the appropriate control using one-way ANOVA with Dunnett's post test (* = $p < 0.05$, ** = $p < 0.01$). Each time point was also analysed individually testing all data columns against each other using one way ANOVA with Bonferroni's post test (a = untreated vs. 1% DMSO is $p < 0.05$, b = 1% DMSO vs. treatment 2 is $p < 0.05$, c = untreated vs. treatment 2 is $p < 0.05$).

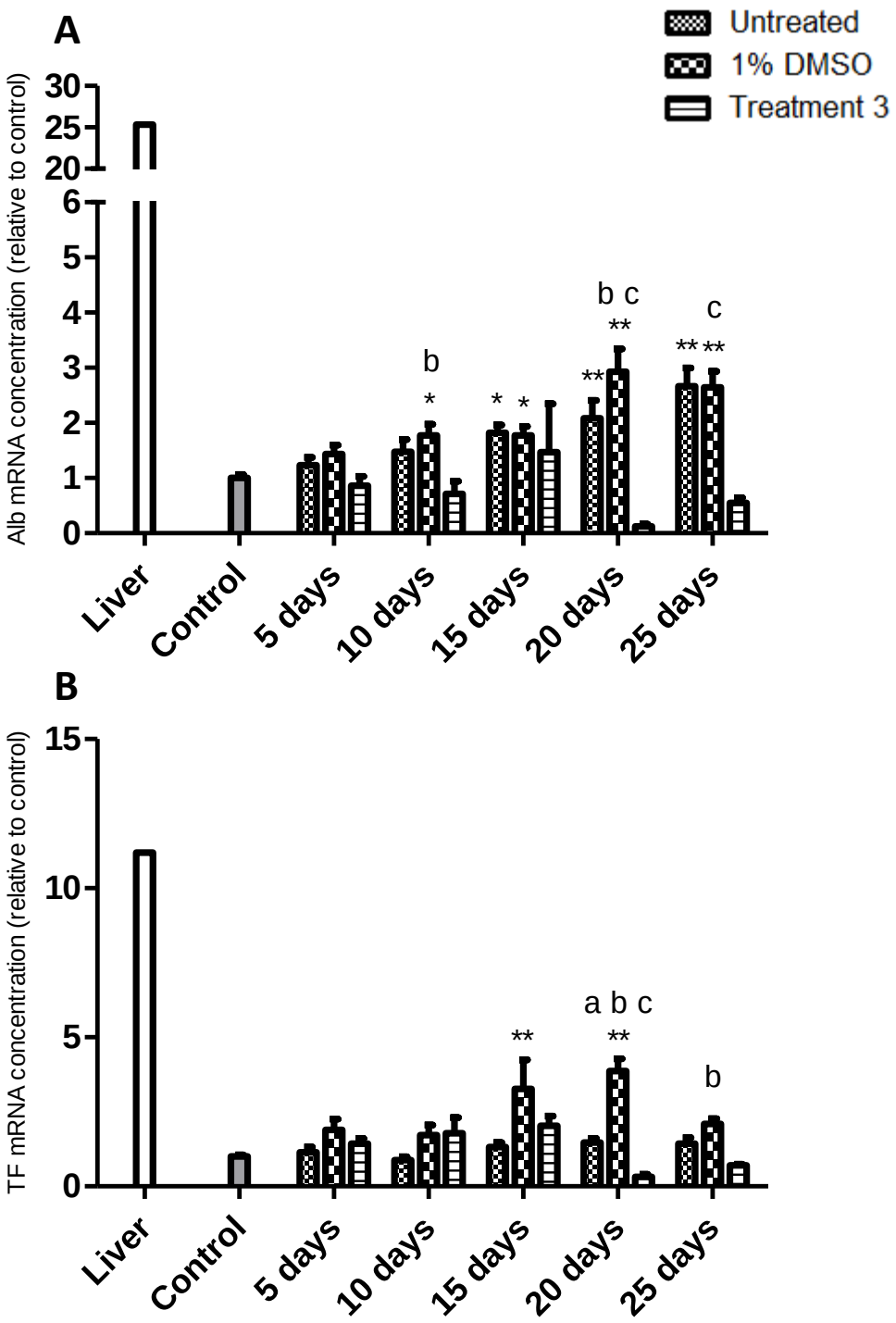
A
Untreated
1% DMSO
Treatment 3
Alb mRNA concentration (relative to control)
30
25
20
6
5
4
3
2
1
0
b
*
* *
** b c
**
** **
c
Liver
Control
5 days
10 days
15 days
20 days
25 days
B
TF mRNA concentration (relative to control)
15
10
5
0
**
a b c
**
b
Liver
Control
5 days
10 days
15 days
20 days
25 days

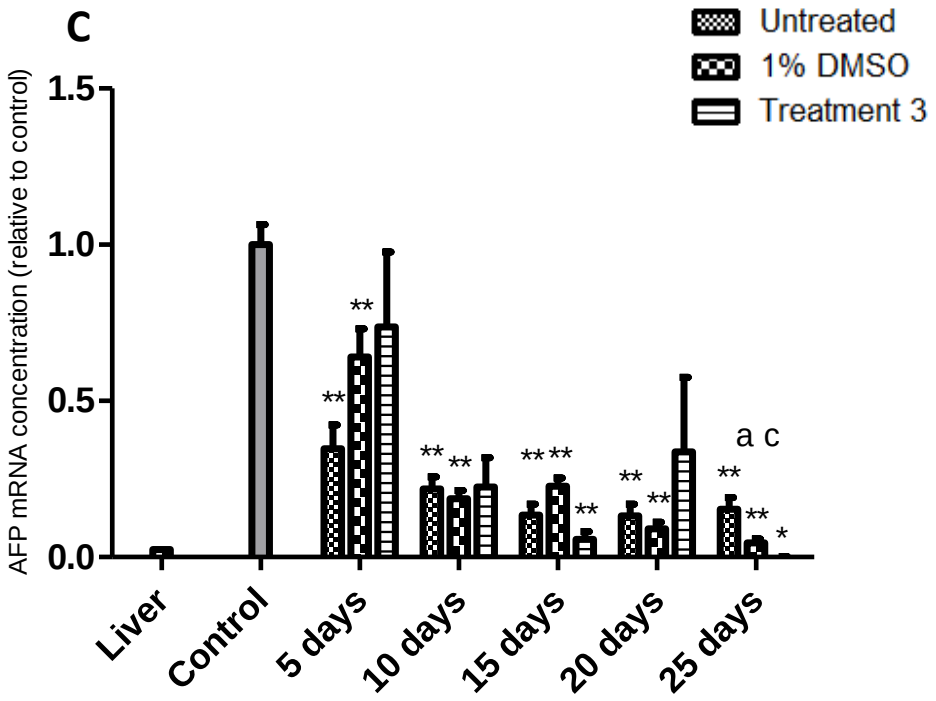

Figure 4.14 – Untreated and DMSO treated Huh7 cells with treatment 3 analysed for differentiation markers. Results for albumin, transferrin and AFP are shown in graphs A, B and C respectively. Cells were grown to 90% confluence and treated with 1% DMSO, 10^{-7}M dexamethasone, 20 ng/ml hepatic growth factor (HGF) and 10 ng/ml oncostatin M (OSM) for up to 25 days; untreated cells were allowed to continue growing without treatment and extracted at the same time points. RNA was harvested, reverse transcribed and analysed for the appropriate genes using qPCR. Cells grown to confluence were used as a control. Data from untreated cells and 1% DMSO treatment is included for comparison. Whole liver cDNA is included as an indication of *in vivo* hepatic mRNA levels. Results for treated cells are from two experiments with a minimum of three total replicates (N = 2, n = 3). Control data from all three experiments was pooled and experiments normalised to this pool of data; total control replicates number a minimum of 36 from eight experiments (N = 8, n = 36). Data is displayed as mean ± SEM and analysed statistically against the appropriate control using one-way ANOVA with Dunnett's post test (* = $p < 0.05$, ** = $p < 0.01$). Each time point is analysed individually testing all data columns against each other using one way ANOVA with Bonferroni's post test (a = untreated vs. 1% DMSO is $p < 0.05$, b = 1% DMSO vs. treatment 3 is $p < 0.05$, c = untreated vs. treatment 3 is $p < 0.05$).

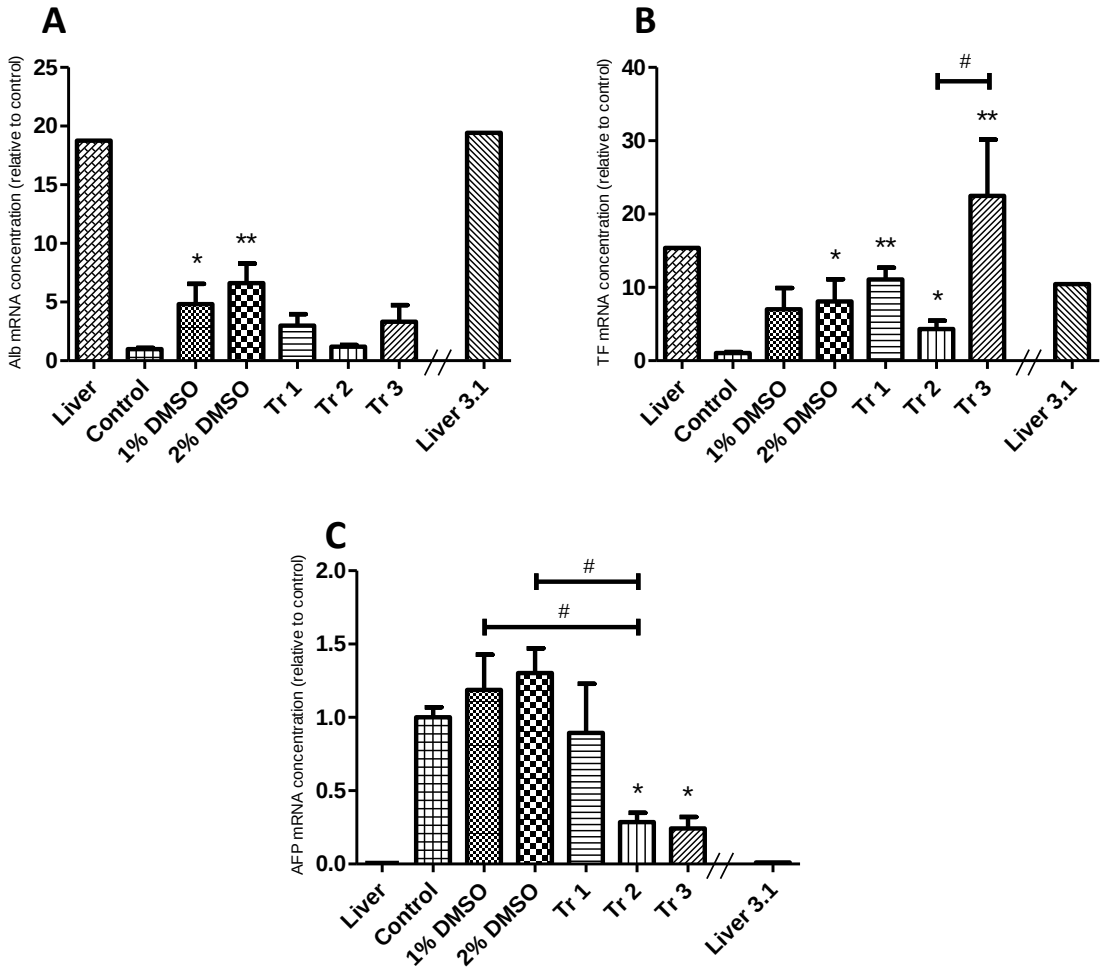

Figure 4.15 – Albumin, transferrin and AFP mRNA levels in 1% DMSO, 2% DMSO and treatments 1, 2 and 3 applied to HepG2 cells for 15 days. These graphs are an amalgamation of data from figures 4.5, 4.7, 4.9, 4.10 and 4.11, showing only data from 15 days of treatment to allow comparison. Data labelled "Liver 3.1" has been recalculated from table 3.1 to be expressed as relative to confluent HepG2 levels. Data has been analysed statistically using one way ANOVA with Dunnett's post test to assess changes from control (* = $p < 0.05$, ** = $p < 0.01$) and also by one way ANOVA with Bonferroni's post test to test all treated pairs of columns against each other (control and liver data excluded) (# = $p < 0.05$, ## = $p < 0.01$).

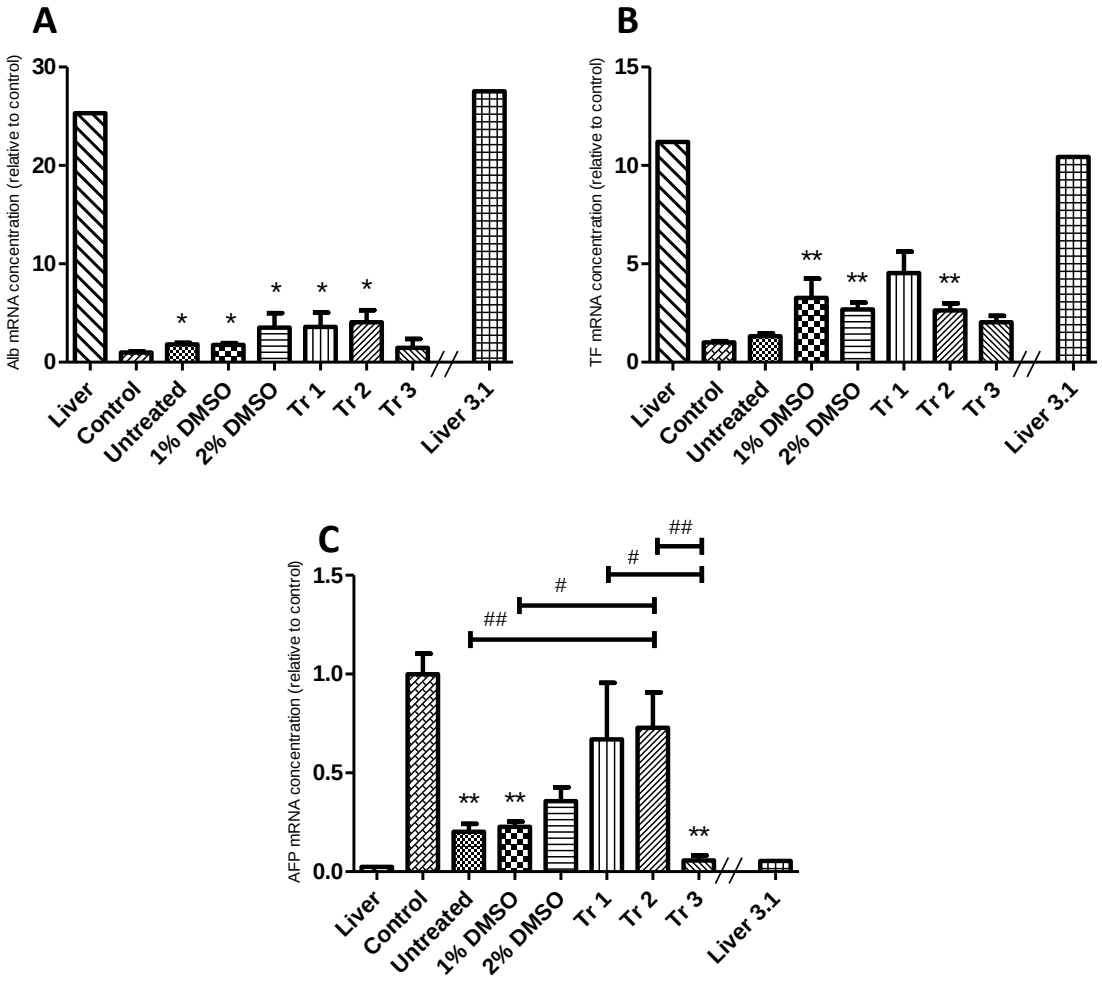

Figure 4.16 – Albumin, transferrin and AFP mRNA levels in untreated, 1% DMSO, 2% DMSO and treatments 1, 2 and 3 applied to Huh7 cells for 15 days. These graphs are an amalgamation of data from figures 4.6, 4.8, 4.12, 4.13 and 4.14, showing only data from 15 days of treatment to allow comparison between the treatments. Data labelled "Liver 3.1" has been recalculated from table 3.1 to be expressed as relative to confluent Huh7 levels. Data has been analysed statistically using one way ANOVA with Dunnett's post test to assess changes from control (* = $p < 0.05$, ** = $p < 0.01$) and also by one way ANOVA with Bonferroni's post test to test all pairs of treated columns against each other (control and liver excluded) (# = $p < 0.05$, ## = $p < 0.01$).

Chapter 5 – Transporter and enzyme levels in DMSO-treated HepG2 and Huh7 cells.

Chapter aim: To characterise the expression levels of selected phase I and II drug metabolising enzymes plus influx and efflux transporters in 1% DMSO-treated HepG2 and Huh7 cells.

5.1 – Introduction

The results described in the previous chapters indicate that a 15 day or longer exposure to 1% DMSO may cause an increase in the differentiation status of both HepG2 and Huh7 cells. However, this has only been assessed by measuring mRNA expression of three markers of differentiation – albumin, transferrin and AFP. Although these provide valuable information regarding the maturation status of the cell, more evidence is required in order to verify that these cells are in fact closer to the *in vivo* hepatocyte in relation to functionality (drug processing). Transcript and protein expression levels along with functional capabilities of various transporters and metabolising enzymes are extremely important to the overall function of a true hepatocyte. An overview of hepatocyte-defining criteria which should always be seen in hepatocytes is given by Hengstler *et al.* (Hengstler *et al.*, 2005) and includes synthesis of albumin, functional assessment of both phase I and II metabolic enzymes and evidence of enzyme induction. As the next step in satisfying these criteria, the work presented in this chapter investigates the basal and DMSO stimulated mRNA levels of several important transporters and phase I and II metabolising enzymes and compares these to levels in mature human liver.

Increases in mRNA level and functional activity of CYP3A4 have been observed in 20 day DMSO-treated Huh7 cells (Choi *et al.*, 2009) and in CYP1A2 and CYP3A4 in Huh7 cells grown in standard media for four weeks (Sivertsson *et al.*, 2010). Sivertsson *et al.* (Sivertsson *et al.*, 2010) investigated the effect of prolonged standard (untreated) growth on both HepG2 and Huh7 cells. The main finding was an increase in mRNA, protein and functional levels of CYP3A4 in Huh7 cells grown for 4 weeks. No similar change was observed in corresponding HepG2 cells. Huh7 cells treated with 1% DMSO for twenty days were assessed for drug metabolising enzyme activity and expression by Choi *et al.* (Choi *et al.*, 2009) with some positive results. mRNA levels of several important enzymes including CYP1A2, 2B6, 2D6 and 3A4 and UGT1A1 were seen to increase towards levels seen in primary hepatocytes (Choi *et al.*, 2009) and metabolic rates of several key enzymes including CYP1A2 and 3A4 were also increased in comparison to control cells. These two papers give a solid indication that both prolonged

untreated growth and 1% DMSO are effective in promoting a more hepatic profile in Huh7 cells at the mRNA, protein and functional levels.

5.1.1 – Influx transporters

General information on influx transporters, their locations and substrates can be found in chapter 1.3.1 and in table 1.1. Four influx transporters were chosen to be investigated in treated HepG2 and Huh7 cells and in untreated Huh7 cells. These were selected from the OATP and the OCT families; namely OATPB, C and 8 plus OCT3. All four of these transporters are expressed in the liver on the basolateral membrane of the hepatocyte, transporting substrates between the blood and hepatocytes (Koepsell et al., 2007; Tamai et al., 2001; Konig et al., 2000a; Konig et al., 2000b).

Substrates of OATP transporters do overlap; for example, both OATPC and -8 transport anticancer drugs such as methotrexate (Abe *et al.*, 2001; Abe *et al.*, 1999) and the antihistamine fexofenadine (Matsushima *et al.*, 2008). Within these categories of substrates there are some compounds which are specific to each OATP transporter such as the antidiabetic drug repaglinide, which utilises the OATPC transporter (Niemi *et al.*, 2005), the cardioactive drug digoxin, which is transported by OATP8 (Kullak-Ublick *et al.*, 2001) and the leukotriene receptor antagonist montelukast, which is transported by OATPB (Mougey *et al.*, 2009). A more extensive list of these transporters and their substrates can be found in table 5.1 (adapted from (Fahrmayr *et al.*, 2010)). Substrates of OCT3 include endogenous neurotransmitters such as epinephrine and xenobiotics introduced into the body such as nicotine, verapamil and quinine (Koepsell *et al.*, 2007). A more in depth list of these transporters and their substrates can be found in table 5.1 (adapted from (Fahrmayr et al., 2010)).

Earlier data from chapter 3 analysed basal mRNA levels of these influx transporters in both HepG2 and Huh7 cells in comparison to liver (figures 3.10 – 3.13, table 3.2). OCT3 mRNA levels were much closer to liver in HepG2 cells (approximately 70% of liver, Huh7 125-fold lower than liver), as were OATPB mRNA levels albeit by a smaller margin (HepG2 levels over 4-fold lower than liver, Huh7 levels 12-fold lower than liver). Huh7 cells showed levels of OATPC and -8 which were closer to liver levels than those in HepG2, although levels of OATPC mRNA in both cell lines was particularly low. If the 1% DMSO treatment has promoted differentiation of HepG2 and Huh7 cells, levels of all four of these transporters must increase with treatment.

5.1.2 – Efflux transporters

Four efflux transporters from the ABC superfamily of transporters, MRP1, MRP2, MDR1 (P-gp) and BCRP were assessed in treated HepG2 and Huh7 cells. General information on these transporters can be found in section 1.3.4 and in table 1.6. In the hepatocyte, P-gp, MRP2 and BCRP are located on the canalicular (apical) membrane, while MRP1 is located on the sinusoidal (basolateral) membrane. P-gp is known to confer multidrug resistance to carcinoma cells and transports steroid hormones and xenobiotic substrates such as digoxin, verapamil and cyclosporin A (Leslie *et al.*, 2005). MRP1 and -2 are known to transport both endogenous and xenobiotic substances which are the products of phase II conjugating enzymes (Haimeur *et al.*, 2004; Leslie *et al.*, 2004). MRP1 is know to efflux substances such as daunorubicin, a chemotherapeutic drug (Leslie *et al.*, 2005), whilst MRP2 effluxes a broad range of conjugated drug metabolites along with anticancer drugs such as cisplatin (Nies and Keppler, 2007; Cui *et al.*, 1999). The spectrum of substances transported by BCRP is smaller and does overlap with the three other efflux transporters studied here. For example, efflux of methotrexate is conducted by P-gp and BCRP along with several MRP proteins; however, BCRP also transports the polyglutamated forms of methotrexate whereas the MRP proteins are known not to (Hooijberg *et al.*, 2004; Ifergan *et al.*, 2004; Hooijberg *et al.*, 2003). Further substrates of these four transporters are detailed in table 5.2.

Basal levels of efflux transporters were analysed in figures 3.6 to 3.9 and displayed relative to liver in table 3.2. HepG2 cells had mRNA levels of MDR1 (P-gp), MRP1 and MRP2 higher than those in liver and BCRP mRNA levels almost 3-fold lower than liver. MRP1 levels in particular were significantly raised from liver, showing over 2100-fold increased mRNA levels. MRP1 and -2 were less markedly raised with levels 2.7-fold and 2.6-fold higher than liver respectively. In Huh7 cells, only basal levels of MRP1 were increased over those in liver, showing an 89-fold increase over liver. Although this is still markedly higher than liver, it is much lower than levels observed in HepG2. MDR1, MRP2 and BCRP levels were 5-fold, 12-fold and 20-fold decreased from liver respectively. For 1% DMSO treatment induction of a more differentiated cell, HepG2 levels of MDR1, MRP1 and -2 must be decreased with an increase in BCRP, while all except MRP1 need to increase in Huh7 cells.

5.1.3 – Phase I metabolising enzymes

Four phase I drug metabolising enzymes (DMEs), cytochrome P450 (CYP) -1A2, -2E1 and -3A4 and flavin containing mono-oxygense 3 (FMO3) were investigated in treated HepG2 and Huh7 cells. General information on the CYP and FMO families, locations and substrates can be found in section 1.3.3 and tables 1.2 and 1.3. The CYP superfamily, in particular families 1, 2 and 3 are

heavily involved in xenobiotic metabolism; for example, CYP3A4 is responsible for full or partial metabolism of over 50% of all therapeutic drugs (Guengerich, 1999; Shimada *et al.*, 1994). As a result, bottlenecks can occur with CYP enzymes and cause drug-drug interactions as well as potentially introducing inhibition and induction problems; inter-individual variations in expression may exacerbate this (Lin, 2006). Drugs metabolised by CYP3A4 include verapamil, diazepam, cyclosporin and tamoxifen (Kacevska *et al.*, 2008; Lin, 2006). CYP1A2 has been shown to increase with maturity and is either absent or present at very low levels in foetal liver, with expression still 10-fold lower in post natal liver up to 10 months of age than in adult liver (Cazeneuve *et al.*, 1994). Substrates of this enzyme include caffeine, melatonin, phenacetin and paracetamol (Zhou *et al.*, 2010). Similarly to CYP1A2, CYP2E1 protein levels increase after birth with newborn levels approximately 10% of those seen in adult liver (Vieira *et al.*, 1996). Many of the drugs metabolised by CYP2E1 are procarcinogens or release a toxic by-product, which can result in a build-up of toxicity if a bottleneck or previous enzyme induction event has taken place. Substances metabolised by CYP2E1 include paracetamol, benzene (Tanaka *et al.*, 2000) and carbon tetrachloride (Cederbaum, 2006). Like many of the genes in the CYP family, FMO3 expression is specific to developmental stage and is absent at birth, failing to reach adult levels until after the onset of puberty (Hines, 2006). Mutations in FMO3 are responsible for the disorder trimethylaminuria, where the substrate of trimethylamine is not broken down correctly. Other substrates of FMO3 include nicotine and tamoxifen (Krueger and Williams, 2005). Table 5.3 consists of an overview of substrates of these four phase I DMEs.

Basal levels of these enzymes were analysed in chapter 3 in both HepG2 and Huh7 cells in comparison to liver (figures 3.14, 3.15, 3.16 and 3.20, table 3.2). Overall, expression levels were much lower than those in liver in both cell lines for all four genes. Although it can be said that, for example, expression of CYP1A2 is closer to liver in Huh7 cells, it remains over 45,000-fold reduced from the *in vivo* level. These vast reductions are apparent for all of these enzymes in both cell lines; increases of several thousand fold would be required with DMSO treatment to produce cells with levels that would begin to be comparable to liver.

5.1.4 – Phase II metabolising enzymes

Phase II DMEs are mainly conjugating enzymes consisting of families such as the glutathione-S-transferases (GSTs), sulphotransferases (SULTs) and UDP glucuronosyltransferases (UGTs); general information on family, location and substrates can be found in chapter 1.3.3 and tables 1.4 and 1.5. The three phase II DME assays described in this chapter assess UGT1A1 and GSTA4

mRNAs specifically along with a third assay named GSTA which measures GSTA1, 2 and 5 mRNAs.

UGT1A1 metabolises a wide range of both xenobiotic and endogenous substrates including paracetamol, the chemotherapeutic drug irinotecan and thyroxine (Bock, 2010). It is also a major route in the metabolism of bilirubin, an accumulation of which can cause both Crigler-Najjar and Gilbert's syndromes (Tukey and Strassburg, 2000). Substrates of individual GST enzymes have not been as thoroughly defined as some enzymes such as CYPs and many characterisations are related to anti-cancer or cancer-related drugs. GSTA2 polymorphisms are known to be associated with cancer of the upper aerodigestive tract cancers (Canova *et al.*, 2010) and it is known to metabolism the immune system suppressant azathioprine (Eklund *et al.*, 2006). GSTA4 is involved in the metabolism of arachidonic acid (Hubatsch *et al.*, 1998) and GSTA1 in the metabolism of the chemotherapeutic compound chlorambucil (Hayes *et al.*, 2005). Known substrates of UGT1A1 and GSTA enzymes are listed in table 5.4.

In chapter 3 the basal levels of these genes in HepG2 and Huh7 cells in comparison to liver were analysed (table 3.2). Levels of GSTA and GSTA4 mRNAs were higher in HepG2 than Huh7 cells and were reasonably close to liver levels at 6-fold and 1.6-fold lower than liver respectively. UGT1A1 mRNA levels were over 1000-fold reduced from liver in both HepG2 and Huh7 cells. In order for the DMSO treatment to promote a more hepatocyte-like cell from either cell line, levels of these genes would all need to increase.

In the previous chapter 1% DMSO applied to HepG2 and Huh7 cells appeared to result in differentiation to a more mature hepatic state after a minimum of 15 days of treatment. However, this was assessed using only three markers of differentiation. While this does provide some valuable information it would be unwise to declare these cells more mature without further assessment of other salient features of the cell. Assessment of the expression levels of these described transport and metabolising GOI in treated HepG2 and Huh7 cells with comparison to liver expression will generate a more informative overview of the maturation status of these cells and their relevance as a model in drug development regime.

5.2 – Methods

Data generated in this chapter utilises the same samples as were assessed for levels of differentiation markers in chapter 4. HepG2 and Huh7 cells were cultured in six-well plastic plates for up to 30 days while being treated with 1% DMSO. Huh7 cells were also grown for up to 30 days in standard growth medium to provide time-matched controls. During these experiments Huh7 cells reached confluence after four days of growth as previously described;

during a further period of growth (3-6 days) during which cells became over-confluent, cell proliferation appeared to slow and eventually cease. Conversely, HepG2 cells did not cease to proliferate with prolonged untreated growth, becoming so over-confluent that maintenance was impossible and cells began to die after roughly 8-10 days of total growth (4-6 days post-confluence). Experimental layout is shown in figures 2.1 and 2.2. qPCR assays were conducted as outlined in chapters 2 and 3. Data from human liver is shown relative to HepG2 and Huh7 confluent control cells. Data from days 5 and 30 of treatment are not shown as differentiation analysis from the previous chapter revealed that any changes would be expected to take place after 15 to 20 days of treatment. Data was analysed by one-way ANOVA with Dunnett's post test when comparisons are to a single control point, and by Student's T-test for matched time points in treated and untreated Huh7 cells.

5.3 – Results

5.3.1 – Influx transporters

The four influx transporters assessed in this chapter were OATPB, C and 8 and OCT3. The mRNA levels of these transporters in HepG2 and Huh7 cells following 1% DMSO treatment are shown in figures 5.1 and 5.2 respectively. Levels in Huh7 cells in standard growth medium are also shown in figure 5.2. Graph A in figure 5.1 shows that OATPB mRNA levels in HepG2 cells were almost 5-fold lower in confluent control cells than in liver and remained close to control level throughout the treatment period. OATPC mRNA level (graph B) was approximately 40,000-fold lower in control HepG2 cells than in liver and although there were significant increases from control after 20 and 25 days of treatment, these did not result in levels approaching that observed in the liver sample. OATP8 mRNA expression (graph C) was also much higher in liver with the level approximately 20,000-fold higher than that in control HepG2 cells and was not significantly increased in the cells at any point during the 1% DMSO treatment. Finally, graph D in figure 5.1 shows that OCT3 mRNA levels in liver and HepG2 control cells are very similar and that a significant increase is observed in cell expression following 25 days of treatment.

Results for Huh7 cells treated with 1% DMSO or grown in standard media alone for up to 25 days and subsequently analysed for mRNA levels of the four influx transporters are shown in figure 5.2. OATPB mRNA levels were roughly 12-fold lower in control cells than in liver and remained stable throughout 1% DMSO treatment (graph A). In untreated cells, OATPB mRNA levels were decreased significantly compared to control after 10 days, but increased at subsequent time points to become comparable to control after 20 and 25 days of treatment. Expression in treated cells tended to be higher than in untreated cells but the difference was

significant only after 15 days of treatment and by day 25 levels in treated and untreated cells were comparable. OATPC mRNA in liver was approximately 300-fold higher than in Huh7 control cells and the level of expression in the cells did not change significantly over 25 days of untreated growth (graph B). However, 1% DMSO treated cells showed significantly decreased mRNA level from the control at every time point and were also significantly lower in OATPC mRNA than time-matched, untreated cells. OATP8 mRNA level was roughly 70-fold higher in liver than in control Huh7 cells and decreased significantly in both prolonged untreated growth and 1% DMSO treated cells in comparison to control at all time points (graph C). t-tests on these data revealed that over longer growth periods, 1% DMSO resulted in OATPC mRNA levels significantly lower than in time matched untreated cells; however this is unlikely to be of any physiological significance since levels in both treated and untreated cells were much lower than those in liver. Finally, OCT3 mRNA level was approximately 300-fold higher in liver than in control Huh7 cells (graph D). Both prolonged untreated growth and 1% DMSO resulted in cells with significant increases in OCT3 levels compared to control after 15-25 days and 25 days respectively. The level in untreated Huh7 cells remained significantly higher than that in control cells from 15 days onwards and was also significantly increased over the corresponding DMSO treated cells at 15 and 20 days. In both sets of cells, OCT3 mRNA expression was roughly 5-fold higher than in controls after 25 days of growth; however this still did not result in a concentration approaching the measured liver level.

Summary

- OATPB – no significant change with 1% DMSO treatment in HepG2 cells. Untreated Huh7 cells decreased significantly after 10 days but this was not sustained; no change in DMSO-treated Huh7 cells.

- OATPC – significant increase in HepG2 cells after 20 and 25 days of treatment but remained much lower than liver. No significant changes in untreated Huh7 cells, significant decreases from control at all time points in DMSO-treated Huh7 cells.

- OATP8 – no significant change with 1% DMSO treatment in HepG2 cells. Both untreated and DMSO-treated Huh7 cells were significantly decreased from control at all time points; DMSO-treated cells had significantly lower expression than matched untreated cells.

- OCT3 – significant increase in HepG2 cells treated for 25 days with 1% DMSO which elevated levels above those in liver. Untreated Huh7 cells showed significant increases

from control at 15, 20 and 25 days, while DMSO-treated cells were significantly increased from control only after 25 days.

5.3.2 – Efflux transporters

The four efflux transporters assayed were MRP1, MRP2, MDR1 and BCRP. The results for these assays from 1% DMSO treated HepG2 and Huh7 cells are shown in figures 5.3 and 5.4 respectively. Prolonged growth of Huh7 cells in standard growth medium is also shown in figure 5.4. Graph A in figure 5.3 shows that MRP1 mRNA level in control HepG2 cells was calculated to be over 2100-fold higher than in liver and that no significant change from control occurred with 1% DMSO treatment Although liver value for MRP1 is too low to be shown visually on the graph in comparison to HepG2 values, it was detectable and the actual value was $2.7x10^{-4}$. MRP2 mRNA level (graph B) in control HepG2 cells was roughly double that in liver and did not significantly change with 1% DMSO treatment. MDR1 mRNA (graph C) was over 3-fold higher in control HepG2 cells than in liver and treatment with 1% DMSO resulted in no significant change from control throughout the experiment. Finally, graph D in figure 5.3 shows BCRP mRNA levels in liver and HepG2 cells. Control HepG2 cells had roughly half the BCRP mRNA of liver and levels decreased significantly from control at 10, 15 and 20 days of treatment with 1% DMSO.

Results from Huh7 cells analysed for mRNA levels of MRP1 are shown in graph A of figure 5.4. In control cells the level of MRP1 was approximately 10-fold higher than in liver and extended growth either with or without 1% DMSO did not result in a significant change from control level. MRP1 mRNA levels in DMSO treated cells were significantly lower at 15 and 25 days than in untreated cells of the same age. MRP2 mRNA level in liver was approximately 200-fold higher than in control Huh7 cells. No significant changes from control were seen in either untreated or 1% DMSO treated cells, nor were any significant differences seen between the two treatments at any time point. MDR1 mRNA level was roughly 9-fold higher in liver than in control Huh7 cells. Prolonged growth in standard medium resulted in a steady increase in MDR1 level culminating in a significant increase after 25 days. However, MDR1 levels in cells treated with 1% DMSO remained close to control and did not significantly alter. Finally, graph D of figure 5.4 shows that BCRP mRNA level in Huh7 control cells was roughly 20-fold lower than liver level and, with prolonged untreated growth, BCRP expression was decreased significantly from control at every time point. Following 1% DMSO treatment BCRP mRNA levels in Huh7 cells did not change significantly from control but were significantly higher than untreated cells at 10 and 15 days of treatment.

Summary

- MRP1 – no significant change from control was observed in HepG2 cells, untreated Huh7 or DMSO-treated Huh7 cells. However, levels in untreated Huh7 cells were significantly higher at matched timepoints than those in DMSO-treated cells after 15 and 25 days.

- MRP2 – no significant change from control was observed in HepG2 cells, untreated Huh7 or DMSO-treated Huh7 cells.

- MDR1 – no significant change from control was observed in HepG2 cells. A significant increase was observed after 25 days in untreated Huh7 cells, while no significant changes were observed in DMSO-treated Huh7 cells.

- BCRP – significant decreases from control were observed at 10, 15 and 20 days in HepG2 cells. Untreated Huh7 cells were significantly decreased from control at all timepoints, while no significant changes from control were observed in DMSO-treated Huh7 cells.

5.3.3 – Phase I metabolising enzymes

The phase I DMEs assayed in this chapter were CYP1A2, 2E1, 3A4 and FMO3. The results from these assays on 1% DMSO treated HepG2 and Huh7 cells are shown in figures 5.5 and 5.6 respectively. Results for prolonged untreated culture of Huh7 cells in standard growth medium are also shown in figure 5.6. Graph A in figure 5.5 shows that the liver level of CYP1A2 mRNA was approximately 2000-fold higher than that in control HepG2 cells. CYP1A2 level in HepG2 cells treated with 1% DMSO decreased from control at all time points, however none reached significance. CYP2E1 mRNA level (graph B) was roughly 130-fold higher in liver than in control HepG2 cells. In cells treated with 1% DMSO, levels of CYP2E1 increased and reached significance compared to control at 20 days; however, this was not sustained at 25 days of treatment. CYP3A4 mRNA level (graph C) was approximately 30-fold higher in liver than in HepG2 control cells and with 1% DMSO treatment applied to cells for 10, 15 and 20 days increased significantly to roughly 4-fold control level. Finally, graph D in figure 5.5 shows that the liver level of FMO3 was approximately 2700-fold higher than in control HepG2 cells; although 1% DMSO increased mRNA expression, the differences to control did not reach significance.

Results from Huh7 cells assessed for levels of CYP1A2 mRNA are displayed in graph A in figure 5.6. Liver CYP1A2 level was approximately 40-fold higher than in control Huh7 cells and

prolonged untreated growth of Huh7 cells resulted in an increase in CYP1A2 mRNA expression, which was significant at 20 and 25 days. At these time points, CYP1A2 mRNA was approximately 60-fold higher than control and exceeded the level observed in liver. Huh7 cells treated with 1% DMSO showed no significant change in CYP1A2 mRNA from control level at any point during the experiment. CYP1A2 mRNA levels were significantly higher in untreated cells in comparison to 1% DMSO treated cells at 15, 20 and 25 days of treatment and were markedly increased, being some 40-70 fold higher. CYP2E1 mRNA level in liver was approximately 35,000-fold higher than in Huh7 control cells. Following 10 and 20 days of untreated growth, cells showed significant increases over control of approximately 3-fold. 1% DMSO increased CYP2E1 mRNA throughout the experiment, with the increase reaching significance compared to control cells after 25 days when levels were roughly 20-fold greater than control. Although all DMSO-treated cells had increases at least equal to those which were increased significantly in untreated cells (over 3-fold), bigger error margins prevented the data from reaching significance until the much larger increase after 25 days. CYP2E1 mRNA level in 1% DMSO treated Huh7 cells was significantly higher than in untreated cells at 15 and 25 days of treatment. CYP3A4 mRNA level was roughly 72-fold higher in liver than in control Huh7 cells and in untreated and 1% DMSO treated cells were roughly 3-fold higher than control at all time points, with significant increases compared to control at 15 and 25 days for untreated and 1% DMSO treated cells respectively. Comparing time matched DMSO treated and untreated cells showed no effect of DMSO treatment at any time point. Finally, FMO3 mRNA level in liver was approximately 770-fold higher than that in control Huh7 cells. Extended growth resulted in significant decreases from control at all time points, whilst the level in 1% DMSO treated cells remained around control level throughout the experiment. 1% DMSO treated Huh7 cells had significantly higher levels of FMO3 mRNA than were found in untreated cells of the same age at 10 and 15 days of treatment.

Summary

- CYP1A2 – mRNA levels in DMSO-treated HepG2 cellsdid not significantly change. Untreated Huh7 cells significantly increased from control after 15, 20 and 25 days, while DMSO-treatment of Huh7 cells did not result in any significant changes.

- CYP2E1 – levels in 20-day DMSO-treated HepG2 cells increased significantly. Untreated Huh7 cells are significantly increased from control after 10 and 20 days, while levels in DMSO-treated Huh7 cells significantly increased after 25 days.

- CYP3A4 – significant increases were observed after 10, 15 and 20 days of DMSO treatment on HepG2 cells. Levels in both untreated and DMSO-treated Huh7 cells

were approximately double of those in control at all time points, but only reached significance at 15 and 25 days of treatment respectively.

- FMO3 – no significant changes were observed in DMSO-treated HepG2 cells. Levels in untreated Huh7 cells were significantly decreased from control at all time points, while those in DMSO-treated Huh7 cells did not significantly change.

5.3.4 – Phase II metabolising enzymes

The assays measuring mRNA levels of phase II DMEs included specific assays for GSTA4 and UGT1A1 and one assay encompassing GSTA1, 2 and 5, referred to here as GSTA. The results from these assays on 1% DMSO treated HepG2 and Huh7 cells are shown in figures 5.7 and 5.8 respectively. Results for prolonged untreated culture of Huh7 cells in standard growth medium are also shown in figure 5.8. Graph A in figure 5.7 shows GSTA mRNA level in liver was almost 40-fold higher than that in control HepG2 cells and in 1% DMSO treated cells levels decreased significantly from control at all time points. GSTA4 mRNA level in liver (graph B) was almost double that seen in control HepG2 cells. HepG2 cells with 1% DMSO treatment showed a significant increase in GSTA4 over control after 15 days, when the level increased to approximately those in liver. At other time points GSTA4 mRNA levels remained around control level. UGT1A1 mRNA level in liver (graph C) was approximately 4,600-fold higher than in HepG2 control cells. Large increases from control were seen in all 1% DMSO treated cells and reached significance at 20 days of treatment with a level approximately 1,500-fold higher than control. Although control levels cannot be visualised on the graph whilst displaying the much larger HepG2 and liver levels, UGT1A1 mRNA was detectable and control was set at a value of 1.

Results from Huh7 cells treated with 1% DMSO and grown in standard media assayed for phase II DMEs are shown in figure 5.8. GSTA mRNA level was over 600-fold higher in liver than control Huh7 cells (graph A); untreated Huh7 cells showed significantly reduced GSTA mRNA from control at all time points. This was reversed by 1% DMSO treatment, which resulted in increased expression over control at all time points, reaching significance at 20 days of treatment when a level roughly 12-fold higher than control was observed. Comparing 1% DMSO treated to age-matched untreated cells showed that 1% DMSO significantly increased GSTA mRNA at 10, 15 and 20 days. GSTA4 mRNA level was approximately 15-fold higher in liver than in control Huh7 cells and did not change significantly from control with either extended growth or DMSO. Treatment with 1% DMSO for 25 days resulted in a significantly higher GSTA4 level than untreated Huh7 cells at the same time point. Finally, UGT1A1 mRNA level in liver was approximately 1000-fold higher than in control Huh7 cells. Levels in untreated

Huh7 cells did not change significantly from control whereas 1% DMSO treated cells had significantly higher UGT1A1 mRNA levels than control after 20 and 25 days of treatment.

Summary

- GSTA – levels in DMSO-treated HepG2 cells were significantly decreased from control at all time points. Untreated Huh7 cells were significantly decreased from control at all time points, while in DMSO-treated cells a significant increase was observed after 20 days.

- GSTA4 – levels in DMSO-treated HepG2 cells remained similar at most time points, with a solitary significant increase at 15 days. No significant changes were observed in either untreated or DMSO-treated Huh7 cells.

- UGT1A1 – a significant increase in DMSO-treated HepG2 cells was observed at 20 days. No significant changes were seen in untreated Huh7 cells, while significant increases were observed after 20 and 25 days of DMSO treatment in Huh7 cells.

5.3.5 – GOI mRNA levels in HepG2 cells

Table 5.5 shows accumulated data from figures 5.1, 5.3, 5.5 and 5.7 along with data from table 3.1 recalculated to show liver levels relative to control. Column 1 shows data from table 3.1 – these data are from preliminary experiments in assay development (chapter 3) using samples from two confluent HepG2 experiments and a pooled liver sample; values have been recalculated to show liver levels relative to HepG2 cells. Column 2 shows data for the same liver sample relative to different control HepG2 samples. These two data sets essentially allow comparison of mRNA levels in confluent control cell samples and indicate how stable basal expression is between passages. Columns 3 and 4 show data from HepG2 cells treated with 1% DMSO expressed relative to control. In column 3 data from 15 days of treatment is shown as this was the time point at which most treatment effects were observed when assaying differentiation markers (chapter 4). Column 4 shows the data point for each gene which was closest to liver level along with the time point at which this was observed.

Comparison of the values for columns 1 and 2 which show expression in liver relative to control cells shows that influx transporter mRNA levels remained similar in the two separate sets of experiments. Although the level of OATPB mRNA was just under 5-fold higher in liver than in control cells only a very small increase over control was seen following 15 days of growth, which was the biggest difference at any time point. After 15 days of DMSO treatment the OATPC mRNA level was over 2-fold higher than control and this increased to over 4-fold

higher than control after 25 days of treatment. However, neither of these values approached liver level. OATP8 mRNA levels increased slightly from control after 15 days of treatment, which was the biggest increase seen throughout the treatment, but this also did not approach the level in liver. OCT3 mRNA levels in liver relative to confluent cells were not vastly different from each other or from levels seen after 15 days of treatment.

Efflux transporter mRNA levels are fairly similar in the first two columns of table 5.5 displaying liver levels relative to control HepG2 cells and calculated from two separate sets of experiments. MRP1 mRNA levels showed a difference between the two values for liver relative to confluent cells but both values were much lower than those observed in control and after 15 days of treatment with 1% DMSO, which was the closest of the treated values to that seen in liver. Both liver values show MRP2 mRNA levels of approximately half those seen in control HepG2 cells with the closest treated value to liver seen at 10 days. However, none of the time points showed large variations from control and at 20 days MRP2 levels were also close to those observed at 10 days. MDR1 mRNA levels in liver relative to confluence were roughly one third of those seen in control HepG2 cells and values were close, indicating relatively stable mRNA levels of this gene between passages. Treated HepG2 cells did show slight decreases in MDR1 mRNA at 10 and 15 days but these did not reach liver levels. Finally, BCRP mRNA levels in liver relative to confluent HepG2 cells were between 2- to 3-fold increased, remaining relatively stable with passaging. With 1% DMSO treatment levels did not increase and were consistently lower than control.

Phase I and II DMEs showed much wider variation in confluent levels of the GOI than were seen in the transporters with the exception of GSTA4, which showed fairly stable basal levels. Other enzymes varied widely; for example, CYP1A2 mRNA levels varied by over 600-fold when measuring liver relative to the two confluent data sets. mRNA levels of CYP2E1, CYP3A4 and FMO3 had variations similar to or even larger than this, indicating either that basal levels of these genes were very variable or that the genes were expressed at such a low level that consistent measurements were difficult to obtain. Of the genes which did show substantial increases with DMSO treatment such as CYP2E1 and 3A4, FMO3, GSTA4 and UGT1A1, all except UGT1A1 and GSTA4 remained much lower than their respective liver levels even if the lowest relative liver level calculated was taken as the true level. The GSTA4 mRNA level in 15 day treated HepG2 cells was roughly equal to liver. UGT1A1 mRNA after 20 days of treatment was almost half of that in liver if the lowest relative liver level is used, and just under one third of the higher relative liver level. The CYP1A2 and GSTA assay results both showed mRNA levels in treated cells lower than those in control cells whilst liver levels of both genes were higher than control.

Summary

- In most cases liver levels relative to HepG2 at confluence were similar in experiments in this chapter and previous ones in chapter 3, indicating that basal levels do not change with passaging. Some exceptions were CYP2E1, CYP3A4 and FMO3.
- For most genes the closest expression to liver did occur after at least 15 days of treatment which agrees with results from chapter 4.
- While increases in some low expression genes such as CYP2E1 and -3A4 did increase, they remained much lower than liver levels. MRP1, which should have decreased if a more mature cell line was produced, did not do so.

5.3.6 – GOI mRNA levels in Huh7 cells

The mRNA levels of the three OATP influx transporters assayed were very close in both measurements of liver relative to confluent Huh7 levels, indicating that basal expression is stable with passage number of the cells (Table 5.6). OCT3 mRNA levels were slightly more variable than the OATP levels observed with a 2.4-fold difference seen between the two values for liver relative to confluence. Although increases in OCT3 mRNA levels were seen in treated and untreated Huh7 cells, neither approached liver values. Of the OATP genes assayed, increases were seen in OATPB and C mRNA levels in treated and untreated cells respectively but again neither approached levels in liver. Levels of OATPB and 8 in untreated cells and OATPC and 8 in treated cells all decreased when an increase was required to match levels in liver.

Levels of MRP1 and MRP2 mRNA differed between the two measurements of liver relative to confluent Huh7 cells by approximately 7-fold and 13-fold respectively. MDR1 and BCRP mRNA levels were similar in the two measurements indicating a more stable basal level of these genes. Notable responses in DMSO treated Huh7 cells were seen at 15 days when MRP1 mRNA levels fell from control and were closer to liver levels; untreated cells increased in MRP1 mRNA which was the opposite effect to that desired. Slight increases from control were observed in MRP2 mRNA in both untreated and treated cells but these did not approach those seen in liver. MDR1 mRNA levels in untreated Huh7 cells approached those seen in liver after 25 days; in DMSO treated cells the largest increase was observed after 20 days but this was only about 50% of the magnitude seen in untreated cells. BCRP mRNA levels in both treated and untreated cells decreased after 15 days when a minimal increase of 20-fold would be required to come close to liver levels.

Levels of phase I DMEs in confluent Huh7 cells did appear to differ significantly between passages as was observed in HepG2 cells; for example, a 50-fold difference is apparent between the two liver calculations in CYP2E1 mRNA levels. The largest differences out of all of the GOIs assayed were observed between confluent values for CYP2E1, 3A4 and FMO3 in HepG2 cells, and in CYP1A2, 3A4 and FMO3 in Huh7 cells. This demonstrates that the apparent variability of expression between passages in confluent cells does have some similarity between the two cell lines, noticeably in those GOIs which had low expression. mRNA levels in the phase II DMEs appeared to be more stable with only a 2-fold difference between liver relative to confluence in the GSTA assay and negligible differences in GSTA4 and UGT1A1 mRNA levels. Large increases in CYP1A2 mRNA in comparison to control can be seen at 15 and 10 days of the experiment in untreated and treated cells respectively; however, with the discrepancy between the values for liver relative to control it cannot be determined whether these are close to true liver levels or not. CYP2E1 and 3A4 mRNA levels increased compared to control in both treated and untreated cells but did not approach those in liver, while FMO3 levels were lower than control with both growth conditions. No real increase from control was observed in GSTA4 mRNA levels in either untreated or treated Huh7 cells. This was also true for GSTA levels in untreated cells. However, an 11-fold increase in GSTA mRNA level was observed in DMSO treated cells after 20 days but this did not approach the 300- to 600-fold increase over control cells which was observed in liver. Small increases in UGT1A1 mRNA levels were also observed in both untreated and treated Huh7 cells but again these did not approach the 1000-fold plus increase shown in liver over confluent cells.

Summary

- Gene levels in liver relative to confluent Huh7 cells from data in this chapter and chapter 3 showed that most were stable with passaging, the exceptions being the CYPs and FMO3 which are also the lowest in expression.

- The majority of genes showed the closest expression to liver after 15-20 days of treatment which agrees with results from chapter 4.

- As with HepG2 cells, the majority of genes did not markedly change towards liver levels either with prolonged untreated or DMSO-treated growth, which indicates that a more hepatocyte-like cell has not been produced.

5.4 – Discussion

In the previous chapter it was observed that 1% DMSO prompted changes in the mRNA expression levels of certain markers of differentiation in both HepG2 and Huh7 cells indicating that a more hepatocyte-like cell resulted from the treatment. The aim of this chapter was to determine whether this apparent maturation was also apparent as changes in the mRNA levels of selected transporters and enzymes to a more liver-like expression level. HepG2 cells in particular are known to have poorly expressed levels of important DMEs such as CYP3A4 (Hart *et al.*, 2010; Jennen *et al.*, 2010; Slany *et al.*, 2010; Guillouzo *et al.*, 2007; Cederbaum, 2006; Hewitt and Hewitt, 2004). Although Huh7 cells have not been characterised to as great an extent as HepG2 cells, published data do indicate that DME levels here and in hepatocarcinoma cell lines in general are lower than in primary and *in vivo* hepatocytes (Hart *et al.*, 2010; Jennen *et al.*, 2010; Slany *et al.*, 2010).

Data from this set of experiments comparing the expression in confluent control cells scaled to expression in liver were compared to an earlier set of experiments described in Chapter 3. mRNA levels in HepG2 cells for all three CYP enzymes along with FMO3 and GSTA showed wide variation between the two sets of data. This may indicate that basal expression of these genes varies between cultures, however it was noted that expression levels of these genes were very low in HepG2 cells which made measurement difficult, which may account for some of the variability.

In HepG2 cells the majority of genes assessed showed no significant positive change in expression from control cells as a result of DMSO treatment. Of those which showed increased expression from a starting point below that in liver, such as OATPC and FMO3, the achieved expression level remained well below liver level and so the physiological relevance of these results is questionable. MRP1, MRP2 and MDR1 levels in HepG2 cells before treatment were higher compared to liver but did not decrease to levels similar to liver in response to 1% DMSO. UGT1A1 mRNA levels were significantly increased and became a lot closer to liver levels as a result of 1% DMSO treatment. Depending on the more likely level of CYP1A2 mRNA in liver relative to confluent cells, this may also be true of CYP1A2 levels in 1% DMSO treated cells.

Both prolonged untreated Huh7 cells and 1% DMSO treated Huh7 cells were assessed for levels of GOIs. In contrast to what was seen in HepG2 cells, only MRP1 mRNA levels were higher in confluent Huh7 cells than in liver. In untreated Huh7 cells, several instances of decreases in mRNA levels over time were observed when an increase would be expected with a more mature hepatic phenotype – these include OATP8, BCRP and GSTA. Significant

increases in MDR1 mRNA over time revealed mRNA levels approaching those in liver. Another notable result was a 36-fold increase in CYP1A2 levels which may or may not result in expression approaching that in liver depending on the calculated values of liver relative to the potentially variable, low expression basal levels in confluent cells. Huh7 cells treated with 1% DMSO showed notable increases in OCT3, MDR1, CYP1A2, CYP2E1 and GSTA mRNA levels. However, only MDR1 approached liver mRNA level. Interestingly, OATP8 mRNA levels decreased significantly from control in both untreated and treated cells while liver expression was at least 70-fold higher than that in control cells.

The results obtained here agree with those published by Choi *et al.* (Choi *et al.*, 2009) where the two data-sets overlap, as increases in the mRNA levels of CYP1A2, CYP3A4 and UGT1A1 were seen in DMSO treated cells in comparison to confluent Huh7 cells while not reaching those measured in primary human hepatocytes. However, this publication showed that functional protein levels were vastly improved upon by DMSO in comparison to growing Huh7 cells, indicating that a small mRNA increase could result in a much more appropriate hepatic model being produced. Aspects of the data shown here also agree with that for prolonged untreated growth as published by Sivertsson *et al.* (Sivertsson *et al.*, 2010) such as the slight increase in OATPC and MDR1 and the relatively unchanged MRP2 mRNA levels. Although a 3-fold increase in CYP3A4 was seen, this did not compare to the near *in vivo* levels of the gene with an increase of at least 100-fold over confluence observed in this publication. However, other increases observed here such as the 36-fold increase in CYP1A2 mRNA were not observed by Sivertsson. This could be due to their classification of changes in expression into groups rather than expressing an individual value for each gene, as if a change was not large enough to change categories it would not be apparent; for example, if an exceptionally low-expression gene displayed a large fold change but did not enter the next group (i.e. from <0.001 to 0.001-0.01) it would not be seen. Alternatively, the Huh7 cell lines used by the two laboratories could be responding differently due to inherent differences in tissue culture and laboratory regimes as discussed previously.

Changes in expression of certain genes as a result of DMSO treatment has been observed in both rat and human hepatocytes (Sumida *et al.*, 2011; Nishimura *et al.*, 2003). Some of these results do support data presented here; for example, Nishimura *et al.* (Nishimura *et al.*, 2003) reported a 1.5-2 fold increase and a 2-3 fold increase in CYP3A4 mRNA over control with 0.5% and 2.5% DMSO treatments respectively, which are comparable to changes observed here in both HepG2 and Huh7 cells. Results for induction of CYP1A2 were again much lower than those observed in both treated and untreated Huh7 cells with increases less than 2-fold at all concentrations. Some inconsistencies are also apparent when comparing with Sumida *et al.*

(Sumida *et al.*, 2011). Although these results are not associated with any fold-change values, the data suggest that some genes such as CYP3A4 and CYP2E1 are up-regulated with DMSO treatment, which agrees with data presented here. However, their data also suggests that MRP2 is down-regulated, while results obtained here suggests there is little change in either cell line. Although both of these papers investigate the direct effects of DMSO on a cell system, no potential mechanism of action by the compound is discussed. Indeed, it seems that very little in general is known about the potential effects of DMSO on signalling pathways or cellular systems and communications, which could be a potential avenue for future research.

Overall, 1% DMSO treatment is not effective at inducing a hepatocyte-like expression profile of key transporters and drug metabolising enzymes in either HepG2 or Huh7 cells. There are some indications that expression levels of certain genes have been made more like the hepatic level, such as UGT1A1 in 1% DMSO treated HepG2 cells, MDR1 in untreated Huh7 cells and MRP1 in 1% DMSO treated Huh7 cells. This may indicate that although the mature hepatic phenotype has not been induced across all genes there may be certain areas in which these cells are more true to the hepatocyte than confluent cells 4-days post plating and suggest that the identified treatments or growth regimes may be useful in producing models for studying specific aspects of drug metabolism. However, so far only mRNA levels have been investigated and it is possible that changes in protein expression or transporter/enzyme activity occur independently of changes in mRNA expression, for example in translation, activation or translocation of the protein, resulting in a functional hepatocyte-like phenotype. In subsequent chapters, effects in these areas are investigated by using induction assays with phenobarbital, rifampicin and β-naphthoflavone and by functional assays and Western blots to assess protein levels and functionality.

Transporter	Substrate Class	Substrate
OATPB	Antibiotic	Benzylpenicillin
	Antihistamine	Fexofenadine
	Antihypertensive	Bosentan
	Leukotriene receptor-antagonist	Montelukast
	Statins	Atorvastatin
		Fluvastatin
		Rosuvastatin
OATPC	Antibiotic	Benzylpenicillin
		Rifampicin
	Anticancer	Atrasentan
		Methotrexate
	Antidiabetic	Repaglinide
	Antihistamine	Fexofenadine
	Antihypertensive	Bosentan
		Valsartan
	Diuretic	Torasemide
	Fungicide	Capsofungin
	Statins	Atorvastatin
		Fluvastatin
		Pravastatin
	Endogenous	Bile salts
		Hormone conjugates
		Bilirubin
OATP8	Analgesic	Deltorphin II
	Antibiotic	Rifampicin
	Anticancer	Atrasentan
		Methotrexate
	Antihistamine	Fexofenadine
	Antihypertensive	Bosentan
		Telmisartan
		Valsartan
	Cardioactive	Digoxin
		Ouabain
	Statins	Fluvastatin
		Pravastatin
	Endogenous	Bile salts
		Hormone conjugates
		Bilirubin
OCT3	Cholinergic receptor antagonist	Atropine
		Nicotine
	Cholinergic receptor agonist	Etilefrine
	Adrenergic receptor antagonist	Quinine
		Verapamil
	Antimalarial	Epinephrine
	Ca^{2+} channel blocker	Histamine
	Neurotransmitters	Norepinephrine

Table 5.1 – Substrates of influx transporters. Information adapted from tables presented in Koepsell *et al.* (Tompkins *et al.*, 2010; Koepsell *et al.*, 2007) and Fahrmayer *et al.* (Fahrmayr *et al.*, 2010) and data from Konig *et al.* (Urquhart *et al.*, 2007; Konig *et al.*, 2000a; Konig *et al.*, 2000b) and Cui *et al.* (Cui *et al.*, 2001).

Transporter	Substrate class	Substrate
MRP1	Anticancer	Daunorubicin Etoposide Vincristine Chlorambucil metabolites Cyclophosphamide metabolites
MRP2	Antidiabetic Statins Protease inhibitor Anticancer Histamine receptor antagonist Endogenous	Conjugated drug metabolites Glibenclamide Pravastatin Indinavir Irinotecan Cisplatin Cimetidine Bilirubin glucouronide Leukotrine C_4
MDR1	Antihypertensive Antihistamine Anticancer Protease inhibitor Immunosuppressant Ca^{2+} channel blocker Endogenous	Digoxin Quinidine Losartan Mibefradil Fexofenadine Paclitaxel Daunorubicin Doxorubicin Irinotecan Saquinavir Cyclosporin A Verapamil Steroid hormones
BCRP	Anticancer Statins Histamine receptor antagonist Endogenous	Sulphate metabolites Topotecan Daunorubicin Irinotecan Mitoxantrone Rosuvastatin Pitavastatin Cimetidine Estrone sulphate Folic acid

Table 5.2 – Substrates of efflux transporters. Information from Leslie *et al.* (Urquhart *et al.*, 2007; Leslie *et al.*, 2005)and Funk (Funk, 2008).

Transporter	Substrate class	Substrate
CYP1A2	Analgesic	Paracetamol
		Phenacetin
		Aminopyrine
	CNS stimulant	Caffeine
		Paraxanthine
	Anticancer	Dacarbazine
	Antidepressant	Duloxetine
	Anti-inflammatory	Leflunomide
	Beta-blocker	Propranolol
	Bronchodilator	Theophylline
	Ca^{2+} channel blocker	Verapamil
CYP2E1	Anaesthetic	Halothane
		Isoflurane
	Analgesic	Paracetamol
	Antidepressant	Fluoxetine
	Anti-epileptic	Phenobarbital
	CNS stimulant	Caffeine
	Bronchodilator	Theophylline
	Alcohol	Ethanol
		Methanol
	Beta-blocker	Propranolol
	Ketones	Acetone
	Aromatic hydrocarbons	Benzene
	Halogenated hydrocarbons	Carbon tetrachloride
CYP3A4	Anticancer	Docetaxel
		Irinotecan
		Topotecan
		Mitoxantrone
		Vincristine
		Vinblastine
		Tamoxifen
		Letrozole
		Imatinib
	Immunosuppressant	Cyclosporin A
	Synthetic opioid, analgesic	Methadone
	Antihypertensive	Quinidine
	Ca^{2+} channel blocker	Verapamil
	Anti-anxiety	Diazepam
FMO3	Endogenous	Methionine
		Trimethylamine
		Tyramine
	Psychostimulant	Methamphetamine
	Analgesic	Benzydamine
	Alkaloid	Nicotine
	Agonist/antagonist	Tamoxifen

Table 5.3 – Substrates of phase I metabolising enzymes. Information from Zhou *et al.* (Zhou *et al.*, 2010), Tanaka *et al.* (Tanaka *et al.*, 2000), Kacevska *et al.* (Kacevska *et al.*, 2008), Lin (Lin, 2006) and Krueger *et al.* (Krueger and Williams, 2005).

Transporter	Substrate class	Substrate
UGT1A1	Antihypertensive	Carvedilol
	Synthetic thyroxine	Levothyroxine
	Anticancer	Irinotecan
	Analgesic	Paracetamol
	Estrogen receptor modulator	Raloxifene
	Endogenous	Thyroxine
		Bilirubin
		Eicosanoids
GSTA1	Anticancer	Chlorambucil
		Busulfan
		Melphalan
		Thiotepa
		Brostallicin
		Doxorubicin
		Vincristine
		Mitoxantrone
	Glutathione depletion	Chlorodinitrobenzene
GSTA4	Lipid peroxidation product	4-hydroxynonenal
	Glutathione depletion	Chlorodinitrobenzene
	Anticancer, autoimmune disease blockers	Thiopurines
	Endogenous	Arachidonic acid

Table 5.4 – Substrates of phase II metabolising enzymes. Information from Williams *et al.* (Williams *et al.*, 2004), Bock (Bock, 2010), Lo *et al.* (Lo and Ali-Osman, 2007) and Hayes *et al.* (Hayes *et al.*, 2005).

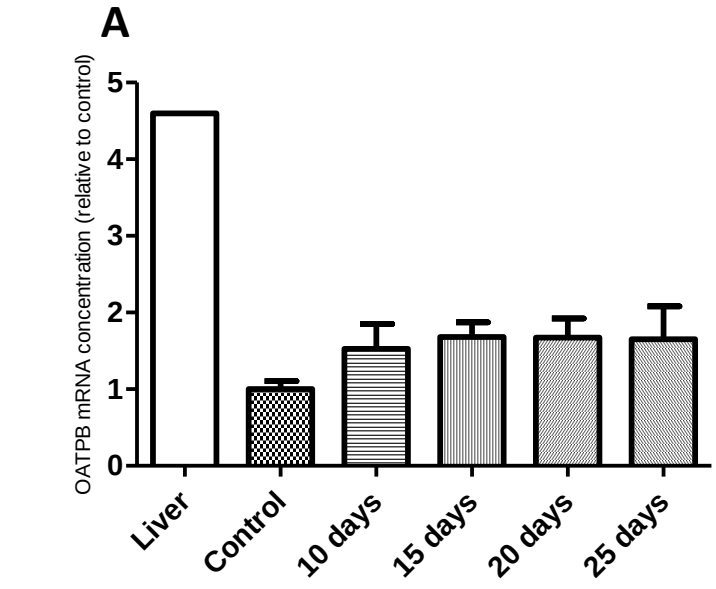
A
OATPB mRNA concentration (relative to control)
5
4
3
2
1
0
Liver
Control
10 days
15 days
20 days
25 days

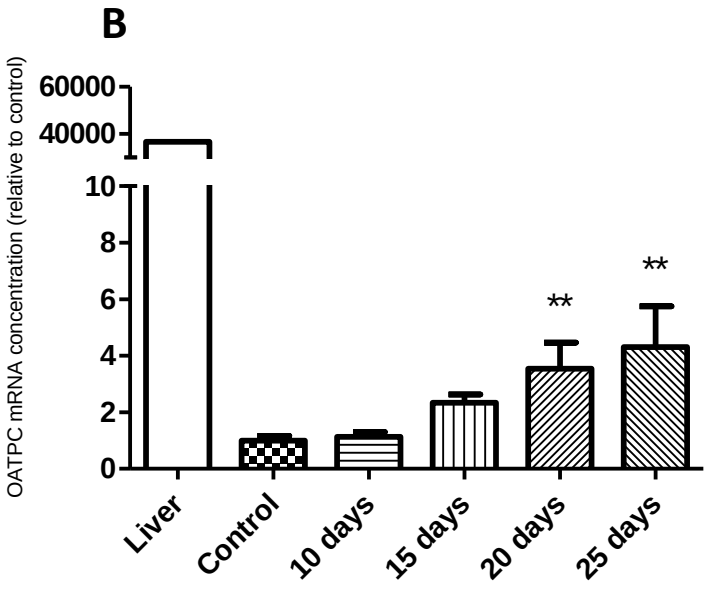
B
OATPC mRNA concentration (relative to control)
60000
40000
10
8
6
4
2
0
**
**
Liver
Control
10 days
15 days
20 days
25 days

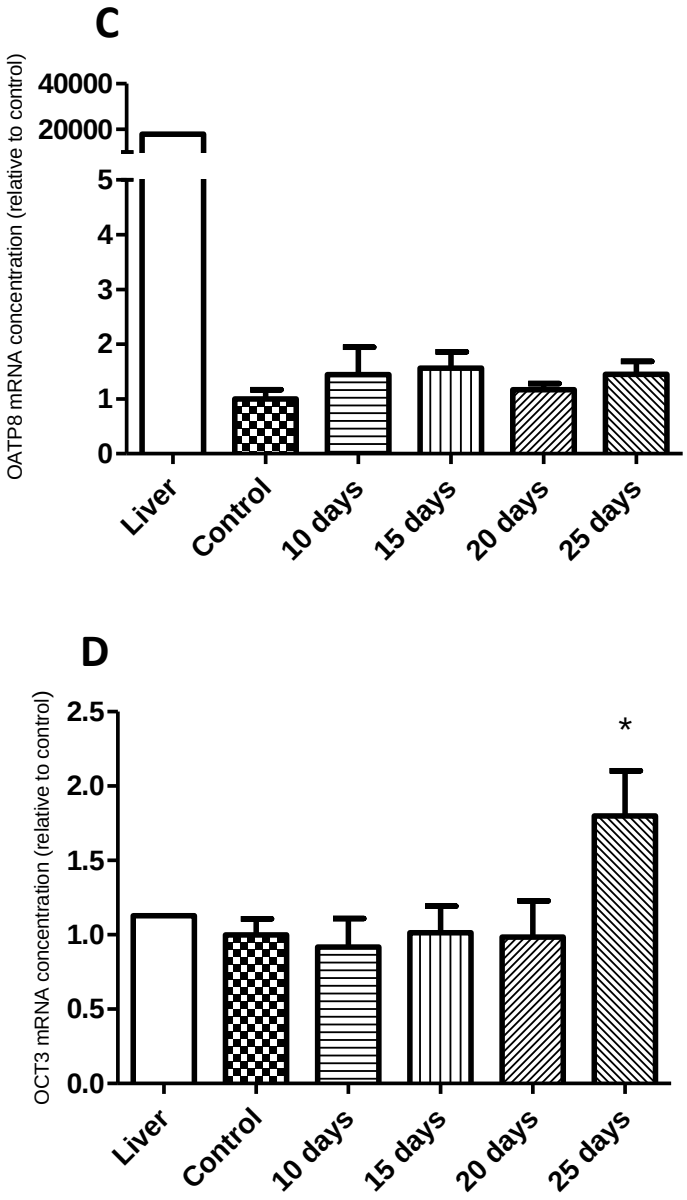

Figure 5.1 – DMSO treated HepG2 cells – OATPB, OATPC, OATP8 and OCT3 mRNA levels. Results for these four influx transporters are shown in graphs A to D. Cells were treated with 1% DMSO for up to 25 days and assessed for the appropriate gene by qPCR. Cells grown to confluence are used as a control and whole liver cDNA is included as an indication of hepatic mRNA levels. Results shown are from three experiments with a minimum of nine total replicates (N = 3, n = 9), confluent cells having twelve replicates (N = 3, n = 12). Data is displayed as mean ± SEM and analysed statistically against control using one-way ANOVA with Dunnett's post test (* = $p < 0.05$, ** = $p < 0.01$).

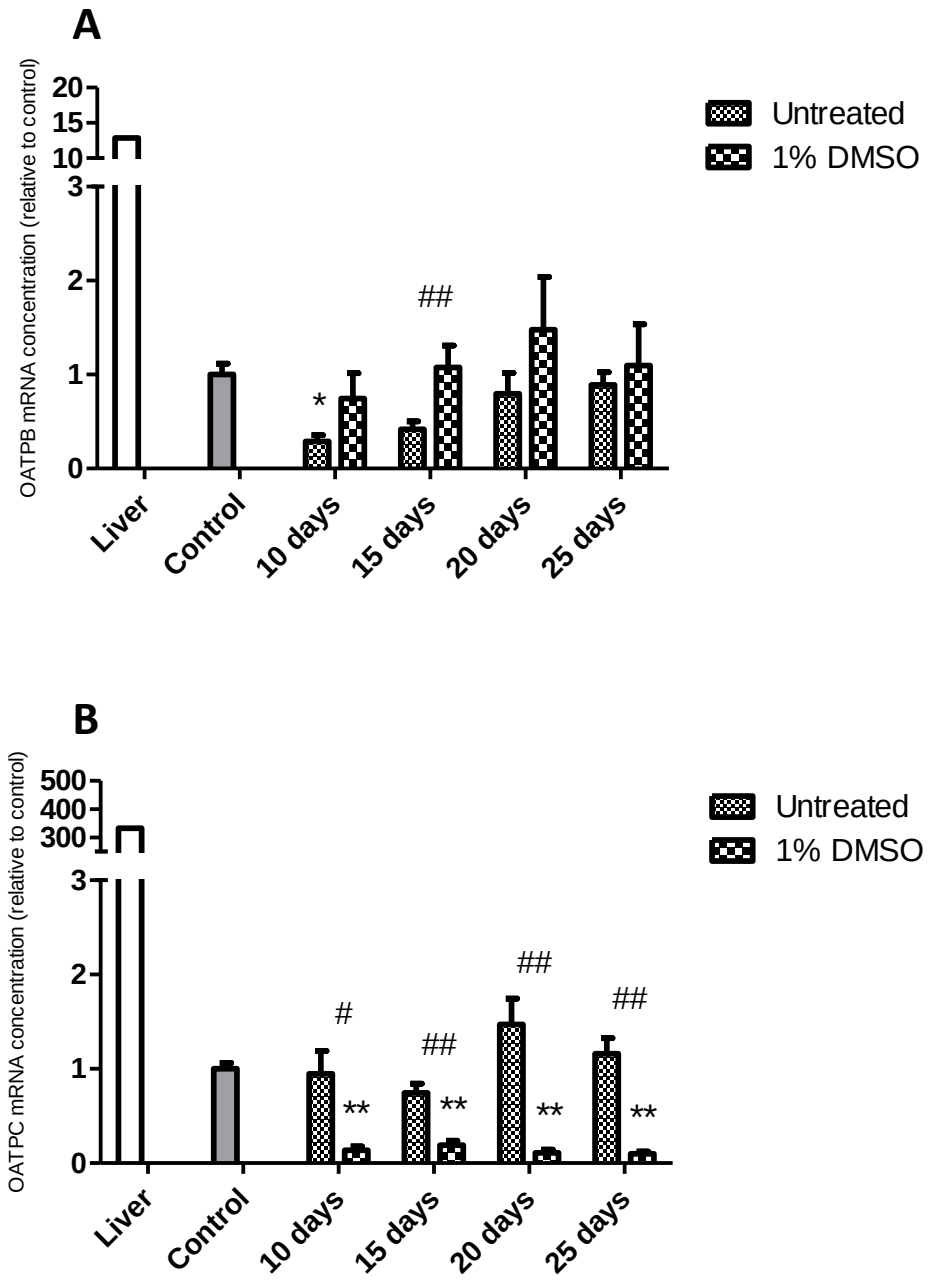
A
OATPB mRNA concentration (relative to control)
20
15
10
3
2
1
0
*
##
Untreated
1% DMSO
Liver
Control
10 days
15 days
20 days
25 days
B
OATPC mRNA concentration (relative to control)
500
400
300
3
2
1
0
#
##
##
##
**
**
**
**
Untreated
1% DMSO
Liver
Control
10 days
15 days
20 days
25 days

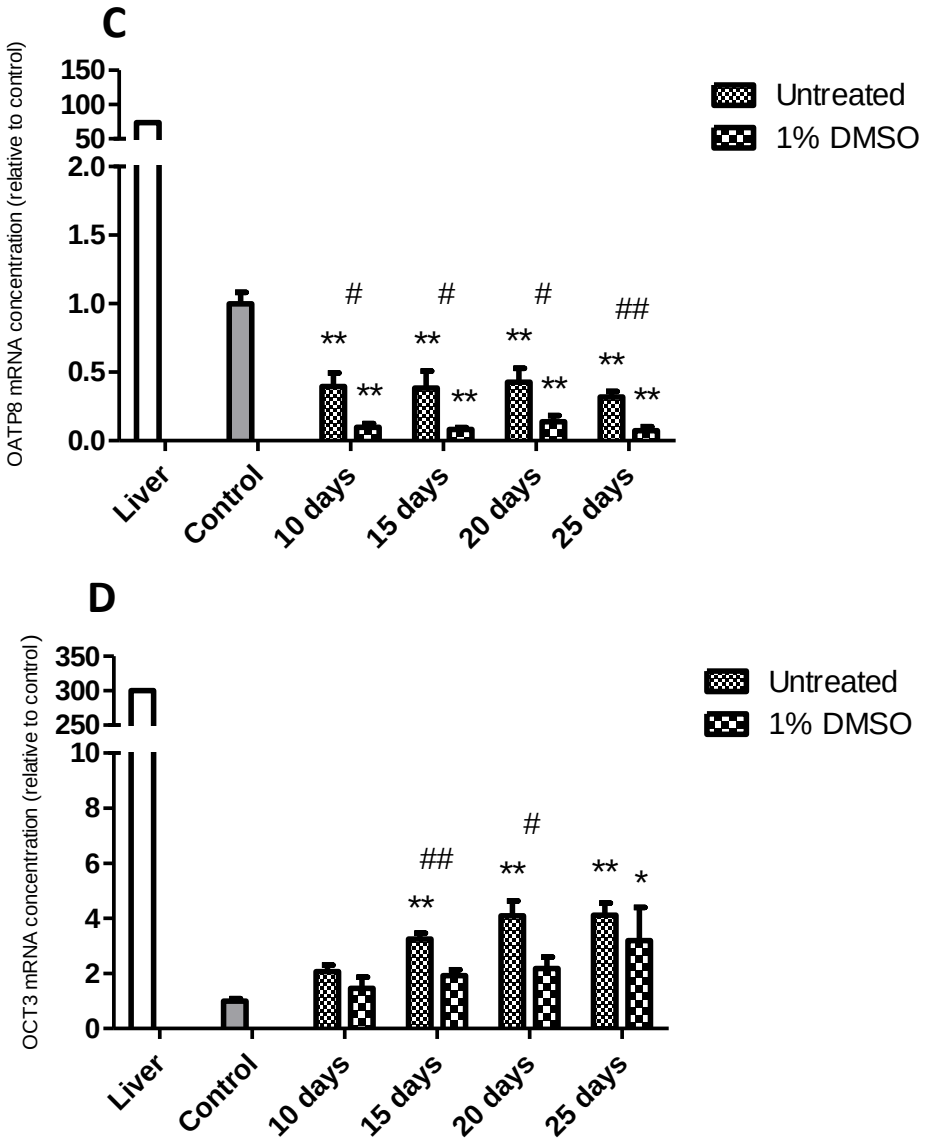

Figure 5.2 – Untreated and DMSO treated Huh7 cells – OATPB, OATPC, OATP8 and OCT3 mRNA levels. Results for these four influx transporters are shown in graphs A to D. Cells were treated with 1% DMSO for up to 25 days and assessed for the appropriate gene by qPCR. Cells grown to confluence are used as a control and whole liver cDNA is included as an indication of hepatic mRNA levels. Results shown are from three experiments with a minimum of nine total replicates (N = 3, n = 9). Control data was pooled and experiments normalised to this pool of data; total control replicates number a minimum of 30 from six experiments (N = 6, n = 30). Data is displayed as mean ± SEM and analysed statistically against control using one-way ANOVA with Dunnett's post test (* = $p < 0.05$, ** = $p < 0.01$). Analysis of untreated against treated cells was done using Student's t-test (# = $p < 0.05$, ## = $p < 0.01$).

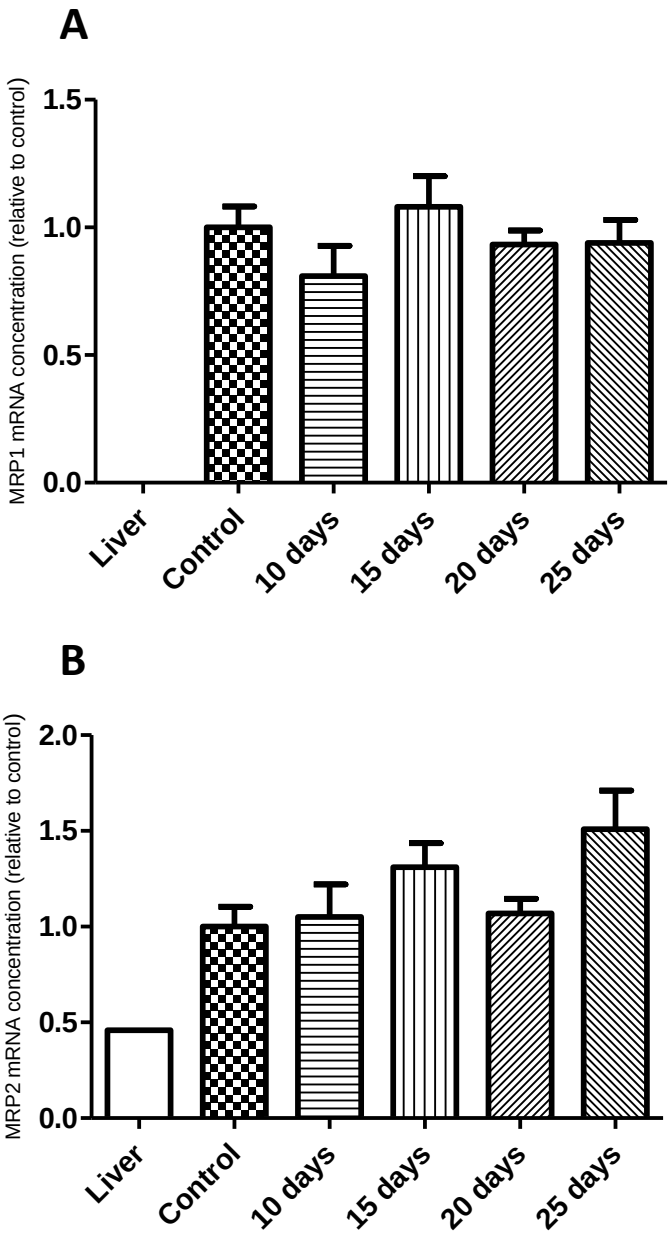
A
MRP1 mRNA concentration (relative to control)
1.5
1.0
0.5
0.0
Liver
Control
10 days
15 days
20 days
25 days
B
MRP2 mRNA concentration (relative to control)
2.0
1.5
1.0
0.5
0.0
Liver
Control
10 days
15 days
20 days
25 days

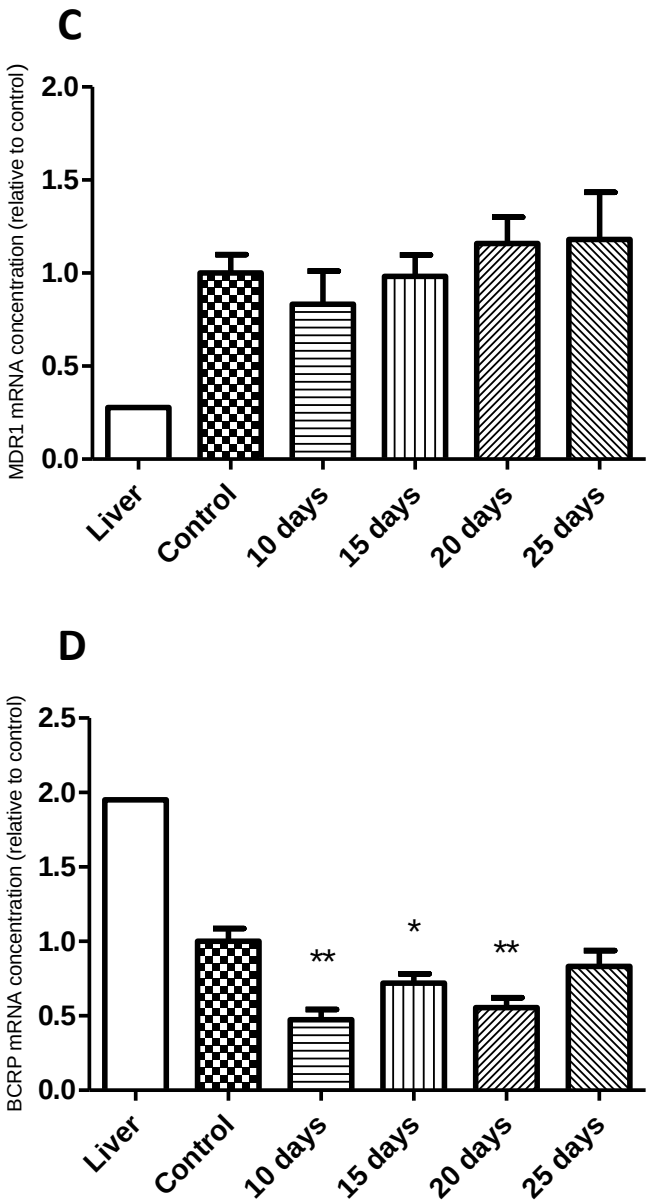

Figure 5.3 – DMSO treated HepG2 cells – MRP1, MRP2, MDR1 and BCRP mRNA levels. Results for these four efflux transporters are shown in graphs A to D. Cells were treated with 1% DMSO for up to 25 days and assessed for the appropriate gene by qPCR. Cells grown to confluence are used as a control and whole liver cDNA is included as an indication of hepatic mRNA levels. Results shown are from three experiments with a minimum of nine total replicates (N = 3, n = 9), confluent cells having twelve replicates (N = 3, n = 12). Data is displayed as mean ± SEM and analysed statistically against control using one-way ANOVA with Dunnett's post test (* = $p < 0.05$, ** = $p < 0.01$).

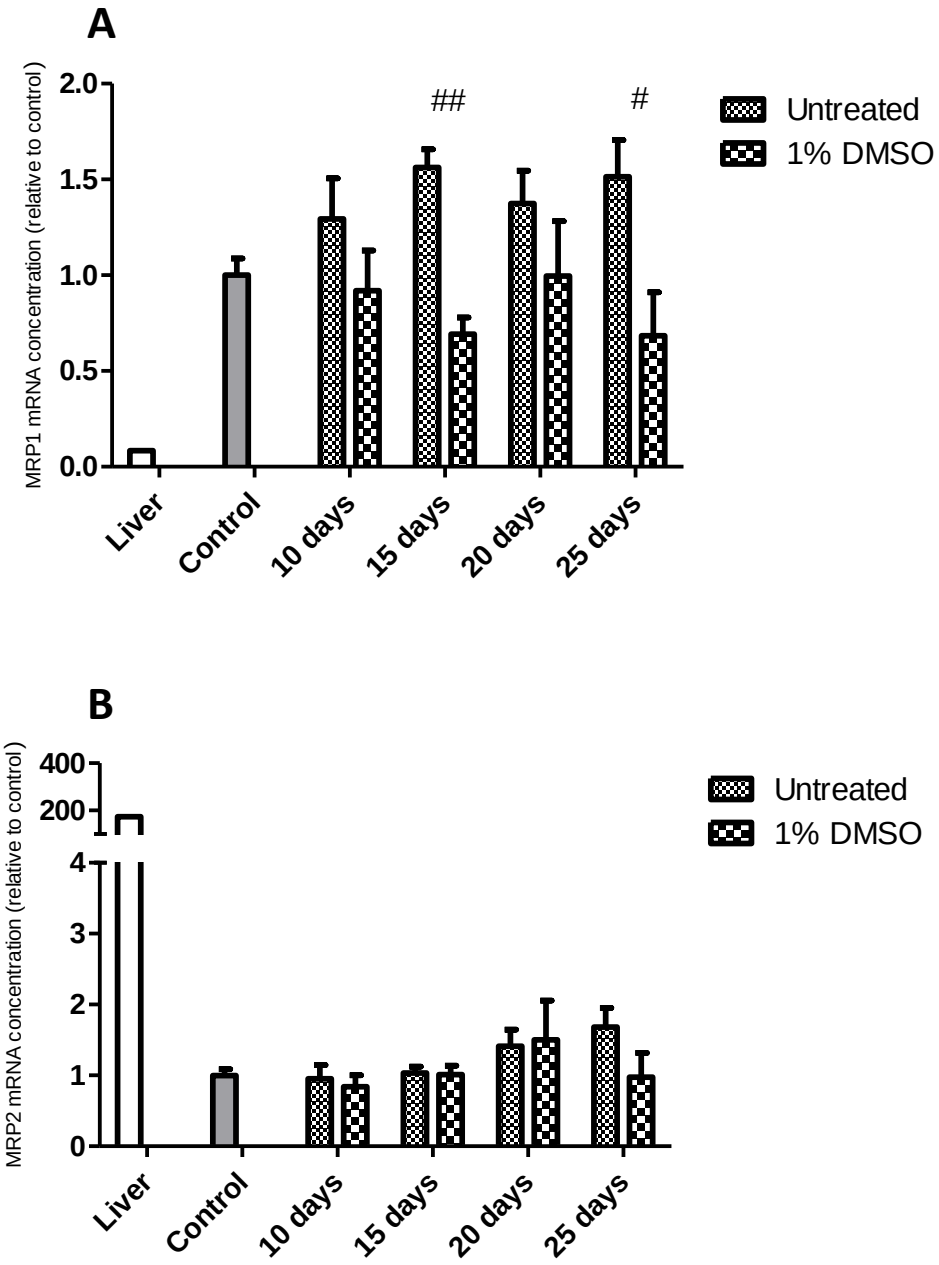
A
MRP1 mRNA concentration (relative to control)
2.0
1.5
1.0
0.5
0.0
##
#
Untreated
1% DMSO
Liver
Control
10 days
15 days
20 days
25 days
B
MRP2 mRNA concentration (relative to control)
400
200
4
3
2
1
0
Untreated
1% DMSO
Liver
Control
10 days
15 days
20 days
25 days

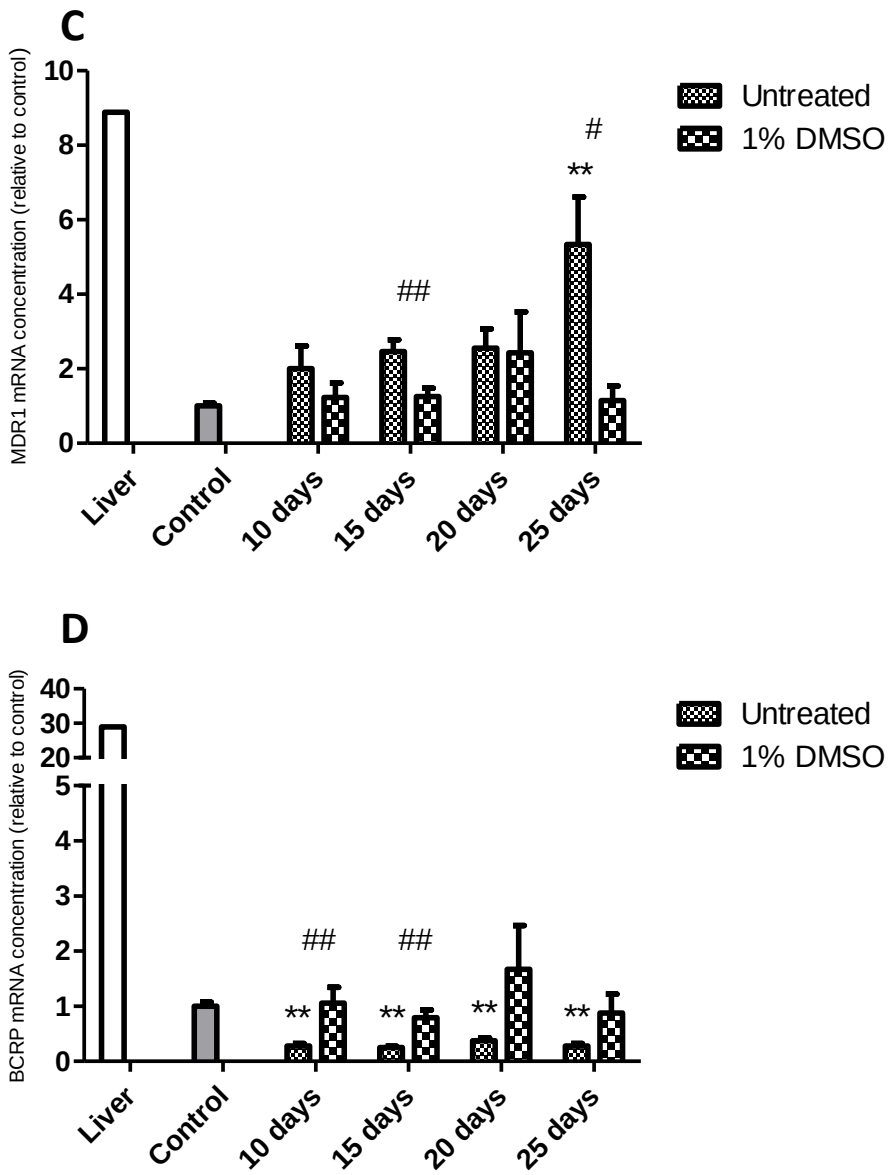

Figure 5.4 – Untreated and DMSO treated Huh7 cells – MRP1, MRP2 MDR1 and BCRP mRNA levels. Results for these four efflux transporters are shown in graphs A to D. Cells were treated with 1% DMSO for up to 25 days and assessed for the appropriate gene by qPCR. Cells grown to confluence are used as a control and whole liver cDNA is included as an indication of hepatic mRNA levels. Results shown are from three experiments with a minimum of nine total replicates (N = 3, n = 9). Control data was pooled and experiments normalised to this pool of data; total control replicates number a minimum of 30 from six experiments (N = 6, n = 30). Data is displayed as mean ± SEM and analysed statistically against control using one-way ANOVA with Dunnett's post test (* = $p < 0.05$, ** = $p < 0.01$). Analysis of untreated against treated cells was done using Student's t-test (# = $p < 0.05$, ## = $p < 0.01$).

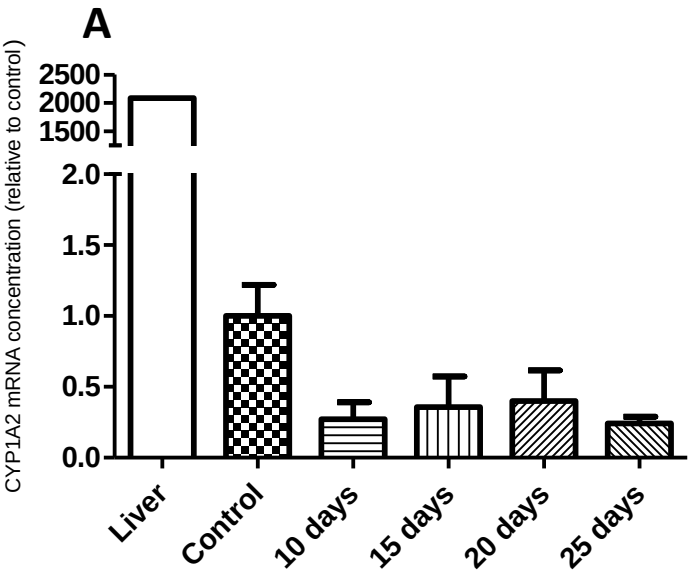
A
CYP1A2 mRNA concentration (relative to control)
2500
2000
1500
2.0
1.5
1.0
0.5
0.0
Liver
Control
10 days
15 days
20 days
25 days

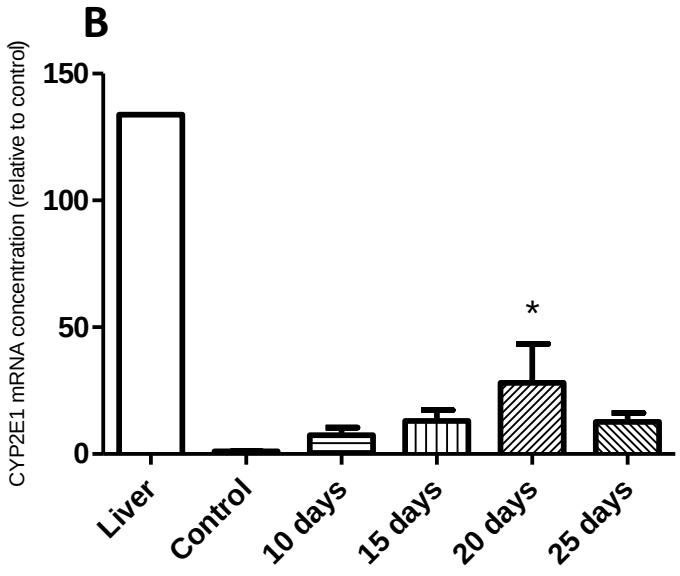
B
CYP2E1 mRNA concentration (relative to control)
150
100
50
0
*
Liver
Control
10 days
15 days
20 days
25 days

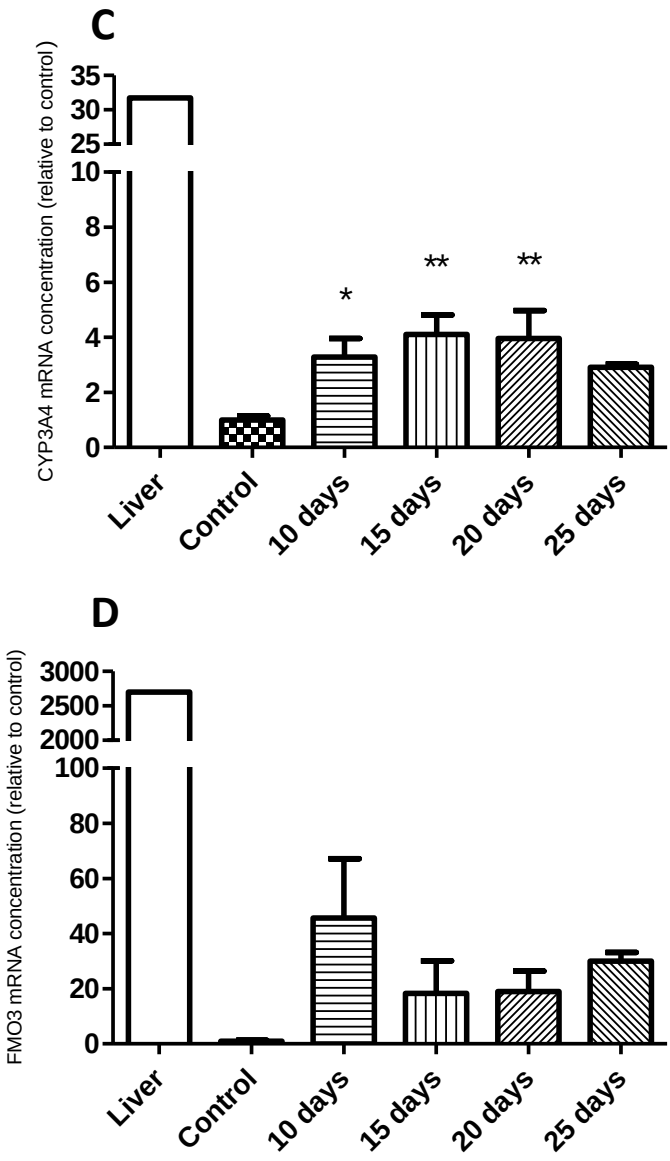

Figure 5.5 – DMSO treated HepG2 cells – CYP1A2, 2E1, 3A4 and FMO3 mRNA levels. Results for these four metabolising enzymes are shown in graphs A to D. Cells were treated with 1% DMSO for up to 25 days and assessed for the appropriate gene by qPCR. Cells grown to confluence are used as a control and whole liver cDNA is included as an indication of hepatic mRNA levels. Results shown are from three experiments with a minimum of nine total replicates (N = 3, n = 9), confluent cells having twelve replicates (N = 3, n = 12). Data is displayed as mean ± SEM and analysed statistically against control using one-way ANOVA with Dunnett's post test (* = $p < 0.05$, ** = $p < 0.01$).

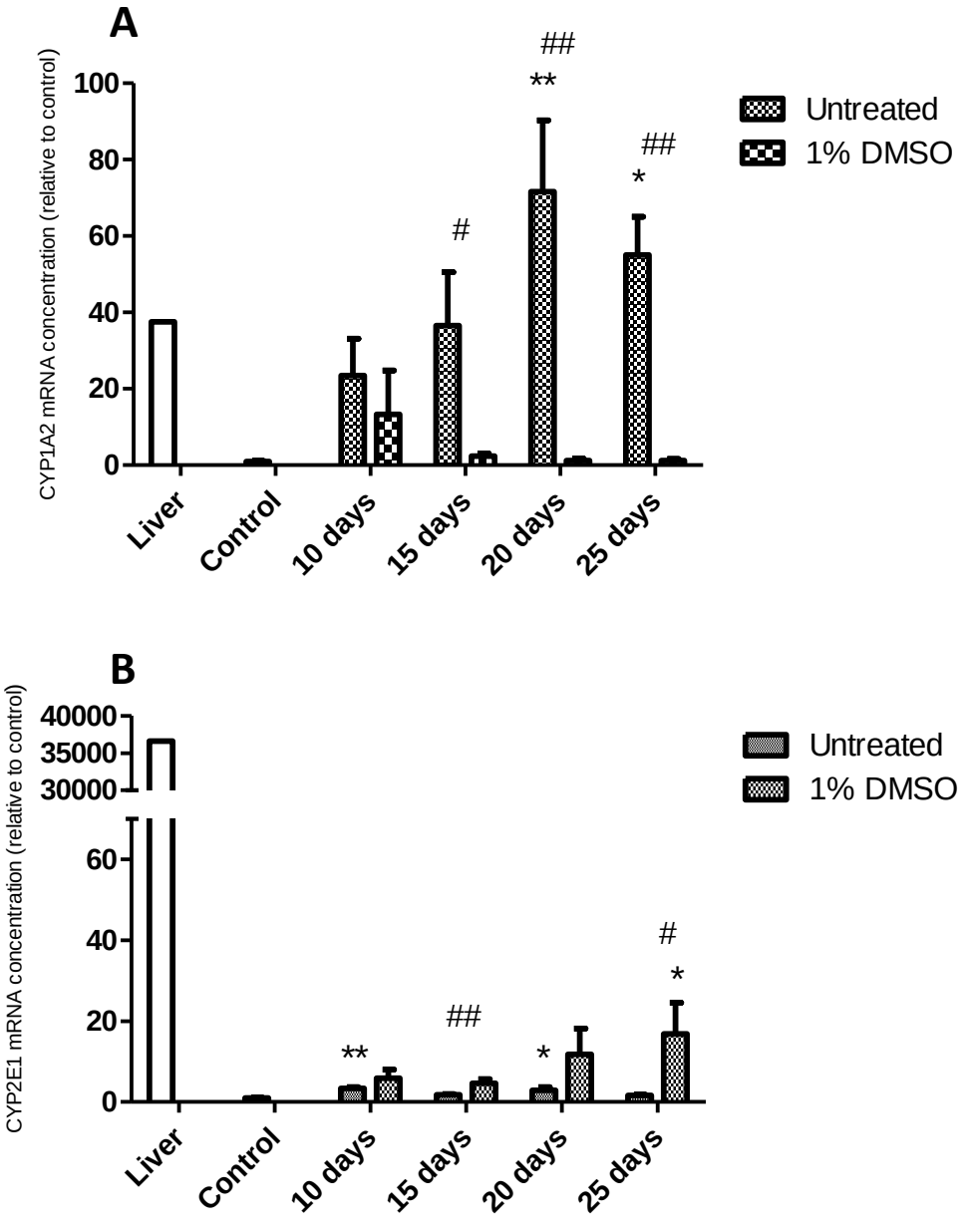
A
CYP1A2 mRNA concentration (relative to control)
100
80
60
40
20
0
Liver
Control
10 days
15 days
20 days
25 days
**
##
#
##
*
Untreated
1% DMSO
B
CYP2E1 mRNA concentration (relative to control)
40000
35000
30000
60
40
20
0
Liver
Control
10 days
15 days
20 days
25 days
**
##
*
#
*
Untreated
1% DMSO

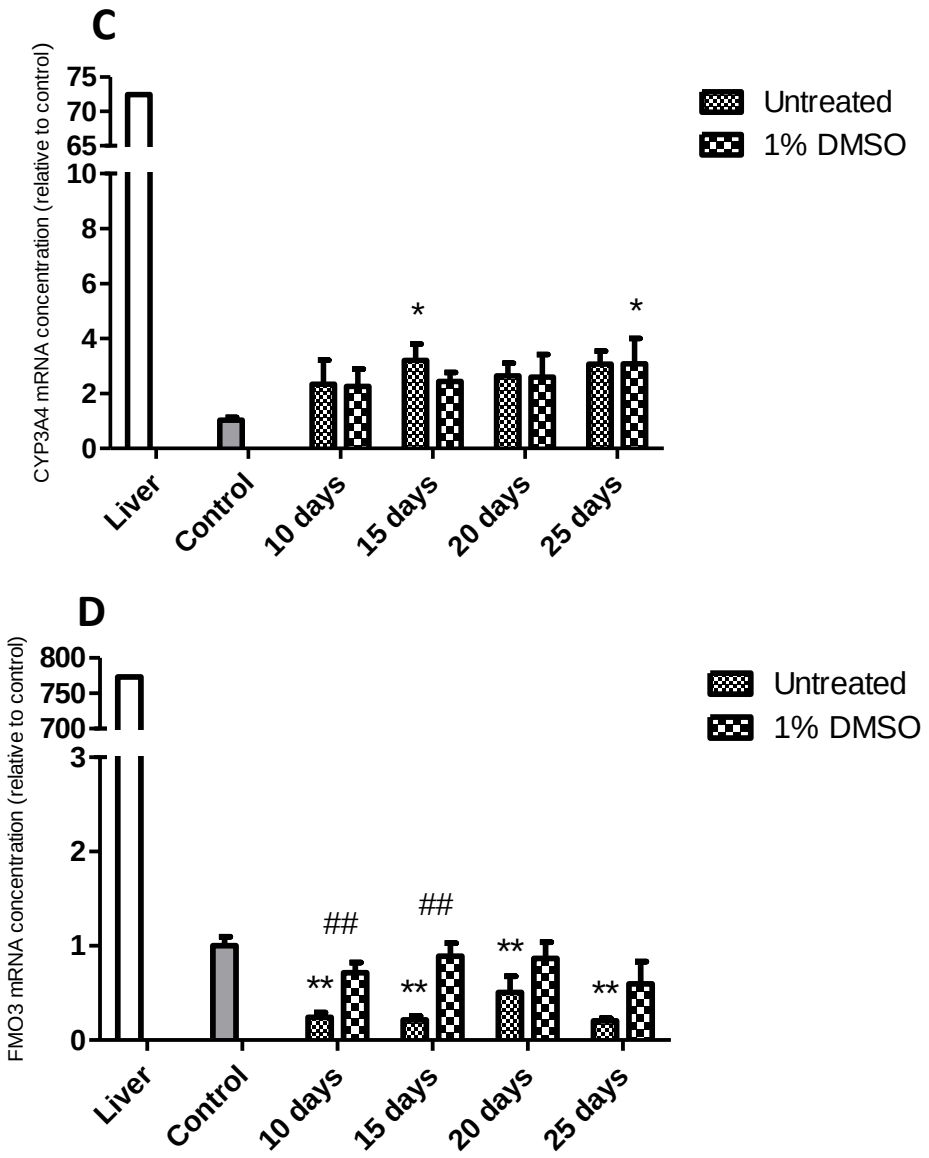

Figure 5.6 – Untreated and DMSO treated Huh7 cells – CYP1A2, 2E1, 3A4 and FMO3 mRNA levels. Results for these four metabolising enzymes are shown in graphs A to D. Cells were treated with 1% DMSO for up to 25 days and assessed for the appropriate gene by qPCR. Cells grown to confluence are used as a control and whole liver cDNA is included as an indication of hepatic mRNA levels. Results shown are from three experiments with a minimum of nine total replicates (N = 3, n = 9). Control data was pooled and experiments normalised to this pool of data; total control replicates number a minimum of 30 from six experiments (N = 6, n = 30). Data is displayed as mean ± SEM and analysed statistically against control using one-way ANOVA with Dunnett's post test (* = $p < 0.05$, ** = $p < 0.01$). Analysis of untreated against treated cells was done using Student's t-test (# = $p < 0.05$, ## = $p < 0.01$).

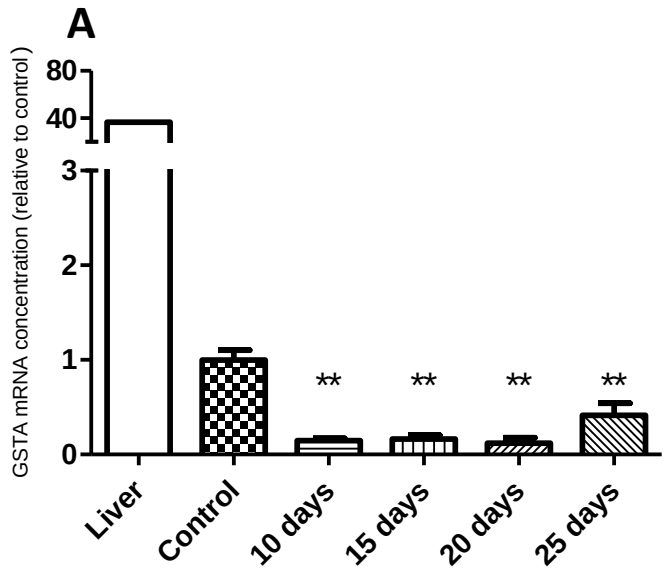
A
GSTA mRNA concentration (relative to control)
80
40
3
2
1
0
**
**
**
**
Liver
Control
10 days
15 days
20 days
25 days

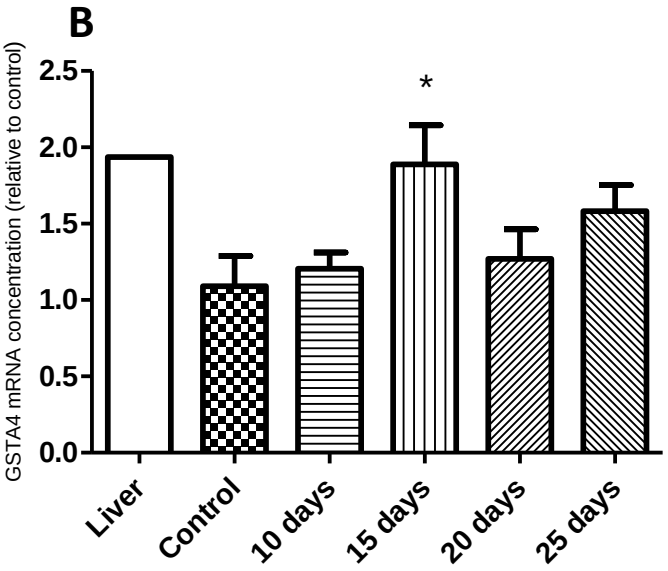
B
GSTA4 mRNA concentration (relative to control)
2.5
2.0
1.5
1.0
0.5
0.0
*
Liver
Control
10 days
15 days
20 days
25 days

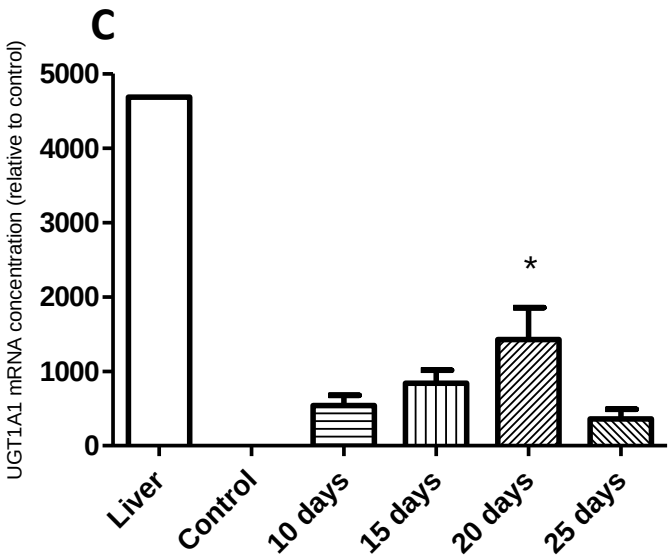

Figure 5.7 – DMSO treated HepG2 cells – GSTA, GSTA4 and UGT1A1 mRNA levels. Results for these three conjugating enzymes are shown in graphs A to C. Cells were treated with 1% DMSO for up to 25 days and assessed for the appropriate gene by qPCR. Cells grown to confluence are used as a control and whole liver cDNA is included as an indication of hepatic mRNA levels. Results shown are from three experiments with a minimum of nine total replicates (N = 3, n = 9), confluent cells having twelve replicates (N = 3, n = 12). Data is displayed as mean ± SEM and analysed statistically against control using one-way ANOVA with Dunnett's post test (* = $p < 0.05$, ** = $p < 0.01$).

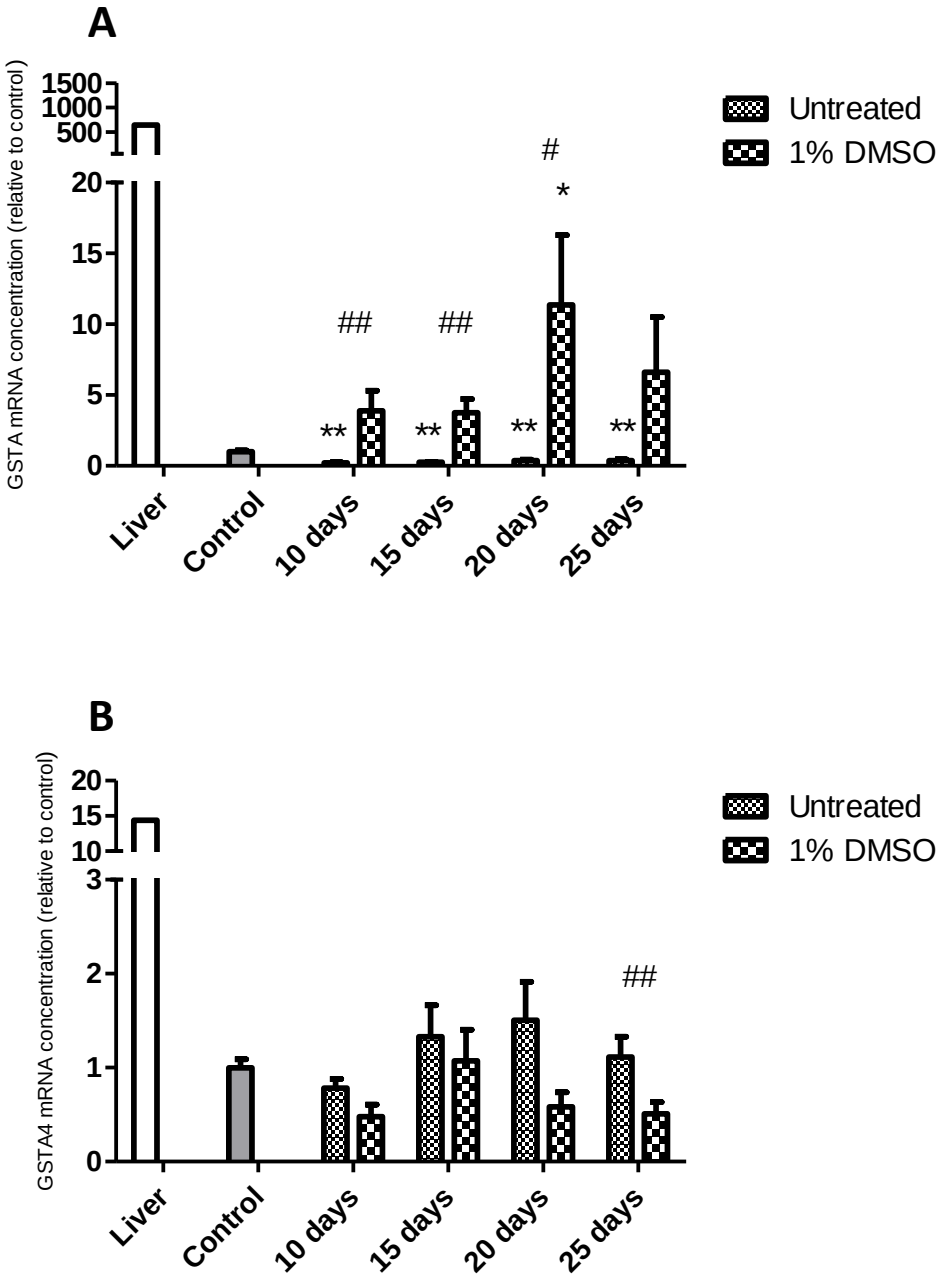
A
GSTA mRNA concentration (relative to control)
1500
1000
500
20
15
10
5
0
##
##
#
*
**
**
**
**
Liver
Control
10 days
15 days
20 days
25 days
Untreated
1% DMSO
B
GSTA4 mRNA concentration (relative to control)
20
15
10
3
2
1
0
##
Liver
Control
10 days
15 days
20 days
25 days
Untreated
1% DMSO

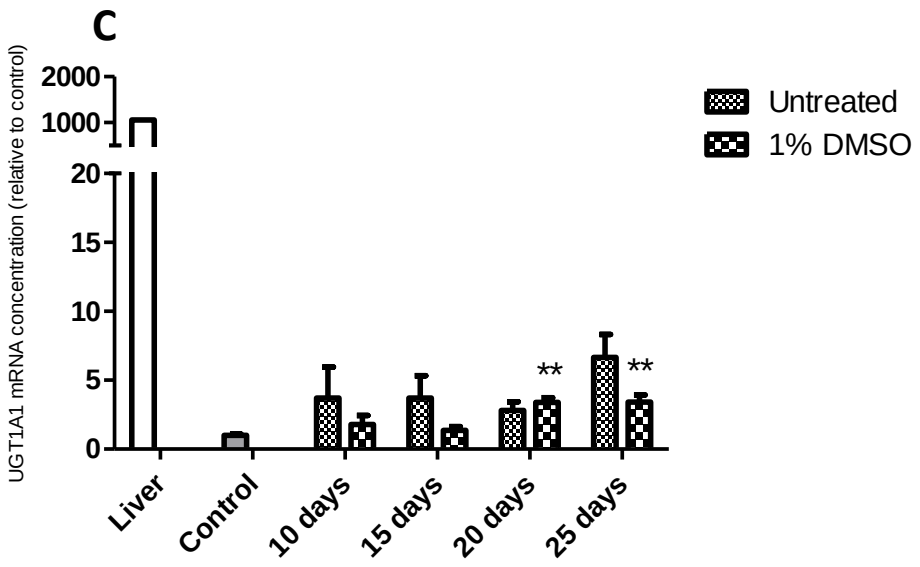

Figure 5.8 – Untreated and DMSO treated Huh7 cells – GSTA, GSTA4 and UGT1A1 mRNA levels. Results for these three conjugating enzymes are shown in graphs A to C. Cells were treated with 1% DMSO for up to 25 days and assessed for the appropriate gene by qPCR. Cells grown to confluence are used as a control and whole liver cDNA is included as an indication of hepatic mRNA levels. Results shown are from three experiments with a minimum of nine total replicates (N = 3, n = 9). Control data was pooled and experiments normalised to this pool of data; total control replicates number a minimum of 30 from six experiments (N = 6, n = 30). Data is displayed as mean ± SEM and analysed statistically against control using one-way ANOVA with Dunnett's post test (* = $p < 0.05$, ** = $p < 0.01$). Analysis of untreated against treated cells was done using Student's t-test (# = $p < 0.05$, ## = $p < 0.01$).

	Liver levels relative to HepG2 cells at confluence **	Liver levels relative to control *	HepG2 + 1% DMSO levels at 15 days relative to control *	HepG2 + 1% DMSO – closest expression to liver (days) relative to control *
OATPB	4.81	4.60	1.68	1.68 (15 days)
OATPC	$5.2x10^{5}$	$3.7x10^{5}$	2.34	4.31 (25 days)
OATP8	$1.9x10^{5}$	$1.8x10^{5}$	1.57	1.57 (15 days)
OCT3	1.44	1.13	1.01	1.01 (15 days)
MRP1	$4.74x10^{-4}$	$2.7x10^{-4}$	1.08	1.08 (15 days)
MRP2	0.61	0.46	1.31	1.05 (10 days)
MDR1	0.37	0.28	0.98	0.83 (10 days)
BCRP	2.86	1.95	0.72	0.83 (25 days)
CYP1A2	$1.4x10^{6}$	$2.1x10^{3}$	0.36	0.40 (20 days)
CYP2E1	$2.6x10^{6}$	133	13.05	28.01 (20 days)
CYP3A4	$1.3x10^{5}$	31.71	4.11	4.11 (15 days)
FMO3	$4.7x10^{9}$	$2.7x10^{3}$	18.25	45.65 (10 days)
GSTA	6.29	36.74	0.17	0.41 (25 days)
GSTA4	1.64	1.94	1.89	1.89 (15 days)
UGT1A1	2900	4700	841	1428 (20 days)

* Experimental control cells are confluent, control values are set at 1. Data taken from figures 5.1, 5.3, 5.5 and 5.7.

** Data recalculated from table 3.1.

Table 5.5 – Transporter and enzyme mRNA levels in HepG2 cells relative to control. This data shows relative change in the level of a gene in comparison to control. Control values are always 1. Data for liver in comparison to confluent levels in HepG2 cells has been recalculated from table 3.1.

	Liver levels relative to Huh7 cells at confluence **	Liver levels relative to control *	Untreated Huh7 levels at 15 days relative to control *	Untreated Huh7 – closest expression to liver (days) relative to control *	Huh7 + 1% DMSO levels at 15 days relative to control *	Huh7 + 1% DMSO – closest expression to liver (days) relative to control *
OATPB	11.98	12.86	0.42	0.89 (25 days)	1.08	1.48 (20 days)
OATPC	363	332	0.75	1.47 (20 days)	0.19	0.19 (15 days)
OATP8	82.64	73.64	0.38	0.43 (20 days)	0.081	0.14 (20 days)
OCT3	124	300	3.24	4.12 (25 days)	1.92	3.19 (25 days)
MRP1	0.011	0.085	1.56	1.29 (10 days)	0.69	0.69 (15 days)
MRP2	12.59	173	1.03	1.68 (25 days)	1.01	1.50 (20 days)
MDR1	5.68	8.89	2.46	5.34 (25 days)	1.25	2.43 (20 days)
BCRP	21.46	28.94	0.25	0.37 (20 days)	0.79	1.06 (10 days)
CYP1A2	$4.5x10^4$	37.56	36.57	36.57 (15 days)	2.34	13.27 (10 days)
CYP2E1	$1.9x10^6$	$3.7x10^4$	1.76	3.36 (10 days)	4.65	16.83 (25 days)
CYP3A4	$3.2x10^5$	72.45	3.20	3.20 (15 days)	2.44	3.08 (25 days)
FMO3	$4.0x10^5$	773	0.89	0.51 (20 days)	0.89	0.89 (15 days)
GSTA	357	641	0.26	0.38 (20 days)	3.76	11.35 (20 days)
GSTA4	13.83	14.39	1.33	1.50 (20 days)	1.07	1.07 (15 days)
UGT1A1	1095	1055	3.70	6.65 (25 days)	1.35	3.41 (25 days)

* Experimental control cells are confluent, control values are set at 1. Data taken from figures 5.2, 5.4, 5.6 and 5.8.

** Data recalculated from table 3.1.

Table 5.6 – Transporter and enzyme mRNA levels in Huh7 cells relative to control. This data shows relative change in the level of a gene in comparison to control. Control values are always 1. Data for liver in comparison to confluent levels in Huh7 cells has been recalculated from table 3.1.

Chapter 6 – Induction via CAR, PXR and AhR nuclear receptor pathways

Chapter aim: To investigate the effects of the model inducing compounds rifampicin, phenobarbital and beta-naphthoflavone in confluent and DMSO-treated HepG2 and Huh7 cells.

6.1 – Introduction

The induction of enzymes and transporters is key in a fully functioning cell, enabling it to respond to changing levels of endogenous and xenobiotic compounds by altering expression of metabolising enzymes and transporters. Appropriate responses to inducing agents are also indicative of a high degree of phenotypic differentiation and are achieved by changes in both transcription and post-transcriptional mechanisms. Correctly functioning induction is especially important in hepatocytes as they are responsible for a large proportion of drug metabolism. Although short term responses to stimuli can be managed via post-transcriptional mechanisms, more complex, longer term responses require changes in the transcription of genes. This involves a ligand interacting with the cell and creating a response via nuclear receptors which bind to the genomic DNA and cause either repression or stimulation of transcription.

The effects of typical activating compounds of three nuclear receptor pathways were examined in HepG2 and Huh7 cells to enable assessment of induction functionality in both confluent and DMSO- treated cells; the receptors selected were the aryl hydrocarbon receptor (AhR), the constitutive androstane receptor (CAR) and the pregnane X receptor (PXR). These three receptor pathways are well established as being involved in the regulation of many important proteins in the hepatocyte. Examples of protein targets of these receptors can be seen in table 6.1. However, cross-talk and interaction between nuclear receptor pathways is inevitable due to built-in redundancy mechanisms within the cell. Several studies have investigated this issue with regard to the three receptors being addressed here and will be outlined below.

The AhR is usually found in the cytoplasm of the cell and translocates into the nucleus in response to treatment with a suitable ligand. Here it can form a complex with the AhR nuclear translocator (Arnt) and bind to DNA, initiating increases in levels of affected genes (Xu *et al.*, 2005). One of a number of genes known to respond to AhR stimulation is breast cancer restistance protein (BCRP) (Tan *et al.*, 2010; Tompkins *et al.*, 2010; Dauchy *et al.*, 2008) and the

compound beta-naphthoflavone (BNF) is known to act predominantly via the AhR pathway (Patel *et al.*, 2007; Urquhart *et al.*, 2007; Xu *et al.*, 2005). However, BNF activation of the AhR could result in additional pathways besides AhR being activated by an extended cascade of events. This is demonstrated by Patel *et al.* (Patel *et al.*, 2007) where it was found that an increase in AhR can result in an increase in CAR levels. This could potentially mean that application of BNF results in induction via AhR and CAR even if BNF solely interacted with AhR and would be unavoidable with any AhR agonist. As BNF acts predominantly via AhR and AhR activating compounds have been routinely used in the literature to increase BCRP levels, cells here were treated with three concentrations of BNF and assessed for BCRP mRNA levels.

PXR and CAR are both orphan nuclear receptors which have two distinctive domains; a DNA binding domain and a ligand binding domain (Wang and LeCluyse, 2003). PXR has been studied in several organisms and are predominantly expressed in the liver and intestine, whilst CAR is found mainly in hepatocytes and to a lesser extent in the intestine (Mottino and Catania, 2008; Xu *et al.*, 2005). Cross-talk between the PXR and CAR receptor pathways is recognised and many genes have been observed to respond to inducers of both pathways. Many ligands are also recognised to activate both pathways, and although some are seen as typical inducers of one or the other cross-talk may still be apparent.

PXR responds to a wide variety of ligands including both endogenous and xenobiotic compounds. One of the most widely utilised PXR activators is rifampicin which is used here to attempt to induce MDR1 (multidrug resistance protein 1) mRNA levels, a known target of the PXR pathway (Mottino and Catania, 2008; Urquhart *et al.*, 2007; Xu *et al.*, 2005; Mills *et al.*, 2004). Rifampicin itself has been reported as both acting predominantly via PXR and as having no activating effect on the CAR receptor (Gibson *et al.*, 2006; Xu *et al.*, 2005; Moore and Kliewer, 2000). Although MDR1 is recognised as a PXR pathway target and has been used as such alongside rifampicin induction in a number of publications, it is also recognised that it can be activated by other mechanisms such as the CAR pathway if activated (Kohle and Bock, 2009; Urquhart *et al.*, 2007). Data from Haslam *et al.* (Haslam *et al.*, 2008) reports that rifampicin successfully increased levels of MDR1 mRNA, total protein and apically expressed protein alongside increases in functional activity in the T84 epithelial cell line. A similar reduction of digoxin accumulation with a rifampicin-induced increase in MDR1 protein expression was observed *in vivo* in humans by Greiner *et al.* (Greiner *et al.*, 1999). Despite the potential for increased expression as a result of activation of more than one pathway, potentially useful information can still be extracted from assessment of confluent and DMSO-treated cells treated with rifampicin and analysed for MDR1 mRNA levels in comparison to previously published data indicating levels of induction in liver and primary hepatocytes.

A well-known activator of CAR is phenobarbital (PB) which has been used on multiple occasions to analyse gene responses to CAR induction (Mottino and Catania, 2008; Xu *et al.*, 2005; Sidhu *et al.*, 2004). Sidhu *et al.* (Sidhu *et al.*, 2004) also suggested that the responsiveness of an hepatocyte to phenobarbital may be a reliable indicator of the maturation status of the cell. Phenobarbital has been stated to cause induction predominantly by CAR activation (Xu *et al.*, 2005) and is known to have the ability to induce several transporters in the MRP family (Urquhart *et al.*, 2007). MRP2 (multidrug resistance associated protein 2) has been demonstrated in several previous publications as being responsive to phenobarbital induction (Antherieu *et al.*, 2010; Mottino and Catania, 2008; Urquhart *et al.*, 2007; Courtois *et al.*, 2002). As with rifampicin/PXR induction of MDR1, the induction of MRP2 can be achieved via more than one pathway; for example, Kast *et al.* (Kast *et al.*, 2002) reported MRP2 induction by CAR, PXR and FXR (farnesoid X receptor). It has also been observed that CAR and PXR bind to similar response elements once activation has occurred, indicating likely cross-talk between these two pathways (Burk *et al.*, 2005; Kast *et al.*, 2002). Although phenobarbital could potentially result in activation of more than just the CAR pathway and cross-talk between the activated CAR and other response pathways is likely, the number of previous publications utilising this compound to analyse MRP2 induction allows a useful comparison to be made between results in the literature obtained for primary hepatocytes and other hepatic cell lines and the induction profile of the confluent and DMSO-treated HepG2 and Huh7 cells here. Cells were treated with several concentrations of phenobarbital and were subsequently assessed for mRNA levels of MRP2.

MDR1, MRP2 and BCRP were chosen to be assessed for induction by the three compounds in question partly because there is evidence in the literature that thesewill show induction, and also because all three are highly expressed in both cell lines both at confluence and after DMSO treatment. MDR1 mRNA levels are almost 3-fold higher than liver in confluent HepG2 cells and approximately 5-fold lower than liver in confluent Huh7 cells. This does not change after 15 days of DMSO treatment in either HepG2 or Huh7 cells. MRP2 mRNA levels were approximately 2-fold of those in liver in confluent HepG2 cells but were between 170-fold and 12-fold reduced from liver in confluent Huh7 cells. DMSO treatment for 15 days did not significantly change MRP2 levels in HepG2 or Huh7 cells. Finally, BCRP mRNA levels in confluent HepG2 cells were between 2- and 3-fold lower than liver, while those in confluent Huh7 cells were between 20- and 30-fold lower than liver. A significant reduction in BCRP mRNA level was observed in 15-day DMSO-treated HepG2 cells, while no significant difference was observed in DMSO-treated Huh7 cells.

In the following experiments, both 15 day DMSO-treated cells and untreated confluent cells from each cell line were subjected to incubation with rifampicin, phenobarbital and BNF. Analysis of mRNA levels by qPCR was used to assess induction of the target genes MDR1, MRP2 and BCRP respectively in confluent and DMSO-treated cells, providing more information on the maturation status of the cells.

6.2 – Methods

HepG2 and Huh7 cells were seeded and grown in 6-well plastic plates as described in chapter 2.2. Cells were either grown to confluence or treated with 1% DMSO for 15 days (as described in chapter 2.2 and figures 2.1 and 2.2) and incubated with rifampicin, phenobarbital or BNF for 24 hours as described in chapter 2.3. Concentrations used were ones previously reported as having an effect in published papers, together with a higher concentration in the event that no effect was observed at lower concentrations. Rifampicin at 10, 50 and 100 µM and BNF at 1, 10 and 100 µM were applied in standard growth medium to confluent cells or in standard growth medium supplemented with 1% DMSO to DMSO treated cells, with both compounds dissolved in a vehicle of DMSO. DMSO concentration was maintained at a constant level between all treated and control cells. Phenobarbital at 0.5, 1.5 and 3.0 mM was applied to cells in standard growth media and in media containing 1% DMSO with all containing an equivalent volume of vehicle, in this case water. Incubations were continued for 24 hours, after which total RNA was extracted, reverse transcribed and mRNA levels of GOI assessed by qPCR (as described previously in chapters 2 and 3). Data from a purchased human liver cDNA sample are shown relative to HepG2 and Huh7 confluent control cells.

6.3 – Results

6.3.1 – Rifampicin treatments

Figures 6.1 and 6.2 show results for rifampicin treated HepG2 and Huh7 cells respectively. MDR1 mRNA levels in confluent and DMSO treated cells are shown in each figure (parts A and B respectively). MDR1 mRNA levels in human liver cDNA were less than half of those observed in both confluent control and in 1% DMSO control HepG2 cells (fig 6.1). In confluent HepG2 cells no significant change was seen with 10 or 50 µM rifampicin but at 100 µM a significant increase from control level was observed. In cells pre-treated with 1% DMSO for 15 days a very different response to rifampicin was observed, as MDR1 mRNA levels decreased to around half that seen in control cells at all concentrations of the compound although no significant changes were observed.

Data from Huh7 cells treated with rifampicin and analysed for MDR1 mRNA levels at confluence are shown in figure 6.2 part A, with results from 1% DMSO-treated cells in part B. MDR1 mRNA level was higher in liver than in control cells both at confluence and following DMSO treatment. The difference between control and liver levels was slightly less in DMSO-treated cells than in confluent cells demonstrating the slight induction in MDR1 mRNA level by 1% DMSO described in Ch5, figure 5.4 part C. No significant changes from control with rifampicin at 10 or 50 µM were seen in confluent cells, while a significant increase in MDR1 mRNA occurred following 100 µM rifampicin treatment. As in HepG2 cells all concentrations of rifampicin appeared to decrease the MDR1 mRNA level in DMSO treated Huh7 cells, however none of the observed changes were found to be statistically significant.

Summary

- MDR1 increased significantly with 100 µM rifampicin in confluent HepG2 cells; levels in DMSO-treated HepG2 cells decreased from control at all concentrations but no significant changes were observed.
- MDR1 mRNA increased significantly with 100 µM rifampicin in confluent Huh7 cells but no significant changes were observed in DMSO-treated Huh7 cells.

6.3.2 – Phenobarbital treatments

Figures 6.3 and 6.4 show results for phenobarbital treated HepG2 and Huh7 cells respectively. MRP2 mRNA levels in both confluent and DMSO treated cells are shown in each figure (parts A and B respectively). Figure 6.3 shows that liver MRP2 mRNA level was around half of that in control confluent and DMSO treated cells. In confluent HepG2 cells, 0.5 and 1 mM phenobarbital had no significant effect on MRP2 mRNA levels, however a significant increase to approximately two-fold control level was observed with 3 mM phenobarbital. A similar set of results was observed for DMSO treated HepG2 cells, with the only significant change observed an approximate doubling of expression following 3 mM phenobarbital.

Results from Huh7 cells treated with phenobarbital are shown in figure 6.4. Comparison of MRP2 mRNA level in liver to that in control cells showed similar values for both confluent and DMSO treated cells, with the liver level approximately 160-fold that seen in the cells. Both sets of cells, confluent and DMSO treated, showed very similar responses to phenobarbital in terms of MRP2 mRNA level, with significant increases, to approximately double that of the respective control, seen only following the drug at 3 mM.

Summary

- Results in confluent and DMSO-treated HepG2 cells were very similar, with the only significant increases in MRP2 mRNA seen after 3 mM phenobarbital treatment.
- The only phenobarbital concentration to significantly increase MRP2 mRNA levels in both confluent and DMSO-treated Huh7 cells was 3 mM.

6.3.3 – BNF treatments

Figures 6.5 and 6.6 show results for BNF treated HepG2 and Huh7 cells respectively. BCRP mRNA levels in both confluent and DMSO treated cells are shown in each figure (parts A and B respectively). In liver, the BCRP mRNA level was approximately double that of control confluent HepG2 cells, whereas it was approximately three-fold that of control DMSO treated cells. Although this difference between untreated and DMSO treated cells is relatively small, it reflects the change in BCRP mRNA level resulting from 15 days of 1% DMSO treatment shown in figure 5.3 part D. In confluent HepG2 cells increases in BCRP mRNA to levels similar to those in liver were observed at all concentrations of BNF but none reached significance in comparison with the control. In HepG2 cells treated with 1% DMSO for 15 days prior to BNF incubation, BCRP mRNA expression was significantly increased compared to that in control cells and to a level slightly higher than found in liver when using the compound at 10 µM. This was not sustained at 100 µM BNF.

Results for Huh7 cells treated with three concentrations of BNF are shown in figure 6.6. The liver level of BCRP mRNA was approximately 30- and 36-fold higher than that in control confluent and DMSO treated cells respectively. Again, this mirrors results shown in figure 5.4 part D where BCRP mRNA level after 15 days exposure to 1% DMSO is lower than in confluent control cells. Figure 6.6 part A displays results for BCRP mRNA levels in confluent Huh7 cells treated with BNF and shows significant increases from control with both 1 and 10 µM treatments. A lesser increase was seen with 100 µM BNF which, while still roughly 5-fold higher than control, did not reach significance. DMSO treated Huh7 cells showed significantly increased BCRP mRNA levels compared with control at all concentrations of BNF, and exhibited a concentration dependent increase over 1-100 µM BNF. This is in contrast to results from confluent Huh7 cells and to those from both HepG2 experiments, which showed no significant effect with 100 µM BNF treatment.

Summary

- Although BCRP mRNA levels in confluent HepG2 cells were increased over control with BNF treatment, results were not significant. In DMSO-treated HepG2 cells, 10 µM BNF did result in a significant increase of BCRP; this was not sustained at 100 µM.
- Significant increases in BCRP mRNA were observed after 1 and 10 µM BNF treatment in confluent Huh7 cells. In DMSO-treated Huh7 cells, all three BNF concentrations produced a significant increase, but to a lesser extent than was observed in confluent cells.

6.4 – Discussion

Overall, the effects of rifampicin, phenobarbital and BNF on MDR1, MRP2 and BCRP mRNA levels respectively in confluent HepG2 and Huh7 cells were those expected in a properly functioning hepatocyte; however, some differences in effective concentrations of inducers were observed. Significant increases were observed in all confluent cells after exposure to the appropriate compound with the exception of BNF induction of BCRP mRNA in HepG2 cells, which displayed a trend of increase over control but failed to reach significance. DMSO treated cells appeared to respond similarly to confluent cells with phenobarbital and BNF treatments but failed to induce MDR1 mRNA with rifampicin treatment. DMSO treatment of cells would ideally have led to responses to the inducing compounds occurring at concentrations closer to results from the literature observed in liver or primary hepatocytes. These results and comparisons to the literature will be analysed in more detail below.

The effect of rifampicin on MDR1 mRNA levels was similar in HepG2 and Huh7 confluent cells, with 100 µM treatment increasing expression by 2-fold compared with control. In contrast to this neither cell line responded to rifampicin when pre-treated with 1% DMSO. In the literature there are several reports of rifampicin treatment on various cell lines and human hepatocytes. Mills *et al.* (Mills *et al.*, 2004) reported a 3-fold increase in MDR1 mRNA after 10 µM rifampicin for 48 hours in Fa2N-4 cells, an artificially immortalised hepatocyte cell line. An increase in MDR1 mRNA of between 1.5- and 10-fold over control was reported after an identical rifampicin treatment to that by Mills *et al.* (Mills *et al.*, 2004) in the HepaRG cell line (Antherieu *et al.*, 2010), whilst in human liver an increase in MDR1 mRNA of 2.3-fold over control after 10µM rifampicin for 24 hours was observed (Olinga *et al.*, 2008). These results reveal an increase in MDR1 mRNA after exposure to much lower concentrations of rifampicin than observed here. No significant difference in MDR1 mRNA was observed here after 24 hours incubation with 10 µM rifampicin in either cell line with or without prior 1% DMSO treatment.

This suggests that confluent HepG2 and Huh7 cells are not as sensitive to induction by rifampicin as these other cells types and that exposure to 1% DMSO for 15 days does not improve the observed responses towards those seen in human hepatocytes. A longer period of incubation may result in induction at lower concentrations of rifampicin.

Phenobarbital induction of MRP2 mRNA was similar in confluent and 1% DMSO treated HepG2 and Huh7 cells. All showed a significant increase over control at 3 mM phenobarbital of between 2- and 3-fold. Induction of MRP2 by phenobarbital has been reported in several publications. For example, in HepaRG cells induction of between 1.5- and 10-fold over control was seen with 1 mM PB applied for 48 hours (Antherieu *et al.*, 2010). In experiments with human hepatocytes, incubation with 3.2 mM PB for 96 hours produced noticeable increases in both RNA and protein levels of MRP2 (Courtois *et al.*, 2002), whilst a treatment of only 50 µM PB for 24 hours resulted in a 12.4-fold increase in mRNA levels of MRP2 in human liver slices (Olinga *et al.*, 2008). Although induction in HepaRG cells was achieved at a lower PB concentration than in HepG2 and Huh7 cells, the shorter incubation time used here could account for the difference. The publication of Courtois *et al.* (Courtois *et al.*, 2002) does not give definitive fold changes but a similar PB concentration to that used here was used in those experiments. However, much larger increases in MRP2 mRNA were seen in human liver slices (12.4-fold) in the publication by Olinga *et al.* (Olinga *et al.*, 2008) with a much lower PB concentration (50 µM) than was used here in HepG2 and Huh7 cells, indicating that hepatocytes *in situ* are much more sensitive to the ligand than are hepatocyte like cell lines and isolated hepatocytes.

BNF did not result in significantly induced expression of BCRP mRNA at any concentration in confluent HepG2 cells, whereas 10 µM BNF produced a significant increase in 1% DMSO treated cells; however, this was not sustained. Both confluent and DMSO-treated Huh7 cells showed significant increases in BCRP following 1 and 10 µM BNF which were sustained only in DMSO-treated cells at 100 µM. Results in the literature for BCRP induction with the compound 2,3,7,8-tetrachlorodibenzo-p-dioxin (TCDD or dioxin), which also acts via the AhR, showed mRNA and protein increases of 2- and 2.7-fold respectively in human hepatocytes (Tan *et al.*, 2010), a similar level of induction to that seen in this work.

In HepG2 cells DMSO treatment appeared to improve the cellular response to AhR activation, as an increase was seen following 10µM BNF in DMSO-treated but not confluent cells. Similarly, 100µM BNF produced a significant change in DMSO-treated but not in confluent Huh7 cells. However, the magnitude of induction with 1 and 10 µM BNF was much larger in confluent Huh7 cells than in DMSO-treated cells, suggesting no simple positive effect of DMSO

treatment. As reports of work specifically using BNF to target the AhR in human liver were unavailable in the literature it is difficult to determine whether the 10-fold induction over control in confluent Huh7 cells is the expected result, or whether the more modest 2-fold increase seen in DMSO-treated cells with 1 µM BNF is the appropriate response.

Although appropriate induction of genes by the compounds has been demonstrated for confluent cells of both lines (with the exception of BNF induction of BCRP mRNA in HepG2 cells, which did not reach significance), it cannot be automatically assumed that activation of the single target pathway caused the observed responses. Due to built in redundancy mechanisms, if a compound was introduced to a cell in which the predominantly activated pathway was deficient or absent it would be feasible to potentially observe activation of an alternate nuclear receptor pathway in order to facilitate clearance of the compound. Various techniques have been employed to study nuclear receptor activation such as mRNA and protein analysis, luciferase reporter gene assays and electrophoretic gel mobility shift assays to determine functional motif binding (Faucette *et al.*, 2006; Owen *et al.*, 2006; Ripp *et al.*, 2006). Differences in reported findings of which nuclear receptors are activated by compounds and subsequently produce gene responses can be accounted for by differences in cell types, sources, culture conditions, reagents and laboratory practices during experimentation as well as many other factors; to thoroughly define which nuclear receptor pathway was active in a particular cell type would need to be established in each laboratory. However, for the purposes required here a demonstration of gene response to a typical inducing compound was sufficient to demonstrate whether cells were responding positively or negatively with DMSO in comparison to confluent cells and published results.

The effects of the DMSO treatment itself must also be considered as the mechanism through which it can potentially be used to promote differentiation or halt de-differentiation is largely unknown. Nuclear receptor responses could realistically be negated or impeded by DMSO; it has been observed previously that a DMSO concentration of 1% inhibits functional activity of CYP3A4 in pooled human liver microsomes (Iwase *et al.*, 2006). Nuclear receptors also regulate basal expression of many of the genes they can induce as demonstrated in the case of AhR by Tijet *et al.* (Tijet *et al.*, 2006). If DMSO does affect nuclear receptors or their subsequent pathways, basal gene expression may be affected as well as the ability of the cell to respond via that pathway.

Overall, it can be concluded that rifampicin induction of MDR1 mRNA has been adversely affected by DMSO treatment in comparison to confluent cells in both cell lines and did not show a significant increase with 10 µM treatment observed in Fa2N-4 cells, HepaRG cells and

in human liver slices. This indicates that both HepG2 and Huh7 cells have less hepatocyte-like functionality than the aforementioned cell types and liver slices, and that DMSO treatment did not improve the response to lower levels of inducer. Phenobarbital induction of MRP2 mRNA appears to be unaffected in both cell lines by DMSO treatment and did not exhibit increased sensitivity to phenobarbital at lower concentrations as were observed in liver slices. BNF induction of BCRP remained similar in confluent and DMSO treated HepG2 cells, whilst the response in Huh7 cells at lower concentrations was of a lesser magnitude after DMSO treatment than was observed in confluent cells. However, conclusions can only be drawn regarding response to a particular compound rather than successful induction via a specific nuclear receptor pathway due to no direct analysis of nuclear receptor mobilisation, protein or mRNA levels being undertaken. Further analysis of these DMSO treated cells in the form of functional transport studies and Western blots are presented in the following chapters.

Receptor	Protein Targets
CAR	CYP3A1 CYP3A4 CYP2B1 CYP2B2 CYP2B6 CYP2C7 CYP2C9 CYP2C19 UGT1A1 UGT2B1 GSTA1 GSTA2 GSTA3 GSTM1 MRP2 MRP3 (hepatocytes only) MRP4 OATPC P-gp
PXR	CYP3A4 CYP2B6 CYP2C9 UGT1A1 P-gp (MDR1) OATPC OATPA MRP2 MRP3 SULT2A1
AhR	CYP1A1 CYP1A2 CYP1B1 UGT1A1 UGT1A6 GSTA1 GSTA2 GSTM OATPC (decrease) BCRP

Table 6.1 – Protein targets of CAR, PXR and AhR. Protein targets of the three selected receptors are listed here; although this is not an exhaustive list, it gives and impression of the range of proteins that a particular receptor has been shown to affect. Data extracted from Xu *et al.*, Dauchy *et al.*, Tan *et al.*, Tompkins *et al.* and Urquhart *et al.* (Tan *et al.*, 2010; Tompkins *et al.*, 2010; Dauchy *et al.*, 2008; Urquhart *et al.*, 2007; Xu *et al.*, 2005).

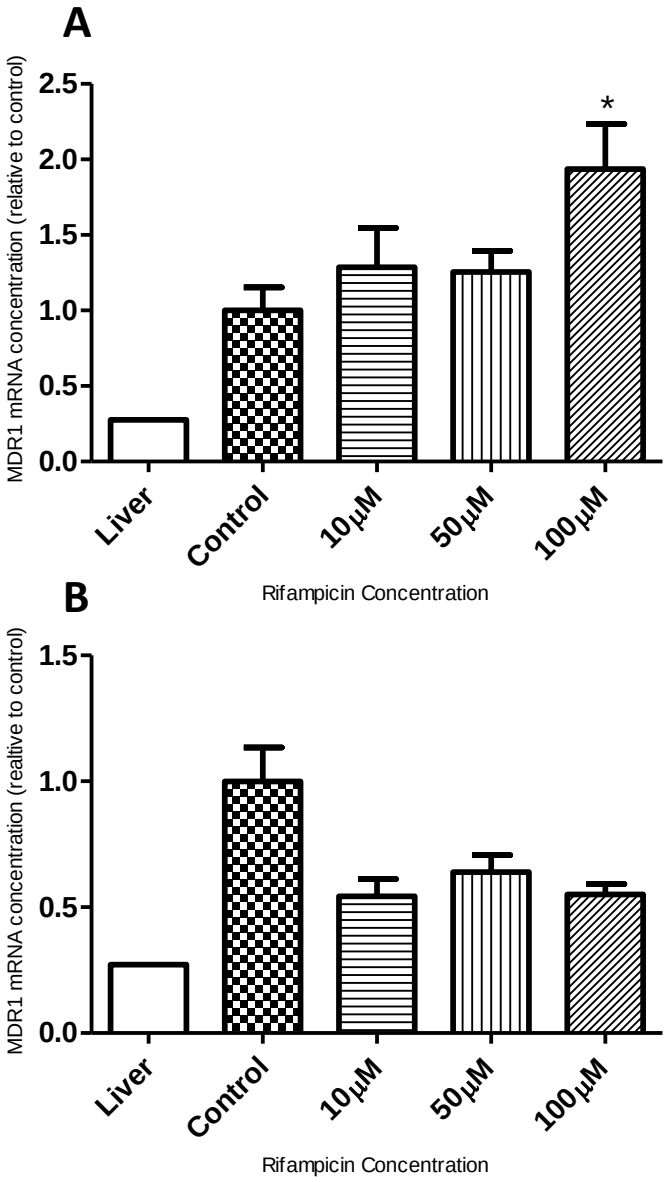

Figure 6.1 – Rifampicin induction of MDR1 mRNA levels in confluent and 15 day 1% DMSO treated HepG2 cells. Cells were grown either to confluence (A) or with 1% DMSO for 15 days (B) in 6 well plastic plates as described previously. Rifampicin, 10-100 µM, was applied as described in chapter 2. RNA was harvested, processed and assessed by qPCR for MDR1 mRNA. All data was normalised to two reference genes. Results shown are from three experiments with a minimum of nine total replicates for confluent cells (N = 3, n = 9) and one experiment with three replicates for DMSO treated cells (N = 1, n = 3). Liver values from whole liver cDNA are shown as relative to control. Data is presented as mean ± SEM and was analysed statistically against control by one-way ANOVA with Dunnett's post test. * = $p < 0.05$, ** = $p < 0.01$.

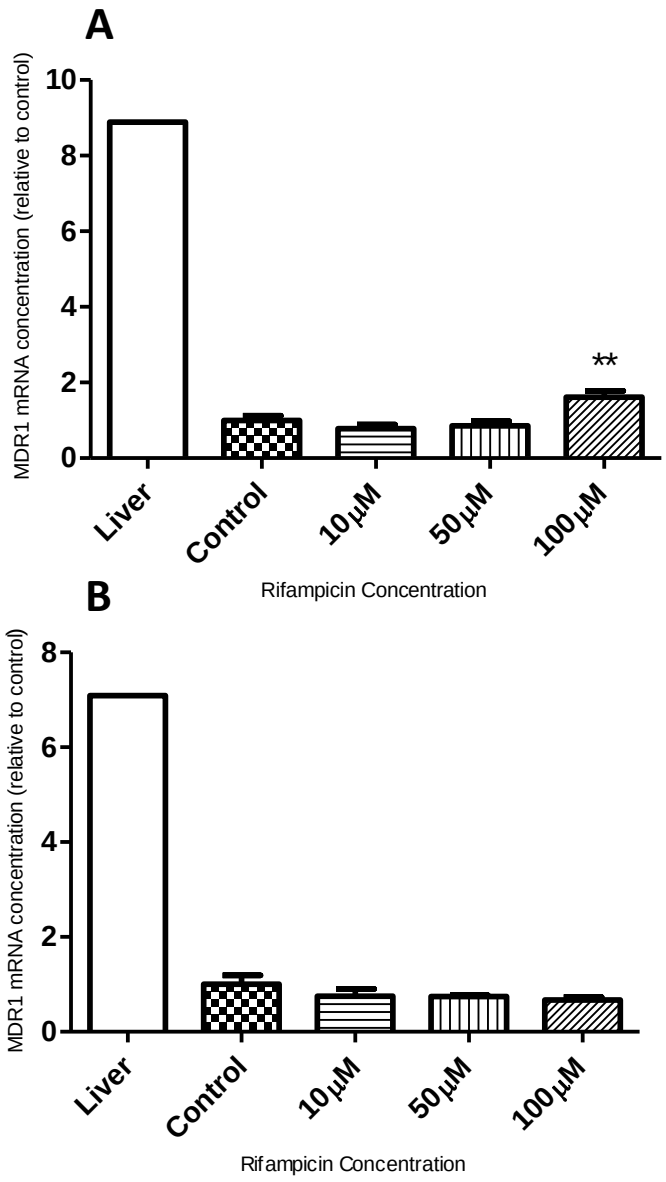

Figure 6.2 – Rifampicin induction of MDR1 mRNA levels in confluent and 15 day 1% DMSO treated Huh7 cells. Cells were grown either to confluence (A) or with 1% DMSO for 15 days (B) in 6 well plastic plates as described previously. Rifampicin, 10-100 µM, was applied as described in chapter 2. RNA was harvested, processed and assessed by qPCR for MDR1 mRNA. All data was normalised to two reference genes. Results shown are from three experiments with a minimum of ten total replicates for confluent cells (N = 3, n = 10) and one experiment with three replicates for DMSO treated cells (N = 1, n = 3). Liver values from whole liver cDNA are shown as relative to control. Data is presented as mean ± SEM and was analysed statistically against control by one-way ANOVA with Dunnett's post test. * = $p < 0.05$, ** = $p < 0.01$.

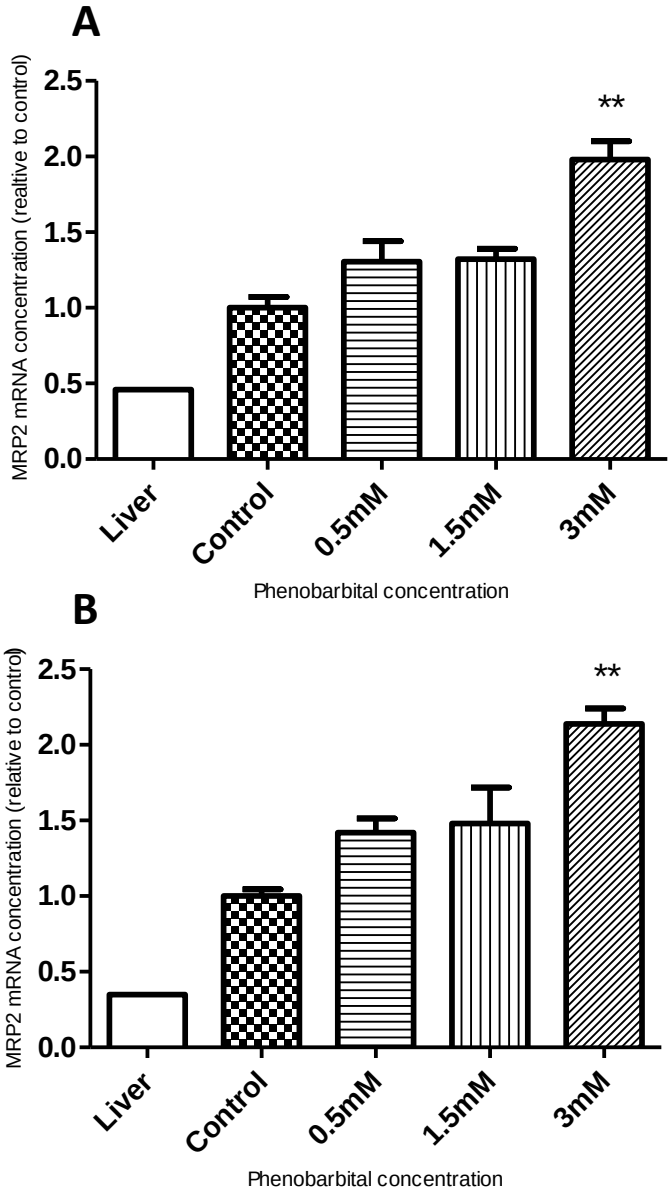

Figure 6.3 – Phenobarbital induction of MRP2 mRNA levels in confluent and 15 day 1% DMSO treated HepG2 cells. Cells were grown either to confluence (A) or with 1% DMSO for 15 days (B) in 6 well plastic plates as described previously. Phenobarbital, 0.5-3 mM, was applied as described in chapter 2. RNA was harvested, processed and assessed by qPCR for MRP2 mRNA. All data was normalised to two reference genes. Results shown are from three experiments with a minimum of nine total replicates for confluent cells (N = 3, n = 9) and one experiment with three replicates for DMSO treated cells (N = 1, n = 3). Liver values from whole liver cDNA are shown as relative to control. Data is presented as mean ± SEM and was analysed statistically against control by one-way ANOVA with Dunnett's post test. * = $p < 0.05$, ** = $p < 0.01$.

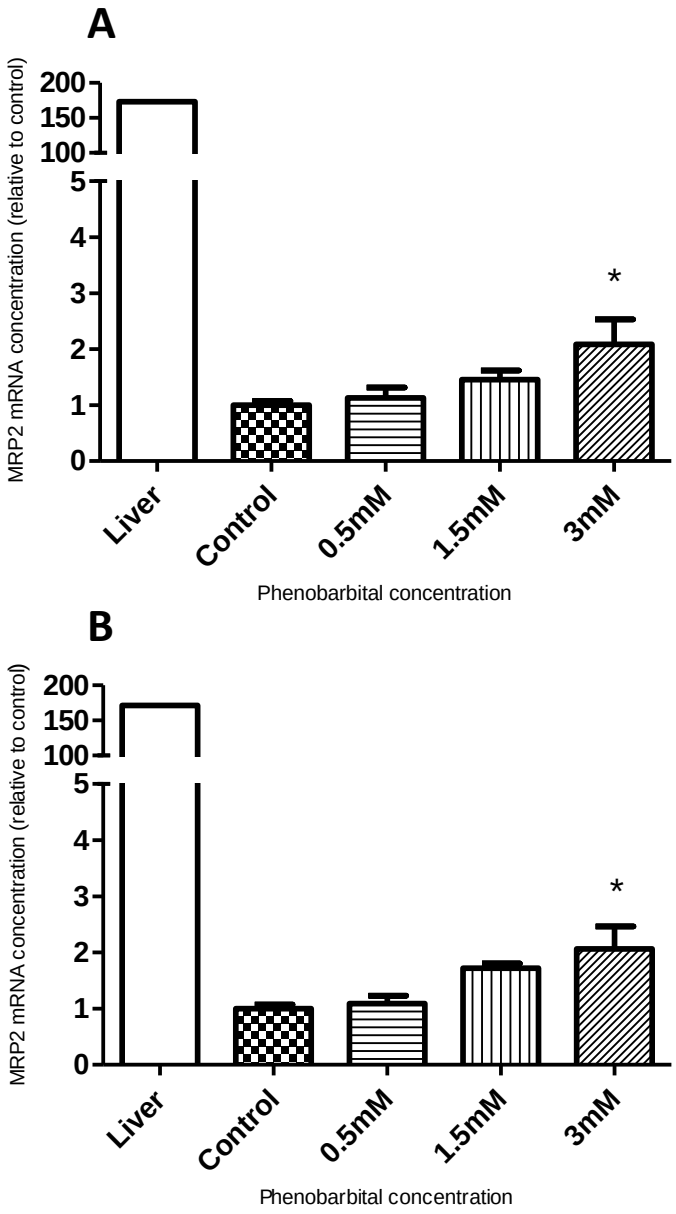

Figure 6.4 – Phenobarbital induction of MRP2 mRNA levels in confluent and 15 day 1% DMSO treated Huh7 cells. Cells were grown either to confluence (A) or with 1% DMSO for 15 days (B) in 6 well plastic plates as described previously. Phenobarbital, 0.5-3 mM, was applied as described in chapter 2. RNA was harvested, processed and assessed by qPCR for MRP2 mRNA. All data was normalised to two reference genes. Results shown are from three experiments with a minimum of ten total replicates for confluent cells (N = 3, n = 10) and one experiment with three replicates for DMSO treated cells (N = 1, n = 3). Liver values from whole liver cDNA are shown as relative to control. Data is presented as mean ± SEM and was analysed statistically against control by one-way ANOVA with Dunnett's post test. * = $p < 0.05$, ** = $p < 0.01$.

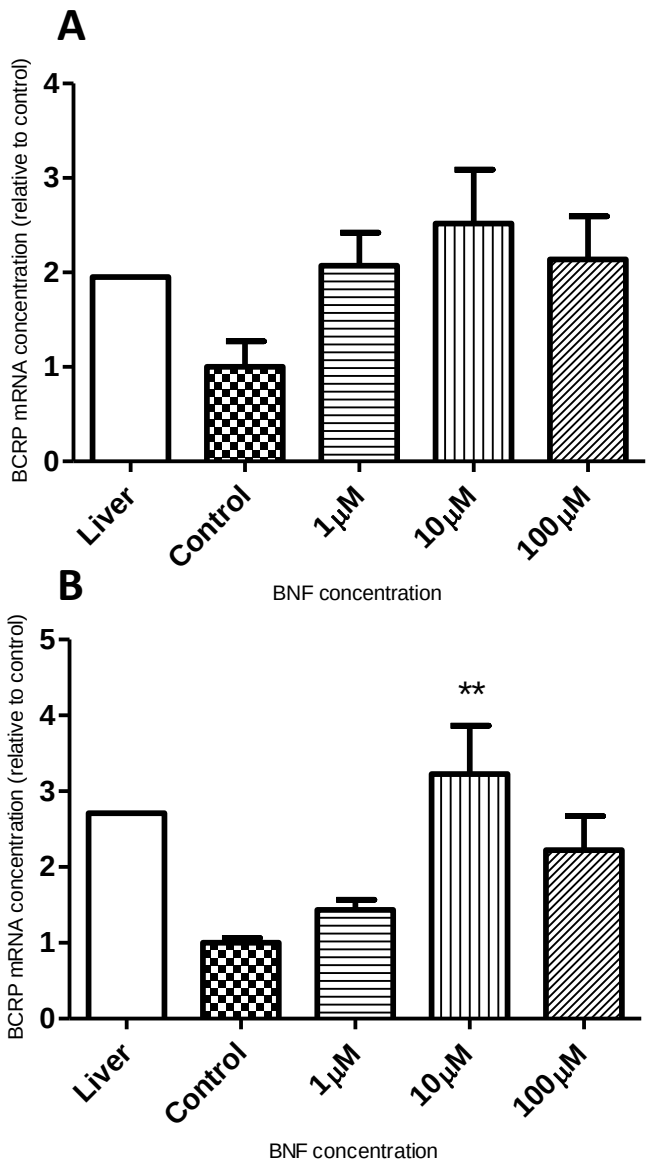

Figure 6.5 – Beta-naphthoflavone (BNF) induction of BCRP mRNA levels in confluent and 15 day 1% DMSO treated HepG2 cells. Cells were grown either to confluence (A) or with 1% DMSO for 15 days (B) in 6 well plastic plates as described previously. BNF, 1-100 µM, was applied as described in chapter 2. RNA was harvested, processed and assessed by qPCR for BCRP mRNA. All data was normalised to two reference genes. Results shown are from three experiments with a minimum of nine total replicates for confluent cells (N = 3, n = 9) and one experiment with three replicates for DMSO treated cells (N = 1, n = 3). Liver values from whole liver cDNA are shown as relative to control. Data is presented as mean ± SEM and was analysed statistically against control by one-way ANOVA with Dunnett's post test. * = $p < 0.05$, ** = $p < 0.01$.

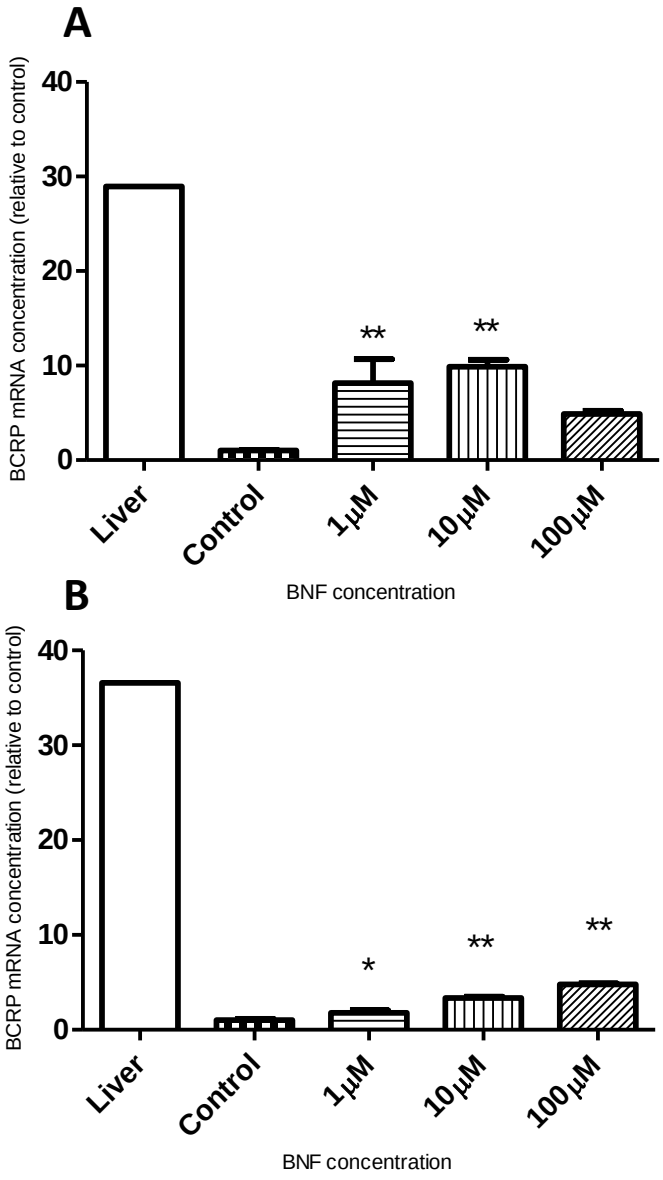

Figure 6.6 – Beta-naphthoflavone (BNF) induction of BCRP mRNA levels in confluent and 15 day 1% DMSO treated Huh7 cells. Cells were grown either to confluence (A) or with 1% DMSO for 15 days (B) in 6 well plastic plates as described previously. BNF, 1-100 µM, was applied as described in chapter 2. RNA was harvested, processed and assessed by qPCR for BCRP mRNA. All data was normalised to two reference genes. Results shown are from three experiments with a minimum of ten total replicates for confluent cells (N = 3, n = 10) and one experiment with three replicates for DMSO treated cells (N = 1, n = 3). Liver values from whole liver cDNA are shown as relative to control. Data is presented as mean ± SEM and was analysed statistically against control by one-way ANOVA with Dunnett's post test. * = $p < 0.05$, ** = $p < 0.01$.

Chapter 7 – Functional studies using Hoechst 33342 and calcein-AM

Chapter aim: To conduct Hoechst 33342 and calcein-AM functional studies on confluent and 15-day DMSO-treated HepG2 and Huh7 cells, along with prolonged untreated Huh7 cells in order to assess function of the cells and key efflux transporters before and after DMSO treatment.

7.1 – Introduction

Hoechst 33342 is a fluorescent dye which binds to double-stranded DNA. It is often used to estimate cell number by nuclear staining or to assess the function of P-glycoprotein (P-gp, MDR1) and breast cancer resistance protein (BCRP, ABCG2), both of which efflux the compound from the cell. Hoechst 33342 is one of the more lipophilic members of the Hoechst family and enters the cell easily by diffusion through the lipid membrane. Unbound Hoechst dye can then be effluxed from the cell by P-gp and BCRP, with the rate of efflux being higher when more copies of the transporter are present (Brown *et al.*, 2008; Ozvegy *et al.*, 2002). Inhibitors of P-gp such as verapamil and cyclosporin A (CSA) (reviewed by Perez-Tomas, Yang *et al.* and Colabufo *et al.* (Colabufo *et al.*, 2010; Yang *et al.*, 2008; Perez-Tomas, 2006)) and BCRP inhibitors such as Ko143 (Pick *et al.*, 2011; Ni *et al.*, 2010; Pick *et al.*, 2010; Matsson *et al.*, 2009; Allen *et al.*, 2002) can be applied to demonstrate that transport is indeed being conducted by these proteins.

Calcein-AM is not fluorescent and enters the cell by diffusion through the lipid membrane. Once inside the cell it is cleaved by intracellular esterases into calcein, which is both hydrophilic, so it cannot diffuse out of the cell through the lipid membrane, and fluorescent. Before calcein-AM is cleaved it is a substrate of the P-gp and multidrug resistance associated protein 1 (MRP1) transporters so the addition of inhibitors such as CSA and verapamil can be used to increase loading of the cell (Vellonen *et al.*, 2004). Once fluorescent calcein has been produced it is no longer a P-gp substrate; instead the only routes out of the cell are via MRP1 and MRP2 transporters (Vellonen *et al.*, 2004). These can be inhibited by ligands such as MK571, a potent MRP inhibitor (Matsson *et al.*, 2009; Gekeler *et al.*, 1995).

Basal MDR1 (P-gp), MRP1, MRP2 and BCRP mRNA levels were analysed in chapters 3 and 5, and levels in DMSO-treated HepG2 and Huh7 cells along with prolonged untreated Huh7 cells were also assessed in chapter 5. MDR1 mRNA levels were approximately 3-fold higher in confluent HepG2 cells than in liver and did not change after 15 days of DMSO treatment. In

confluent Huh7 cells, MDR1 mRNA levels were roughly 5-fold lower than in liver, which again did not change with 15 days of DMSO treatment. Confluent HepG2 cells had BCRP levels 2- to 3-fold lower than in liver, which were significantly reduced following 15 day DMSO treatment. Confluent Huh7 cells had BCRP mRNA levels 20- to 30-fold lower than liver but these did not change with DMSO treatment. MRP1 and -2 mRNA levels in confluent HepG2 cells were approximately 2100- to 3500-fold of those in liver and roughly 2-fold of those in liver respectively, neither of which changed significantly with DMSO treatment. In confluent Huh7 cells MRP1 mRNA levels were between 10- and 90-fold of those in liver, while MRP2 mRNA levels were between 12- and 170-fold lower than those in liver; neither gene showed significant changes with DMSO treatment. These previous results demonstrate that only BCRP levels in HepG2 cells appear to have changed with DMSO treatment; functional experiments conducted here could reveal whether the lack of changes in mRNA are a true reflection of the effects of DMSO treatment, or whether in fact there are post-translational events occurring which affect expression and functional levels of the proteins.

Efflux activity in confluent and treated cells can be determined using these two assays both by quantifying the amount of compound effluxed over a given period of time and by lysing the cells to measure the stored compound. With the Hoechst assay, cells were lysed and the fluorophore retained inside the cell measured. In the calcein-AM assay both calcein effluxed throughout the experiment and that remaining inside the cells was quantified.

7.2 – Methods

HepG2 and Huh7 cells were grown to confluence and, in the case of Huh7 cells, for a further 15 days in standard growth media in 24-well plastic plates. For DMSO treatment, HepG2 and Huh7 cells were grown in 12-well and 24-well plastic plates respectively. This was due to physical limitation of the volume of media that could be applied to HepG2 cells in 24-well plates, which was not sufficient to sustain the cells throughout the 15 day DMSO treatment period. Cell culture was as described in chapter 2.2.2 and figures 2.1 and 2.2.

Both Hoechst 33342 and calcein-AM experimental procedures are described in chapter 2.6. Briefly, in Hoechst experiments, cells were washed with warm Krebs solution and kept on a hotplate at 37^{o}C in Krebs with or without the inhibitors CSA (10 µM), verapamil (100 µM) or Ko143 (10 µM) for 30 minutes. Hoechst 33342 was dissolved in water, added to Krebs solution at concentrations ranging from 0.1 to 30 µM and applied to cells with or without inhibitors as appropriate for a further 60 minutes. Cells were then washed twice in cold Krebs solution and lysed (buffer detailed in appendix A) before quantification of the fluorescent signal using either

a Perkin-Elmer LS-5 luminescence spectrometer (Perkin Elmer, Massachusetts, USA) at excitation wavelength 360 nm and emission wavelength 480 nm or a fluorescent plate reader (FLUOstar Omega, BMG Labtech, Germany) in black plastic 96-well plates using excitation filter 355 ± 10 nm and emission filter 480 ± 20 nm. Protein quantification was by the method of Bradford as described in chapter 2.6 (Bradford, 1976). Data were corrected for background fluorescence and normalised to protein concentration for each individual well.

Cells used in calcein-AM experiments were washed in warm Krebs solution before incubation with 1 nmole calcein-AM in 500 µl Krebs (final concentration of 2 µM) with or without 100 µM verapamil or 10 µM CSA as required for 30 minutes. Cells were washed again with warm Krebs solution and incubated with efflux buffer comprised of 500 µl Krebs with or without inhibitors (100 µM verapamil, 10 µM CSA or 20 µM MK571). Solutions were harvested and replaced every 20 minutes four times (total efflux time of 80 minutes) before cells were lysed overnight in water. Lysed cells were harvested and centrifuged at 1200 rpm (9660 x g) for 10 minutes after which the supernatant was collected and all samples were analysed for fluorescence using either a Perkin-Elmer LS-5 luminescence spectrometer (Perkin Elmer, Massachusetts, USA) at excitation wavelength 492 nm and emission wavelength 518 nm or on a fluorescent plate reader (FLUOstar Omega, BMG Labtech, Germany) in black plastic 96-well plates using excitation filter 480 ± 20 nm and emission filter 520 ± 10 nm. Protein quantification was by the method of Bradford as described previously. Data were corrected for background fluorescence then normalised to protein concentration for each individual well. The sum of the four efflux values is displayed in the figures as efflux; the lysate value is displayed separately, with the sum of efflux and lysate values representing the total calcein retained by cells after loading.

Data are displayed as mean ± SEM and all statistical analyses were carried out in GraphPad Prism using Student's t-test or one-way ANOVA with either Dunnett's or Bonferroni's post test where appropriate.

8.3 – Results

7.3.1 – Hoechst 33342 – confluent HepG2 cells

Figures 7.1-7.5 show results for Hoechst 33342 experiments on confluent and 15 day DMSO-treated HepG2 and Huh7 cells, along with 15 day untreated Huh7 cells. Statistical analyses of the data by Student's t-test are displayed in tables 7.1-7.5. Figure 7.1 shows data from confluent HepG2 cells loaded with 0.1-30 µM Hoechst along with either verapamil, CSA, Ko143 or with no inhibitor present (control); table 7.1 displays results from statistical analysis of these data. The different graphs in the figure display efflux data for Hoechst 33342 or along with one

of three inhibitors. Graphs A and B display data for the P-gp inhibitors verapamil and CSA respectively, while data in graph C shows the effect of Ko143, a BCRP inhibitor. Both of these transporters are major contributors to Hoechst efflux from cells where they are functional and therefore, as they are inhibited, the amount of dye remaining in the cells following loading should increase.

However, statistical analysis of the data from these experiments did not show consistent increases in Hoechst loading by the inhibitors. Loading was slightly but significantly increased by verapamil at concentrations of 0.1 to 3 µM Hoechst but lost significance at 5 and 10 µM. CSA did not produce any significant increase in Hoechst loading and in fact resulted in a significant decrease in comparison to Hoechst alone at 3 and 5 µM Hoechst despite both verapamil and CSA being inhibitors of P-gp. The effect of Ko143 was dependent on the concentration of Hoechst, with small but significant increases at 0.1 and 0.5 µM Hoechst; however, a significant decrease in accumulation in comparison to Hoechst alone was produced at 5 µM Hoechst. Results for 30 µM Hoechst were excluded from the statistical analysis due to results which did not fit with the rest of the data, indicating a possible toxic effect on the cells.

Of the three inhibitors, only verapamil gave results similar to those expected. However, much larger increases might have been expected than are observed here; Brown *et al.* (Brown *et al.*, 2008) showed an increase in Hoechst retention of almost 4-fold compared to control in human renal tubular cells with 1 µM Hoechst and 10 µM CSA, and a 2-fold increase compared to control with 1 µM Hoechst and 10 µM verapamil. These results could indicate that functional levels of P-gp and BCRP were low in the cells under the particular culture conditions used or that an alternative mechanism effluxed the Hoechst from the cell so quickly that inhibition of P-gp or BCRP made no difference to the overall amount retained.

Summary

- Verapamil inhibited efflux effectively at Hoechst concentrations of 0.1-3 µM. Ko143 inhibited efflux only at 0.1 and 0.5 µM of Hoechst, while CSA did not effectively inhibit Hoechst efflux.

7.3.2 – Hoechst 33342 – DMSO-treated HepG2 cells

Data for Hoechst uptake experiments in HepG2 cells treated with 1% DMSO for 15 days are displayed in figure 7.2, with statistical analysis displayed in table 7.2. Again, the results from cells incubated with Hoechst alone are shown alongside results from Hoechst plus verapamil, CSA or Ko143. As in confluent HepG2 cells, Hoechst accumulation was not consistently increased with verapamil, CSA or Ko143 inhibition. Again, some small but statistically

significant increases in Hoechst accumulation were observed with each inhibitor; at 0.5 and 1 µM Hoechst with verapamil, at 1 and 3 µM Hoechst with CSA and at 0.5, 1 and 3 µM Hoechst with Ko143. However, these increases were not sustained at higher Hoechst concentrations and at 30 µM Hoechst a significant reduction in loading was observed with all three inhibitors in comparison to control, indicating a possible toxic effect of Hoechst. The substantial sustained increases in Hoechst accumulation expected of the three inhibitors were not observed in confluent HepG2 cells and treatment with DMSO for 15 days did not improve upon that result.

Summary

- Although some increases in retained Hoechst were seen at low Hoechst concentrations with each inhibitor, these were not sustained.
- DMSO treatment did not improve upon results in confluent HepG2 cells. Sustained inhibition of Hoechst efflux was not observed in either cell type.

7.3.3 – Hoechst 33342 – confluent Huh7 cells

Results for confluent Huh7 cells incubated with Hoechst 33342 either alone or with verapamil, CSA or Ko143 are shown in figure 7.3, with statistical analysis displayed in table 7.3. In contrast to results seen in confluent HepG2 cells, significant increases in Hoechst accumulation in comparison to control were observed at the majority of Hoechst concentrations with all three inhibitors. With the inclusion of verapamil, significant increases over control were observed at all Hoechst concentrations except 8 µM. Not only were these increases sustained over the whole concentration range unlike in HepG2 cells, the magnitude of increases was larger. For example, 3 µM Hoechst with verapamil in confluent Huh7 cells showed a statistically significant increase of approximately 2-fold compared to Hoechst alone, whereas in confluent HepG2 cells the increase with verapamil remained significant but was only approximately 1.2-fold of levels seen with Hoechst alone. Hoechst accumulation was also significantly increased with CSA at all but two of the tested Hoechst concentrations (8 and 10 µM). This is vastly different from results obtained using HepG2 cells, where no significant increases in Hoechst accumulation were observed when CSA was added. Significant increases in Hoechst accumulation with Ko143 in Huh7 cells were observed over Hoechst alone at the majority of Hoechst concentrations. Again, these results were different to those in HepG2 cells as larger increases were seen over a wider range of Hoechst concentrations. These results indicate that P-gp and BCRP transporters in confluent Huh7 cells are functional and expressed at a sufficiently high level that their inhibition is effective in increasing the amount of retained

Hoechst; they also demonstrate a difference between the two cell lines at confluence in terms of the magnitude and consistency of the increases produced via inhibition of P-gp and BCRP.

Summary

- Successful inhibition of Hoechst efflux was observed with all three inhibitors over a range of Hoechst concentrations.

7.3.4 – Hoechst 33342 – prolonged untreated Huh7 cells

Results from Hoechst accumulation experiments in prolonged untreated Huh7 cells are shown in figure 7.4, with results of statistical analysis displayed in table 7.4. Significant increases in Hoechst accumulation were observed in comparison to control with the inclusion of verapamil between 0.1 and 5 µM Hoechst but not at the three highest concentrations. In comparison to results from confluent Huh7 cells the magnitude of increases here are lower; for example, at 3 µM Hoechst verapamil inclusion in confluent Huh7 cells resulted in values approximately 2-fold of those in Hoechst alone, whereas here in prolonged untreated growth of Huh7 cells the accumulation observed under the same conditions was approximately 1.4-fold of those observed with Hoechst alone. The inclusion of CSA during Hoechst loading in these prolonged untreated Huh7 cells did not result in a sustained significant increase in Hoechst accumulation; only three of the eight comparisons were significant (0.1, 5 and 10 µM Hoechst). This is a noticeable change from results obtained in confluent Huh7 cells, where significant increases in accumulated Hoechst were observed with CSA in the majority of data points. These data indicate that a change in P-gp expression or functionality may have occurred as a result of prolonged untreated growth of Huh7 cells, as inhibition of Hoechst efflux via this transporter is less effective. However, no significant change in MDR1 mRNA, which encodes the P-gp protein, was observed after 15 days DMSO treatment in either cell line, or in prolonged untreated Huh7 cells in comparison to control (see figures 5.3 and 5.4). This could indicate that mRNA and protein levels did not correlate and post-translational mechanisms may be responsible for protein changes.

Summary

- Verapamil did successfully inhibit Hoechst efflux via P-gp up to 5 µM Hoechst, but no inhibition of efflux via P-gp with CSA was observed.

- Prolonged untreated culture did not retain the characteristics of inhibition observed in confluent Huh7 cells.

7.3.5 – Hoechst 33342 – DMSO-treated Huh7 cells

Results from Hoechst accumulation experiments in DMSO-treated Huh7 cells are shown in figure 7.5, with results of statistical analysis displayed in table 7.5. Statistically significant increases in Hoechst accumulation were seen with both verapamil and CSA compared to Hoechst alone at Hoechst concentrations of 0.1, 0.5 and 5 µM; addition of CSA also resulted in increased accumulation at 8 µM Hoechst. However, the magnitude of the changes observed in these DMSO-treated cells were smaller than those recorded previously in confluent cells with both verapamil and CSA; the effect of CSA was similar in prolonged untreated and DMSO-treated cells, while inclusion of verapamil during Hoechst loading appeared to have a greater effect in prolonged untreated than in DMSO-treated cells. Inhibition of Hoechst efflux with Ko143 resulted in only one significant increase over Hoechst alone at 0.5 µM Hoechst and two significant decreases at 3 and 10 µM Hoechst. Although there were three concentrations at which inhibition resulted in a significant increase in Hoechst retention, both those and DMSO-treated cells had a reduced response to Ko143 in comparison to that seen in confluent Huh7 cells. The reduced effect of Ko143 could indicate that transporter levels have decreased with prolonged growth with and without DMSO, which Western blotting of BCRP protein in these cells could reveal.

Summary

- Although some significant inhibition of Hoechst efflux was seen with all three inhibitors, this was not sustained and was of a smaller magnitude than that observed in confluent Huh7 cells.
- DMSO-treatment results in less inhibition of Hoechst efflux than in confluent Huh7 cells, indicating a less representative cell model.

7.3.6 – Calcein-AM – preliminary experiments

Calcein-AM experiments were conducted on confluent and DMSO-treated HepG2 and Huh7 cells and on Huh7 cells with prolonged untreated growth for up to 15 days. Briefly, cells were loaded with calcein-AM with the inhibitors verapamil or CSA where applicable for 30 minutes then washed, followed by four efflux periods of 20 minutes each in Krebs with inhibitors where applicable. After each efflux period the buffer was removed, kept for analysis and replaced with identical efflux solution. After the final efflux stage, cells were washed in cold Krebs and lysed in water overnight. Data displayed in figures 7.7 – 7.11 shows total calcein (all four efflux measurements plus lysate) and efflux separately (all four efflux measurements combined). Total calcein (efflux plus lysate) was analysed using one-way ANOVA with Dunnett's post test

using cells incubated with calcein-AM during loading with no additional inhibitors during either loading or efflux as control. The results of these statistical tests are shown in figures 7.7 – 7.11. Efflux alone was also statistically analysed by one way ANOVA with Bonferroni's post test, selected results of which are shown in tables 7.6 – 7.10.

Figure 7.6 displays results from confluent HepG2 and Huh7 cells incubated with 1 nmol of calcein in 500 µl Krebs solution for 20 minutes then lysed overnight. This experiment was necessary to demonstrate that re-uptake of calcein, previously effluxed from the cell, was not significant over the time frame in which efflux was being measured. Results are shown for calcein uptake alongside those for calcein efflux over 20 minutes and total calcein (efflux plus lysate) for each cell line when loaded with calcein-AM in the presence of verapamil. As calcein-AM is cleaved directly to calcein by esterases, the maximum amount of intracellular calcein possible is 1 nmol when cells are loaded with 1 nmol calcein-AM. These results showed that 15-20% of total intracellular calcein was effluxed during the initial 20 minutes of the experiment, demonstrating that the maximum amount of calcein likely to be outside of the cell during this time is 0.2 nmol (20% of 1 nmol). Even with 5 times the likely maximum amount of calcein present in the extracellular fluid, the fluorescence released from lysed cells following 20 minutes of incubation with calcein was only a fraction of that found in the efflux buffer after 20 minutes from cells loaded with calcein-AM, indicating that calcein is not subject to significant uptake during 20 minutes of efflux and the experimental conditions are appropriate.

Summary

- The experimental design is appropriate as calcein influx into the cells during the 20 efflux period is not large enough to obscure efflux results.

7.3.7 – Calcein-AM – confluent HepG2 cells

Data from experiments with calcein-AM in confluent HepG2 cells are displayed in figure 7.7. Statistical analysis of total calcein revealed that levels were significantly raised over control with the addition of either verapamil or CSA to the loading buffer. Calcein fluorescence in efflux and lysate ranged from 1.5- to 2-fold that seen in control cells with the inclusion of either inhibitor. This reflects the ability of verapamil and CSA to inhibit efflux of calcein-AM via the P-gp transporter during loading, resulting in more calcein being generated via esterase cleavage of calcein-AM and retained in the cells.

Table 7.6 displays selected results from statistical analysis of efflux values alone. Efflux data are displayed in figure 7.7 as the lower, darker proportion of the column. Compared to

measurements made in cells with verapamil present only during the loading stage, inclusion of any of the three inhibitors in the efflux buffer reduced calcein efflux. The most potent inhibitor was MK571 and the weakest was verapamil. These results agree with the known inhibitory actions of the inhibitors, where verapamil inhibits only MRP1 but CSA and MK571 inhibit both MRP1 and 2. Addition of both MK571 and CSA to the efflux buffer showed no significant difference in comparison to efflux with MK571 alone but significantly reduced efflux in comparison to CSA alone. This indicates that 20 µM MK571 inhibits MRP1 and 2 more effectively than 10 µM CSA. The ratio of efflux to lysate also reflected changes to inhibitors in the loading and efflux buffers. Control cells and those loaded with verapamil saw 60% and 66% of the cellular calcein effluxed respectively; addition of verapamil to the efflux buffer reduced this to 54% of calcein effluxed, while addition of CSA and MK571 separately caused a reduction in calcein efflux to 40% and 25% of total calcein respectively. These data support the statistical analysis and show that the inhibitors do indeed change the proportion of calcein effluxed from the cell when the slightly variable total calcein levels are taken into account. Overall these results indicate that P-gp, MRP1 and MRP2 are all functional and are expressed at a sufficiently high level to be useful in assessing transport and inhibition via these proteins.

Summary

- Addition of verapamil or CSA to loading buffer resulted in significant increases in calcein-AM loading (total calcein) over control (no inhibitor), demonstrating P-gp inhibition.
- Verapamil, CSA and MK571 all significantly reduced calcein efflux from control.
- Efflux of calcein via both MRP1 and -2 was demonstrated as MK571 increased cellular calein in comparison to verapamil during efflux.

7.3.8 – Calcein-AM – confluent Huh7 cells

Data from experiments using calcein-AM on confluent Huh7 cells are shown in figure 7.8. Statistical analysis of total calcein levels showed that the inclusion of either verapamil or CSA during loading significantly increased accumulated calcein in comparison to cells loaded with calcein-AM in the absence of inhibitors. As in confluent HepG2 cells, the addition of either verapamil or CSA during loading increased the calcein in both efflux and lysate to 1.5- to 2-fold that in control cells. This demonstrates that P-gp is functioning as expected.

Table 7.7 displays selected results from statistical analysis of efflux values. The addition of either verapamil, CSA or MK571 to the efflux buffer caused reduced efflux in comparison to

cells similarly loaded with verapamil present but with no inhibitor included in the efflux buffer, indicating that inhibition of at least one MRP transporter occurred. Comparison of the effects of verapamil, MK571, CSA and MK571 plus CSA during efflux revealed no significant differences between efflux levels. This is in contrast to results for confluent HepG2 cells, where efflux levels were affected differently by verapamil, CSA and MK571. The lack of difference between verapamil and both CSA and MK571 indicates that the MRP1 transporter is dominating efflux of calcein in these cells as no additional effect is seen with the MRP2 inhibitors. The percentage of effluxed calcein in confluent Huh7 cells was 61% in control cells and 63% in cells loaded in the presence of verapamil, which indicates that verapamil is not retained during efflux after loading and that transporters continue to efflux calcein at the same rate with and without verapamil loading. Although this did reduce to 49% of calcein effluxed with verapamil in the efflux buffer, addition of CSA and MK571 in subsequent experiments resulted in 46% and 42% of calcein effluxed respectively. This was not the big reduction seen in HepG2 cells, where efflux more than halved during incubation with MK571 in comparison to verapamil. These data support the statistical analyses of effluxed calcein and support the conclusion of a lack of functional MRP2 at physiologically relevant levels in the cells.

Overall, these cells demonstrated the presence of functional P-gp and MRP1, but MRP2 is either non-functional or is expressed at such low levels that it is not contributing to calcein efflux at a detectable rate. This is in contrast to HepG2 cells, where all three transporters appear to be expressed at a sufficiently high level that the applied inhibitors had a visible effect.

Summary

- P-gp inhibition by both verapamil and CSA was observed due to increased total calcein during loading with these inhibitors.
- Verapamil, CSA and MK571 all significantly reduced calcein efflux by the same degree, indicating that only MRP1 is functionally expressed or that MRP2 is expressed at such low levels that the effect cannot be observed.

7.3.9 – Calcein-AM – DMSO treated HepG2 cells

Data from experiments using calcein-AM on DMSO-treated HepG2 cells are shown in figure 7.9. Statistical analysis of total calcein levels showed that the inclusion of either verapamil or CSA in the loading buffer resulted in a significantly higher total calcein level than was observed in control. As was observed in confluent HepG2 cells, inclusion of either inhibitor in the loading buffer lead to an increase in total calcein in the range of 1.5- to 2-fold of that in control.

Results here indicate that P-gp function has been retained with DMSO treatment and the function has not altered noticeably from that observed in confluent cells.

Selected results from statistical analysis of efflux data are shown in table 7.8. Efflux was significantly reduced with the addition of MK571 and CSA to the efflux buffer when compared to cells loaded similarly with verapamil but with no inhibitors included during efflux, whilst the reduction observed with verapamil included during efflux did not reach significance. Although the reductions in efflux caused by MK571 in comparison to CSA and verapamil are visible on the graph in figure 7.9, none of these comparisons reach significance when analysed statistically in table 7.8. This is in contrast to results observed in confluent HepG2 cells, where these differences were both visually apparent and statistically significant. The percentage of calcein effluxed in control cells and cells loaded in the presence of verapamil is 64% and 56% respectively. Although the reduction in efflux with verapamil is marked at only 37%, this has not reached significance due to the wider spread of data than was observed in confluent HepG2 cells. Addition of CSA to the efflux buffer resulted in a slightly lower percentage of calcein effluxed at 31%, while MK571 resulted in a marked decrease at only 18%, less than half of that effluxed with verapamil in the buffer. These support findings from the statistical analyses which indicated that although the pattern of inhibition was similar to that observed in confluent HepG2 cells, the possible negative effects of DMSO on the ability of the cells to remain attached affected the data collected and in some cases prevented statistical significance from being achieved.

Overall, results from DMSO-treated HepG2 cells indicate that P-gp function is retained and whilst the same pattern of changes is apparent regarding efflux differences with the inhibitor combinations, statistical significance has been lost in some cases. This is likely due to the larger spread of data values; although the error bars remain fairly small they are larger than those obtained from analysis of data from confluent cells and this may contribute to the lack of significance in some cases. A factor in this may be that HepG2 cells were observed to occasionally wash away from the well during the repeated washing and changing of solutions in this experimental protocol. To compensate for this a larger number of experiments were conducted than for confluent cells and wells with clear patches where cells had washed away were disregarded from analysis. Although all wells were corrected for background fluorescence and normalised to total protein for each well specifically, it appears that more variable results were obtained compared to experiments with confluent cells where cell attachment was not an issue. This was not as apparent in Hoechst experiments, where the number of washes and addition/removal of buffers are less numerous and so less likely to cause mechanical disruption of cell adhesion to the plastic plates.

Summary

- Both verapamil and CSA increased calcein-AM loading over control, indicating that functional P-gp was present.
- Inhibition of calcein efflux by CSA and MK571 was observed, but no significant reduction in efflux occurred with verapamil. This may be due to a proportion of cells becoming detatched, resulting in slightly more variable data.
- DMSO-treated HepG2 cells are not a better model than confluent cells.

7.3.10 – Calcein-AM – prolonged untreated Huh7 cells

Data from experiments with calcein-AM on prolonged untreated Huh7 cells are shown in figure 7.10. Statistical analysis of total calcein levels showed that inclusion of either verapamil or CSA in the loading buffer significantly increased total calcein in comparison to control. In comparison to results from confluent Huh7 cells, the proportion of calcein present in efflux buffer versus lysate has reduced in these experiments. Approximately 25% of total calcein was effluxed here in comparison to approximately 60% of total calcein effluxed in confluent Huh7 cells. These results indicate that P-gp was present and functional as total calcein did increase with inhibition of calcein-AM efflux. However, indications are that functional levels of a calcein efflux protein, MRP1 or 2, have altered as a result of prolonged untreated growth in comparison to function in confluent cells. No detachment of cells during the experiment was observed.

Table 7.9 shows selected results from statistical analysis of efflux values. Efflux was significantly decreased in comparison to control by the addition of MK571 to the efflux buffer, while neither verapamil nor CSA significantly affected efflux of calcein. MK571 also caused a significant reduction in calcein efflux in comparison to CSA; addition of both MK571 and CSA to the efflux buffer simultaneously reduced efflux significantly compared to CSA alone, indicating a dominant effect of MK571 over CSA. The proportion of calcein effluxed in control cells and cells loaded in the presence of verapamil was very similar at 34% and 30% respectively. Inclusion of either verapamil or CSA in the efflux buffer did not affect calcein efflux much, with percentages of calcein effluxed 25% and 23% respectively. However, addition of MK571 to the efflux buffer results in only 16% of total calcein effluxed, a marked reduction from other experimental conditions. These data support the statistical analyses of efflux data, showing that only MK571 had a marked effect on calcein efflux.

These results indicate that although MRP-mediated efflux of calcein did occur and it could be effectively reduced by MK571, a potent MRP1 and 2 inhibitor, neither verapamil nor CSA were

effective in inhibition of MRP. This indicates that prolonged untreated Huh7 cells may not be responding as would be expected to CSA during efflux but did respond to P-gp inhibition by the compound during loading. As verapamil successfully inhibited P-gp efflux of calcein-AM, the lack of a significant reduction in calcein efflux via MRP1, which is inhibited by verapamil, indicates that efflux of calcein via MRP1 is reduced or absent. In confluent Huh7 cells verapamil did significantly reduce calcein efflux but no further reduction was seen with MK571. This could indicate a more prominent role of MRP2 in calcein efflux in these cells in conjunction with a reduction in MRP1 function. Indeed, it could be that MRP2 functionality has been revealed purely due to a severe reduction/absence of functional MRP1, with the actual level of functional MRP2 remaining similar to that in confluent cells. The change in the proportion of efflux to lysate in total calcein in these cells compared to confluent cells may indicate that there is a reduction in efflux via MRP, leaving more of the loaded calcein inside the cell.

Summary

- P-gp inhibition by verapamil and CSA was successful and increased total calcein.
- MK571 did decreased inhibition of calcein efflux in comparison to control and verapamil, indicating that MRP2 is now playing a functional role in efflux.
- The percentage of total calcein in the lysate has increased substantially in all conditions, indicating a decrease in calcein efflux which could be caused by a reduction in the functional levels of MRP1.
- Prolonged untreated Huh7 cells appear to be a better efflux transporter model than confluent Huh7 cells.

7.3.11 – Calcein-AM – DMSO treated Huh7 cells

Data from experiments using calcein-AM in DMSO-treated Huh7 cells are shown in figure 7.11. Analysis of total calcein levels showed that inclusion of either verapamil or CSA in the loading buffer significantly increased total calcein in comparison to control. This indicates that P-gp is functional and was successfully inhibited in these cells by both verapamil and CSA. As observed in previous results for prolonged untreated Huh7 cells, the proportion of total calcein represented by efflux measurement is much lower than in confluent cells, with approximately 80% of total calcein remaining inside the cell in control cells.

Selected results from statistical analysis of efflux values are shown in table 7.10. MK571 significantly reduced efflux of calcein in comparison to control, whilst inclusion of verapamil or CSA in the efflux buffer had no significant effect. The addition of MK571 to the efflux buffer

also reduced efflux significantly in comparison to efflux with verapamil or CSA. MK571 plus CSA in efflux significantly reduced efflux of calcein in comparison to CSA alone but no difference was observed in efflux from cells with MK571 alone. The percentage of calcein efflux from control cells and cells loading in the presence of verapamil was 25% and 20% respectively; addition of verapamil to the efflux buffer did not appear to affect efflux, with 19% of total calcein effluxed. CSA also had little effect on calcein efflux with 14% of total calcein effluxed from the cell. As indicated by statistical analyses, MK571 did have a significant effect on calcein efflux, causing a reduction in efflux to only 9% of total calcein.

The results indicate that P-gp is functional and can be inhibited in these cells. Efflux inhibition results were very similar to those observed in prolonged untreated Huh7 cells and indicated an increased role for MRP2 during calcein efflux compared to confluent cells. As also observed in the prolonged untreated Huh7 cells, the decreased proportion of efflux in total calcein indicates that a change in MRP expression or function has been precipitated by this treatment, although no change in mRNA level of either MRP1 or MRP2 was observed in previous experiments (figure 5.4).

Summary

- Both verapamil and CSA increased loading of calcein-AM, demonstrated by the increase in total calcein over control.
- MK571 inhibited efflux more effectively than verapamil and CSA, indicating that MRP2 was effectively inhibited as well as MRP1, and that MRP2 was present in sufficient amounts in comparison to MRP1 that it was functionally effective during efflux.
- The proportion of calcein retained in the lysate was increased over that observed in confluent cells, similar to results in prolonged untreated cells. This could indicate that functional levels of MRP1 were reduced.
- Although this model is preferable to the confluent Huh7 cells in terms of efflux, no significant advantage over the prolonged untreated cells is apparent.

7.4 – Discussion

The Hoechst 33342 and calcein-AM assays utilised in this chapter have been described in various cellular systems (Brown *et al.*, 2008; Goda *et al.*, 2007; Schoonen *et al.*, 2005; Wortelboer *et al.*, 2005; Ifergan *et al.*, 2004; Vellonen *et al.*, 2004; Allen and Schinkel, 2002; Allen *et al.*, 2002; Scharenberg *et al.*, 2002). Hoechst 33342 is a lipophilic compound which enters the cell via diffusion across the cell membrane; once inside the cell it binds to double stranded DNA, with the remaining unbound compound subsequently effluxed by the

transporters P-gp and BCRP. Three inhibitors were used here to attempt to block this efflux: CSA, verapamil and Ko143. CSA enters the cell via diffusion (Leonardi *et al.*, 2001) and inhibits its targets via competitive inhibition (Saeki *et al.*, 1993); this is also the case for verapamil (Saeki *et al.*, 1993). Ko143 inhibition of BCRP transport is not as clearly understood as the more established compounds such as verapamil and CSA; however, work published by Ozvegy-Laczka *et al.* (Ozvegy-Laczka *et al.*, 2005) demonstrated that addition of Ko143 resulted in a conformational change in BCRP. This was measured by binding of the 5D3 antibody to BCRP, which increased in accordance with certain conformational changes. Inhibition by Ko143 and ATP depletion within the cell gave similar results, indicating that inhibition could be due to disruption of the normal cycling of the transporter. Calcein-AM is a lipophilic compound which diffuses into cells through the cell membrane and can be effluxed via P-gp. Any calcein-AM remaining in the cell is transformed into calcein by intercellular esterases; this cannot diffuse through the membrane and is effluxed primarily by MRP1 and 2. The inhibitior MK571 was used here to block efflux by the MRP pathway, which is known to be a competitive inhibitor of MRP1, 2 and 4 as reviewed by Keppler (Keppler, 2011). The inhibitor CSA is also known to be a non-selective inhibitor of both MRP1 and 2 although it is a more potent inhibitor of P-gp, while verapamil is known to inhibit transport via MRP1 and not MRP2 (reviewed by Keppler (Keppler, 2011)).

7.4.1 – Hoechst 33342 experiments

Inhibition of P-gp in HepG2 cells at confluence and after DMSO treatment was inconsistent, with different results obtained using verapamil and CSA. Ko143 did not produce consistent increases in Hoechst accumulation in either HepG2 cell type. Results obtained in confluent Huh7 cells were more promising and showed significant increases in Hoechst accumulation over a range of concentrations with all three inhibitors. These are well known inhibitors and have been used successfully many times; it would be expected to see successful inhibition in both cell lines (Pick *et al.*, 2010; Brown *et al.*, 2008; Goda *et al.*, 2007; Ifergan *et al.*, 2004; Vellonen *et al.*, 2004; Allen *et al.*, 2002; Saeki *et al.*, 1993). The Hoechst 33342 accumulation assay has been used successfully in HepG2 cells previously with verapamil as an inhibitor (Cheng *et al.*, 2011), which was the inhibitor that had the most effect on increasing accumulation in confluent HepG2 cells here. After DMSO treatment, inhibition in both cell lines is less effective, which may indicate an increase in P-gp and BCRP levels. To further investigate P-gp and two other important functional proteins, MRP1 and 2, the calcein-AM series of experiments were conducted.

7.4.2 – Calcein-AM experiments

Measurement of calcein-AM in confluent HepG2 cells showed that verapamil and CSA both inhibited transport as expected, increasing the level of total calcein retained in the cell and indicating the P-gp activity. It was also shown that verapamil and CSA inhibited efflux, demonstrating MRP function to some extent but that MK571 was a more effective inhibitor, reducing calcein efflux significantly compared to both other inhibitors. DMSO-treated HepG2 cells showed a similar pattern to confluent cells but some efflux inhibitors which had a significant effect in confluent cells were not found to significantly reduce efflux of calcein from the cell; however, the pattern of inhibition seen in the two cell types remained similar. Overall, the results for HepG2 cells indicate that P-gp, MRP1 and MRP2 are present at a level where function can be measured and are inhibited as expected. This points towards Hoechst 33342 being a less informative marker in these cells as although P-gp inhibition was observed with verapamil in confluent cells, CSA did not produce similar results as would be expected. The results from both Hoechst and calcein-AM assays also indicate that some transporter function or effectiveness of the inhibitors may be lost with DMSO treatment; as no significant changes were observed in mRNA levels of any of the transporters involved here in DMSO-treated cells compared to confluent HepG2 cells, a form of post-transcriptional regulation is likely to be involved in regulating expression as was observed for BCRP in both cell lines.

Results from calcein-AM experiments in confluent Huh7 cells indicated that P-gp is functional and can be inhibited successfully. However, differences in inhibition of MRP1 and 2 were observed in these cells in comparison to the patterns seen in both confluent and DMSO-treated HepG2 cells. Inhibition of calcein efflux was seen with verapamil, CSA and MK571 but at an equal level for all, whereas in HepG2 cells, MK571 inhibited efflux more effectively than either verapamil or CSA. This indicates that only MRP1 was contributing to efflux of calcein in Huh7 cells, as verapamil, known to inhibit this transporter but be ineffective against MRP2, was equally as effective at inhibiting efflux as MK571, an inhibitor of both MRPs. This is supported by the mRNA data for these cell lines (figures 5.3 and 5.4) which showed that confluent HepG2 cells had an MRP2 mRNA level double that in liver, while confluent Huh7 cells had an MRP2 mRNA level 200-fold lower than that in liver. This very low expression of MRP2 could explain the lack of changes in efflux of calcein with different inhibitors observed in confluent Huh7 cells, as MRP2 transport could be so low in comparison to MRP1 that no efflux could be detected.

The data indicate that changes in transporter activity levels occur in Huh7 cells maintained in prolonged untreated culture or treated with DMSO. The proportion of effluxed calcein

dropped from roughly 60% of total calcein in confluent cells to approximately 25% and 20% in prolonged untreated and DMSO-treated cells respectively. This could indicate reduced levels of the MRP transporters. Although neither MRP1 nor 2 mRNA level changed significantly with either treatment in Huh7 cells, decreased MRP1 protein level could explain other differences also seen in these cells. In confluent cells there was no difference in effect of verapamil and MK571 but in both prolonged untreated and DMSO treated cells, the pattern seen in HepG2 cells, where inhibition with MK571 was more effective than with verapamil, reappeared. This could be due to either lower MRP1 or higher MRP2 protein or activity reintroducing the balance of efflux between the two and allowing the function of MRP2 to be observed. As the efflux levels are much lower, it would seem that a decrease in MRP1 protein or activity is more likely.

Although no other information regarding Hoechst or calcein-AM transport assays in prolonged DMSO-treated cells has been published, changes in levels of these transporters predicted in other studies can be examined with results obtained here in mind. Unfortunately, Choi *et al.* (Choi *et al.*, 2009) examined mainly metabolising enzyme levels and no other data regarding transporter mRNA or protein levels in DMSO-treated Huh7 cells is available. Information from Sivertsson *et al.* (Sivertsson *et al.*, 2010) revealed that MRP2 mRNA levels in prolonged untreated Huh7 cells did not change from those in confluent cells at any point during a four week growth period, while MDR1 mRNA levels (P-gp) increased very slightly only after four weeks of growth. These data agree with results observed here previously and adds weight to the suggestion that if protein changes are occurring, they are being controlled by a post-translational mechanism. Antherieu *et al.* (Antherieu *et al.*, 2010) and Le Vee *et al.* (Le Vee *et al.*, 2006) both observed that changes in MDR1 and MRP2 mRNA levels were very small in DMSO-treated HepaRG cells from 5-28 days of culture. Le Vee *et al.* (Le Vee *et al.*, 2006) looked at function of P-gp and MRP2 by measuring rhodamine 123 and carboxyffuorescein (CF) diacetate transport respectively with appropriate inhibitors in HepG2 and HepaRG cells at confluence, HepaRG cells after DMSO treatment and in primary human hepatocytes. Results indicated that P-gp function was very similar in both HepaRG cell types and in HepG2 cells, with P-gp activity in all three cell cultures slightly increased over that in primary hepatocytes. MRP2 function did decrease slightly in DMSO-treated HepaRG cells in comparison to confluent ones and showed a level similar to that in primary hepatocytes; HepG2 cells showed increased MRP2 activity in comparison to both DMSO-treated HepaRG cells and primary hepatocytes. This agrees with mRNA data obtained in chapter 5, where initial levels of MRP2 mRNA in confluent HepG2 cells were higher than those in whole liver. It has also been observed that functional MRP2 levels do not change in Caco-2 cells after culture with or without antibiotics

for up to nine weeks, demonstrating that neither prolonged untreated culture nor antibiotic treatment affect expression of functional MRP2 in this cell line (Prime-Chapman *et al.*, 2005). Results here indicate that even if MRP2 protein function is decreased after DMSO-treatment of HepG2 cells, levels remain high enough that function can be detected.

Overall, these functional experiments have produced mixed results. Both confluent and DMSO-treated HepG2 cells gave similar results in terms of inhibition, indicating no advantage of DMSO treatment in HepG2 cells. Huh7 cells did have a more normal response in terms of expected inhibitor effect when they were grown for 15 days regardless of the presence of DMSO, compared with confluent cells where MRP2 functionality could not be detected. However, this was at the expense of a large percentage of efflux function suggesting that functional levels of both transporters were reduced well below the *in vivo* liver levels. These changes in functional activity were not predicted by mRNA analysis, suggesting that the effects seen following prolonged growth of Huh7 cells result from changes at a post-transcriptional level.

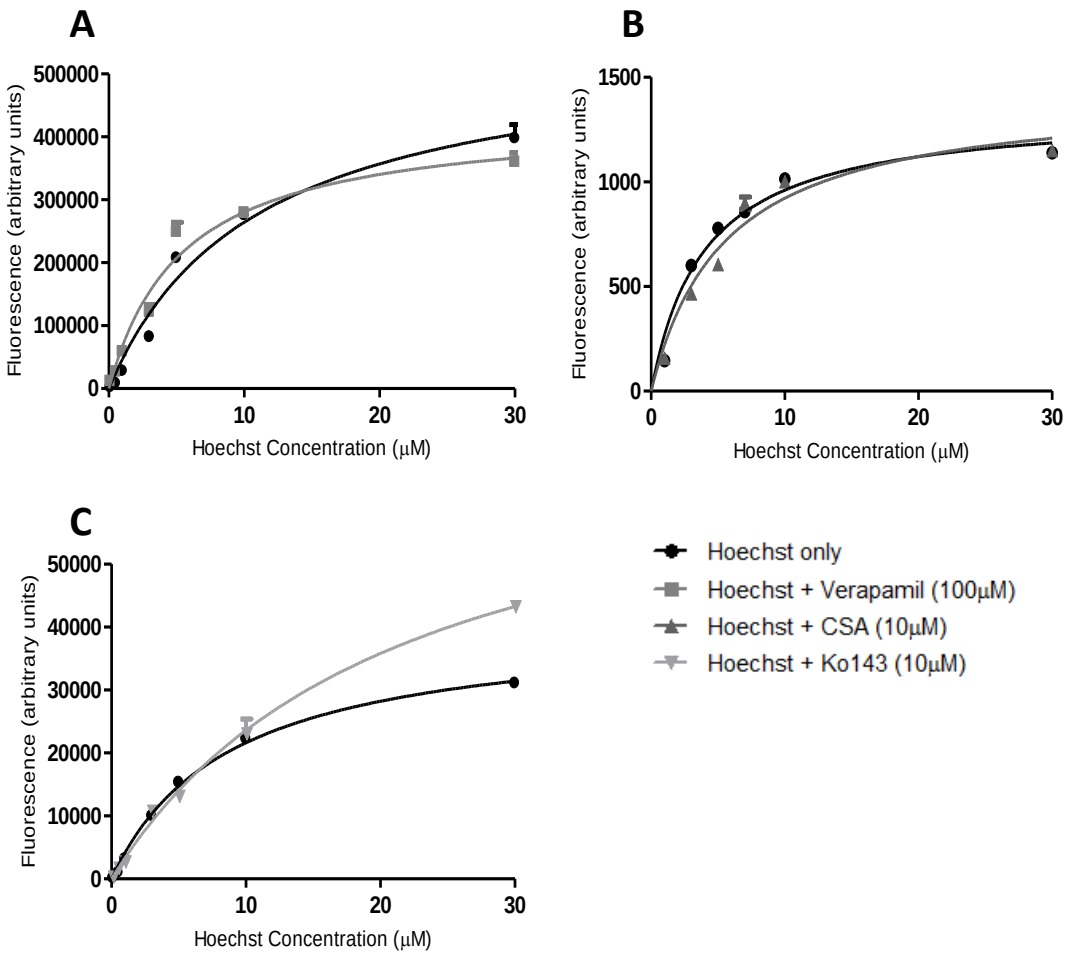

Figure 7.1 – Hoechst 33342 accumulation in confluent HepG2 cells in the presence of P-gp and BCRP inhibitors. Cells were grown in 24-well plastic plates until confluent in standard growth medium. Accumulation of Hoechst dye was assessed as described in chapter 2 with Hoechst alone and with inhibitors verapamil (A), CSA (B) and Ko143 (C). Each graph shows data from one experiment with three repeats (N = 1, n = 3) which was representative of a further two experiments. Data displayed in parts A and C were obtained using a FLUOstar Omega platereader (BMG Labtech) at different intensities, while data in part B was obtained using a Perkin Elmer LS-5 luminescence spectrometer. All data has been normalised to protein levels. Data shown is mean ± SEM with a hyperbola line fitted. Statistical analysis of data displayed here is presented in table 7.1.

Hoechst concentration (μM)	Hoechst only versus Hoechst plus verapamil		Hoechst only versus Hoechst plus CSA		Hoechst only versus Hoechst plus Ko143	
	Significance	Hoechst retention with inhibitor	Significance	Hoechst retention with inhibitor	Significance	Hoechst retention with inhibitor
0.1	*	↑	NS	-	*	↑
0.5	***	↑	NS	-	***	↑
1	**	↑	NS	-	NS	-
3	*	↑	**	↓	NS	-
5	NS	-	**	↓	*	↓
10	NS	-	NS	-	NS	-

Table 7.1 – Statistical analysis of data from figure 7.1. Data from experiments with confluent HepG2 cells incubated with Hoechst 33342 alone and alongside the inhibitors verapamil, CSA and Ko143 are displayed in figure 7.1. Statistical analysis of this data using Student's t-test is displayed here. * = $p < 0.05$, ** = $p < 0.01$, *** = $p < 0.001$, NS = not significant.

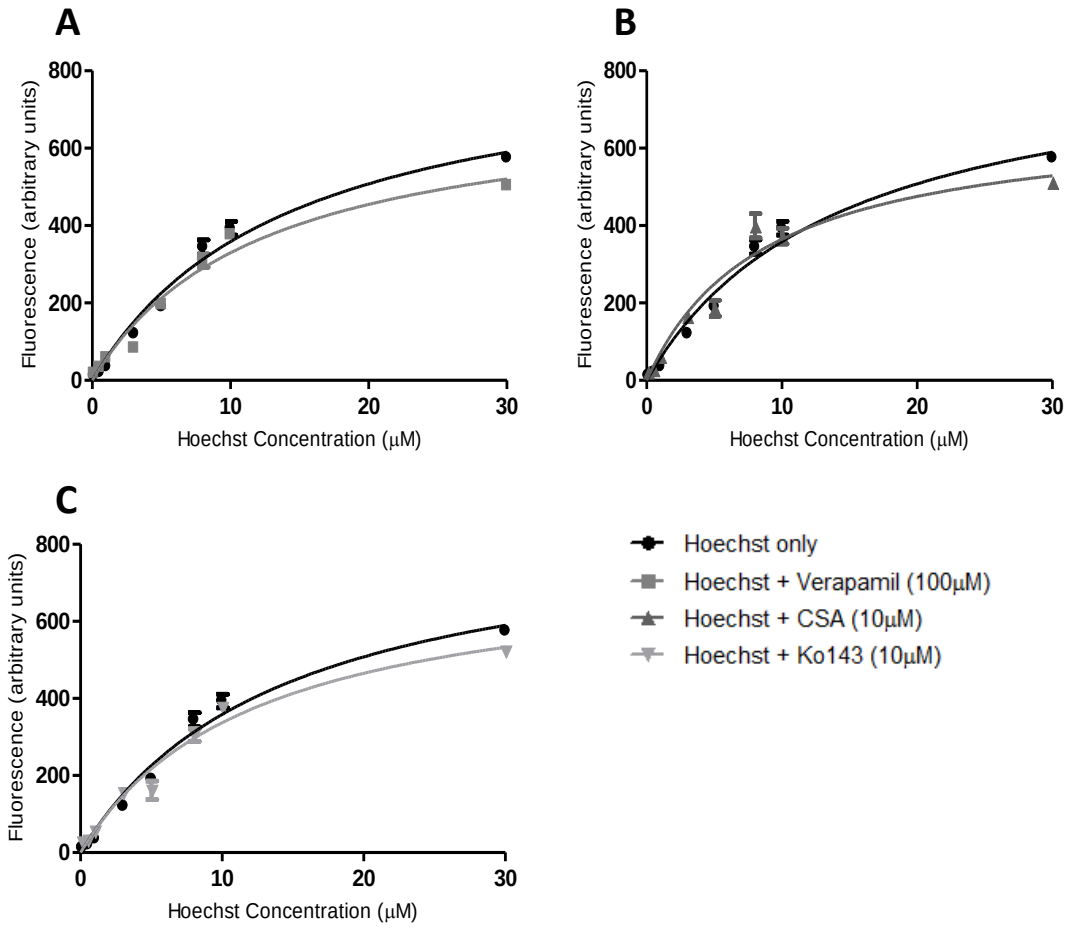

Figure 7.2 – Hoechst 33342 accumulation in 15 day DMSO-treated HepG2 cells in the presence of P-gp and BCRP inhibitors. Cells were grown in 12-well plastic plates for 15 days in standard growth medium plus 1% DMSO. Accumulation of Hoechst dye was assessed as described in chapter 2 with Hoechst alone and with inhibitors verapamil (A), CSA (B) and Ko143 (C). Data is shown from one experiment with three repeats (N = 1, n = 3) which was representative of a total of two experiments. Data displayed in all three parts was obtained using a Perkin-Elmer LS-5 luminescence spectrometer. All data has been normalised to protein levels. Data shown is mean ± SEM with a hyperbola line fitted. Statistical analysis of data displayed here is presented in table 7.2.

Hoechst concentration (μM)	Hoechst only versus Hoechst plus verapamil		Hoechst only versus Hoechst plus CSA		Hoechst only versus Hoechst plus Ko143	
	Significance	Hoechst retention with inhibitor	Significance	Hoechst retention with inhibitor	Significance	Hoechst retention with inhibitor
0.1	NS	-	NS	-	NS	-
0.5	**	↑	NS	-	*	↑
1	***	↑	***	↑	***	↑
3	***	↓	**	↑	***	↑
5	NS	-	NS	-	NS	-
8	NS	-	NS	-	NS	-
10	NS	-	NS	-	NS	-

Table 7.2 – Statistical analysis of data from figure 7.2. Data from experiments with DMSO-treated HepG2 cells incubated with Hoechst 33342 alone and alongside the inhibitors CSA and Ko143 are displayed in figure 7.2. Statistical analysis of this data using Student's t-test is displayed here. * = $p < 0.05$, ** = $p < 0.01$, *** = $p < 0.001$, NS = not significant.

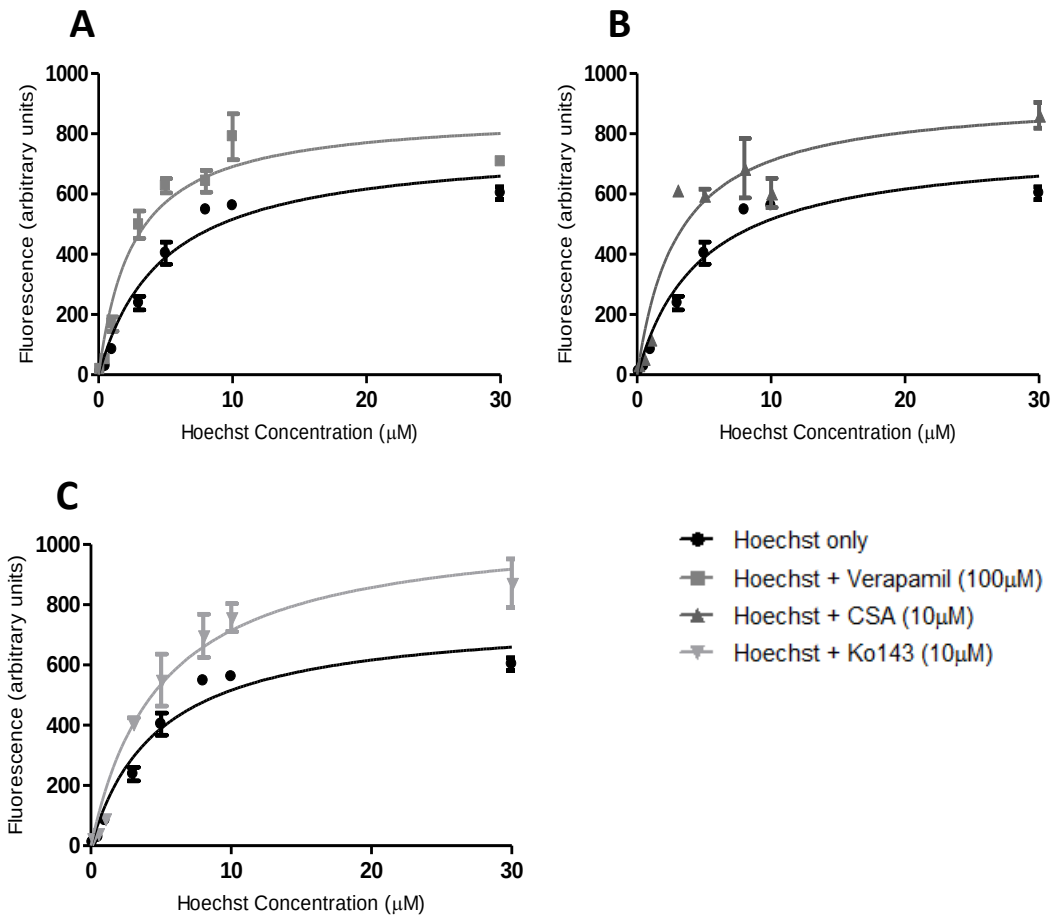

Figure 7.3 – Hoechst 33342 accumulation in confluent Huh7 cells in the presence of P-gp and BCRP inhibitors. Cells were grown in 24-well plastic plates until confluent in standard growth medium. Accumulation of Hoechst dye was assessed as described in chapter 2 with Hoechst alone and with inhibitors verapamil (A), CSA (B) and Ko143 (C). Data is shown from one experiment with three repeats (N = 1, n = 3) which was representative of a further two experiments. Data displayed in all three parts was obtained using a Perkin-Elmer LS-5 luminescence spectrometer. All data has been normalised to protein levels. Data shown is mean ± SEM with a hyperbola line fitted. Statistical analysis of data displayed here is presented in table 7.3.

Hoechst concentration (μM)	Hoechst only versus Hoechst plus verapamil		Hoechst only versus Hoechst plus CSA		Hoechst only versus Hoechst plus Ko143	
	Significance	Hoechst retention with inhibitor	Significance	Hoechst retention with inhibitor	Significance	Hoechst retention with inhibitor
0.1	*	↑	*	↑	***	↑
0.5	**	↑	***	↑	**	↑
1	*	↑	*	↑	NS	-
3	**	↑	***	↑	**	↑
5	**	↑	**	↑	NS	-
8	NS	-	NS	-	NS	-
10	*	↑	NS	-	*	↑
30	*	↑	**	↑	*	↑

Table 7.3 – Statistical analysis of data from figure 7.3. Data from experiments with confluent Huh7 cells incubated with Hoechst 33342 alone and alongside the inhibitors verapamil, CSA and Ko143 are displayed in figure 7.3. Statistical analysis of this data using Student's t-test is displayed here. * = $p < 0.05$, ** = $p < 0.01$, *** = $p < 0.001$, NS = not significant.

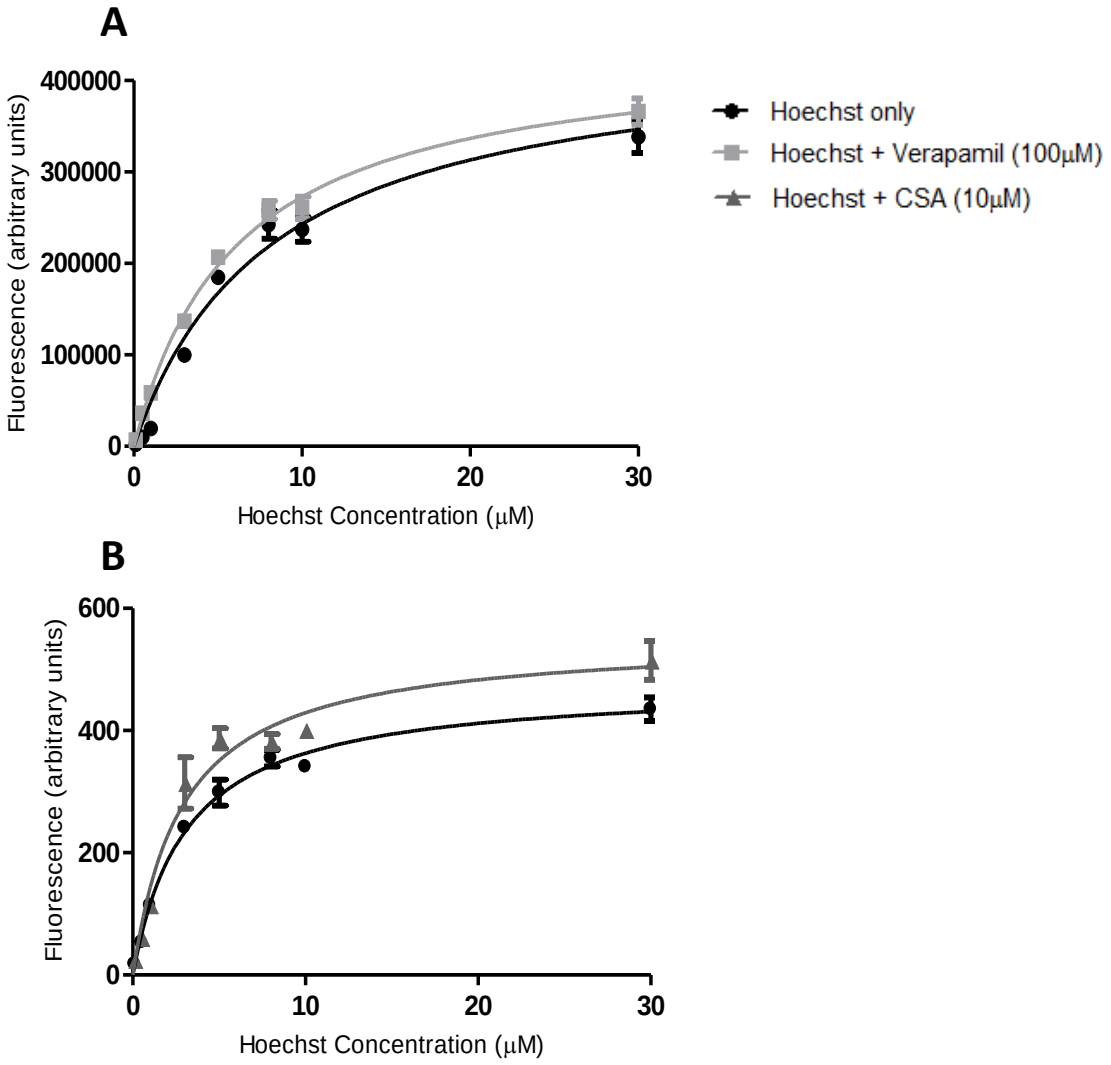

Figure 7.4 – Hoechst 33342 accumulation in 15 day untreated Huh7 cells in the presence of P-gp inhibitors. Cells were grown in 24-well plastic plates until confluent followed by growth for a further 15 days in standard growth medium. Accumulation of Hoechst dye was assessed as described in chapter 2 with Hoechst alone and with inhibitors verapamil (A) and CSA (B). Each graph shows data from one experiment with three repeats (N = 1, n = 3) which was representative of a total of two experiments. Data displayed in part A was obtained using a FLUOstar Omega platereader (BMG Labtech) at different intensities, while data in part B was obtained using a Perkin Elmer LS-5 luminescence spectrometer. All data has been normalised to protein levels. Data shown is mean ± SEM with a hyperbola line fitted. Statistical analysis of data displayed here is presented in table 7.4.

Hoechst concentration (μM)	Hoechst only versus Hoechst plus verapamil		Hoechst only versus Hoechst plus CSA	
	Significance	Hoechst retention with inhibitor	Significance	Hoechst retention with inhibitor
0.1	***	↑	**	↑
0.5	***	↑	NS	-
1	***	↑	NS	-
3	**	↑	NS	-
5	*	↑	*	↑
8	NS	-	NS	-
10	NS	-	*	↑
30	NS	-	NS	-

Table 7.4 – Statistical analysis of data from figure 7.4. Data from experiments with prolonged untreated Huh7 cells incubated with Hoechst 33342 alone and alongside the inhibitors verapamil and CSA are displayed in figure 7.4. Statistical analysis of this data using Student's t-test is displayed here. * = $p < 0.05$, ** = $p < 0.01$, *** = $p < 0.001$, NS = not significant.

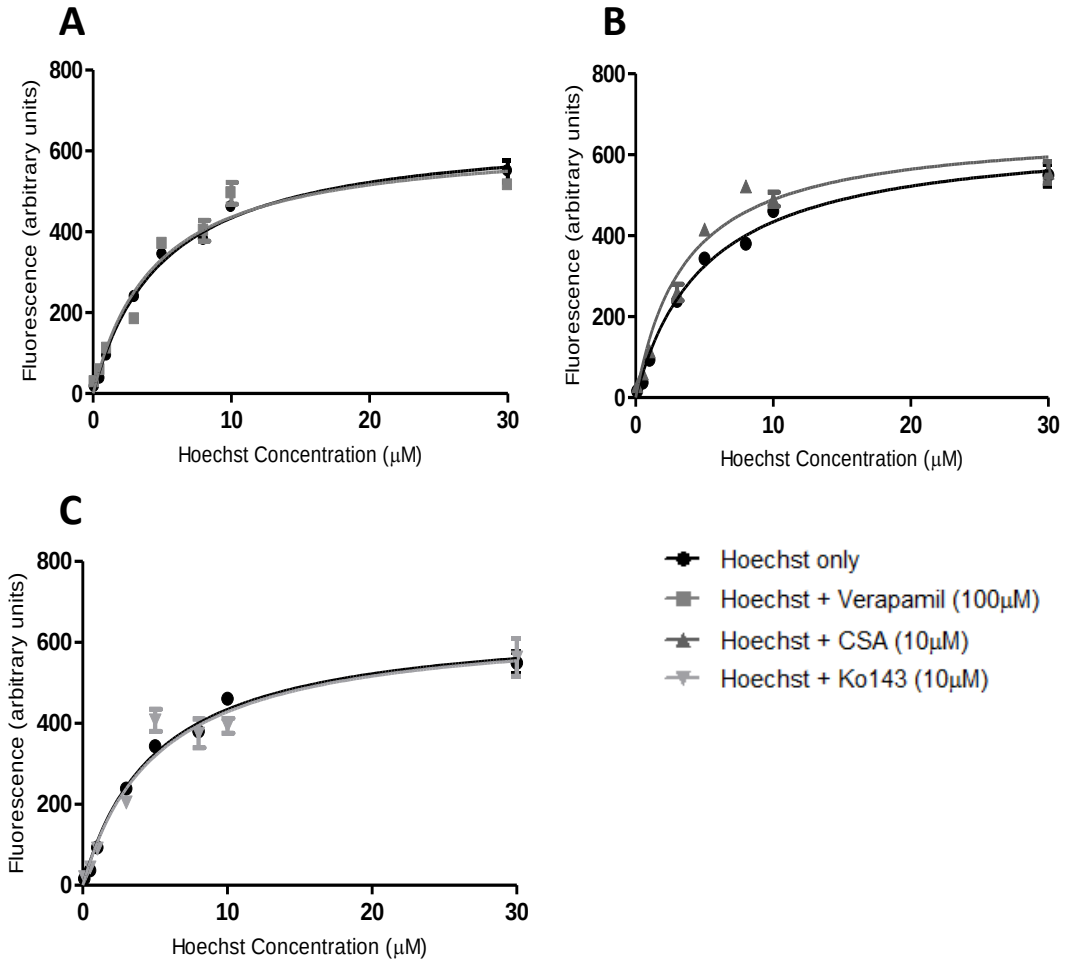

Figure 7.5 – Hoechst 33342 accumulation in 15 day DMSO-treated Huh7 cells in the presence of P-gp and BCRP inhibitors. Cells were grown in 24-well plastic plates until confluent followed by growth for a further 15 days in standard growth medium plus 1% DMSO. Accumulation of Hoechst dye was assessed as described in chapter 2 with Hoechst alone and with inhibitors verapamil (A), CSA (B) and Ko143 (C). Data is shown from one experiment with three repeats (N = 1, n = 3) which was representative of a total of two experiments. Data displayed in all three parts was obtained using a Perkin-Elmer LS-5 luminescence spectrometer. All data has been normalised to protein levels. Data shown is mean ± SEM with a hyperbola line fitted. Statistical analysis of data displayed here is presented in table 7.5.

Hoechst concentration (μM)	Hoechst only versus Hoechst plus verapamil		Hoechst only versus Hoechst plus CSA		Hoechst only versus Hoechst plus Ko143	
	Significance	Hoechst retention with inhibitor	Significance	Hoechst retention with inhibitor	Significance	Hoechst retention with inhibitor
0.1	**	↑	*	↑	NS	-
0.5	**	↑	***	↑	*	↑
1	NS	-	NS	-	NS	-
3	***	↓	NS	-	*	↓
5	**	↑	**	↑	NS	-
8	NS	-	***	↑	NS	-
10	NS	-	NS	-	*	↓
30	NS	-	NS	-	NS	-

Table 7.5 – Statistical analysis of data from figure 7.5. Data from experiments with DMSO-treated Huh7 cells incubated with Hoechst 33342 alone and alongside the inhibitors verapamil, CSA and Ko143 are displayed in figure 7.5. Statistical analysis of this data using Student's t-test is displayed here. * = $p < 0.05$, ** = $p < 0.01$, *** = $p < 0.001$, NS = not significant.

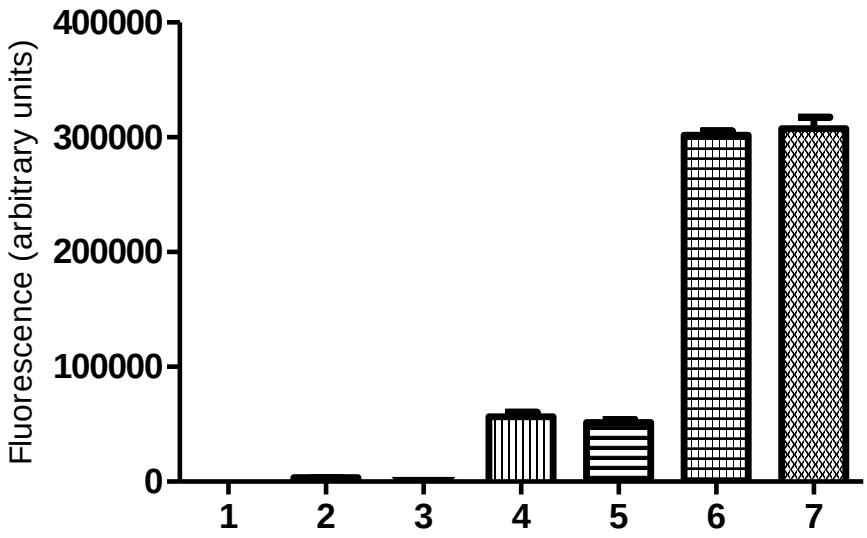

Figure 7.6 – Calcein uptake into confluent HepG2 and Huh7 cells. A solution of 1 nmole calcein in 500 µl Krebs was incubated with confluent HepG2 and Huh7 cells for 20 minutes to assess whether calcein could effectively travel back into the cells during the efflux period. These data are shown alongside those from confluent cells loaded with calcein-AM showing calcein present in the efflux buffer after 20 minutes and the total calcein from both efflux and lysate. Cells in each column were treated as follows:

Column	Treatment
1	Krebs only (no cells)
2 & 3	HepG2 (2) and Huh7 (3) cells lysed after exposure to 1 nmole calcein for 20 minutes
4 & 5	Efflux of calcein from HepG2 (4) and Huh7 (5) cells after 20 minutes with no inhibitors included in efflux buffer. Cells were initially loaded with 1 nmole calcein-AM alongside 100 µM verapamil as described in chapters 2 and 8.
6 & 7	Total calcein (efflux plus lysate) from HepG2 (6) and Huh7 (7) cells loaded with 1 nmole calcein-AM alongside 100 µM verapamil with no inhibitors included in the efflux buffer.

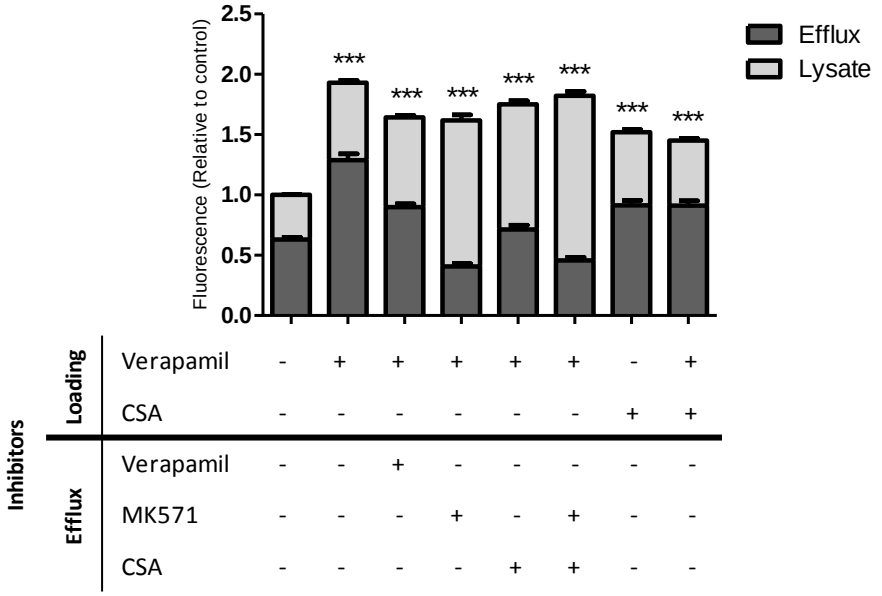

Inhibitor	Relevant proteins inhibited	
	Loading	Efflux
Verapamil	P-gp	MRP1
CSA	P-gp	MRP1, MRP2
MK571	-	MRP1, MRP2

Figure 7.7 – Confluent HepG2 cells analysed for calcein-AM uptake and calcein efflux. Cells were grown on 24-well plastic plates until confluent. Calcein-AM experiments were conducted as described in chapter 2 and chapter 8. Data shown are from three experiments with a total of nine replicates (N = 3, n = 9) and is displayed as mean ± SEM. Statistical analysis of total calcein levels (efflux plus lysate) was by one-way ANOVA with Dunnett's post test using values from cells loaded with calcein-AM alongside verapamil and no inhibitors in efflux as the control (first column). Selected data are compared in table 7.6. *** = $p < 0.001$.

Experiment 1		vs	Experiment 2		Significance	Calcein efflux in experiment 2
Loading	Efflux		Loading	Efflux		
Verapamil	-	vs	Verapamil	Verapamil	***	↓
Verapamil	-	vs	Verapamil	MK571	***	↓
Verapamil	-	vs	Verapamil	CSA	***	↓
Verapamil	Verapamil	vs	Verapamil	MK571	***	↓
Verapamil	Verapamil	vs	Verapamil	CSA	**	↓
Verapamil	CSA	vs	Verapamil	MK571	***	↓
Verapamil	CSA	vs	Verapamil	CSA, MK571	***	↓
Verapamil	MK571	vs	Verapamil	CSA, MK571	NS	-

Table 7.6 – Statistical analysis of efflux data from figure 7.7. Data for confluent HepG2 cells incubated with calcein-AM with or without inhibitors during loading and efflux were analysed to show the effect of efflux inhibition. Selected results are displayed. Statistical analysis of data was carried out using one-way ANOVA with Bonferroni's post-test. ** = $p < 0.01$, *** = $p < 0.001$, NS = not significant, ↓ = decrease.

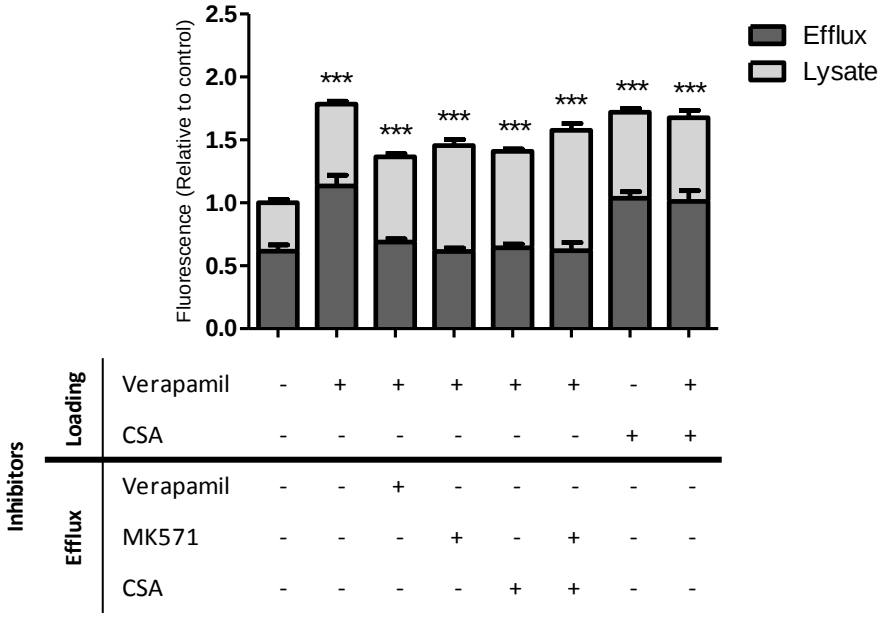

Inhibitor	Relevant proteins inhibited	
	Loading	Efflux
Verapamil	P-gp	MRP1
CSA	P-gp	MRP1, MRP2
MK571	-	MRP1, MRP2

Figure 7.8 – Confluent Huh7 cells analysed for calcein-AM uptake and calcein efflux. Cells were grown on 24-well plastic plates until confluent. Calcein-AM experiments were conducted as described in chapter 2 and chapter 8. Data shown is from three experiments with a total of nine replicates (N = 3, n = 9) and is displayed as mean ± SEM. Statistical analysis of total calcein levels (efflux plus lysate) was by one-way ANOVA with Dunnett's post test using values from cells loaded with calcein-AM alongside verapamil and no inhibitors in efflux as the control (first column). Selected data are compared in table 7.7. *** = $p < 0.001$.

Experiment 1		vs	Experiment 2		Significance	Calcein efflux in experiment 2
Loading	Efflux		Loading	Efflux		
Verapamil	-	vs	Verapamil	Verapamil	***	↓
Verapamil	-	vs	Verapamil	MK571	***	↓
Verapamil	-	vs	Verapamil	CSA	***	↓
Verapamil	Verapamil	vs	Verapamil	MK571	NS	-
Verapamil	Verapamil	vs	Verapamil	CSA	NS	-
Verapamil	CSA	vs	Verapamil	MK571	NS	-
Verapamil	CSA	vs	Verapamil	CSA, MK571	NS	-
Verapamil	MK571	vs	Verapamil	CSA, MK571	NS	-

Table 7.7 – Statistical analysis of efflux data from figure 7.8. Data for confluent Huh7 cells incubated with calcein-AM with or without inhibitors during loading and efflux were analysed to show the effect of efflux inhibition. Selected results are displayed. Statistical analysis of data was carried out using one-way ANOVA with Bonferroni's post-test. *** = $p < 0.001$, NS = not significant, ↓ = decrease.

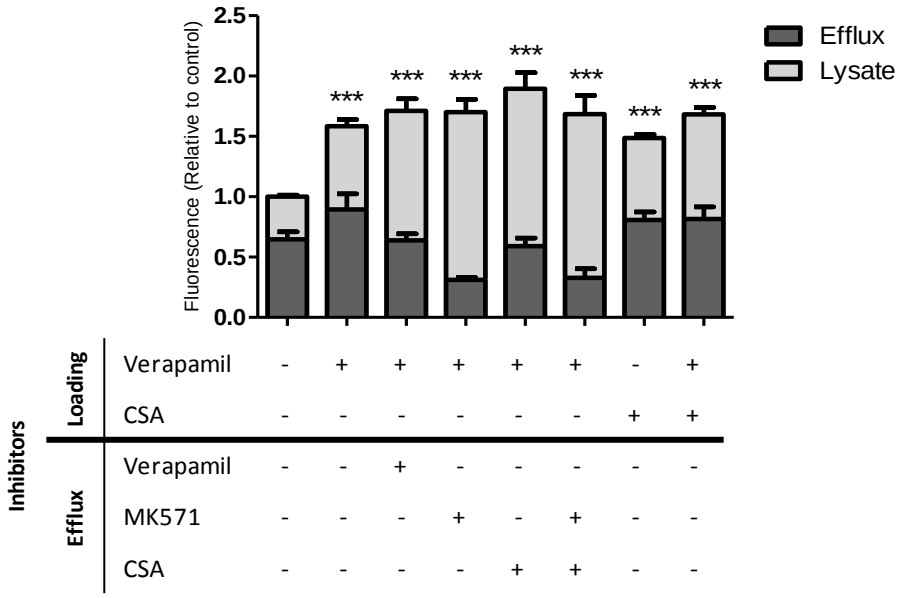

Inhibitor	Relevant proteins inhibited	
	Loading	Efflux
Verapamil	P-gp	MRP1
CSA	P-gp	MRP1, MRP2
MK571	-	MRP1, MRP2

Figure 7.9 – HepG2 cells treated for 15 days with 1% DMSO and analysed for calcein-AM uptake and calcein efflux. Cells were grown on 12-well plastic plates. Calcein-AM experiments were conducted as described in chapter 2 and chapter 8. Data shown are from five experiments with a minimum of eight total replicates (N = 5, n = 8) and is displayed as mean ± SEM. Statistical analysis of total calcein levels (efflux plus lysate) was by one-way ANOVA with Dunnett's post test using values from cells loaded with calcein-AM alongside verapamil and no inhibitors in efflux as the control (first column). Selected data are compared in table 7.8. *** = $p < 0.001$.

Experiment 1		vs	Experiment 2		Significance	Calcein efflux in experiment 2
Loading	Efflux		Loading	Efflux		
Verapamil	-	vs	Verapamil	Verapamil	NS	-
Verapamil	-	vs	Verapamil	MK571	***	↓
Verapamil	-	vs	Verapamil	CSA	*	↓
Verapamil	Verapamil	vs	Verapamil	MK571	NS	-
Verapamil	Verapamil	vs	Verapamil	CSA	NS	-
Verapamil	CSA	vs	Verapamil	MK571	NS	-
Verapamil	CSA	vs	Verapamil	CSA, MK571	NS	-
Verapamil	MK571	vs	Verapamil	CSA, MK571	NS	-

Table 7.8 – Statistical analysis of efflux data from figure 7.9. Data for DMSO-treatedHepG2 cells incubated with calcein-AM with or without inhibitors during loading and efflux were analysed to show the effect of efflux inhibition. Selected results are displayed. Statistical analysis of data was carried out using one-way ANOVA with Bonferroni's post-test. * = $p < 0.05$, *** = $p < 0.001$, NS = not significant, ↓ = decrease.

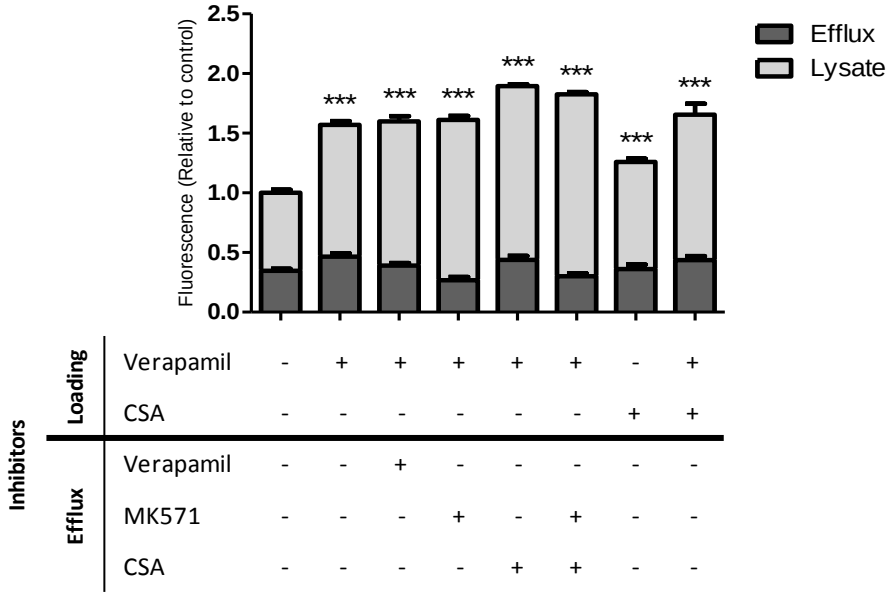

Inhibitor	Relevant proteins inhibited	
	Loading	Efflux
Verapamil	P-gp	MRP1
CSA	P-gp	MRP1, MRP2
MK571	-	MRP1, MRP2

Figure 7.10 – Huh7 cells grown untreated for 15 days and analysed for calcein-AM uptake and calcein efflux. Cells were grown on 24-well plastic plates. Calcein-AM experiments were conducted as described in chapter 2 and chapter 8. Data shown are from three experiments with a total of nine replicates (N = 3, n = 9) and is displayed as mean ± SEM. Statistical analysis of total calcein levels (efflux plus lysate) was by one-way ANOVA with Dunnett's post test using values from cells loaded with calcein-AM alongside verapamil and no inhibitors in efflux as the control (first column). Selected data are compared in table 7.9. *** = $p < 0.001$.

Experiment 1		vs	Experiment 2		Significance	Calcein efflux in experiment 2
Loading	Efflux		Loading	Efflux		
Verapamil	-	vs	Verapamil	Verapamil	NS	-
Verapamil	-	vs	Verapamil	MK571	***	↓
Verapamil	-	vs	Verapamil	CSA	NS	-
Verapamil	Verapamil	vs	Verapamil	MK571	NS	-
Verapamil	Verapamil	vs	Verapamil	CSA	NS	-
Verapamil	CSA	vs	Verapamil	MK571	**	↓
Verapamil	CSA	vs	Verapamil	CSA, MK571	*	↓
Verapamil	MK571	vs	Verapamil	CSA, MK571	NS	-

Table 7.9 – Statistical analysis of efflux data from figure 7.10. Data for prolonged untreated Huh7 cells incubated with calcein-AM with or without inhibitors during loading and efflux were analysed to show the effect of efflux inhibition. Selected results are displayed. Statistical analysis of data was carried out using one-way ANOVA with Bonferroni's post-test. * = $p < 0.05$, ** = $p < 0.01$, *** = $p < 0.001$, NS = not significant, ↓ = decrease.

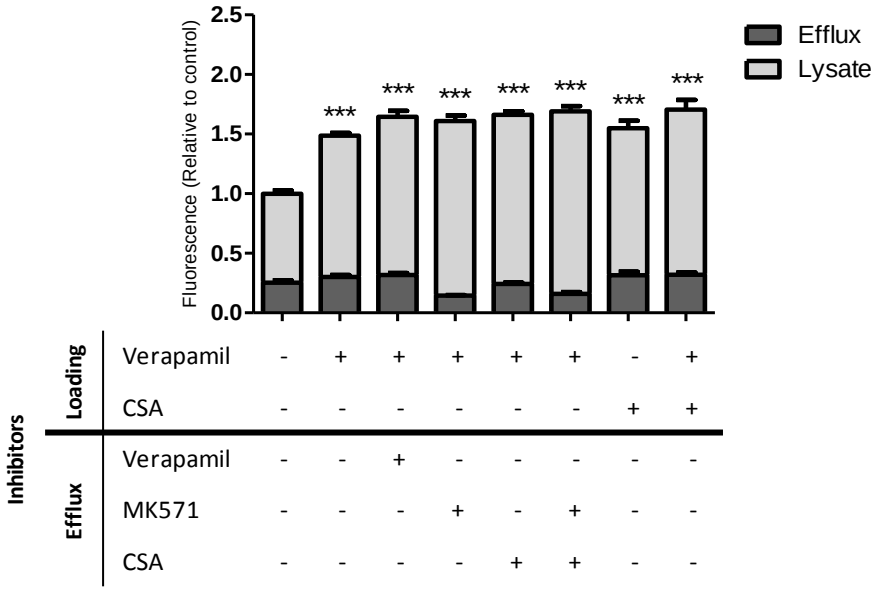

Inhibitor	Relevant proteins inhibited	
	Loading	Efflux
Verapamil	P-gp	MRP1
CSA	P-gp	MRP1, MRP2
MK571	-	MRP1, MRP2

Figure 7.11 – Huh7 cells treated for 15 days with 1% DMSO and analysed for calcein-AM uptake and calcein efflux. Cells were grown on 24-well plastic plates. Calcein-AM experiments were conducted as described in chapter 2 and chapter 8. Data shown are from three experiments with a total of nine replicates (N = 3, n = 9) and is displayed as mean ± SEM. Statistical analysis of total calcein levels (efflux plus lysate) was by one-way ANOVA with Dunnett's post test using values from cells loaded with calcein-AM alongside verapamil and no inhibitors in efflux as the control (first column). Selected data are compared in table 7.10. *** = $p < 0.001$.

Experiment 1		vs	Experiment 2		Significance	Calcein efflux in experiment 2
Loading	Efflux		Loading	Efflux		
Verapamil	-	vs	Verapamil	Verapamil	NS	-
Verapamil	-	vs	Verapamil	MK571	***	↓
Verapamil	-	vs	Verapamil	CSA	NS	-
Verapamil	Verapamil	vs	Verapamil	MK571	***	↓
Verapamil	Verapamil	vs	Verapamil	CSA	NS	-
Verapamil	CSA	vs	Verapamil	MK571	**	↓
Verapamil	CSA	vs	Verapamil	CSA, MK571	*	↓
Verapamil	MK571	vs	Verapamil	CSA, MK571	NS	-

Table 7.10 – Statistical analysis of efflux data from figure 7.11. Data for DMSO-treated Huh7 cells incubated with calcein-AM with or without inhibitors during loading and efflux were analysed to show the effect of efflux inhibition. Selected results are displayed. Statistical analysis of data was carried out using one-way ANOVA with Bonferroni's post-test. * = $p < 0.05$, ** = $p < 0.01$, *** = $p < 0.001$, NS = not significant, ↓ = decrease.

Chapter 8 – Detection of proteins by Western blotting

Chapter aim: To determine the absence or presence of selected proteins by Western blotting in confluent and DMSO-treated HepG2 and Huh7 cells. Results to be analysed in comparison to mRNA data to determine whether post-transcriptional regulation is affecting expression.

8.1 – Introduction

In this chapter results from Western blot processing of samples are displayed and analysed. The method for Western blotting using sodium dodecyl sulphate (SDS)-polyacrylamide gels was first developed by Burnette *et al.* (Burnette, 1981) and published in 1981. Despite being rejected for publication upon its first submission (Burnette, 2009), this technique was widely accepted and is utilised to this day for separation and identification of proteins, analysis of relative molecular mass and determination of relative abundance of proteins to name but a few applications. As the technique has been utilised, improvements and alterations to the initial methods have been suggested. These include choices to be made in every area including sample source, lysis conditions, separating and denaturing buffers, gel and membrane type, transfer method, blocking of the membrane post-transfer, polyclonal versus monoclonal antibodies, secondary antibody conjugation, detection method and quantification of protein. These variables will be briefly discussed here and the decisions made in terms of techniques used explained, followed by presentation and analysis of blots undertaken.

Lysis buffers and techniques vary according to the original sample source used; for example, a whole cell lysate will require a different extraction procedure to that of a tissue sample or a nuclear extract. Reagents can be included to aid in extraction of proteins from the membrane and cytoskeleton of the cell such as SDS, NP40 and Triton X-100, all of which are considered denaturing detergents. More stringent buffers such as RIPA (Radio Immuno Precipitation Assay) can be used to further disrupt protein-protein interactions for nuclear or mitochondrial extracts. However, the antibodies to be used must be taken into consideration at this early stage as some do not recognise denatured proteins, thus rendering a buffer containing, for example, SDS unsuitable. Another element which improves protein recovery is the addition of protease inhibitors to the lysis buffer, which halt the degradation of protein. An easy addition to this is to carry out sample lysis on ice or at 4^{o}C at all times, reducing the efficiency of the proteases. In these experiments a whole cell lysate was required. Lysis buffer, as described in appendix A, included SDS, NP40, DTT and protease inhibitors to aid in protein recovery and during protein extraction samples were kept at 4^{o}C or on ice at all times.

The antibodies to be used are an important factor to consider when preparing samples for gel loading. Antibodies raised against a short peptide sequence within the protein of interest identify a particular sequence of consecutive amino acids and require the protein to be denatured in order to have access to that epitope. However, other antibodies recognise an epitope only found in the 3D protein conformation – these require non-reducing conditions in both the lysis and sample loading buffers. As all antibodies used here required denaturing conditions (further information can be found in table 8.1), the loading buffer used was NuPAGE LDS sample buffer (Invitrogen) which is denaturing and is also slightly alkaline in pH, further contributing to ideal denaturing conditions. A 10x reducing agent containing 500 mM dithiothreitol (DTT) (Invitrogen) was also added to the sample loading mixture and the complete mixture was heated at 70^{o}C for 10 minutes.

While the use of pre-cast gels can be prohibitively expensive if a large number of blots are to be performed, they pose several advantages over self-made ones. Pre-cast gels of a single percentage are much more likely to have a consistent pore size throughout the gel, whereas ones made in the laboratory using acrylamide and bisacrylamide may set unevenly. Additionally, pre-cast gels using a percentage gradient, for example, ranging from 4-12% acrylamide, can be purchased to enable a variety of protein sizes to be separated efficiently on the same gel whereas in a self-made gel only a single percentage is easy to produce. In these experiments pre-cast NuPAGE Novex 4-12% Bis-Tris gels (Invitrogen) were utilised. Once samples have been loaded onto the gel they are separated by electrophoresis. This process requires a buffer, the components of which are another variable in Western blotting. Gel migration charts which demonstrate the likely migration of proteins with various gel and buffer combinations are widely available, especially for pre-cast gels and buffer systems purchased from the same supplier. These can be used as a guide when selecting reagents and conditions for different sized proteins. The vast majority of running buffers contain SDS to sustain the denatured state of the sample proteins; this is the case in the buffer used here which was NuPAGE MOPS-SDS running buffer, purchased from Invitrogen. A specific antioxidant (NuPAGE Antioxidant, Invitrogen) is available to use with this Invitrogen system which migrates down the gel with the sample, maintaining proteins in a reduced form during electrophoresis. This product is utilised only in this system as it is carried out at a lower pH than other gel systems and so is not effective under different conditions. Other substances can be included to maintain reduction in alternative gel systems such as DTT and β-mercaptoethanol; however, in a lower pH gel system such as is used here, these chemicals have a tendency to remain at the top of the gel rather than migrate with the sample. Electrophoresis voltages and times vary with equipment and gel or running buffer type and are

also dependent on the size of the protein to be detected; here a voltage of 200V was applied for 50-55 minutes when samples had migrated sufficiently for the range of proteins of interest.

Once electrophoresis has been carried out protein bands can be visualised on the gel itself or transferred to a membrane to enable the use of antibodies for more specific identification. A Coomassie stain is commonly used to visualise protein separation but involves precipitation of the proteins, which prevents further transfer of protein to a membrane. For this reason, Coomassie staining of a gel is generally carried out on a duplicate of the gel, allowing one gel to be continued through the blotting process, or after transfer of the separated proteins to a membrane to check transfer efficiency. Other commonly-used protein visualising stains include silver staining and fluorescent stains such as the SYPRO-Ruby and Coomassie Fluor-Orange techniques. Since the Western blotting protocol used was well established in our laboratory and sample volume was limited, gel staining for protein visualisation was not carried out. However, in the event that ladders and visualised bands did not appear to be separating correctly, protein visualisation using these techniques is a viable troubleshooting step. Transfer of the protein can be to either a nitrocellulose or a PVDF (polyvinylidene fluoride) membrane. Nylon membranes are not recommended for Western blotting as these tend to produce a very high background protein reading. Generally, background signals are lower on nitrocellulose membranes and these were used here as recommended by Licor, the manufacturer of the Odyssey system used here for detection of antibodies. Transfer of proteins can be conducted in either wet or semi-dry conditions. If large proteins are to be transferred it is preferable to use a wet transfer procedure; however, since the majority of proteins considered in this study were under 100 kDa in size the semi-dry method was used as it is considerably quicker than wet-blotting.

Once transfer of protein to the membrane has been achieved the membrane must be blocked to prevent indiscriminate binding of primary or secondary antibodies. Common examples of blocking agents are non-fat dry milk and BSA; however, with the Licor Odyssey detection system it is recommended to use a proprietary blocking buffer containing 0.1% sodium azide (Odyssey Blocking Buffer) to reduce background fluorescence. This has some additional advantages over using milk-based blocking solutions – the Odyssey buffer can be re-used and stored at $4^{o}C$ with or without antibodies in solution and it is useful when using anti-goat antibodies, as these have been known to react with milk-based reagents. Both primary and secondary antibodies can be applied to blocked membranes using milk or blocking buffer as a vehicle as appropriate.

Primary antibodies are available in polyclonal or monoclonal formats. Polyclonal antibodies are generated by injection of an antigen into an animal followed by collection and purification of

serum, whereas monoclonal antibodies are generated by clonal cells. Polyclonal antibodies have advantages as they can recognise multiple epitopes of an antigen, with the resultant signal amplification being especially useful for detection of low expression proteins. Production of polyclonal antibodies is much cheaper and less time consuming than that of monoclonal antibodies but the process can result in generation of less specific antibodies and high background signals. A further problem can be batch to batch variability, something which is not seen with monoclonal antibodies as once the production system is set up the cloned cells are guaranteed to produce the same antibody each time. However, this monoclonal specificity can be a disadvantage if the antibody fails to recognise epitopes with minor variations from the published amino acid sequence. In the experiments described here, a mixture of mono- and polyclonal antibodies were used (table 8.1).

Antibody incubation conditions and titre are extremely wide ranging, dependent on the antibody itself and the target sample among other things and will often require experimental determination; however, a starting dilution or range of concentrations will generally be suggested in the information sheet provided with the antibody by most manufacturers. Here, most primary antibodies were initially tested at 1:1000 dilution for a minimum of 1 hour at room temperature followed by an overnight incubation at 4^{o}C. The method of antibody visualisation depends on the marker molecule conjugated to the secondary antibody. Many laboratories use horseradish peroxidase (HRP) conjugated secondary antibodies as standard, which are usually visualised using photographic film or detected using a phosphor imager. A Licor Odyssey scanner which utilises fluorescently labelled secondary antibodies was used here to visualise bound proteins on the membrane. The conjugated labels are in the near infra-red range which provides advantages over traditional fluorescent probes as most biological systems produce little or no signal in this range, which reduces background signals and enhances assay sensitivity. A fluorescent system has some notable advantages over HRP, a major one being that two detection channels with different wavelengths are available, enabling simultaneous detection of two separate proteins providing they are labelled with different secondary antibodies with different fluorescent labels. This is very useful when measurement of both a reference and a target protein is required, for example in quantification of two similarly sized proteins. The Licor Odyssey also allows repeated scans with different intensities and sensitivities unique to each channel. Secondary antibodies utilised here were goat anti-mouse IgG (680LT labelled), donkey anti-rabbit IgG (680LT labelled) and donkey anti-goat IgG (800CW labelled) (Licor) and were applied at a dilution of 1:5000 for 1 hour at room temperature (detailed in table 8.2).

Several primary antibodies were tested for experimental use in the work described in this chapter. These included antibodies to proteins which have already been analysed for mRNA levels in previous chapters, specifically anti-BCRP (using BXP-21 antibody), transferrin and albumin; antibodies to the reference proteins GAPDH and actin and to the protein ADPGK (ADP-dependent glucokinase). A qPCR assay for ADPGK mRNA has not been developed or used here but it is a member of the key hexokinase family of enzymes in the liver which catalyse the phosphorylation of glucose to glucose-6-phosphate, the first step in glycolysis, thus the presence or absence of this protein would provide useful information on the maturation status of the cells. Measurement of protein levels of genes tested for previously by qPCR will indicate whether response patterns observed at the mRNA level are being replicated in protein production.

BCRP mRNA levels in both confluent and DMSO-treated HepG2 and Huh7 cells have previously been measured in chapters 3 and 5. In HepG2 cells BCRP mRNA levels at confluence were approximately 2- to 3-fold lower than those in liver, with DMSO-treatment for 15 days resulting in a small but significant decrease to roughly 70% of confluent levels. BCRP mRNA levels in confluent Huh7 cells were approximately 20- to 30-fold lower than those in liver and were not significantly different after DMSO-treatment. BCRP mRNA levels were also measured after induction with the ahryl hydrocarbon receptor (AhR) agonist beta-naphthoflavone (BNF) (chapter 6); results indicated no effect on BCRP mRNA level in confluent HepG2 cells, while DMSO-treated HepG2 cells responded to 10 µM BNF with an approximate doubling in BCRP transcripts. Confluent Huh7 cells showed significant induction of BCRP mRNA at both 1 and 10 µM BNF, while after DMSO-treatment significant induction was observed with all three BNF concentrations (1, 10 and 100 µM). Transferrin mRNA levels at confluence and after DMSO treatment were analysed in both HepG2 and Huh7 cells and were presented in chapters 3 and 4. Confluent HepG2 transferrin level was approximately 15-fold lower than liver, with DMSO treatment for 15 days producing an increase of approximately 6-fold over control. Confluent Huh7 transferrin level was approximately 11-fold lower than that in liver, while DMSO treatment for 15 days resulted in a significant increase to roughly 3- to 4-fold of control level.

8.2 – Methods

HepG2 and Huh7 cells were grown on 6-well plastic plates to confluence and subsequently treated for up to 20 days with 1% DMSO as previously described. Experimental layout for HepG2 and Huh7 cells is shown in figures 2.1 and 2.2 respectively. Protein extraction was carried out as described in chapter 2.7 and concentrations determined using Bradford reagent and read using a spectrometer at 595 nm. Precipitation and concentration of protein using

acetone was carried out where necessary as described in chapter 2.7. Western blotting was carried out using 20 µg of loaded protein per sample as described in chapter 2.7 with images generated using a Licor Odyssey and numerical densitometry data determined using ImageJ software (version 1.44p, http://imagej.nih.gov/ij). Serial dilutions of samples were carried out for all antibodies. Results for proteins of interest were normalised to the reference protein GAPDH or to a normalisation factor using both actin and GAPDH levels where applicable. Details of primary and secondary antibodies used can be seen in tables 8.1 and 8.2 respectively.

8.3 – Results

8.3.1 – Assessment of antibodies

Several antibodies were initially tested with protein extracted from confluent and 15 day DMSO treated HepG2 and Huh7 cells. Those which gave reliable and strong detection were BCRP (BXP-21, Abcam), ADPGK (Genetex), transferrin (TF, Genetex), actin (I-19, Santa Cruz) and GAPDH (Genetex); results using these antibodies are shown in figures 8.1-8.8. Other antibodies tried were UGT1A1 (1:30 dilution, D-16, Santa Cruz), MDR1 (1:100 dilution, C219, Abcam) and albumin (1:100 dilution, Abcam); unfortunately no bands could be detected with these antibodies even when using protein samples concentrated ten-fold over stocks. Membranes which failed to show signals with these antibodies were subsequently stripped using Restore Western Blot Stripping Buffer (Thermo Fisher Scientific, Illinois, USA) and probed with anti-GAPDH, which consistently produced strong bands with this antibody.

BCRP, ADPGK, TF, actin and GAPDH antibodies were tested against serial dilutions of stock protein (protein extracted from confluent cells) in order to determine the accuracy with which protein could be quantified both visually and numerically; results are shown in figures 8.1-8.3. The initial amount of protein loaded, 10 µl, is equal to approximately 20 µg of protein. Results from 1 in 2 serial dilutions of Huh7 protein from both confluent and 15 day DMSO treated cells probed with BCRP antibody are shown in figure 8.1. The image in part A displays results for the five dilutions of each protein sample, with the graph in part B showing semi-quantitative data extracted using ImageJ software. The band shown in the image was detected at around the 75 kDa marker; the predicted size for BCRP is 72.3 kDa, which indicates that this antibody is detecting the correct protein. The intensity of the band in the image appeared to decrease with increasing sample dilution and became very faint in the fifth, most dilute sample from confluent cells. The numerical data for these results mirrors this observed decrease with measured BCRP level decreasing with each dilution (figure 8.1 part B). Measurement of protein level was fairly accurate throughout the dilution series with numerical data approximately

halving with each dilution. This result leads to the conclusion that this antibody is likely to be correctly identifying BCRP and that levels can be accurately assessed throughout a range of dilutions.

Figure 8.2 shows results from 1 in 2 serial dilutions of confluent and 15 day 1% DMSO treated Huh7 cell lysates analysed with transferrin, ADPGK and GAPDH antibodies. The transferrin antibody detected three bands in Huh7 cells as shown in A and the magnified image – these included a doublet (TF bands 1 and 2) slightly higher than the 75 kDa molecular weight marker and an additional band at around 60-65 kDa (TF band 3). The expected molecular weight of transferrin is 77 kDa, indicating that the higher doublet contains the correct product. This lower band of the doublet (TF band 2) is not as clear in the lysates from confluent cells, however it is still faintly visible in the first sample dilution. This could indicate that this second band is more highly expressed with DMSO treatment, but normalisation to reference proteins would be required to substantiate this. As all three bands decrease similarly in intensity with increasing dilution it is possible that the lowest band at 60-65 kDa (band 3) is an alternatively spliced or degraded form of the protein or that some post-translational modification such as glycosylation, phosphorylation or modification of leading sequences and binding proteins has taken place. As it is reduced in line with decreased protein loading it could also be a non-specific protein being detected. For quantification purposes, the higher doublet (bands 1 and 2) was measured as separation of the two bands was difficult to accomplish accurately. Graph B shows data for TF protein levels; data did not quite half from dilution to dilution but a noticeable difference could be quantified, particularly in the more concentrated samples.

The molecular weight of ADPGK is 54 kDa and a very faint band of this size was seen on Western blots probed with anti-ADPGK antibody (figure 8.2 part A) in both protein samples, although it is more clearly visible in the 15 day DMSO treated cells. Since no normalisation to reference protein level has been conducted here, it cannot be concluded from this initial data whether this indicates a specific ADPGK increase or simply an overall increase in global protein. As only the more concentrated dilutions of each sample produced a clearly visible band, a high loading concentration was required for further experiments utilising this antibody. Numerical data (figure 8.2 part C) indicated that where bands were detected they could be accurately quantified with an approximate halving of protein being detected through the first three dilutions.

GAPDH has a molecular weight of 37 kDa and the anti-GAPDH antibody produced a very clear band of this size (figure 8.2 part A) in both samples at all dilutions tested which visibly lessened with each dilution. Numerical data (figure 8.2 part D) showed that between the first two dilutions GAPDH protein detected did not quite half but a noticeable lessening of protein to

approximately 65% was detected. However, with subsequent dilutions the detectable change in protein levels by numerical assessment was not as marked, indicating that a higher protein loading concentration is more suitable for this antibody.

Figure 7.3 shows results from 1 in 2 dilutions of confluent Huh7 cell lysates analysed with anti-actin and a 1:5000 dilution of the anti-GAPDH antibody. A more dilute anti-GAPDH antibody was assessed due to some smearing of bands detected with the previous 1:1000 dilution, as this can be an indicator of over-exposure. Actin has a molecular weight of approximately 43 kDa which matches with the band size observed in image A. The intensity of this band clearly diminished visibly with increasing sample dilution, which is also shown by numerical data in part B of figure 8.3 where each dilution shows approximately half the signal intensity of the previous dilution, with the exception of the final dilution where no band was detected. These data indicate that actin can be reliably quantified over a wide range of protein loading levels. A 1:5000 dilution of anti-GAPDH antibody detects a band at 37 kDa as was seen previously in figure 8.2. However, very little change was seen between dilutions (figure 8.3 part C) where halving of protein level was not seen between any pair of dilutions. This indicates that a 1:5000 dilution of GAPDH cannot be used to accurately quantify protein levels here and is less sensitive in terms of quantifying protein levels than the initial 1:1000 dilution used previously.

8.3.2 – Effect of DMSO on BCRP levels

Figure 8.4 shows results for BCRP levels in HepG2 and Huh7 cells at confluence and treated with 1% DMSO for up to 20 days. These membranes were also probed for the reference proteins actin and GAPDH to allow normalisation of numerical data with respect to protein loading differences and reveal potential increases in BCRP level. Part A of figure 8.4 clearly shows that the BCRP level in HepG2 lysates was quite low as the bands were not very strong. However, signal intensity at all time points was sufficient to gather numerical data. This was normalised to GAPDH levels and is presented in part B of the figure. This membrane was also probed with actin antibody, however, a faint band was only observed with the confluent cell sample and no actin detection was evident in protein extracts from DMSO treated cells, despite fairly strong GAPDH bands and evidence of BCRP expression in all samples. BCRP increased in comparison to confluence at all time points; approximately 4-fold and 7-fold increases were observed after 10 and 20 days of DMSO treatment respectively. However, the increase in BCRP after 15 days of treatment was lower than both of the other time points showing an increase of approximately 1.8-fold over the confluent cell sample.

Figure 8.4 also shows samples from Huh7 cells at confluence and after DMSO treatment assessed for levels of BCRP, actin and GAPDH. The membrane image in part A clearly shows

strong bands with all three antibodies with all samples. Both actin and GAPDH appeared to stay fairly constant from confluence throughout the DMSO treatment while the BCRP level looked higher in DMSO-treated samples than in confluent cell lysates. Data for BCRP normalised using a normalisation factor representative of both actin and GAPDH levels can be seen in part C of this figure. An increase in BCRP was observed in all DMSO-treated samples in comparison to confluent levels, with expression levels 4-fold, 5-fold and 7-fold higher than confluence in 10, 15 and 20 day DMSO-treated samples respectively. Both visual assessment of the membrane image and numerical data generated indicate that BCRP expression increased in a time-dependent manner with DMSO treatment.

Summary

- DMSO-treated HepG2 cells showed increases at all time points but they were not sustained at comparable levels, with the level at the 15 day time point much reduced from those at 10 and 20 days. Actin was only detected in the confluent sample.
- DMSO-treated Huh7 cells showed increased BCRP levels at all three DMSO treatment time points, which increased after each time point to a maximum of 6-fold over confluence.

8.3.3 – Effect of BNF on BCRP levels

Figure 8.5 shows results from lysates of confluent HepG2 and Huh7 cells treated with three concentrations of BNF and a control (experimental protocol as described previously (chapter 6.2)), which were then analysed using anti-BCRP, anti-actin and anti-GAPDH antibodies. Images obtained are shown in part A. BCRP level did not appear to increase from control in either cell line with BNF treatment with regard to the membrane image alone. Graphs B and C show results for HepG2 and Huh7 samples normalised to both actin and GAPDH. Neither cell line showed a consistent increase or decrease from control levels with BNF treatment.

Figure 8.6 shows results from lysates of HepG2 and Huh7 cells treated for 15 days with 1% DMSO and subsequently treated with three concentrations of BNF with a relevant control as described previously (chapter 6.2). Results from HepG2 cells (part A) revealed that neither GAPDH nor actin were detected in the control or 1 µM samples even though a BCRP signal was present. The gel electrophoresis, blotting and staining of these samples was conducted several times with each sample from each experiment showing the same outcome (n=6, N=2). Concentration of these two protein samples using acetone precipitation failed to reveal either actin or GAPDH protein at detectable concentrations. Consequently, normalisation could not be conducted for this experiment. BCRP level did appear to be higher in these samples than in

the 10 and 100 µM BNF treated samples but without a loading control it cannot be determined whether this was a true result or simply a global protein increase. BCRP, GAPDH and actin levels in Huh7 cells appeared to be fairly constant throughout BNF treatment. Graph B shows numerical data for BCRP levels in Huh7 cells normalised to both actin and GAPDH which revealed small decreases in BCRP in comparison to control with all concentrations of BNF.

Summary

- Neither HepG2 nor Huh7 cells showed an increase in BCRP protein with any concentration of BNF at confluence. Actin was only detected in the 100 µM sample.
- DMSO-treated Huh7 cells did not show increased expression of BCRP with any concentration of BNF. BCRP levels in DMSO-treated HepG2 cells could not be quantified accurately due to absence of GAPDH in some samples.

8.3.4 – Transferrin and ADPGK protein levels

Figure 8.7 displays results for lysates from HepG2 and Huh7 cells at confluence or treated for 10, 15 and 20 days with 1% DMSO and analysed with anti-transferrin, anti-actin and anti-GAPDH antibodies. HepG2 cells again did not respond well to the actin antibody and no bands were evident in these samples (part A). Although GAPDH and TF bands were present in all samples they varied in intensity. Numerical data for HepG2 TF levels normalised to GAPDH (part B) showed a 3.5-fold increase over confluence at 10 days which was not sustained at later time points; after 15 and 20 days of DMSO treatment TF levels were decreased in comparison to the confluent sample. All three proteins were detected in Huh7 samples. Data were normalised to GAPDH and actin levels (part C) and showed a TF level after 10 days which was approximately equal to confluent cells, decreasing after 15 and 20 days to approximately 75% and 25% of the confluent level respectively. Interestingly, the lower 60-65 kDa band seen with the TF antibody in Huh7 cells was not detected in HepG2 cells indicating that it could be a variant of the protein or non-specific binding seen solely in these Huh7 cells.

Figure 8.8 shows results for lysates from HepG2 and Huh7 cells at confluence or after treatment for 10, 15 and 20 days with 1% DMSO and analysed with anti-ADPGK, anti-actin and anti-GAPDH antibodies. As observed previously, HepG2 samples did not display uniform expression when exposed to the actin antibody; in this case actin was only seen clearly in confluent cells. Although GAPDH was detected in all HepG2 samples, ADPGK was only present in confluent cells, indicating a loss of expression of ADPGK at protein level with DMSO treatment in HepG2 cells. All three proteins were detected in Huh7 cell lysates; results for ADPGK normalised to actin and GAPDH are shown in graph B and show no large change from

control at 10 and 15 days of treatment, with a reduction to approximately 75% of confluent levels after 20 days of DMSO treatment. An additional band was visible in the confluent HepG2 and 20 day DMSO treated Huh7 samples between those for ADPGK and actin – this could indicate a different form or alternative processing of ADPGK under certain conditions or could be the result of antibody detection of non-specific protein.

Summary

- HepG2 transferrin levels appeared to increase only after 10 days of DMSO treatment; however, some bands were very faint and data was difficult to extract from the blot. No actin was detected on the blot.
- Transferrin levels in DMSO-treated Huh7 cells were stable after 10 days of DMSO treatment but decreased steadily at the two time points afterwards.
- ADPGK expression in HepG2 cells was only apparent in confluent cells and was not observed with any DMSO treatment. GAPDH expression also decreased in the three DMSO samples, while actin expression was only apparent in confluent HepG2 cells.
- ADPGK expression in Huh7 cells remained fairly stable with DMSO treatment and both actin and GAPDH expression was strong and consistant.

8.4 – Discussion

The work described in this chapter has confirmed the presence of BCRP, ADPGK and transferrin protein in confluent HepG2 and Huh7 cells and attempted to quantify the changes in protein expression in response to 1% DMSO treatment for up to 20 days. Changes in BCRP levels in response to BNF treatment both at confluence and after 15 days DMSO pre-treatment were quantified where possible in both cell lines. However, variations in protein level in response to treatment could not always be successfully measured due to expression of certain proteins being absent with certain treatments. The findings and limitations encountered during this work are discussed below.

Initially it was intended to analyse data from these experiments in a similar way to that used previously for qPCR analysis – two reference genes/proteins would be measured and a normalisation factor would be derived from these data to allow more accurate representation of the data for the expression of the protein in question. Anti-GAPDH and anti-actin antibodies were applied to blotted lysates from both cell lines in order to apply this technique. However, a major impediment to data analysis was soon discovered with the lack of actin detection in some HepG2 cells, mainly those which had received a DMSO treatment. In the majority of

HepG2 samples GAPDH could still be detected and so normalisation to one reference protein was possible. However, in a limited number of samples neither GAPDH nor actin was detected – in this case, no normalisation of protein level was possible and so loading differences could not be accounted for which would make any analysis of the target protein alone questionable.

The lack of actin detection in the majority of DMSO-treated HepG2 samples is unexplained, as actin is an integral protein involved in cell structure and motility which should be present in all cells. Actin is commonly used as a loading control for Western blotting as it should show stable expression. Additionally, the anti-actin antibody used here detects several different isoforms of the protein; considering this and the fact that actin was detected in some HepG2 samples, it is unlikely that HepG2 cells are expressing an undetectable isoform of the protein. It is possible that the protein was lost during the extraction process; however, protein was extracted from HepG2 and Huh7 cells simultaneously using the same methodology and solutions, and produced consistent yields of total protein as estimated via the Bradford assay. Since actin has been reliably detected in all Huh7 samples regardless of growth stage or treatment, it seems unlikely that this specific protein could be lost during sample processing for one cell line and not another. As the majority of HepG2 lysates lacking actin expression did show GAPDH and/or target protein expression, a general absence or loss of protein does not explain the lack of actin detected.

A literature search investigating whether similar issues had occurred in other groups looking at prolonged exposure of cells to DMSO or loss of actin mRNA or protein expression in general yielded few results. A paper published in 1983 by Farmer *et al.* (Farmer *et al.*, 1983) showed that in suspended mouse fibroblast cells (3T3 line) the amount of actin detected fell from 12% to 6% of total cellular protein in comparison to fibroblasts grown in contact with a surface. This change in actin protein occurred independently of actin mRNA levels which remained constant in attached and suspended cells, only increasing once cells in suspension were re-introduced to a contact-culture system. Another paper by the same group in 1988 looked at cytoskeletal mRNA and protein including that of actin in primary rat hepatocyte cultures (Ben-Ze'ev *et al.*, 1988). Results here indicated that growth conditions using matrigel promoted expression of liver-specific mRNA and proteins whilst simultaneously reducing expression of cytoskeletal proteins including actin. However, although actin decreases were observed, complete absence of expression as seen in some HepG2 samples here was not apparent. Nishimura *et al.* (Nishimura *et al.*, 2008) observed that in C2C12 myotubes (derived from mouse skeletal muscle) treated with concentrations of up to 2.5% DMSO for up to 24 hours, β-actin mRNA expression decreased significantly in comparison to an untreated control. Indeed, significant decreases were also observed with 2.5% DMSO treatment for 4 and 8 hours, and with 0.5%

DMSO treatment for 24 hours. This publication also described results from the same experiments measuring GAPDH mRNA expression and found no significant differences from control with any concentration of DMSO after 24 hours of treatment. However, no protein analysis was undertaken so it remains unknown whether this change in actin mRNA translated directly to similar changes in protein level. It is also unknown whether these changes in different systems are relevant to hepatic cells.

Several publications using mouse, rat and human hepatocytes have shown that actin is present at a constant and stable level (Caja *et al.*, 2011; Glaros *et al.*, 2010; Shay and Hagen, 2009; Gkretsi *et al.*, 2007); two of these in particular show stable actin protein expression in both highly differentiated and more de-differentiated hepatocytes (Caja *et al.*, 2011; Glaros *et al.*, 2010). Glaros *et al.* (Glaros *et al.*, 2010) also showed strong actin protein expression in HepG2 cells. Of the papers published where Western blotting or qPCR analysis have been used in cells which have been treated for prolonged periods of time with 1% DMSO, many have opted for alternatives to actin as either a protein or cDNA reference gene. However, there is no mention of whether this is because problems were encountered using actin or because other traditional reference genes such as 18S or GAPDH were utilised with no need to also measure actin. For example, many of the publications regarding the cell line HepaRG, which requires a 2% DMSO treatment for two weeks to aid differentiation, utilise qPCR with normalisation to the reference gene 18S (Antherieu *et al.*, 2010; Dumont *et al.*, 2010a; Dumont *et al.*, 2010b; Le Vee *et al.*, 2010; Tuoi Do *et al.*, 2010; Le Vee *et al.*, 2006). Prolonged 1% DMSO treatment of Huh7 cells was carried out by Choi *et al.* (Choi *et al.*, 2009) where analysis used qPCR with β-actin as the reference gene. This publication reported no unusual or adverse effects on actin expression at mRNA level, which agrees with results observed here where no disproportionate decrease or absence of actin protein expression was observed in any of the DMSO-treated Huh7 samples.

Overall, no evidence has been reported previously that any growth condition or treatment, including DMSO, has resulted in compete loss of actin expression in a cell system as appears to have occurred in some HepG2 samples here. It may be that the effect observed here is a previously undiscovered effect of prolonged DMSO treatment on certain cell types; as observed by Hewitt and Hewitt in HepG2 cells (Hewitt and Hewitt, 2004), not all cells given the same name will remain identical due to differences in tissue culture regimes and extended passaging. It is also possible that there simply was not enough actin protein present in the HepG2 samples to be detected by Western blotting and a more sensitive technique is required, although fluorescent detection is one of the most sensitive methods of detecting blotted proteins.

Serial dilutions of protein samples revealed that less dilute samples produced the most reliable results in terms of detecting protein reduction with all of the tested antibodies, therefore in all subsequent experiments 20 μg of protein was loaded onto the gel. Detection of BCRP in confluent and DMSO-treated cells showed an increase in protein level with DMSO after normalisation to reference proteins in both HepG2 and Huh7 samples at all time points, although to a lesser extent in the 15 day DMSO-treated HepG2 sample. This is in contrast to mRNA levels displayed previously in chapter 5 (figures 5.3 and 5.4 part D, HepG2 and Huh7 respectively), which showed significant decreases from control in BCRP mRNA level in DMSO treated HepG2 cells, and remained unchanged in Huh7 cells. The lack of correlation between BCRP mRNA and protein levels indicates that the apparent increase in protein level is probably due to a post-transcriptional mechanism stimulated or initiated by DMSO. Post-transcriptional regulation of BCRP has been observed previously in rat intestinal cells where a reduction in protein after organ damage was not mirrored by a similar mRNA reduction (Ogura *et al.*, 2008), and in MCF-7 cells after oestrogen treatment (Imai *et al.*, 2005). Pan *et al.* (Pan *et al.*, 2009) reported that micro-RNAs (miRNAs) could successfully be used to inhibit expression of BCRP protein at a post-transcriptional level via modification of the 3'-UTR section of the transcript. Since miRNAs are expressed at certain developmental stages or in response to cellular stress, it is feasible to consider that DMSO treatment could be contributing to the lack of co-ordination between mRNA and protein levels due to both stress and the attempted push towards a more differentiated cell model.

Neither cell line showed a sustained increase in BCRP when cells were treated with BNF at confluence. Previous data from chapter 6 (figures 6.5 and 6.6 part A, HepG2 and Huh7 respectively) showed that mRNA levels of BCRP in BNF treated HepG2 and Huh7 cells were consistently higher than control if not always significant. With a DMSO pre-treatment the BNF effect on BCRP protein level in HepG2 cells could not be measured due to the apparent lack of GAPDH and actin expression which persisted even after sample concentration. However, looking at the BCRP band alone does not indicate that expression increased with BNF treatment. Pre-treatment of Huh7 cells with DMSO followed by BNF treatment did not result in any changes in BCRP protein; previous data from chapter 6 (figure 6.6 part B) indicated that significant increases in BCRP mRNA occurred with all three BNF concentrations. The reduced effect of the BCRP inhibitor Ko143 in treated Huh7 cells could indicate that BCRP levels have decreased with prolonged growth with and without DMSO in comparison to confluence (figures 7.3-5); however, Western blotting of BCRP protein in 15 day DMSO-treated Huh7 cells revealed an increase compared to confluent Huh7 cells. Again, these results for BCRP protein and mRNA expression do not correlate and indicate that some form of post-transcriptional regulation is occurring within each cell line, both at confluence and after DMSO treatment.

Alternatively, as both Huh7 and to a lesser extent HepG2 did show increased levels of BCRP protein in Western blots, this could point towards the reduced inhibition of BCRP seen in DMSO-treated Huh7 cells being a result of increased transporter levels which were not inhibited as completely as in confluent Huh7 cells. Following this, it is possible that an increase in P-gp protein is responsible for the reduced ability of both verapamil and CSA to inhibit Hoechst efflux in DMSO-treated cells.

In a more differentiated hepatic state TF levels would be expected to increase. However, the only TF increase observed was unsustained and occurred after 10 days of DMSO treatment in HepG2 cells; this was followed by levels lower than control at subsequent time points. No increase in TF protein was observed in Huh7 samples. Previous assessment of TF mRNA in DMSO-treated cells revealed that substantial increases were seen after 15 and 20 days of treatment in both cell lines (figures 4.5 and 4.6). As observed with previous results for BCRP, it could be that some form of post-transcriptional regulation of TF is taking place. Alternatively, since TF is secreted from the cell it is possible that any increase in protein production cannot be detected due to the excess protein being transported out of the cell (Zakin, 1992).

ADPGK plays a role in glycolysis, a key function of the liver. An increase in this protein would indicate a more mature cell type – unfortunately, this was not observed in either HepG2 or Huh7 cells. ADPGK was detected in confluent HepG2 cells along with both actin and GAPDH but expression of both ADPGK and actin decreased to an undetectable level or were absent from DMSO-treated cells, indicating a less hepatocyte-like profile in terms of ADPGK expression. Although Huh7 cells did express ADPGK throughout DMSO treatment, no increase indicative of a more mature hepatic profile was observed. The detection of a lower molecular weight band at approximately 45-50 kDa in the confluent HepG2 and 20-day DMSO-treated Huh7 samples may point towards an alternative form of the protein being detected, for example if cleaving of a leader sequence has occurred. It could also point towards some non-reduced protein or modifications such as glycosylation remaining in the sample, although why this would occur in some samples and not others when all were treated identically is unclear.

Overall, results from this chapter indicate no differentiation of cells towards a more hepatic profile in DMSO-treated cells in terms of increased transferrin or ADPGK expression. Although increased BCRP protein expression was detected with DMSO treatment, no increase in mRNA transcripts was detected in matching samples. However, data comparing mRNA levels of liver to confluent HepG2 and Huh7 cells did indicate that liver levels of BCRP are increased over those observed in these cell lines at confluence, so an increase in BCRP protein may be a positive indication of a more hepatocyte-like profile in some aspects of the cellular profile. Conversely, where BNF initiated an increase in BCRP mRNA levels it failed to increase protein

levels both with and without DMSO treatment. These results point strongly towards post-transcriptional modifications being a major factor in the expression of BCRP rather than being driven mainly by levels of mRNA expression.

Antibody	Company/ Number	Peptide	Host species	Antigen species	Cross-reactivity	Mono/polyclonal	Dilution	Incubation	Predicted size
Actin (I-19)	Santa Cruz (sc-1616)	Region within the C-terminus of human actin (detects a broad range of isoforms)	Goat	Human	Mouse, rat, human, zebrafish, C. elegans, drosophila and xenopus	Polyclonal	1:2000	3 hours at room temperature	43 kDa
ADPGK	Genetex (GTX106029)	Region within amino acids 103 and 493 of human ADPGK	Rabbit	Human	None known	Polyclonal	1:500	1 hour at room temperature followed by overnight at 4^{o}C	54 kDa
BCRP (BXP-21)	Abcam (ab3380)	Fusion of E. Coli maltose binding protein and amino acids 271 to 396 of human BCRP	Mouse	Human	None known	Monoclonal	1:50	1 hour at room temperature followed by overnight at 4^{o}C	72.3 kDa
GAPDH	Genetex (GTX100118)	Region within amino acids 134 and 145 of human GAPDH	Rabbit	Human	Zebrafish	Polyclonal	1:1000	1 hour at room temperature	36 kDa
Transferrin	Genetex (GTX101035)	Region within amino acids 339 and 638 of human transferrin	Rabbit	Human	None known	Polyclonal	1:500	1 hour at room temperature followed by overnight at 4^{o}C	77 kDa

Table 8.1 – Primary antibodies used for the detection of protein in Western blots. This table includes technical details for all primary antibodies used to successfully detect protein after Western blotting of lysate samples alongside dilution factors and incubation durations utilised in these experiments.

Antibody	Company	Host species	Antigen species	Label	Dilution	Incubation
Anti-rabbit secondary	Licor	Donkey	Rabbit	680LT (red)	1:5000	1 hour at room temperature
Anti-mouse secondary	Licor	Goat	Mouse	680LT (red)	1:5000	1 hour at room temperature
Anti-goat secondary	Licor	Donkey	Goat	800CW (green)	1:5000	1 hour at room temperature

Table 8.2 – Secondary antibodies used for the detection of protein in Western blots. This table includes technical details for all secondary antibodies used to successfully detect protein after Western blotting of lysate samples alongside dilution factors and incubation durations utilised in these experiments.

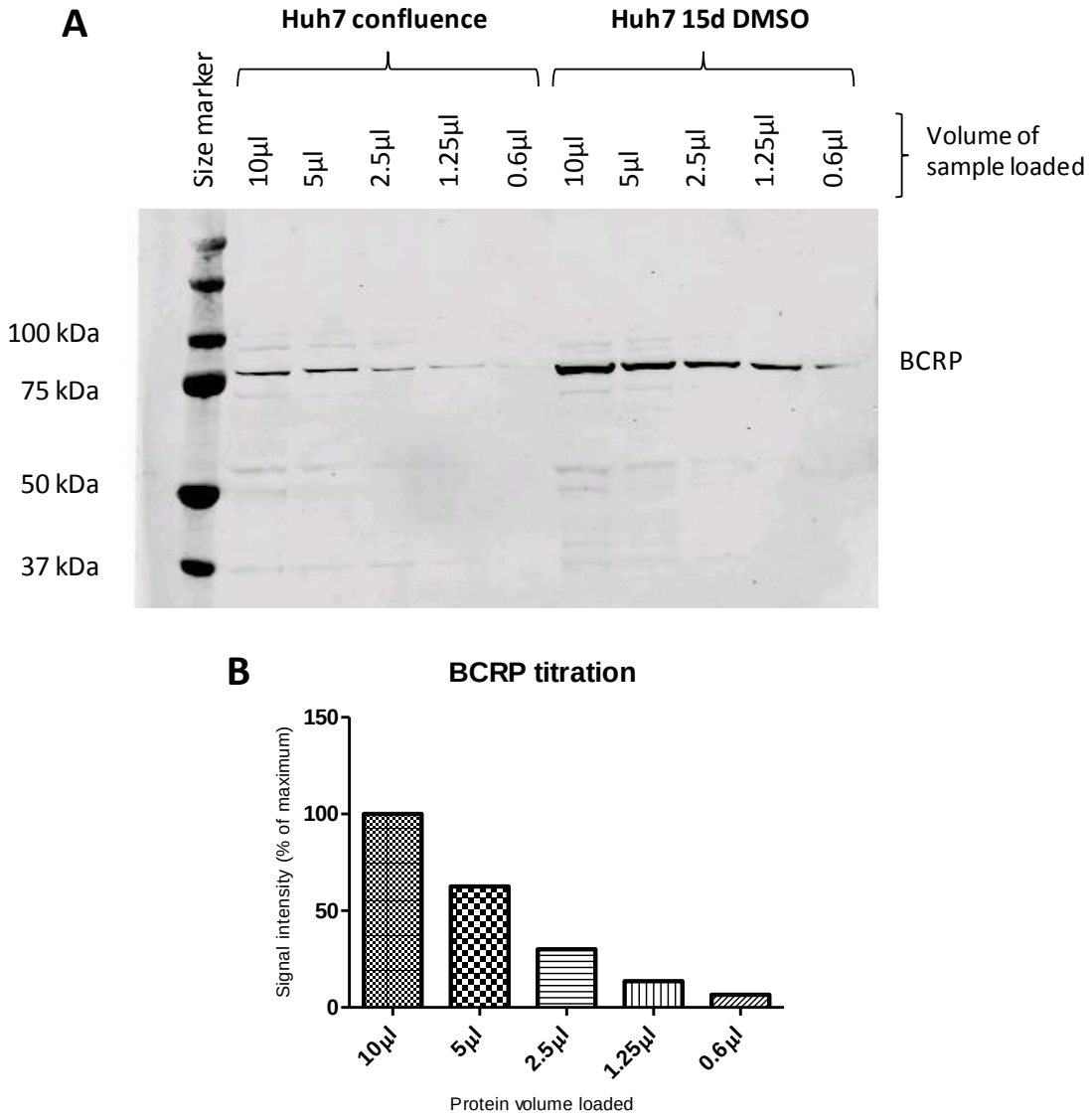

Figure 8.1 – Titration of sample for Western blot analysis using anti-BCRP. Protein was extracted from Huh7 cells at confluence and after 15 days of treatment with 1% DMSO as described in chapter 2.7. Samples were prepared, serially diluted, separated by electrophoresis, transferred to nitrocellulose membrane and incubated with a 1:50 dilution of anti-BCRP (Abcam, USA), followed by a 1:5000 incubation with goat anti-mouse IgG secondary antibody (Licor). The image (A) was captured using a Licor Odyssey scanner and analysed with ImageJ software, generating the displayed graphical data (B). Data displayed is the mean of serial dilutions from both samples with the first sample in each set given a value of 100%. Data is representative of two serial dilutions for each sample.

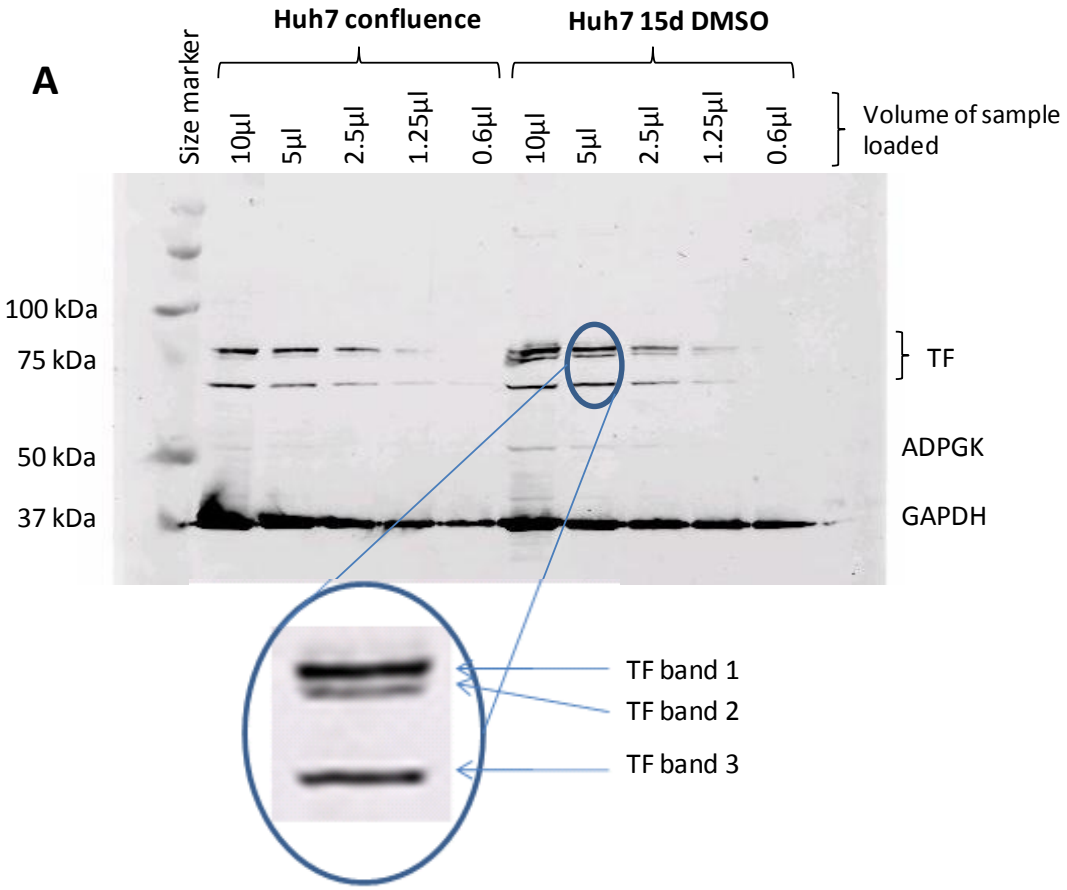
A
Huh7 confluence
Huh7 15d DMSO
Size marker
10µl
5µl
2.5µl
1.25µl
0.6µl
10µl
5µl
2.5µl
1.25µl
0.6µl
Volume of sample loaded
100 kDa
75 kDa
50 kDa
37 kDa
TF
ADPGK
GAPDH
TF band 1
TF band 2
TF band 3

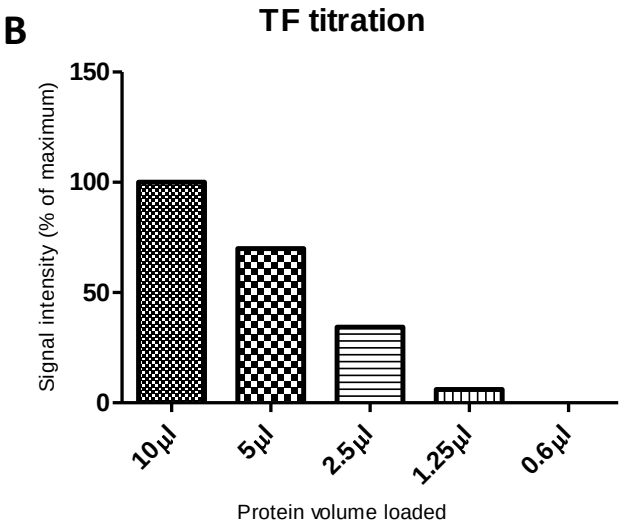
B
TF titration
Signal intensity (% of maximum)
150
100
50
0
10µl
5µl
2.5µl
1.25µl
0.6µl
Protein volume loaded

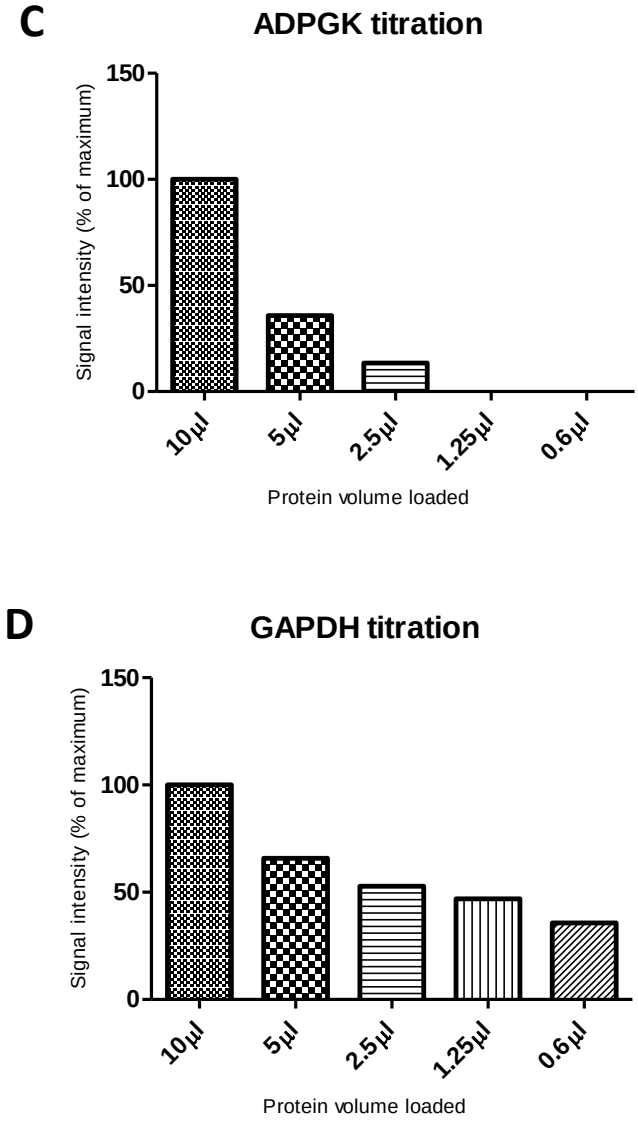

Figure 8.2 – Titration of sample for Western blot analysis using anti-transferrin, anti-ADPGK and anti-GAPDH. Protein was extracted from Huh7 cells at confluence and after 15 days of treatment with 1% DMSO as described in chapter 2.7. Samples were prepared, serially diluted, separated by electrophoresis, transferred to nitrocellulose membrane and incubated with the antibodies transferrin, ADPGK and GAPDH (Genetex, USA) at dilutions of 1:500 (TF), 1:1000 (GAPDH) and 1:500 (ADPGK), followed by a 1:5000 incubation with donkey anti-rabbit IgG secondary antibody (Licor). The image (A) was captured using a Licor Odyssey scanner and analysed with ImageJ software, generating the displayed graphical data (B, C and D). Data displayed is the mean of serial dilutions from both samples with the first sample in each set given a value of 100%. Data is representative of two serial dilutions for each sample.

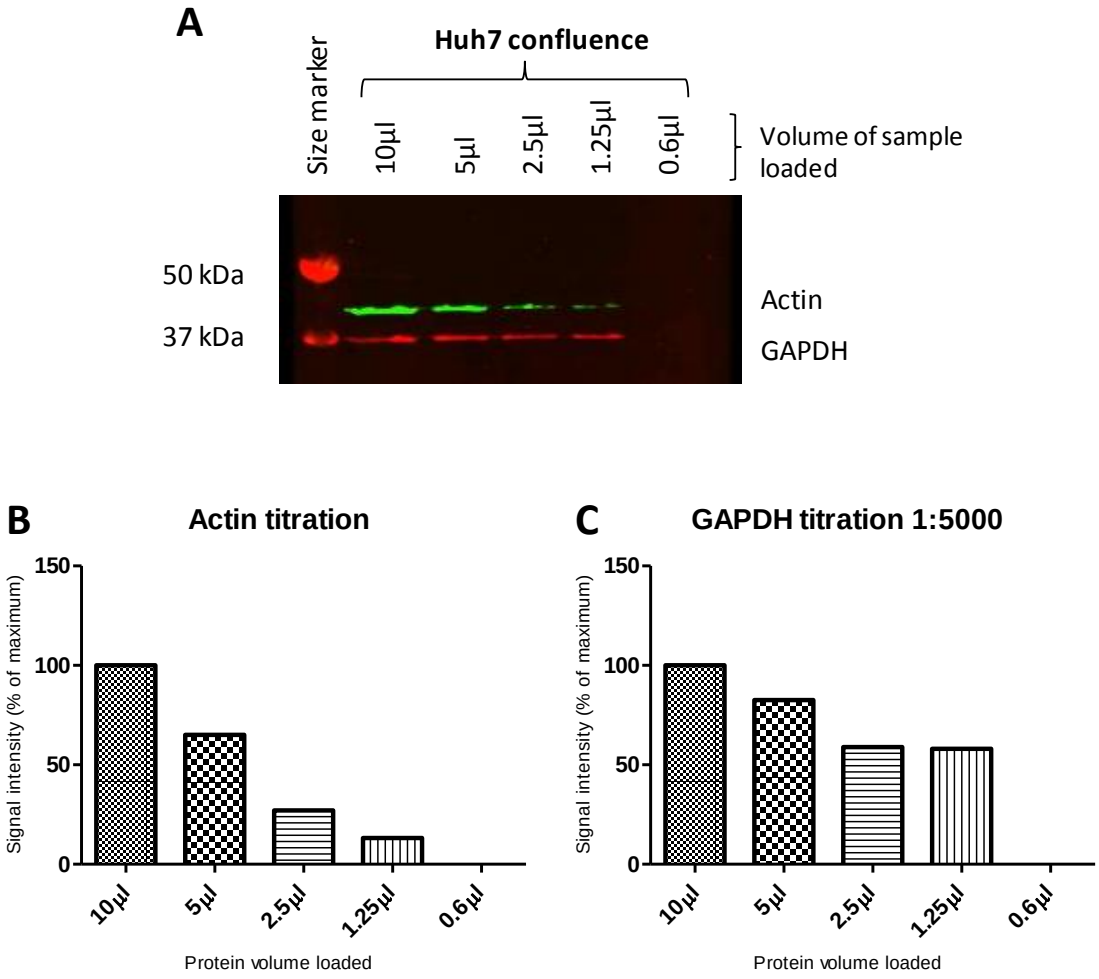

Figure 8.3 – Titration of sample for Western blot analysis using anti-actin and anti-GAPDH. Protein was extracted from Huh7 cells at confluence as described in chapter 2.7. Samples were prepared, serially diluted, separated by electrophoresis, transferred to nitrocellulose membrane and incubated with the antibodies actin (Santa Cruz, USA) and GAPDH (Genetex, USA) at diltuions of 1:5000 (GAPDH) and 1:2000 (actin), followed by a 1:5000 incubation with donkey anti-rabbit IgG secondary antibody (GAPDH) and donkey anti-goat IgG secondary antibody (actin) (Licor). The image (A) was captured using a Licor Odyssey scanner and analysed with ImageJ software, generating the displayed graphical data (B and C). Data is representative of two serial dilutions for the sample.

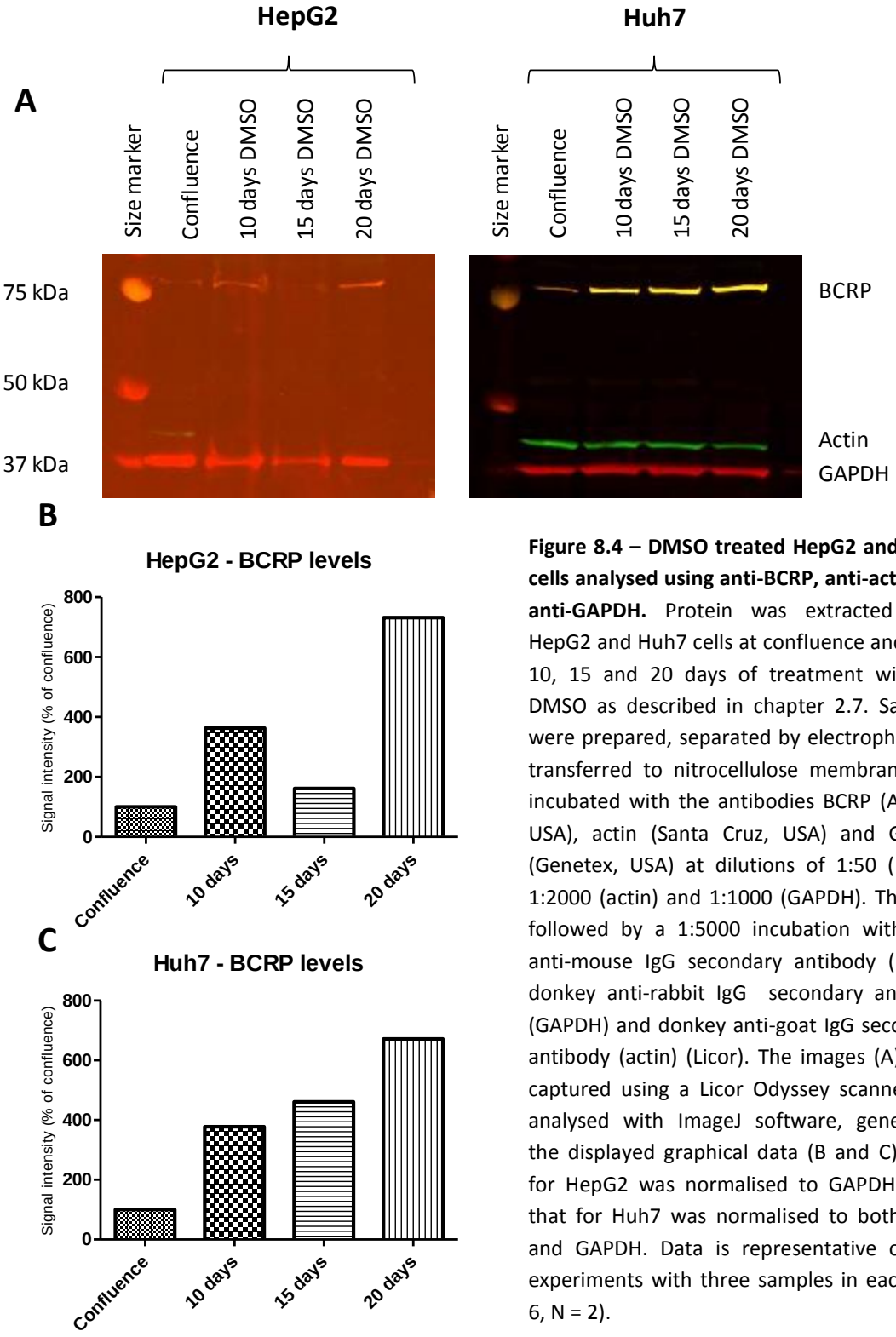

Figure 8.4 – DMSO treated HepG2 and Huh7 cells analysed using anti-BCRP, anti-actin and anti-GAPDH. Protein was extracted from HepG2 and Huh7 cells at confluence and after 10, 15 and 20 days of treatment with 1% DMSO as described in chapter 2.7. Samples were prepared, separated by electrophoresis, transferred to nitrocellulose membrane and incubated with the antibodies BCRP (Abcam, USA), actin (Santa Cruz, USA) and GAPDH (Genetex, USA) at dilutions of 1:50 (BCRP), 1:2000 (actin) and 1:1000 (GAPDH). This was followed by a 1:5000 incubation with goat anti-mouse IgG secondary antibody (BCRP), donkey anti-rabbit IgG secondary antibody (GAPDH) and donkey anti-goat IgG secondary antibody (actin) (Licor). The images (A) were captured using a Licor Odyssey scanner and analysed with ImageJ software, generating the displayed graphical data (B and C). Data for HepG2 was normalised to GAPDH while that for Huh7 was normalised to both actin and GAPDH. Data is representative of two experiments with three samples in each (n = 6, N = 2).

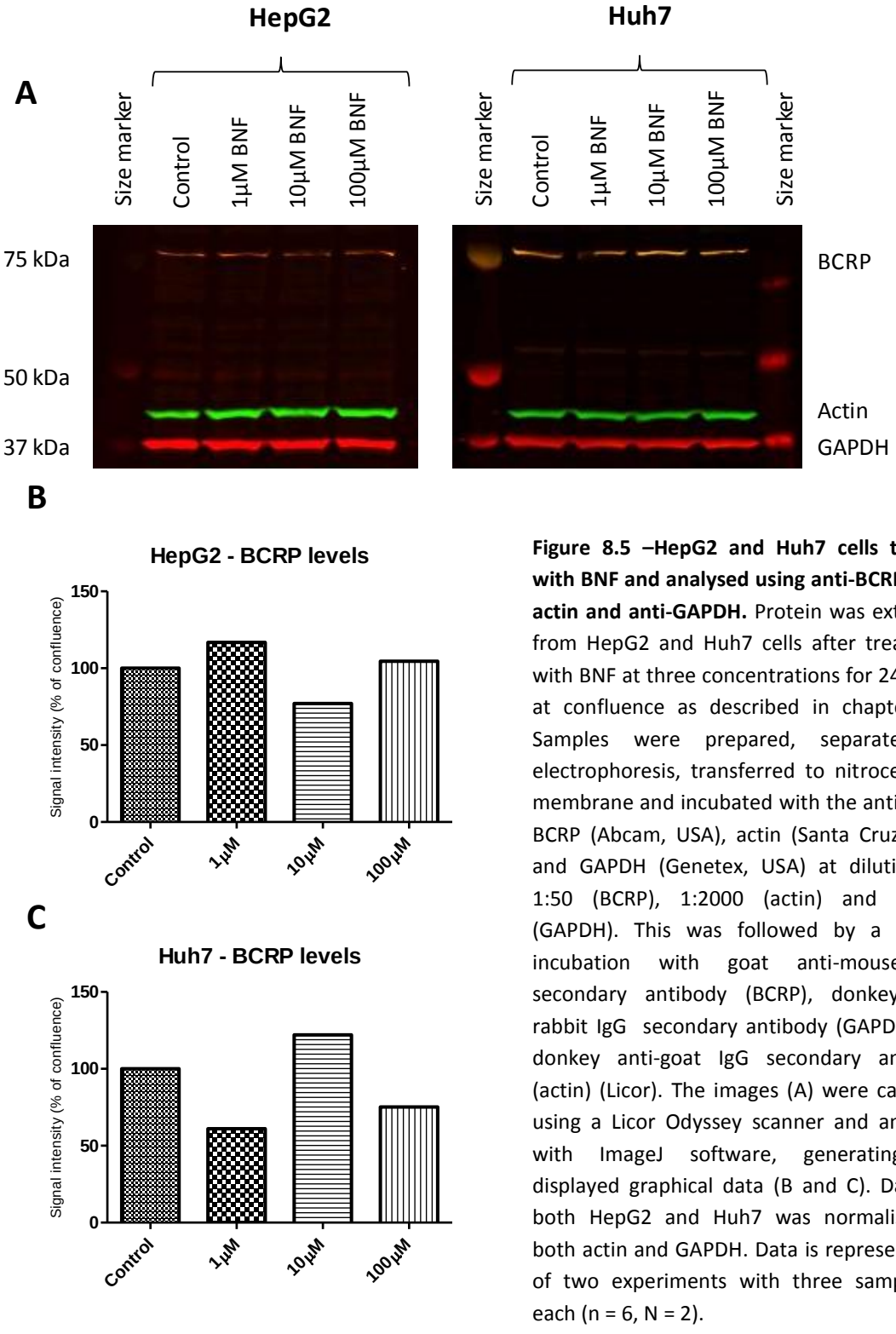

Figure 8.5 –HepG2 and Huh7 cells treated with BNF and analysed using anti-BCRP, anti-actin and anti-GAPDH. Protein was extracted from HepG2 and Huh7 cells after treatment with BNF at three concentrations for 24 hours at confluence as described in chapter 2.7. Samples were prepared, separated by electrophoresis, transferred to nitrocellulose membrane and incubated with the antibodies BCRP (Abcam, USA), actin (Santa Cruz, USA) and GAPDH (Genetex, USA) at dilutions of 1:50 (BCRP), 1:2000 (actin) and 1:1000 (GAPDH). This was followed by a 1:5000 incubation with goat anti-mouse IgG secondary antibody (BCRP), donkey anti-rabbit IgG secondary antibody (GAPDH) and donkey anti-goat IgG secondary antibody (actin) (Licor). The images (A) were captured using a Licor Odyssey scanner and analysed with ImageJ software, generating the displayed graphical data (B and C). Data for both HepG2 and Huh7 was normalised to both actin and GAPDH. Data is representative of two experiments with three samples in each (n = 6, N = 2).

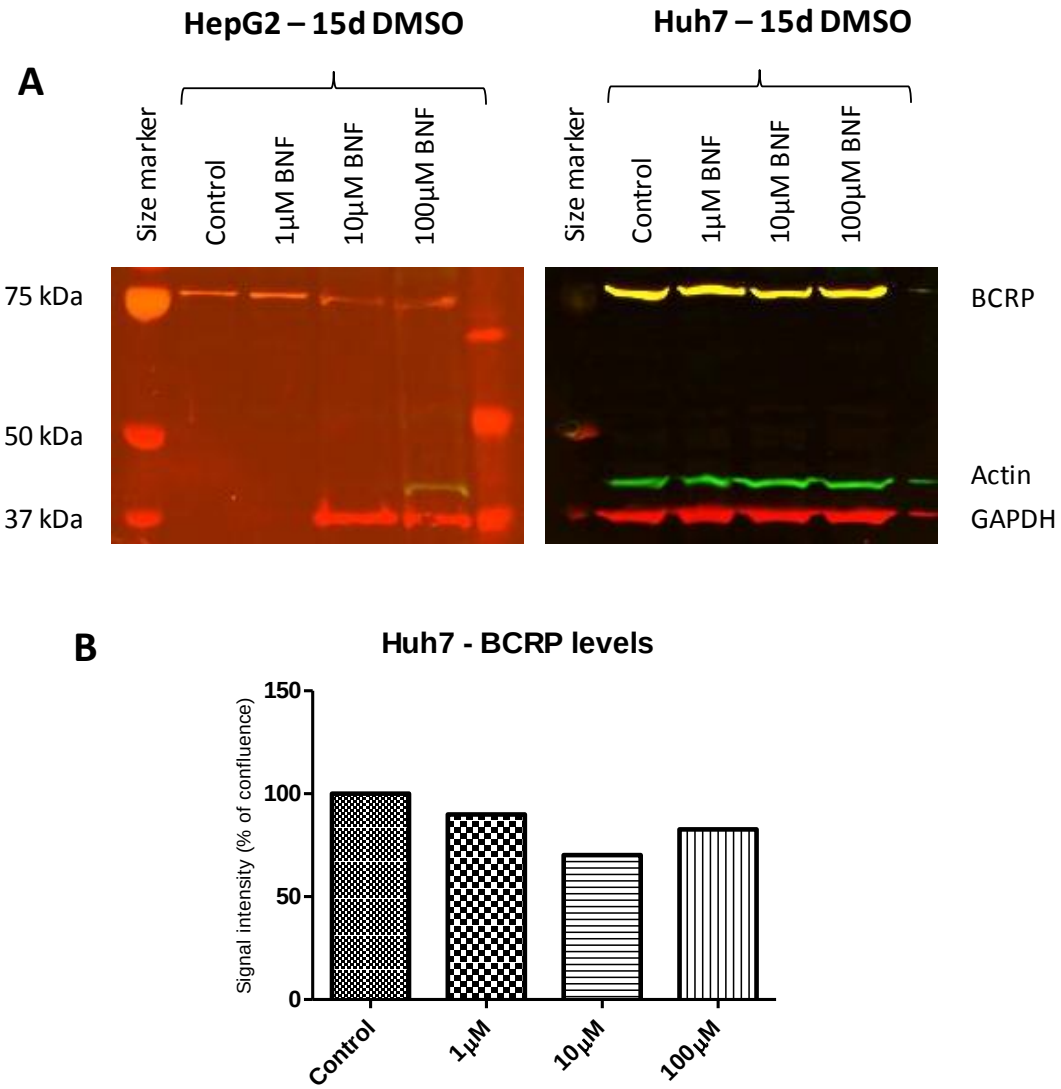

Figure 8.6 –HepG2 and Huh7 cells treated with DMSO plus BNF and analysed using anti-BCRP, anti-actin and anti-GAPDH. Protein was extracted from HepG2 and Huh7 cells after treatment with 1% DMSO for 15 days followed by BNF at three concentrations for 24 hours as described in chapter 2.7. Samples were prepared, separated by electrophoresis, transferred to nitrocellulose membrane and incubated with the antibodies BCRP (Abcam, USA), actin (Santa Cruz, USA) and GAPDH (Genetex, USA) at dilutions of 1:50 (BCRP), 1:2000 (actin) and 1:1000 (GAPDH). This was followed by a 1:5000 incubation with goat anti-mouse IgG secondary antibody (BCRP), donkey anti-rabbit IgG secondary antibody (GAPDH) and donkey anti-goat IgG secondary antibody (actin) (Licor). The images (A) were captured using a Licor Odyssey scanner and analysed with ImageJ software, generating the displayed graphical data (B). Data for Huh7 was normalised to both actin and GAPDH. Data is representative of two experiments with two samples in each (n = 4, N = 2).

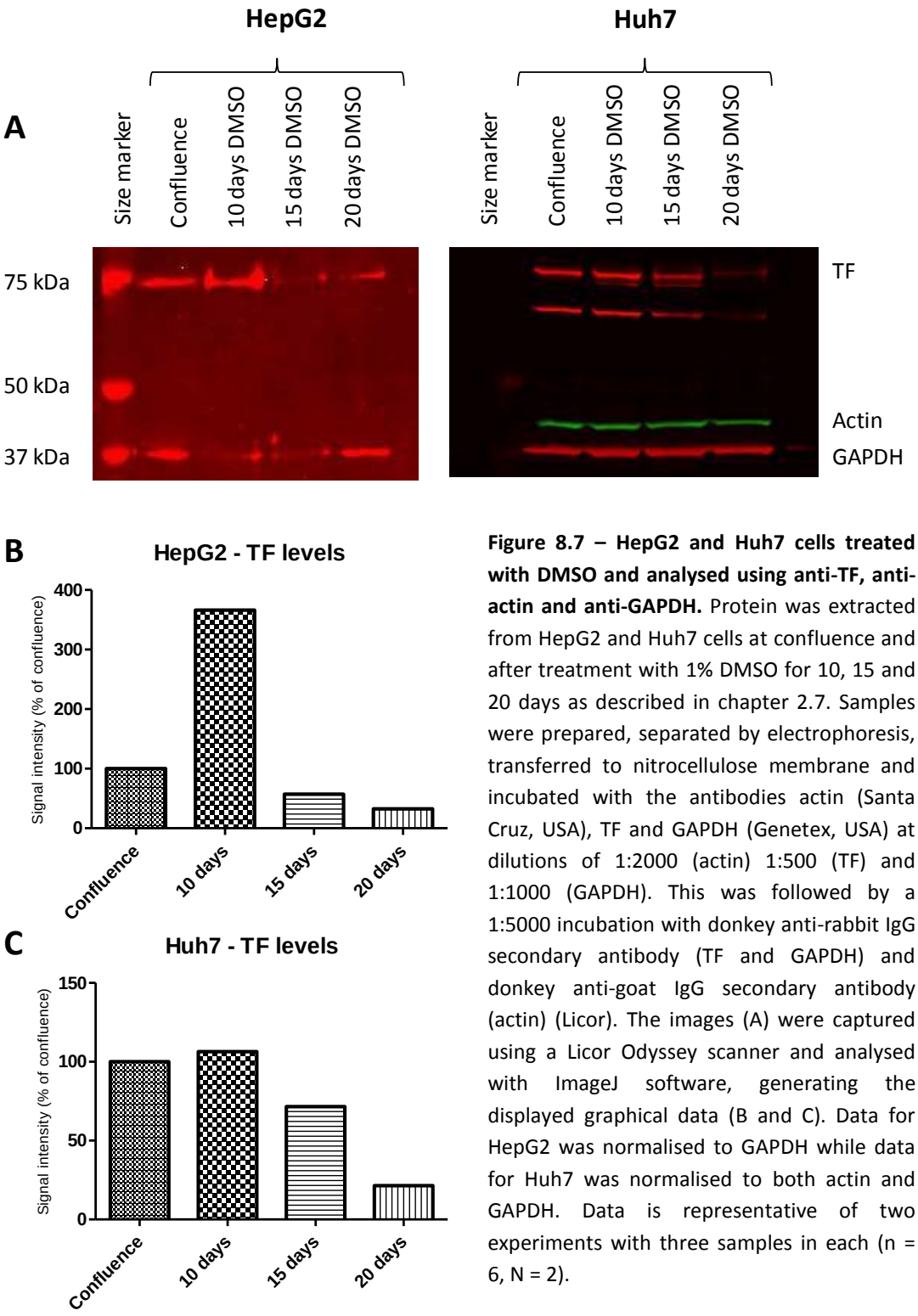

Figure 8.7 – HepG2 and Huh7 cells treated with DMSO and analysed using anti-TF, anti-actin and anti-GAPDH. Protein was extracted from HepG2 and Huh7 cells at confluence and after treatment with 1% DMSO for 10, 15 and 20 days as described in chapter 2.7. Samples were prepared, separated by electrophoresis, transferred to nitrocellulose membrane and incubated with the antibodies actin (Santa Cruz, USA), TF and GAPDH (Genetex, USA) at dilutions of 1:2000 (actin) 1:500 (TF) and 1:1000 (GAPDH). This was followed by a 1:5000 incubation with donkey anti-rabbit IgG secondary antibody (TF and GAPDH) and donkey anti-goat IgG secondary antibody (actin) (Licor). The images (A) were captured using a Licor Odyssey scanner and analysed with ImageJ software, generating the displayed graphical data (B and C). Data for HepG2 was normalised to GAPDH while data for Huh7 was normalised to both actin and GAPDH. Data is representative of two experiments with three samples in each (n = 6, N = 2).

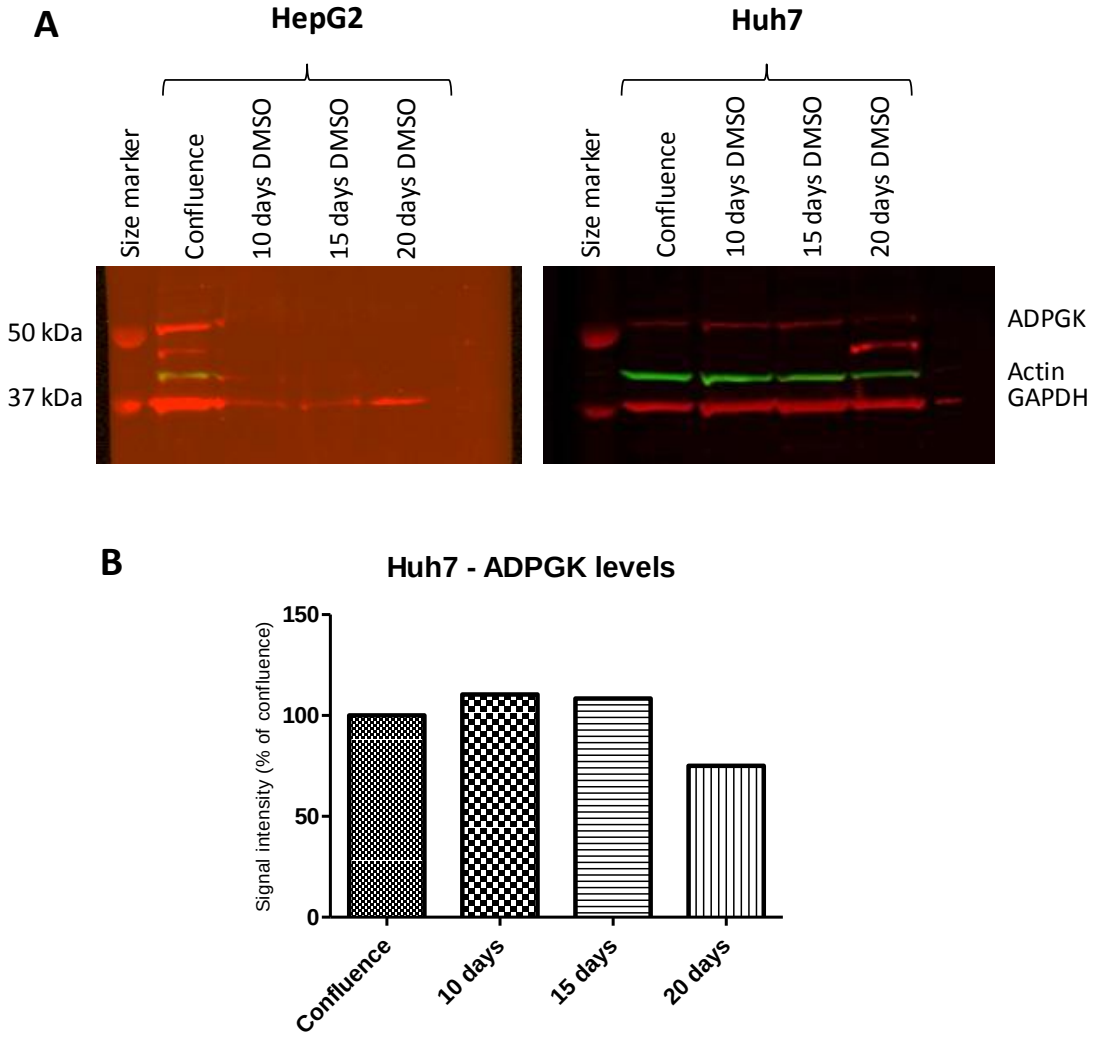

Figure 8.8 – HepG2 and Huh7 cells treated with DMSO and analysed using anti-ADPGK, anti-actin and anti-GAPDH. Protein was extracted from HepG2 and Huh7 cells at confluence and after treatment with 1% DMSO for 10, 15 and 20 days as described in chapter 2.7. Samples were prepared, separated by electrophoresis, transferred to nitrocellulose membrane and incubated with the antibodies actin (Santa Cruz, USA), ADPGK and GAPDH (Genetex, USA) at dilutions of 1:500 (ADPGK), 1:2000 (actin) and 1:1000 (GAPDH). This was followed by a 1:5000 incubation with donkey anti-rabbit IgG secondary antibody (ADPGK and GAPDH) and donkey anti-goat IgG secondary antibody (actin) (Licor). The images (A) were captured using a Licor Odyssey scanner and analysed with ImageJ software, generating the displayed graphical data (B). Data for Huh7 was normalised to both actin and GAPDH. Data is representative of two experiments with three samples in each (n = 6, N = 2).

Chapter 9 – Concluding discussion

The primary aim of this work was to investigate whether an *in vitro* system could be developed which could accurately predict toxicity of novel compounds in hepatocytes and provide an inexpensive, reliable and readily available screening system to be employed before testing in more expensive and difficult to obtain primary hepatocytes. To do this, the baseline expression of differentiation markers, transporters and enzymes in HepG2 and Huh7 human hepatic carcinoma cell lines was analysed and compared to expression in whole liver. Changes in gene expression following induction of key metabolic pathways, Western blotting and finally functional assays were employed in order to determine whether any of an array of growth regimes and treatments resulted in differentiation of these immortalised cell lines to a more hepatocyte-like profile.

A whole cell system is the most relevant one to employ when potential *in vivo* effects are to be determined. Although they lack the interactions with other cell types found in tissues and organs, a much clearer picture of transport and metabolic routes can be obtained than with a partial cell system such as microsomes. The gold standard of *in vitro* whole cell hepatic systems is the freshly isolated primary hepatocyte; however, as these are sourced directly from liver donors availability is unpredictable. These cells also de-differentiate rapidly *in vitro* so cannot be reliably used long-term – fresh cells are needed on a regular basis. Clearly this is a valuable but costly resource, one which ideally would not be used until the later stages of drug development if a more reliable whole cell system could be sourced. Cryopreserved hepatocytes can be more reliably sourced as they can be stored in liquid nitrogen until needed. Although these are not as expensive as primary hepatocytes, they remain substantially more costly than a sustainable secondary cell line and do not show the full hepatic profile observed in freshly obtained primary cells. Currently available secondary cell lines such as HepG2 do not express a full complement of hepatic proteins (Sivertsson *et al.*, 2010; Ek *et al.*, 2007; Hilgendorf *et al.*, 2007; Olsavsky *et al.*, 2007; Westerink and Schoonen, 2007a; Westerink and Schoonen, 2007b; Elizondo and Medina-Diaz, 2003) and more promising lines such as HepaRG (Hart *et al.*, 2010; Jennen *et al.*, 2010; Kanebratt and Andersson, 2008a; Kanebratt and Andersson, 2008b; Aninat *et al.*, 2006; Gripon *et al.*, 2002) have only recently become widely available through commercial routes and so are not yet fully characterised. This niche between available secondary cell lines and cryopreserved hepatocytes is one a more highly differentiated cell line could fill.

Several groups have attempted to define the baseline expression of key genes for one or both of the two cell lines, HepG2 and Huh7, utilised in the current work (Hart *et al.*, 2010; Sivertsson

et al., 2010; Choi *et al.*, 2009; Ek *et al.*, 2007; Hilgendorf *et al.*, 2007; Lim *et al.*, 2007; Olsavsky *et al.*, 2007). However, as observed and documented in the literature, changes in the phenotype of a cell line can and do occur during use in different laboratories, possibly as a result of small variations in culture conditions (Hewitt and Hewitt, 2004). Although it is generally agreed that expression of many important enzymes and transporters is reduced in the HepG2 and Huh7 lines, it is not clear which most resembles the *in vivo* hepatocyte. For example, both mRNA and protein of the key metabolising enzyme CYP3A4 are reported as being expressed in HepG2 at levels 80-1000 fold lower than in liver and as being either 1000-fold lower than liver or completely absent from Huh7 cells (Sivertsson *et al.*, 2010; Ek *et al.*, 2007; Olsavsky *et al.*, 2007). Expression at mRNA and protein level of several other CYPs such as CYP1A2 and 2E1 have also been reported as being very low or absent from HepG2 and Huh7 cells at confluence (Choi *et al.*, 2009; Ek *et al.*, 2007; Lim *et al.*, 2007; Olsavsky *et al.*, 2007). mRNA expression of the major efflux transporters such as MDR1 and MRP2 appears to deviate less from levels observed in liver and primary hepatocytes, while mRNA levels of influx transporters such as OCT3 and OATPB and C have been reported as being absent or fairly close to liver levels (Sivertsson *et al.*, 2010; Ek *et al.*, 2007; Hilgendorf *et al.*, 2007; Olsavsky *et al.*, 2007). Values for expression of these transporters and enzymes relative to liver measured in this project generally fell within the range of those cited from the literature, although as discussed above these are on occasion very wide-ranging. Overall, analysis of the literature shows that neither cell line should be considered more hepatocyte-like than the other as both have substantial deficiencies in expression of metabolising enzymes and transporters, an observation supported by the current study where neither cell line stood out as a superior system with respect to basal expression levels of these key genes.

Attempts to create a more hepatocyte-like cell using cell lines as a starting point have been described in the literature. Of these, two in particular have applied differentiation protocols to Huh7 cells similar to those employed here on both cell lines. Choi *et al.* (Choi *et al.*, 2009) built on initial work from that group (Sainz and Chisari, 2006) where Huh7 cells were treated with 1% DMSO in order to create a more differentiated cell model for studies of hepatitis C virus infection. Over the two publications, mRNA levels of certain maturation markers, transporters and enzymes such as albumin, CYP1A2, -2E1 and -3A4 and UGT1A1 were quantified by qPCR alongside functional assessment of selected enzymes. Sivertsson *et al.* (Sivertsson *et al.*, 2010) grew both HepG2 and Huh7 cells for up to four weeks in standard media, comparable to the treatment described here as prolonged untreated growth. While both cell lines showed an increase in albumin mRNA after four weeks of growth, only Huh7 cells showed increased CYP3A4 mRNA, protein and activity with these remaining at initial levels in HepG2 cells.

Prolonged untreated growth of Huh7 cells in 3D culture for up to 26 days was also examined for expression of selected genes by Sainz *et al.* (Sainz *et al.*, 2009). Results showed increased mRNA expression of maturation markers such as albumin and enzymes such as CYP3A4 and UGT1A1; however, these were not compared to levels in liver or primary hepatocytes. HepG2 cells have also been grown in 3D spheroid cultures with increases in CYP1A2 activity as well as improved basic functional aspects of the hepatocyte such as bilirubin detoxification, urea synthesis and glucose consumption, although this was also accompanied by an increase in AFP production (Coward et al., 2009).

Aspects of these published results, such as increased albumin and CYP3A4 mRNA expression, are mirrored in data described in this thesis, which demonstrates similar increases in these mRNAs after 15 days of untreated growth or DMSO treatment. However, although an increase in CYP3A4 mRNA was observed in all studies including this, the attained levels remained much lower than those in primary hepatocytes or human liver. Although this is not ideal, the increase in CYP3A4 expression seen in this work and increases in both expression and activity in that of Choi *et al.* and Sivertsson *et al.* (Sivertsson *et al.*, 2010; Choi *et al.*, 2009) suggest an improvement in the suitability of DMSO-treated cells and prolonged untreated growth of Huh7 cells for use as a model in toxicity testing.

However, a study by Antherieu *et al.* (Antherieu *et al.*, 2010) using the HepaRG cell line showed that mRNA, protein and activity levels of some transporters and metabolising enzymes (which remained lowered in Huh7 and HepG2 cells following DMSO-treatment and prolonged untreated growth (Sivertsson 2010, Choi 2009 and this work)), were close to or even elevated above those in human hepatocytes cultured for one day. Although it has also been shown that levels in primary hepatocytes after one day of culture can be substantially lower than in fresh hepatocytes, this remains a much higher level of expression than observed here and in other studies using HepG2 and Huh7.

The response of a cell to induction of specific pathways and receptors can elicit important information relating to whether it is functioning as expected. Here, comparison with results from the literature for induction profiles of model compounds in primary hepatocytes and liver slices can be utilised to determine the relative functionality of confluent and treated HepG2 and Huh7 cells. Increases in MDR1 and MRP2 mRNA levels elicited by rifampicin and phenobarbital respectively were seen in liver slices at a much lower concentration of the ligands than in cell lines used here both at confluence and after DMSO treatment (Olinga *et al.*, 2008). Significant responses to rifampicin were observed with a 10 µM treatment in liver slices, whereas significant increases in MDR1 mRNA as a result of rifampicin induction were observed

in HepG2 and Huh7 cells only with a 100 µM treatment (Olinga *et al.*, 2008). MDR1 mRNA increases in response to rifampicin were also observed in other cell lines (Fa2N-4 and HepaRG) at a similar concentration to that used in liver slices (Antherieu *et al.*, 2010; Mills *et al.*, 2004). Although all three examples from the literature showed significant responses to a lower concentration of rifampicin than were observed here, the magnitude of induction at these relevant concentrations were similar, ranging from a 2-fold increase over control in confluent HepG2 and Huh7 cells used here, to a 2.3-fold increase in liver slices (Olinga *et al.*, 2008), a 3-fold increase over control in Fa2N-4 cells (Mills *et al.*, 2004) and an increase between 1.5- and 10-fold over control in HepaRG cells (Antherieu *et al.*, 2010). In contrast, with DMSO pre-treated cells, rifampicin resulted in a decrease in MDR1 mRNA at all concentrations tested in both cell lines and so did not improve upon results observed in confluent cells. These comparisons show that although the effective concentration of rifampicin used here is higher than in other studies cited in the literature, the magnitude of induction is similar which indicates that these cells retain the PXR pathway initiated by rifampicin if not the sensitivity.

With phenobarbital an increase in MRP2 mRNA level has been reported in HepaRG cells, human hepatocyte and liver slices and was seen in experiments here with HepG2 and Huh7 cells both at confluence and after DMSO pre-treatment. As with rifampicin, changes were generated at a lower concentration of phenobarbital in liver slices (50 µM) than in cell lines used here (3 mM) (Olinga *et al.*, 2008). HepaRG cells also required a higher concentration (1 mM) for a response than that used in liver slices (Antherieu *et al.*, 2010). Courtois *et al.* (Courtois *et al.*, 2002) used a similar phenobarbital concentration to that used here (3.2 mM) in primary human hepatocytes to induce both MRP2 mRNA and protein but did not specify fold differences observed. In both confluent and DMSO-treated HepG2 and Huh7 cells here, increases in MRP2 mRNA were between 2- and 3-fold higher than control; increases in HepaRG cells were in the same range, 1.5- to 10-fold higher than control, albeit with a slightly lower concentration of the ligand than that which produced an effective increase here. However, the increase observed with only 50 µM phenobarbital in liver slices was 12.4-fold higher than control, a much greater increase than observed with cells in experiments here. These results show that while confluent HepG2 and Huh7 cells responded appropriately to rifampicin and phenobarbital, the concentrations of reagents required to induce a response indicate that the cells are less sensitive than liver slices and the HepaRG line. DMSO treatment did not improve these responses relative to liver and in the case of rifampicin, no response to the compound was observed after treatment in either cell line. This loss of response after DMSO treatment suggests that some aspect of DMSO action is interfering with the cellular response to rifampicin, which was functional in confluent cells. As stated earlier, it is not known exactly

how DMSO might act to cause maturation or other effects in cells (Aninat *et al.*, 2006; Sainz and Chisari, 2006). Possible results of DMSO treatment include increased ROS scavenging (Villa *et al.*, 1991), anti-apoptosis actions (Gilot *et al.*, 2002), altered cell-cell signalling (Fiore and Degrassi, 1999), effects on cell membrane integrity (Melkonyan *et al.*, 1996) and alternative cellular splicing (Bolduc *et al.*, 2001). Any of these actions alone or together or others currently unknown could contribute to the differences resulting from DMSO treatment seen both in experiments here and in other cell types where it sustains primary hepatocyte maturation and HepaRG differentiation.

Several factors could precipitate the difference in effects seen here with those reported elsewhere. Cells were cultured in different media and were derived from different sources. HepG2 and Huh7 cells are both derived from males with well-differentiated hepatocellular carcinoma, HepG2 from a 15 year old Caucasian and Huh7 from a 57 year old Japanese donor (Nakabayashi *et al.*, 1982; Aden *et al.*, 1979). HepaRG cells were derived from a female of unspecified age and ethnicity, also with hepatocellular carcinoma and Hepatitis C infection (Gripon *et al.*, 2002). Fa2N-4 cells were derived from hepatocytes from a 12 year old female donor of unspecified ethnicity and were artificially immortalised using simian virus 40 large T antigen (Mills *et al.*, 2004). These differences in age, gender, ethnicity and disease state all introduce potential differences in basal gene expression, which is why experiments using primary hepatocytes or liver slices often use several donors of differing age and gender; for example, Olinga *et al.* (Olinga *et al.*, 2008) used 3 male and 3 female donors with an age range of 3-51 years for liver slice experiments. Although HepaRG cells are always used at confluence due to the prolonged growth periods required to further differentiate the cells (up to 28 days with 2% DMSO after high density seeding), Fa2N-4 cells were cultured in serum-free medium and exposed to the inducer only 48 hours after plating. Although no statement on level of confluence was made at this point, my experience with HepG2 and Huh7 cells suggests that confluence would not have been attained at the time of ligand application; however, since all cells grow at different rates it is possible that confluent Fa2N-4 cells were used. HepaRG cells were grown for up to 28 days in medium containing 10% serum and 2% DMSO; this was replaced by medium containing 2% serum and no DMSO 3 days before induction experiments were commenced, whereas here experiments were conducted in standard growth medium containing 10% serum and 1% DMSO. Another notable difference was that both HepaRG and Fa2N-4 cells were incubated with rifampicin for 48 hours (Antherieu *et al.*, 2010; Mills *et al.*, 2004), while in liver slices (Olinga *et al.*, 2008) and in experiments here RNA was extracted after 24 hours of treatment.

Differences in cell-cell communication and the expression of nuclear receptors themselves will also play a role in how a cell responds to an inducer. Liver slices do contain liver cell types other than hepatocytes (for example, stellate cells and cholangiocytes) and retain the extracellular matrix components which are lost with preparations containing hepatocytes only (Olinga *et al.*, 2008); this could alter the reactions and the sensitivities observed in the tissue. HepaRG cells have been shown to have higher mRNA levels of key nuclear receptors such as CAR, PXR and AhR than HepG2 cells and in the case of PXR, higher than that in freshly isolated human hepatocytes (Aninat *et al.*, 2006). This could account for the differences in sensitivities observed here; for example, levels of CAR mRNA in highly differentiated HepaRG cells are reported to be 30% of those in human hepatocytes, while HepG2 cells express CAR at only 2.4% of the hepatic level (Aninat *et al.*, 2006). These differences may themselves explain data discussed previously, where liver slices responded to phenobarbital, a CAR activator, at a concentration of 50 µM while HepaRG and HepG2 showed significant responses at 1 mM and 3 mM respectively (Antherieu *et al.*, 2010; Olinga *et al.*, 2008).

In Huh7 cells both at confluence and treated with DMSO, BCRP mRNA increased significantly with BNF activation of the AhR pathway at concentrations of 1 and 10 µM. In confluent HepG2 cells no significant increase was observed with BNF treatment whereas in DMSO treated cells a significant increase was observed with 10 µM BNF. This could indicate that response to BNF via the AhR pathway was improved with DMSO treatment, but it is difficult to say conclusively that this is the case when significance was only observed at one concentration and not sustained across the concentration range. Although comparable experiments using BNF to induce BCRP in hepatic cells are not available, the compound TCDD has been used to activate the AhR pathway by Tan *et al.* (Tan *et al.*, 2010) and showed a 2-fold mRNA and 2.7-fold protein increase in human hepatocytes. This is similar to results here, where induction of BCRP mRNA in DMSO-treated Huh7 cells ranged from 2- to 5-fold of control levels and in confluent Huh7 cells ranged from 8- to 10-fold of control levels. While responses to BNF in confluent HepG2 cells did not reach significance, the magnitude of change was 2- to 3-fold of control levels across the concentration range.

Protein detection by Western blotting was also carried out for BCRP. Detection of BCRP in HepG2 and Huh7 cells at confluence and treated with DMSO for 10, 15 and 20 days showed increases in protein levels with DMSO at all time points; however, this did not correlate with observed mRNA data which showed significant decreases in DMSO-treated HepG2 cells and no significant change in either prolonged untreated or DMSO-treated Huh7 cells. Protein extracts from both confluent and DMSO-treated HepG2 and Huh7 cells incubated with the inducer BNF were also probed for BCRP. BCRP mRNA abundance was increased by BNF in both confluent

and DMSO-treated Huh7 cells, while results for HepG2 cells showed only one significant increase in BCRP mRNA at 10 µM BNF in DMSO-treated cells, with no significant changes in confluent HepG2 cells. Protein detection revealed that BCRP did not increase with BNF treatment in confluent HepG2 or Huh7 cells, or in DMSO-treated Huh7 cells. Unsatisfactory protein detection in DMSO-treated HepG2 cells incubated with BNF meant that protein could not be accurately determined here.

These results may indicate a substantial role for post-transcriptional regulation of BCRP in both cell lines. Post-transcriptional regulation of this gene has been observed previously (Pan *et al.*, 2009; Ogura *et al.*, 2008; Imai *et al.*, 2005) but data looking specifically at both mRNA and protein upregulation of BCRP by an inducer in hepatocytes is lacking. Both Ogura *et al.* (Ogura *et al.*, 2008) and Imai *et al.* (Imai *et al.*, 2005) observed protein reduction alongside no change in mRNA transcript levels in rat intestinal cells and MCF-7 (human breast cancer) cells respectively. Pan *et al.* (Pan *et al.*, 2009) showed evidence of miRNA inhibition of BCRP expression, also in MCF-7 cells. Since miRNA are known to be expressed at certain developmental stages or under conditions of cellular stress, it is feasible to consider that they could be active in experiments described here also. Another possible explanation for the discrepancy between mRNA and protein levels of BCRP observed here is that protein levels have already been increased and are stabilised at a higher level after 10 -20 days of DMSO treatment, resulting in mRNA levels which are no longer elevated. It is also possible that incubation times used for BNF treatment (24 hours) were sufficient to observe an mRNA increase but not an increase in protein levels. Disagreement between levels of transferrin mRNA and protein were also observed with DMSO-treated HepG2 and Huh7 cells, where increases in mRNA were observed with decreases in protein at corresponding time points; indeed, although significant increases in transferrin mRNA were seen after 15 days of DMSO treatment in Huh7 cells, protein increases were not observed at either 15 or 20 days. This could illustrate delays in protein synthesis, although a five day lag between mRNA and protein increase would seem to be quite extended. However, as transferrin can be secreted from the cell into the medium this may be the explanation for the discrepancies observed (Zakin, 1992). Protein assessment from the medium may reveal an increase in transferrin, but the presence of serum in the medium could mask any change in secreted human transferrin.

Assessment of BCRP and P-gp function using Hoechst 33342 and of P-gp, MRP1 and MRP2 function using calcein-AM was carried out on confluent and DMSO-treated HepG2 and Huh7 cells and on prolonged untreated Huh7 cells. A lack of effective inhibition in confluent HepG2 cells by CSA and Ko143, which inhibit P-gp and BCRP respectively, was not improved upon in DMSO-treated cells. Verapamil, also a P-gp inhibitor, was more effective at inhibiting P-gp

function in confluent than in DMSO-treated HepG2 cells. Hoechst efflux by both P-gp and BCRP was effectively inhibited using verapamil, CSA and Ko143 in confluent Huh7 cells, but the effectiveness of the inhibitors was reduced after both prolonged untreated growth and DMSO treatment. This could be indicative of increased protein expression; in the case of BCRP, increased protein was observed after 15 days of DMSO treatment in both cell lines which could account for the reduced effectiveness of Ko143 in inhibiting Hoechst efflux in DMSO-treated Huh7 cells in comparison to confluent cells as more BCRP protein is present with an equal concentration of inhibitor. The lack of effective inhibition with CSA and Ko143 in HepG2 cells could be indicative of decreased expression of the respective transporters in comparison to Huh7 cells. mRNA data showed that the MDR1 level in HepG2 at confluence was over 2-fold higher than in liver, while the BCRP mRNA level was approximately half of that in liver in confluent HepG2 cells. Confluent Huh7 cells had an MDR1 mRNA level 8-fold lower than that in liver and a BCRP mRNA level 30-fold lower than in liver. This difference in potential expression levels between the two cell types could explain why inhibition of transporters was successful in Huh7 cells but not in HepG2 cells with the same ligand concentrations if protein levels in HepG2 were increased over those in Huh7 to such an extent that effective inhibition did not take place.

Calcein-AM was used to study functional P-gp, MRP1 and MRP2 in HepG2 and Huh7 cells. P-gp function was demonstrated in HepG2 and Huh7 cells at confluence, after DMSO treatment and after prolonged untreated growth of Huh7 cells. DMSO treatment of HepG2 cells did not alter activity of P-gp; when using various MRP inhibitors (CSA, verapamil and MK571) some significant differences to confluent cells were lost with DMSO treatment but the overall pattern of responses remained the same. This indicates that function of MRP1 and 2 in DMSO-treated HepG2 cells did not change from that in confluent cells and agrees with mRNA levels shown here and in Sivertsson *et al.* (Sivertsson *et al.*, 2010) where these three transporter levels remained consistent in both cell lines after 4 weeks of untreated growth.

In confluent Huh7 cells MRP2 functional activity appeared to be very low as verapamil, an MRP1 inhibitor, produced the same inhibition of calcein efflux as MK571, which inhibits both MRP1 and 2. When calcein efflux is mediated by both MRP1 and 2 transporters, MK571 should have a greater inhibitory effect than verapamil, which was seen in both confluent and DMSO-treated HepG2 cells. After both DMSO treatment and prolonged untreated growth of Huh7 cells, the proportion of total calcein effluxed decreased from 60% in confluent cells to 20-25%. Additionally, the differences in efflux seen in HepG2 cells by inhibiting MRP1 alone (verapamil) or MRP1 and 2 together (MK571) were also seen in both prolonged untreated and DMSO-treated Huh7 cells, indicating that a more even balance of the transporters has been achieved.

This could be either by MRP1 decreasing, MRP2 increasing or a combination of both; mRNA data indicated that the MRP1 level in confluent Huh7 cells was approximately 10-fold higher than liver, while the MRP2 mRNA level was approximately 200-fold lower than in liver. This suggests that MRP1 is expressed at a much higher level in confluent Huh7 cells. As the proportion of calcein effluxed was decreased following treatment it is likely that MRP1 protein levels or activity were decreased allowing MRP2 activity to become visible. Such changes in protein abundance were not predicted by a change in mRNA levels, where MRP1 and 2 mRNA abundances remained unchanged from control following both DMSO and prolonged untreated growth. In their work, Sivertsson *et al.* (Sivertsson *et al.*, 2010) saw a slight increase in MDR1 (P-gp) but no change in MRP2 mRNA; protein and functional data were not presented in this paper. These protein and functional data indicate a high degree of post-translational modification for a number of important genes in these cells which would require more analysis of protein generation, modification and transport to the membrane in these cells and collection of comparative data from primary hepatocytes in order to fully evaluate their potential as an effective *in vitro* hepatocyte model.

Overall, the results described do not indicate that a substantially more hepatocyte-like, more differentiated cell type has been created from either cell line with 1% DMSO treatment or with prolonged untreated growth in Huh7 cells. This is disappointing as a cell with a more hepatic profile could be an extremely useful, relatively inexpensive whole cell system for use in early stage testing of new compounds in the pharmaceutical industry. Results gained here indicate that the effective differentiation of every aspect of a hepatic carcinoma cell would be quite difficult to achieve. Initial promising results gained with assessment of differentiation markers were not followed by sustained alteration at either mRNA or protein levels of many key enzymes and transporters towards levels more indicative of the *in vivo* hepatocyte. This leaves HepG2 and Huh7 cells much where they began, with no definite advantage being achieved by prolonged untreated growth or DMSO treatment in terms of the functionality of the cell system as a vehicle for assessment of toxicity.

The HepaRG cell line is a relatively new lineage of cells generated from donated female hepatocarcinoma cells. This was first reported by Gripon *et al.* (Gripon *et al.*, 2002) and initial reports of expression of key genes such as CYPs in the cells were promising (Guillouzo *et al.*, 2007; Aninat *et al.*, 2006; Le Vee *et al.*, 2006). Attempts were made to obtain some of these cells from the authors of the papers at the beginning of this project in October-December 2007 but unfortunately responses were not received to e-mails from myself, Professor Barry Hirst (supervisor) and at least one colleague in another department of the university. Although initial published results for HepaRG indicated that it was a promising model for hepatic

function, publications at the time were not as numerous as those for HepG2 in particular. A search on Pubmed shows that between January 2002 and December 2007 a total of 19 publications mention HepaRG cells; of these, ten discuss differentiation, nuclear receptor activation or enzyme and transporter expression and a further eight discuss infection, the majority with Hepatitis B virus. Over the span of this project use of these cells has become more widespread and they are now commercially available through Invitrogen; unfortunately this came too late to utilise the cells here.

Since the commercialisation of HepaRG there have been many more publications using the cells – 15 from January to the end of April 2011 alone. These indicate that HepaRG is a strong candidate for use in drug metabolism and toxicity studies when seeded at high density and differentiated with 2% DMSO. In particular, the expression of many CYP enzymes has been confirmed at mRNA, protein and functional level by several groups; a search in Pubmed with the key words HepaRG and CYP3A4 produces 17 relevant publications, but HepaRG plus MDR1, P-gp or P-glycoprotein reveals only two matches. This is understandable as a known issue with other hepatic cell lines including HepG2 is the low expression of CYPs, especially CYP3A4, a key metabolic pathway in *in vivo* hepatocytes which can also be lost early after primary hepatic isolation (Sivertsson *et al.*, 2010; Olsavsky *et al.*, 2007). Nevertheless, transport proteins are important in metabolic studies and need to be analysed in these cells. Recent advances in the knowledge of the HepaRG gene expression profile have involved whole genome comparisons of HepaRG, HepG2 and primary human hepatocytes (Hart *et al.*, 2010; Jennen *et al.*, 2010). Hart *et al.* (Hart *et al.*, 2010) showed that both the HepaRG whole genome expression profile and the expression profile of drug-processing genes in particular are more similar to those of a primary hepatocyte than are those of HepG2. Jennen *et al.* (Jennen *et al.*, 2010) analysed whole genome expression after exposure to toxic substances and surmised that HepaRG cells were more suitable than HepG2 for identifying further biological consequences of toxin exposure, while HepG2 cells were more suitable for some cases of substance classification. Additional analysis of baseline genome expression in this publication agreed with Hart *et al.* (Hart *et al.*, 2010) in that HepaRG expression was closer to that of liver and primary human hepatocytes than was HepG2.

Publications are now being released which show attempts to improve HepaRG further. Darnell *et al.* (Darnell *et al.*, 2011) have cultured HepaRG cells in a 3D bioreactor which enabled maintenance of the differentiated state without continued DMSO presence in the media and also prompted the cells to polarise similarly to the state in which they are found *in vivo*. Bednarkiewicz *et al.* (Bednarkiewicz *et al.*, 2010) have experimented with eliminating the biliary cells found in all terminally differentiated HepaRG cell populations by increasing

photosensitivity and subsequently selecting specific cells for elimination by applying UV light. McGill *et al.* (McGill *et al.*, 2011) have shown that HepaRG is a suitable model to study the effects of paracetamol toxicity showing comparable results to those observed in primary mouse hepatocytes and rodent *in vivo* models. However, caution must be used when looking into results for these cells. Ceelen *et al.* (Ceelen *et al.*, 2011) noted that many of the previous publications analysing mRNA levels in HepaRG cells used 18S rRNA as a reference gene. Upon conducting analysis of the suitability of reference genes in HepaRG cells with three different algorithms, including the GeNorm software used here, 18S rRNA was ranked among the least stable by all three. This could call into question previous claims of superiority of this cell line based on mRNA alone, making it especially important that relevant protein and functional data are produced.

Another promising avenue of research centres around transdifferentiation of pancreatic cells into hepatocytes. This was first reported by Shen *et al.* (Shen *et al.*, 2000) where the rat pancreatic cell line AR42J-B13 was shown to progressively develop hepatic markers in culture with 1 μM dexamethasone for up to 14 days. Addition of 10 ng/ml OSM further improved the expression of hepatic markers such as albumin and glucose-6-phosphatase (G6P). This paper also demonstrated a similar effect of dexamethasone on pancreatic buds isolated from mice, showing that the observed generation of hepatocyte-like features was not limited to a particular cell line. This work has been continued further since the original publication, with subsequent data showing detection of CYP3A1, CYP2B1/2, glucokinase and aryl sulfotransferase IV by immunostaining after treatment with dexamethasone for up to 28 days (Tosh *et al.*, 2002). Marek *et al.* (Marek *et al.*, 2003) also analysed protein levels of various CYP enzymes in transdifferentiated AR42J-B13 cells by Western blotting and found that CYP 2C11, 2A, 2E and 3A1 levels were similar to those in freshly-isolated rat hepatocytes. Continued analysis has revealed the presence of transferrin, UGT, CYP2E1 and carbamoyl phosphate synthetase-I (CPS) protein along with sensitivity to paracetamol toxicity, all of which indicate a hepatic phenotype (Wallace *et al.*, 2009; Burke *et al.*, 2006; Marek *et al.*, 2003). Prospective signalling pathways involved in the transdifferentiation process have also been investigated, notably the transcription factor CCAAT enhancer binding protein β (C/EBPβ) and the WNT signalling pathway. Repression of the WNT pathway was found to be concurrent with increased hepatic marker expression, while increased C/EBPβ expression correlated with an increase in albumin and G6P; over-expression of this transcription factor reduced the number of ductal cells generated during the transdifferentiation process, potentially giving a more pure hepatic population (Al-Adsani *et al.*, 2010; Wallace *et al.*, 2009; Shen *et al.*, 2000). This technique has also been applied to human foetal pancreatic cells, where treatment with

dexamethasone and fibroblast growth factor 2 (FGF2) led to increased levels of liver markers such as albumin and cytokeratin 19 at both mRNA and protein level (Sumitran-Holgersson *et al.*, 2009). When transplanted into nude mice with chemical-induced liver injury, these transdifferentiated hepatocyte-like cells successfully engrafted and proceeded to differentiate further, indicating that this may be an option for transdifferentiation of pancreatic cells to hepatocytes not only for *in vitro* use but also with possibilities for transplantation.

Future work

Several possibilities for future experiments are presented in these publications with regard to the cell lines used here, such as extended treatment with dexamethasone alone. Although dexamethasone was included here in early experiments with growth factors and in prolonged treatments with both growth factors and DMSO (chapter 4), experiments with this compound alone were not carried out. It would also be interesting to see if disruption of the WNT pathway or over-expression of C/EBPβ induced differentiation more effectively than the DMSO treatments used here.

Stem cells have been considered as a promising avenue for the creation of a sustainable source of hepatocyte-like cells. In theory, stem cells could be isolated from sources such as human embryos, umbilical cord blood, adipose tissue and bone marrow, and kept in an undifferentiated state until required for use. At this point, stem cells could be directed through the desired differentiation process, for example to endoderm followed by hepatic specification and maturation, by a series of specific treatments at pre-determined time points. This would allow the generation of hepatocyte-like cells for use when desired from a continually proliferating stem cell store by a standard culture procedure, resulting in an easily accessible and reproducible model for toxicity studies. Although attempts to induce differentiation of hepatocyte-like cells have been made by a number of groups, the endpoint of a cell which fully represents an *in vivo* hepatocyte has yet to be reached. Common observations are increased levels of hepatic markers such as albumin, AFP and G6P (Agarwal *et al.*, 2008; Hay *et al.*, 2008; Hossein Baharvand, 2008; Philippe A. Lysy, 2008; Baharvand *et al.*, 2006; Snykers *et al.*, 2006). Although such markers will increase during differentiation from a stem cell to an hepatocyte-like cell, markers of a foetal liver phenotype such as AFP should then decrease with further maturation towards the true hepatic lineage (Cascio and Zaret, 1991). This increase and subsequent decrease in AFP was observed by Snykers *et al.* (Snykers *et al.*, 2006) using rat BMSCs, along with detection of CYP1A1 and 2B1/2 protein, but has not been mentioned in many of the other publications which report only an increase in AFP (Agarwal *et al.*, 2008; Hay *et al.*, 2008; Hossein Baharvand, 2008; Philippe A. Lysy, 2008; Baharvand *et al.*, 2006). Levels of

key hepatic proteins such as CYP3A4 do not reach levels observed in primary hepatocytes; Lysy *et al.* (Philippe A. Lysy, 2008) report no detection of CYP3A4 mRNA, whilst Agarwal *et al.* (Agarwal *et al.*, 2008) report levels lower than that in HepG2 cells, which have been shown in work here to be much lower than those in liver. More recent publications have continued in this vein and attempted to develop improved differentiation protocols. Protocols used by Duan *et al.* (Duan *et al.*, 2010) demonstrated more success using fibroblast growth factor 4 (FGF4), hepatocyte growth factor (HGF), bone morphogenic proteins 2 and 4 (BMP2, BMP4) and 0.5% DMSO, with differentiated hepatocyte-like cells shown to express several important phase I and II metabolising proteins such as CYP3A4, -1A2 and UGT1A1 and the transporters MRP1 and OATPC. Confirmation of functional expression of CYP3A4, -1A2, -2C9 and -2D6 was also documented and was similar to that observed in primary hepatocytes. Expression here appears to be an improvement over that in past differentiation regimes and this or other similar protocols could be a major improvement in the similarity of stem cell-derived hepatocyte-like cells to the *in vivo* ideal.

Attempts to further improve upon this technology have been made, in particular in improving the culture environment of the cells. 2D growth on plastic, often with coatings of substances such as collagen, allows the cells to survive and differentiate to an extent but does not mimic the *in vivo* conditions. Baharvand *et al.* (Baharvand *et al.*, 2006) observed that markers of differentiation were detected earlier and higher levels of urea production were obtained when hESC-derived hepatocyte-like cells were grown in a 3D environment with collagen scaffolds rather than a 2D one. More recently, Miki *et al.* (Miki *et al.*, 2011) also observed that more functional maturation was seen in 3D cultured hESCs than in 2D cultured ones. These observations indicate that if differentiation to genuine hepatocyte-like status in a 2D system does prove to be unattainable, moving the differentiation process to a 3D system may give an additional functional boost to the cells. Alternatively, if the maturation process can be accelerated by moving to a 3D system, this would add to the usefulness of the cells overall.

A common feature in the many published differentiation protocols is the use of growth factors in the media. Here, preliminary and extended growth factor treatments were applied to both HepG2 and Huh7 cells. Initial growth factor experiments, with media formulae based on final-step maturation cocktails from the literature, were not successful as the cells proliferated extensively and could not be maintained successfully for the extended time periods indicated in other publications (10 days plus) (Agarwal *et al.*, 2008; Hay *et al.*, 2008; Hossein Baharvand, 2008; Philippe A. Lysy, 2008; Jun Cai, 2007; Baharvand *et al.*, 2006; Snykers *et al.*, 2006; Kurash *et al.*, 2004). When 1% DMSO was added to the growth factor mixtures cells could be maintained for longer; however, little additional effect above that of DMSO alone was seen.

Although the final step from multi-step protocols was applied, it could be that these hepatic carcinoma cells are already differentiated beyond the point at which the selected growth factors (HGF, OSM or HGF plus OSM all with dexamethasone and 1% DMSO) can improve upon the phenotype and a different maturation protocol is required to improve the cells further. The relevant receptors could be expressed at low levels in these cell lines, or the serum content of the media could be limiting the observed response due to the presence of similar growth factors already having had an effect. One way to limit the impact of additional factors in serum would be to use dialysed serum and add in hormones and growth factors as required. 3D growth of these cell lines, with or without DMSO, may also have a maturation effect. Increases in albumin production and in CYP enzymes were observed in HepG2 cells cultured in a rotating bioreactor in comparison to those grown in 2D conditions (Chang and Hughes-Fulford, 2009). Similar functional changes were observed by Lee *et al.* (Lee *et al.*, 2009) with HepG2 cells grown on inverted colloid crystal (ICC) scaffolds in 96 well plates. Huh7 cells grown in 3D conditions using microcarrier beads in a bioreactor were shown to have increased expression of albumin, CYP3A4, CYP2D6 and UGT1A1 mRNAs as well as other relevant hepatic genes over a period of 26 days and in comparison to confluent 2D-cultured cells (Sainz *et al.*, 2009).These results indicate that 3D growth of the cell lines used here may elicit a more hepatocyte-like cell and is a future direction which could yield promising results.

Bioartificial liver (BAL) systems consist of a combination of mechanical and biological features which function as a substitute during instances of liver failure. These systems incorporate living primary or secondary cell line hepatocytes, generally from either human or porcine sources, into a bioreactor system where the cells are immobilised and cultured. Blood or plasma from the patient is passed through the BAL system which aims to provide enough hepatic function to bridge the gap between liver failure and transplant or regeneration (Carpentier *et al.*, 2009; Yu *et al.*, 2009; Park and Lee, 2005; Strain and Neuberger, 2002; Cao *et al.*, 1998; Mito, 1986). Current BAL systems used clinically have large scope for improvement which could be aided by finding a more suitable cell population. The extracorporeal liver assist device (ELAD) utilises the C3A cell line, which is derived from the HepG2 cell line (Ellis *et al.*, 1996; Sussman *et al.*, 1994; Kelly and Darlington, 1989) and is the one of the only devices to utilise a cell line rather than primary hepatocytes. However, initial clinical trials showed that no distinct advantage was gained by use of this BAL with increases observed in plasma levels of both ammonia and bilirubin (Park and Lee, 2005). The reasoning behind the use of C3A was that unlike HepG2, it does produce urea, an essential function of the hepatocyte. However, it was assumed that this urea production was via the urea cycle, whereby ammonia is detoxified and urea is a by-product. This was found to be an incorrect assumption as reported by Mavri-Damelin *et al.*

(Mavri-Damelin *et al.*, 2008) where urea was instead produced via a mechanism independent of the urea cycle and the urea cycle in C3A cells is non-functional, making it unsuitable for use as an ammonia-detoxifying component in BAL systems. Several other systems currently in development utilise porcine primary hepatocytes but these present problems with immunorejection and the possibility of animal pathogen transmission; in clinical trials these have also been shown to provide no significant improvement in survival rates of patients with acute liver failure (Demetriou *et al.*, 2004).

Improving the culture conditions of the cellular component in BAL systems to promote the desired characteristics, whether using cell lines such as HepG2 or primary hepatocytes, may allow for vast improvement in the BAL without continual harvesting of human primary hepatocytes. For example, Coward *et al.* (Coward *et al.*, 2009) demonstrated that HepG2 cells stably transfected with both ornithine carbamyl transferase and arginase 1, which are key components of the urea cycle absent from standard Hepg2 cells, followed by encapsulation in alginate and culture in a microgravity environment before being used in a fluidised bed bioreactor could efficiently carry out all metabolic, synthetic and detoxification functions required from a BAL device. This system would be a viable option to expand and test in a BAL device in a clinical setting and could potentially yield cells which would be useful in the drug development industry. Further experiments using these encapsulated HepG2 cells have attempted to cryopreserve the cells in this state, eliminating the process of encapsulation before use and potentially making these cells more easily available for use in BAL systems (Massie *et al.*, 2011).

So far, primary hepatocytes remain as the gold standard cellular system for assessment of drug toxicity. However, as outlined previously, high costs, unpredictable availability and failure to thrive *in vitro* means another system is required for early stage, routine testing. Potentially an improvement in the culturing conditions of primary hepatocytes could prolong their useful life; alternatively, a change in the culture of cryopreserved hepatocytes could result in that system improving. Factors which may improve expression and lifespan of these cells are similar to those identified for cell line culture and stem cell differentiation, such as specialised culture media, co-culture alongside other liver cell types and 3D culture to mimic the *in vivo* structure.

Co-culture of hepatocytes with endothelial, stellate and Kupffer cells have all been shown to improve the function or longevity of hepatocytes *in vitro* (as reviewed by Dash *et al.* (Dash *et al.*, 2009)). This is widely thought to be a result of secreted growth factors and cell-cell signalling; for example, HGF, which promotes hepatocyte mitosis, is synthesised by hepatic stellate cells and co-culture has been shown to result in continued expression of albumin and

CYP enzymes in hepatocytes after two months in culture (Riccalton-Banks *et al.*, 2003). 3D co-culture systems have also been investigated for improvements in hepatic function. An example of such a system is described by Kim *et al.* (Kim and Rajagopalan, 2010), where hepatocytes were cultured alongside liver sinusoidal epithelial cells using a construct designed to mimic the physical separation seen *in vivo*. This resulted in increased expression of albumin and stable levels of urea production after 12 days of culture, whereas hepatic monolayers showed a 65% decrease in albumin after 12 days of culture. Ideas such as these may be useful in cell line differentiation in the future, however if the aim is to use the resulting cells as early drug toxicity models, other mechanisms such as 3D culture alone may provide sufficient advantage over existing models while further development is undertaken.

The study of liver development and regeneration processes may provide vital clues to the types and timing of growth factor applications required to develop a truly representative hepatic model. It is thought that fibroblast growth factors (FGFs) and bone morphogenic proteins (BMPs) along with activation of several hepatocyte nuclear factors (HNFs) are required for initial liver cell differentiation during early foetal liver development (Rossi *et al.*, 2001; Darlington, 1999). This information is reflected in attempts to differentiate stem cells *in vitro*, several of which incorporate these factors (Tuleuova *et al.*, 2010; Agarwal *et al.*, 2008; Snykers *et al.*, 2007; Schuldiner *et al.*, 2000). Liver regeneration relies on a large number of factors such as IL-6, TNFα, EGF, HGF, FGF1, TGFα, TGFβ, insulin and norepinephrine (Michalopoulos and DeFrances, 1997; Evarts *et al.*, 1993). Although these generate important information on the required factors for differentiation, the precise manner in which they influence a cell to regenerate is unknown and so cannot be directly applied to *in vitro* hepatocytes, where this process could potentially be used to expand and maintain populations. The same is true for differentiation of liver stem cells and hepatic progenitor cells, which are difficult to isolate and in the case of progenitor cells, in short supply in a healthy liver, as reviewed in Tosh *et al.* (Tosh and Strain, 2005) and Sangan *et al.* (Sangan and Tosh, 2010). Evidence of successful maturation of progenitor cells using co-culture with hepatic stellate cells was presented recently with raised expression of albumin and HNF4α and decreased expression of AFP and CK19 indicating a more mature hepatocyte (Chen *et al.*, 2009). Additional work to investigate enzyme and transporter levels in comparison to primary hepatocytes is required to confirm maturation and suitability for drug transport and metabolism studies.

In conclusion, I suggest that greater success is more likely to be gained from attempted differentiation of cells which are already closer in expression to that of a true hepatocyte than HepG2 and Huh7 used here; perhaps an immortalised line or transdifferentiated cells which do

not have the inherent changes of carcinoma cells. Although analysis of the HepaRG cell line at this stage is not complete, available data are indicative of a cell system more comparable to primary hepatocytes than either the HepG2 or Huh7 lines both before and after treatment. More may be gained by continued evaluation and development of HepaRG rather than attempted refining of the models created here. Alternatively, advances in the understanding of the differentiation and regeneration processes may result in sufficient knowledge to enhance protocols for application to stem cells from various sources and allow hepatocyte-like cells to be reliably produced from that avenue of research. Co-cultures of hepatic cell types also appear to have promise in prolonging the effective life of both cryopreserved and primary hepatocytes; for now, primary hepatocytes remain the gold standard toxicology prediction model.

Appendix A

Krebs and lysis buffer recipes used in experiments in chapters 7 and 8 are detailed here. All reagents were purchased from Sigma (Dorset, UK) unless otherwise stated.

Krebs buffer

NaCl	137mM
KCl	5.4mM
$CaCl_2$	2.8mM
$MgSO_4$	1mM
NaH_2PO_4	0.3mM
KH_2PO_4	0.3mM
Glucose	10mM
HEPES	10mM

pH to 7.4 with Tris base in 1L of deionised water

Lysis buffer for Hoechst 33342 experiments

EDTA (pH 8)	0.625mM
EGTA (pH 8)	1mM
Sucrose	0.64mM
Tris (pH 7.6)	1mM
Triton X-100	0.05%

Made up to 40ml in deionised water.

Protein lysis buffer (samples for Western blots)

SDS	0.002%

Nonidet P-40 0.2ml

DTT 1µM

Complete protease inhibitor cocktail tablets – 1 per 10ml (Roche)

Made up to 10ml with 1x PBS.

Appendix B

Sigma datasheet I2521

3050 Spruce Street
Saint Louis, Missouri 63103 USA
Telephone 800-325-8832 • (314) 771-5765
Fax (314) 286-7828
email: techservice@sial.com
sigma-aldrich.com

SIGMA

ProductInformation

Media Supplements:

ITS, SITE, SPIT, SPITE, Fatty Acid-Albumin Supplements

INTRODUCTION

Most cells will not survive or exhibit optimal phenotypic properties for any length of time when cultured in basal medium alone. They require supplementation with additional growth and survival factors, such as hormones, transport proteins, trace elements or ECM factors. Traditionally, serum has been the supplement of choice to provide these factors. However, many investigators prefer to work in a serum-free culture environment to avoid the variability and contaminants that can be introduced by serum.
Serum-free formulations that substitute a purified form of the factors normally supplied by serum are suitable for many *in vitro* growth and differentiation studies. These factors include insulin, transferrin, selenium, pyruvate, and ethanolamine. Addition of other components varies greatly, depending on the cell type being studied and the basal medium employed.

ROLE OF COMPONENTS

INSULIN is a polypeptide hormone that promotes the uptake of glucose and amino acids and may owe observed mitogenic effect to this property.

TRANSFERRIN is an iron-transport protein. Iron is an essential trace element, but can be toxic in the free form. To nourish cells in culture, it is supplied bound to transferrin in serum.

SELENIUM is an essential trace element normally provided by serum.

SODIUM PYRUVATE has been shown to be beneficial as an additional energy source in some instances.

ETHANOLAMINE is a fatty acid that plays a significant role in the proliferation of hybridoma cells and frequently is added to supplements used for culturing these cells.

MEDIA SUPPLEMENTS

Nutritional studies indicate that the supplement components described are utilized by most mammalian cells. They enhance cell proliferation and decrease the serum requirement of many cell types. When the following supplements are used with 2 to 4 percent serum, proliferation is reported to be similar to medium supplemented with 10 percent serum.

ITS is a mixture of bovine insulin, human transferrin (partially iron-saturated), and sodium selenite. It is a general cell supplement designed for use in non-complex media (e.g. MEM, RPMI-1640) and complex media (e.g. Ham□s F-12, DME/F-12, MEM) *with* sodium pyruvate.

SITE is a mixture of bovine insulin, human transferrin (partially iron-saturated), sodium selenite, and ethanolamine. It is a general cell supplement designed for use in non-complex media (e.g. MEM, RPMI-1640) and complex media (e.g. Ham□s F-12, DME/F-12, MEM) *with* sodium pyruvate.

SPIT is a mixture of bovine insulin, human transferrin (partially iron-saturated), sodium selenite, and sodium pyruvate. It is designed for cell cultures in which media *without* sodium pyruvate are used.

SPITE is a mixture of bovine insulin, human transferrin (partially iron-saturated), sodium selenite, sodium pyruvate and ethanolamine. It is designed for cell cultures in which media *without* sodium pyruvate are used.

FATTY ACID-ALBUMIN complexes have been employed as alternative sources of lipids in the development of serum-free media. Fatty acids bind to serum proteins in high proportions. Such proteins may release beneficial fatty acids and bind those that are inhibitory. Oleic acid bound to BSA has been shown to be beneficial to the growth of a variety of cell types (e.g. BHK, hybridoma). Similar observations have been made regarding linoleic acid, a precursor of prostaglandins. A mixture of poly- unsaturated and monosaturated fatty acids (i.e. linoleic acid and oleic acid) used as a medium supplement has been reported to exhibit a synergistic effect.

MEDIUM SUPPLEMENT FORMULATION TABLE

Final Conc. [1X]	ITS I 1884	SPIT S 5791	SPITE S 5666	SITE S 4920	ITS I 3146	ITS +1 I 2521	ITS +2 I 2646	ITS +3 I 2771	SITE +1 S 5045	SITE +2 S 5170	SITE +3 S 5295	FAC +LO L 9655	FAC +L L 9530	FAC +0 O 3008
insulin mg/L	5	10	10	10	10	10	10	10	10	10	10	□	□	□
transferrin mg/L	5	5.5	5.5	5.5	5.5	5.5	5.5	5.5	5.5	5.5	5.5	□	□	□
selenium µg/L	5	5	5	5	5	5	5	5	5	5	5	□	□	□
pyruvate mg/L	□	110	110	□	□	□	□	□	□	□	□	□	□	□
ethanolamine mg/L	□	□	2	2	□	□	□	□	2	2	2	□	□	□
BSA mg/mL	□	□	□	□	□	0.5	0.5	0.5	0.5	0.5	0.5	1.0	1.0	1.0
linoleic acid µg/mL	□	□	□	□	□	4.7	□	4.7	4.7	□	4.7	9.4	9.4	□
oleic acid µg/mL	□	□	□	□	□	□	4.7	4.7	□	4.7	4.7	9.4	□	9.4

NOTE: These products are sold at [100X] concentration. The concentration in the vial is [100X] value shown in the Table.

REFERENCES

1. Guilbert, L. J. and Iscove, N. N. (1976) Partial replacement of serum be selenite, transferrin, albumin, and lecithin on haemopoietic cell culture. Nature, 263: 594-595.
2. Ham, R. G. and McKeehan, W. L. (1979) Media and growth requirements. Methods in Enzymology, 58: 44-93.
3. Hinman, J. W. (1972) Prostaglandins. Ann. Rev. Biochem., 41: 161-178.
4. Kano-Sueoka, T. and Errick, J. E. (1981) Effects of phosphoethanolamine and ethanolamine on growth of mammalian carcinoma cells in culture. Exp. Cell Res., 97: 120-126.
5. Kelley, D. S., Becker, J. E., and Porter, V. R. (1978) Effects of insulin, dexamethasone, and glucagon on the amino acid transport ability of four rat hepatoma cell lines and rat hepatocytes in culture. Cancer Res., 38: 4591-4601. s, NY, p. 103.
6. McKeehan, W. L., Hamilton, W. G., and Ham, R. G. (1976) Selenium is an essential trace nutrient for the growth of WI-38 diploid human fibroblasts. Proc. Natl. Acad. Sci., USA 73: 2023-2027.
7. McKeehan, W. L. and McKeehan, K. A. (1979) Oxocarboxylic acids, pyrimidine nucleotide-linked oxidoreductase and serum factors in regulation of cell proliferation. J. Cell Physiol., 101: 9-16.
8. Murikami, H., Masui, H., Sato, G. H., Sueoka, N., Chow, T. P., and Sueoka, T. K. (1982) Growth of hybridoma cells in serum-free medium: ethanolamine is an essential component. Proc. Natl. Acad. Sci., USA 79: 1158-1162.
9. Wolpe, S. D. (1984) In: Mammalian Cell Culture. J. P. Mather ed. Plenum Pres.

References

Abe, T., Kakyo, M., Tokui, T., Nakagomi, R., Nishio, T., Nakai, D., Nomura, H., Unno, M., Suzuki, M., Naitoh, T., Matsuno, S. and Yawo, H. (1999) 'Identification of a novel gene family encoding human liver-specific organic anion transporter LST-1', *J Biol Chem,* 274, (24), pp. 17159-63.

Abe, T., Unno, M., Onogawa, T., Tokui, T., Kondo, T. N., Nakagomi, R., Adachi, H., Fujiwara, K., Okabe, M., Suzuki, T., Nunoki, K., Sato, E., Kakyo, M., Nishio, T., Sugita, J., Asano, N., Tanemoto, M., Seki, M., Date, F., Ono, K., Kondo, Y., Shiiba, K., Suzuki, M., Ohtani, H., Shimosegawa, T., Iinuma, K., Nagura, H., Ito, S. and Matsuno, S. (2001) 'LST-2, a human liver-specific organic anion transporter, determines methotrexate sensitivity in gastrointestinal cancers', *Gastroenterology,* 120, (7), pp. 1689-99.

Aden, D. P., Fogel, A., Plotkin, S., Damjanov, I. and Knowles, B. B. (1979) 'Controlled synthesis of HBsAg in a differentiated human liver carcinoma-derived cell line', *Nature,* 282, (5739), pp. 615-6.

Adjei, A. A., Gaedigk, A., Simon, S. D., Weinshilboum, R. M. and Leeder, J. S. (2008) 'Interindividual variability in acetaminophen sulfation by human fetal liver: implications for pharmacogenetic investigations of drug-induced birth defects', *Birth Defects Res A Clin Mol Teratol,* 82, (3), pp. 155-65.

Agarwal, S., Holton, K. L. and Lanza, R. (2008) 'Efficient Differentiation of Functional Hepatocytes from Human Embryonic Stem Cells', *Stem Cells,* 26, (5), pp. 1117-1127.

Al-Adsani, A., Burke, Z. D., Eberhard, D., Lawrence, K. L., Shen, C. N., Rustgi, A. K., Sakaue, H., Farrant, J. M. and Tosh, D. (2010) 'Dexamethasone treatment induces the reprogramming of pancreatic acinar cells to hepatocytes and ductal cells', *PLoS One,* 5, (10), pp. e13650.

Al-Waiz, M., Ayesh, R., Mitchell, S. C., Idle, J. R. and Smith, R. L. (1987) 'A genetic polymorphism of the N-oxidation of trimethylamine in humans', *Clin Pharmacol Ther,* 42, (5), pp. 588-94.

Allen, J. D. and Schinkel, A. H. (2002) 'Multidrug resistance and pharmacological protection mediated by the breast cancer resistance protein (BCRP/ABCG2)', *Mol Cancer Ther,* 1, (6), pp. 427-34.

Allen, J. D., van Loevezijn, A., Lakhai, J. M., van der Valk, M., van Tellingen, O., Reid, G., Schellens, J. H., Koomen, G. J. and Schinkel, A. H. (2002) 'Potent and specific inhibition of the breast cancer resistance protein multidrug transporter in vitro and in mouse intestine by a novel analogue of fumitremorgin C', *Mol Cancer Ther,* 1, (6), pp. 417-25.

Alvaro, D., Alpini, G., Onori, P., Franchitto, A., Glaser, S., Le Sage, G., Gigliozzi, A., Vetuschi, A., Morini, S., Attili, A. F. and Gaudio, E. (2002a) 'Effect of ovariectomy on the proliferative capacity of intrahepatic rat cholangiocytes', *Gastroenterology,* 123, (1), pp. 336-44.

Alvaro, D., Onori, P., Metalli, V. D., Svegliati-Baroni, G., Folli, F., Franchitto, A., Alpini, G., Mancino, M. G., Attili, A. F. and Gaudio, E. (2002b) 'Intracellular pathways mediating estrogen-induced cholangiocyte proliferation in the rat', *Hepatology,* 36, (2), pp. 297-304.

Ameen, C., Strehl, R., Bjorquist, P., Lindahl, A., Hyllner, J. and Sartipy, P. (2008) 'Human embryonic stem cells: Current technologies and emerging industrial applications', *Critical Reviews in Oncology/Hematology,* 65, (1), pp. 54-80.

Aninat, C., Piton, A., Glaise, D., Le Charpentier, T., Langouet, S., Morel, F., Guguen-Guillouzo, C. and Guillouzo, A. (2006) 'EXPRESSION OF CYTOCHROMES P450, CONJUGATING ENZYMES AND NUCLEAR RECEPTORS IN HUMAN HEPATOMA HepaRG CELLS', *Drug Metab Dispos,* 34, (1), pp. 75-83.

Antherieu, S., Chesne, C., Li, R., Camus, S., Lahoz, A., Picazo, L., Turpeinen, M., Tolonen, A., Uusitalo, J., Guguen-Guillouzo, C. and Guillouzo, A. (2010) 'Stable expression, activity, and inducibility of cytochromes P450 in differentiated HepaRG cells', *Drug Metab Dispos,* 38, (3), pp. 516-25.

Anzai, N., Kanai, Y. and Endou, H. (2006) 'Organic anion transporter family: current knowledge', *J Pharmacol Sci,* 100, (5), pp. 411-26.

Asseffa, A., Smith, S. J., Nagata, K., Gillette, J., Gelboin, H. V. and Gonzalez, F. J. (1989) 'Novel exogenous heme-dependent expression of mammalian cytochrome P450 using baculovirus', *Arch Biochem Biophys,* 274, (2), pp. 481-90.

Baharvand, H., Hashemi, S. M., Kazemi Ashtiani, S. and Farrokhi, A. (2006) 'Differentiation of human embryonic stem cells into hepatocytes in 2D and 3D culture systems in vitro', *Int J Dev Biol,* 50, (7), pp. 645-52.

Bain, M. A., Fornasini, G. and Evans, A. M. (2005) 'Trimethylamine: metabolic, pharmacokinetic and safety aspects', *Curr Drug Metab,* 6, (3), pp. 227-40.

Bednarkiewicz, A., Rodrigues, R. M. and Whelan, M. P. (2010) 'Enrichment of hepatocytes in a HepaRG culture using spatially selective photodynamic treatment', *J Biomed Opt,* 15, (2), pp. 028002.

Ben-Ze'ev, A., Robinson, G. S., Bucher, N. L. and Farmer, S. R. (1988) 'Cell-cell and cell-matrix interactions differentially regulate the expression of hepatic and cytoskeletal genes in primary cultures of rat hepatocytes', *Proc Natl Acad Sci U S A,* 85, (7), pp. 2161-5.

Berasain, C., Garcia-Trevijano, E. R., Castillo, J., Erroba, E., Lee, D. C., Prieto, J. and Avila, M. A. (2005) 'Amphiregulin: an early trigger of liver regeneration in mice', *Gastroenterology,* 128, (2), pp. 424-32.

Bhatia, S. N., Balis, U. J., Yarmush, M. L. and Toner, M. (1999) 'Effect of cell-cell interactions in preservation of cellular phenotype: cocultivation of hepatocytes and nonparenchymal cells', *FASEB J,* 13, (14), pp. 1883-900.

Bhatia, S. N., Yarmush, M. L. and Toner, M. (1997) 'Controlling cell interactions by micropatterning in co-cultures: hepatocytes and 3T3 fibroblasts', *J Biomed Mater Res,* 34, (2), pp. 189-99.

Bird, T. G., Lorenzini, S. and Forbes, S. J. (2008) 'Activation of stem cells in hepatic diseases', *Cell Tissue Res,* 331, (1), pp. 283-300.

Bock, K. W. (2010) 'Functions and transcriptional regulation of adult human hepatic UDP-glucuronosyl-transferases (UGTs): Mechanisms responsible for interindividual variation of UGT levels', *Biochemical Pharmacology,* 80, (6), pp. 771-777.

Bode, G., Clausing, P., Gervais, F., Loegsted, J., Luft, J., Nogues, V. and Sims, J. (2010) 'The utility of the minipig as an animal model in regulatory toxicology', *J Pharmacol Toxicol Methods,* 62, (3), pp. 196-220.

Bokhari, M., Carnachan, R. J., Cameron, N. R. and Przyborski, S. A. (2007a) 'Culture of HepG2 liver cells on three dimensional polystyrene scaffolds enhances cell structure and function during toxicological challenge', *J Anat,* 211, (4), pp. 567-76.

Bokhari, M., Carnachan, R. J., Cameron, N. R. and Przyborski, S. A. (2007b) 'Novel cell culture device enabling three-dimensional cell growth and improved cell function', *Biochem Biophys Res Commun,* 354, (4), pp. 1095-100.

Bolduc, L., Labrecque, B., Cordeau, M., Blanchette, M. and Chabot, B. (2001) 'Dimethyl sulfoxide affects the selection of splice sites', *J Biol Chem,* 276, (20), pp. 17597-602.

Boyer, J. L., Ng, O. C., Ananthanarayanan, M., Hofmann, A. F., Schteingart, C. D., Hagenbuch, B., Stieger, B. and Meier, P. J. (1994) 'Expression and characterization of a functional rat liver Na+ bile acid cotransport system in COS-7 cells', *Am J Physiol,* 266, (3 Pt 1), pp. G382-7.

Bozina, N., Bradamante, V. and Lovric, M. (2009) 'Genetic polymorphism of metabolic enzymes P450 (CYP) as a susceptibility factor for drug response, toxicity, and cancer risk', *Arh Hig Rada Toksikol,* 60, (2), pp. 217-42.

Bradford, M. M. (1976) 'A rapid and sensitive method for the quantitation of microgram quantities of protein utilizing the principle of protein-dye binding', *Anal Biochem,* 72, pp. 248-54.

Brown, C. D. A., Sayer, R., Windass, A. S., Haslam, I. S., De Broe, M. E., D'Haese, P. C. and Verhulst, A. (2008) 'Characterisation of human tubular cell monolayers as a model of proximal tubular xenobiotic handling', *Toxicology and Applied Pharmacology,* 233, (3), pp. 428-438.

Bucher, N. L., Patel, U. and Cohen, S. (1977) 'Hormonal factors concerned with liver regeneration', *Ciba Found Symp*, (55), pp. 95-107.

Burchell, B., Lockley, D. J., Staines, A., Uesawa, Y. and Coughtrie, M. W. (2005) 'Substrate specificity of human hepatic udp-glucuronosyltransferases', *Methods Enzymol,* 400, pp. 46-57.

Burk, O., Arnold, K. A., Geick, A., Tegude, H. and Eichelbaum, M. (2005) 'A role for constitutive androstane receptor in the regulation of human intestinal MDR1 expression', *Biol Chem,* 386, (6), pp. 503-13.

Burke, Z. D., Shen, C. N., Ralphs, K. L. and Tosh, D. (2006) 'Characterization of liver function in transdifferentiated hepatocytes', *Journal of Cellular Physiology,* 206, (1), pp. 147-159.

Burnette, W. N. (1981) '"Western blotting": electrophoretic transfer of proteins from sodium dodecyl sulfate--polyacrylamide gels to unmodified nitrocellulose and radiographic detection with antibody and radioiodinated protein A', *Anal Biochem,* 112, (2), pp. 195-203.

Burnette, W. N. (2009) 'Western blotting : remembrance of past things', *Methods Mol Biol,* 536, pp. 5-8.

Bustin, S. A., Benes, V., Garson, J. A., Hellemans, J., Huggett, J., Kubista, M., Mueller, R., Nolan, T., Pfaffl, M. W., Shipley, G. L., Vandesompele, J. and Wittwer, C. T. (2009) 'The MIQE guidelines: minimum information for publication of quantitative real-time PCR experiments', *Clin Chem,* 55, (4), pp. 611-22.

Caja, L., Bertran, E., Campbell, J., Fausto, N. and Fabregat, I. (2011) 'The transforming growth factor-beta (TGF-beta) mediates acquisition of a mesenchymal stem cell-like phenotype in human liver cells', *J Cell Physiol,* 226, (5), pp. 1214-23.

Canova, C., Richiardi, L., Merletti, F., Pentenero, M., Gervasio, C., Tanturri, G., Garzino-Demo, P., Pecorari, G., Talamini, R., Barzan, L., Sulfaro, S., Franchini, G., Muzzolini, C., Bordin, S., Pugliese, G. N., Macri, E. and Simonato, L. (2010) 'Alcohol, tobacco and genetic susceptibility in relation to cancers of the upper aerodigestive tract in northern Italy', *Tumori,* 96, (1), pp. 1-10.

Cao, S., Esquivel, C. O. and Keeffe, E. B. (1998) 'New approaches to supporting the failing liver', *Annu Rev Med,* 49, pp. 85-94.

Carlile, D. J., Zomorodi, K. and Houston, J. B. (1997) 'Scaling Factors to Relate Drug Metabolic Clearance in Hepatic Microsomes, Isolated Hepatocytes, and the Intact Liver', *Drug Metabolism and Disposition,* 25, (8), pp. 903-911.

Carpentier, B., Gautier, A. and Legallais, C. (2009) 'Artificial and bioartificial liver devices: present and future', *Gut,* 58, (12), pp. 1690-702.

Cascio, S. and Zaret, K. S. (1991) 'Hepatocyte differentiation initiates during endodermal-mesenchymal interactions prior to liver formation', *Development,* 113, (1), pp. 217-25.

Cazeneuve, C., Pons, G., Rey, E., Treluyer, J. M., Cresteil, T., Thiroux, G., D'Athis, P. and Olive, G. (1994) 'Biotransformation of caffeine in human liver microsomes from foetuses, neonates, infants and adults', *Br J Clin Pharmacol,* 37, (5), pp. 405-12.

Cederbaum, A. I. (2006) 'Cytochrome P450 2E1-dependent oxidant stress and upregulation of anti-oxidant defense in liver cells', *Journal of Gastroenterology and Hepatology,* 21, pp. S22-S25.

Ceelen, L., De Spiegelaere, W., David, M., De Craene, J., Vinken, M., Vanhaecke, T. and Rogiers, V. (2011) 'Critical selection of reliable reference genes for gene expression study in the HepaRG cell line', *Biochem Pharmacol,* 81, (10), pp. 1255-61.

Chang, T. T. and Hughes-Fulford, M. (2009) 'Monolayer and spheroid culture of human liver hepatocellular carcinoma cell line cells demonstrate distinct global gene expression patterns and functional phenotypes', *Tissue Eng Part A,* 15, (3), pp. 559-67.

Chen, L., Chen, X. P., Zhang, W., Liang, H. F., Lin, Y. Z., Dong, H. H. and Zhou, Q. D. (2009) '[Differentiation of hepatic oval cell into mature hepatocyte induced by hepatic stellate cells]', *Zhonghua Gan Zang Bing Za Zhi,* 17, (10), pp. 765-70.

Chen, Z. S., Lee, K. and Kruh, G. D. (2001) 'Transport of cyclic nucleotides and estradiol 17-beta-D-glucuronide by multidrug resistance protein 4. Resistance to 6-mercaptopurine and 6-thioguanine', *J Biol Chem,* 276, (36), pp. 33747-54.

Cheng, J., Meziani, M. J., Sun, Y.-P. and Cheng, S. H. (2011) 'Poly(ethylene glycol)-conjugated multi-walled carbon nanotubes as an efficient drug carrier for overcoming multidrug resistance', *Toxicology and Applied Pharmacology,* 250, (2), pp. 184-193.

Childs, S., Yeh, R. L., Hui, D. and Ling, V. (1998) 'Taxol resistance mediated by transfection of the liver-specific sister gene of P-glycoprotein', *Cancer Res,* 58, (18), pp. 4160-7.

Chodon, D., Ramamurty, N. and Sakthisekaran, D. (2007) 'Preliminary studies on induction of apoptosis by genistein on HepG2 cell line', *Toxicol In Vitro,* 21, (5), pp. 887-91.

Choi, S., Sainz, B., Jr., Corcoran, P., Uprichard, S. and Jeong, H. (2009) 'Characterization of increased drug metabolism activity in dimethyl sulfoxide (DMSO)-treated Huh7 hepatoma cells', *Xenobiotica,* 39, (3), pp. 205-17.

Chung, W. G., Park, C. S., Roh, H. K., Lee, W. K. and Cha, Y. N. (2000) 'Oxidation of ranitidine by isozymes of flavin-containing monooxygenase and cytochrome P450', *Jpn J Pharmacol,* 84, (2), pp. 213-20.

Ciaccio, P. J., Tew, K. D. and LaCreta, F. P. (1991) 'Enzymatic conjugation of chlorambucil with glutathione by human glutathione S-transferases and inhibition by ethacrynic acid', *Biochem Pharmacol,* 42, (7), pp. 1504-7.

Colabufo, N. A., Berardi, F., Perrone, M. G., Capparelli, E., Cantore, M., Inglese, C. and Perrone, R. (2010) 'Substrates, inhibitors and activators of P-glycoprotein: candidates for radiolabeling and imaging perspectives', *Curr Top Med Chem,* 10, (17), pp. 1703-14.

Cole, S. P., Bhardwaj, G., Gerlach, J. H., Mackie, J. E., Grant, C. E., Almquist, K. C., Stewart, A. J., Kurz, E. U., Duncan, A. M. and Deeley, R. G. (1992) 'Overexpression of a transporter gene in a multidrug-resistant human lung cancer cell line', *Science,* 258, (5088), pp. 1650-4.

Comer, K. A., Falany, J. L. and Falany, C. N. (1993) 'Cloning and expression of human liver dehydroepiandrosterone sulphotransferase', *Biochem J,* 289 (Pt 1), pp. 233-40.

Court, M. H. (2005) 'Isoform-selective probe substrates for in vitro studies of human UDP-glucuronosyltransferases', *Methods Enzymol,* 400, pp. 104-16.

Courtois, A., Payen, L., Le Ferrec, E., Scheffer, G. L., Trinquart, Y., Guillouzo, A. and Fardel, O. (2002) 'Differential regulation of multidrug resistance-associated protein 2 (MRP2) and cytochromes P450 2B1/2 and 3A1/2 in phenobarbital-treated hepatocytes', *Biochemical Pharmacology,* 63, (2), pp. 333-341.

Coward, S. M., Legallais, C., David, B., Thomas, M., Foo, Y., Mavri-Damelin, D., Hodgson, H. J. and Selden, C. (2009) 'Alginate-encapsulated HepG2 cells in a fluidized bed bioreactor maintain function in human liver failure plasma', *Artif Organs,* 33, (12), pp. 1117-26.

Cruise, J. L., Houck, K. A. and Michalopoulos, G. K. (1985) 'Induction of DNA synthesis in cultured rat hepatocytes through stimulation of alpha 1 adrenoreceptor by norepinephrine', *Science,* 227, (4688), pp. 749-51.

Cui, Y., Konig, J., Buchholz, J. K., Spring, H., Leier, I. and Keppler, D. (1999) 'Drug resistance and ATP-dependent conjugate transport mediated by the apical multidrug resistance protein, MRP2, permanently expressed in human and canine cells', *Mol Pharmacol,* 55, (5), pp. 929-37.

Cui, Y., Konig, J., Leier, I., Buchholz, U. and Keppler, D. (2001) 'Hepatic uptake of bilirubin and its conjugates by the human organic anion transporter SLC21A6', *J Biol Chem,* 276, (13), pp. 9626-30.

Dannenberg, L. O. and Edenberg, H. J. (2006) 'Epigenetics of gene expression in human hepatoma cells: expression profiling the response to inhibition of DNA methylation and histone deacetylation', *BMC Genomics,* 7, pp. 181.

Darlington, G. J. (1999) 'Molecular mechanisms of liver development and differentiation', *Curr Opin Cell Biol,* 11, (6), pp. 678-82.

Darnell, M., Schreiter, T., Zeilinger, K., Urbaniak, T., Soderdahl, T., Rossberg, I., Dillner, B., Berg, A. L., Gerlach, J. and Andersson, T. B. (2011) 'Cytochrome P450 (CYP) dependent metabolism in HepaRG cells cultured in a dynamic three-dimensional (3D) bioreactor', *Drug Metab Dispos*.

Dash, A., Inman, W., Hoffmaster, K., Sevidal, S., Kelly, J., Obach, R. S., Griffith, L. G. and Tannenbaum, S. R. (2009) 'Liver tissue engineering in the evaluation of drug safety', *Expert Opin Drug Metab Toxicol,* 5, (10), pp. 1159-74.

Dauchy, S., Dutheil, F., Weaver, R. J., Chassoux, F., Daumas-Duport, C., Couraud, P. O., Scherrmann, J. M., De Waziers, I. and Decleves, X. (2008) 'ABC transporters, cytochromes P450 and their main transcription factors: expression at the human blood-brain barrier', *J Neurochem,* 107, (6), pp. 1518-28.

Dean, M., Rzhetsky, A. and Allikmets, R. (2001) 'The human ATP-binding cassette (ABC) transporter superfamily', *Genome Res,* 11, (7), pp. 1156-66.

Demetriou, A. A., Brown, R. S., Jr., Busuttil, R. W., Fair, J., McGuire, B. M., Rosenthal, P., Am Esch, J. S., 2nd, Lerut, J., Nyberg, S. L., Salizzoni, M., Fagan, E. A., de Hemptinne, B., Broelsch, C. E., Muraca, M., Salmeron, J. M., Rabkin, J. M., Metselaar, H. J., Pratt, D., De La Mata, M., McChesney, L. P., Everson, G. T., Lavin, P. T., Stevens, A. C., Pitkin, Z. and Solomon, B. A. (2004) 'Prospective, randomized, multicenter, controlled trial of a bioartificial liver in treating acute liver failure', *Ann Surg,* 239, (5), pp. 660-7; discussion 667-70.

Desmots, F., Rissel, M., Loyer, P., Turlin, B. and Guillouzo, A. (2001) 'Immunohistological analysis of glutathione transferase A4 distribution in several human tissues using a specific polyclonal antibody', *J Histochem Cytochem,* 49, (12), pp. 1573-80.

Deutsch, G., Jung, J., Zheng, M., Lora, J. and Zaret, K. S. (2001) 'A bipotential precursor population for pancreas and liver within the embryonic endoderm', *Development,* 128, (6), pp. 871-81.

DiMasi, J. A., Hansen, R. W. and Grabowski, H. G. (2003) 'The price of innovation: new estimates of drug development costs', *Journal of Health Economics,* 22, (2), pp. 151-185.

Doyle, L. A., Yang, W., Abruzzo, L. V., Krogmann, T., Gao, Y., Rishi, A. K. and Ross, D. D. (1998) 'A multidrug resistance transporter from human MCF-7 breast cancer cells', *Proc Natl Acad Sci U S A,* 95, (26), pp. 15665-70.

Duan, Y., Ma, X., Zou, W., Wang, C., Bahbahan, I. S., Ahuja, T. P., Tolstikov, V. and Zern, M. A. (2010) 'Differentiation and characterization of metabolically functioning hepatocytes from human embryonic stem cells', *Stem Cells,* 28, (4), pp. 674-86.

Dumont, J., Josse, R., Lambert, C., Antherieu, S., Laurent, V., Loyer, P., Robin, M. A. and Guillouzo, A. (2010a) 'Preferential induction of the AhR gene battery in HepaRG cells after a single or repeated exposure to heterocyclic aromatic amines', *Toxicol Appl Pharmacol,* 249, (1), pp. 91-100.

Dumont, J., Josse, R., Lambert, C., Antherieu, S., Le Hegarat, L., Aninat, C., Robin, M. A., Guguen-Guillouzo, C. and Guillouzo, A. (2010b) 'Differential toxicity of heterocyclic aromatic amines and their mixture in metabolically competent HepaRG cells', *Toxicol Appl Pharmacol,* 245, (2), pp. 256-63.

Dunn, J. C., Tompkins, R. G. and Yarmush, M. L. (1992) 'Hepatocytes in collagen sandwich: evidence for transcriptional and translational regulation', *J Cell Biol,* 116, (4), pp. 1043-53.

Dunn, J. C., Yarmush, M. L., Koebe, H. G. and Tompkins, R. G. (1989) 'Hepatocyte function and extracellular matrix geometry: long-term culture in a sandwich configuration', *FASEB J,* 3, (2), pp. 174-7.

Eberhard, D., O'Neill, K., Burke, Z. D. and Tosh, D. (2010) 'In vitro reprogramming of pancreatic cells to hepatocytes', *Methods Mol Biol,* 636, pp. 285-92.

Ek, M., Soderdahl, T., Kuppers-Munther, B., Edsbagge, J., Andersson, T. B., Bjorquist, P., Cotgreave, I., Jernstrom, B., Ingelman-Sundberg, M. and Johansson, I. (2007) 'Expression of drug metabolizing enzymes in hepatocyte-like cells derived from human embryonic stem cells', *Biochem Pharmacol,* 74, (3), pp. 496-503.

Eklund, B. I., Moberg, M., Bergquist, J. and Mannervik, B. (2006) 'Divergent activities of human glutathione transferases in the bioactivation of azathioprine', *Mol Pharmacol,* 70, (2), pp. 747-54.

Elizondo, G. and Medina-Diaz, I. M. (2003) 'Induction of CYP3A4 by 1alpha,25-dyhydroxyvitamin D3 in HepG2 cells', *Life Sci,* 73, (2), pp. 141-9.

Ellis, A. J., Hughes, R. D., Wendon, J. A., Dunne, J., Langley, P. G., Kelly, J. H., Gislason, G. T., Sussman, N. L. and Williams, R. (1996) 'Pilot-controlled trial of the extracorporeal liver assist device in acute liver failure', *Hepatology,* 24, (6), pp. 1446-51.

Enomoto, A., Wempe, M. F., Tsuchida, H., Shin, H. J., Cha, S. H., Anzai, N., Goto, A., Sakamoto, A., Niwa, T., Kanai, Y., Anders, M. W. and Endou, H. (2002) 'Molecular identification of a novel carnitine transporter specific to human testis. Insights into the mechanism of carnitine recognition', *J Biol Chem,* 277, (39), pp. 36262-71.

Evarts, R. P., Hu, Z., Fujio, K., Marsden, E. R. and Thorgeirsson, S. S. (1993) 'Activation of hepatic stem cell compartment in the rat: role of transforming growth factor alpha, hepatocyte growth factor, and acidic fibroblast growth factor in early proliferation', *Cell Growth Differ,* 4, (7), pp. 555-61.

Fahrmayr, C., Fromm, M. F. and KÃ¶nig, J. r. (2010) 'Hepatic OATP and OCT uptake transporters: their role for drug-drug interactions and pharmacogenetic aspects', *Drug Metabolism Reviews,* 0, (0), pp. 1-22.

Falany, C. N., Krasnykh, V. and Falany, J. L. (1995) 'Bacterial expression and characterization of a cDNA for human liver estrogen sulfotransferase', *J Steroid Biochem Mol Biol,* 52, (6), pp. 529-39.

Farmer, S. R., Wan, K. M., Ben-Ze'ev, A. and Penman, S. (1983) 'Regulation of actin mRNA levels and translation responds to changes in cell configuration', *Mol Cell Biol,* 3, (2), pp. 182-9.

Faucette, S. R., Sueyoshi, T., Smith, C. M., Negishi, M., Lecluyse, E. L. and Wang, H. (2006) 'Differential regulation of hepatic CYP2B6 and CYP3A4 genes by constitutive androstane receptor but not pregnane X receptor', *J Pharmacol Exp Ther,* 317, (3), pp. 1200-9.

Fiore, M. and Degrassi, F. (1999) 'Dimethyl sulfoxide restores contact inhibition-induced growth arrest and inhibits cell density-dependent apoptosis in hamster cells', *Exp Cell Res,* 251, (1), pp. 102-10.

Fleige, S., Walf, V., Huch, S., Prgomet, C., Sehm, J. and Pfaffl, M. W. (2006) 'Comparison of relative mRNA quantification models and the impact of RNA integrity in quantitative real-time RT-PCR', *Biotechnol Lett,* 28, (19), pp. 1601-13.

Funk, C. (2008) 'The role of hepatic transporters in drug elimination', *Expert Opin Drug Metab Toxicol,* 4, (4), pp. 363-79.

Galbraith, R. A., Sassa, S. and Kappas, A. (1986) 'Induction of haem synthesis in Hep G2 human hepatoma cells by dimethyl sulphoxide. A transcriptionally activated event', *Biochem J,* 237, (2), pp. 597-600.

Gamage, N., Barnett, A., Hempel, N., Duggleby, R. G., Windmill, K. F., Martin, J. L. and McManus, M. E. (2006) 'Human sulfotransferases and their role in chemical metabolism', *Toxicol Sci,* 90, (1), pp. 5-22.

Gaudio, E., Carpino, G., Cardinale, V., Franchitto, A., Onori, P. and Alvaro, D. (2009) 'New insights into liver stem cells', *Dig Liver Dis,* 41, (7), pp. 455-62.

Gebhardt, R. (1992) 'Metabolic zonation of the liver: regulation and implications for liver function', *Pharmacol Ther,* 53, (3), pp. 275-354.

Gekeler, V., Ise, W., Sanders, K. H., Ulrich, W. R. and Beck, J. (1995) 'The leukotriene LTD4 receptor antagonist MK571 specifically modulates MRP associated multidrug resistance', *Biochem Biophys Res Commun,* 208, (1), pp. 345-52.

Gerlach, J. H., Endicott, J. A., Juranka, P. F., Henderson, G., Sarangi, F., Deuchars, K. L. and Ling, V. (1986a) 'Homology between P-glycoprotein and a bacterial haemolysin transport protein suggests a model for multidrug resistance', *Nature,* 324, (6096), pp. 485-9.

Gerlach, J. H., Kartner, N., Bell, D. R. and Ling, V. (1986b) 'Multidrug resistance', *Cancer Surv,* 5, (1), pp. 25-46.

Gibson, G. G., Phillips, A., Aouabdi, S., Plant, K. and Plant, N. (2006) 'Transcriptional regulation of the human pregnane-X receptor', *Drug Metab Rev,* 38, (1-2), pp. 31-49.

Gilot, D., Loyer, P., Corlu, A., Glaise, D., Lagadic-Gossmann, D., Atfi, A., Morel, F., Ichijo, H. and Guguen-Guillouzo, C. (2002) 'Liver protection from apoptosis requires both blockage of initiator caspase activities and inhibition of ASK1/JNK pathway via glutathione S-transferase regulation', *J Biol Chem,* 277, (51), pp. 49220-9.

Gkretsi, V., Bowen, W. C., Yang, Y., Wu, C. and Michalopoulos, G. K. (2007) 'Integrin-linked kinase is involved in matrix-induced hepatocyte differentiation', *Biochem Biophys Res Commun,* 353, (3), pp. 638-43.

Glaros, E. N., Kim, W. S. and Garner, B. (2010) 'Myriocin-mediated up-regulation of hepatocyte apoA-I synthesis is associated with ERK inhibition', *Clinical Science,* 118, (12), pp. 727-736.

Glaser, S. S., Gaudio, E., Miller, T., Alvaro, D. and Alpini, G. (2009) 'Cholangiocyte proliferation and liver fibrosis', *Expert Rev Mol Med,* 11, pp. e7.

Goda, K., Fenyvesi, F., Bacso, Z., Nagy, H., Marian, T., Megyeri, A., Krasznai, Z., Juhasz, I., Vecsernyes, M. and Szabo, G., Jr. (2007) 'Complete inhibition of P-glycoprotein by simultaneous treatment with a distinct class of modulators and the UIC2 monoclonal antibody', *J Pharmacol Exp Ther,* 320, (1), pp. 81-8.

Gomez-Lechon, M. J., Donato, M. T., Castell, J. V. and Jover, R. (2003a) 'Human hepatocytes as a tool for studying toxicity and drug metabolism', *Curr Drug Metab,* 4, (4), pp. 292-312.

Gomez-Lechon, M. J., Donato, M. T., Castell, J. V. and Jover, R. (2004) 'Human hepatocytes in primary culture: the choice to investigate drug metabolism in man', *Curr Drug Metab,* 5, (5), pp. 443-62.

Gomez-Lechon, M. J., Donato, T., Ponsoda, X. and Castell, J. V. (2003b) 'Human hepatic cell cultures: in vitro and in vivo drug metabolism', *Altern Lab Anim,* 31, (3), pp. 257-65.

Greenhough, S., Medine, C. N. and Hay, D. C. (2010) 'Pluripotent stem cell derived hepatocyte like cells and their potential in toxicity screening', *Toxicology,* 278, (3), pp. 250-5.

Greiner, B., Eichelbaum, M., Fritz, P., Kreichgauer, H. P., von Richter, O., Zundler, J. and Kroemer, H. K. (1999) 'The role of intestinal P-glycoprotein in the interaction of digoxin and rifampin', *J Clin Invest,* 104, (2), pp. 147-53.

Gripon, P., Rumin, S., Urban, S., Le Seyec, J., Glaise, D., Cannie, I., Guyomard, C., Lucas, J., Trepo, C. and Guguen-Guillouzo, C. (2002) 'Infection of a human hepatoma cell line by hepatitis B virus', *Proc Natl Acad Sci U S A,* 99, (24), pp. 15655-60.

Guengerich, F. P. (1999) 'Cytochrome P-450 3A4: regulation and role in drug metabolism', *Annu Rev Pharmacol Toxicol,* 39, pp. 1-17.

Guillouzo, A., Corlu, A., Aninat, C., Glaise, D., Morel, F. and Guguen-Guillouzo, C. (2007) 'The human hepatoma HepaRG cells: A highly differentiated model for studies of liver metabolism and toxicity of xenobiotics', *Chemico-Biological Interactions,* 168, (1), pp. 66-73.

Guo, L., Song, L., Wang, Z., Zhao, W., Mao, W. and Yin, M. (2009) 'Panaxydol inhibits the proliferation and induces the differentiation of human hepatocarcinoma cell line HepG2', *Chemico-Biological Interactions,* In Press, Corrected Proof.

Gutierrez, L., Mauriat, M., Guenin, S., Pelloux, J., Lefebvre, J. F., Louvet, R., Rusterucci, C., Moritz, T., Guerineau, F., Bellini, C. and Van Wuytswinkel, O. (2008) 'The lack of a systematic validation of reference genes: a serious pitfall undervalued in reverse transcription-polymerase chain reaction (RT-PCR) analysis in plants', *Plant Biotechnol J,* 6, (6), pp. 609-18.

Hagenbuch, B. and Meier, P. J. (2004) 'Organic anion transporting polypeptides of the OATP/ SLC21 family: phylogenetic classification as OATP/ SLCO superfamily, new nomenclature and molecular/functional properties', *Pflugers Arch,* 447, (5), pp. 653-65.

Haimeur, A., Conseil, G., Deeley, R. G. and Cole, S. P. (2004) 'The MRP-related and BCRP/ABCG2 multidrug resistance proteins: biology, substrate specificity and regulation', *Curr Drug Metab,* 5, (1), pp. 21-53.

Hariparsad, N., Carr, B. A., Evers, R. and Chu, X. (2008) 'COMPARISON OF IMMORTALIZED Fa2N-4 CELLS AND HUMAN HEPATOCYTES AS IN VITRO MODELS FOR CYTOCHROME P450 INDUCTION', *Drug Metab Dispos*.

Hart, S. N., Li, Y., Nakamoto, K., Subileau, E.-a., Steen, D. and Zhong, X.-b. (2010) 'A Comparison of Whole Genome Gene Expression Profiles of HepaRG Cells and HepG2 Cells to Primary Human Hepatocytes and Human Liver Tissues', *Drug Metabolism and Disposition,* 38, (6), pp. 988-994.

Haslam, I. S., Jones, K., Coleman, T. and Simmons, N. L. (2008) 'Rifampin and digoxin induction of MDR1 expression and function in human intestinal (T84) epithelial cells', *Br J Pharmacol,* 154, (1), pp. 246-55.

Hay, D. C., Zhao, D., Fletcher, J., Hewitt, Z. A., McLean, D., Urruticoechea-Uriguen, A., Black, J. R., Elcombe, C., Ross, J. A., Wolf, R. and Cui, W. (2008) 'Efficient Differentiation of Hepatocytes from Human Embryonic Stem Cells Exhibiting Markers Recapitulating Liver Development In Vivo', *Stem Cells,* 26, (4), pp. 894-902.

Hay, D. C., Zhao, D., Ross, A., Mandalam, R., Lebkowski, J. and Cui, W. (2007) 'Direct differentiation of human embryonic stem cells to hepatocyte-like cells exhibiting functional activities', *Cloning Stem Cells,* 9, (1), pp. 51-62.

Hayes, J. D., Flanagan, J. U. and Jowsey, I. R. (2005) 'Glutathione transferases', *Annu Rev Pharmacol Toxicol,* 45, pp. 51-88.

Hayes, J. D. and Pulford, D. J. (1995) 'The glutathione S-transferase supergene family: regulation of GST and the contribution of the isoenzymes to cancer chemoprotection and drug resistance', *Crit Rev Biochem Mol Biol,* 30, (6), pp. 445-600.

Hayes, J. D. and Strange, R. C. (2000) 'Glutathione S-transferase polymorphisms and their biological consequences', *Pharmacology,* 61, (3), pp. 154-66.

Hein, D. W., McQueen, C. A., Grant, D. M., Goodfellow, G. H., Kadlubar, F. F. and Weber, W. W. (2000) 'Pharmacogenetics of the arylamine N-acetyltransferases: a symposium in honor of Wendell W. Weber', *Drug Metab Dispos,* 28, (12), pp. 1425-32.

Henderson, N. C. and Forbes, S. J. (2008) 'Hepatic fibrogenesis: from within and outwith', *Toxicology,* 254, (3), pp. 130-5.

Hengstler, J. G., Brulport, M., Schormann, W., Bauer, A., Hermes, M., Nussler, A. K., Fandrich, F., Ruhnke, M., Ungefroren, H., Griffin, L., Bockamp, E., Oesch, F. and von Mach, M. A. (2005) 'Generation of human hepatocytes by stem cell technology: definition of the hepatocyte', *Expert Opin Drug Metab Toxicol,* 1, (1), pp. 61-74.

Hewitt, N. J. and Hewitt, P. (2004) 'Phase I and II enzyme characterization of two sources of HepG2 cell lines', *Xenobiotica,* 34, (3), pp. 243-56.

Hewitt, N. J., Lechon, M. J., Houston, J. B., Hallifax, D., Brown, H. S., Maurel, P., Kenna, J. G., Gustavsson, L., Lohmann, C., Skonberg, C., Guillouzo, A., Tuschl, G., Li, A. P., LeCluyse, E., Groothuis, G. M. and Hengstler, J. G. (2007) 'Primary hepatocytes: current understanding of the regulation of metabolic enzymes and transporter proteins, and pharmaceutical practice for the use of hepatocytes in metabolism, enzyme induction, transporter, clearance, and hepatotoxicity studies', *Drug Metab Rev,* 39, (1), pp. 159-234.

Hilgendorf, C., Ahlin, G., Seithel, A., Artursson, P., Ungell, A. L. and Karlsson, J. (2007) 'Expression of thirty-six drug transporter genes in human intestine, liver, kidney, and organotypic cell lines', *Drug Metab Dispos,* 35, (8), pp. 1333-40.

Hines, R. N. (2006) 'Developmental and tissue-specific expression of human flavin-containing monooxygenases 1 and 3', *Expert Opin Drug Metab Toxicol,* 2, (1), pp. 41-9.

Hines, R. N. (2008) 'The ontogeny of drug metabolism enzymes and implications for adverse drug events', *Pharmacology & Therapeutics,* 118, (2), pp. 250-267.

Hodgson, E., Rose, R. L., Cao, Y., Dehal, S. S. and Kupfer, D. (2000) 'Flavin-containing monooxygenase isoform specificity for the N-oxidation of tamoxifen determined by product measurement and NADPH oxidation', *J Biochem Mol Toxicol,* 14, (2), pp. 118-20.

Hodgson, E., Rose, R. L., Ryu, D. Y., Falls, G., Blake, B. L. and Levi, P. E. (1995) 'Pesticide-metabolizing enzymes', *Toxicol Lett,* 82-83, pp. 73-81.

Hooijberg, J. H., Jansen, G., Assaraf, Y. G., Kathmann, I., Pieters, R., Laan, A. C., Veerman, A. J., Kaspers, G. J. and Peters, G. J. (2004) 'Folate concentration dependent transport activity of the Multidrug Resistance Protein 1 (ABCC1)', *Biochem Pharmacol,* 67, (8), pp. 1541-8.

Hooijberg, J. H., Peters, G. J., Assaraf, Y. G., Kathmann, I., Priest, D. G., Bunni, M. A., Veerman, A. J., Scheffer, G. L., Kaspers, G. J. and Jansen, G. (2003) 'The role of multidrug resistance proteins MRP1, MRP2 and MRP3 in cellular folate homeostasis', *Biochem Pharmacol,* 65, (5), pp. 765-71.

Hossein Baharvand, S. M. H. M. S. (2008) 'Differentiation of human embryonic stem cells into functional hepatocyte-like cells in a serum-free adherent culture condition', *Differentiation,* 76, (5), pp. 465-477.

Huang, P., He, Z., Ji, S., Sun, H., Xiang, D., Liu, C., Hu, Y., Wang, X. and Hui, L. (2011) 'Induction of functional hepatocyte-like cells from mouse fibroblasts by defined factors', *Nature*.

Huang, W., Ma, K., Zhang, J., Qatanani, M., Cuvillier, J., Liu, J., Dong, B., Huang, X. and Moore, D. D. (2006) 'Nuclear receptor-dependent bile acid signaling is required for normal liver regeneration', *Science,* 312, (5771), pp. 233-6.

Hubatsch, I., Ridderstrom, M. and Mannervik, B. (1998) 'Human glutathione transferase A4-4: an alpha class enzyme with high catalytic efficiency in the conjugation of 4-hydroxynonenal and other genotoxic products of lipid peroxidation', *Biochem J,* 330 (Pt 1), pp. 175-9.

Ifergan, I., Shafran, A., Jansen, G., Hooijberg, J. H., Scheffer, G. L. and Assaraf, Y. G. (2004) 'Folate deprivation results in the loss of breast cancer resistance protein (BCRP/ABCG2) expression. A role for BCRP in cellular folate homeostasis', *J Biol Chem,* 279, (24), pp. 25527-34.

Ilias, A., Urban, Z., Seidl, T. L., Le Saux, O., Sinko, E., Boyd, C. D., Sarkadi, B. and Varadi, A. (2002) 'Loss of ATP-dependent transport activity in pseudoxanthoma elasticum-associated mutants of human ABCC6 (MRP6)', *J Biol Chem,* 277, (19), pp. 16860-7.

Imai, Y., Ishikawa, E., Asada, S. and Sugimoto, Y. (2005) 'Estrogen-mediated post transcriptional down-regulation of breast cancer resistance protein/ABCG2', *Cancer Res,* 65, (2), pp. 596-604.

Iwase, M., Kurata, N., Ehana, R., Nishimura, Y., Masamoto, T. and Yasuhara, H. (2006) 'Evaluation of the effects of hydrophilic organic solvents on CYP3A-mediated drug-drug interaction in vitro', *Hum Exp Toxicol,* 25, (12), pp. 715-21.

Jancova, P., Anzenbacher, P. and Anzenbacherova, E. (2010) 'Phase II drug metabolizing enzymes', *Biomed Pap Med Fac Univ Palacky Olomouc Czech Repub,* 154, (2), pp. 103-16.

Jedlitschky, G., Leier, I., Buchholz, U., Barnouin, K., Kurz, G. and Keppler, D. (1996) 'Transport of glutathione, glucuronate, and sulfate conjugates by the MRP gene-encoded conjugate export pump', *Cancer Res,* 56, (5), pp. 988-94.

Jedlitschky, G., Leier, I., Buchholz, U., Hummel-Eisenbeiss, J., Burchell, B. and Keppler, D. (1997) 'ATP-dependent transport of bilirubin glucuronides by the multidrug resistance protein MRP1 and its hepatocyte canalicular isoform MRP2', *Biochem J,* 327 (Pt 1), pp. 305-10.

Jedlitschky, G., Tirschmann, K., Lubenow, L. E., Nieuwenhuis, H. K., Akkerman, J. W., Greinacher, A. and Kroemer, H. K. (2004) 'The nucleotide transporter MRP4 (ABCC4) is highly expressed in human platelets and present in dense granules, indicating a role in mediator storage', *Blood,* 104, (12), pp. 3603-10.

Jennen, D. G. J., Magkoufopoulou, C., Ketelslegers, H. B., van Herwijnen, M. H. M., Kleinjans, J. C. S. and van Delft, J. H. M. (2010) 'Comparison of HepG2 and HepaRG by Whole-Genome Gene Expression Analysis for the Purpose of Chemical Hazard Identification', *Toxicol. Sci.,* 115, (1), pp. 66-79.

Jun Cai, Y. Z. Y. L. F. Y. Z. S. H. Q. S. M. Y. C. R. Z. X. S. Y. G. M. D. H. D. (2007) 'Directed differentiation of human embryonic stem cells into functional hepatic cells', *Hepatology,* 45, (5), pp. 1229-1239.

Jung, J., Zheng, M., Goldfarb, M. and Zaret, K. S. (1999) 'Initiation of mammalian liver development from endoderm by fibroblast growth factors', *Science,* 284, (5422), pp. 1998-2003.

Kacevska, M., Robertson, G. R., Clarke, S. J. and Liddle, C. (2008) 'Inflammation and CYP3A4-mediated drug metabolism in advanced cancer: impact and implications for chemotherapeutic drug dosing', *Expert Opinion on Drug Metabolism & Toxicology,* 4, (2), pp. 137-149.

Kamisako, T., Leier, I., Cui, Y., Konig, J., Buchholz, U., Hummel-Eisenbeiss, J. and Keppler, D. (1999) 'Transport of monoglucuronosyl and bisglucuronosyl bilirubin by recombinant human and rat multidrug resistance protein 2', *Hepatology,* 30, (2), pp. 485-90.

Kanebratt, K. P. and Andersson, T. B. (2008a) 'Evaluation of HepaRG Cells as an In Vitro Model for Human Drug Metabolism Studies', *Drug Metab Dispos*, pp. dmd.107.020016.

Kanebratt, K. P. and Andersson, T. B. (2008b) 'HepaRG Cells as an In Vitro Model for Evaluation of Cytochrome P450 Induction in Humans', *Drug Metab Dispos*, pp. dmd.107.017418.

Kast, H. R., Goodwin, B., Tarr, P. T., Jones, S. A., Anisfeld, A. M., Stoltz, C. M., Tontonoz, P., Kliewer, S., Willson, T. M. and Edwards, P. A. (2002) 'Regulation of multidrug resistance-associated protein 2 (ABCC2) by the nuclear receptors pregnane X receptor, farnesoid X-activated receptor, and constitutive androstane receptor', *J Biol Chem,* 277, (4), pp. 2908-15.

Katoonizadeh, A., Nevens, F., Verslype, C., Pirenne, J. and Roskams, T. (2006) 'Liver regeneration in acute severe liver impairment: a clinicopathological correlation study', *Liver Int,* 26, (10), pp. 1225-33.

Kawamura, A., Graham, J., Mushtaq, A., Tsiftsoglou, S. A., Vath, G. M., Hanna, P. E., Wagner, C. R. and Sim, E. (2005) 'Eukaryotic arylamine N-acetyltransferase. Investigation of

substrate specificity by high-throughput screening', *Biochem Pharmacol,* 69, (2), pp. 347-59.

Kekuda, R., Prasad, P. D., Wu, X., Wang, H., Fei, Y. J., Leibach, F. H. and Ganapathy, V. (1998) 'Cloning and functional characterization of a potential-sensitive, polyspecific organic cation transporter (OCT3) most abundantly expressed in placenta', *J Biol Chem,* 273, (26), pp. 15971-9.

Kelly, J. and Darlington, G. (1989) 'Modulation of the liver specific phenotype in the human hepatoblastoma line Hep G2', *In Vitro Cellular & Developmental Biology - Plant,* 25, (2), pp. 217-222.

Keppler, D. (2011) 'Multidrug resistance proteins (MRPs, ABCCs): importance for pathophysiology and drug therapy', *Handb Exp Pharmacol*, (201), pp. 299-323.

Keppler, D., Jedlitschky, G. and Leier, I. (1998) 'Transport function and substrate specificity of multidrug resistance protein', *Methods Enzymol,* 292, pp. 607-16.

Kidambi, S., Yarmush, R. S., Novik, E., Chao, P., Yarmush, M. L. and Nahmias, Y. (2009) 'Oxygen-mediated enhancement of primary hepatocyte metabolism, functional polarization, gene expression, and drug clearance', *Proc Natl Acad Sci U S A,* 106, (37), pp. 15714-9.

Kim, Y. and Rajagopalan, P. (2010) '3D hepatic cultures simultaneously maintain primary hepatocyte and liver sinusoidal endothelial cell phenotypes', *PLoS One,* 5, (11), pp. e15456.

Kimura, H., Takeda, M., Narikawa, S., Enomoto, A., Ichida, K. and Endou, H. (2002) 'Human organic anion transporters and human organic cation transporters mediate renal transport of prostaglandins', *J Pharmacol Exp Ther,* 301, (1), pp. 293-8.

Kinoshita, T. and Miyajima, A. (2002) 'Cytokine regulation of liver development', *Biochim Biophys Acta,* 1592, (3), pp. 303-12.

Kinoshita, T., Sekiguchi, T., Xu, M. J., Ito, Y., Kamiya, A., Tsuji, K., Nakahata, T. and Miyajima, A. (1999) 'Hepatic differentiation induced by oncostatin M attenuates fetal liver hematopoiesis', *Proc Natl Acad Sci U S A,* 96, (13), pp. 7265-70.

Kiso, S., Kawata, S., Tamura, S., Higashiyama, S., Ito, N., Tsushima, H., Taniguchi, N. and Matsuzawa, Y. (1995) 'Role of heparin-binding epidermal growth factor-like growth factor as a hepatotrophic factor in rat liver regeneration after partial hepatectomy', *Hepatology,* 22, (5), pp. 1584-90.

Kmiec, Z. (2001) 'Cooperation of liver cells in health and disease', *Adv Anat Embryol Cell Biol,* 161, pp. III-XIII, 1-151.

Koepsell, H. and Endou, H. (2004) 'The SLC22 drug transporter family', *Pflugers Arch,* 447, (5), pp. 666-76.

Koepsell, H., Lips, K. and Volk, C. (2007) 'Polyspecific organic cation transporters: structure, function, physiological roles, and biopharmaceutical implications', *Pharm Res,* 24, (7), pp. 1227-51.

Koepsell, H., Schmitt, B. M. and Gorboulev, V. (2003) 'Organic cation transporters', *Rev Physiol Biochem Pharmacol,* 150, pp. 36-90.

Kohle, C. and Bock, K. W. (2009) 'Coordinate regulation of human drug-metabolizing enzymes, and conjugate transporters by the Ah receptor, pregnane X receptor and constitutive androstane receptor', *Biochem Pharmacol,* 77, (4), pp. 689-99.

Konig, J., Cui, Y., Nies, A. T. and Keppler, D. (2000a) 'Localization and genomic organization of a new hepatocellular organic anion transporting polypeptide', *J Biol Chem,* 275, (30), pp. 23161-8.

Konig, J., Cui, Y., Nies, A. T. and Keppler, D. (2000b) 'A novel human organic anion transporting polypeptide localized to the basolateral hepatocyte membrane', *Am J Physiol Gastrointest Liver Physiol,* 278, (1), pp. G156-64.

Krueger, S. K. and Williams, D. E. (2005) 'Mammalian flavin-containing monooxygenases: structure/function, genetic polymorphisms and role in drug metabolism', *Pharmacol Ther,* 106, (3), pp. 357-87.

Kullak-Ublick, G. A., Ismair, M. G., Stieger, B., Landmann, L., Huber, R., Pizzagalli, F., Fattinger, K., Meier, P. J. and Hagenbuch, B. (2001) 'Organic anion-transporting polypeptide B (OATP-B) and its functional comparison with three other OATPs of human liver', *Gastroenterology,* 120, (2), pp. 525-33.

Kung, J. W., Currie, I. S., Forbes, S. J. and Ross, J. A. (2010) 'Liver development, regeneration, and carcinogenesis', *J Biomed Biotechnol,* 2010, pp. 984248.

Kurash, J. K., Shen, C. N. and Tosh, D. (2004) 'Induction and regulation of acute phase proteins in transdifferentiated hepatocytes', *Exp Cell Res,* 292, (2), pp. 342-58.

Kusama, M., Kubota, T., Matsukura, Y., Matsuno, K., Ogawa, S., Kanda, Y. and Iga, T. (2006) 'Influence of glutathione S-transferase A1 polymorphism on the pharmacokinetics of busulfan', *Clin Chim Acta,* 368, (1-2), pp. 93-8.

Kuwahara, R., Kofman, A. V., Landis, C. S., Swenson, E. S., Barendswaard, E. and Theise, N. D. (2008) 'The hepatic stem cell niche: identification by label-retaining cell assay', *Hepatology,* 47, (6), pp. 1994-2002.

Landry, J., Bernier, D., Ouellet, C., Goyette, R. and Marceau, N. (1985) 'Spheroidal aggregate culture of rat liver cells: histotypic reorganization, biomatrix deposition, and maintenance of functional activities', *J Cell Biol,* 101, (3), pp. 914-23.

Larionov, A., Krause, A. and Miller, W. (2005) 'A standard curve based method for relative real time PCR data processing', *BMC Bioinformatics,* 6, pp. 62.

Lasser, K. E., Allen, P. D., Woolhandler, S. J., Himmelstein, D. U., Wolfe, S. M. and Bor, D. H. (2002) 'Timing of New Black Box Warnings and Withdrawals for Prescription Medications', *JAMA,* 287, (17), pp. 2215-2220.

Le Vee, M., Jigorel, E., Glaise, D., Gripon, P., Guguen-Guillouzo, C. and Fardel, O. (2006) 'Functional expression of sinusoidal and canalicular hepatic drug transporters in the differentiated human hepatoma HepaRG cell line', *European Journal of Pharmaceutical Sciences,* 28, (1-2), pp. 109-117.

Le Vee, M., Jouan, E. and Fardel, O. (2010) 'Involvement of aryl hydrocarbon receptor in basal and 2,3,7,8-tetrachlorodibenzo-p-dioxin-induced expression of target genes in primary human hepatocytes', *Toxicol In Vitro,* 24, (6), pp. 1775-81.

Le Vee, M., Lecureur, V., Moreau, A., Stieger, B. and Fardel, O. (2009) 'Differential regulation of drug transporter expression by hepatocyte growth factor in primary human hepatocytes', *Drug Metab Dispos,* 37, (11), pp. 2228-35.

LeCouter, J., Moritz, D. R., Li, B., Phillips, G. L., Liang, X. H., Gerber, H. P., Hillan, K. J. and Ferrara, N. (2003) 'Angiogenesis-independent endothelial protection of liver: role of VEGFR-1', *Science,* 299, (5608), pp. 890-3.

Lee, J., Cuddihy, M. J., Cater, G. M. and Kotov, N. A. (2009) 'Engineering liver tissue spheroids with inverted colloidal crystal scaffolds', *Biomaterials,* 30, (27), pp. 4687-94.

Lee, K. D., Kuo, T. K., Whang-Peng, J., Chung, Y. F., Lin, C. T., Chou, S. H., Chen, J. R., Chen, Y. P. and Lee, O. K. (2004a) 'In vitro hepatic differentiation of human mesenchymal stem cells', *Hepatology,* 40, (6), pp. 1275-84.

Lee, Y. M., Cui, Y., Konig, J., Risch, A., Jager, B., Drings, P., Bartsch, H., Keppler, D. and Nies, A. T. (2004b) 'Identification and functional characterization of the natural variant MRP3-Arg1297His of human multidrug resistance protein 3 (MRP3/ABCC3)', *Pharmacogenetics,* 14, (4), pp. 213-23.

Leier, I., Jedlitschky, G., Buchholz, U., Cole, S. P., Deeley, R. G. and Keppler, D. (1994) 'The MRP gene encodes an ATP-dependent export pump for leukotriene C4 and structurally related conjugates', *J Biol Chem,* 269, (45), pp. 27807-10.

Leonardi, A., DeFranchis, G., Fregona, I. A., Violato, D., Plebani, M. and Secchi, A. G. (2001) 'Effects of cyclosporin A on human conjunctival fibroblasts', *Arch Ophthalmol,* 119, (10), pp. 1512-7.

Leslie, E. M., Deeley, R. G. and Cole, S. P. C. (2005) 'Multidrug resistance proteins: role of P-glycoprotein, MRP1, MRP2, and BCRP (ABCG2) in tissue defense', *Toxicology and Applied Pharmacology,* 204, (3), pp. 216-237.

Leslie, E. M., Haimeur, A. and Waalkes, M. P. (2004) 'Arsenic transport by the human multidrug resistance protein 1 (MRP1/ABCC1). Evidence that a tri-glutathione conjugate is required', *J Biol Chem,* 279, (31), pp. 32700-8.

Lewis, D. F., Ioannides, C. and Parke, D. V. (1998) 'Cytochromes P450 and species differences in xenobiotic metabolism and activation of carcinogen', *Environ Health Perspect,* 106, (10), pp. 633-41.

Li, A. P. (2007) 'Human hepatocytes: Isolation, cryopreservation and applications in drug development', *Chemico-Biological Interactions,* 168, (1), pp. 16-29.

Libbrecht, L. and Roskams, T. (2002) 'Hepatic progenitor cells in human liver diseases', *Semin Cell Dev Biol,* 13, (6), pp. 389-96.

Lim, P. L. K., Tan, W., Latchoumycandane, C., Mok, W. C., Khoo, Y. M., Lee, H. S., Sattabongkot, J., Beerheide, W., Lim, S. G., Tan, T. M. C. and Boelsterli, U. A. (2007) 'Molecular and functional characterization of drug-metabolizing enzymes and transporter expression in the novel spontaneously immortalized human hepatocyte line HC-04', *Toxicology in Vitro,* 21, (8), pp. 1390-1401.

Lin, J. H. (1995) 'Species similarities and differences in pharmacokinetics', *Drug Metab Dispos,* 23, (10), pp. 1008-21.

Lin, J. H. (2006) 'CYP induction-mediated drug interactions: in vitro assessment and clinical implications', *Pharm Res,* 23, (6), pp. 1089-116.

Lin, J. H. and Yamazaki, M. (2003) 'Role of P-glycoprotein in pharmacokinetics: clinical implications', *Clin Pharmacokinet,* 42, (1), pp. 59-98.

Lindroos, P. M., Zarnegar, R. and Michalopoulos, G. K. (1991) 'Hepatocyte growth factor (hepatopoietin A) rapidly increases in plasma before DNA synthesis and liver regeneration stimulated by partial hepatectomy and carbon tetrachloride administration', *Hepatology,* 13, (4), pp. 743-50.

Little, J. M., Kurkela, M., Sonka, J., Jantti, S., Ketola, R., Bratton, S., Finel, M. and Radominska-Pandya, A. (2004) 'Glucuronidation of oxidized fatty acids and prostaglandins B1 and

E2 by human hepatic and recombinant UDP-glucuronosyltransferases', *J Lipid Res,* 45, (9), pp. 1694-703.

Liu, Z., Sakamoto, T., Ezure, T., Yokomuro, S., Murase, N., Michalopoulos, G. and Demetris, A. J. (1998) 'Interleukin-6, hepatocyte growth factor, and their receptors in biliary epithelial cells during a type I ductular reaction in mice: interactions between the periductal inflammatory and stromal cells and the biliary epithelium', *Hepatology,* 28, (5), pp. 1260-8.

Lloyd, T. D., Orr, S., Skett, P., Berry, D. P. and Dennison, A. R. (2003) 'Cryopreservation of hepatocytes: a review of current methods for banking', *Cell Tissue Bank,* 4, (1), pp. 3-15.

Lo, H. W. and Ali-Osman, F. (2007) 'Genetic polymorphism and function of glutathione S-transferases in tumor drug resistance', *Curr Opin Pharmacol,* 7, (4), pp. 367-74.

Loe, D. W., Almquist, K. C., Deeley, R. G. and Cole, S. P. (1996) 'Multidrug resistance protein (MRP)-mediated transport of leukotriene C4 and chemotherapeutic agents in membrane vesicles. Demonstration of glutathione-dependent vincristine transport', *J Biol Chem,* 271, (16), pp. 9675-82.

Loe, D. W., Deeley, R. G. and Cole, S. P. (2000) 'Verapamil stimulates glutathione transport by the 190-kDa multidrug resistance protein 1 (MRP1)', *J Pharmacol Exp Ther,* 293, (2), pp. 530-8.

Malato, Y., Sander, L. E., Liedtke, C., Al-Masaoudi, M., Tacke, F., Trautwein, C. and Beraza, N. (2008) 'Hepatocyte-specific inhibitor-of-kappaB-kinase deletion triggers the innate immune response and promotes earlier cell proliferation during liver regeneration', *Hepatology,* 47, (6), pp. 2036-50.

Marek, C. J., Cameron, G. A., Elrick, L. J., Hawksworth, G. M. and Wright, M. C. (2003) 'Generation of hepatocytes expressing functional cytochromes P450 from a pancreatic progenitor cell line in vitro', *Biochem J,* 370, (Pt 3), pp. 763-9.

Martin, H., Sarsat, J. P., Lerche-Langrand, C., Housset, C., Balladur, P., Toutain, H. and Albaladejo, V. (2002) 'Morphological and biochemical integrity of human liver slices in long-term culture: effects of oxygen tension', *Cell Biol Toxicol,* 18, (2), pp. 73-85.

Massie, I., Selden, C., Hodgson, H. and Fuller, B. (2011) 'Cryopreservation of encapsulated liver spheroids for a bioartificial liver: reducing latent cryoinjury using an ice nucleating agent', *Tissue Eng Part C Methods,* 17, (7), pp. 765-74.

Matsson, P., Pedersen, J. M., Norinder, U., Bergstrom, C. A. and Artursson, P. (2009) 'Identification of novel specific and general inhibitors of the three major human ATP-binding cassette transporters P-gp, BCRP and MRP2 among registered drugs', *Pharm Res,* 26, (8), pp. 1816-31.

Matsushima, S., Maeda, K., Hayashi, H., Debori, Y., Schinkel, A. H., Schuetz, J. D., Kusuhara, H. and Sugiyama, Y. (2008) 'Involvement of multiple efflux transporters in hepatic disposition of fexofenadine', *Mol Pharmacol,* 73, (5), pp. 1474-83.

Mavri-Damelin, D., Damelin, L. H., Eaton, S., Rees, M., Selden, C. and Hodgson, H. J. (2008) 'Cells for bioartificial liver devices: the human hepatoma-derived cell line C3A produces urea but does not detoxify ammonia', *Biotechnol Bioeng,* 99, (3), pp. 644-51.

McGill, M. R., Yan, H. M., Ramachandran, A., Murray, G. J., Rollins, D. E. and Jaeschke, H. (2011) 'HepaRG cells: a human model to study mechanisms of acetaminophen hepatotoxicity', *Hepatology,* 53, (3), pp. 974-82.

McGuckin, C. P., Forraz, N., Baradez, M. O., Navran, S., Zhao, J., Urban, R., Tilton, R. and Denner, L. (2005) 'Production of stem cells with embryonic characteristics from human umbilical cord blood', *Cell Proliferation,* 38, (4), pp. 245-255.

Mead, J. E. and Fausto, N. (1989) 'Transforming growth factor alpha may be a physiological regulator of liver regeneration by means of an autocrine mechanism', *Proc Natl Acad Sci U S A,* 86, (5), pp. 1558-62.

Medine, C. N., Greenhough, S. and Hay, D. C. (2010) 'Role of stem-cell-derived hepatic endoderm in human drug discovery', *Biochem Soc Trans,* 38, (4), pp. 1033-6.

Meinl, W., Meerman, J. H. and Glatt, H. (2002) 'Differential activation of promutagens by alloenzymes of human sulfotransferase 1A2 expressed in Salmonella typhimurium', *Pharmacogenetics,* 12, (9), pp. 677-89.

Melkonyan, H., Sorg, C. and Klempt, M. (1996) 'Electroporation efficiency in mammalian cells is increased by dimethyl sulfoxide (DMSO)', *Nucleic Acids Res,* 24, (21), pp. 4356-7.

Michalopoulos, G. K. (2007) 'Liver regeneration', *J Cell Physiol,* 213, (2), pp. 286-300.

Michalopoulos, G. K. (2010) 'Liver regeneration after partial hepatectomy: critical analysis of mechanistic dilemmas', *Am J Pathol,* 176, (1), pp. 2-13.

Michalopoulos, G. K. and DeFrances, M. C. (1997) 'Liver regeneration', *Science,* 276, (5309), pp. 60-6.

Miki, T., Ring, A. and Gerlach, J. (2011) 'Hepatic differentiation of human embryonic stem cells is promoted by three-dimensional dynamic perfusion culture conditions', *Tissue Eng Part C Methods,* 17, (5), pp. 557-68.

Mills, J. B., Rose, K. A., Sadagopan, N., Sahi, J. and de Morais, S. M. F. (2004) 'Induction of Drug Metabolism Enzymes and MDR1 Using a Novel Human Hepatocyte Cell Line', *J Pharmacol Exp Ther,* 309, (1), pp. 303-309.

Mitchell, C., Nivison, M., Jackson, L. F., Fox, R., Lee, D. C., Campbell, J. S. and Fausto, N. (2005) 'Heparin-binding epidermal growth factor-like growth factor links hepatocyte priming with cell cycle progression during liver regeneration', *J Biol Chem,* 280, (4), pp. 2562-8.

Mito, M. (1986) 'Hepatic assist: present and future', *Artif Organs,* 10, (3), pp. 214-8.

Mohammed, F. F. and Khokha, R. (2005) 'Thinking outside the cell: proteases regulate hepatocyte division', *Trends Cell Biol,* 15, (10), pp. 555-63.

Molderings, G. J., Bruss, M., Bonisch, H. and Gothert, M. (2003) 'Identification and pharmacological characterization of a specific agmatine transport system in human tumor cell lines', *Ann N Y Acad Sci,* 1009, pp. 75-81.

Monga, S. P., Mars, W. M., Pediaditakis, P., Bell, A., Mule, K., Bowen, W. C., Wang, X., Zarnegar, R. and Michalopoulos, G. K. (2002) 'Hepatocyte growth factor induces Wnt-independent nuclear translocation of beta-catenin after Met-beta-catenin dissociation in hepatocytes', *Cancer Res,* 62, (7), pp. 2064-71.

Moore, J. T. and Kliewer, S. A. (2000) 'Use of the nuclear receptor PXR to predict drug interactions', *Toxicology,* 153, (1-3), pp. 1-10.

Morin, O. and Normand, C. (1986) 'Long-term maintenance of hepatocyte functional activity in co-culture: requirements for sinusoidal endothelial cells and dexamethasone', *J Cell Physiol,* 129, (1), pp. 103-10.

Mottino, A. D. and Catania, V. A. (2008) 'Hepatic drug transporters and nuclear receptors: regulation by therapeutic agents', *World J Gastroenterol,* 14, (46), pp. 7068-74.

Mougey, E. B., Feng, H., Castro, M., Irvin, C. G. and Lima, J. J. (2009) 'Absorption of montelukast is transporter mediated: a common variant of OATP2B1 is associated with reduced plasma concentrations and poor response', *Pharmacogenet Genomics,* 19, (2), pp. 129-38.

Nahmias, Y., Berthiaume, F. and Yarmush, M. L. (2007) 'Integration of technologies for hepatic tissue engineering', *Adv Biochem Eng Biotechnol,* 103, pp. 309-29.

Nahmias, Y., Kramvis, Y., Barbe, L., Casali, M., Berthiaume, F. and Yarmush, M. L. (2006) 'A novel formulation of oxygen-carrying matrix enhances liver-specific function of cultured hepatocytes', *FASEB J,* 20, (14), pp. 2531-3.

Nakabayashi, H., Taketa, K., Miyano, K., Yamane, T. and Sato, J. (1982) 'Growth of human hepatoma cells lines with differentiated functions in chemically defined medium', *Cancer Res,* 42, (9), pp. 3858-63.

Nelson, D. R., Koymans, L., Kamataki, T., Stegeman, J. J., Feyereisen, R., Waxman, D. J., Waterman, M. R., Gotoh, O., Coon, M. J., Estabrook, R. W., Gunsalus, I. C. and Nebert, D. W. (1996) 'P450 superfamily: update on new sequences, gene mapping, accession numbers and nomenclature', *Pharmacogenetics,* 6, (1), pp. 1-42.

Ni, Z., Bikadi, Z., Rosenberg, M. F. and Mao, Q. (2010) 'Structure and function of the human breast cancer resistance protein (BCRP/ABCG2)', *Curr Drug Metab,* 11, (7), pp. 603-17.

Niemi, M., Backman, J. T., Kajosaari, L. I., Leathart, J. B., Neuvonen, M., Daly, A. K., Eichelbaum, M., Kivisto, K. T. and Neuvonen, P. J. (2005) 'Polymorphic organic anion transporting polypeptide 1B1 is a major determinant of repaglinide pharmacokinetics', *Clin Pharmacol Ther,* 77, (6), pp. 468-78.

Nies, A. T. and Keppler, D. (2007) 'The apical conjugate efflux pump ABCC2 (MRP2)', *Pflugers Arch,* 453, (5), pp. 643-59.

Nishimura, M., Nikawa, T., Kawano, Y., Nakayama, M. and Ikeda, M. (2008) 'Effects of dimethyl sulfoxide and dexamethasone on mRNA expression of housekeeping genes in cultures of C2C12 myotubes', *Biochem Biophys Res Commun,* 367, (3), pp. 603-8.

Nishimura, M., Ueda, N. and Naito, S. (2003) 'Effects of dimethyl sulfoxide on the gene induction of cytochrome P450 isoforms, UGT-dependent glucuronosyl transferase isoforms, and ABCB1 in primary culture of human hepatocytes', *Biol Pharm Bull,* 26, (7), pp. 1052-6.

Oda, M., Yokomori, H. and Han, J. Y. (2003) 'Regulatory mechanisms of hepatic microcirculation', *Clin Hemorheol Microcirc,* 29, (3-4), pp. 167-82.

Oertel, M. and Shafritz, D. A. (2008) 'Stem cells, cell transplantation and liver repopulation', *Biochim Biophys Acta,* 1782, (2), pp. 61-74.

Ogura, J., Kobayashi, M., Itagaki, S., Hirano, T. and Iseki, K. (2008) 'Post-transcriptional regulation of breast cancer resistance protein after intestinal ischemia-reperfusion', *Biol Pharm Bull,* 31, (5), pp. 1032-5.

Olinga, P., Elferink, M. G. L., Draaisma, A. L., Merema, M. T., Castell, J. V., Pérez, G. and Groothuis, G. M. M. (2008) 'Coordinated induction of drug transporters and phase I and II metabolism in human liver slices', *European Journal of Pharmaceutical Sciences,* 33, (4-5), pp. 380-389.

Olsavsky, K. M., Page, J. L., Johnson, M. C., Zarbl, H., Strom, S. C. and Omiecinski, C. J. (2007) 'Gene expression profiling and differentiation assessment in primary human hepatocyte cultures, established hepatoma cell lines, and human liver tissues', *Toxicol Appl Pharmacol,* 222, (1), pp. 42-56.

Orloff, J., Douglas, F., Pinheiro, J., Levinson, S., Branson, M., Chaturvedi, P., Ette, E., Gallo, P., Hirsch, G., Mehta, C., Patel, N., Sabir, S., Springs, S., Stanski, D., Evers, M. R., Fleming, E., Singh, N., Tramontin, T. and Golub, H. (2009) 'The future of drug development: advancing clinical trial design', *Nat Rev Drug Discov,* 8, (12), pp. 949-57.

Oswald, M., Kullak-Ublick, G. A., Paumgartner, G. and Beuers, U. (2001) 'Expression of hepatic transporters OATP-C and MRP2 in primary sclerosing cholangitis', *Liver,* 21, (4), pp. 247-53.

Owen, A., Goldring, C., Morgan, P., Park, B. K. and Pirmohamed, M. (2006) 'Induction of P-glycoprotein in lymphocytes by carbamazepine and rifampicin: the role of nuclear hormone response elements', *Br J Clin Pharmacol,* 62, (2), pp. 237-42.

Ozaki, I., Zhang, H., Mizuta, T., Ide, Y., Eguchi, Y., Yasutake, T., Sakamaki, T., Pestell, R. G. and Yamamoto, K. (2007) 'Menatetrenone, a vitamin K2 analogue, inhibits hepatocellular carcinoma cell growth by suppressing cyclin D1 expression through inhibition of nuclear factor kappaB activation', *Clin Cancer Res,* 13, (7), pp. 2236-45.

Ozvegy-Laczka, C., Varady, G., Koblos, G., Ujhelly, O., Cervenak, J., Schuetz, J. D., Sorrentino, B. P., Koomen, G. J., Varadi, A., Nemet, K. and Sarkadi, B. (2005) 'Function-dependent conformational changes of the ABCG2 multidrug transporter modify its interaction with a monoclonal antibody on the cell surface', *J Biol Chem,* 280, (6), pp. 4219-27.

Ozvegy, C., Varadi, A. and Sarkadi, B. (2002) 'Characterization of drug transport, ATP hydrolysis, and nucleotide trapping by the human ABCG2 multidrug transporter. Modulation of substrate specificity by a point mutation', *J Biol Chem,* 277, (50), pp. 47980-90.

Page, J. L., Johnson, M. C., Olsavsky, K. M., Strom, S. C., Zarbl, H. and Omiecinski, C. J. (2007) 'Gene expression profiling of extracellular matrix as an effector of human hepatocyte phenotype in primary cell culture', *Toxicol Sci,* 97, (2), pp. 384-97.

Pan, Y. Z., Morris, M. E. and Yu, A. M. (2009) 'MicroRNA-328 negatively regulates the expression of breast cancer resistance protein (BCRP/ABCG2) in human cancer cells', *Mol Pharmacol,* 75, (6), pp. 1374-9.

Paranjpe, S., Bowen, W. C., Bell, A. W., Nejak-Bowen, K., Luo, J. H. and Michalopoulos, G. K. (2007) 'Cell cycle effects resulting from inhibition of hepatocyte growth factor and its receptor c-Met in regenerating rat livers by RNA interference', *Hepatology,* 45, (6), pp. 1471-7.

Park, J. K. and Lee, D. H. (2005) 'Bioartificial liver systems: current status and future perspective', *J Biosci Bioeng,* 99, (4), pp. 311-9.

Parkinson, A., Mudra, D. R., Johnson, C., Dwyer, A. and Carroll, K. M. (2004) 'The effects of gender, age, ethnicity, and liver cirrhosis on cytochrome P450 enzyme activity in human liver microsomes and inducibility in cultured human hepatocytes', *Toxicol Appl Pharmacol,* 199, (3), pp. 193-209.

Patel, R. D., Hollingshead, B. D., Omiecinski, C. J. and Perdew, G. H. (2007) 'Aryl-hydrocarbon receptor activation regulates constitutive androstane receptor levels in murine and human liver', *Hepatology,* 46, (1), pp. 209-18.

Perez-Tomas, R. (2006) 'Multidrug resistance: retrospect and prospects in anti-cancer drug treatment', *Curr Med Chem,* 13, (16), pp. 1859-76.

Pfeifer, A. M., Cole, K. E., Smoot, D. T., Weston, A., Groopman, J. D., Shields, P. G., Vignaud, J. M., Juillerat, M., Lipsky, M. M., Trump, B. F. and et al. (1993) 'Simian virus 40 large tumor antigen-immortalized normal human liver epithelial cells express hepatocyte characteristics and metabolize chemical carcinogens', *Proc Natl Acad Sci U S A,* 90, (11), pp. 5123-7.

Philippe A. Lysy, F. S. M. N. E. M. S. (2008) 'Leukemia inhibitory factor contributes to hepatocyte-like differentiation of human bone marrow mesenchymal stem cells', *Differentiation,* 76, (10), pp. 1057-1067.

Phillips, B. W. and Crook, J. M. (2010) 'Pluripotent human stem cells: A novel tool in drug discovery', *BioDrugs,* 24, (2), pp. 99-108.

Pick, A., Klinkhammer, W. and Wiese, M. (2010) 'Specific inhibitors of the breast cancer resistance protein (BCRP)', *ChemMedChem,* 5, (9), pp. 1498-505.

Pick, A., Muller, H., Mayer, R., Haenisch, B., Pajeva, I. K., Weigt, M., Bonisch, H., Muller, C. E. and Wiese, M. (2011) 'Structure-activity relationships of flavonoids as inhibitors of breast cancer resistance protein (BCRP)', *Bioorg Med Chem,* 19, (6), pp. 2090-102.

Pierce, R. H., Campbell, J. S., Stephenson, A. B., Franklin, C. C., Chaisson, M., Poot, M., Kavanagh, T. J., Rabinovitch, P. S. and Fausto, N. (2000) 'Disruption of redox homeostasis in tumor necrosis factor-induced apoptosis in a murine hepatocyte cell line', *Am J Pathol,* 157, (1), pp. 221-36.

Prime-Chapman, H., Moore, V. and Hirst, B. H. (2005) 'Antibiotic exposure does not influence MRP2 functional expression in Caco-2 cells', *J Drug Target,* 13, (1), pp. 1-6.

Raucy, J. L. and Lasker, J. M. (1991) 'Isolation of P450 enzymes from human liver', *Methods Enzymol,* 206, pp. 577-87.

Raul Cassia, L. B. L. F. A. E. d. l. M. P. A. M.-C. P. M. H. J. d. V. M. M. Z. F. G. (1997) 'Transferrin is an early marker of hepatic differentiation, and its expression correlates with the postnatal development of oligodendrocytes in mice', *Journal of Neuroscience Research,* 50, (3), pp. 421-432.

Riccalton-Banks, L., Liew, C., Bhandari, R., Fry, J. and Shakesheff, K. (2003) 'Long-term culture of functional liver tissue: three-dimensional coculture of primary hepatocytes and stellate cells', *Tissue Eng,* 9, (3), pp. 401-10.

Ripp, S. L., Mills, J. B., Fahmi, O. A., Trevena, K. A., Liras, J. L., Maurer, T. S. and de Morais, S. M. (2006) 'Use of immortalized human hepatocytes to predict the magnitude of clinical drug-drug interactions caused by CYP3A4 induction', *Drug Metab Dispos,* 34, (10), pp. 1742-8.

Rius, M., Hummel-Eisenbeiss, J. and Keppler, D. (2008) 'ATP-dependent transport of leukotrienes B4 and C4 by the multidrug resistance protein ABCC4 (MRP4)', *J Pharmacol Exp Ther,* 324, (1), pp. 86-94.

Rius, M., Nies, A. T., Hummel-Eisenbeiss, J., Jedlitschky, G. and Keppler, D. (2003) 'Cotransport of reduced glutathione with bile salts by MRP4 (ABCC4) localized to the basolateral hepatocyte membrane', *Hepatology,* 38, (2), pp. 374-84.

Rius, M., Thon, W. F., Keppler, D. and Nies, A. T. (2005) 'Prostanoid transport by multidrug resistance protein 4 (MRP4/ABCC4) localized in tissues of the human urogenital tract', *J Urol,* 174, (6), pp. 2409-14.

Rossi, J. M., Dunn, N. R., Hogan, B. L. and Zaret, K. S. (2001) 'Distinct mesodermal signals, including BMPs from the septum transversum mesenchyme, are required in combination for hepatogenesis from the endoderm', *Genes Dev,* 15, (15), pp. 1998-2009.

Rotem, A., Toner, M., Bhatia, S., Foy, B. D., Tompkins, R. G. and Yarmush, M. L. (1994) 'Oxygen is a factor determining in vitro tissue assembly: Effects on attachment and spreading of hepatocytes', *Biotechnol Bioeng,* 43, (7), pp. 654-60.

Roymans, D., Annaert, P., Van Houdt, J., Weygers, A., Noukens, J., Sensenhauser, C., Silva, J., Van Looveren, C., Hendrickx, J., Mannens, G. and Meuldermans, W. (2005) 'EXPRESSION AND INDUCTION POTENTIAL OF CYTOCHROMES P450 IN HUMAN CRYOPRESERVED HEPATOCYTES', *Drug Metab Dispos,* 33, (7), pp. 1004-1016.

Saeki, T., Ueda, K., Tanigawara, Y., Hori, R. and Komano, T. (1993) 'Human P-glycoprotein transports cyclosporin A and FK506', *J Biol Chem,* 268, (9), pp. 6077-80.

Sainz, B., Jr. and Chisari, F. V. (2006) 'Production of Infectious Hepatitis C Virus by Well-Differentiated, Growth-Arrested Human Hepatoma-Derived Cells', *J. Virol.,* 80, (20), pp. 10253-10257.

Sainz, B., Jr., TenCate, V. and Uprichard, S. L. (2009) 'Three-dimensional Huh7 cell culture system for the study of Hepatitis C virus infection', *Virol J,* 6, pp. 103.

Sakamoto, T., Liu, Z., Murase, N., Ezure, T., Yokomuro, S., Poli, V. and Demetris, A. J. (1999) 'Mitosis and apoptosis in the liver of interleukin-6-deficient mice after partial hepatectomy', *Hepatology,* 29, (2), pp. 403-11.

Samokyszyn, V. M., Gall, W. E., Zawada, G., Freyaldenhoven, M. A., Chen, G., Mackenzie, P. I., Tephly, T. R. and Radominska-Pandya, A. (2000) '4-hydroxyretinoic acid, a novel substrate for human liver microsomal UDP-glucuronosyltransferase(s) and recombinant UGT2B7', *J Biol Chem,* 275, (10), pp. 6908-14.

Sanchez-Munoz, D., Castellano-Megias, V. M. and Romero-Gomez, M. (2007) 'Expression of bcl-2 in ductular proliferation is related to periportal hepatic stellate cell activation and fibrosis progression in patients with autoimmune cholestasis', *Dig Liver Dis,* 39, (3), pp. 262-6.

Sangan, C. B. and Tosh, D. (2010) 'Hepatic progenitor cells', *Cell Tissue Res,* 342, (2), pp. 131-7.

Santoni-Rugiu, E., Jelnes, P., Thorgeirsson, S. S. and Bisgaard, H. C. (2005) 'Progenitor cells in liver regeneration: molecular responses controlling their activation and expansion', *APMIS,* 113, (11-12), pp. 876-902.

Scharenberg, C. W., Harkey, M. A. and Torok-Storb, B. (2002) 'The ABCG2 transporter is an efficient Hoechst 33342 efflux pump and is preferentially expressed by immature human hematopoietic progenitors', *Blood,* 99, (2), pp. 507-12.

Schirmacher, P., Geerts, A., Jung, W., Pietrangelo, A., Rogler, C. E. and Dienes, H. P. (1993) 'The role of Ito cells in the biosynthesis of HGF-SF in the liver', *EXS,* 65, pp. 285-99.

Schmelzer, E., Zhang, L., Bruce, A., Wauthier, E., Ludlow, J., Yao, H. L., Moss, N., Melhem, A., McClelland, R., Turner, W., Kulik, M., Sherwood, S., Tallheden, T., Cheng, N., Furth, M. E. and Reid, L. M. (2007) 'Human hepatic stem cells from fetal and postnatal donors', *J Exp Med,* 204, (8), pp. 1973-87.

Schoonen, W. G. E. J., Westerink, W. M. A., de Roos, J. A. D. M. and Debiton, E. (2005) 'Cytotoxic effects of 100 reference compounds on Hep G2 and HeLa cells and of 60 compounds on ECC-1 and CHO cells. I Mechanistic assays on ROS, glutathione depletion and calcein uptake', *Toxicology in Vitro,* 19, (4), pp. 505-516.

Schroeder, A., Eckhardt, U., Stieger, B., Tynes, R., Schteingart, C. D., Hofmann, A. F., Meier, P. J. and Hagenbuch, B. (1998) 'Substrate specificity of the rat liver Na(+)-bile salt cotransporter in Xenopus laevis oocytes and in CHO cells', *Am J Physiol,* 274, (2 Pt 1), pp. G370-5.

Schuldiner, M., Yanuka, O., Itskovitz-Eldor, J., Melton, D. A. and Benvenisty, N. (2000) 'Effects of eight growth factors on the differentiation of cells derived from human embryonic stem cells', *Proc Natl Acad Sci U S A,* 97, (21), pp. 11307-12.

Schwartz, R. E., Reyes, M., Koodie, L., Jiang, Y., Blackstad, M., Lund, T., Lenvik, T., Johnson, S., Hu, W. S. and Verfaillie, C. M. (2002) 'Multipotent adult progenitor cells from bone marrow differentiate into functional hepatocyte-like cells', *J Clin Invest,* 109, (10), pp. 1291-302.

Sekine, T., Cha, S. H. and Endou, H. (2000) 'The multispecific organic anion transporter (OAT) family', *Pflugers Arch,* 440, (3), pp. 337-50.

Sekine, T., Cha, S. H., Tsuda, M., Apiwattanakul, N., Nakajima, N., Kanai, Y. and Endou, H. (1998) 'Identification of multispecific organic anion transporter 2 expressed predominantly in the liver', *FEBS Lett,* 429, (2), pp. 179-82.

Senoo, H., Yoshikawa, K., Morii, M., Miura, M., Imai, K. and Mezaki, Y. (2010) 'Hepatic stellate cell (vitamin A-storing cell) and its relative--past, present and future', *Cell Biol Int,* 34, (12), pp. 1247-72.

Sensken, S., Waclawczyk, S., Knaupp, A. S., Trapp, T., Enczmann, J., Wernet, P. and Kogler, G. (2007) 'In vitro differentiation of human cord blood-derived unrestricted somatic stem cells towards an endodermal pathway', *Cytotherapy,* 9, (4), pp. 362-78.

Shay, K. P. and Hagen, T. M. (2009) 'Age-associated impairment of Akt phosphorylation in primary rat hepatocytes is remediated by alpha-lipoic acid through PI3 kinase, PTEN, and PP2A', *Biogerontology,* 10, (4), pp. 443-56.

Sheehan, D., Meade, G., Foley, V. M. and Dowd, C. A. (2001) 'Structure, function and evolution of glutathione transferases: implications for classification of non-mammalian members of an ancient enzyme superfamily', *Biochem J,* 360, (Pt 1), pp. 1-16.

Shen, C. N., Slack, J. M. and Tosh, D. (2000) 'Molecular basis of transdifferentiation of pancreas to liver', *Nat Cell Biol,* 2, (12), pp. 879-87.

Shen, C. N. and Tosh, D. (2010) 'Transdifferentiation of pancreatic cells to hepatocytes', *Methods Mol Biol,* 640, pp. 273-80.

Shimada, T., Yamazaki, H., Mimura, M., Inui, Y. and Guengerich, F. P. (1994) 'Interindividual variations in human liver cytochrome P-450 enzymes involved in the oxidation of

drugs, carcinogens and toxic chemicals: studies with liver microsomes of 30 Japanese and 30 Caucasians', *J Pharmacol Exp Ther,* 270, (1), pp. 414-23.

Shin, D., Shin, C. H., Tucker, J., Ober, E. A., Rentzsch, F., Poss, K. D., Hammerschmidt, M., Mullins, M. C. and Stainier, D. Y. (2007) 'Bmp and Fgf signaling are essential for liver specification in zebrafish', *Development,* 134, (11), pp. 2041-50.

Sidhu, J. S., Liu, F. and Omiecinski, C. J. (2004) 'Phenobarbital responsiveness as a uniquely sensitive indicator of hepatocyte differentiation status: requirement of dexamethasone and extracellular matrix in establishing the functional integrity of cultured primary rat hepatocytes', *Experimental Cell Research,* 292, (2), pp. 252-264.

Singh, S. S. (2006) 'Preclinical pharmacokinetics: an approach towards safer and efficacious drugs', *Curr Drug Metab,* 7, (2), pp. 165-82.

Sivertsson, L., Ek, M., Darnell, M., Edebert, I., Ingelman-Sundberg, M. and Neve, E. P. A. (2010) 'CYP3A4 Catalytic Activity Is Induced in Confluent Huh7 Hepatoma Cells', *Drug Metabolism and Disposition,* 38, (6), pp. 995-1002.

Skett, P., Tyson, C., Guillouzo, A. and Maier, P. (1995) 'Report on the international workshop on the use of human in vitro liver preparations to study drug metabolism in drug development. Held at Utrecht, The Netherlands, 6-8 September 1994', *Biochem Pharmacol,* 50, (2), pp. 280-5.

Slany, A., Haudek, V. J., Zwickl, H., Gundacker, N. C., Grusch, M., Weiss, T. S., Seir, K., Rodgarkia-Dara, C., Hellerbrand, C. and Gerner, C. (2010) 'Cell characterization by proteome profiling applied to primary hepatocytes and hepatocyte cell lines Hep-G2 and Hep-3B', *J Proteome Res,* 9, (1), pp. 6-21.

Smit, J. J., Schinkel, A. H., Oude Elferink, R. P., Groen, A. K., Wagenaar, E., van Deemter, L., Mol, C. A., Ottenhoff, R., van der Lugt, N. M., van Roon, M. A. and et al. (1993) 'Homozygous disruption of the murine mdr2 P-glycoprotein gene leads to a complete absence of phospholipid from bile and to liver disease', *Cell,* 75, (3), pp. 451-62.

Snykers, S., De Kock, J., Vanhaecke, T. and Rogiers, V. (2007) 'Differentiation of neonatal rat epithelial cells from biliary origin into immature hepatic cells by sequential exposure to hepatogenic cytokines and growth factors reflecting liver development', *Toxicology in Vitro,* 21, (7), pp. 1325-1331.

Snykers, S., Vanhaecke, T., Papeleu, P., Luttun, A., Jiang, Y., Vander Heyden, Y., Verfaillie, C. and Rogiers, V. (2006) 'Sequential Exposure to Cytokines Reflecting Embryogenesis: The Key for in vitro Differentiation of Adult Bone Marrow Stem Cells into Functional Hepatocyte-like Cells', *Toxicol. Sci.,* 94, (2), pp. 330-341.

Soars, M. G., Grime, K., Sproston, J. L., Webborn, P. J. and Riley, R. J. (2007a) 'Use of hepatocytes to assess the contribution of hepatic uptake to clearance in vivo', *Drug Metab Dispos,* 35, (6), pp. 859-65.

Soars, M. G., McGinnity, D. F., Grime, K. and Riley, R. J. (2007b) 'The pivotal role of hepatocytes in drug discovery', *Chem Biol Interact,* 168, (1), pp. 2-15.

Stephenne, X., Najimi, M. and Sokal, E. M. (2010) 'Hepatocyte cryopreservation: is it time to change the strategy?', *World J Gastroenterol,* 16, (1), pp. 1-14.

Stocker, E. and Heine, W. D. (1971) 'Regeneration of liver parenchyma under normal and pathological conditions', *Beitr Pathol,* 144, (4), pp. 400-8.

Stocker, E., Wullstein, H. K. and Brau, G. (1973) '[Capacity of regeneration in liver epithelia of juvenile, repeated partially hepatectomized rats. Autoradiographic studies after continous infusion of 3H-thymidine (author's transl)]', *Virchows Arch B Cell Pathol,* 14, (2), pp. 93-103.

Strain, A. J. and Neuberger, J. M. (2002) 'A bioartificial liver--state of the art', *Science,* 295, (5557), pp. 1005-9.

Strassburg, C. P., Strassburg, A., Kneip, S., Barut, A., Tukey, R. H., Rodeck, B. and Manns, M. P. (2002) 'Developmental aspects of human hepatic drug glucuronidation in young children and adults', *Gut,* 50, (2), pp. 259-65.

Strom, S. C., Davila, J. and Grompe, M. (2010) 'Chimeric mice with humanized liver: tools for the study of drug metabolism, excretion, and toxicity', *Methods Mol Biol,* 640, pp. 491-509.

Suleiman, S. A. and Stevens, J. B. (1987) 'The effect of oxygen tension on rat hepatocytes in short-term culture', *In Vitro Cell Dev Biol,* 23, (5), pp. 332-8.

Sumida, K., Igarashi, Y., Toritsuka, N., Matsushita, T., Abe-Tomizawa, K., Aoki, M., Urushidani, T., Yamada, H. and Ohno, Y. (2011) 'Effects of DMSO on gene expression in human and rat hepatocytes', *Hum Exp Toxicol*.

Sumitran-Holgersson, S., Nowak, G., Thowfeequ, S., Begum, S., Joshi, M., Jaksch, M., Kjaeldgaard, A., Jorns, C., Ericzon, B. G. and Tosh, D. (2009) 'Generation of hepatocyte-like cells from in vitro transdifferentiated human fetal pancreas', *Cell Transplant,* 18, (2), pp. 183-93.

Sun, W., Wu, R. R., van Poelje, P. D. and Erion, M. D. (2001) 'Isolation of a family of organic anion transporters from human liver and kidney', *Biochem Biophys Res Commun,* 283, (2), pp. 417-22.

Sussman, N. L., Gislason, G. T., Conlin, C. A. and Kelly, J. H. (1994) 'The Hepatix extracorporeal liver assist device: initial clinical experience', *Artif Organs,* 18, (5), pp. 390-6.

Svegliati-Baroni, G., De Minicis, S. and Marzioni, M. (2008) 'Hepatic fibrogenesis in response to chronic liver injury: novel insights on the role of cell-to-cell interaction and transition', *Liver Int,* 28, (8), pp. 1052-64.

Takeda, M., Khamdang, S., Narikawa, S., Kimura, H., Hosoyamada, M., Cha, S. H., Sekine, T. and Endou, H. (2002a) 'Characterization of methotrexate transport and its drug interactions with human organic anion transporters', *J Pharmacol Exp Ther,* 302, (2), pp. 666-71.

Takeda, M., Khamdang, S., Narikawa, S., Kimura, H., Kobayashi, Y., Yamamoto, T., Cha, S. H., Sekine, T. and Endou, H. (2002b) 'Human organic anion transporters and human organic cation transporters mediate renal antiviral transport', *J Pharmacol Exp Ther,* 300, (3), pp. 918-24.

Tamai, I., Nezu, J., Uchino, H., Sai, Y., Oku, A., Shimane, M. and Tsuji, A. (2000) 'Molecular identification and characterization of novel members of the human organic anion transporter (OATP) family', *Biochem Biophys Res Commun,* 273, (1), pp. 251-60.

Tamai, I., Nozawa, T., Koshida, M., Nezu, J., Sai, Y. and Tsuji, A. (2001) 'Functional characterization of human organic anion transporting polypeptide B (OATP-B) in comparison with liver-specific OATP-C', *Pharm Res,* 18, (9), pp. 1262-9.

Tan, K. P., Wang, B., Yang, M., Boutros, P. C., Macaulay, J., Xu, H., Chuang, A. I., Kosuge, K., Yamamoto, M., Takahashi, S., Wu, A. M., Ross, D. D., Harper, P. A. and Ito, S. (2010) 'Aryl hydrocarbon receptor is a transcriptional activator of the human breast cancer resistance protein (BCRP/ABCG2)', *Mol Pharmacol,* 78, (2), pp. 175-85.

Tanaka, E., Terada, M. and Misawa, S. (2000) 'Cytochrome P450 2E1: its clinical and toxicological role', *J Clin Pharm Ther,* 25, (3), pp. 165-75.

Tanaka, M., Itoh, T., Tanimizu, N. and Miyajima, A. (2011) 'Liver stem/progenitor cells: their characteristics and regulatory mechanisms', *J Biochem,* 149, (3), pp. 231-9.

Teramoto, K., Asahina, K., Kumashiro, Y., Kakinuma, S., Chinzei, R., Shimizu-Saito, K., Tanaka, Y., Teraoka, H. and Arii, S. (2005) 'Hepatocyte differentiation from embryonic stem cells and umbilical cord blood cells', *J Hepatobiliary Pancreat Surg,* 12, (3), pp. 196-202.

Tew, K. D. (1994) 'Glutathione-associated enzymes in anticancer drug resistance', *Cancer Res,* 54, (16), pp. 4313-20.

Tietz, P. S. and Larusso, N. F. (2006) 'Cholangiocyte biology', *Curr Opin Gastroenterol,* 22, (3), pp. 279-87.

Tijet, N., Boutros, P. C., Moffat, I. D., Okey, A. B., Tuomisto, J. and Pohjanvirta, R. (2006) 'Aryl hydrocarbon receptor regulates distinct dioxin-dependent and dioxin-independent gene batteries', *Mol Pharmacol,* 69, (1), pp. 140-53.

Tilles, A. W., Baskaran, H., Roy, P., Yarmush, M. L. and Toner, M. (2001) 'Effects of oxygenation and flow on the viability and function of rat hepatocytes cocultured in a microchannel flat-plate bioreactor', *Biotechnol Bioeng,* 73, (5), pp. 379-89.

Tompkins, L. M., Li, H., Li, L., Lynch, C., Xie, Y., Nakanishi, T., Ross, D. D. and Wang, H. (2010) 'A novel xenobiotic responsive element regulated by aryl hydrocarbon receptor is involved in the induction of BCRP/ABCG2 in LS174T cells', *Biochem Pharmacol,* 80, (11), pp. 1754-61.

Tosh, D., Shen, C. N. and Slack, J. M. (2002) 'Differentiated properties of hepatocytes induced from pancreatic cells', *Hepatology,* 36, (3), pp. 534-43.

Tosh, D. and Strain, A. (2005) 'Liver stem cells--prospects for clinical use', *J Hepatol,* 42 Suppl, (1), pp. S75-84.

Tukey, R. H. and Strassburg, C. P. (2000) 'Human UDP-glucuronosyltransferases: metabolism, expression, and disease', *Annu Rev Pharmacol Toxicol,* 40, pp. 581-616.

Tuleuova, N., Lee, J. Y., Lee, J., Ramanculov, E., Zern, M. A. and Revzin, A. (2010) 'Using growth factor arrays and micropatterned co-cultures to induce hepatic differentiation of embryonic stem cells', *Biomaterials,* 31, (35), pp. 9221-31.

Tuoi Do, T. H., Gaboriau, F., Ropert, M., Moirand, R., Cannie, I., Brissot, P., Loreal, O. and Lescoat, G. (2010) 'Ethanol Effect on Cell Proliferation in the Human Hepatoma HepaRG Cell Line: Relationship With Iron Metabolism', *Alcohol Clin Exp Res*.

Urquhart, B. L., Tirona, R. G. and Kim, R. B. (2007) 'Nuclear Receptors and the Regulation of Drug-Metabolizing Enzymes and Drug Transporters: Implications for Interindividual Variability in Response to Drugs', *J Clin Pharmacol,* 47, (5), pp. 566-578.

Van de Bovenkamp, M., Groothuis, G. M., Meijer, D. K. and Olinga, P. (2007) 'Liver fibrosis in vitro: cell culture models and precision-cut liver slices', *Toxicol In Vitro,* 21, (4), pp. 545-57.

VandenBranden, M., Wrighton, S. A., Ekins, S., Gillespie, J. S., Binkley, S. N., Ring, B. J., Gadberry, M. G., Mullins, D. C., Strom, S. C. and Jensen, C. B. (1998) 'Alterations of the catalytic activities of drug-metabolizing enzymes in cultures of human liver slices', *Drug Metab Dispos,* 26, (11), pp. 1063-8.

Vandesompele, J., De Preter, K., Pattyn, F., Poppe, B., Van Roy, N., De Paepe, A. and Speleman, F. (2002) 'Accurate normalization of real-time quantitative RT-PCR data by geometric averaging of multiple internal control genes', *Genome Biol,* 3, (7), pp. RESEARCH0034.

Vellonen, K. S., Honkakoski, P. and Urtti, A. (2004) 'Substrates and inhibitors of efflux proteins interfere with the MTT assay in cells and may lead to underestimation of drug toxicity', *Eur J Pharm Sci,* 23, (2), pp. 181-8.

Vermeir, M., Annaert, P., Mamidi, R. N., Roymans, D., Meuldermans, W. and Mannens, G. (2005) 'Cell-based models to study hepatic drug metabolism and enzyme induction in humans', *Expert Opin Drug Metab Toxicol,* 1, (1), pp. 75-90.

Vessey, C. J. and de la Hall, P. M. (2001) 'Hepatic stem cells: a review', *Pathology,* 33, (2), pp. 130-41.

Vieira, I., Sonnier, M. and Cresteil, T. (1996) 'Developmental expression of CYP2E1 in the human liver. Hypermethylation control of gene expression during the neonatal period', *Eur J Biochem,* 238, (2), pp. 476-83.

Villa, P., Arioli, P. and Guaitani, A. (1991) 'Mechanism of maintenance of liver-specific functions by DMSO in cultured rat hepatocytes', *Exp Cell Res,* 194, (1), pp. 157-60.

Wagenaar, G. T., Chamuleau, R. A., Pool, C. W., de Haan, J. G., Maas, M. A., Korfage, H. A. and Lamers, W. H. (1993) 'Distribution and activity of glutamine synthase and carbamoylphosphate synthase upon enlargement of the liver lobule by repeated partial hepatectomies', *J Hepatol,* 17, (3), pp. 397-407.

Wallace, K., Marek, C. J., Currie, R. A. and Wright, M. C. (2009) 'Exocrine pancreas trans-differentiation to hepatocytes--a physiological response to elevated glucocorticoid in vivo', *J Steroid Biochem Mol Biol,* 116, (1-2), pp. 76-85.

Wang, H. and LeCluyse, E. L. (2003) 'Role of orphan nuclear receptors in the regulation of drug-metabolising enzymes', *Clin Pharmacokinet,* 42, (15), pp. 1331-57.

Webber, E. M., Bruix, J., Pierce, R. H. and Fausto, N. (1998) 'Tumor necrosis factor primes hepatocytes for DNA replication in the rat', *Hepatology,* 28, (5), pp. 1226-34.

Webber, E. M., Wu, J. C., Wang, L., Merlino, G. and Fausto, N. (1994) 'Overexpression of transforming growth factor-alpha causes liver enlargement and increased hepatocyte proliferation in transgenic mice', *Am J Pathol,* 145, (2), pp. 398-408.

Westerink, W. M. A. and Schoonen, W. G. E. J. (2007a) 'Cytochrome P450 enzyme levels in HepG2 cells and cryopreserved primary human hepatocytes and their induction in HepG2 cells', *Toxicology in Vitro,* 21, (8), pp. 1581-1591.

Westerink, W. M. A. and Schoonen, W. G. E. J. (2007b) 'Phase II enzyme levels in HepG2 cells and cryopreserved primary human hepatocytes and their induction in HepG2 cells', *Toxicology in Vitro,* 21, (8), pp. 1592-1602.

Wietholtz, H., Marschall, H. U., Sjovall, J. and Matern, S. (1996) 'Stimulation of bile acid 6 alpha-hydroxylation by rifampin', *J Hepatol,* 24, (6), pp. 713-8.

Williams, J. A., Hyland, R., Jones, B. C., Smith, D. A., Hurst, S., Goosen, T. C., Peterkin, V., Koup, J. R. and Ball, S. E. (2004) 'Drug-drug interactions for UDP-glucuronosyltransferase substrates: a pharmacokinetic explanation for typically observed low exposure (AUCi/AUC) ratios', *Drug Metab Dispos,* 32, (11), pp. 1201-8.

Winau, F., Hegasy, G., Weiskirchen, R., Weber, S., Cassan, C., Sieling, P. A., Modlin, R. L., Liblau, R. S., Gressner, A. M. and Kaufmann, S. H. (2007) 'Ito cells are liver-resident antigen-presenting cells for activating T cell responses', *Immunity,* 26, (1), pp. 117-29.

Wobus, A. M. and Loser, P. (2011) 'Present state and future perspectives of using pluripotent stem cells in toxicology research', *Arch Toxicol,* 85, (2), pp. 79-117.

Wortelboer, H. M., Usta, M., van Zanden, J. J., van Bladeren, P. J., Rietjens, I. M. C. M. and Cnubben, N. H. P. (2005) 'Inhibition of multidrug resistance proteins MRP1 and MRP2 by a series of [alpha],[beta]-unsaturated carbonyl compounds', *Biochemical Pharmacology,* 69, (12), pp. 1879-1890.

Wu, X., Kekuda, R., Huang, W., Fei, Y. J., Leibach, F. H., Chen, J., Conway, S. J. and Ganapathy, V. (1998) 'Identity of the organic cation transporter OCT3 as the extraneuronal monoamine transporter (uptake2) and evidence for the expression of the transporter in the brain', *J Biol Chem,* 273, (49), pp. 32776-86.

Xu, C., Li, C. Y. and Kong, A. N. (2005) 'Induction of phase I, II and III drug metabolism/transport by xenobiotics', *Arch Pharm Res,* 28, (3), pp. 249-68.

Yamamoto, T., Nakamura, H., Liu, W., Cao, K., Yoshikawa, S., Enomoto, H., Iwata, Y., Koh, N., Saito, M., Imanishi, H., Shimomura, S., Iijima, H., Hada, T. and Nishiguchi, S. (2009) 'Involvement of hepatoma-derived growth factor in the growth inhibition of hepatocellular carcinoma cells by vitamin K(2)', *J Gastroenterol,* 44, (3), pp. 228-35.

Yanagi, K. and Ohshima, N. (2001) 'Improvement of metabolic performance of cultured hepatocytes by high oxygen tension in the atmosphere', *Artif Organs,* 25, (1), pp. 1-6.

Yang, K., Wu, J. and Li, X. (2008) 'Recent advances in the research of P-glycoprotein inhibitors', *Biosci Trends,* 2, (4), pp. 137-46.

Yu, C. B., Pan, X. P. and Li, L. J. (2009) 'Progress in bioreactors of bioartificial livers', *Hepatobiliary Pancreat Dis Int,* 8, (2), pp. 134-40.

Zakin, M. M. (1992) 'Regulation of transferrin gene expression', *FASEB J,* 6, (14), pp. 3253-8.

Zaret, K. S. (2002) 'Regulatory phases of early liver development: paradigms of organogenesis', *Nat Rev Genet,* 3, (7), pp. 499-512.

Zeng, H., Liu, G., Rea, P. A. and Kruh, G. D. (2000) 'Transport of amphipathic anions by human multidrug resistance protein 3', *Cancer Res,* 60, (17), pp. 4779-84.

Zhang, L., Dresser, M. J., Gray, A. T., Yost, S. C., Terashita, S. and Giacomini, K. M. (1997) 'Cloning and functional expression of a human liver organic cation transporter', *Mol Pharmacol,* 51, (6), pp. 913-21.

Zhang, L., Gorset, W., Dresser, M. J. and Giacomini, K. M. (1999) 'The interaction of n-tetraalkylammonium compounds with a human organic cation transporter, hOCT1', *J Pharmacol Exp Ther,* 288, (3), pp. 1192-8.

Zhang, W., Yatskievych, T. A., Baker, R. K. and Antin, P. B. (2004) 'Regulation of Hex gene expression and initial stages of avian hepatogenesis by Bmp and Fgf signaling', *Dev Biol,* 268, (2), pp. 312-26.

Zheng, Z. Y., Weng, S. Y. and Yu, Y. (2009) 'Signal molecule-mediated hepatic cell communication during liver regeneration', *World J Gastroenterol,* 15, (46), pp. 5776-83.

Zhou, J. and Shephard, E. A. (2006) 'Mutation, polymorphism and perspectives for the future of human flavin-containing monooxygenase 3', *Mutation Research/Reviews in Mutation Research,* 612, (3), pp. 165-171.

Zhou, S.-F., Wang, B., Yang, L.-P. and Liu, J.-P. (2010) 'Structure, function, regulation and polymorphism and the clinical significance of human cytochrome P450 1A2', *Drug Metabolism Reviews,* 42, (2), pp. 268-354.

Ziegler-Skylakakis, K., Nill, S., Pan, J. F. and Andrae, U. (1998) 'S-oxygenation of thiourea results in the formation of genotoxic products', *Environ Mol Mutagen,* 31, (4), pp. 362-73.